Lecture Notes in Civil Engineering

Lelitha Devi
Madhu Errampalli
Avijit Maji
Gitakrishnan Ramadurai *Editors*

Proceedings of the Sixth International Conference of Transportation Research Group of India

CTRG 2021 Volume 3

Springer

Lecture Notes in Civil Engineering

Volume 273

Lecture Notes in Civil Engineering (LNCE) publishes the latest developments in Civil Engineering—quickly, informally and in top quality. Though original research reported in proceedings and post-proceedings represents the core of LNCE, edited volumes of exceptionally high quality and interest may also be considered for publication. Volumes published in LNCE embrace all aspects and subfields of, as well as new challenges in, Civil Engineering. Topics in the series include:

- Construction and Structural Mechanics
- Building Materials
- Concrete, Steel and Timber Structures
- Geotechnical Engineering
- Earthquake Engineering
- Coastal Engineering
- Ocean and Offshore Engineering; Ships and Floating Structures
- Hydraulics, Hydrology and Water Resources Engineering
- Environmental Engineering and Sustainability
- Structural Health and Monitoring
- Surveying and Geographical Information Systems
- Indoor Environments
- Transportation and Traffic
- Risk Analysis
- Safety and Security

To submit a proposal or request further information, please contact the appropriate Springer Editor:

– Pierpaolo Riva at pierpaolo.riva@springer.com (Europe and Americas);
– Swati Meherishi at swati.meherishi@springer.com (Asia—except China, Australia, and New Zealand);
– Wayne Hu at wayne.hu@springer.com (China).

All books in the series now indexed by Scopus and EI Compendex database!

Lelitha Devi · Madhu Errampalli · Avijit Maji ·
Gitakrishnan Ramadurai
Editors

Proceedings of the Sixth International Conference of Transportation Research Group of India

CTRG 2021 Volume 3

Springer

Editors
Lelitha Devi
Department of Civil Engineering
Indian Institute of Technology Madras
Chennai, Tamil Nadu, India

Avijit Maji
Department of Civil Engineering
Indian Institute of Technology Bombay
Mumbai, India

Madhu Errampalli
CSIR-Central Road Research Institute
New Delhi, India

Gitakrishnan Ramadurai
Department of Civil Engineering
Indian Institute of Technology Madras
Chennai, Tamil Nadu, India

ISSN 2366-2557 ISSN 2366-2565 (electronic)
Lecture Notes in Civil Engineering
ISBN 978-981-19-4203-7 ISBN 978-981-19-4204-4 (eBook)
https://doi.org/10.1007/978-981-19-4204-4

This Springer imprint is published by the registered company Springer Nature Singapore Pte Ltd.
The registered company address is: 152 Beach Road, #21-01/04 Gateway East, Singapore 189721, Singapore

Preface

The Transportation Research Group of India (TRG) has put together the edited book titled Proceedings of the Sixth International Conference of Transportation Research Group of India—CTRG 2021 in three volumes. This is the third volume with 26 selected papers on themes TCT-E01: Environment (including energy) and sustainability in transportation, TCT-F01: Transportation safety and security, and TCT-H01: Emerging travel technology. Six of these papers are on theme TCT-E01, 11 on TCT-F01, and 9 on TCT-H01. All the selected papers went through a double-blind review process prior to the selection. We acknowledge the support of Prof. Manoranjan Parida and Prof. P. Vedagiri, in managing the review process. We also thank all the anonymous reviewers for the valuable and timely review comments.

The CTRG 2021 was held at Trichy, India, from 14 to 17 December 2021 in the decennial year of the TRG. It provided a platform for academicians, professionals, and researchers from India and abroad working on transportation-related problems and their solutions. The compiled papers in this book represent cutting-edge research work from various parts of the world. This volume, like the other two volumes, will provide insights that the readers will find helpful in solving a variety of transportation problems.

Chennai, India — Lelitha Devi
New Delhi, India — Madhu Errampalli
Mumbai, India — Avijit Maji
Chennai, India — Gitakrishnan Ramadurai

About TRG and CTRG

Transportation Research Group of India (TRG) is a not-for-profit registered society with the mission to aid India's overall growth through focused transportation research, education, and policies in the country. It was formally registered on 28 May 2011 and has completed 10 years of its journey this year. The following are the vision and objectives of TRG:

Vision

- To provide a unique forum within India for the interchange of ideas among transportation researchers, educators, managers, and policymakers from India and all over the world, with the intention of covering all modes and sectors of transport (road, rail, air, and water; public and private; motorized and non-motorized) as well as all levels (urban, regional, inter-city, and rural transport) and for both passenger as well as freight movement, in India. At the same time, to also address the transportation-related issues of safety, efficiency, economic and social development, local and global environmental impact, energy, land use, equity and, access for the widest range of travelers with special needs, etc.

- To serve as a platform to guide and focus transportation research, education, and policies in India towards satisfying the country's needs and assist in its overall growth.

Objectives

- To conduct a regular peer-reviewed conference in India so as to provide a dedicated platform for the exchange of ideas and knowledge among transportation researchers, educators, managers, and policymakers from India and all over the world, from a perspective which is multimodal, multidisciplinary, multilevel, and multi-sectoral, but with an India-centric focus. Initially, this conference will be held every 2 years; however, the frequency may change as per the decision of the society from time to time.
- To publish a peer-reviewed journal of good international standard that considers and recognizes quality research work done for Indian conditions, but which also encourages quality research focused on other developing and developed countries that can potentially provide useful learning lessons to address Indian issues.
- To conduct other activities such as seminars, training and research programs, meetings, discussions, etc., as decided by the society from time to time, towards fulfilling the mission and vision of the society.
- To identify pertinent issues of national importance, related to transportation research, education, and policy through various activities of the society, and promote transportation researchers, educators, managers, and policymakers in an appropriate manner to address the same.
- To collaborate with other international societies and organizations, like WCTRS, ASCE, TRB, etc., in a manner that works towards fulfilling the mission and vision of the society.

The Conference of Transportation Research Group of India (CTRG) is the premier event of TRG. It is held every 2 years and traditionally moves around India. In the past, CTRG has been organized in Bangalore (Dec. 2011), Agra (Dec. 2013), Kolkata (Dec. 2015), Mumbai (Dec. 2017), Bhopal (Dec. 2019), Trichy (Dec. 2021), and Surat (upcoming in Dec. 2023 jointly with SVNIT Surat). CTRG has been getting a wide-scale recognition from reputed Indian and international institutions/organizations, like IIT Kanpur, IIT Kharagpur, IIT Guwahati, IIT Bombay (Mumbai), SVNIT Surat, MANIT Bhopal, NIT Trichy, TRB, WCTRS, CSIR-CRRI, ATPIO, T&DI-ASCE, and EASTS, to name a few. CTRG is a large conference typically attended by around 400–500 participants, usually from 12 to 15 countries, with about 200 double-blind peer-reviewed technical papers being presented. The conference provides a wide range of executive courses, tutorials, workshops, technical tours, keynote sessions, and special sessions.

Transportation in Developing Economies (TiDE) is the official journal of TRG and is published by Springer. TiDE was formally launched in 2014 and has so far published eight volumes.

Prof. Akhilesh Kumar Maurya
Indian Institute of Technology Guwahati
Current President, TRG

Reviewers

Ammu Gopalakrishnan, School of planning and architecture, Delhi, India
Ankit Gupta, Shiv Nadar University Dadri, India
Niraj Sharma, CRRI, Delhi, India
Padmarekha, SRM, Chennai, India
Saurabh Dandapat, PwC India, India
Yogeshwar Navandar, NIT Calicut, India
Abdul Pinjari, IISc Bangalore, India
Abdullah Ahmad, NIT Srinager, India
Aboelkasim Diab, Aswan University, Egypt
Aditya Kumar Das, S'O'A University Bhubaneswar, India
Aditya Medury, IIT Kanpur, India
Agnivesh Pani, IIT (BHU) Varanasi, India
Akhilesh Chepuri, GITAM School of technology Hyderabad, India
Akhilesh Kumar Maurya, IIT Guwahati, India
Ambika Behl, CRRI, New Delhi, India
Ambika Kuity, NIT Silchar, India
Amit Agarwal, IIT Roorkee, India
Amit Kumar Yadav, Central University of Jharkhand, India
Aneena Mohan, IIT Bombay, India
Aninda Bijoy Paul, SVNIT, Surat, India
Anjan Kumar Siddagangaiah, IIT Guwahati, India
Ankit Kathuria, IIT Jammu, India
Ankit Kumar Yadav, IIT Bombay, India
Ankit Yadav, IIT Bombay, India
Anna Charly, IIT Bombay, India
Anuj Budhkar, IIEST, Shibpur, India
Anush Chandrappa, IIT Bhubaneswar, India
Anusha S. P., College of Engineering Trivandrum, India
Apparao Gandi, NICMAR Hyderabad, India
Aravind Krishna Swamy, IIT Delhi, India
Arkopal Goswami, IIT Kharagpur, India

Arpan Mehar, NIT Warangal, India
Arpita Saha, VNIT, India
Arpita Suchismita, IIT Bombay, India
Arun Rajkumar, IIT Madras, India
Asha Latha, College of Engineering Trivandrum, India
Ashish Dhamaniya, NIT Surat, India
Ashish Verma, IISc Banglore, India
Ashok Julaganti, NIT Warangal, India
Ashutosh Arun, Queensland University of Technology, Brisbane, Australia
Avijit Maji, IIT Bombay, India
Avinash Chaudhari, Government Engineering College Daman, India
Ayyanna Habal, PDEU Gandhinagar, India
B. Raghuram Kadali, NIT Warangal, India
B. K. Bhavathrathan, IIT Palakkad, India
Babak Mehran, University of Manitoba, Winnipeg, Canada
Bachu Anil Kumar, IIT Patna, India
Balaji Ponnu, The Ohio State University, USA
Bandhan Majumdar, BITS Pilani Hyderabad, India
Bharat Pathivada, IIT Bombai, India
Bharat Rajan, IIT Bombai, India
Bhargava Chilukuri, IIT Madras, India
Bhaswati Bora, IIT Kanpur, India
Bhupendra Singh, IIT Jalandhar, India
Binanda Khungur Narzary, Tezpur University Assam, India
Bishwajit Bhattacharjee, IIT Delhi, India
Bivina G R, MANIT Bhopal, India
Burhan Showkat, NIT Surathkal, India
Darshana Othayoth, NIT Trichy, India
Debapratim Pandit, IIT Kharagpur, India
Debashish Roy, NIT Sikkim, India
Debasis Basu, IIT Bhubaneswar, India
Deepa L, IISC Banglore, India
Digvijay Pawar, IIT Hyderabad, India
Dipanjan Mukherjee, IIT Kharagpur, India
Emanuele Renzi, Ministry of Sustainable Infrastructure and Mobility, Italy
Fabio Croccolo, Ministry of Sustainable Infrastructure and Mobility, Italy
Gaurang Joshi, SVNIT Surat, India
Gavadakatla Vamsikrishna, IIT Bombay, India
Gopal Patil, IIT Bombay, India
Gottumukkala Bharath, CSIR-CRRI New Delhi, India
Gourab Sil, IIT Indore, India
Goutham Sarang, VIT Chennai, India
Gowri Asaithambi, IIT Tirupati, India
Gunasekaran Karuppanan, Anna University, Chennai, India
Hareshkumar Golakiya, Govt. Engineering College Surat, India

Hari Krishna Gaddam, National Rail and Transportation Institute, India
Harikrishna Madhavan, NIT Calicut, India
Harish Puppala, BML Munjal University Haryana, India
Harsha Vajjarapu, iCED CAG Jaipur, India
Hemanth Kumar, IIT Bombay, India
Hyuk-Jae Roh, University of Regina, Canada
Indrajit Ghosh, IIT Roorkee, India
Ipsita Banerjee, University of California, Berkeley
Jaikishan Damani, IIT Bombay, India
Jakkula Nataraju, CSIR-CRRI Delhi, India
Jaydip Goyani, SVNIT Surat, India
Jiten Shah, IITRAM Ahmedabad, India
Jithin Raj, IIT Bombay, India
Kalaanidhi Sivagnanasundaram, Technion-Isreal Institute of Technology, Isreal
Kinjal Bhattacharyya, LICIT-ECO7, Université Gustave Eiffel, France
Kirti Mahajan, IIT Bombay, India
Kranthi Kuna, IIT Kharagpur, India
Kshama Puntambekar, SPA, Bhopal, India
Lekhaz Devulapalli, Technion-Isreal Institute of Technology, Isreal
M. N. Sharath, IIT Bombay, India
M. Sivakumar, NIT Calicut, India
M. R. Nivitha, PSG, Coimbatore, India
Madhu Errampalli, CRRI, NewDelhi, India
Madhumita Paul, IIT Kharagpur, India
Madhuri Kashyap N R, IIT Thirupathi, India
Malavika Jayakumar, IIT Bombay, India
Mallikarjuna Chunchu, IIT Guwahati, India
Manoj Malayath, IIT Delhi, India
Manoranjan Parida, IIT Roorkee, India
Marisamynathan S, NIT Trichy, India
Minal Minal, CRRI, Delhi, India
Mithun Mohan, NITK, Surathkal, India
Mohan Rao, CRRI, Delhi, India
Monalisa Patra, IIT Bombay, India
Mounisai Siddartha Middela, IIT Madras, India
Mukti Advani, CSIR-CRRI, India
Munavar Fairooz Cheranchery, TKM College of Engineering, India
Muthulingam Subramaniyan, IIT Ropar, India
Naga Siva Pavani Peraka, IIT Tirupati, India
Nagendra Velaga, IIT Bombay, India
Nandan Dawda, SVNIT Surat, India
Narayana Raju, TU Delft, Netherlands
Naveen Kumar Chikkakrishna, VNRVJIET Hyderabad, India
Nikhil Bugalia, IIT Madras, India
Nikhil Saboo, IIT Roorkee, India

Ninad Gore, Ryerson University, Toronto, Canada
Nipjyoti Bharadwaj, IIT Guwahati, India
Nishant Pawar, IIT Bombay, India
Nivedya M K, Worcester Polytechnic Institute, USA
Nur Izzi Md. Yusoff, Universiti Kebangsaan, Malaysia
Padma Seetharaman, CRRI, Delhi, India
Pallav Kumar, MIT Muzaffarpur, India
Partha Pratim Dey, IIT Bhubaneswar, India
Parthan K, BMS, Bangalore, India
Phani Kumar Chintakayala, University of Leeds, England
Phani Kumar Patnala, University of Manitoba, Canada
Pooja Raj, Gopalan College of Engineering and Management, India
Prabin Ashish, IIT Kanpur, India
Pranamesh Chakraborty, IIT Kanpur, India
Prasanta Sahu, BITS Pilani, Hyderabad Campus, India
Prateek Bansal, National University of Singapore, Singapore
Pravin Telang, IIT Bombay, India
Pritikana Das, MANIT Bhopal, India
Priyansh Singh, IIT Palakkad, India
Pushpa Choudhary, IIT Roorkee, India
R Sivanandan, IIT Madras, India
Rahul T M, IIT Ropar, India
Rajan Choudhary, IIT Guwahati, India
Rajat Rastogi, IIT Roorkee, India
Rajeev Mishra, Delhi Technological University, India
Rajiv Kumar, NIT Jalandhar, India
Ramachandra Rao K, IIT Delhi, India
Ramesh Anbanandam, IIT Roorkee, India
Ramya Sri Mullapudi, IIT Hyderabad, India
Ranja Bandyopadhyaya, NIT Patna, India
Ranju Mohan, IIT Jodhpur, India
Raunak Mishra, University of North Carolina, USA
Ravi Sekhar Chalumuri, CRRI, New Delhi, India
Ravindra Kumar, CRRI, New Delhi, India
Reema Bera, IIT Kharagpur, India
Remya K P, IIT Bombay, India
Rupali Zope, COEP, Pune, India
Rushikesh Amrutsamanvar, TU Dresden, Germany
S. P. Atul Narayan, IIT Madras, India
S.Vasantha Kumar, VIT,Vellore, India
Sadguna Nuli, Vardhaman College of Engineering, Hyderabad, India
Saladi Sv Subbarao, Mahindra University Hyderabad, India
Sandeepan Roy, IIT Bombay, India
Sanhita Das, IIT Roorkee, India
Sanjay Dave, MSU Baroda, India

Sarah Mariam, BITS Pilani, India
Sarfaraz Ahmed, NUST, Pakistan
Shahana A, IIT Bombay, India
Shankar Sabavath, NIT Warangal, India
Shashi Bhushan Girimath, IIT Bombay, India
Shobhit Saxena, IISc Banglore, India
Shriniwas Arkatkar, SVNIT Surat, India
Shubhajit Sadhukhan, IIT Roorkee, India
Siddharth S M P, IIT Bombay, India
Siddhartha Rokade, MANIT, Bhopal, India
Siksha Swaroopa Kar, CSIR-CRRI, India
Sita Rami Reddy, VNIT, Nagpur, India
Smruti Mohapatra, ISM Dhanbad, India
Sonu Mathew, University of North Carolina at Charlotte, USA
Sridhar Raju, BITS Pilani, Hyderabad Campus, India
Srinath Mahesh, IIT Madras, India
Srinivas Geedipally, Texas A&M Transportation Institute, USA
Subhojit Roy, IIT Bhubaneswar, India
Sudhakar Reddy Kusam, IIT Kharagpur, India
Sudhir Varma, IIT Patna, India
Sunitha K Nayar, IIT Palakkad, India
Sunitha V, NIT Trichy, India
Suresha S. N., NIT Suratkal, India
Sushma Mb, IIT Bombay, India
Suvin P. Venthuruthiyil, IIT Guwahati, India
Swati Maitra, IIT Kharagpur, India
Tarun Rambha, IISc Bangalore, India
Tushar Choudhari, IIT Bombay, India
Udit Jain, VNIT Nagpur, India
Uma M. Arepalli, SRM University AP, Andhra Pradesh, India
Umesh Sahoo, IIT Bhubaneswar, India
Vasudevan N, SV NIT, Surat, India
Vedagiri Perumal, IIT Bombay, India
Veena Venudharan, IIT Palakkad, India
Velmurugan S, CRRI, India
Venkaiah Chowdary, NIT Warangal, India
Venkatesan Kanagaraj, IIT Kanpur, India
Vinamra Mishra, IIT Bombay, India
Vinayaka Ram V, BITS Pilani-Hyderabad, India
Vinayaraj V S, IIT Bombay, India
Vishwas Sawant, IIT roorkee, India
Vivek R Das, Ramaiah Institute of Technology, India
Yawar Ali, S V NIT, Surat, India
Yogesh Shah, IITRAM Ahmedabad, India

Contents

About the Editors

Dr. Lelitha Devi is a Professor in the Transportation Division of the Department of Civil Engineering at IIT Madras and holds a Ph.D. from Texas A&M University, USA. Her teaching and research interests are in the general area of transportation systems with emphasis on traffic flow modelling, traffic operations, and Intelligent Transportation systems. She has published around 90 referred journal papers and more than 100 conference papers. She serves in various editorial boards and is a member of various national and international societies. She has been involved in 15 research projects and has graduated more than 10 MS/Ph.D. scholars.

Dr. Madhu Errampalli is a Senior Principal Scientist in Transportation Planning and Environment Division at CSIR-Central Road Research Institute (C.R.R.I.), New Delhi, India. He has more than 22 years of experience of R&D and Consultancy works in the areas of Transportation Planning, Traffic Engineering and Road Safety. His main research interests are microscopic traffic simulation and fuzzy logic. He did Ph.D. in Transportation Engineering from Gifu University, Gifu, Japan. He completed about 38 R&D and Consultancy Projects and published a total of 132 Research Publications. He also guided 24 M.Tech/ ME students and 1 Ph.D. Student. He has received number of recognitions and awards namely Pt. Jawaharlal Nehru Birth Centenary Award 2017 from IRC, Vishwakarma Award 2016 of CIDC for the category of Scientist, SKOCH Order of Merit Award 2015 for SUSTRANS Project on being a Champion of the Project, Young Scientist Award 2011–2012 from CSIR-CRRI, Two times Bronze Medal Award from IRC in 2005 and 2011, Best Article Award in Indian Journal of Traffic Management by ASRTU in 2009, Session Best Presentation Award in SCIS & ISIS 2006, Tokyo, Japan, Japanese Government Scholarship (Monbugakusho) for 2004–2008, etc. He served as Member Secretary, IRC H-1 Committee on Transport Planning & Traffic Engineering, 2018–2021.

Dr. Avijit Maji is a Professor in the Department of Civil Engineering, IIT Bombay, India. He received Doctor of Engineering from Morgan State University, USA in 2008; M.Tech. from IIT Kanpur in 2004; and B.E. from Bengal Engineering College (now known as Indian Institute of Engineering Science and Technology) in 2000. He

has more than eighteen years of academia and industry experience working for organizations in India and USA. At present, he is a member of Transportation Research Board's Standing Committee on Performance Effects of Geometric Design (AKD 10), Co-Chair of Performance-Based Approaches and Applications Subcommittee and Chair of Technical Committee of the Transportation Research Group of India on Transportation Safety and Security. His area of expertise includes design, operations, and safety of transportation infrastructure. He has published more than eighty technical research papers in journals, edited books, and conferences. For his contribution, Maryland Society of Professional Engineers conferred him with the "Young Engineer of the Year Award" in 2011. He is a licensed Professional Engineer (PE) in Maryland, USA and Transportation Professional Certification Board's certified Professional Traffic Operations Engineer (PTOE).

Dr. Gitakrishnan Ramadurai is an Associate Professor in the Transportation Engineering Division, Department of Civil Engineering, IIT Madras, and a core faculty member in the Robert Bosch Center for Data Science and AI at IIT Madras. He received his Ph.D. in Transportation Engineering from Rensselaer Polytechnic Institute, Troy, NY, in June 2009, M.S. in Civil Engineering from the University of Texas at Austin in December 2003, and B.Tech. with honors in Civil Engineering from Indian Institute of Technology, Roorkee in May 2002. His overarching goal is to develop technological and management solutions for a safe and sustainable transportation system. His primary research interests are in network modeling, dynamic traffic simulation and assignment, Intelligent Transport Systems (ITS), vehicular emissions, urban freight, public transit systems, and road safety. He was awarded First Place in the 2009 Dissertation Prize by Transportation Science and Logistics Society, Institute for Operations Research and Management Science (INFORMS) in San Diego, USA. He is a recipient of New York Metropolitan Transportation Commission's September 11 Memorial Program Fellowship in 2007-08. He has co-authored over 65 conference and journal papers. He has served as a principal/co-investigator in Government of India funded projects on ITS and urban transportation. He has advised Chennai Port Trust, JNPT, Kolkata Port Trust and CIDCO, Navi Mumbai on improving congestion of trucks destined to ports, and various government organizations including Chennai Corporation, Tamil Nadu Police, TNHSP/EMS on ITS technology implementation, transportation planning, and management, and road safety. He was a corresponding member of the IRC H-8 committee on urban roads from 2015–17.

Environment and Sustainability in Transportation

Estimating Impacts and Cost of Air Pollution Due to Road Infrastructure Projects

Ranjan Sharma and Anush K. Chandrappa

Abstract Economic activities in the world are growing at an enormous pace and thus it is required to connect with the areas never touched before, leading to high-scale infrastructure development. This is a good thing from a normal human perspective as it is giving an opportunity to the lower income people to earn the bread on their own but this development has its own consequences. With an objective to improve the connectivity between two points, the infrastructure projects are awarded without significant consideration towards environment. This study presents an estimate of damage produced by vehicle operations in terms of monetary values. This gives an opportunity to the Indian infrastructure planners to take environmental damage cost into account for selecting a suitable alignment between two nodes, which is not a common practice in India. The study included a two-fold objective to quantify the emissions from vehicles of typical national highway traffic in terms of capital cost and to compare the changes in the cost associated with the emissions by shifting vehicle operation from BS IV to BS VI. In order to achieve the objectives, secondary data from an alignment of Maharashtra and Karnataka was utilized. The study adopts a methodology of finding out the difference in the cost between BS IV and BS VI vehicular operation based on standard emission norms and unit costs of pollutants suggested by researchers around the globe. This gives us an approximate estimate of how much damage is posed to the environment and health effects on nearby residents or users of the link by operating a vehicle for one km. Data collected from various reports give an indication of the total overhead cost to upgrade the fuel technology and vehicles as per BS VI norms.

Keywords Air pollution cost · Emission quantification · Energy · Traffic

R. Sharma (✉) · A. K. Chandrappa
IIT Bhubaneswar, Bhubaneswar, India
e-mail: rs43@iitbbs.ac.in

L. Devi et al. (eds.), *Proceedings of the Sixth International Conference of Transportation Research Group of India*, Lecture Notes in Civil Engineering 273,
https://doi.org/10.1007/978-981-19-4204-4_1

1 Introduction

1.1 Background

The enormous growth in industry is leading to urbanization of rural areas and formation of new cities. More road networks are being developed for faster and more comfortable travel routes. This is all good from the perspective of economic growth of the country but this is just one side of the entire story. On the other hand, we are emitting huge amount of greenhouse gases (GHGs) from the industries like vehicle manufacturing, fuel extraction, travel, road construction, and traffic congestion. This pollution in short term does not mean much, but in the long run, it is creating imbalance in the environment. The imbalances can be seen everywhere around the globe, e.g., loss of coastal lands due to rise in sea level, melting of permanent glaciers, devastating cyclones in the Bay of Bengal each year, extinction of species, and origin of deadly viruses, etc. These are just preliminary warnings; the threat in the coming future can be far more dangerous than it is today.

As per International Energy Agency, the transportation sector itself contributed approximately 8 Giga tonnes of GHG emissions, which is approximately 1/4th of the entire GHG emission in that year. Out of this, approximately 74% is contributed by road transportation which consists of construction, maintenance, and rehabilitation of roads/highways, operation of vehicles, etc. Several methodologies/tools such as RoadCO2 [1], COPERT4, MOVES, CHANGER, and CO2NSTRUCT are developed around the world to estimate the amount of GHG emitted during each phase of the road infrastructure's life cycle. If the unit cost of each type of pollutant can be determined based on the severity of each pollutant on human health, animal species, and environment, then the output from the various tools can be directly used to estimate the mitigation cost. This cost can be imposed on public or concerned industrial bodies to reverse the damage done by the transportation sector. The present study focuses on understanding the effects of air pollution on environment and human health by relating it to monetary values.

1.2 Literature Review

Small and Kazimi [17] determined the air pollution costs for the city of Los Angeles. The cost of the average car towards air pollution was found to be $0.03 considering 1990s class of vehicles. It was observed that diesel cars and trucks resulted in higher cost towards air pollution. The study indicated that substantial cost savings can be achieved by changes in vehicle and fuel technology. Chatterjee et al. [4] divided the cost into two parts, one for the cost incurred for technological advancement of the vehicles and compatible fuel production and the other required to operate and upgrade the vehicle by the user. Kuik et al. [11] conducted a meta-analysis on 62 papers and estimated the marginal abatement cost as € 74–227 for 2025 and € 132–381 per

tonne for a target reduction of CO_2 to 350 ppmv. Maibach et al. (2008) considered the current impact on the environment such as sea level rise, common health issues due to pollution, damage to the ecosystem and biodiversity, and extreme weather events such as floods, droughts, cyclones, and collapse of Amazon forests. The estimated damage cost came out to be € 50–100 t/CO_2 to maintain a safe gap between the threshold limit of catastrophic events. Litman [12, 13] evaluated the carbon tax as an energy conservation strategy, which would also result in consumption of the fossil fuels. Various fossil fuels were provided a certain amount of carbon tax, which the user has to pay for the consumption. The collected tax money was utilized in the economic upliftment of low-income groups, where it was first introduced in British Columbia. Litman et al. (2018) divided this environmental cost into two parts for a simplified view: Damage Cost and Control Cost. Damage cost reflects the monetary valuation of damage done to environment and risks, while control cost reflects the amount that can be incurred to reduce emissions. These costs are estimated considering various factors such as discount rate, current global factors, uncertainty of the extent of the damage, vehicle type and road condition, etc. Čokorilo et al. [5] developed a methodology to calculate the exhaust emission cost with the help of traffic data, vehicle and fuel type, length of road network, and unit cost of each pollutant. For the base year, the total exhaust emission cost was estimated to be € 354,238,894 per year for the chosen road segment.

1.3 Significance of Research

The way we are expanding ourselves to the edge of advancements, the environment should not be neglected in the process. Developed nations are putting an effort to find a way to reduce the damage. India can also follow the same path and start by developing a methodology to estimate the unit cost of each pollutant to estimate the damage cost. This data can also be helpful in selecting the best alignment while designing a road network from both perspective environment as well as development cost. Further, this cost can be included in the total transportation cost in order to assess the damage to the environment, which will help the policymakers to make a decision on various aspects.

2 Methodology

2.1 Vehicle Emission Standards

The government of India formed Bharat Stage Emission Standards (BSES) to regulate the air pollution created by motor vehicles. The Central Pollution Control

Table 1 Indian emission standard roll-out timeline for 4-wheelers (DieselNet.com) [6]

Standard	Reference	Year	Region
India 2000	Euro 1	2000	Nationwide
Bharat Stage II	Euro 2	2001	NCR*, Mumbai, Kolkata, Chennai
		2003	NCR and 14 Cities#
		2005	Nationwide
Bharat Stage III	Euro 3	2005-04	NCR*, 14 Cities#
		2010	Nationwide
Bharat Stage IV	Euro 4	2010	NCR, 14 Cities#
		2017	Nationwide
Bharat Stage V	Euro 5	Skipped	
Bharat Stage VI	Euro 6	2018	Delhi
		2019	NCR*
		2020	Nationwide

*National Capital Region (Delhi)
#Mumbai, Kolkata, Chennai, Bengaluru, Hyderabad, Ahmedabad, Pune, Surat, Kanpur, Lucknow, Jamshedpur, Agra and Guwahati

Board (CPCB) under the Ministry of Environment sets the standard policy and its implementation plan throughout the nation.

The emission standard was first introduced in 2000 on the basis of European emission standards. Bharat Standard (BS) IV emission standard has been enforced to the entire states on 1 April 2017, with a deadline to vehicle manufacturers to jump to BS VI standard 1 April 2020 [3]. New emission standards come with a motivation to have a stricter control over the air pollutants ejected from the tail-pipe in comparison to its previous version. The Indian emission standard roll-out is shown in Table 1.

The current work uses secondary data from the traffic survey of a national highway in plain terrain in the region of Maharashtra and Karnataka to arrive at an abatement cost. The abatement cost is divided into two parts: *vehicle operation cost* or *exhaust emission cost* and *technology advancement cost* as shown in Fig. 1.

The *vehicle operation cost* is calculated with the help of the cost estimation model developed by Čokorilo et al. [5] because of some similarities between India and Serbia and suitability of the model. This model makes use of network length and traffic data, fuel emission technology, and type of vehicle which is very helpful in estimating the amount of pollution that can be generated due to traffic operation.

Technology advancement cost can be directly obtained from the financial reports of various oil refining companies.

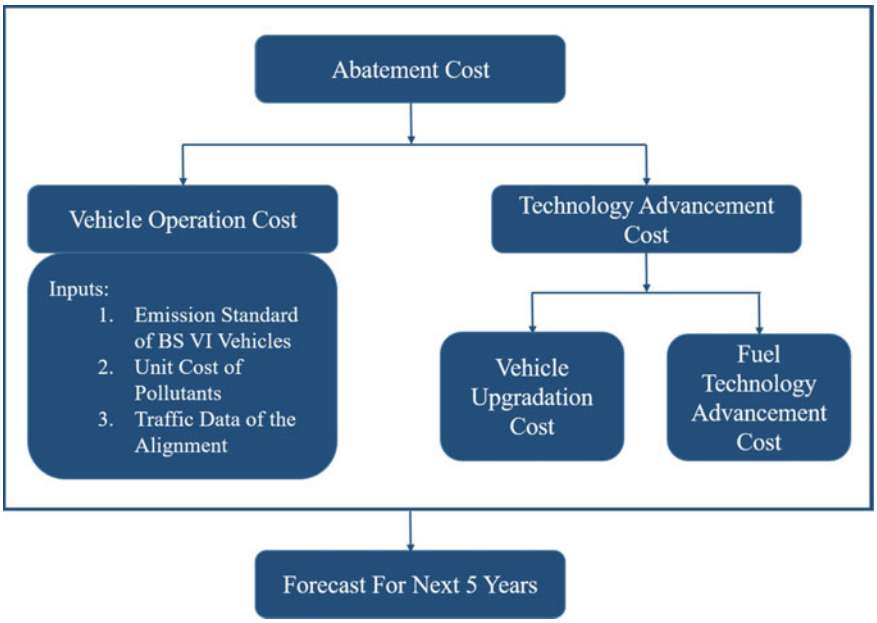

Fig. 1 Methodology to estimate EEC

2.2 Exhaust Emission Cost (EEC) Estimation Method

The EEC is estimated with the help of Eq. (1) as per Čokorilo et al. [5]:

$$EEC = \sum_{i,j,k} \text{const} * DT_{i,j} * FC_{i,j} * f_{(FC)_{i,j}} * \rho_f * L_j * EF_{i,k} * f_{EF_{i,j,k}} * UC_k \tag{1}$$

where

EEC	Exhaust emission cost for the road network (₹/year)
DT	Average Annual Daily Traffic (AADT) per vehicle category (vehicle/day)
FC	Fuel consumption of vehicle (L/km)
f_{FC}	Correction factor of fuel consumption (1–1.25 for passenger vehicles and 1–1.8 for freight vehicles)
ρ_f	Density of fuel (petrol = 0.71 kg/L, diesel = 0.835 kg/L, LPG = 0.56 kg/L)
const	3.65×10^{-4}
L	Length of road section (km)
EF	Emission factors ($g_{pollutant}/kg_{fuel}$)
f_{EF}	Factor of change in the emission of pollutants, depending on the different engine mode
UC	Unit cost of pollutant (€/tonne)

i Index of vehicle category
j Index of road section
k Index of pollutants

The EEC is calculated for BS IV and BS VI vehicles as these two engine technologies are currently in use in India. The difference in the amount would suggest that shifting from one technology to the other the amount of environmental cost that can be saved in terms of emission cost. Further, this data is projected for the next 5 years to determine the increment of the cost over the time span. A period of 5 years is considered as beyond 5 years, the growth rate of vehicles may change depending on various factors associated with politics, natural disasters, economic changes, etc.

Traffic forecast is done with the help of econometric modeling taking historical national state domestic product (NSDP) data and vehicle counts in the states considered for this study.

2.3 Traffic Growth Rate Estimation

Traffic growth rate for two alignments is estimated with the help of econometric modeling as per IRC:108-2015.

$$\ln P = c + m * \ln(\text{Economic Indicator}) \tag{2}$$

where P is the traffic count, m is the coefficient of traffic demand elasticity.

$$\text{Traffic Growth Rate} = \text{Elasticity} * \text{Growth Rate of Economic Indicator} \tag{3}$$

$$\text{Growth Rate of Economic Indicator} = \frac{(\text{Current Year Value} - \text{Previous Year Value})}{\text{Previous Year Value}} \times 100\% \tag{4}$$

$$P_n = P_0(1 + r)^n \tag{5}$$

where P_n and P_0 are the traffic population in the nth year and the base year, respectively, and r is the traffic growth rate in the state.

3 Result and Discussion

3.1 Vehicle Operation Cost

National State Domestic Product (NSDP) is chosen as the economic indicator for this study for a period of 9 years from 2006 to 2014 for Maharashtra state and 2009 to 2015 for Karnataka state as shown in Tables 2 and 3, respectively.

Average growth rate of the economic indicator is the statistical mean of year-on-year growth of NSDP, yearly growth is calculated with the help of Eq. (4). Equation (2) can be used to estimate the traffic demand elasticity which is further used in Eq. (3) to determine the average traffic growth rate [10]. The regression statistics and growth rates of different vehicle categories are shown in Tables 4 and 5 for Maharashtra and Karnataka state, respectively. Average growth rate of NSDP in Maharashtra was estimated to be 7.44% and 13.15% for Karnataka.

Table 6 shows the traffic volume at the stretch of selected highway in the region of Maharashtra (NH 361) and Karnataka (NH 648) and Table 7 shows the forecasted

Table 2 Historical vehicle count and NSDP (in INR Crore) data of Maharashtra (Ministry of statistics and programme implementation) [15]

Year	2 Wheelers	Cars	Buses	Trucks	NSDP
2006	8,573,679	1,648,379	71,187	316,502	481,983
2007	9,394,869	1,822,458	77,042	344,267	538,081
2008	10,212,360	1,979,191	79,073	366,642	546,533
2009	11,181,762	2,182,969	83,816	374,705	599,338
2010	12,429,011	2,440,404	89,861	389,941	667,625
2011	13,921,763	2,750,167	100,097	411,418	695,904
2012	15,457,123	2,592,565	110,121	402,366	749,137
2013	16,910,395	2,834,847	120,886	47,128	805,593
2014	18,603,835	3,113,773	120,750	491,582	852,451

Table 3 Historical vehicle count and NSDP (in INR Crore) data of Karnataka (Ministry of statistics and programme implementation) [15]

Year	2 Wheelers	Cars	Buses	Trucks	NSDP
2009	4,796,587	892,160	44,308	366,597	278,534
2010	6,404,905	1,005,291	53,874	377,495	300,747
2011	7,033,045	1,131,201	58,012	415,491	368,338
2012	7,737,366	1,269,430	62,501	454,582	406,821
2013	8,575,104	1,420,767	69,718	506,340	462,395
2014	9,533,892	1,572,521	75,529	555,255	516,516
2015	10,644,368	1,741,831	80,911	606,352	581,741

Table 4 Econometric model output for Maharashtra

Regression statistics	2-Wheelers	Cars	Buses	Trucks
Multiple R	0.995	0.979	0.987	0.963
R square	0.990	0.958	0.973	0.928
Adjusted R square	0.989	0.952	0.970	0.918
Standard error	0.028	0.047	0.035	0.040
Observations	9	9	9	9
Elasticity	1.372	1.082	1.001	0.688
Intercept	−2.012	0.185	−1.959	3.676
Traffic growth rate (%)	10.21	8.05	7.45	5.12

Table 5 Econometric model output for Karnataka

Regression statistics	2-Wheelers	Cars	Buses	Trucks
Multiple R	0.924	0.955	0.928	0.964
R Square	0.854	0.912	0.860	0.928
Adjusted R square	0.824	0.894	0.832	0.914
Standard error	0.112	0.079	0.085	0.056
Observations	7	7	7	7
Intercept	7.123	5.883	4.205	6.485
Elasticity	0.673	0.630	0.528	0.506
Traffic growth rate (%)	8.85	8.28	6.94	6.65

Table 6 AADT of Maharashtra (NH 361) and Karnataka (NH 648)

Vehicle	AADT (veh/day)	
	Karnataka	Maharashtra
PC petrol	2929	2493
PC diesel	517	440
Buses	285	550
Trucks	2858	3531
TWs	6047	1763
Total	12,636	8777

Table 7 Base year and forecasted year traffic data

P_0 (veh/day)		P_5 (veh/day)	
Maharashtra	Karnataka	Maharashtra	Karnataka
8777	12,506	12,724	18,711

Table 8 Unit cost of pollutants [5]

Pollutant	Unit cost (₹/kg)
CO	8.09
NOx	763.97
NMVOC	42.79
CH_4	75.54
PM	1954.86
CO_2	2.70
SOx	699.13

traffic population if the traffic grows by the growth rate predicted by the econometric model output (as shown in Tables 4 and 5) in the year 2025.

Unit cost (Table 8) was estimated by Čokorilo et al. [5] to estimate the EEC using Eq. (1).

Based on the unit cost shown in Table 8, the exhaust emission cost due to BS IV and BS VI emission categories is shown in Table 9. The year-wise total EEC for Maharashtra and Karnataka is shown in Figs. 2 and 3, respectively.

Traffic growth is forecasted for five consecutive years from 2020 and the exhaust emission cost is calculated per unit km length per year of the selected highway link. Results indicate that the EEC varies linearly for the next 5 years for both Maharashtra and Karnataka regions (Figs. 2 and 3) assuming the calculated growth rate of vehicles in this study. The vehicle category-wise EEC for the states of Maharashtra and Karnataka is shown in Figs. 4, 5, 6, 7, 8 and 9. A saving of ₹33.19 thousand/km, 2.53 lakh/km, and 2.19 lakh/km can be made by switching from BS IV to BS VI vehicles for Maharashtra region, while a saving of ₹1.39 lakh/km, ₹2.43 lakh/km, and ₹10.53

Table 9 Exhaust emission cost (in INR) due to various fuel emission technologies

Emission technology	State	Maharashtra		Karnataka	
	Year	Base year 2020	Forecasted year 2025	Base year 2020	Forecasted year 2025
	Vehicle type				
BS IV	Cars	1028533.44	1514754.57	1208438.90	1798729.82
	Buses and trucks	926283.10	1207532.34	713380.98	985516.34
	2-Wheelers	881456.82	877517.14	3023351.90	4619881.83
	Total	2836273.36	3599804.05	4945171.78	7404127.99
BS VI	Cars	995340.86	1465870.78	1169444.24	1740687.27
	Buses and trucks	673132.53	877517.14	518415.96	716177.49
	2-Wheelers	652561.70	1061027.38	2238253.32	3420199.22
	Total	2321035.09	3404415.30	3926113.52	5877063.98

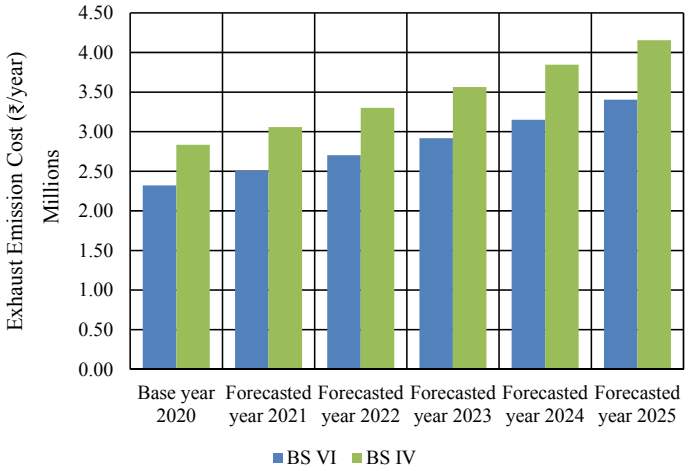

Fig. 2 Total exhaust emission cost for base and forecasted year in Maharashtra region

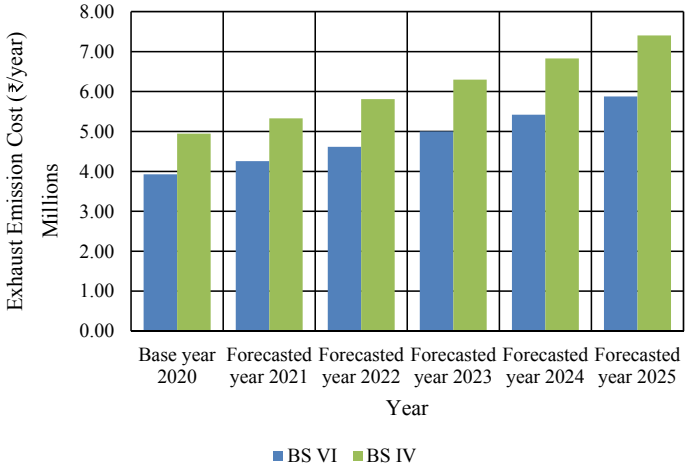

Fig. 3 Total exhaust emission cost for base and forecasted year in Karnataka region

lakh/km can be saved in the base year 2020 for Karnataka region for cars, buses and trucks and two-wheelers, respectively.

For the projected period, the difference in the EEC by shifting from BS IV to BS VI technology grew by 7.45%, 5.15%, and 9.26% for cars, buses and trucks, and two-wheelers, respectively, for Maharashtra, while for Karnataka, the difference grew by 7.65%, 6.26%, and 8.13% for cars, buses and trucks, and two-wheelers, respectively.

Results indicate that the EEC difference between BS IV and BS VI is negligible for cars for the entire projected years (Figs. 4 and 5) but the same is not true for buses

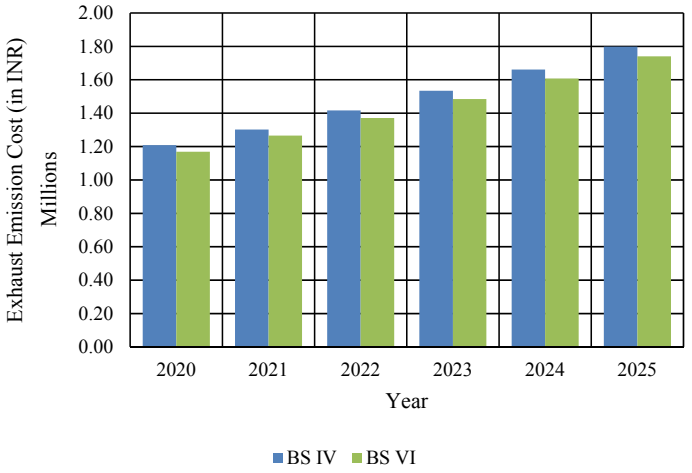

Fig. 4 Year-wise EEC for cars in Karnataka

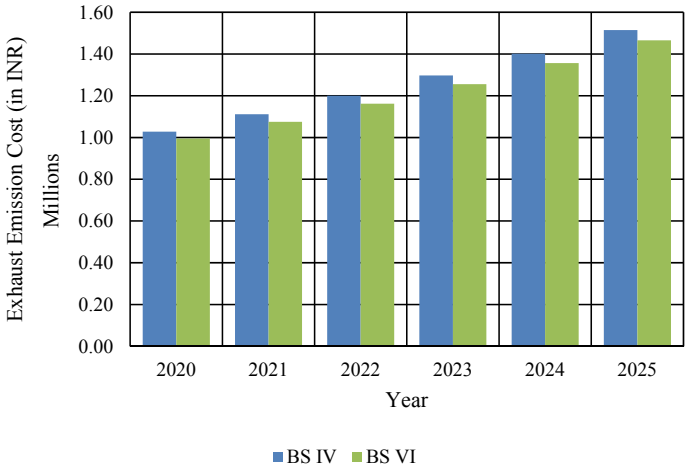

Fig. 5 Year-wise EEC for cars in Maharashtra

and trucks (Figs. 6 and 7) and two-wheelers (Figs. 8 and 9). This is mainly because car engine emission standards are already heavily regulated and buses and trucks emit a high amount of poisonous NOx gases which pose a huge threat to human life, hence their unit cost is kept high, which ultimately leads to very high environmental cost for the operation of buses and trucks. Further, the two-wheelers amount to a high cost associated with air pollution. Therefore, adopting electric two-wheelers may considerably bring down this cost in the near future. Note that we cannot compare

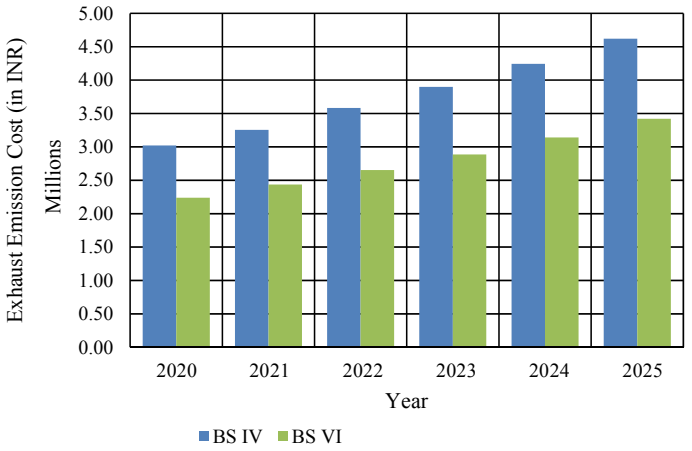

Fig. 6 Year-wise EEC for 2-wheelers in Karnataka

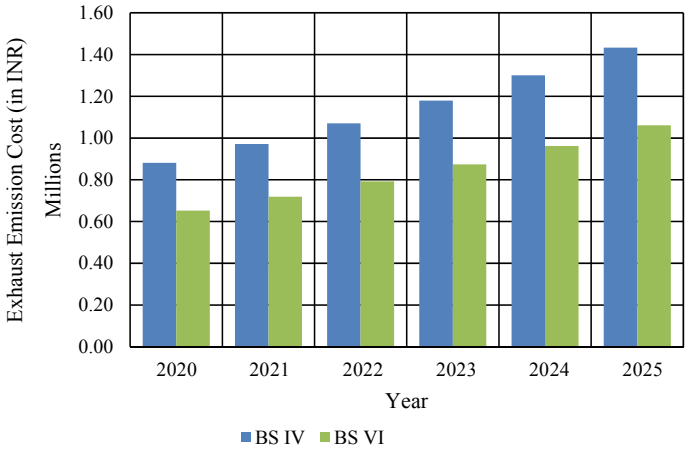

Fig. 7 Year-wise EEC for 2-wheelers in Maharashtra

here, which state is resulting in higher EEC or lower EEC considering various factors such as AADT obtained, local factors, etc.

3.2 Technology Advancement Cost

Technology advancement cost consists of vehicle up-gradation cost and fuel technology advancement cost. These costs are one-time cost that needs to be borne by either owner of the vehicle with the help of lending institutions or their own money

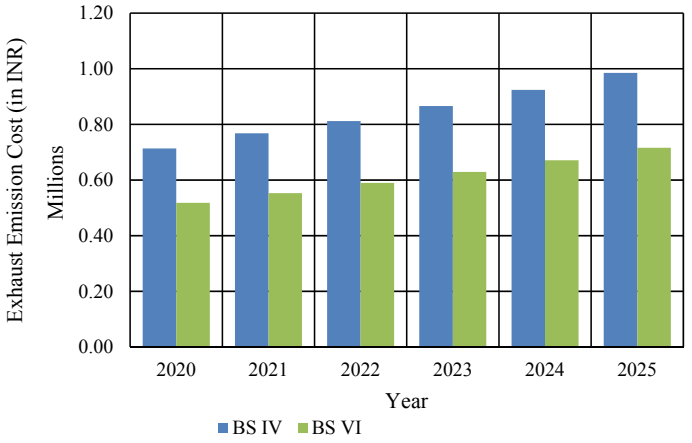

Fig. 8 Year-wise EEC for buses and trucks in Karnataka

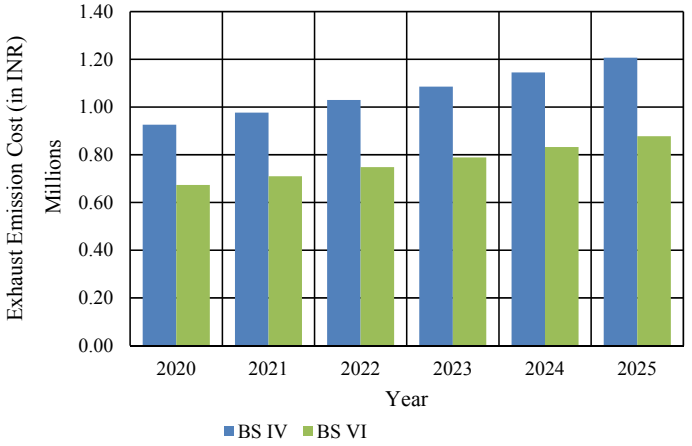

Fig. 9 Year-wise EEC for buses and trucks in Maharashtra

or by the government by subsidizing the shifting cost. These costs can vary on the basis of company, vehicle class, and financing schemes of the lending institutions.

As per Live Mint [14], Sanjeev Singh, chairman of IOCL reported that the oil refineries around the country spent a sum of ₹35,000 crore to upgrade their machinery across the nation to produce fuels as per the norms of BS VI from 1 April 2020.

As per the methodology worked out by Chatterjee et al. [4], the states of Maharashtra and Karnataka would need a sum of ₹97.71 crore and ₹82.60 crore per year, respectively, for the next 5 years at a 10% discount rate to finance all the vehicle owners to switch to new technology vehicles in the base year.

4 Conclusions

This study included a two-fold objective:

- To quantify the emissions from vehicles of typical national highway traffic in terms of capital cost.
- To compare the changes in the cost associated with the emissions by shifting vehicle operation from BS IV to BS VI.

It was observed that upgrading the vehicles from BS IV to BS VI would cost around ₹97.71 and ₹82.60 crores per year for a period of 5 years for Maharashtra and Karnataka, respectively. Upgrading fuel technology for BS VI standard vehicles has cost around ₹35,000 crore for oil refineries as per the statements of Sanjeev Singh, chairman of IOCL. These technological advancement costs would be borne by the road users either with the help of a bank or independently.

India formally switched to BS VI vehicles on 1 April 2020, skipping BS V category of vehicles. Therefore, currently, most of the vehicles on the road are either BS IV standard vehicle or BS VI standard vehicle. There is a significant improvement in tail-pipe emission technology in the new standard vehicles. The operation of all BS IV vehicles on the highway traffic considered in this study would create damage worth ₹28.36 lakh, while BS VI vehicles would create a damage of ₹23.21 lakh for each km of distance traveled per year. This study suggests that upgrading to new norms can save a sum of ₹33.19 thousand/km from passenger car operation, ₹2.53 lakh/km from buses and trucks operation, and ₹2.29 lakh/km from two-wheelers operation, i.e., approximately ₹5 lakh/km can be saved annually if all vehicles using this alignment located in Maharashtra switch to the latest emission standard for the vehicles and the same for an alignment located in Karnataka was found to be approximately ₹10.19 lakh/km from all vehicles (passenger car: ₹38.99 thousand/km, buses and trucks: ₹1.95 lakh/km, and two-wheelers: ₹7.85 lakh/km). Based on the study, it is interesting to note that the two-wheelers resulted in a significant reduction in air pollution cost, or in other words, their contribution towards air pollution will be significant. The savings while using cars and two-wheelers would be significant if we consider the traffic data from an urban road as the traffic data considered in this study was obtained from a national highway. Therefore, this result can help policymakers in promoting electrical vehicles, which are already gaining the attention of many automobile owners.

The exhaust emission cost increases linearly primarily because of the nature of the model presented by Čokorilo et al. [5]. This model can help the regulatory bodies to evaluate the trend and determine the right time to switch from the current emission standard to a new one which can aggressively cut down the air pollution.

4.1 Scope of Future Work

From literature survey, it was found that this kind of cost estimation methodology is still far away from being realized especially in India. The researchers should definitely look into this direction to propose a suitable methodology to estimate unit costs of various gases from vehicles for Indian conditions as the air pollution problem has already started creating a havoc on the eco-system. Moreover, air pollution is considered the first significant threat towards the environment and human health.

References

1. Alzard MH, Maraqa MA, Chowdhury R, Sherif M, Mauga TI, De Albuquerque FB, Aljunadi KN (2019) RoadCO2: A web-based tool for estimation of greenhouse gas emissions of road projects. In: 2019 advances in science and engineering technology international conferences (ASET). IEEE, pp 1–6
2. Bak M (2007) Handbook on estimation of external cost in the transport sector, CE Delft, European Commission. Energy and Transport DG, Delft
3. BusinessLine Bookmark. https://www.thehindubusinessline.com/companies/what-bs-6-means-for-auto-buyers/article29633593.ece. Accessed 17 Nov 2020
4. Chatterjee S, Dhavala KK, Murty MN (2007) Estimating cost of air pollution abatement for road transport in India: case studies of Andhra Pradesh and Himachal Pradesh. Econ Polit Wkly 3662–3668
5. Čokorilo O, Ivković I, Kaplanović S (2019) Prediction of exhaust emission costs in air and road transportation. Sustainability 11(17):4688
6. DieselNet. https://dieselnet.com/standards/in/. Accessed 23 Aug 2021
7. El-Fadel M, Bou-Zeid E (1999) Transportation GHG emissions in developing countries: the case of Lebanon. Transp Res Part D Transp Environ 4(4):251–264
8. Huang Y, Hakim B, Zammataro S (2013) Measuring the carbon footprint of road construction using CHANGER. Int J Pavement Eng 14(6):590–600
9. International Energy Agency. CO_2 emissions from fuel combustion 2017 highlights. https://webstore.iea.org/co2-emissions-from-fuel-combustion-highlights-2017. Accessed 14 Nov 2020
10. IRC: 108-2015. Guidelines for traffic prediction in rural highways. Indian Roads Congress, New Delhi
11. Kuik O, Tol RS, Brander L (2008) Marginal abatement costs of carbon-dioxide emissions: a meta-analysis. ESRI WP248, June 2008
12. Litman T (2009a) Evaluating carbon taxes as an energy conservation and emission reduction strategy. Transp Res Rec, J Transp Res Board 2139:125–132
13. Litman T (2009b) Transportation cost and benefit analysis. Victoria Transp Policy Inst 31:1–19
14. Live Mint Bookmark. https://www.livemint.com/industry/energy/get-ready-to-pay-more-for-bs-vi-fuel-11582892655560.html. Accessed 15 Apr 2021
15. Ministry of Statistics and Programme Implementation. http://mospi.nic.in/data. Accessed 23 Aug 2021
16. Ntziachristos L, Gkatzoflias D, Kouridis C, Samaras Z (2009) COPERT: A European road transport emission inventory model. In: Information technologies in environmental engineering. Springer, Berlin, Heidelberg, pp 491–504

17. Small KA, Kazimi C (1995) On the costs of air pollution from motor vehicles. J Transp Econ Policy 29(1):7–32
18. US EPA, "MOVES2014a: Latest version of motor vehicle emission simulator (MOVES)", US EPA, 10 May 2016. https://www.epa.gov/moves/moves2014a-latest-version-motor-vehicle-emission-simulator-moves. Accessed 14 Nov 2020

Benefits from Active Transportation—A Case Study of Bangalore Metropolitan Region

Hemanthini Allirani, Ashish Verma, and Sajitha Sasidharan

Abstract Rapid urbanization in developing economies like India has led to an increase in motorized modes of transport, even for shorter trips replacing Non-Motorized Transport (NMT). The urban lifestyle has made most of the adult population physically less active leading to adverse health impacts. Studies suggest that active transportation, usually through bicycling and walking, can potentially increase Physical Activity (PA) and improve health. In this study, an attempt has been made to quantify PA in terms of Metabolic Equivalent of Task (MET) for NMT. Two scenarios, such as base case and mode shift to NMT, are evaluated in which the latter scenario shows a 5% increase in the active population and 3% increase in the physically benefitted individuals due to the shift to active transportation. Thus, the population commuting through NMT are sufficiently physically active than other road users and, hence, are less subjected to obesity and other non-communicable diseases.

Keywords Active transportation · Non-motorized transport · Physical activity · Metabolic equivalent of task

1 Introduction

Transportation plays a vital role in the economic and social development of a country. Enhanced mobility has a positive impact through efficient movement of goods and passengers, but the mobility achieved through increased motor vehicle usage leads to worse physical and environmental impacts [18]. The related negative impacts include physical inactivity, air pollution, chronic illness, traffic collision, and traffic congestion. Globally, physical inactivity is estimated to cause some 3.2 million deaths annually [1]. Insufficient Physical Activity (PA) increases the risk of cardiovascular diseases, cancers, diabeteQuerys, and mental health problems [1]. According to 2012 obesity reviews by the International Association, increment in car ownership in the

H. Allirani · A. Verma (✉) · S. Sasidharan
Indian Institute of Science, Bengaluru, Karnataka, India
e-mail: ashishv@iisc.ac.in

L. Devi et al. (eds.), *Proceedings of the Sixth International Conference of Transportation Research Group of India*, Lecture Notes in Civil Engineering 273,
https://doi.org/10.1007/978-981-19-4204-4_2

developing economies has increased vehicle kilometers traveled and declined the distance walked per year. In developing economies such as India, a sedentary lifestyle is observed because of rapid unplanned urbanization and increment in the number of private vehicles owned [9]. However, the impact of intensified car ownership is less severe due to the promotion of active mode of travel and the urban design being more conducive to walking and cycling. The active mode of transport, which includes walking and cycling, plays a crucial role in improving an individual's wellbeing.

In India, sedentary time is projected to increase from 18.6 h per week in 2000 to 20 h per week by 2030 [15]. According to the study conducted by 'Down to Earth' in 2015 [21] regarding the attitude of road user's mode choice in Indian cities, among respondents from the rural area, 68.3 percent bicycled, and 11.9 percent walked to work; on the contrary, 15.9 percent bicycled, and 12.5 percent walked to work in urban areas, respectively. Physical activity is often measured in terms of Metabolic Equivalent of Task (MET), i.e., energy spent in various activities [11, 17]. The study pointed out a need for encouraging commuters to utilize a physically active mode of transport which might lessen the risk of chronic diseases. The poor condition of footpaths and cycle lanes act as a disincentive to active transport; in addition, pedestrians and two-wheeler users are more prone to traffic collision.

Bangalore being the fifth major metropolis in India, is one of the fastest-growing cities in Asia. As per the report Bangalore mobility indicators (2010–2011) [4], rapid growth in registered vehicles is observed from 0.4 million in 1987 to 3.7 million in 2010. It is expected that Bangalore will have 10.6 million motorized vehicles by the year 2022 which might create a marked shift of travel from public transport and active modes to privately owned motor vehicles exceeding the capacity of existing road network. The rise in the travel demand and inadequacy of the public transit system encourages more and more commuters to shift to cars and two-wheelers. The extension in time spent on motorized transportation modes would mean an absence of PA, leading to a sedentary lifestyle [19]. There is a lack of importance given to NMT, such as walking and cycling infrastructure in Bangalore [13]. Consequently, there is a need for an intervention to encourage mode shift toward the active mode of travel. Active transportation is mostly preferred for shorter trip distances by road users. Apart from the trip distance, an individual's attitude toward physical exercise also plays a predominant role in preference for their active mode of travel.

The main objective of the present investigation is to quantify the PA due to active transportation in terms of Metabolic Equivalent of Task (MET) to assess health benefits. Secondly, to assess the effect of mode shift based on the acceptable trip distance for walking and bicycling on the commuters' intensity of PA. Two scenarios, such as base case and mode shift to NMT, are evaluated. Thirdly, to assess the gender-wise and age-wise variation in the number of active transport trips followed by calculation and comparison of MET values for two defined scenarios. Finally, to evaluate the share of physically benefitted individuals due to the shift to active transportation. The subsequent sections illustrate a summary of the literature review followed by data description, methodology, technical analysis, results, and conclusions.

2 Literature Review

Physical Activity (PA) can be broadly defined as an action delivered due to skeletal movements that require energy consumption [12]. Physical activities are executed throughout the day for various purposes. The occupation domain of PA is the prime focus for initial epidemiologic studies. Later, leisure time or recreational physical activities gained importance as occupational activities requiring higher energy declined. However, recently PA, which includes transportation-related such as walking and bicycling activities, has gained importance.

2.1 Physical Activity and Transportation

Numerous studies have focused on the relation between inactivity and related disease costs [7, 14, 22]. The diseases caused by inactivity are very expensive; thus, transportation policies can reduce these costs by providing opportunities for people to be physically active [7]. The physical activities associated with different transport scenarios were compared using the exposure model in many studies. In one such study conducted by Tainio et al. [20], the health benefits of transport related to walking and cycling are computed considering different scenarios. Higher potential toward the increase in the fraction of people cycling compared to walking is identified because of the low base and the greater distance covered by cycling. Web TAG tool has been implemented to estimate the active mode health benefits assessment [20].

Population distributions of exposure to non-transport and transport-related physical activities are estimated for each age and sex group [14]. Estimated the impact of mode shift from car to walking and cycling and associated health benefits using relative-risk response model. Physical activity in the form of active mode of transportation tends to decrease as one moves farther from city center [19]. According to Saelens et al. [16], a compact mixed-use urban development and a high-quality pedestrian and bicycle networks with good connectivity can promote travel by walking and bicycling. Moreover, a good integrated public transit networks with proper infrastructure for active transportation can indirectly stimulate walking and cycling. Higher density land use is more energy efficient [22], as it shortens the trip length. Mixed land use development with better housing location can reduce the travel distance to employment, health services and other amenities thus encouraging a mode shift from motorized to non-motorized transport.

2.2 Measurement of Energy Expenditure

MET concept is used for measuring PA, as the concept being simple, practical and an easy method of expressing the energy expenditure of physical activities as multiples of Resting Metabolic Rate (RMR) [6]. One of the early studies conducted by Sidney and Blumchent [17] aims at defining MET and its comparison with the energy expenditure in terms of watts for selected household and recreational activities. One MET is defined as one kilocalorie/kilogram/hour and is "equivalent to the amount of energy you spend when you are just sitting quietly". MET has been defined by Morris et al. [11] as "on an average, the quantity of oxygen consumed by the body from inspired air under basal conditions is equal to 3.5 ml oxygen/kg/minute". In case of an average adult, this works out to be about one calorie for every one kilogram of body weight per hour. MET values are represented by corresponding physical activities using a five-digit code in the Compendium of Physical Activities study conducted in 2011 [3]. Standard MET in this compendium directly translates the weight-specific energy costs computed by taking the energy costs and dividing them by 3.5 ml/kg/min, thus giving a weight-specific approach to the energy cost of the activity [2, 3].

The measurements of total PA mostly rely on questionnaires which are routinely used as surveillance tools [5]. Recently, Physical Activity Questionnaire (RPAQ) is developed aiming to assess the usual PA in the previous month of the survey. The PA questionnaire makes it easy to measure the energy expenditure for large population at low cost and in assessing the variety of physical activities. The health and ecological effects due to increase in active modes of transport were evaluated using Integrated Transport and Health Impact Modeling tool (ITHIM) [23]. Misra et al. [10] has recommended that for Indian context, the general PA must include a minimum of one hour and up to several hours of at least moderate-intensity aerobic PA daily. This activity may comprise of sports activities, active transport, and usual PA. Watching television and working on computer which are considered as sedentary behavior should be restricted to less than two hours per day during leisure time.

3 Data Description

The data used in the study is from the household travel survey conducted on working days for Bangalore Metropolitan Region (BMR) in 2009. The data was obtained from Bangalore Metropolitan Land Transport Authority. 50,000 household samples from 384 Traffic Analysis Zones (TAZs) were collected and the data is validated using cordon and screen line surveys. Data on household information, travel patterns, and trip details are collected. The survey was focused on different trip purposes and corresponding daily commute trip details. Work and school trips were constituting majority of the trips. A total of 79,335 trips are selected after cleaning the data set for the present study. Table 1 gives the age-wise and gender-wise distribution of the

Table 1 Age-wise and gender-wise share of the observed cycling and walking trips

Age group	Cycling			Walking		
	Male (%)	Female (%)	Total (%)	Male (%)	Female (%)	Total (%)
0–14	14	9	23	13	11	24
15–19	6	5	11	7	5	12
20–29	16	3	19	15	7	22
30–60	44	3	46	31	9	40
60 +	1	0	1	1	1	2
Total	81	19	100	68	32	100

observed cycling and walking trips out of 79,335 trips. It is inferred from Table 1 that the percentage of female using active transportation is comparatively lower than that of male. The reason may be due to lesser number of work trips carried out by women comparing to men. The fact that city lacks infrastructural facilities, related traffic collision risks and poor enforcement of policies make active transport mode less desirable.

4 Methodology

A complete travel information for 79,335 trips obtained from the household travel survey is used for analysis. Computation of MET values is done by considering walking and cycling as distinctive intensity actions. The PA of individuals using active mode of transportation is estimated using the calculated MET value. It is assumed that all cycling had an intensity of 6.8 METs [8, 23]. For walking, an algorithm was created to convert mean walking speed ('S') to MET values, as given in Eq. 1 [23].

$$\text{MET (Walking)} = 1.4594 \text{ x } \exp(0.19 \text{ x S}) \quad (1)$$

The present study is aimed at estimating the PA of people with reference to MET hours per week. Since the health benefits are computed based on weekly activity, the average weekly activity is estimated assuming that the individuals had 250 active days per year. Thus, the individuals are active 4.79 days per week. The mean distance covered by a person per week is obtained as the product of 4.79 days per week and the mean distance covered by a person in a day. This measured distance is converted into time with the use of average speed of active transportation obtained from the trip survey data. The obtained time in terms of hours per week is multiplied with the MET value giving the average measure of PA of the mode of transportation chosen by the individual.

Trip Distance is a determining factor in most of the previous studies for mode choice. This distance can vary with the infrastructural facilities available in the city.

So, the authors considered a transport scenario in which the road users shift to active modes for trip distance less than the acceptable distance [13] for Bangalore. As per the study, an agreeable distance was "0.5 km for walking as the access mode, 1 km for walking as the main mode, and 2 km for cycling as the main mode". Keeping this acceptable trip distance as a base, it is found that about 7.3% of the trips having stage distance of less than 2 km are commuted using modes other than active mode of travel.

Physical activities of different energy expenditures can be grouped under different MET categories namely Light (less than 3 METs), Moderate (3–6 METs), and Vigorous (more than 6 METs). The light physical activities with less than 3 METs include slow walking, sitting, and standing. Moderate intensity activities include brisk walking, slow bicycling, and sports. Vigorous activity includes walking or jogging, carrying heavy loads, fast bicycling. The average shift in the intensity of PA due to shift to active mode of transport is also determined. The guidelines provided by Office of Disease Prevention and Health Promotion (ODPHP) are utilized to understand the health benefits due to PA (MET hours per week). A range of 8.33 MET hours (500 MET minutes) to 16.66 MET hours (1000 MET minutes) of total weekly activity is essential for a good health condition especially for adults. Based on these guidelines, the energy expenditure for the population of the BMR is evaluated to estimate the health gain while shifting to active transportation from other modes of transportation based on the acceptable trip distance for walking and cycling.

5 Analysis of Data and Results

The impact of mode of travel on the physical condition of people is the prime focus of the study. Stage distance, age, and gender are the three important criteria when it comes to choice of bicycling or walking. The active mode of travel is usually adopted for the lesser trip distance. Based on the acceptable distance for active transportation in Bangalore city, it is seen that 7.3% of the potential users of active mode are still relying on motorized travel modes. The scenario considered assumes that the proportion of trips less than acceptable trip distance shifts to active transportation. The summary of data used for analysis is given in Table 2.

The variations in MET calculated for both base case and considered transport scenario is presented in Fig. 1. Activities with MET value less than 3 MET are considered physically inactive and people in this category have higher probability of health risks. The scenario considered shows a decline in population with less than 3 METs and a 5% increase in more active population.

Gender-wise and age-wise variation in a number of trips and its MET is also evaluated and studied. The comparison of these with respect to base case and scenario considered is shown in Fig. 2. Age is categorized into 5 groups where; more active trips are made by age group 30–60 when compared to other age groups. Both females and males make more trips with MET value of 3–6. Considering both genders, more trips are made in the category of 3–6 MET and >6 MET after 7.3% shift to active

Table 2 Summary of dataset

		Base case	Scenario considered
Observed mean stage distance	Walking	1.04 km	0.98 km
	Cycling	2.96 km	2.45 km
Active days per week		250.00 days	250.00 days
Active days per year		4.79 days	4.79 days
Total distance covered by the user in a week	Walking	4.98 km	4.69 km
	Cycling	14.18 km	11.74 km
Average speed	Walking	5.79 km/h	5.79 km/h
	Cycling	8.19 km/h	8.19 km/h
%Share of walking		92	86
%Share of cycling		8	14

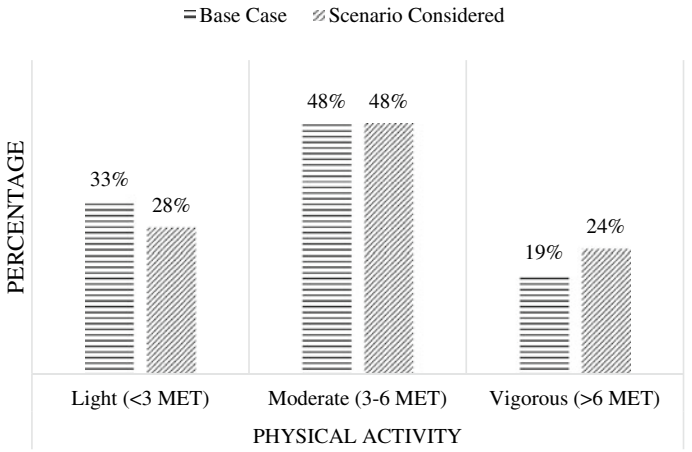

Fig. 1 Comparison of energy expenditure from active transportation

mode transport when compared to base scenario. Although, very little change is observed in trips with MET value less than 3 METs.

Another important feature seen after shift is that, in case of adults above 60 years of age, there is a comparative increase in the vigorous activity trips (>6 MET value), which might reduce the risk to many diseases associated with inactive lifestyle. Women of age between 20 and 60 years are more benefitted due to shift to active transportation as there seems to be an increase in high intensity PA, whereas for male, the shift to vigorous activity is profound for people younger than 20 years old. Result show that 67% of the population commuting through non-motorized transport is sufficiently physically active than other road users who use motorized modes and hence less subjected to obesity and other non-communicable diseases. Compared to

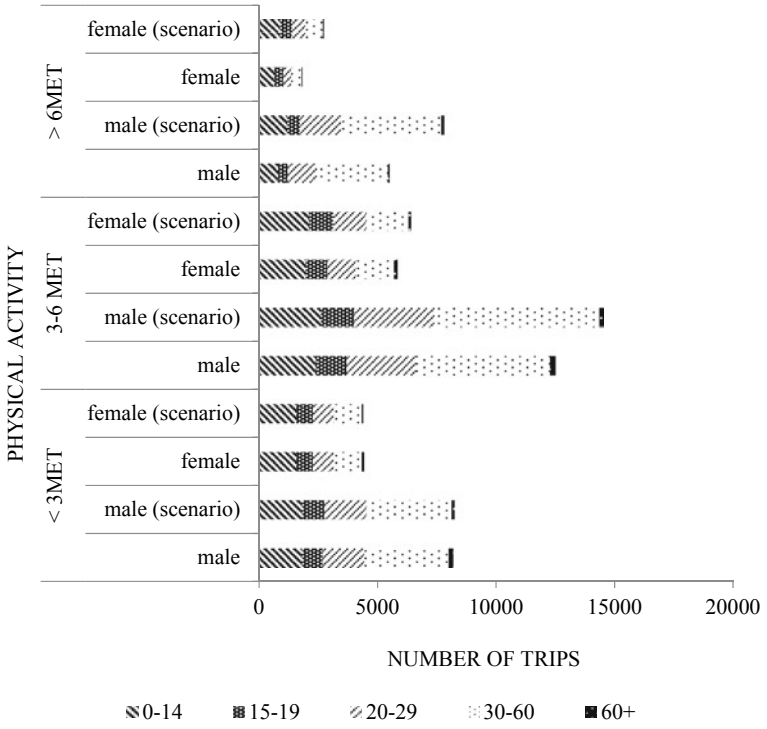

Fig. 2 Age-wise and gender-wise comparison of MET

the base case, the scenario considered has 72% of the commuting population being benefited because of PA.

In the light of the estimated MET hours per week, percentage of active mode users who achieve a minimum of 8.33 MET hours per week activity level is expected to achieve health benefits. The improvement in the health achieved due to mode shift to active transportation is also quantified. Figure 3 shows the percentage of road users using active modes (walking and cycling) achieving minimum standards of active life according to the standard guideline of 8.33 MET hours per week. From the analysis of the data, it is observed that for the base case 28% of the pedestrians are physically benefited whereas 99% of cyclists achieved the minimum standards for active life.

Proportion of active mode users who are potentially benefitted due to mode shift is presented in Table 3. It can be observed from Table 3 that for the base case, out of the total active mode users, 25% of cyclists and 75% of pedestrians are benefited because of active mode of travel, respectively. After the mode shift based on the scenario considered, percentage of cyclists is found to increase to 40%. This increase in the percentage of cyclists is reflected in the increase in the percentage of total percentage of physically benefited active mode users from 34 to 37%.

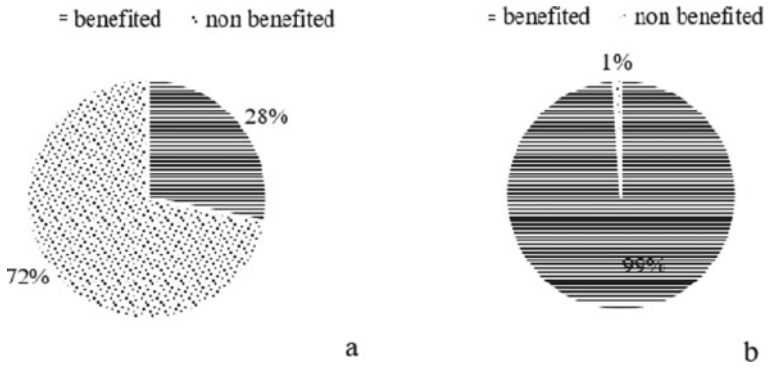

Fig. 3 Percentage of physically benefitted active mode users **a** Walking **b** Cycling

Table. 3 Proportion of physically active road users as per estimated MET hr. per week

	% of physically benefited active mode users	Mode-wise composition of active road users	
		Cyclist (%)	Pedestrians (%)
Base case	34	25	75
Scenario considered	37	40	60

6 Summary and Conclusions

Active transportation has a critical effect in improving the quality of life, physical health, and environmental quality. The study emphasizes the importance of non-motorized modes of transport in achieving health benefits for BMR. Energy expenditure of each trip by active mode is estimated as METs. Major observations from the study are as follows:

- The mean speed of walking is observed as 5.34 km/h, this may be due to abundance of motorized vehicles and resulting friction with the pedestrians [13]. This also shows insufficient attention given to pedestrians and cyclists as the speeds are high and trips are less in number especially cycling. The reason may be because of the related risk of high friction with the motorized traffic leading to road traffic injuries. Thus, proper infrastructure facilities can help in reducing the physical inactivity related health risks as well as the environmental problems to a greater extent.
- Based on the acceptable distance for active transportation, the change in intensity of PA is studied. 7.3% of the total trips are under the acceptable trip distance and is assumed possible for a shift to active transport mode.
- The age-wise and gender-wise split in the commuters give an idea about the current condition that there is less percentage of women using active mode of transportation.

- For base case physically active commuter population was 67% and for the scenario it increased to 72%. Hence the proportion of population engaged in vigorous intensity physical activity showed an upward trend. The increase in participation in active transportation is more for cycling compared to walking.
- Based on the PA computation in terms of MET hours per week it is concluded that about 28% of the pedestrians and 99% of the cyclists are physically benefited and thus fulfill the minimum standard of physically active life.
- Based on the scenario considered, a shift to active transportation from other modes with a stage distance within the acceptable distance for Bangalore resulted in a 3% increase in the individuals who are physically benefited due to active mode of travel.

Health benefits from active transportation are crucial, as this can decrease private vehicle plying on road helping to decrease pollution and traffic congestion. Providing separate infrastructure will be helpful in less exposure of non-motorized modes to other motorized modes thus increasing safety. Hence a future study integrating all these effects together will provide a better inference in promoting active transports. Study shows non-linear relation between physical activity and health outcome [20], which makes it necessary to measure the total volume of physical activity rather than focusing on one domain. Therefore, not only physical activity from transport but PA from different domains must be estimated and studied to understand the overall health benefit of PA.

Acknowledgements The work reported in this paper is part of the Indo-UK collaborative project titled "Toward an Integrated Global Transport and Health Assessment Tool" (TIGTHAT), project (UOCG-0001) sponsored by Medical Research Council (MRC). The authors express their sincere thanks toward the funding agency and other project partners for their valuable inputs and supports.

References

1. A global strategy on diet, physical activity and health, 2019. World health organization
2. Ainsworth BE, Haskell WL, Whitt MC, Irwin ML, Swartz AM, Strath SJ, O'brien WL, Bassett DR, Schmitz KH, Emplaincourt P, Jacobs DR, JR, Leon AS (2000) Compendium of physical activities: an update of activity codes and MET intensities. Med Sci Sports Exerc 32:S498–S516
3. Ainsworth BE, Haskell WL, Herrmann SD, Meckes N, Bassett JR, DR, Tudor-Locke C, Greer JL, Vezina J, Whitt-glover MC, Leon AS (2011) Compendium of physical activities: a second update of codes and MET values. Medicine and Science in Sports & Exercise. Am CollE Sport Med:1575–1581
4. Bangalore mobility indicators (2010–2011), Urban mass transit company limited. (July 23, 2019)
5. Besson H, Brage S, Jakes RW, Ekelund U, Wareham NJ (2010) Estimating physical activity energy expenditure, sedentary time, and physical activity intensity by self-report in adults. Am J Clin Nutr 91:106–114
6. Byrne NM, Andrew P, Hills AP, Hunter GR, Roland L, Weinsier RL, Schutz Y (2005) Metabolic equivalent: one size does not fit all. J Appl Physiol 99:1112–1119

7. Keall M, Randal E, Guria J, Woodward AA (2016) Health outcomes projected from transportation modelling for the new zealand transport outlook
8. Kelly P, Kahlmeier S, Götschi T, Orsini N, Richards J, Roberts N, Scarborough P, Foster C (2014) Systematic review and meta-analysis of reduction in all-cause mortality from walking and cycling and shape of dose response relationship. Int J Behav Nutr Phys Act 11**:**132
9. Millett C, Agrawal S, Sullivan R, Vaz M, Kurpad A, Bharathi AV, Prabhakaran D, Reddy KS, Kinra S, Smith GD, Ebrahim S (2013) Associations between active travel to work and overweight, Hypertension, and diabetes in India. A Cross-Sect Study PLoS Med 10(6)
10. Misra A, Nigam P, Hills AP, Chadha DS, Sharma V, Deepak KK, Vikram NK, Joshi S, Chauhan A, Khanna K, Sharma R, Mittal K, Passi SJ, Seth V, Puri S, Devi R, Dubey AP, Gupta S (2012) Consensus Physical Activity Guidelines for Asian Indians. Diabetes Technol & Ther
11. Morris C, Myers J, Froelicher V, Kawaguchi T, Ueshima K, Hideg A (1993) Nomogram based on metabolic equivalents and age for assessing aerobic exercise capacity in men. J Am CollE Cardiol. 22:175–182
12. Powell KE (2018) Physical activity guidelines advisory committee scientific report
13. Rahul TM, Verma A (2014) A study of acceptable trip distances using walking and cycling in Bangalore. J Transp Geogr 38:106–113
14. Rabl A, Nazelle A (2012) Benefits of shift from car to active transport. Transp Policy 19:121–131
15. Ng SW, Popkin BM Time use and physical activity: A shift away from movement across the globe. Obes Rev Int Assoc Study Obes:659–680
16. Saelens BE, Sallis JF, Black JB, Chen D (2003) Neighborhood-based differences in physical activity: An environment scale evaluation. Am J Public Health 93(9):1552–1558
17. Sidney MJK, Blumchent G (1990) Metabolic equivalents (METS) in exercise testing, exercise prescription and evaluation of functional capacity. Clin Cardiol 13:555–565
18. Sperling D, Clausen E (2002) The developing world's motorization challenge. Issues Sci Technol 19(1)
19. Stefansdottira H, Næss P, Ihlebæk CM (2018) Built environment, non-motorized travel and overall physical activity. Travel Behav Soc
20. Tainio M, Woodcock J, Brage S, Götschi T, Goodman A, Kelly P, Nazelle A (2017) Research into valuing health impacts in transport appraisal
21. Walking or cycling to work reduces health risks in India, 2015, Jyotsna Singh(2019) Down To Earth. <www.downtoearth.org.in/news/walking-or-cycling-to-work-reduces-health-risks-in-india-41320>
22. Woodcock J, Banister D, Edwards P, Prentice AM, Roberts I (2007) Energy and Transport. Lancet 370:1078–1088
23. Woodcock J, Givoni M, Morgan AS (2013) Health impact modelling of active travel visions for England and wales using an integrated transport and health impact modelling tool (ITHIM). Plos One 8(1), e51462. https://doi.org/10.1371/journal.pone.0051462

Framework for Evaluating Traffic Impact of a New Large Commercial Land use—A Case Study from Bengaluru, India

Harihara Subramanian Gayathri, Ashish Verma, G. S. Vishwas, and Raksha Krishnamurthy

Abstract Indian cities are witnessing rampant growth in terms of population and economic growth. The urban population percentage increased from 28.6% in 2001 to 37.7% in 2011. Being a leading IT exporter, Bengaluru sees an increasing number of commercial buildings burdening the existing road infrastructure, leading to heavy congestion in particular areas of Bengaluru. This calls for an understanding of any upcoming commercial development before it is thoroughly established to take adequate measures to reduce the negative impacts. However, the Traffic Impact Assessment (TIA) using the traditional four-stage modeling cannot be used in the current context due to the impact of COVID-19 on the existing traffic. This paper adopts an improved methodological framework that can be used to evaluate the impact of traffic in any situation. An average of 6.6% percentage increase (maximum 25% on some roads) in V/Cs is observed before and after the new development on the adjoining roads. To improve the level of service, several scenarios are considered and analyzed to provide the best mitigation strategies. This improved methodological framework can help to evaluate a new development's impact for any given situation, and what mitigation strategies and types of transportation improvements may be essential to maintain a smooth moving traffic with a satisfactory level of service.

Keywords Traffic Impact Analysis (TIA) · Traffic forecast · Commercial land use · Travel demand model · Scenario analysis

H. S. Gayathri
Research Scholar, Department of Civil Engineering, Indian Institute of Science, Bangalore 560012, India
e-mail: gayathrih@iisc.ac.in

A. Verma (✉)
Professor, Department of Civil Engineering, Indian Institute of Science, Bangalore 560012, India
e-mail: ashishv@iisc.ac.in

G. S. Vishwas · R. Krishnamurthy
Intern, B.M.S College of Engineering, Bengaluru 560019, India
e-mail: vishwasgs.ctm19@bmsce.ac.in

R. Krishnamurthy
e-mail: raksha.ctm19@bmsce.ac.in

L. Devi et al. (eds.), *Proceedings of the Sixth International Conference of Transportation Research Group of India*, Lecture Notes in Civil Engineering 273,
https://doi.org/10.1007/978-981-19-4204-4_3

1 Introduction

Indian cities are witnessing rampant growth in terms of population and economic growth. The urban population percentage increased from 28.6% in 2001 to 37.7% in 2011. There is a substantial increase in India's GDP for most of the last two decades, leading to rising per capita incomes and a reduction in absolute poverty. This growth is physically manifested in increasing employment offices and the associated housing and retail development in the Indian cities. Land use is a fundamental determining factor for movement and activity. The nature of land use influences the source and nature of travel, and consequently, the traffic generation and distribution processes. Among the various land uses, commercial land use contributes more to the traffic flow in cities due to its trip-making nature (built-up area and occupancy are more for commercial [4]). Bengaluru, also known as Silicon Valley of India, is a leading IT exporter, where the number of commercial buildings is more. This rapid growth of employment offices in the city acts as a hub for trip generation and attraction, potentially impacting the existing road infrastructure. This is seen to reflect on the urbanization trends and the mobility choices of people which in turn have resulted in an exponential rise in motorization. This leads to heavy congestion in particular areas of Bengaluru. According to the ninth edition of the Tom Tom Traffic Index report, Bengaluru has the world's worst traffic congestion [13]. Therefore, it is imperative to understand the effect of any upcoming commercial development before it is thoroughly established, to take adequate measures to reduce the negative impacts, if any.

Traffic Impact Assessment (TIA) is a technical analysis of traffic problems and safety issues relating to a specific development. This is done to estimate the impact of a new development's site-generated traffic on the adjoining roads. Upcoming or new projects require a comprehensive TIA to help determine the forecasted traffic on the adjoining roads, identify the potential problems associated with the new development, provide suitable mitigation strategies to tone down the negative impacts, and provide suggestions/ recommendations for hassle-free movement of vehicles on roads. TIA, though recently being studied in India due to the need for developing sustainable solutions to ease out congestion, a few researchers across the world have studied this widely. Most of the studies have used the conventional four-stage modeling [3, 8, 9]. Wagner [17] has studied the impact of logistics-related land use and suggested a methodological improvement of integrating the trip generation and trip distribution estimation into the regional land use and transport models. In a similar study by Sharmeen et al. [11], a generic methodology for TIA is developed by forecasting the background and the developing traffic for a mixed land use in Dhaka city. Mihans et al. [6] did a TIA in the neighborhood of Skudai Town in the Johor Bahru region in which the entry mean trip rate was estimated using trip rate analysis, cross-classification analysis and regression analysis and did a comparison of values obtained from Highway Planning Unit (HPU) Malaysian manual.

Regidor and Teodoro [10] mentioned that detailed description of the traffic conditions around the study site's vicinity is required. At least a few kilometers around

the site should be studied for its impact. Also, the future projected year should be at least 10 years down the line [1] with base year ideally varying by location, extent and purpose of development. To ensure that predictions of traffic impacts are accurate, the TIA should include technical guidance about baseline conditions and key assumptions, with a full assessment of existing transport infrastructure [14]. Environment impacts should also be taken into consideration, as more sustainable solutions are required [1, 15]. The methodology used for predicting trips would have a significant effect on a TIA [7]. Therefore, a more comprehensive methodology which is inclusive of all situations is required.

However, the existing methodologies in the literature cannot be used for the present COVID-19 situation as the traffic is not the same as in the pre-COVID situation, which can overestimate the model values. This necessitates an improved methodological framework that can evaluate the impact of traffic in any situation. A new large commercial land use in Bengaluru is considered the case study to apply the proposed methodology and framework. Therefore, the objectives of this paper are (a) to develop an improved methodological framework to evaluate the traffic impact (b) to perform a traffic impact assessment of a new large commercial land use which is under development in Bengaluru (c) to assess the level of service (LOS) on roads adjoining the new commercial development based on the estimated traffic loads and suggest road improvement measures to maintain a given LOS, wherever possible, and (d) to propose possible ways to reduce traffic loads in the present and near future and ways to integrate with upcoming Bengaluru metro rail station near the new commercial development.

The remainder of the paper is organized as follows: In the next section, details of the case study and data collection are presented. Section 4 describes the methodological framework adopted, and Sect. 5 discusses the results. Finally, we conclude with the discussions of the study and possible future work.

2 Description of the Case Study

2.1 Study Site

ITC Green Centre is an ongoing commercial complex with predominantly office space (buildings 1–6) and a hotel (building 7) in which building 1 and 2 are already existing. It is located on a 13.7-hectare (33.98 acres) site and is approximately 5.5 km northeast of Bengaluru's central business district. The major land use near the campus is residential. The proposed development is planned to be built in 4 phases and will be replacing the existing old buildings on the site, phase-wise. Phase 1 of the campus includes building 1 and 2, which is existing with the ground and 11 floors, and four basement floors for parking in common. Phase 2 includes building 3 with the ground and 12 floors and three basement floors for parking. Phase 3 includes building 4 and 5 with ground and 12 floors each, 2 basements in each building for parking,

and a Multi-Level Car Parking (MLCP) in building 4 to accommodate the overall campus's deficit car parks. Phase 4 includes building 6 with the ground and 11 floors, four basements for parking, and the ITC hotel. Two scenarios are considered for hotel building: (a) Scenario 1–150 rooms with 600 occupancies (includes staff and guest) and (b) Scenario 2–350 rooms with 1400 occupancies (includes staff and guest) The project site in Bengaluru and the layout is shown in Figs. 1 and 2 respectively, and the details of all phases are given in Table 1.

Fig. 1 Project site and the adjoining roads

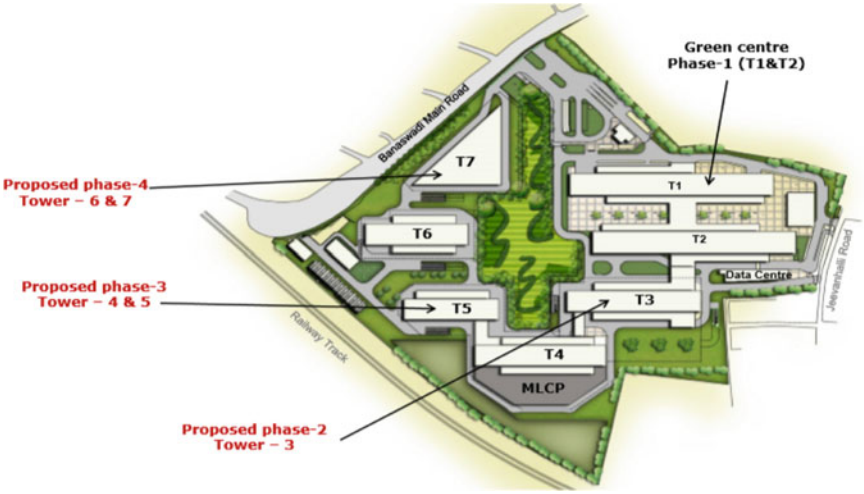

Fig. 2 ITC green centre layout

Table 1 Details of ITC green centre buildings

Phase no	Building no	Landuse type	Built-up area (Sqft)	Occupancy
Phase 1	Building-1 and 2	Office	23,33,994	10,500
Phase 2	Building-3	Office	9,51,237	5870
Phase 3	Building-4	Office	14,69,510	5865
	Building-5	Office	5,01,384	3750
Phase 4	Building-6	Office	5,23,093	3950
	Building-7 (Scenario 1)	Hotel	5,46,619	600
	Building-7 (Scenario 2)	Hotel	5,46,619	1400

2.2 Data Collection and Assumptions Made

Data collection included both primary and secondary data. The secondary data collected from ITC Green Centre were the entry/exit time of vehicles to ITC, pin codes of cars entering ITC for January 2020 (before lockdown) and the vehicle circulation plan inside the ITC campus. Pin codes represent the area of residence of the car users. The pin code details of the car users were collected to identify the shortest route from their location to ITC Green Centre. For validation, a peak hour volume count survey was done on the three roads adjoining the ITC campus.

Due to the non-availability of data, the following assumptions were made.

i. Mode split for hotel employees was assumed to be the same as office buildings.
ii. From the data gathered for hotel guests and visitors, the maximum entries and exits in one-hour interval were assumed as the entries and exits in peak hour as a worst-case scenario.
iii. Directional split percentages of other modes (except two-wheelers) were assumed to be the same as car distribution.
iv. Directional split percentage of two-wheelers from Gate 4 was assumed based on its connectivity to the main road.
v. The occupancy value of a 13-seater tempo traveler was assumed to be 9.75 (75% occupancy).

3 Methodology

The conventional four-stage modeling involves collecting the volume count data from the adjoining roads and adding the additional volume induced due to the new development. However, in the current pandemic situation, collecting the existing volume count data would give wrong figures due to increasing percentage of people opting for work from home, change in travel patterns, etc. Therefore, a generic methodology using the forecasted values from the Regional Travel Demand Model (TDM) developed for Bengaluru using TransCAD [16] was adopted to assess the

traffic impact of the new development. The flow chart depicting the steps involved in developing Travel Demand Model is shown in Fig. 3. The volume on the adjoining roads of the development center was linearly forecasted for the year 2020 for all 384 Traffic Analysis Zones considered in the TDM. The forecasting was done using the growth rates from the Comprehensive Traffic and Transportation Study for Bengaluru Metropolitan Region, which was determined from the primary data (sixteen different types of surveys pertaining to the network, users and operator) and secondary data (Revised Structure Plan-2031, Draft Master Plan-2015, Plan Bengaluru-2020, Census Data, Public transport, fare structure, etc.) (CTTS Report 2010). Using the volume obtained from the TDM model, the impact of the new development on the adjoining roads was assessed. The methodology adopted for the case study is depicted in Fig. 4.

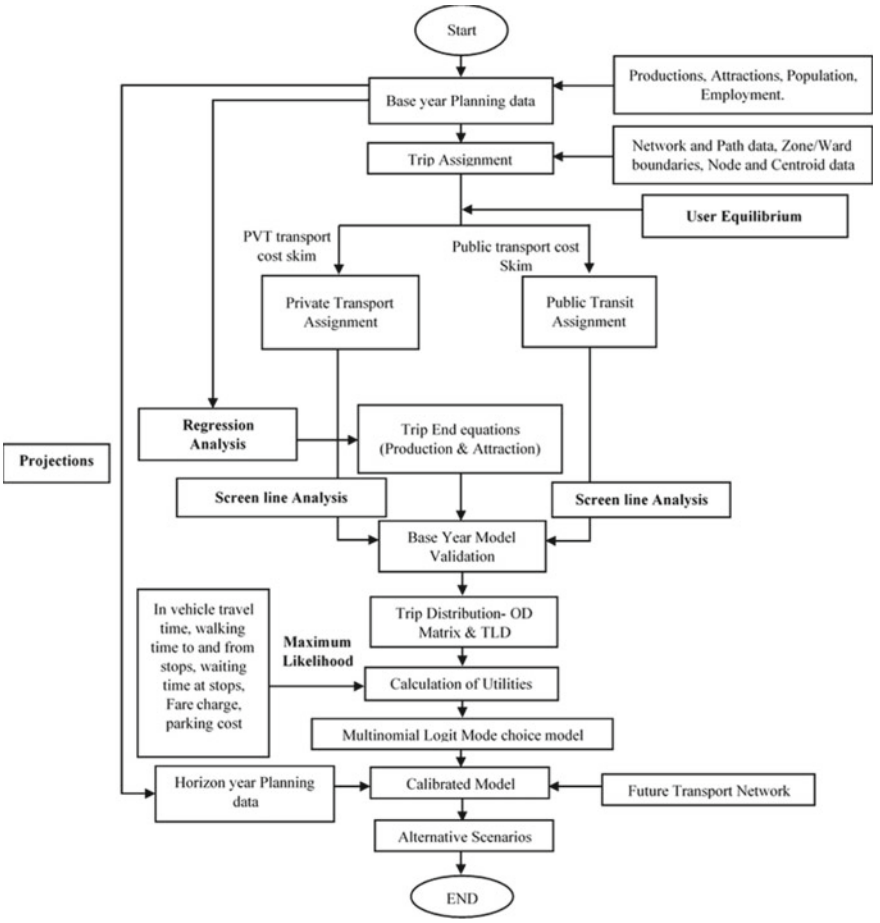

Fig. 3 Process flow chart of the travel demand model [16]

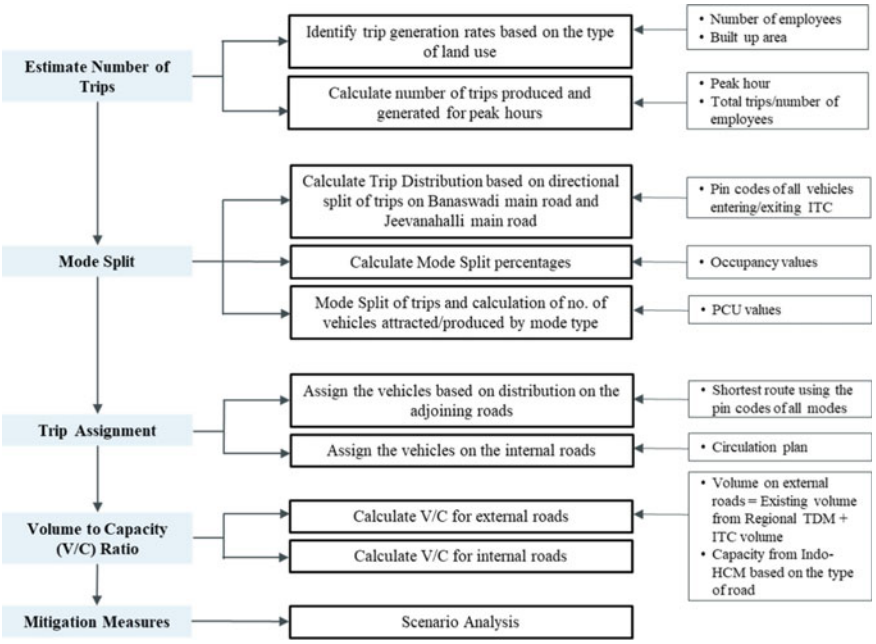

Fig. 4 Methodology adopted for the case study

4 Results

4.1 Trip Rate Analysis

From the built-up area and occupancy details of ITC Green Centre and old campus buildings, average trip generation rates for the peak period of a typical weekday and the number of trips produced and attracted to the development were calculated using the formula

$$Triprate = \frac{Occupancy}{Builtuparea}$$

This is presented in Table 2.

The following representations are to be noted:

a. Scenario 1 a—Employees in scenario 1 of hotel
b. Scenario 1 b—Guests in scenario 1 of hotel
c. Scenario 2 a—Employees in scenario 2 of hotel
d. Scenario 2 b—Guests in scenario 2 of hotel

Table 2 Average trip rates

Buildings	Trip rate (No/1000Sft)
ITC Green Centre	
Building-1 and 2	4.5
Building-3	6.17
Building-4	3.99
Building-5	7.48
Building-6	7.55
Building-7 (Scenario 1 a)	0.55
Building-7 (Scenario 1 b)	0.55
Building-7 (Scenario 2 a)	1.28
Building-7 (Scenario 2 b)	1.28
Old campus	
Corresponding Phase 2 buildings	14.68
Corresponding Phase 3 buildings	11.62
Corresponding Phase 4 buildings	0

4.2 Peak Hour Calculation

The morning peak was identified to be between 9 and 10 AM, and the evening peak was identified to be between 6 and 7 PM for both ITC Green Centre and the old campus. It is seen from Figs. 5 and 6 that 20 and 30% of the total trips in a day were attracted to ITC Green Centre and old campus, respectively, in the morning peak hour and 20% and 24% of the total trips in a day were produced from ITC

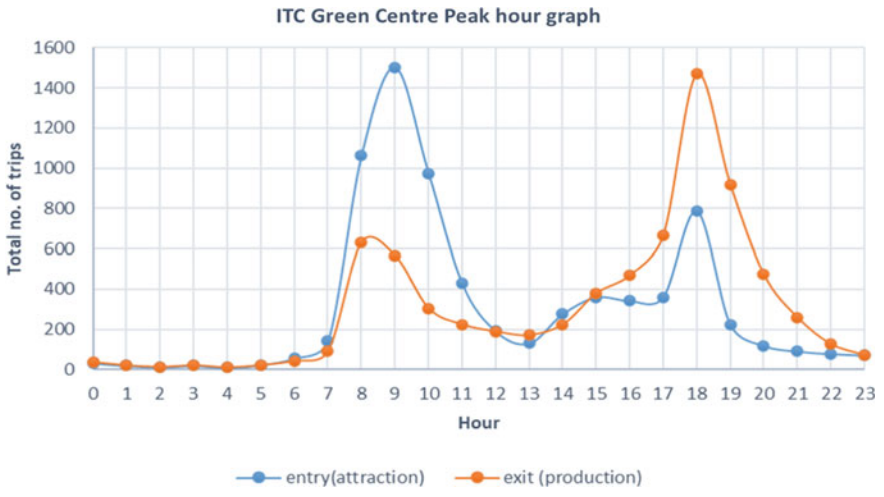

Fig. 5 Peak hour calculation for ITC green centre

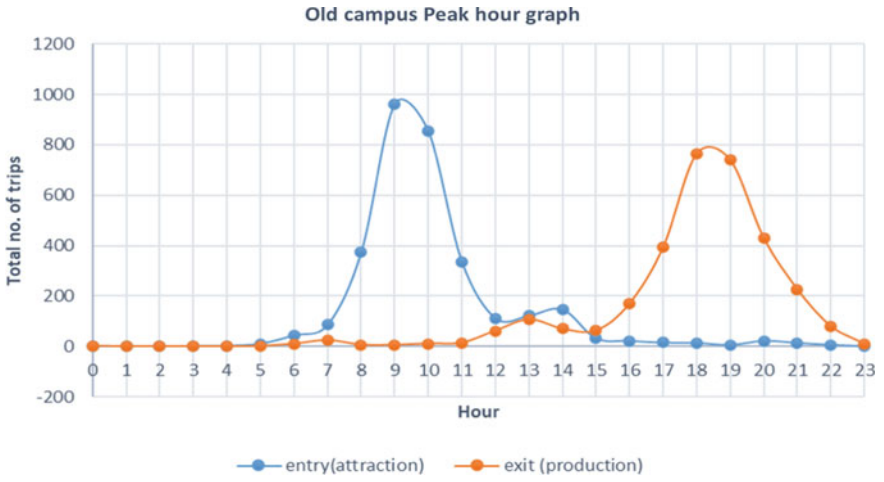

Fig. 6 Peak hour calculation for old campus

Green Centre and old campus, respectively, in the evening peak hour. Similarly, 8% of the total trips in a day were produced from ITC Green Centre in the morning peak hour, and 11% of the total trips in a day were attracted to ITC Green Centre in the evening peak hour. Productions from old campus during morning peak and attraction during evening peak were almost 0%. From this and the total trips in a day, the trips produced and attracted to ITC Green Centre and old campus during the morning and evening peak period were calculated, which is summarized in Table 3. The morning trip production and evening trip attraction of ITC Green Centre are more when compared to the old campus trips. This could be due to a greater number of shift-based trips from ITC Green Centre than from the old campus buildings, which needs a further understanding.

4.3 Mode Split

The mode-wise trips were then calculated using the average occupancy values [5]. The mode split percentages considered are reported in Tables 4 and 5. Mode split for hotel employees was assumed to be the same as office buildings. Only two-wheeler and car were considered, and all other modes were distributed to two-wheeler and car according to their percentages.

Using the mode split percentages, the peak hour trips and the average occupancy values, the vehicle trips by mode were calculated for AM and PM peaks. Using the Passenger Car Units (PCU) from the Indo-HCM manual, 2017, the vehicle trips were converted to their equivalent passenger car values.

Table 3 Trips produced and attracted to ITC Green Centre and old campus during peak hour

Buildings	AM Peak Hour(trips)		PM Peak Hour(trips)	
	Produced	Attracted	Produced	Attracted
ITC Green Centre				
Building-1 and 2	803	2149	2086	1128
Building-3	449	1202	1166	631
Building-4	448	1201	1165	630
Building-5	287	768	745	403
Building-6	302	809	785	424
Building-7 (Scenario 1 a)	23	61	60	32
Building-7 (Scenario 1 b)	43	44	43	44
Building-7 (Scenario 2 a)	54	143	139	75
Building-7 (Scenario 2 b)	100	102	100	102
Old campus				
Corresponding Phase 2 buildings	3	546	434	8
Corresponding Phase 3 buildings	5	974	774	14
Corresponding Phase 4 buildings	0	0	0	0

Table 4 Mode split percentages for office buildings

Mode	Percentage
ITC Green Centre	
Two-wheeler	22%
Car	17%
Cab	31%
Bus	22%
Tempo traveler	8%
Old campus	
Two-wheeler	73%
Car	22%
Cab	5%

Table 5 Mode split percentages for employees and guests of hotel

Mode	Percentage
For hotel employees	
Two-wheeler	57%
Car	43%
For hotel guests	
Car	100%

4.4 Trip Assignment

The trips were assigned using User Equilibrium (UE) trip assignment method. The UE method is based on Wardrop's first principle which assumes that "no user can unilaterally reduce their travel costs by shifting to another route". For a given OD pair, the UE conditions can be represented as

$$f_k(c_k - u) = 0 : \forall k \tag{i}$$

$$c_k - u \geq 0 : \forall k \tag{ii}$$

where f_k is the flow on path k, c_k is the travel cost on path k, and u is the minimum cost. Equation (ii) can have two states:

1. If $c_k - u = 0$, from Eq. (i), $f_k \geq 0$. This means that all used paths will have the same travel time.
2. If $c_k - u > 0$, the from Eq. (i), $f_k = 0$.

This means that all unused paths will have travel time greater than the minimum cost path [12].

The initial OD matrix used for assigning the trips included only the existing Phase 1 buildings of ITC and does not include the trips from the other phases. To add the additional trips from the new phase, about 23 links around ITC were considered which is shown in Fig. 7. The pin codes of cars were gathered, and their route to ITC from the origin was identified from google maps. It was observed that 60% of the cars

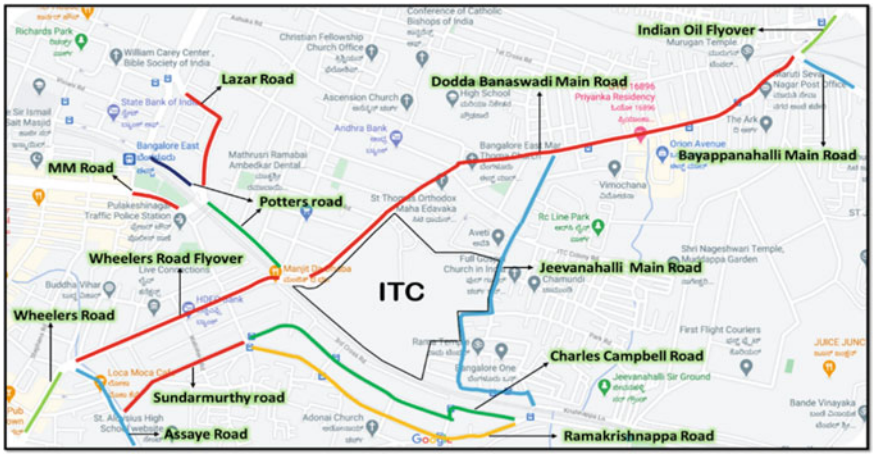

Fig. 7 Adjoining roads considered for assessing the impact of traffic

entered from Wheeler's flyover side and the remaining 40% from Dodda Banaswadi roadside (opposite to Wheeler's flyover side), which was assumed to be the same for all the vehicles entering through the main gate (Gate 1). Similarly, the directional split percentage for two-wheelers entering the campus from Jeevanahalli main road (Gate 4) was also assumed to be 80% from Banaswadi to Jeevanahalli main road and 20% from Ramakrishnappa and Charles Campbell Road, due to unavailability of data.

From the pin codes, it was observed that 60% of the trips came from Wheeler's flyover. Out of the 60%, 78% came straight from Wheeler's flyover and 22% came from pottery to Wheeler's flyover side. Out of the 78%, 67% again came straight from Wheeler's flyover side, and 33% came from Assaye road. Out of the 22%, 95% of the trips were from Lazar road, and 5% were from MM road. Similarly, out of the 40% trips coming from Dodda Banaswdi main road, 95% of the trips came from Indian oil flyover and 5% from Bayappanahalli main road.

For two-wheeler trips, it was assumed that 80% of the trips came from Banaswadi main road to Jeevanahalli main road and 20% from the railway line side. Out of the 80% trips from Banaswadi main road, 60% was from Wheeler's flyover side and 40% from Banaswadi roadside. The 20% from railway line side came from Ramkrishnappa road (one-way road) which diverged from Wheeler's road. The trips were assigned according to these directional split percentages except for one-way roads, where the respective trips were assigned to their alternate roads.

The Regional Travel Demand Model (TDM) was then used to forecast the existing travel demand for 2020 for peak hour, and the existing flow values were derived from the model for the existing condition. Then (Volume/ Capacity) V/C ratio for the adjoining roads was calculated for the existing condition (phase 1 of ITC Green Centre and existing buildings of old campus) to assess the current Level of Service (LOS) on the roads adjoining the campus. The capacity values were obtained from the Indian Highway Capacity Manual (Central Road Research Institute 2017). Similarly, the traffic volume on the adjoining roads was forecasted for the year 2030 using Regional Travel Demand Model (TDM), and the flow values for peak hour were derived from the model.

The peak period classified traffic volume estimates based on the TDM for Bengaluru for the adjoining roads and their corresponding V/C ratios and LOS, for an existing condition, were calculated. Then the incremental impact of traffic due to the development of each phase was also assessed. For this, both the ITC Green Centre and old campus buildings were considered. When a new building was included, the corresponding old buildings that will be replaced were excluded from the assessment. For the existing 2020, in most of the links, volume exceeds the capacity with V/C more than 1 representing LOS F. According to Indo-HCM, this symbolizes a zone of forced or breakdown flow which may result in long queues and delays. For the projected year 2030, the volume to capacity ratio was worse than the current 2020 year. This can lead to queues that are characterized by stop and go waves, which are extremely unstable. Long queues and delays are highly likely. Therefore, proper measures are to be taken to improve the level of service. An average of 6.6%

(maximum 25% on some roads) increase in V/Cs of the adjoining roads was observed due to the development of ITC (before phase 1 and after phase 4).

4.5 Validation

A peak hour traffic volume count survey was done to validate the volumes derived from the Travel Demand Model. The survey was done on a typical working day (Wednesday, 30 December 2020) and under normal weather conditions. Six adjoining roads to ITC were chosen for the survey. The vehicles are counter mode-wise and converted to one unit using PCU values. The total trips are then compared with the volumes derived from TDM and it is seen from Table 6 that the predicted volumes from TDM are higher than the actual volumes on the day of count. Therefore, the calculations are done using TDM volumes which represents a worst-case scenario. However, the survey was done during COVID-19 situation, which is a limitation.

Table 6 Volumes from traffic volume count survey and TDM

Sl no	Road name	Morning peak hour volume (PCU/hr)	Evening peak hour volume (PCU/hr)	Morning peak hour volume from TDM (PCU/hr)	Evening peak hour volume from TDM (PCU/hr)
1	Banaswadi road from Indian oil flyover	1627	1263	3602	3492
2	Banaswadi road from Wheeler's flyover	1584	3294	4118	3954
3	From Banaswadi to jeevanahalli	425	361	4002	3955
4	From Jeevanahalli to banaswadi	472	445	1863	1834
5	From Banaswadi to jeevanahalli gate 4	439	667	4072	3956
6	Railway line to Jeevanahalli gate 4	591	492	1863	1834

4.6 Scenario Analysis

The following scenarios were analyzed to check the effect of those on the estimated traffic volumes, V/C ratios and LOS.

a. Work from Home (30 and 50% of the employees).
b. Staggered time

Morning peak hour trips (8-9 AM, 9-10 AM, 10-11 AM) and evening peak hour trips (5-6 PM, 6-7 PM, 7-8 PM).

c. Mode shift

i. Change in mode shares of ITC

(10% car, 10% TW, 37% office cabs, 29% office bus, 14% office tempo travelers).

ii. Mode share used in bundle 3 of CLIMATRANS [16].

Based on the Intergovernmental Panel on Climate Change (IPCC) definition, inputs from multiple stakeholder meetings and a Delphi survey with various government officials of Bengaluru, 4 policy bundles were formulated in CLIMATRANS. Those mitigation policy bundles' main objective was to attain an optimum balance of push and pull strategy by developing policies that encourage public transportation and other sustainable modes. This can help reduce the vehicle kilometers traveled, which lead to a reduction in emissions and traffic congestion compared to the Business-as-usual scenario, thereby improving the quality of life of people in Bengaluru city.

Bundle 3 of CLIMATRANS is a mixture of Planning, Regulatory, and Economic instrument and includes the following policies:

- *Increasing network coverage of Public Transit.*
- *Defining car restricted roads.*
- *Congestion Pricing.*
- *Park and Ride.*
- *Cycling and Walking infrastructure.*
- *Encouraging car-pooling and High Occupancy Lanes.*
- *High-density mix building use along main transport corridors.*

Bundle 3 was identified as the best bundle in CLIMATRANS and so, the mode share percentages of bundle 3 were adopted for this scenario. The mode share percentages were 16% TW, 2% Car, 3% Auto, 40% Bus, 19% Metro, 6% Walk, and 16% Cycle.

d. Combination of the above scenarios

The following combinations were analyzed.

i. 30% of the employees WFH and staggered time.
ii. 50% of the employees WFH and staggered time.

iii. 30% of the employees WFH and change in the mode share of ITC.
iv. 50% of the employees WFH and change in the mode share of ITC.
v. Staggered time and change in the mode share of ITC.
vi. 30% of the employees WFH, staggered time and change in the mode share of ITC with the existing volumes on adjoining roads.
vii. 50% of the employees WFH, staggered time and change in the mode share of ITC with the existing volumes on adjoining roads.
viii. 30% of the employees WFH, staggered time and change in the mode share of ITC with estimated volumes on adjoining roads, using the mode shares of bundle 3 of CLIMATRANS.
ix. 50% of the employees WFH, staggered time and change in the mode share of ITC with the estimated volumes on adjoining roads, using the mode shares of bundle 3 of CLIMATRANS.

The combination of three scenarios provided better results out of which while comparing the BAU with the existing volume on the adjoining roads, the scenarios (30% WFH, staggering work time from 10 AM to 7 PM and mode shift in ITC trips) and (50% WFH, staggering work time from 10 AM to 7 PM and mode shift in ITC trips) were best for AM trips and the scenarios (30% WFH, staggering work time from 8 AM to 5 PM and mode shift in ITC trips) and (50% WFH, staggering work time from 8 AM to 5 PM and mode shift in ITC trips) were best for PM trips, for both 2020 and 2030. This is because the morning peak hour is 9 AM–10 AM, and so trips will be proportionately less from 10 AM than in 8–9 AM (as this also has a good number of trips). Similarly, the evening peak hour is 6 PM–7 PM and so the trips will be proportionately less around 5 PM than in 6–7 PM (as this also has a good number of trips). It was also seen that there was not much reduction in V/Cs during the peak hour time as 9 AM–6 PM is the general work time. Also, the percentage decrease in V/Cs due to 30% WFH and 50% WFH were almost similar. Therefore, a combination of staggering the work hours before and after the peak hours, with a proportion of employees working from home, and a proportion of employees shifting to shared modes provided by ITC can substantially reduce the V/Cs on the adjoining roads. Decrease in PM was more than AM could be due to external factors (such as school timings). Percentage decrease of V/C from BAU scenario's V/C and projected 2030s V/Cs due to the combination of three scenarios with the existing volumes on adjoining roads are summarized in Table 7.

Similarly, while comparing the BAU with the volumes obtained from bundle 3 scenario of CLIMATRANS, the scenarios (30% WFH, staggering 10 AM–7 PM and bundle 3 mode shift) and (50% WFH, staggering 10 AM–7 PM and bundle 3 mode shift) were best for AM trips, and the scenarios (30% WFH, staggering 8 AM–5 PM and ITC mode shift) and (50% WFH, staggering 8 AM–5 PM ITC mode shift) were best for PM trips, for both 2020 and 2030. It was also seen that there was not much reduction in V/Cs during the peak hour time. Also, the percentage decrease in V/Cs due to 30% WFH and 50% WFH were almost similar. As bundle 3 mode share values from CLIMATRANS were used for adjoining roads' volumes, the percentage decrease in V/Cs were more (Table 8), as it was more toward using public

Table 7 Percentage decrease of V/C from BAU scenario's V/C and projected 2030s V/Cs due to the combination of three scenarios with the existing volumes on adjoining roads

Phase	Combination of scenarios					
	30% WFH, Staggering 8AM–5PM and ITC mode shift	50% WFH, Staggering 8AM–5PM and ITC mode shift	30% WFH, Staggering 9AM–6PM and ITC mode shift	50% WFH, Staggering 9AM–6PM and ITC mode shift	30% WFH, Staggering 10AM–7PM and ITC mode shift	50% WFH, Staggering 10AM–7PM and ITC mode shift
AM 2020						
Phase 1	29	30	2	3	35	35
Phase 2	30	30	3	4	35	36
Phase 3	31	31	5	5	36	37
Phase 4 (Scenario 1)	31	32	5	6	36	37
Phase 4 (Scenario 2)	31	32	5	6	36	37
PM 2020						
Phase 1	55	56	3	3	38	37
Phase 2	55	55	4	4	38	38
Phase 3	55	56	6	6	39	39
Phase 4 (Scenario 1)	55	56	7	7	39	40
Phase 4 (Scenario 2)	55	56	7	7	39	40
AM 2030						
Phase 1	29	29	2	2	34	35
Phase 2	30	30	3	3	35	35
Phase 3	30	31	4	4	35	36
Phase 4 (Scenario 1)	31	31	5	5	36	36
Phase 4 (Scenario 2)	31	31	5	5	36	36
PM 2030						
Phase 1	55	55	2	3	38	39
Phase 2	54	54	3	4	37	38
Phase 3	54	55	5	5	38	38
Phase 4 (Scenario 1)	55	55	6	6	38	39

(continued)

Table 7 (continued)

Phase	Combination of scenarios					
	30% WFH, Staggering 8AM–5PM and ITC mode shift	50% WFH, Staggering 8AM–5PM and ITC mode shift	30% WFH, Staggering 9AM–6PM and ITC mode shift	50% WFH, Staggering 9AM–6PM and ITC mode shift	30% WFH, Staggering 10AM–7PM and ITC mode shift	50% WFH, Staggering 10AM–7PM and ITC mode shift
Phase 4 (Scenario 2)	54	55	6	6	38	39

transportation and sustainable modes. Therefore, a combination of staggering the work hours before and after the peak hours, with a proportion of employees working from home, and shift of ITC employees and the public to more sustainable modes can substantially reduce the V/Cs on the adjoining roads. Decrease in PM was more than AM could be due to external factors (such as school timings). Percentage decrease of V/C from BAU scenario's V/C and projected 2030s V/Cs due to combination of three scenarios with bundle 3 volumes on adjoining roads is summarized in Table 8.

As the bundle 3 mode shift cannot be attained immediately, the best scenario would be the 50% work from home, staggering of work hours from 8–11 AM to 5–8 PM, and ITC mode shift.

4.7 Effect of Metro on the Best Scenario Results

Bengaluru metro has proposed Pottery town metro station, which is approximately 2.5Kms from ITC Green Centre. Therefore, 6% from two-wheelers trips and 4% from cars trips were shifted to the metro. This analysis was done for the best scenario (50% WFH, staggering 8–11 AM to 5–8 PM, and ITC mode shift), and the results are summarized in Table 9. It was seen that there was a 1%–2% reduction on an average in V/Cs from the best scenario V/Cs due to the shift of trips to the metro. If an exclusive skywalk is provided between ITC and the metro station, then there could be more shift of trips toward the metro.

5 Conclusion

This paper discusses the methodological framework adopted to assess the impact of an upcoming commercial development (ITC Green Centre) in Bengaluru. The Regional Travel Demand Model (TDM) that was developed for Bengaluru using TransCAD [16] was adopted to assess the traffic impact of the new development. The forecasted values from this model were considered for the assessment, which rules

Table 8 Percentage decrease of V/C from BAU scenario's V/C and projected 2030's V/Cs due to the combination of three scenarios with the existing volumes on adjoining roads

Phase	Combination of scenarios					
	30% WFH, Staggering 8AM–5PM and ITC mode shift	50% WFH, Staggering 8AM–5PM and ITC mode shift	30% WFH, Staggering 9AM–6PM and ITC mode shift	50% WFH, Staggering 9AM–6PM and ITC mode shift	30% WFH, Staggering 10AM–7PM and ITC mode shift	50% WFH, Staggering 10AM–7PM and ITC mode shift
AM 2020						
Phase 1	36	36	11	11	41	41
Phase 2	36	37	12	13	41	41
Phase 3	37	38	12	13	42	42
Phase 4 (Scenario 1)	38	38	13	13	42	42
Phase 4 (Scenario 2)	37	38	13	13	42	42
PM 2020						
Phase 1	59	60	11	12	44	45
Phase 2	58	59	13	13	43	44
Phase 3	59	60	14	15	44	45
Phase 4 (Scenario 1)	59	60	15	16	45	45
Phase 4 (Scenario 2)	59	60	15	15	45	45
AM 2030						
Phase 1	35	35	11	11	40	41
Phase 2	35	36	11	11	40	41
Phase 3	36	37	13	13	41	42
Phase 4 (Scenario 1)	37	37	13	14	41	42
Phase 4 (Scenario 2)	37	37	13	14	41	42
PM 2030						
Phase 1	59	59	11	11	44	44
Phase 2	58	58	12	12	43	43
Phase 3	58	59	13	13	43	44
Phase 4 (Scenario 1)	58	59	14	14	44	44

(continued)

Table 8 (continued)

Phase	Combination of scenarios					
	30% WFH, Staggering 8AM–5PM and ITC mode shift	50% WFH, Staggering 8AM–5PM and ITC mode shift	30% WFH, Staggering 9AM–6PM and ITC mode shift	50% WFH, Staggering 9AM–6PM and ITC mode shift	30% WFH, Staggering 10AM–7PM and ITC mode shift	50% WFH, Staggering 10AM–7PM and ITC mode shift
Phase 4 (Scenario 2)	58	59	14	14	44	44

Table 9 Percentage decrease of V/C from best scenario to V/Cs due to shift of trips to metro

50% WFH, staggering 8 AM–5 PM, ITC mode shift (including metro)				
	AM 2020	PM 2020	AM 2030	PM 2030
Phase 1	0	1	0	0
Phase 2	0	1	0	0
Phase 3	1	1	1	1
Phase 4(Scenario 1)	1	2	1	2
Phase 4 (Scenario 2)	1	2	1	2
50% WFH, staggering 9 AM–6 PM, ITC mode shift (including metro)				
	AM 2020	PM 2020	AM 2030	PM 2030
Phase 1	0	0	0	0
Phase 2	0	0	1	0
Phase 3	0	1	1	0
Phase 4 (Scenario 1)	1	1	1	1
Phase 4 (Scenario 2)	1	1	1	1
50% WFH, staggering 10 AM–7 PM, ITC mode shift (including metro)				
	AM 2020	PM 2020	AM 2030	PM 2030
Phase 1	0	1	0	0
Phase 2	0	0	1	1
Phase 3	2	2	1	0
Phase 4 (Scenario 1)	2	2	1	2
Phase 4 (Scenario 2)	2	2	1	2

out the necessity for data collection in the conventional techniques, which cannot be done during the pandemic. The same can also be used in the post-pandemic situation by forecasting the volume of the background traffic.

An average of 6.6% percentage increase (maximum 25% on some roads) in V/Cs was observed before and after the new development on the adjoining roads. This might lead to heavy congestion on those roads with a poor level of service. Therefore, several scenarios were considered and analyzed to provide the best mitigation

strategies to improve the level of service. The scenarios considered include work from home (30 and 50% employees), staggered time (ITC trips divided equally between 8–11 AM and 5–8 PM), mode share (shifting toward public transportation and other sustainable modes) and combinations of the three. The best scenario obtained from this was a combination of 50% work from home, staggering of work hours from 8–11 AM to 5–8 PM, and ITC mode shift has brought down the V/Cs to an average of 30% during AM and 50% during PM from BAU scenario. This scenario is suggested for implementation for more congestion and hassle-free movement of vehicles on the adjoining roads. Using the methodological framework developed, this work can help evaluate how appropriate a particular development is for a location, for any given situation, and what mitigation strategies and types of transportation improvements may be essential to maintain smooth moving traffic with a satisfactory level of service. The recommended scenarios have to be further investigated to see how feasible these are, post-COVID. Although work from home can continue to some extent, further study on the possibility of 30 and 50% work from home is required.

References

1. Abley S, Durdin P, Douglass M (2010) Integrated transport assessment guidelines, Research Report 422, NZ Transport Agency, Wellington, New Zealand
2. Chandra S, Gangopadhyay S, Velmurugan S, Ravinder K (2017) Indian highway capacity manual (Indo-HCM)
3. Diliman QC (2005) Traffic impact assessment for sustainable traffic management and transportation planning in urban areas. In Proceedings of the *Eastern Asia Society for Transportation Studies* (Vol. 5, pp. 2342–2351)
4. Izanloo A, Rafsanjani AK, Ebrahimi SP (2017) Effect of commercial land use and accessibility factor on traffic flow in Bojnourd. J Urban Plann Devel 143(2):05016016
5. Karnataka Urban Infrastructure Development and Finance Corporation, Comprehensive Traffic & Transportation Study (2011)
6. Minhans A, Zaki NH, Belwal R (2013) Traffic impact assessment: a case of proposed hypermarket in Skudai town of Malaysia. Jurnal Teknologi, 65(3)
7. Muldoon D, Bloomberg L (2008) Development of best practices for traffic impact studies. Transp Res Record: J Transp Res Board 2077:32–38
8. Padma S, Velmurugan S, Kalsi N, Ravinder K, Erramapalli M, Kannan S (2020) Traffic impact assessment for sustainable development in urban areas. Transp Res Proc 48:3173–3187
9. Ponnurangam P, Umadevi G (2016) Traffic Impact Analysis (TIA) for Chennai IT Corridor. Transp Res Proc 17:234–243
10. Regidor JRF, Teodoro RVR (2003) Institutionalizing traffic impact assessment in the Philippines: some issues and challenges. J Eastern Asia Soc Transp Stud 5:3192–3205
11. Sharmeen N, Sadat K, Zaman N, Mitra SK (2012) Developing a generic methodology for traffic impact assessment of a mixed land use in Dhaka city. J Bangladesh Inst Plann ISSN 2075:9363
12. Tom V Mathew (2019) Trip assignment—lecture notes in transportation systems engineering. https://www.civil.iitb.ac.in/tvm/nptel/206_lnTse/web/web.html#x1-50004
13. TomTom Traffic Index: Global Traffic Congestion Up as Bengaluru takes Crown of 'World's Most Traffic Congested City', January 29, 2020
14. Transport for London (2010) Transport assessment best practice: guidance document. United Kingdom, London

15. van Rensburg JF, van As SC (2004) Issues with traffic impact assessments. Paper presented at 23rd South African Transport Conference (SATC), Pretoria, South Africa
16. Verma A, Harsha V, Hemanthini AR (2018) Sustainable Transport Measures for Liveable Bengaluru. Project Sub Report, IISc Bangalore, India
17. Wagner T (2010) Regional traffic impacts of logistics-related land use. Transp Policy 17(4):224–229. https://doi.org/10.1016/j.tranpol.2010.01.012

Influence of Connectivity of Streets on the Urban Form and Sprawl

Almas Siddiqui and Ashish Verma

Abstract Research on urban expansion, sprawl, and compact city concepts to identify the scope of improvement in master and regional plans has been conducted widely. The changes in the networks of transportation systems have huge impacts on land use. Studies are available which explain the relationship between transportation and land use. But there is a need to understand how these systems' alterations affect the urban form and identify the crucial factors of street connectivity and transport networks contributing to urban and regional growth. Thus, further research is needed to find the influence of the connectivity of transport networks on the urban forms. This paper attempts to review the literature on sprawl indices focusing on transportation factors, street-network sprawl, and linkages of urban form and land use. This study showcases the possibilities of research in street-network sprawl and the relationship between street connectivity and urban form. These research outcomes can bring compelling policy implications in the transport planning of networks.

Keywords Street-network connectivity · Urban form · Urban sprawl · Land-use

1 Introduction

Urbanization and globalization have led people to migrate from villages to cities all over the globe. Its repercussions have been visible in the increase in energy consumption in the urban systems, which have burdened the existing infrastructures. The rise in temperature due to heat island effects in urbanized areas has been discussed and studied at various platforms. United Nations have set the Sustainable Development Goals (SDGs) to reduce and maintain the harmful effects of global warming. Several goals address the importance of identifying urban expansion factors to create more

A. Siddiqui · A. Verma (✉)
Indian Institute of Science, Bengaluru, India
e-mail: ashishv@iisc.ac.in

A. Siddiqui
e-mail: almass@iisc.ac.in

L. Devi et al. (eds.), *Proceedings of the Sixth International Conference of Transportation Research Group of India*, Lecture Notes in Civil Engineering 273,
https://doi.org/10.1007/978-981-19-4204-4_4

resilient and inclusive urban spaces. Different countries have devised different mechanisms and plan to deal with the problems identified in SDGs. One of the most crucial research subjects has been effectively quantifying the measure of sprawl to incorporate sustainability in the development plans. There is no universal definition for urban sprawl. Several scholars have defined it by combining different factors and dimensions of urban sprawl.

Urban forms of cities have also been understood in several studies, and different definitions have been framed for it. Due to the uncertainty of vital universal definitions of urban sprawl and urban form, studies capture similar or various causes of urban sprawl in projecting future urban growth of the cities. In the last few years, attempts have been made to devise sprawl indices with more robustness and efficiency. These indices may or may not have been used by the local bodies while creating the development plans. It was observed that these studies didn't incorporate some of the critical socio-economic and transportation parameters. These parameters require lots of accurate data to predict future urban growth. The factors of transportation have been incorporated in several studies to quantify urban sprawl, which will be discussed extensively in this review paper. Street connectivity or transport networks have been critical ingredients in planning the cities' land use.

The inter-relationship of the street connectivity with urban forms or urban sprawl has been one of the most complex ones. There is a need to understand this relationship at all scales of development to make our master or development plans more effective. Incorporating transportation factors in formulating the urban sprawl indices and indicators would give a better understanding of the interaction effects in an urban area. The objectives of this review paper are to highlight the lack of inclusion of important transport parameters in the studies of urban sprawl indices, identify the research gaps in the studies conducted in understanding the inter-relationship of the street connectivity with urban forms, and identify the possibilities and constraints in replicating the studies of street connectivity sprawl in Indian cities.

Literature has been reviewed to understand the influence of street connectivity on urban form and sprawl, and the paper has been divided into three different sections. The first section consists of the introduction to urban forms and urban sprawl and their dimensions. The second section consists of urban sprawl measures with details of a few sprawl indices and acknowledgment of the causes of urban sprawl, which have been incorporated in the methodology of those sprawl indices. Section 3 explains how urban form affects the sustainability of urban transportation. Section 4 has the information about street-connectivity sprawl and how these have been calculated. The paper ends with the research implications and limitations with a focus to improve the relationship between transportation and urban form and concluding remarks with the possibilities and constraints in conducting similar studies for Indian cities.

2 Urban Form, Urban Sprawl, and Their Dimensions

Urban expansion, growth, and sprawl have been widely discussed, defined, and quantified in several ways in the last few decades. The transport demand and the capacity of transportation systems are directly affected by the structure of land use. Also, the land use is planned according to the present transportation systems to curb population growth in the urban fringes. Spatial form, spatial pattern, and spatial interaction are the three dimensions that influence the environmental impacts of land use and transportation (Fig. 1). The spatial arrangement of a city can be defined by spatial form. This research has led to urban expansion and motorization in cities. The spatial organization of land use is said to be the spatial pattern of the city. Incompatible land uses nearby can be mitigated by planning buffers in between them. Urban land uses generate a specific structure of movements, which are known as the spatial interaction [1] (Figs. 2 and 3).

Half of the population on less than 1% of the world's surface is covered by the cities. Urban sprawl has a high demand for transportation demand, and the cities

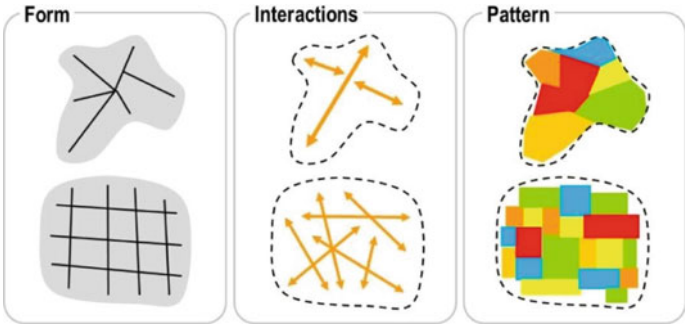

Fig. 1 Spatial form, pattern and interactions. *Source* Rodrigue [2]

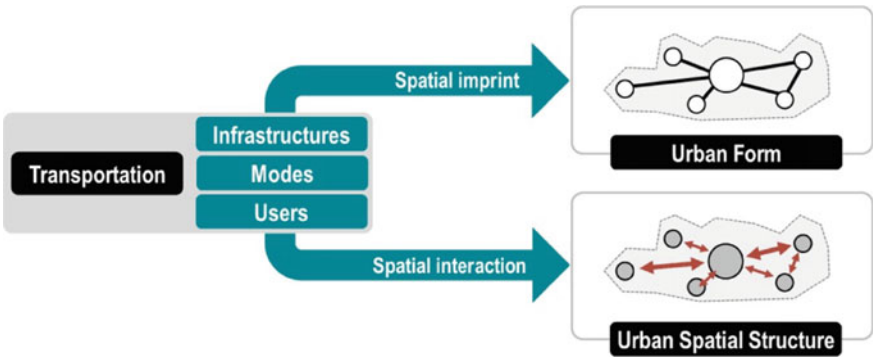

Fig. 2 Spatial structure, urban form, and transportation. *Source* Rodrigue [1]

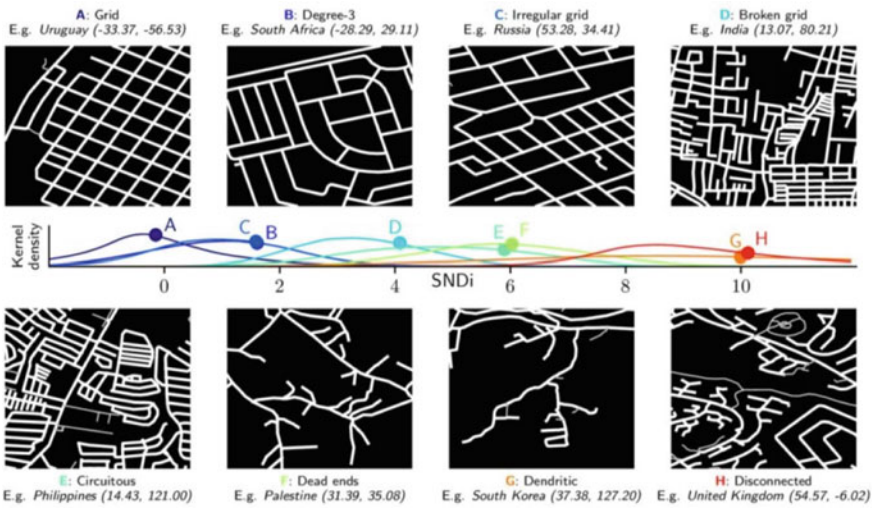

Fig. 3 Examples of eight empirical street-network types. *Source* Barrington-Leigh and Millard-Ball [3]

overall contribute to about 75% of the global total carbon emissions from energy use. By 2050, urban sprawl could consume about 5% of the present cultivated land [4]. Therefore, it is essential to understand the causes and dimensions of the urban growth and sprawl.

Several causes of urban growth have been mentioned in different studies. Dimensions identified for this study are population growth, industrialization, economic growth, development and property tax, physical geography, the demand for more living space, lack of affordable housing, public regulation, transportation, Government developmental policies, and lack of proper planning policies [5]. Dimensions of urban sprawl have been identified as density, continuity, concentration, clustering, centrality, nuclearity, mixed uses, and proximity. Density is defined as the average number of residential units per square mile of developable land where new construction can be made. Continuity is defined as the degree to which developable land has been built upon at urban densities in an unbroken fashion. Concentration is defined as the degree to which development has been tightly bunched to minimize amount of land occupied by residential or non-residential uses. Centrality is defined as the degree to which residential and/or non-residential development is located close to a central business district. Nuclearity is defined as the extent to which an area is characterized by a mononuclear development pattern. The mixed uses dimension is defined as the extent to which multiple land uses exist within the same small area and its prevalence throughout a region. Proximity is defined as the degree to which different land uses are close to each other.

Luciano identified dispersion, land use mix, and accessibility as the dimensions of sprawl [6]. Dispersion or scatteredness of the built-up land use irrespective of the actual land use can be quantified by identifying the unused spaces in between the

Table 1 Review on dimensions of urban sprawl in different studies

Dimensions	George Galster [7]	Fina [8]	Luciano Gervasoni [6]	Christian Gerten [9]	Dragic´evic [10]	Lu Liu [11]
Density	✔	✔		✔		✔
Continuity	✔					
Concentration						
Compactness	✔					
Centrality	✔					
Nuclearity	✔					
Diversity	✔					
Proximity	✔					
Size						✔
Fragmentation/Dispersion			✔			
Pattern/LU mix/LU pattern		✔	✔	✔		
Surface		✔		✔		
Accessibility			✔			

buildings. For accessibility, the street network and activity uses are extracted from Open Street Maps at a given input location. This depicts whether there is a mixed land use or higher dependency on cars. The land use mix indicator measures the extent of the distribution of the spatial configuration and co-occurrence of different land uses in local neighborhoods.

Table 1 summarizes how five relevant studies on urban sprawl have included different dimensions in their analysis. There is no such rule to follow when sprawl is being quantified. There are several reasons for considering different dimensions and not having a standard set to identify sprawl pattern. Lack of data and its transparency is a major reason to incorporate all the dimensions in the studies of urban sprawl. There is a need to define a set of standards while measuring sprawl of any area on earth in order to quantify, predict and plan future cities in more inclusive manner.

3 Measures of Sprawl: Indices

Various measures are available in the literature to quantify sprawl based on several indicators and methods. The factor of transportation has been included in many studies in different forms. The impacts of connectivity and disconnectivity of streets have also been studied with different approaches and dimensions of the urban sprawl phenomenon[12–15]. Table 9 depicts some of the most relevant studies which explain how urban form, urban sprawl, and transportation are interconnected (Table 9 can be found at the end of this paper). This shows the importance of measuring sprawl

Table 2 Sprawl indices and the related causes of urban sprawl (1)

Causes of urban growth	Sierra club ranking 1998	USA today's sprawl index 2001	US sustainable city ranking 2008 [12, 13]	New sprawl index (IN10) [14]	Population-weighted density (CPB)
Population growth	✔	✔	✔	✔	✔
Industrialization	✔	✔	✔	✔	✔
Economic growth	✔	✔	✔	✔	✔
Development and property tax	✔	✔	✔		✔
Physical geography					✔
Demand of more living space	✔		✔		
Lack of affordable housing			✔		
Public regulation			✔		✔
Transportation					
Government developmental policies					
Lack of proper planning policies			✔		

at different scales with relevant findings of regulations, framework, and climate resiliency of transportation infrastructure.

Many sprawl indices have been devised, framed, and calculated in different studies. An attempt has been made to list them (most recent and relevant) down along with the related causes of the urban growth. This listing has been done to understand how several indices have incorporated several parameters based on different causes of the urban growth.

Tables 2, 3, 4 and 5 highlight the causes of urban sprawl, which are usually taken into account for measuring sprawl. In Table 2, it can be observed that the sprawl index given by US Sustainable City Ranking 2008 has addressed most of the causes of urban sprawl and measured them. Transportation has not been incorporated in the index except Sierra Club ranking 1998. It is important to note that government developmental policies and lack of proper planning policies have not been included in any studies.

In Table 3, again, the factor of transportation has not been addressed in the studies except in Ewing and Hamidi's Composite Sprawl Index as a Street Network Density

Table 3 Sprawl indices and the related causes of urban sprawl (2)

Causes of urban growth	Location affordability index—housing cost as percentageof income for home owners (HDO)	Lopez and Hynes' sprawl index (LH)	Ewing and Hamidi's composite sprawl index, and sub-indices (ECS, ED, EM, ECN, and EST)	Tsai's sprawl index (first-difference model only)
Population growth	✔	✔	✔	✔
Industrialization	✔	✔	✔	✔
Economic growth	✔	✔	✔	✔
Development and property tax	✔	✔	✔	✔
Physical geography			✔	✔
Demand of more living space			✔	
Lack of affordable housing	✔			
Public regulation	✔	✔	✔	✔
Transportation			✔	
Government developmental policies		✔	✔	
Lack of proper planning policies			✔	

Subindex. Government developmental policies and lack of proper planning policies have been addressed in a few of them. It is pretty interesting to note that in Tables 4 and 5, all the indices address transportation in their studies for measuring sprawl. All the indices have been calculated by using remote sensing applications [5, 6].

4 How Urban Form affect the Sustainability of Urban Transportation?

The transportation modes, infrastructures, and users are considered to be the elements of an urban transport system. The spatial imprint (i.e., the size, shape, and configuration of an urban area) of the urban transportation system and adjacent physical infrastructures is known as Urban Form [16]. It varies for different cities based on diversity in their geographical and socio-economic characteristics. The urban form

Table 4 Sprawl indices and the related causes of urban sprawl (3)

Causes of urban growth	Area index	Shape index	Discontinuous development index	Strip development index	Leapfrog development index
Population growth	✔	✔			
Industrialization	✔	✔	✔	✔	✔
Economic growth	✔	✔	✔	✔	✔
Development and property tax	✔	✔	✔	✔	✔
Physical geography	✔	✔	✔	✔	✔
Demand of more living space	✔	✔			
Lack of affordable housing					
Public regulation	✔	✔		✔	✔
Transportation		✔	✔	✔	✔
Government developmental policies	✔		✔	✔	✔
Lack of proper planning policies	✔	✔	✔		✔

is shaped by the space consumed by the transportation infrastructures, technical and operational characteristics of the transport modes, and passenger and freight movements generated by the users. The passenger and freight movements' circulation patterns represent the spatial interactions that form the urban spatial structure. All of these spatial imprints and interactions affect the sustainability of urban transportation.

Any change in the development plans requires changes in the transportation networks. In the conventional four-step modeling process, urban form has been implied in it [17]. The density pattern is considered an important criterion for urban form in the first three steps of modeling. It determines how the generated trips are distributed in several city sections and how the modes are allotted in these sections. In the trip generation process, concentricity and homogeneity are the criteria for urban spatial form as they expose the areas where trips would either generate or end based on the diversity of land uses and the degree to which these are organized zonally around the centers of a city. Connectivity and density gradient affect the trip distribution as they are defined by the transportation networks and the changes in the density pattern around a central business district in a city or a multiple center in a polycentric city.

Along with density pattern and density gradient, sectorality has been used as a criterion for urban form in the modal split. However, traffic assignment used directionality and connectivity as criteria for urban form. The following Table 6 explains how these criteria were defined in the Des Moines metropolitan area case study.

Table 5 Sprawl indices and the related causes of urban sprawl (4)

Causes of urban growth	Planning consistency index	Population or vertical density index	Horizontal density index	GDP density index	Open or agriculture space index	Traffic impact index
Population growth	✔	✔	✔		✔	✔
Industrialization	✔			✔	✔	
Economic growth	✔			✔	✔	✔
Development and property tax	✔	✔	✔			
Physical geography					✔	
Demand of more living space		✔	✔		✔	✔
Lack of affordable housing	✔	✔	✔			✔
Public regulation	✔			✔	✔	✔
Transportation		✔	✔			✔
Government developmental policies	✔	✔		✔	✔	✔
Lack of proper planning policies	✔	✔	✔		✔	✔

Table 6 Generalized form of seven spatial measurements in the urban form of Des Moines metropolitan area

Spatial measurements	Urban form
Homogeneity	Distribution of Land uses in a city along the transport routes and in core or peri-urban areas
Density pattern	High, medium, and low-density patterns in different parts of city
Connectivity	Connection of transport routes in different directions and location of city
Density gradient	Measures population density from CBD
Concentricity	Concentration of trips, housing, population, etc., in the city
Directionality	Direction of movement of work trips across a city w.r.t. location
Sectorality	Analysis of population and trips through CBD and corridor studies

Source Chunlin Cao [17]

5 Linkages Between Street Connectivity or Networks with Urban Land Use, Forms, and/or Sprawl

The need for research on the relationship between transport networks and urban sprawl has already been emphasized and explained in detail in this paper. In the last few years, researchers have made attempts to quantify and measure this relationship through different methodologies, detailed in Table 8. Barrington-Leigh has demonstrated this relationship by measuring the street-network sprawl by Street-Network Disconnectedness index (SNDi), classifying eight types of street networks by k-means cluster analysis, and conducting sensitivity analysis [3, 18]. Interestingly, this study seems to be one of its first kind where urban forms and types of street networks have been extensively studied globally. A suite of measures of street-network sprawl consisted of nodal degree, dendricity, circuity, and sinuosity. It has been found that nodal degree and nodal density do not necessarily indicate how streets are configured at the network level and are sensitive to the scale at which analysis is conducted. It was also discovered that the lack of comparative, cross-national analysis is a significant research gap in the previous literature on urban sprawl. Classification of grid cells over eight measures of street-network sprawl and characterization of aggregate SNDi at high resolution on a global grid with 1 km resolution has been done. These results of quantified street-network sprawl can be reproduced through open-source computer code only for urban areas. For validation of SNDi measuring the characteristics of the built environment, three paradigms of urban street networks (grid, medieval and culs-de-sac) and a qualitative appraisal investigation was conducted [3].

Table 7 showcases the multidimensional classification of street network into eight empirical types [3]. It has been observed that these types discriminate strongly between high- and low-automobility regions. In this study, Indian cities, namely, Ahmedabad (2.7), Belgaum, Coimbatore (3.9), Hindupur, Hyderabad (3.1), Jaipur (3.1), Jalna, Kanpur (2.1), Kolkata (3.9), Kozhikode, Malegaon, Mumbai (3.7), Parbhani, Pune (4.9), Singrauli, Sitapur, Vijayawada (3.2) were also studied. SNDi values are mentioned in brackets along with each city mentioned above. High SNDi represents low connectivity and low SNDi represents high connectivity. 5th percentile (SNDi ≈ -0.6), 50th percentile (SNDi ≈ 2.7), and 95th percentile (SNDi ≈ 9.2) have been considered as low, medium, and high SNDi, respectively. So, among these cities with the available data, Pune has the lowest connectivity with highest SNDi and Kanpur has the highest connectivity.

The cities in Table 7 have been mentioned as per the two largest distributions of empirical street-network types mentioned in the study conducted by Barrington-Leigh and Millard-Ball [3]. It is clear that most of the cities have either irregular or broken grid in their transport networks. Kozhikode, Malegaon, and Sitapur mostly have the regular grids in their street networks. Mumbai and Pune are examples of gated communities with circuitous networks. Dead ends, dendritic and disconnected street types are absent in the Indian cities considered in the study. Kanpur has degree-3 and irregular grids as the largest part of its street network with medium connectivity. On the other hand, Pune has broken grid and circuitous as the largest part of its

Table 7 Multidimensional classification: eight empirical street-network types

Type	Name	Description	Indian cities
A	Grid	Regular grids	Kozhikode, Malegaon, Sitapur
B	Degree-3	B is differentiated from grid cells of similar SNDi by a high proportion of degree-3 nodes	Belgaum, Hindupur, Jalna, Kanpur, Malegaon, Parbhani
C	Irregular grid	Many grid cells in this type do not meet at 90°	Ahmedabad, Belgaum, Kanpur, Kolkata, Kozhikode, Mumbai, Sitapur, Vijayawada
D	Broken grid	Incomplete grids with or without 90° angles	Ahmedabad, Coimbatore, Hyderabad, Jaipur, Kolkata, Mumbai, Pune, Singrauli, Vijayawada
E	Circuitous	Many grid cells in this type are gated communities	Mumbai, Pune
F	Dead ends	F is characterized by a high fraction of deadends	None
G	Dendritic	G has a branched form resembling a tree network has the highest fraction of network bridges	None
H	Disconnected	H is the least connected on almost every dimension, and has the highest proportion of deadends and the most circuitous road networks	None

Source Barrington-Leigh and Millard-Ball [3]

street network with lowest connectivity. Pune has tree and radial road pattern with ribbon sprawl. Ahmedabad has ring and radial road pattern with axial growth and ribbon development. Jaipur has networks of gridded streets with leapfrog urban sprawl. Kolkata has trunk and irregular road pattern with low density, leapfrog, and fragmented urban sprawl. Mumbai has radial and sub-parallel trellis road pattern with high density, leapfrog sprawl. This study also reveals about the need to reduce over-construction of transport networks by investigation the spatial patterns of the street networks.

6 Research Implications and Limitations

To improve the relationship between transportation and urban form Chunlin Cao recommended that the utility lines of cities which generally run through the transportation routes can be measured as the determinants of urban form [17]. There is a need to use the measures explicitly accounting for urban form into transportation models. It is important to examine the effects on urban forms by different types of

Table 8 Literature review on inter-dependency of street network, urban form, and urban sprawl

Title of paper	Need or aim of the study	Findings	Remarks
Barrington-Leigh and Millard-Ball [3]	**Measuring** street-network sprawl and paradigms	• **Index:** Street-Network Disconnectedness index (**SNDi**) • Analysis provides a **framework and data for future research** to help to understand the street-network sprawl and how urban growth policies can move cities onto a less sprawling path	• This study has created a strong foundation for future studies to understand and predict sprawl patterns due to disconnectedness of streets • The paradigms and empirical street classification at a global level can pave ways for more extensive research with inclusion of socio-economic parameters in measuring sprawl
Barrington- Leigh and Millard-Ball [18]	Provide **the foundation** for future work to understand urban processes, predict future pathways of transportation energy consumption and emissions, and identify effective policy responses	• **Index:** Street-Network Disconnectedness index (**SNDi**) • In the long term, low-connectivity street networks lack resilience to adapt to changing pressures and resources and ultimately to densify toward a mixed-use, transit-integrated, energy-efficient urban form	• Regulatory measures to monitor the conversion of agricultural land and green areas into urban land use (including transport routes) could be framed based on the determined transportation energy consumption and emissions

(continued)

Table 8 (continued)

Title of paper	Need or aim of the study	Findings	Remarks
Amnon Frenkel [12] Sprawl Measure: **US Sustainable City Ranking 2008**	**To understand whether a** sustainable city has a compact city form or not Indicator analysis: 'Smart Growth America' data for 84 metropolitan areas: 15 variables were combined into three sprawl factors using a PCA technique, 6 variables to the land use mix factor, 6 variables to degree of centering factor, and 3 variables to the street accessibility factor	• 15 different indicators that represent various aspects of urban planning and sustainability: city commuting, metro public transit ridership, metro street and freeway congestion, air quality, tap water quality, green building, local food and agriculture, waste management, planning and land use, housing affordability, natural disaster risk, green economy, energy and climate change, city innovation, knowledge base and communications, and water supply • Tool used in SPSS: Pearson correlation coefficient was used in the relationship analysis between overall ranking and the ranking of each indicator (Significant if p-values are smaller than 0.05) • Urban form indicator analysis: categories-density, mode of commute to work, mean travel time to work and traffic congestion cost, and planning and land use	• Categories of study areas into urban areas and regional areas can release the limitation of different physical boundaries while ranking the cities which will give a better comparison among those areas at different scales • The weak correlation of street connectivity with overall ranking can be studied further to find the factors responsible for such results • It is difficult to accept the result that the mixed land use, centeredness, and street connectivity do not have an effect on each other. There must be some unobserved factors responsible for such results which need to be checked and re-evaluated

transportation modes. The influence of the transportation policies, building codes, zoning ordinances, building, and master plans should be examined, shaping the transportation network and the urba n form [19]. To statistically understand the relationship between urban pattern and transportation networks, different urban patterns of cities with different sizes should be measured and quantified, focusing on street connectivity. Lu Liu suggested that there is a need for global index to measure the urban sprawl, which can reveal the poor street accessibility in different types of urban forms [11].

One of the most recent and relevant studies by Barrington-Leigh focuses on street connections to address these research gaps [3, 18]. It was based on the well-established principle that disconnected streets promote travel by private car and discourage walking while constructing globally consistent measures of urban form. He highlights that globally comparable and meaningful metrics of street-network sprawl should be proposed that relate to the similar qualitative attributes of the built environment across countries; vary meaningfully within countries and across countries, and have predictive power for cross-sectional variation in transportation and energy outcomes. This analysis provides a framework and data for future research to help to understand how urban growth policies can move cities onto a less sprawling path. Its main results have aggregated the properties of edges and nodes accessible by motor vehicles. Those by walking and cycling paths have been considered only to calculate connectivity. This research limitation has immense possibilities for future studies to make cities more sustainable. The eight empirical street-network types have been extensively studied in cities around the globe. Among them, the Indian cities have been highlighted in this paper in order to understand the future scope of the study. It has been found that the identified Indian cities mostly have irregular or broken grids and the SNDi index has varied from 2.1 to 4.9 which advocates the need of good street connectivity in Indian cities to reduce adverse impacts of urban sprawl on these cities. Luciano Gervasoni highlights the absence of methodology to validate sprawl indices due to lack of ground truth data. To account for the intensity of land use in the land use mix computation, building heights to weight residential and activity use should be considered. Fine-grained worldwide gridded population data should be included [6].

This review paper implies how the inter-relationship between the transportation networks and urban forms can be quantified and analyzed at different scales by different methodologies (Table 9). Different types of studies have been done at urban, regional, national, and global levels. The identified research gaps include the lack of ground truth data, incomplete street connectivity in Open Street Map at local level, socio-economic parameters, and involvement of walkable and cycling paths. This can be replicated in Indian scenarios also. As most of the Indian cities are either densely populated or poorly planned, incorporation of population density separately at each parcel of land in central and peripheral areas of a city into urban form metrics or urban sprawl indices should be considered. While collecting data related to commuting patterns through questionnaires or surveys, the extent of city, differences in socio-economic status and supply of urban infrastructure should be taken into account to avoid large variations in the data.

To address the climate change impacts of transportation in the cities, carbon dioxide emission index can be correlated with specific commuting patterns in the areas with heavy pollution. This can further be associated with the urban form metrices and sprawl indices to achieve sustainability in transportation. Involvement of socio-economic factors into the analysis and classification of urban land use can be be neficial. Quality of life and transport service can be studied in correlation with the sprawl indices to incorporate parameters like safety, ambiance, real-time information with quality, ride quality, and crowding. Transport networks of road, rail, and waterways can be connected and integrated to form a combined transport network in any region or metropolitan area to study the overall impact of connectivity of transport routes on the urban form characteristics and suggest relevant planning practices. Air and noise pollution exposure on these routes can also be correlated (area-wise) with the sprawl indices. The impacts of land development and rehabilitation on different types of urban forms can be studied. The policies and land use plans consisting of the provision of a new tra nsport system can lead to possibilities of new developments along with these systems along with urban renewal of open or unused urban areas. Also, the usage efficiency of the existing street networks should be promoted and seek developmental benefits of society and environment.

Table 9 Review of recent studies with a strong correlation between streets network (and connectivity) and urban growth

Author	Place of study	Year	Type of analysis	Scale of study area	Methodology
Barrington-Leigh [3]	Global worldwide (46 million km of mapped streets worldwide)	2019	• Measuring street-network sprawl (Street-Network Disconnectedness index: SNDi), • Empirical street-network types (k-means cluster analysis), • Sensitivity analysis	Urban areas only	• Calculation of a suite of measures of street-network sprawl that are derived from graph theoretic and spatial principles by using the dataset of approx. 120 million intersections and 171 million edges • A global grid with 1 km resolution to characterize aggregate SNDi at high resolution, and classification of grid cells using k-means similarity grouping over eight measures of street-network sprawl have been done • Construction of three abstracted paradigms of urban street networks, in order to demonstrate how certain distinctive patterns of urban form map to SNDi

(continued)

Table 9 (continued)

Author	Place of study	Year	Type of analysis	Scale of study area	Methodology
Dena Kasraian [20]	The Greater Randstad area	2019	• GEE-analysis to a panel of cells	Metropolitan Area	• Investigated transport networks: rail, and road • Assumptions: transport accessibility, urban proximity, and spatial policies influence urbanization are translated into six hypotheses, further operationalized into eleven indicators • In logit, time-independent and dependent predictor variables are policies, and transport accessibility and urban proximity respectively

(continued)

Table 9 (continued)

Author	Place of study	Year	Type of analysis	Scale of study area	Methodology
Ge Shi [21]	Nanjing, China	2019	• A kernel density estimation model is used to describe the spatiotemporal distribution patterns of the road network • A geographically weighted regression (GWR) is applied to generate the social and environmental variance influenced by the urban road network expansion	City	• The spatial distribution of the road network has been studied by Line Density Estimation Model • Index of road network expansion rate shows the average annual growth rate of the urban road network over the study period • GWR model estimates the parameter for the local level concentration of road network growth based on social and environment variables at a given location by a weighted least squares method
Zhang and Wang [22]	Hubei Province in central China	2017	• The correlation between network density and a total area of built-up land in each administrative unit is analyzed • The distance map of each traffic network is obtained. Area of built-up land of 1990–2010 at different distances from each type of traffic network is calculated and analyzed	Region	• Density of six types of traffic network have been retrieved in ArcGIS • Linear regression representing the relationship between density of transport network and built-up area, the influencing distance and corresponding buffer map for each traffic network, and accumulative built-up land area have been calculated

(continued)

Table 9 (continued)

Author	Place of study	Year	Type of analysis	Scale of study area	Methodology
Bin [23]	40 US cities	2007	• Topological analysis with an approach to merge the adjacent street segments and check street-street intersections to form a topology of an urban street network and a scale-free property for both street length and connectivity degree have been analyzed	Urban areas	• The selection of cities with a diverse set (size and their geographic locations) has been done based on census data • Urban street networks were pre-processed in order to form individual streets based on the Gestalt principle of good continuation For every street segment, its connected segments have been traced, and concatenate the segment and an adjacent one with the smallest deflection angle

References

1. Rodrigue J-P (2020b) Urban transportation: transportation, urban form and spatial structure. In: Rodrigue J-P (ed) The geography of transport systems, Fifth Edition. Routledge, New York, 456 pages. ISBN 978-0-367-36463-2. https://transportgeography.org/con
2. Rodrigue J-P (2020) Environmental footprint of transportation. In: The geography of transport systems. Routledge, New York, 456 pages. ISBN 978-0-367-36463-2. https://transportgeography.org/contents/chapter4/environmental-footprint-of-transportation/spatial-form-pattern-interaction-environment/
3. Barrington-Leigh C, Millard-Ball A (2019) A global assessment of street-network sprawl. PLoS ONE 14(11):e0223078. https://doi.org/10.1371/journal.pone.0223078
4. Plautz J (2019) 100 experts issue dire warning about urban sprawl's impact on climate change. Smart Cities Dive. https://www.smartcitiesdive.com/news/100-experts-issue-dire-warning-about-urban-sprawls-impact-on-climate-chang/560767/
5. Bhatta B (2010) Urban growth and sprawl. In: Analysis of urban growth and sprawl from remote sensing data. Advances in geographic information science. Springer. https://doi.org/10.1007/978-3-642-05299-6_1
6. Luciano Gervasoni MB (2017) Calculating spatial urban sprawl indices using open data. In: 15th International conference on computers in urban planning and urban management, Adelaide, Australia
7. George Galster RH (2001) Wrestling sprawl to the ground: defining and measuring an elusive concept. Hous Policy Debate 12(4):681–717. https://doi.org/10.1080/10511482.2001.9521426
8. Fina SS (2010) Monitoring urban sprawl in Germany: towards a GIS-based measurement and assessment approach. J Land Use Sci 5(2):73–104
9. Christian Gerten SF (2019) The sprawling planet: simplifying the measurement of global urbanization trends. Front Environ Sci. https://doi.org/10.3389/fenvs.2019.00140
10. Dragic´evic OK (2019) A local and regional spatial index for measuring three-dimensional urban compactness growth. Environ Plan B Urban Anal City Sci 46(1):143–164
11. Lu Liu LM (2020) Patterns of urban sprawl from a global perspective. Am Soc Civil Eng. https://doi.org/10.1061/(ASCE)UP.1943-5444.0000558
12. Amnon Frenkel MA (2008) Measuring urban sprawl: how can we deal with It? Environ Plann B Plann Des 35(1):56–79. https://doi.org/10.1068/b32155
13. Boah Kim NM (2012) An empirical test of the relationship between sustainability and urban form: based on indicator comparisons using sustainlane sustainable city rankings. In: Conference: Urban affairs association spatial bias in LUTI models, Doctoral Dissertation. UCL, Louvain-la-Neuve, Belgium
14. Laidley T (2015) Measuring sprawl: a new index, recent trends, and future research. Urban Affairs Review ©The Author(s) 1–32. https://doi.org/10.1177/1078087414568812
15. Susan Handy RP (2003) Techniques for mitigating urban sprawl: goals, characteristics, and suitability factors. Research Report 0-4420-2: conducted for the Texas Department of Transportation by the Center for Transportation Research, The University of Texas at Austin
16. Rodrigue J-P (2020a) The geography of transport systems. In: Rodrigue J-P (ed) Transportation and the urban form, Fifth Edition. Routledge, New York, 456 pages. Retrieved from https://transportgeography.org/contents/chapter8/transportation-urban-f
17. Chunlin Cao TS (1998) Transportation and urban form: a case study of the Des Moines metropolitan area. In: Transportation conference proceedings
18. Barrington-Leigh C, Millard-Ball A (2020) Global trends toward urban street-network sprawl. PNAS 117(4):1941–1950. https://doi.org/10.1073/pnas.1905232116
19. Adedire FM (2018) Peri-urban Expansion in Ikorodu, Lagos: extent, causes, effects, and policy response. Urban Forum, Springer Science+Business Media B.V., part of Springer Nature. https://doi.org/10.1007/s12132-018-9336-5
20. Dena Kasraian KM (2019) The impact of urban proximity, transport accessibility and policy on urban growth: a longitudinal analysis over five decades. Urban Anal City Sci 46(6):1000–1017

21. Ge Shi JS (2019) Urban road network expansion and its driving variables: a case study of Nanjing City. Int J Environ Res Public Health 16:2318. https://doi.org/10.3390/ijerph16132318
22. Zhang W, Wang H (2017) The impact of traffic networks on urban sprawl: a case study for Hubei Province in central China. In: 4th international conference on transportation information and safety (ICTIS). https://doi.org/10.1109/ICTIS.2017.8047745.
23. Bin J (2007) A topological pattern of urban street networks: universality and peculiarity. Phys A 384(2):647–655

Sustainability Assessment of Biomass Within Biofuel Supply Chain in Transport Sector Using Circular Economy Framework

Reema Mohanty, P. Balachandra, and S. Dasappa

Abstract The transport sector contributes to almost 25% of global CO_2 emissions (Hannah Ritchie, October 06, 2020.Our World in data.). In general, transport activities mainly rely on fossil fuels, which results in global warming. The objective is to design a framework based on circular economy to assess the economic and environmental viability of the proposed second-generation (2G) biofuel supply chain system with respect to transport sector as biofuel is a clean and renewable form of energy. To represent economic sustainability, the total revenue generated, the net present value (NPV), and internal rate of return (IRR) followed by a sensitivity analysis are considered and for the environmental indicator, total CO_2 emission is considered as the parameter. The assessment is performed by particle swarm optimization technique. In the future, the proposed work can show a pathway to the industries and government organizations in building 2G ethanol plants.

Keywords Particle swarm optimization · Circular economy · Second-generation · Biofuel supply chain system

1 Introduction

Biofuel comes in the category of renewable energy in the world. As there are various forms of renewable energies available in the world like Solar, Wind, Geothermal, Tidal, etc., biofuel is one among them. It reduces lifecycle greenhouse gas emissions, lowers particulate matter by reducing smog and making our air healthier to breathe, and reduces the hydrocarbon emissions. The burgeoning exigency of transportation due to globalization, changes in the nature of jobs, and increase in tourism have led to a demand for clean fuel. According to the report of the world bank, the transport

R. Mohanty (✉) · S. Dasappa
Center for Sustainable Technologies, Indian Institute of Science, Bangalore, India
e-mail: reemamohanty@iisc.ac.in

P. Balachandra
Department of Management Studies, Indian Institute of Science, Bangalore, India
e-mail: patilb@iisc.ac.in

L. Devi et al. (eds.), *Proceedings of the Sixth International Conference of Transportation Research Group of India*, Lecture Notes in Civil Engineering 273,
https://doi.org/10.1007/978-981-19-4204-4_5

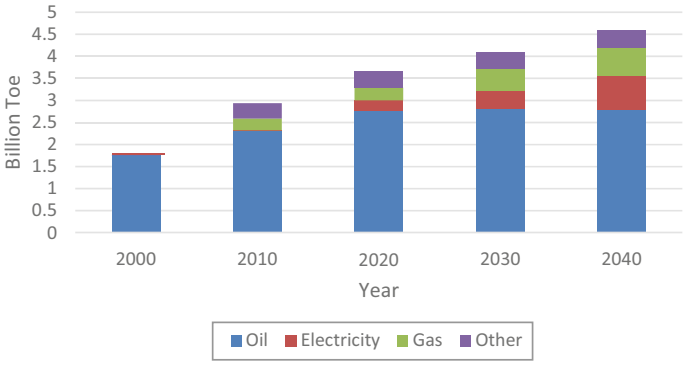

Fig. 1 Consumption of various fuels over the years (Ref. [2])

sector is far away from sustainability. The world bank has produced a first kind of assessment report known as the global mobility report. In the report, all kinds of modes of transportation and progress toward sustainable mobility are being summarized. Out of the four categories, safety and green mobility are the primary concern for sustainable transport [1]. Also, a study in the report describes that to transport a container of avocados from Kenya to the Netherlands, 200 interactions and more than 20 documents are required, at a cost equal to the shipping. The effective supply chain can increase the farmer's income by around 10–100% [1]. The transport sector emits 23% of all energy-related greenhouse gases; its CO_2 emissions could grow by 40% by 2040 [1]. We can see the trend of increased consumption due to the enhanced mobility in transport through land, water, and air. The chart below gives the transport scenario around the world extrapolated till 2040. There are various kinds of fuels such as 1—Oil, 2—Electricity, 3—Gas, and 4—Other associated with it (Fig. 1).

The Y-axis gives information about the consumption of different energy resources around the world [2].

1.1 Literature Review

We can find established literature on power and heat generation by the virtue of biofuel and cooking stoves using biofuel, but there are a few kinds of literature on the sustainability assessment of biofuel in the transport sector. [2] shows that approximately 74% of transport emissions are caused by road transportation. [1] gives the elaborated idea on biochemical pathways of extracting ethanol and biodiesel in first-generation (1G); but in first-generation biofuel supply chain system, the resources are based on crops, which can create food versus fuel problems. Whereas the second-generation biofuel is based on agricultural residues, switchgrass, waste from food crops, wood chips, etc., [3] gives information on the cradle to grave assessment. It has only two blocks: 1—Harvesting site and 2—Bio-refinery. The cradleto grave

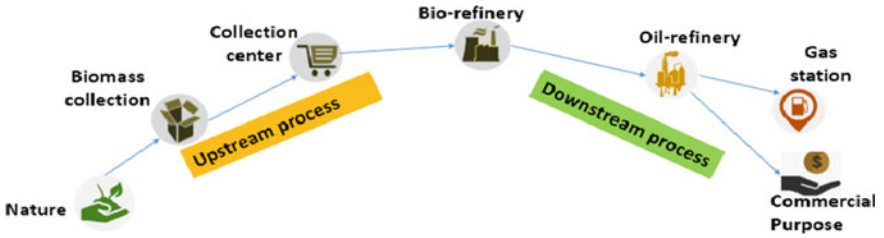

Fig. 2 An example of well to wheel analysis

analysis doesn't include the environmental and social factors. It only deals with resource extraction and utilization, but it doesn't cover the factors associated with it. As a result, the efficiency of the entire system could not be assessed properly. For this reason, the circular economy or cradle to cradle approach is followed in the proposed work. Figure 2 shows a typical cradle to grave or well to wheel-based biofuel supply chain system.

In Fig. 2, the arrow marks are the transportation sector, every block is connected to another block by virtue of transport. The losses in revenue due to transport and the emissions related to transportation need a proper assessment in order to make the entire system sustainable. The evolution of the circular economy with its futuristic implementations has been demonstrated in [4].

1.2 Proposed Work

The proposed circular economy framework or cradle to cradle analogy is based on two major sustainability indicators—Economic and Environmental. The aim is to suggest the feasibility of the proposed biomass supply chain within the system (biofuel supply chain) for the transportation industry. The major blocks of the proposed supply chain are (i) Harvesting Site, (ii) Transport, (iii) Conversion Plant, (iv) Oil Refinery, and (v) Ethanol blended with petrol in IC engine. As a pilot study, we have assessed the first two blocks since it deals with the proposed biomass supply chain. In the sustainability assessment phase, corn cobs have been considered as the biomass or source for ethanol generation. A brief description of the conversion of biomass to biofuel is given in the next section.

Thermochemical Pathway of Conversion for Second-Generation Biofuel

Conversion of biomass to biofuel takes 2 pathways: 1—Thermochemical and 2—Biochemical. The thermochemical conversion route is followed in the later phase of the proposed work. In order to produce ethanol via the thermochemical route, processes like pyrolysis and gasification are followed [5]. The thermochemical route goes through a step-by-step manner and synthetic gas, commonly known as syngas, is an intermediate product in it [6]. The syngas can be directly burned or further

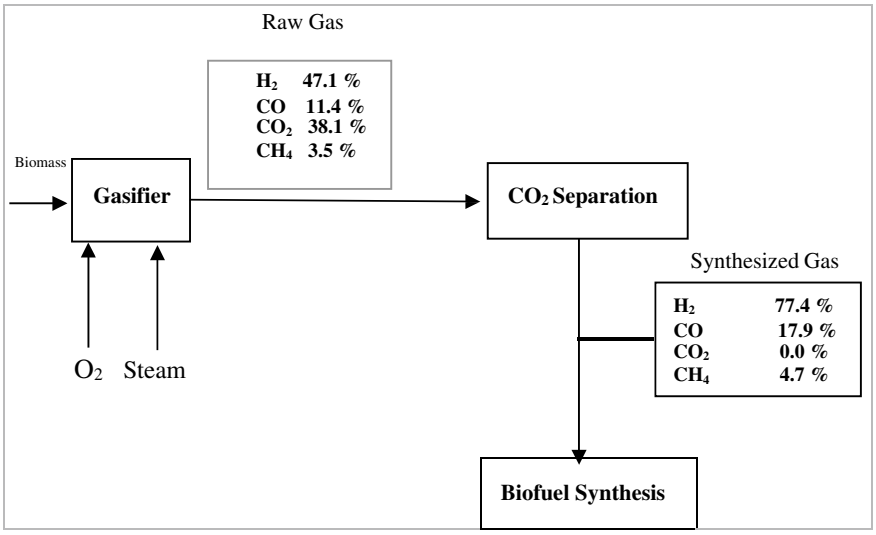

Fig. 3 Extraction of Biofuel in Combustion, Gasification, and Propulsion Lab, IISc

processed for other gaseous or liquid products. For this reason, the thermal or chemical conversion of biomass is very similar to that of coal.

Gasification Process

At CGPL (Combustion Gasification Propulsion Lab, IISc Bengaluru), we work on various pathways for synthesizing biofuel. The overall view of synthesizing biofuel is provided in Fig. 3. The process is known as oxy steam gasification where the biomass (corn cobs) is converted into ethanol at a suitable temperature and pressure. As described before, the intermediate product is syngas, later the syngas is converted into ethanol via a thermochemical or biochemical route with proper temperature, pressure, and a catalyst [5].

1.3 Objective of the Proposed Work

The primary objective is to develop a generalized second-generation ethanol supply chain adopting a circular economy framework. In order to validate the above frame work, corn cobs are taken as the biomass, which is generated in a certain cluster (Ranebennur, Davengaere, Harpanahalli, Anagodu, etc.) in the state of Karnataka.

The main part is to develop and validate an optimization model (Heuristic-based) to assess the cradle to cradle sustainability of the biofuel supply chain. Finally, it will provide inputs for industries and policymakers based on the results and findings. Figure 4 gives a thorough idea of the proposed supply chain within the circular economy framework. The first two blocks are important for the proposed research

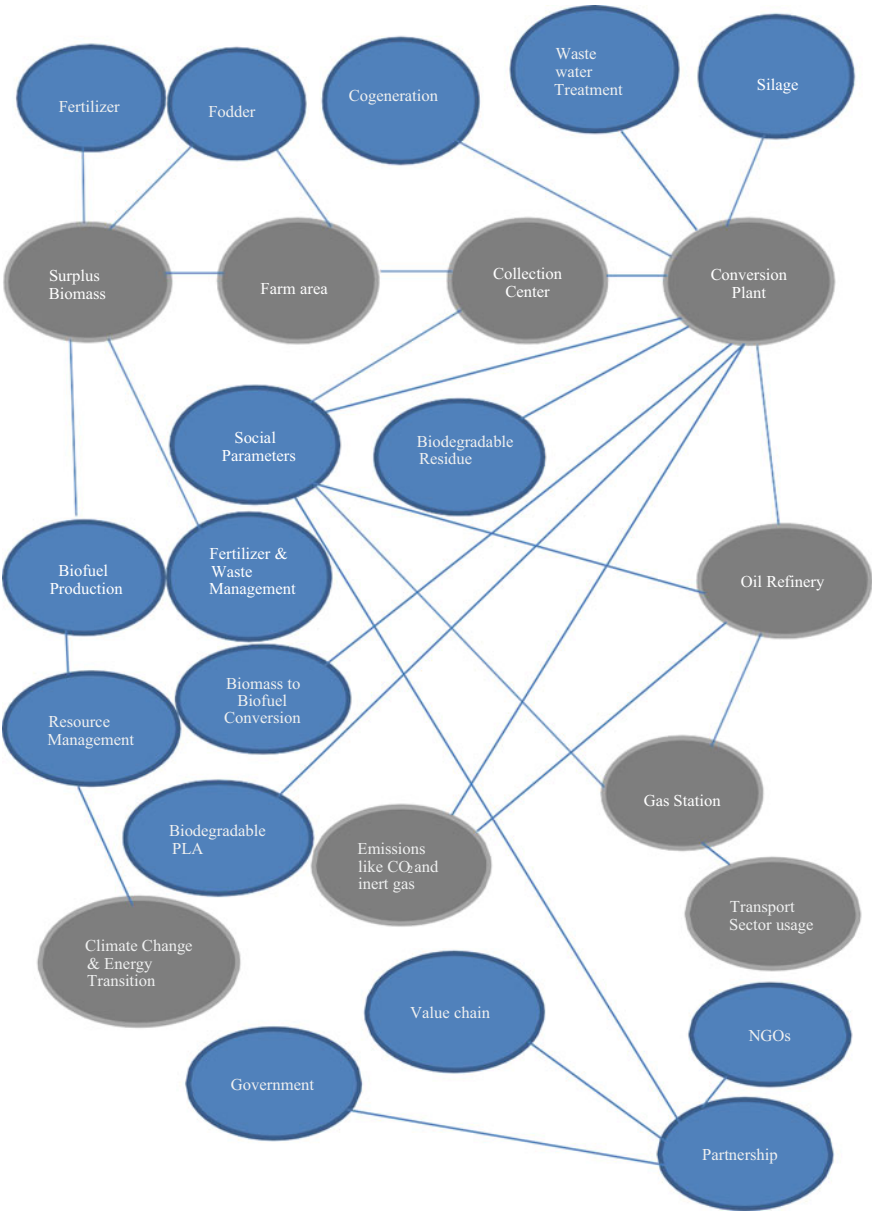

Fig. 4 Proposed supply chain

work. As we simplify those two blocks, we divide them into a simple biomass supply chain system. We will be assessing the sustainability of the proposed work with respect to two indicators: 1—Economic and 2—Environmental. The segment of the supply chain is divided into 3 parts: 1—Harvesting area, 2—Collection Center (CC), and 3—Transportation.

2 Methodology

2.1 Assessment with Respect to Economic Indicator

The assessment in this section covers the entire farm area and the transportation of biomass to the collection center. As mentioned above, the profit of the entire system will be calculated considering corn cobs as the biomass source. The proposed collection centers are selected so that the biomass which is available in the vicinity can be collected. Basically, these are villages/towns, which are accessible, spread out in the area as per biomass availability. The proposed collection centers in this cluster can be seen in Fig. 5.

Maize Cobs are expected to be available from November to April, hence required quantity needs to be purchased and stored during this period for ensuring regular

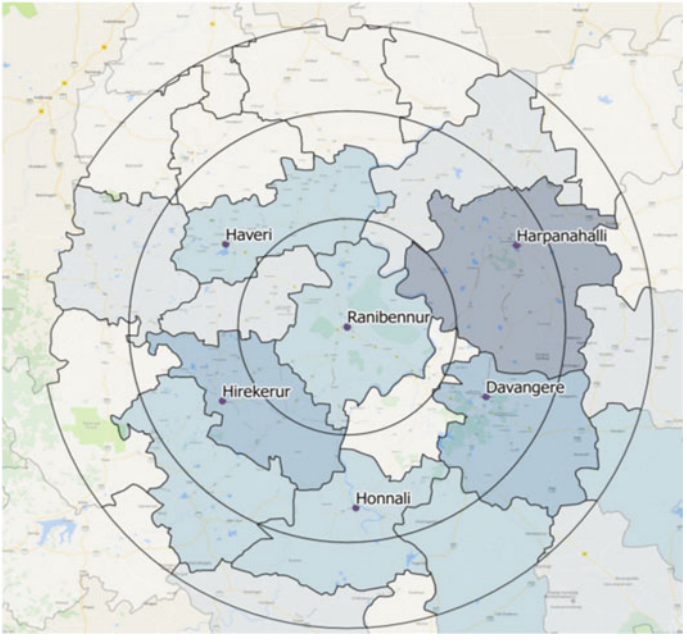

Fig. 5 Proposed area of corn cob cultivation [7]

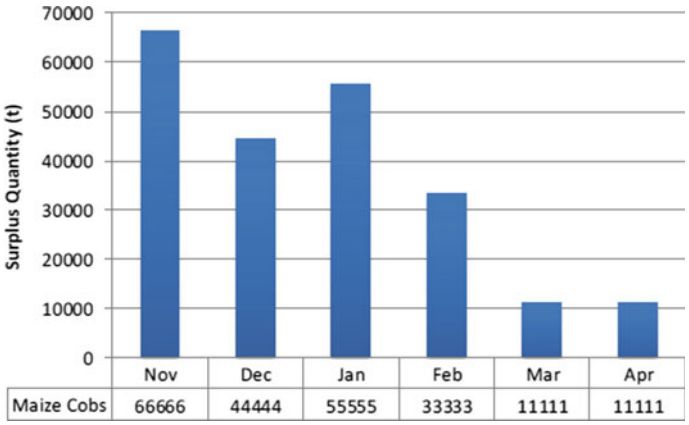

Fig. 6 Corn cob harvesting season [7]

supply. The procurement is expected to be at its peak from November to January. The month-wise estimated surplus quantity of Maize Cobs, the quantity to be purchased, during the season can be seen in Fig. 6.

All the charts and data about the surplus biomass are provided by Punjab Renewable Energy Systems Private Ltd (PRESPL) [7]. In order to expedite the collection of maize cobs during the collection window, CCs at strategic locations having a catchment radius of 20–25 km are formed [7]. The collection and storage system advocated for maize cobs is in bags. Bags of customized material need to be given to village-level entrepreneurs (VLEs) registered with the project developer. These bags would be stored at CC. This act would optimize the handling, brings traceability to the system, and would also put checks on VLEs from the material being diverted to other prospective buyers. During the rainy season, stacks of bags would be covered with good quality plastic sheets to avoid damage from elements of nature. Maximum 4500 MT of Maize cobs are stored in 1 Ha of land, and thus the capacity of CC is 18,000 MT [7].

2.2 Modern Optimization Technique

The first mathematical model corresponds to the maximization of revenue generated in the system containing 1. Harvesting area and 2. Transportation linking harvest area CC, and 3. Collection center (CC). In the analogy, we have implemented a novel technology for the maximization of revenue in the supply chain system. The constraints related to the system are intermittency of surplus biomass, loss in dry weight due to moisture content, rotting away of the corn due to pest attack, spillage due to the transportation, absence of proper storage area, etc. In these cases, it is very difficult to arrive at an optimal solution. So, we have implemented a heuristic-based optimization

technique to evaluate the supply chain with respect to two pillars of sustainability, i.e., economic and environmental. In recent years, some optimization methods which are conceptually different from the previous mathematical programming techniques have been developed. These methods are known as non-traditional methods in the field of optimization techniques. These methods are based on characteristics and behavior of biological, molecular, swarm of insects, and neurobiological systems. The following are the examples of such optimization techniques:1—Genetic algorithms, 2—Simulated annealing, 3—Particle swarm optimization, 4—Ant colony optimization, and 5—Fuzzy optimization.

These algorithms have been developed in recent years and are emerging as one of the best methods for the solution of complex engineering or mathematical problems. They require only the function values and not the derivatives. The genetic algorithm (GA) is based on the ideas of natural genetics and selection. Simulated annealing is based on the simulation of thermal annealing of critically heated solids [8]. In the genetic algorithm, the population size is fixed since it deals with DNA; hence it is not suitable for supply chain-based problems [9]. In case of simulated annealing, it only finds out the minima; it does not address the maximization part [10]. A genetic algorithm is an evolution-based algorithm. Unlike the previous technique, PSO is based on behavior-based algorithm. For this reason, the particle swarm optimization technique has been the best optimization technique to be adopted so far.

The word particle refers to a flock of birds, a colony of ants or a group of insects. The particle swarm optimization algorithm mimics the behavior of social organisms [11]. Each particle is located initially at random locations in the multidimensional space. Each particle has two characteristics: a position and a velocity. It wanders around in the design space and memorizes the best position (in terms of objective function value) it has discovered. When one bird locates a target or location of food (or maximum of the objective function), it will instantaneously transmit the information to all other birds. The other birds gravitate to the target or location of food (or maximum of the objective function), but not directly. There is a component of each bird's own independent thinking as well as its past memory. An algorithm can be defined to demonstrate the PSO model [12]. In the PSO model, there will be two best values.

$p_{\text{best}} \rightarrow$ Best solution (fitness) it has achieved in the last iteration.

$g_{\text{best}} \rightarrow$ Best solution achieved by any particle in the population.

Each particle tries to modify its current position and velocity according to the distance between the current position and p_{best}.

It tries to modify the distance between the current position and g_{best}.

Calculation of position and velocity

Set the initial velocity = 0.

$$\begin{aligned} \text{Velocity, } V_j(i) &= w * V_j(i-1) + c_1 r_1[\, p_{\text{best},j} - X_j(i-1)] \\ &\quad + c_2 r_2[g_{\text{best}} - X_j(i-1)] \\ j &= 1, 2 \ldots N, \ ''i'' \text{ is the iteration count} \end{aligned} \tag{1}$$

$$\text{Position of } j\text{th particle in } i\text{th } iteration\ is\ X_j(i) = X_j(i-1) + V_j(i)$$
$$j = 1,\ 2 \ldots N,\ ''i'' \text{ is the iteration count} \quad (2)$$

c_1, c_2 are cognitive and social learning rates respectively. In the Eq. (1), "w" corresponds to inertia weight.

1. The objective function and constraints attached to the supply chain including harvesting area, transportation of biomass and collection center for calculation of total system profit is:

Maximize profit
Subject to

Each harvesting area has a capacity limit. (1)

Maximum one kind of technology is selected at one time. (2)

Biomass can be transported in unidirectional,

vice versa is not true. (3)

Establish a link between harvesting area and collection center. (4)

An arc is selected by considering certain no of harvesting areas and its flow amount is restricted by imposing arc capacity. (5)

2. The second objective function deals with environmental indicator where the aim is to minimize the emissions:

Minimize the emissions into air
Subject to

All the biomass should go to the collection center from harvesting site. (6)

The availability of biomass should not exceed dry weight. Here the seasonality,

harvesting window and geographical availability of various biomass at different

harvesting areas is taken into account. (7)

The logistics distance must not exceed a maximum transportation distance. (8)

2.3 Model Formulation

The first equation refers to the profit-based objective function.

$$\sum_{k\in K}\sum_{f\in F}\sum_{t\in T1}\sum_{a\in A^{+}_{frt}} C_k Z_{ka} - \sum_{f\in F}\sum_{r\in R}(C_{fr}x_{fr} + V_{fr}q_{fr}) - \sum_{a\in A} C^{a}_{T} y_a - \sum_{k\in K}\sum_{a\in A} V^{a}_{T} Z_{ka} \quad (1)$$

Nomenclature

h	harvesting area
r	technology type
t	time
b	biomass type
k	commodity type
l	layer
j	collection center
$x_{hr} = 1$	if harvesting area "h" of type "r" is open, 0 otherwise
$y_a = 1$	if arc a is directed, 0 otherwise $qhr =$ capacity of facility "f" of type "r"
$P_{bh} =$	flow amount of biomass "b" in harvesting area "h"

Constraints

$$\sum_{r\in R} x_{hr} \le 1 \qquad h \in H_{OB} \text{(At most one technology type can be selected for each facility)} \quad (2)$$

$$q_{hr} - Q^{H}_{b,h,t} x_{hr} \le 0 \qquad h \in H_{OB,} r \in R_h \quad (3)$$

The equation above shows that, if the facility is opened, the amount of flow out of it is restricted by its capacity, $Q^{H}_{b,h,t}$ otherwise, the facility can sustain no flow.

$$\sum_{a\in A^{+}_{hrt}} Y_a \le 1 \qquad h \in H_{b1} \cup H_{b2}, t \in T \quad (4)$$

$Y_a = 1$ if there is a direct link from the facility to the collection center.

$$\sum_{k\in K} P_{bh} - Q^{T}_{b,a} y_a \le 0 \qquad h \in H, r \in R, t \in T, a \in A^{+}_{hrt} \quad (5)$$

If arc a selected, then the flow amount of biomass is restricted by the arc capacity $Q^{T}_{b,a}$, otherwise, flow amount is zero.

$$\sum_{a\in H^{+}_{rt}} P_{bh} \le Q^{H}_{k} \qquad h \in H_{b1}, r \in R_h, t \in T, a \in A^{+}_{hrt} \quad (6)$$

This shows the supply limit in the farm area.

The second equation refers to the emission-based objective function. We are trying to model the emissions pattern till the biomass reaches the collection center. It primarily includes emissions due to CO_2 and NO_x.

Total emission is divided into 2 parts.

Emissions during harvesting area (E^{ha}) and emissions during transport (E^{trans}).

$$Eha = \sum_{b\in B}\sum_{h\in H}\sum_{t\in T} eab_{b,h,t} Pbh_{b,h,t} \tag{7}$$

$$Etrans = \sum_{b\in B}\sum_{h\in H}\sum_{j\in J}\sum_{t\in T} etb_b ds_{i,j} Fbij_{i,j,t} \tag{8}$$

There are 3 types of constraints attached to the mentioned objective function.

$$Pbh_{b,h,j} = \sum_{j\in J} Fbh_{b,h,j} \qquad \forall b \in B, h \in H, t \in T \tag{9}$$

$$Pbh_{b,h,j} \leq Q^{H}_{b,h,t} \qquad \forall h \in H, b \in B, t \in T \tag{10}$$

$$Fbh_{b,h,j} = 0, \qquad \forall (b, h, j, t) | (dsij_{i,j} > mdb_{b,t}) \tag{11}$$

$Fbh_{b,h,j}$ denotes the amount of raw biomass b shipped from harvesting site h to pre-processing facility j in time period t.

2.4 Solution Method

We are implementing a constrained optimization method using the PSO algorithm. We have two stochastic acceleration coefficients c_1 and c_2. Hence, proper control of these two components is very important to find the optimum solution precisely and efficiently. In order to incorporate a better compromise between the exploration and exploitation of the search space in Particle Swarm Optimization, time-variant acceleration coefficients have been introduced in the proposed work [13]. The approach is known as time-variant PSO method where the values of c_1 and c_2 are expressed in terms of initial and final values as

$$c_{1t} = (c_{1f} - c_{1i})\, t/\max(it) + c_{1i} \tag{1}$$

$$c_{2t} = (c_{2f} - c_{2i})\, t/\max(it) + c_{2i} \tag{2}$$

$\max(it)$ refers to maximum iterations and the subscript i and f refer to initial and final values, respectively. Also, a time-variant inertia weight, i.e., "w" is implemented

here.

$$w_t = (w_1 - w_2) * (\max it - it)/\max it + w_2 \tag{3}$$

w_t decreases linearly with iteration from w_1 to w_2. max(it) is the maximum iterations and (it) is the iteration number.

Flowchart of a constrained PSO

1. Assume the swarm size to be N.
2. Set the objective function as $F(x)$ and iteration as i, j, respectively.
3. Evaluate $F[X_1(i)]$, $F[X_2(i)]$, $F[X_3(i)]$, $F[X_N(i)]$.
4. Check whether the constraints are satisfied.
5. Generate position of each particle as $X_j(i)$.
6. Generate the velocity of each particle as $V_j(i)$
7. Set initial velocity = 0
8. Find velocity, $V_j(i) = w * V_j(i-1) + c1r1[p_{\text{best},j} - X_j(i-1)] + c2r2[g\text{best} - X_j(i-1)]$, where $j = 1, 2, \ldots N$
9. Find the position of jth particle in ith iteration as $X_j(i) = X_j(i-1) + V_j(i), j = 1, 2, 3 \ldots N$
10. Check if $p$best = $g$best**.** (only the points in feasible space)
11. If NO then go back to step 5, set $i = i + 1$.
12. If YES then stop iteration

3 Results and Discussions

The data used in plotting of the results have been derived from Sect. 2.1. All these data are primary data provided by a firm known as Punjab Renewable Energy Systems Private Limited (PRESPL) [7]. The constraints are also derived from the assessment report produced by PRESPL [7].

3.1 Minimization of Environmental Emissions

Figures 7 and 8 gives an idea on the reduction of CO_2 emissions in the supply chain using PSO in static and time-varying case. Both the cases have been considered to know the best scenario for the emission analysis. The X-axis and Y-axis corresponds to time in years and emissions in tons CO_2 equivalent per kg.

Case 1. For time-varying PSO, we have plotted various combination of sets of inertia weights and acceleration coefficients. The combination which gives the optimal result is $c1f = 2.0$, $c2f = 2.0$, $c1i = 1.5$, $c2i = 1.5$, $w\max = 0.8$, $w\min = 0.4$. As per

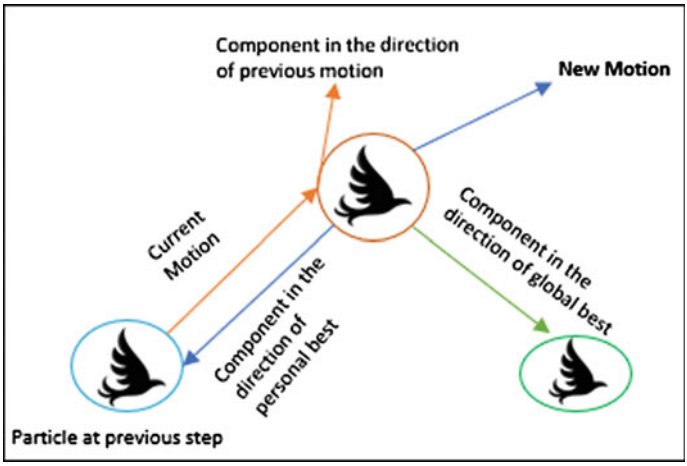

Fig. 7 Illustration of particle swarm optimization technique

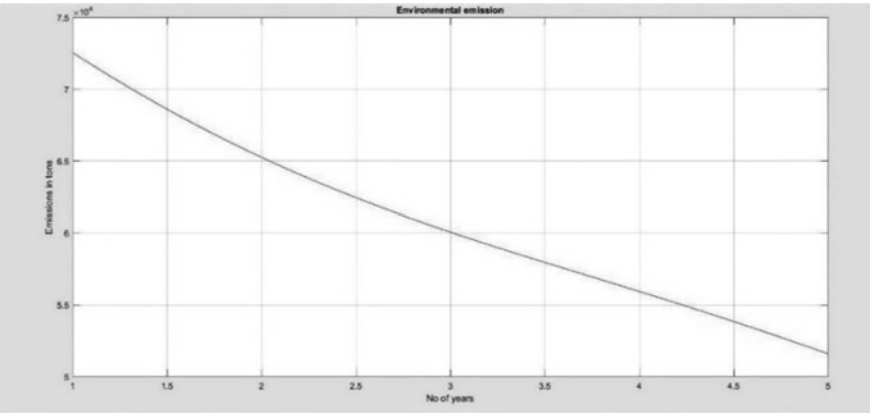

Fig. 8 PSO with time-varying inertia weight and acceleration coefficients

the illustration from the paper by Sermpinis [14], in the dynamic case the c_2 grows linearly from 0.5 to 3.5 and c1 decays from 3.5 to 0.5 in order to ensure $c_1 + c_2 = 4$ and w is at 0.8 initially and then it slowly converges to 0.4.

Case 2. $c_1 = c_2 = 2.05$ and $w = 0.729$

The case of a static PSO-based system is based on the proposed work by Clerc and Kennedy [15], Where $c_1 + c_2 > 4$ and the optimal value of $w = 0.729$ (Fig. 9).

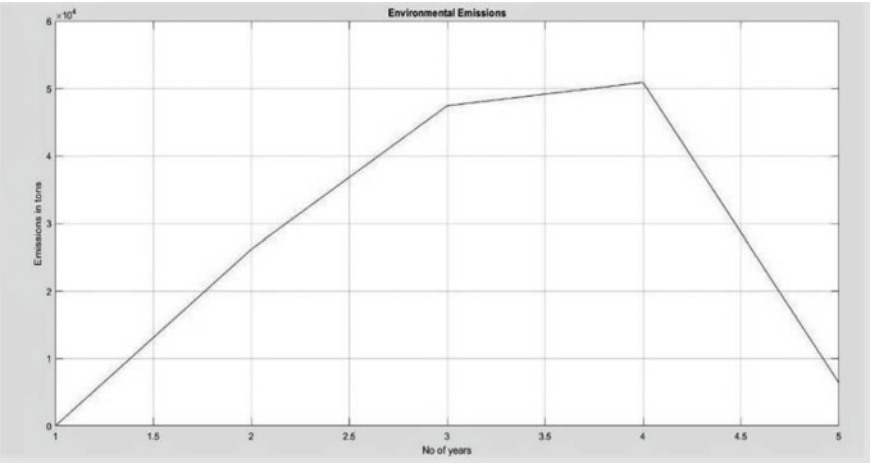

Fig. 9 PSO with non-time-varying inertia weight and acceleration coefficient

3.2 Maximization of System Profit

The maximization of revenue is calculated with respect to the supply chain for 5 years. The best 2 cases are shown in static and time-varying PSO cases.

Case 1. In this plot, the assumptions are for a static PSO algorithm. Hence, $c_1 = c_2 = 2.05$, $w = 0.729$. Here, X-axis corresponds to no. of years and Y-axis corresponds to system profit in INR (Fig. 10).

Case 2. The assumptions made here are based on time-varying PSO.

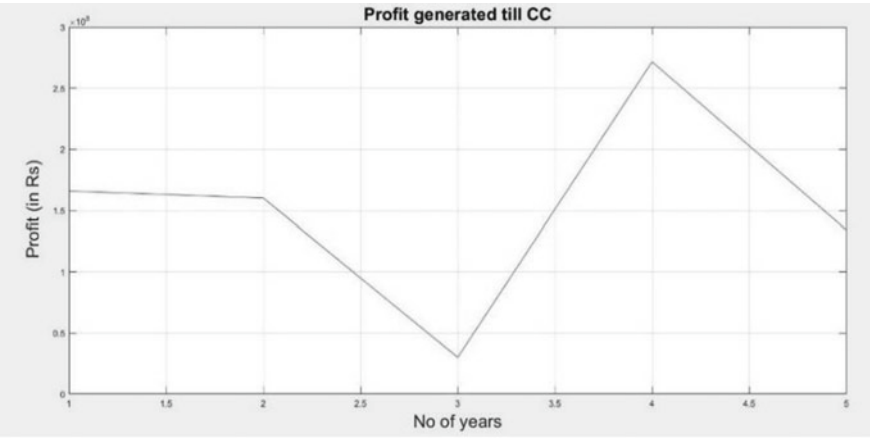

Fig. 10 PSO with non-time-varying inertia weight and acceleration coefficient

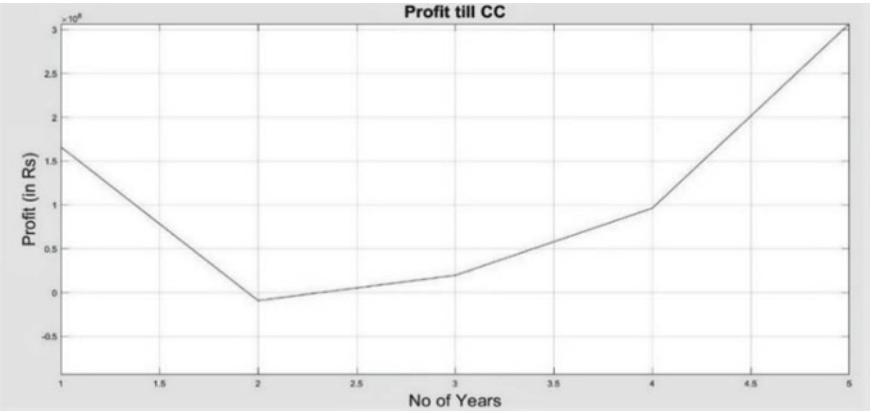

Fig. 11 PSO with time-varying inertia weight and acceleration coefficient

In this plot, $c_{1f} = c2f = 2.5$, $c_{1i} = c_{2i} = 1.5$, and $w\max = 0.8$ $w\min = 0.4$.

The results are plotted with the help of MATLAB2019b. In the environment emissions, the proposed PSO technique gives an optimum minimization curve. The table below gives the distinguished idea between the two methods.

So, it is clear that in the economic indicator perspective, it's a profitable business as break-even occurs at $t = 2$. The total revenue generated for the system is INR 30 Crore by considering the time-varying PSO approach. The decrease in the profit till the 2nd year in Fig. 11 is due to the insertion of uncertainties such as decay in moisture content, pest attack, spillage in transportation, and inefficiency in storage. From the environmental indicator point of view, the annual emissions are nearly 68 tons CO_2 eq/kg [12], but by the proposed methodology, the emission is reduced to 9 tons CO_2 eq/kg.

3.3 Sensitivity Analysis Through the Business Model

Apart from sustainability analysis, a business model is developed for the corresponding biofuel supply chain. In the first scenario, the harvesting area/farm area is considered. The details of the harvesting site along with the sensitivity plot are given in the preceding paragraphs. Table 1 gives the detail of the business model of the harvest area. The data regarding total output biomass, biomass cost, operational expenses, and capital expenses are adapted from the PRESPL paper [7]. The rate and other financial parameters are adapted from the established literature [16, 17]. Table 2 gives an idea on the NPV and IRR which have been found out by detailed analysis using an MS Excel sheet. The internal rate of return is associated with the financial rate of return, and the net present value is a tool of capital budgeting in order to find out the profitability of the project. Further, sensitivity analysis is done

Table 1 Comparison between static and dynamic PSO

	Traditional/Static PSO	Time-varying PSO
Profit maximization	There is no convergence. There is no clear identification of break-even point	Profit increases at $t = 2$. So, break-even occurs in 2nd year
Minimization of emissions	The minimization is non-converging	It's a smooth curve with a value of less than 10 tons of CO_2 equivalent per kg

Table 2 Business model of harvesting area

Business model		
Interest rate	%	14%
Inflation rate	%	5%
Discount rate	%	10%
Depreciation rate	%	20%
Salvage value of machinery and building	%	10%
Equity	%	25%
Debt repayment period	Years	7
Corporate income tax rate	%	30.9%
CER price	INR/CER	0
Total project investment	INR Million	110.00
Equity component	INR Million	27.5
Capital subsidy	INR Million	15
Output biomass per MT	INR	2183.00
Capital expenses	INR Million	385.00
Operational expenses	INR Million	3.51
Total depreciable investment (Rs)	INR Million	275.00
Loan amount	INR Million	188.51
Annual repayment (Rs.)	INR Million	26.93

in an excel environment which gives us an idea regarding the relationship between surplus biomass, NPV, and IRR. Figure 12 gives an idea on sensitivity analysis of surplus biomass, NPV, and IRR. Figure 13 is based on the sensitivity analysis of biomass selling price, NPV, and IRR.

The NPV (Net present value) was found to be INR 82.96 and the IRR (Internal rate of return) is 15%.

As the Table 3 shows, with the increase in surplus biomass quantity, NPV and IRR increases. Hence, it is always a profitable choice for the farmers to invest in biofuel supply chain. The NPV in both the cases is linearly decreasing suggesting that if we are considering the surplus amount of biomass less than 80000 MT, then it is a bad choice (Fig. 11). One of the main reasons for the decreasing NPV is

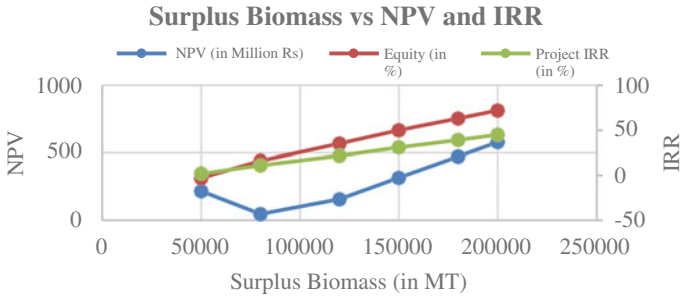

Fig. 12 Sensitivity analysis of Surplus biomass, NPV, and IRR

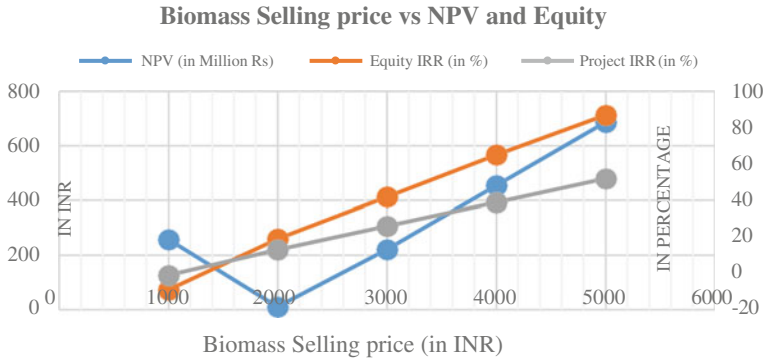

Fig. 13 Sensitivity analysis of biomass selling price, NPV, and IRR

Table 3 Inference from sensitivity analysis in Fig. 12

Surplus biomass (in MT)	NPV (in Million INR)	IRR (in %)
50,000	216	2
80,000	46.12	11
120,000	156.57	22
150,000	314.67	31
180,000	472.78	39
200,000	578.18	45

the uncertainties and randomness associated with the supply chain. Similarly, the inference from Fig. 12 has been drawn and the biomass selling price is found out to be more than INR 2000 per metric ton of biomass. Relative comparison is given in Table 4.

Table 4 Inference from Fig. 13

Biomass selling price (INR/MT)	NPV (in Million INR)	IRR (in %)
1000	258.25	−1
2000	10.76	13
3000	221.78	26
4000	454.48	39
5000	686.87	52

4 Conclusion

The model utilized particle swarm optimization technique-based decision to assess the sustainability of the biofuel supply chain in the transportation sector. It has adapted data from Karnataka, India. Since corn is one of the major crops in the state, the second-generation biofuel assessment study is based on corn cobs as biomass. The invocation of circular economy has helped to perceive waste valorization as a possibility in the Indian scenario while keeping the clean energy concept intact. The objective of the study is to make the farmers and other stakeholders gain from the discussed supply chain. The results of the assessment through the PSO technique show an overall profit in the biomass supply chain with a break-even period of 2 years. Another positive aspect is the lesser amount of CO_2 emission while going for the establishment of a biofuel supply chain. The supply chain includes a harvesting area, a collection center, and transportation of biomass to the center, but the study shows there is a measurable amount of less CO_2 emission. Hence, it is a feasible approach to go for the establishment of a second-generation biofuel supply chain in Karnataka. The distance between the collection center and harvesting area should not be more than 50 km, otherwise, transportation losses will result in loss. In order to showcase the feasibility, a business model is shown which gives an idea that NPV is the sensitive parameter in both the cases of analysis. Based on the results of sensitivity analysis, the price of surplus corn cobs is set to be INR 2183 per metric ton. Through the case study, the proposed work is intended to provide inputs to policymakers, industries, and government organizations.

References

1. Ritchie H (2020) Our World in data, 06 October 2020
2. CO2 emissions: OECD data.
3. Møller F, Slentø E, Frederiksen P (2014) Integrated well-to-wheel assessment of biofuels combining energy and emission LCA and welfare economic cost benefit analysis. Biomass Bioenergy 60:41–49. ISSN 0961-9534
4. Wautelet T (2018) The concept of circular economy: its origins and its evolution
5. Anex RP et al (2010) Techno-economic comparison of biomass-to-transportation fuels via pyrolysis, gasification, and biochemical pathways. Fuel 89:S29–S35

6. Phillips S et al (2007) Thermochemical ethanol via indirect gasification and mixed alcohol synthesis of lignocellulosic biomass. No. NREL/TP-510-41168. National Renewable Energy Lab. (NREL), Golden, CO (United States)
7. Biomass assessment study and proposed supply chain management plan by PRESPL
8. Rao SS (2019) Modern methods of optimization. John Wiley & Sons, Inc
9. Katoch S, Chauhan SS, Kumar V (2021) A review on genetic algorithm: past, present, and future. Multimed Tools Appl 80:8091–8126
10. Grabusts P, Musatovs J, Golenkov V (2019) The application of simulated annealing method for optimal route detection between objects Procedia Comput Sci 149
11. Koohi I, Groza VZ (2014) Optimizing particle swarm optimization algorithm. In: 2014 IEEE 27th Canadian conference on electrical and computer engineering (CCECE), pp 1–5. https://doi.org/10.1109/CCECE.2014.6901057
12. Holka M, Bieńkowski J (2020) carbon footprint and life-cycle costs of maize production in conventional and non-inversion tillage systems. Agronomy 10(12):1877
13. Kennedy J, Eberhart R (1995) Particle swarm optimization. In: Proceedings of ICNN'95 - international conference on neural networks, vol 4, pp 1942–1948
14. Sermpinis G, Theofilatos K, Karathanasopoulos A, Georgopoulos EF, Dunis C, Forecasting foreign exchange rates with adaptive neural networks using radial-basis functions and particle swarm optimization. Eur J Oper Res
15. Clerc M, Kennedy J (2002) The particle swarm — explosion, stability, and convergence in a multidimensional complex space. IEEE Trans Evol Comput 6(1):58–73
16. Reniers G, Talarico L, Paltrinieri N (2016) Cost-benefit analysis of safety measures (Chap. 16). In: Paltrinieri N, Khan F (eds) Dynamic risk analysis in the chemical and petroleum industry. Butterworth-Heinemann, pp 195–205. ISBN 9780128037652
17. International Energy Outlook 2019. https://www.iea.org/reports/world-energy-outlook-2019

Environmental Capacity of Roads Under Mixed Traffic Conditions

Naina Gupta, Sewa Ram, and Bhaskar Gowd Sudagani

Abstract Transportation provides basic mobility and accessibility for people and goods between different origins and destinations. However, this benefit costs us congestion and deteriorated environmental quality. In recent years, road transport has been one of the major contributors of pollutants like hydrocarbons, carbon monoxide, particulate matter, etc. In transport infrastructure planning, one important aspect is determining the need and capacity of roads. Several researches, in this aspect, so far considered different traffic flow theories to estimate the maximum number of vehicles that can be accommodated under certain traffic conditions. However, these researches neglect the impact of traffic on the environment in estimating capacity. Thus, amalgamated research on traffic and the environment is the need of the hour. This research aims to develop a methodology for determining the environmental capacity of roads from three perspectives, namely: road capacity restraints, air pollution restraint, and noise pollution restraint conditions. The environmental capacity, considering the above three conditions, is estimated in the range of 60–70% of its capacity for eight- and six-lane divided roads and approximately 50% for four-lane divided and two-lane undivided roads. Further, a correction factor is derived for four different boundary conditions by carrying out dispersion modelling. The correction factor is estimated to be 0.93 for one-side built up, 1.09 for street canyon and 0.72 for open terrain with respect to both sides built-up boundary conditions. Thus, overall, this research could provide a theoretical and reliable database for traffic optimization, air and noise pollution control, i.e. conducive to transport as well as environmental planning and management.

Keywords General finite line source model (GFLSM) · Dispersion modelling · Capacity

N. Gupta (✉) · S. Ram · B. G. Sudagani
School of Planning and Architecture, Delhi, India
e-mail: nainagupta9793@gmail.com

L. Devi et al. (eds.), *Proceedings of the Sixth International Conference of Transportation Research Group of India*, Lecture Notes in Civil Engineering 273,
https://doi.org/10.1007/978-981-19-4204-4_6

1 Introduction

The aim of planning the development of an area is to improve the quality of the environment. However, an important aspect when planning the road infrastructure is determining its capacities. This capacity, determined using traffic flow theories, completely neglects the vehicular emissions, which are serious health and environmental problems worldwide[18, 24, 25]. Hence, there is a need to carry out research and develop methodologies for planning road infrastructure by estimating the relationship between the environment and transport.

There have been several researches that have been carried out for addressing the concept of Environmental Capacity (EC) starting from the 1960's [1, 6, 7, 15, 26, 27, 28]. The chronology of the researches on the concept of EC is depicted in Table 1. These studies indicate that there is limited research that has considered air pollution for estimating Environmental Capacity. According to Indo-Highway Capacity Manual [21], capacity is defined as 'the maximum number of vehicles that can pass a given point during a specified period under the prevailing roadway, mixed traffic and control conditions'. This does not consider any influence from downstream traffic operation (traffic queues) or environmental constraints. The capacity is defined based on the service quality. However, this research intends to develop a design framework related to the concept of Environment Capacity of Roads considering air and noise pollution.

Table 1 Chronology of research on concept of environmental capacity

Year	Researcher	Parameters used for defining EC
1963	Buchanan [20]	Pedestrian delay and carriageway width
1972	Sharpe [15]	Pedestrian safety; air pollution; road traffic and noise
1979	Holsworth [26]	Pedestrian safety; pedestrian delay; road traffic and noise
1981	Appleyard [19]	Residential amenity and traffic volume
1993	Song and Dunne [17]	Pedestrian delay and accident risk
1997	Commonwealth of Australia [22]	Noise; air pollution; crossing delay and pedestrian safety
2002	City of Palo Alto [21] and RTA [31]	Pedestrian Delay, User perception and traffic volume
2004	Cheng [1]	Pollutants (NOx) emitted from vehicle
2008	Zhu [32]	Emission factors and trip ends
2009	Li [7]	Air pollution and traffic volume
2013	Kebria [6]	Theoretically expressed necessity and importance for estimating road EC and its significance in terms of management and air pollution controlling
2016	Nwoye [10]	Traffic composition and traffic flow

The aim of this paper is to determine not the capacity but the environmental capacity, which is defined as the 'maximum allowable flow', so that the air and noise quality standards are not violated. The results of this research carried out in Delhi will be discussed to make a valuable contribution to further international discussion on this topic.

2 Case Study Area—Delhi

Delhi, the capital of India, covers an area of 1484 square kilometers with a population of 16.7 million (Census 2011). Being the capital city, it has experienced rapid urbanization and phenomenal population growth at a rate of 21.6% over the past decade. The city has also seen rapid growth in vehicle registration and has the highest number of registered cars compared to any other metropolitan city in India.

Delhi, one of the most polluted Indian cities, was considered for this research. Nine locations were considered to conduct primary surveys (video graphic traffic survey, simultaneous monitoring of Carbon Monoxide (CO) concentration with the Langan T15 × CO Measurer and noise pollution levels using decibel meter app). These locations cover different lane configurations of Eight, Six, Four-lane divided and Two-lane undivided roads; different surrounding boundary conditions with open terrain, built on one side and on both sides and all located in predominant commercial areas. Table 2 summarizes the detailed physical characteristics of the surveyed stretches.

3 Capacity of Urban Roads

The speed-flow studies were conducted through videography and spot speed survey at all nine locations. The observed traffic was expressed in terms of Passenger Car Unit (PCU) using the concept of Stream Equivalency Factor (K), which converts mixed traffic to a homogeneous equivalent without using PCU values [2, 21]. This factor is equal to the ratio of traffic flow in PCU/hour and flow in vehicles/hour and also relates to the traffic composition and traffic volume on a road by a regression analysis method, shown in Eqs. (1) and (2). These equations for "K" were taken from the Indian Highway Capacity Manual [21].

$$\begin{aligned} &\text{SEF for Undivided Roads: } K = 1 - 0.62 \times P_{2\ \text{Wheeler}} \\ &- 0.47 \times P_{3\ \text{Wheeler}} + 4.53 \times P_{\text{Bus}} - 4.40 \times P_{\text{Heavy Vehicles}} \\ &- 0.45 \times P_{\text{Non - Motorized}} - 2.83 \times P_{\text{Light Commercial Vehicle}} - 84.87 \times (1/N) \end{aligned} \quad (1)$$

Table 2 Physical characteristics of the nine surveyed stretches

Loc.	Name of the road (latitude, longitude)	Road hierarchy	Type of road	RoW (mts)	Surrounding environment
1	Near Millenium Depot (28.59°, 77.26°)	Arterial road	Eight-Lane divided	70	Open terrain
2	Near Ring Road (28.54°, 77.22°)	Arterial road	Eight-Lane divided	40	Built up
3	Arjangarh Metro Station (28.48°, 77.13°)	Arterial road	Six-Lane divided	40	One side built up
4	Bahadur Shah Zafar Road (28.63°, 77.24°)	Arterial road	Six-Lane divided	40	Built up
5	Near MG Road (28.48°, 77.10°)	Arterial road	Six-Lane divided	65	Built up
6	Zakir Hussain Marg (28.60°, 77.24°)	Arterial road	Four-Lane divided	40	One side built up
7	Tamil Sangam Road (28.56°, 77.18°)	Sub-arterial road	Four-Lane divided	24	Built up
8	GTB Nagar (28.60°, 77.11°)	Local road	Two-Lane undivided	15	Built up
9	Vivek Vihar (28.67°, 77.32°)	Local road	Two-Lane undivided	12	Built up

$$\begin{aligned}\text{SEF for Divided Roads: } K = {} & 1 - 0.77 \times P_{2\text{ Wheeler}} \\ & - 0.28 \times P_{3\text{ Wheeler}} + 0.53 \times P_{\text{Light Commercial Vehicle}} + 2.60 \times P_{\text{Bus}} \\ & + 1.83 \times P_{\text{Heavy Vehicles}} - 0.66 \times P_{\text{Non - Motorized}} - 12.71 \times (1/N)\end{aligned} \quad (2)$$

where P represents percentage composition and N represents total traffic volume in vehicles/h. Thereafter, the capacity of roads was estimated by developing speed-flow equations based on Green-shield Model. The estimated capacity for different test sections were 7177 PCU/h/direction for Eight-lane divided (shown in Fig. 1), 6088 PCU/h/direction for Six-lane divided, 3204 PCU/h/direction for Four-lane divided and 2422 PCU/h for Two-lane undivided roads.

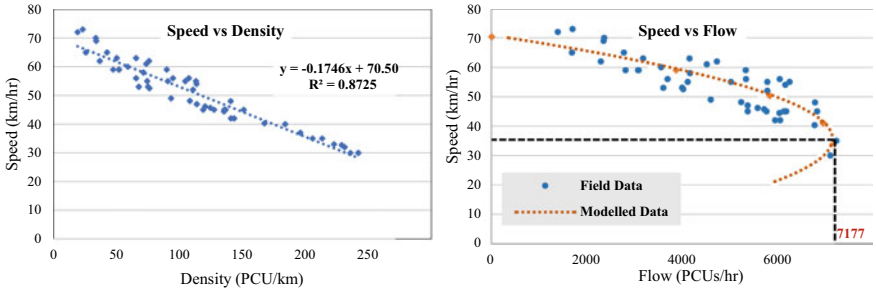

Fig. 1 Capacity for an 8-lane divided road

4 Environmental Capacity (EC) of Urban Roads

The road capacity concept discussed above does not take into account the impact of traffic emissions on the environment. Therefore, a quantifiable concept of environmental capacity is derived, which aims to develop an empirical relationship between environmental parameters and traffic characteristics from three perspectives, namely road capacity restraint, air pollution restraint and noise pollution restraint conditions, and thus determine the environmental capacity of roads. This environmental capacity is defined as the "maximum number of vehicles that can ply on a certain road hierarchy in order to comply with the environmental standards (air and noise quality standards) under specified conditions".

4.1 Environmental Capacity—Air Pollution Restraint Conditions

To estimate the capacity, carbon monoxide (CO) was taken into account as a pollutant under the under air pollutant restraint condition. This pollutant is one of the most heavily emitted pollutants with serious toxicological effects. In order to convert the vehicular emissions into ambient concentration, the General Finite Line Source Model (GFLSM) was adopted[8, 13]which is derived using Eq. (3) [8].

$$\text{Concentration at any point} = \begin{pmatrix} \sqrt{2 \times \text{Emissions}} \\ \times \text{Dispersion Factor} \end{pmatrix} / \begin{pmatrix} \pi \times \text{Mean Wind} \\ \text{Speed} \times \sigma_z \end{pmatrix} \quad (3)$$

where σ_z—$a \times$ (Distance from the line source of the point where concentration is desired)^b; (a, b are stability parameters). The Dispersion Factor was estimated by taking into account the empirical relationship between traffic volume and ambient air quality, given in Eq. (4) [28].

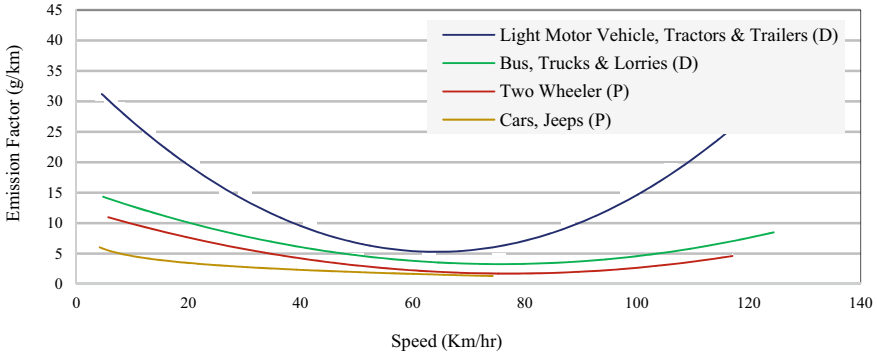

Fig. 2 Emission factor, (CO) for different modes at different speeds

$$\text{Dispersion Factor} = \left[(\text{Avg 8 hour CO conc.})/(1\text{ h max CO conc.})\right] \times \left[(\text{Traffic volume during max observed CO})/(\text{Eight hours traffic volume})\right] \quad (4)$$

Data related to the mean wind speed; Stability parameters were collected from secondary sources. The emissions Q were estimated using the relationship between speed and emission factor shown in Fig. 2, to reflect driving conditions on the ground. For other modes, emission factors with regard to the type of fuel are taken into account using secondary data [11, 14].

The distance from the line source point (x), was considered to be the mixing zone width, which includes a uniform emission zone (carriageway and median width) and an additional 3 m on both sides to account for vehicle-induced turbulence. Based on the above values, the pollutant concentration for various road hierarchies was estimated.

A best-fit curve was created for various road hierarchies, which relates speed vs. flow and speed versus pollutant concentration. The estimated concentrations are compared to their maximum standard limit (prescribed by National Ambient Air Quality Standards, India), i.e. 4 mg/m^3 for 1 h averaging time to derive a relationship between flow- speed-pollutant concentration.

The analysis for an eight-lane divided road depicts that the speed above which the predicted concentration of the pollutant CO would fall below its threshold of 4 mg/m^3 is 52.9 km/h, which corresponds to a flow rate of 5332 PCU/h, shown in Fig. 3. This flow, which complies with environmental standards is 74.3% of its capacity, i.e. 7177 PCU/h, and is defined as EC (under air pollution restraint conditions).

A similar analysis for a six-lane divided road show this maximum CO concentration of 4 mg/m^3 is achieved for speeds above 52.4 km/h which corresponds to a flow rate of 4402 PCU/h, i.e.72.3% of its capacity of 6088 PCU/h. For four-lane divided roads, the maximum flow within the standard is 1907 PCU/h, i.e. 59.5% of the capacity. For two-lane roads, the flow rate of 1462 PCU/h which is 60.4% of the capacity, was found to be within environmental standards.

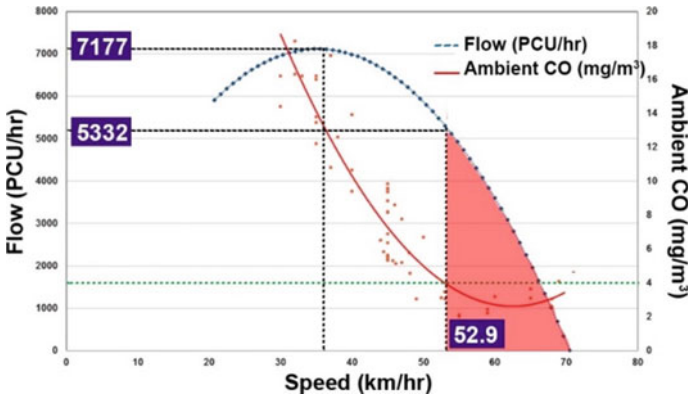

Fig. 3 Flow versus speed versus ambient CO concentration for eight-lane divided roads

It is concluded from this that, taking into account the pollutant concentration of CO, the EC is in the range of 60–74% of its capacity for different road hierarchies. This decreasing trend of the EC with the street width shows its importance for the later discussed pollution dispersion. However, it has been observed that the EC for two-lane roads is relatively higher than for four-lane roads, which is likely due to the different traffic composition.

4.2 Environmental Capacity—Noise Pollution Restraint Conditions

Traffic noise is another important component of pollution with serious effects on human health [5]. It is therefore imperative to pay equal attention to the measurement and control of noise exposure through the regulation of noise emission limits.

In this research, the noise levels along the roadside for every 5 min were measured simultaneously along with other surveys, i.e. videography and CO monitoring. The monitored values such as sound levels and dB(A) were plotted on the x-axis, and the cumulative percentage of time that this sound level was exceeded was plotted on the y-axis. These plots were used to calculate L_x (i.e. noise levels greater than x% of the time) for x = 10, 50, and 90. These L_x values were used to calculate the combined index measuring noise, i.e. equivalent sound level, L_{eq} using Eq. (5).

$$L_{eq} = L_{50} + \left[(L_{10} - L_{90})^2/60\right] \tag{5}$$

In addition, the relationship between L_{eq} and traffic parameters, i.e. traffic volume and speed was derived using the regression tool. The derived linear relationship between these parameters is given in Eqs. (6) and (7).

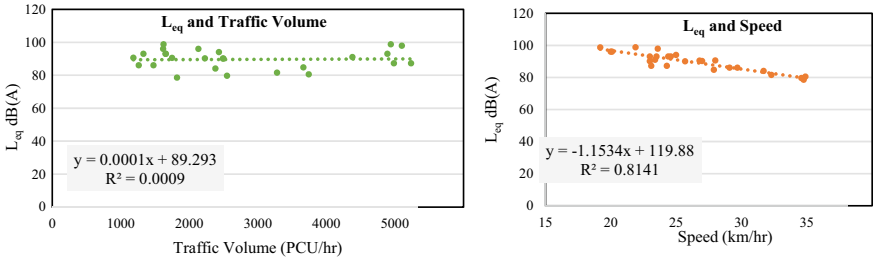

Fig. 4 Relationship between traffic parameters and noise level

$$\text{Equivalent Noise Level} = 0.0001 \times \text{Vehicles/h} + 89.293 \quad (6)$$

$$\text{Equivalent Noise Level} = -1.1543 \times \text{Average speed of vehicles} + 119.88 \quad (7)$$

The decrease in the noise level with increasing traffic speed is probably due to better flow conditions eliminating the need for constant honking for clearance.

Further, using Eq. (5), L_{eq} was estimated for various speeds corresponding to speed-flow curves, as shown in Fig. 4. The estimated noise levels were compared with the maximum standard limit (prescribed by the Central Pollution Control Board, India) of L_{eq} in commercial areas, i.e. 65 dB(A) to estimate the EC.

The analysis for an eight-lane divided road indicated that the speed above which the noise levels are within the standard limit of 65 dB(A) is 47.6 km/h, which corresponds to a flow rate of 6366 PCU/h. It was found that these flow-sustaining noise standards represent 88.7% of their capacity, i.e. 7177 PCU/h and are defined as the EC of roads (under noise pollution restraint conditions), as shown in Fig. 5.

Similarly, for a six-lane divided road, the noise level threshold was reached for speeds above 47.6 km/h, which corresponds to a flow rate of 5348 PCU/h, i.e. 87.8% of the capacity of 6088 PCU/h. For four-lane divided roads, the maximum flow rate was 1597 PCU/h, i.e. 49.8% of the capacity and for two-lane undivided roads, the flow rate was 1251 PCU/h, which is 51.7% of the capacity of 2422 PCU/h is within the environmental limits.

Based on the above results, it was concluded that the environmental capacity, taking into account the noise level norms, ranged from 87 to 89% of its capacity for eight- and six-lane roads and 49–51% for four- and two-lane roads.

4.3 Environmental Capacity

Overall, the environmental capacity was estimated by taking into account the maximum flow that complied with both the environmental standards for air and noise. On this basis, for eight-lane divided roads, a flow of 5332 PCU/h (i.e. 74.3%

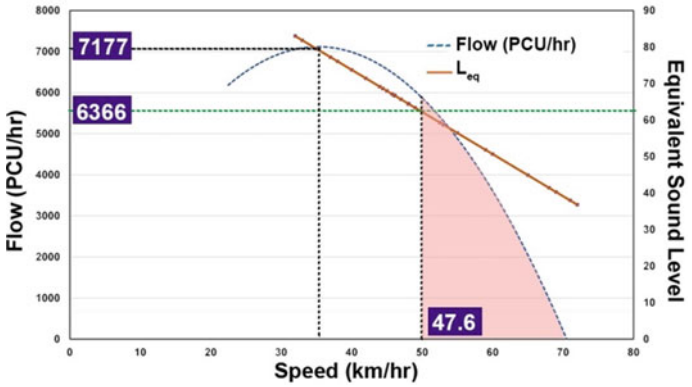

Fig. 5 Flow versus speed versus equivalent sound levels for eight-lane divided roads

of its capacity) was observed as the maximum flow that would meet the air and noise quality standards shown in Fig. 6.

Similarly, for six-lane, four-lane and two-lane roads, a flow of 4402 PCU/h (i.e. 72.3% of its capacity), 1597 PCU/h (i.e. 49.8% of its capacity), and 1251 PCU/h (i.e. 51.7% of its capacity) was observed to be the maximum flow that met air and noise quality standards.

Thus, it was concluded that the environmental capacity for eight, six, and four-lane divided roads and two-lane undivided roads are 74.3%, 72.3%, 49.8%, and 51.7% of their capacity, respectively. In addition, a dispersion modelling was carried out in order to understand the influence of the surrounding environment on the pollutant concentration.

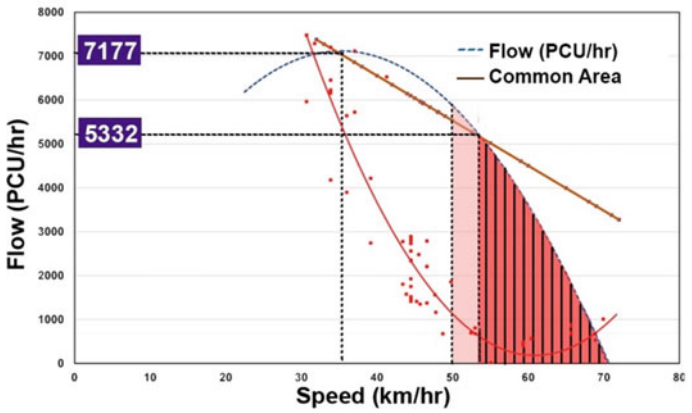

Fig. 6 Overall environmental capacity for an 8-lane divided road

5 Dispersion Modelling

The aim was to predict the future pollutant concentration depending on the boundary conditions and to facilitate the abatement and management of vehicular pollution. This simulation for dispersion of pollutants was carried out with the CALINE [3, 4, 9, 12] and Vissim EnViver software which is based on the Gaussian Plume Dispersion. The Gaussian plume dispersion model is one of the most widely used models for air pollution modelling that uses the Gaussian plume distribution equation to estimate the concentration of pollutants at fixed receptors based on the dispersion of pollutants.

5.1 Input Parameters for Dispersion Modelling

The dispersion of pollutants depends on the site-related properties such as road geometry, traffic characteristics, surrounding conditions, and meteorological parameters. The parameters considered include traffic data for 8 h; weighted emission factors; terrain type; road geometry (i.e. mixing zone width and road type); meteorological data (i.e. wind speed, wind direction, mixing height, stability class and temperature.

5.2 Modelling Results

The following section discusses the estimated model results for one location, i.e. near Millenium Depot (Location-1). This location has an eight-lane divided road configuration with open terrain on both sides. In order to carry out dispersion modelling at this location, a primary road network was first created in Vissim, which defined the vehicle counts, modal compositions, vehicle routes, driving behaviour and vehicle speeds, giving us the simulated network. This output was considered as an input for the add-on software EnViver for pollution modelling which can predict the pollutant concentration under various boundary conditions such as open terrain, built on one side, built on both sides and street canyon. In addition to the parameters listed above, the traffic composition, the age of the vehicles, the type of fuel and the emission standards were also given as input in EnViver. Based on these inputs, the predicted CO pollutant concentration under different boundary conditions, shown in Fig. 7.

The monitored and modelled value shows a deviation of 7.8%, which is acceptable. In addition, the model was also validated with the GEH index (calculated using Eq. (8)) which predicted a value of 9.6, i.e. warranting an investigation of the model.

$$\mathrm{GEH} = \sqrt{\left\{\left[2 \times \begin{pmatrix}\text{Modelled Value} \\ -\,\text{Monitored Value}\end{pmatrix}^2\right] \Big/ \left[\begin{matrix}\text{Modelled Value} \\ +\,\text{Monitored Value}\end{matrix}\right]\right\}} \tag{8}$$

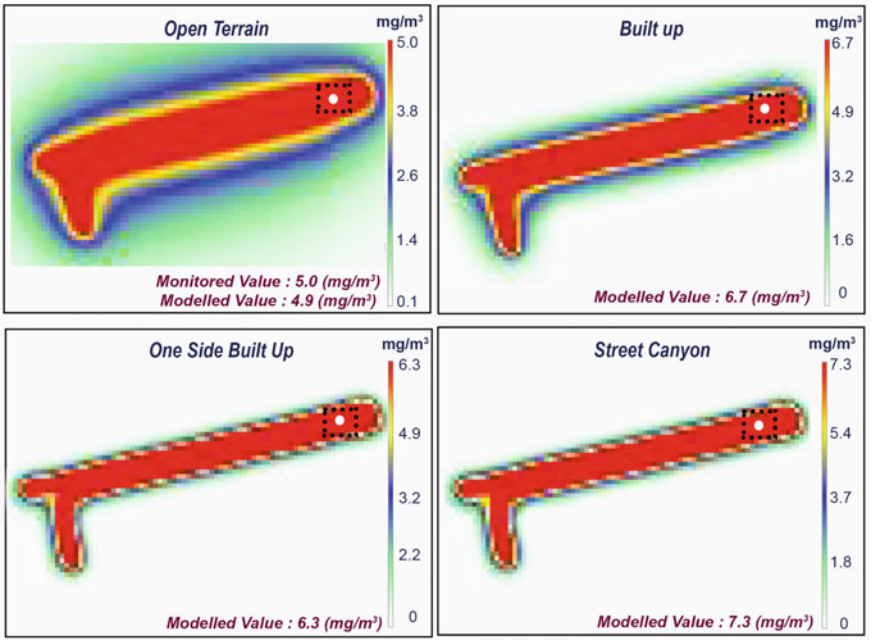

Fig. 7 Dispersion modelling for Location-3 under different boundary conditions

The modelled value under street canyon condition is 7.4 mg/m^3; built-up condition on both sides is 6.8 mg/m^3; one-sided built-up condition is 6.4 mg/m^3 and for open terrain conditions is 5.0 mg/m^3. In other words, the modelled CO concentration under one-sided built-up typology is 0.94 times the modelled concentration under both sides built up. Similarly, under street canyon and open terrain conditions, it is 1.1 and 0.74 times that of the built-up conditions on both sides. It can be concluded from this that the same location could have a higher/lower concentration of pollutants due to its surrounding boundary conditions (Fig. 8).

In addition, the statistical results of the model predicted a correlation coefficient of 0.598; index of agreement as 0.69; fractional bias as 0.05 and normalized mean square error as 0.012. The overall model thus provided statistically satisfactory predictions for CO under defined conditions.

A similar analysis was performed for other locations as shown in Table 3. On this basis, the overall derived correction factor for one-sided built-up boundary condition is 0.93; for street canyon, it is 1.09 and for open terrain, it is 0.72, with respect to built-up on both sides.

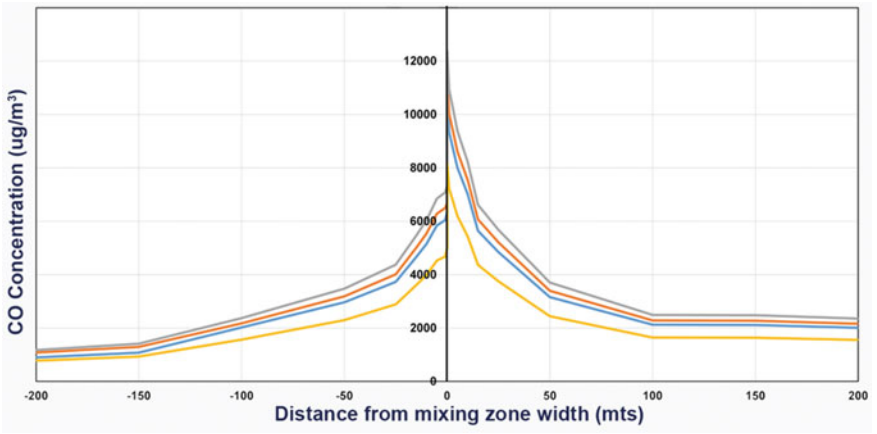

Fig. 8 Dispersion from edge of mixing zone width

Table 3 Summary of dispersion model outcomes for all the locations

Location	Surrounding built up	Monitored CO Conc. (mg/m^3)	Modelled CO concentration (mg/m^3)				% variation	GEH value
			OSBU	BU	OT	SC		
1	OT	5.7	6.4	6.8	**5.0**	7.4	7.8	9.6
2	BU	7.1	6.2	**6.6**	4.9	7.2	7.3	6.2
3	OSBU	6.5	**7.2**	7.8	5.6	8.5	9.9	7.7
4	BU	10.7	10.6	**11.4**	8.3	12	6.8	7
5	BU	6.7	6.6	**7.1**	5.1	7.7	6.1	4.9
6	OSBU	7.4	**6.9**	7.5	5.3	8.1	7.4	6.5
7	BU	8.0	7.2	**7.8**	5.4	8.5	3.0	9.4
8	BU	8.5	7.3	**7.9**	5.6	8.6	6.2	5.8
9	BU	7.5	6.4	**6.9**	4.9	7.5	7.7	7.4

Note Built up (BU); one side built up (OSBU); open terrain (OT); street canyon (SC)

6 Level of Service (LOS)

Further LOS standards were derived using the concept of k-mean clustering to derive a qualitative measure of the quality of transport service based on travel speed and environmental performance measures [32]. Based on this, the data set was divided into 6 clusters with the designations LOS A (best) to LOS F (worst). Based on the analysis, the CO concentration and L_{eq} values for LOS A are up to 2.3 mg/m^3 and 49 dB(A); LOS B: 2.3–4.1 mg/m^3 and 49–61 dB(A); LOS C: 4.1–6.3 mg/m^3 and 61–70 dB(A); LOS D: 6.3–9.1 mg/m^3 and 70–78 dB(A); LOS E: 9.1–12.2 mg/m^3

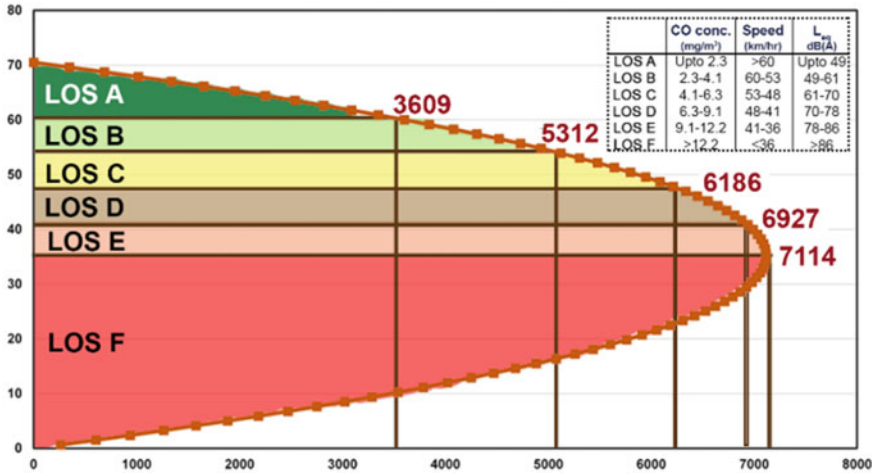

Fig. 9 Environmental LOS for 8-lane divided road

and 78–86 dB(A) and LOS F: greater than 12.2 mg/m^3 and 86 dB(A), respectively. Environmental LOS graph for eight-lane divided road is shown in Fig. 9.

7 Conclusion

The research concludes that the overall environmental capacities are approximately in the range of 60–70% of its capacity for eight, six-lane divided roads and approximately 50% for four-lane divided and two-lane undivided roads. In addition, the result of the dispersion modelling derives a correction factor for predicting CO concentration under various boundary conditions, i.e. 0.93, 1.09 and 0.72 for one-sided built up, street canyon and open terrain with respect to both sides built-up conditions. Therefore, the parameter environment must be taken into account as one of the criteria in terms of air pollution and noise pollution to determine the capacity or level of service of roads that might call for reduced capacities.

Further research in this area is required to understand the effects of other pollutants on the environmental capacity, the effect of seasonal and temporal variations, the effects of changes in vehicle composition and fuel type and to test the applicability of this model in other cities.

References

1. Cheng J (2004) Modeling urban environmental traffic. J Chang'an Univ (Nat Sci Ed) 24(5):94–98
2. Dhamaniya A, Chandra S (2013) Concept of stream equivalency factor for heterogeneous traffic on urban arterial roads. J Transp Eng 139(11):1117–1123
3. Dhyani R, Gulia S, Sharma N, Singh A (2014) Air quality impact assessment of a high-way corridor through vehicular pollution modelling. Int J Renew Energy Environ Eng 2(2):93–99
4. Dubey B, Pal A, Singh G (2013) Assessment of vehicular pollution in Dhanbad city using CALINE4 model. Int J Geol Earth Environ Sci
5. Hunashal RB, Patil YB (2012) Assessment of noise pollution indices in the city of Kolhapur, India. Procedia-Soc Behav Sci 37:448–457
6. Kebria D, Darvishi Y (2013) Assessment of necessity on determining of road environmental capacity with a focus on air pollution due to transport. Glob J Adv Pure Appl Sci 01:275–281
7. Li T, Lin J, Wu M, Wang X (2009) Concept and spatial analysis method of urban environmental traffic capacity. J Transp Eng 135(11):873–879
8. Luhar AK, Patil RS (1989) A general finite line source model for vehicular pollution prediction. Atmos Environ 23(3):555–562
9. Niraj S, Chalapati R (2014) Vehicular pollution prediction modelling: review of highway dispersion models. Transp Rev 24(4):409–435
10. Nwoye CF (2016) An assessment of the carrying capacity of lagos metropolitan roads: a case study of Mile2-Apapa and Lekki-Epe Corridors. Arts Soc Sci J. ISSN: 2151-6200
11. Ramachandra TV, Shwetmala (2009) Emissions from India's transport sector: state wise synthesis. Atmos Environ 43:5510–5517
12. Samitha S, Stever G (2014) Real-time estimation of pollution emissions & dispersion from highway traffic. Comput-Aided Civ Infrastruct Eng 29:546–558
13. Sharad G, Mukesh K (2005) Hybrid model for predicting CO from vehicular exhausts in urban environments. Atmos Environ 39:4025–4040
14. Sharma S, Mathew TV (2016) Developing speed dependent emission factors using on-board emission measuring equipment in India. Int J Traffic Transp Eng 6(3):265–279
15. Sharpe CP, Maxman RJ (1972) A methodology for computation of the environmental capacity of roadway networks. Highway Res Rec 394:33–40
16. Solanki HK, Ahamed F, Gupta SK, Nongkynrih B (2016) Road transport in urban India: its implications on health. Indian J Community Med. Indian Assoc Prev Soc Med 41(1):16–22
17. Song L, Dunne MC, Black JA (1993) Models of delay and accident risk to pedestrians in C. F. Daganzo. In: Proceedings of 12th international symposium on transportation and traffic theory, pp 899–910
18. Srivastava R, Saxena N, Gautam G (2013) Air pollution due to road transportation in India: a review on assessment and reduction strategies. J Environ Res Dev

Technical Reports

19. Appleyard D, Gerson MS, Lintell M (1981) Livable streets. University of California Press, Berkeley, USA
20. Buchanan C (1963) Traffic in towns: a study of the long-term problems of traffic in urban areas. London, England
21. Chandra S, Gangopadhyay S, Velmurugan S, Ravinder K (2017) Indo highway capacity manual. Council of Scientific and Industrial Research (CRRI), India
22. City of Palo Alto (2002) Transportation significance thresholds—study session and new interim standards. Staff Report to the Planning & Transport Commission, Sep 19 2002

23. Commonwealth of Australia (1997) Australian model code for residential development (AMCORD). Local Government & Planning Ministers Council
24. Dahiya S, Myllyvirta L, Sivalingam N (2017) Airpocalypse-assessment of air pollution in Indian cities. GPET, India
25. Ghate AT, Sundar S (2014) Proliferation of cars in Indian cities: let us not ape the west. The Energy and Resources Institute, India
26. Glen K, Rhys C (2010) Assessing environmental capacity of local residential streets. In: 12th WCTR. Lisbon, Portugal
27. Holdsworth J, Singleton DJ (1979) Environmental traffic capacity of roads. In: Papers of the fifth Australia transport research forum, pp 219–238
28. Koorey G, Chesterman R (2010) Assessing the environmental capacity of local residential streets. In: 12th world conference on transport research society (WCTR), Lisbon
29. Meisel WS, Dushane TE (1979) NCHRP report 200, 1979: monitoring carbon monoxide concentrations in urban areas. TRB, National Research Council, Washington, DC
30. Messina D, Bullin JA, Nelli JP, Moe RD (1982) Estimates of air pollution near simple signalized intersections. Texas Transportation Institute, Texas
31. Roads and Traffic Authority (RTA) (2002) Guide to traffic generating developments. Roads and Traffic Authority, NSW, Australia
32. Teja S, Ram S, Shukla A (2017) Environmental consideration in assessing LOS of a signalized intersection. In: 10th urban mobility India conference, Hyderabad, India
33. Zhu Z (2008) Traffic assignment modelling: under the consideration of urban environmental traffic capacity. Southeast University, China

Transportation Safety and Security

A Review on Surrogate Safety Measures in Safety Evaluation and Analysis

Dungar Singh and Pritikana Das

Abstract Road traffic safety has become a major problem, despite developments in technology and infrastructure. Traditionally, road safety is measured using accident data, which is essentially considered a reactive approach, although this method has time and efficiency limitations. Using surrogate safety data allows for a faster evolution of safety than using long-term accident data, according to previous studies. This paper presents an overview of the current surrogate safety measures (SSMs) that explicitly focuses on the potential to analyze vulnerable road users and the areas that previous studies have ratified. In a compressive and quantitative manner, the scope analysis explored how surrogate safety measures (SSMs) have been applied so far in scientific literature and what are their key drawbacks. This study will also help to identify new ideas in this field and identify recommendations for research leading to the emergence of a new use of surrogate safety measures.

Keywords Road safety · Surrogate safety indicators · Traffic conflict technique · Micro-simulation

1 Introduction

Road safety is a major concern in developing countries like India because it influences the people's welfare and the worldwide economy. India is the world's second-largest populated country after China. According to world population prospect 2019, India will surpass China as the world's most populous country in 2027 [1]. An increase in population gradually led to higher traffic safety risks as the current infrastructure is not able to manage higher traffic demand. In 2019, around 449,002 road accidents have been reported in India in which 151,113 people have lost their lives and 451,361

D. Singh · P. Das (✉)
Maulana Azad National Institute of Technology Bhopal, Bhopal, India
e-mail: pritikana.das@gmail.com

D. Singh
e-mail: dsdudi97@gmail.com

L. Devi et al. (eds.), *Proceedings of the Sixth International Conference of Transportation Research Group of India*, Lecture Notes in Civil Engineering 273,
https://doi.org/10.1007/978-981-19-4204-4_7

people were injured [2]. This translates into an average of 1230 accidents and 414 deaths every day and nearly 51 accidents and 17 deaths every hour, this leads to a severity rate of 1.3% points in 2019 over the previous year's persons. It shows a need for a reliable accident prevention strategy. The main reason for high fatality rates in Indian traffic is a heterogeneous condition, which includes various classes of vehicles sharing the same road space where high speed of vehicle sharing with vulnerable road users, unsafe road infrastructure and vehicle in poor condition. The main purpose of safety evaluation is to identify safety issues and provide various opportunities for future improvement.

Over the span of five decades, road safety assessments have evolved. Traditionally road safety assessments were done using the previous year's crash data to improve road safety conditions. The Crash base assessment is a reactive approach because it begins based on previous crash data and focuses on crash-based data identification of the high-risk location and collecting other sources of information to access treat risk [3]. There are significant limitations associated with accident data reporting and recording; this approach tends to be inaccurate globally [4–8]. Furthermore, a reactive process that does not represent the causative variables of incidents. Therefore, observed crashed data, is not a complete prediction of road safety as crashes occurring today may not show where crashes will occur tomorrow. Hence to overcome this problem there is a need to provide an alternative safety evaluation approach.

Safety evaluation using traffic conflict techniques applying different surrogate safety measures (SSMs) is another alternative approach to the crash-based events method. It is a safer approach for resolving all of the above-described difficulties. This approach, which dates back to 1960, is used to characterize the interaction between two road users in a traffic collision and to estimate the likelihood of a crash or the severity of a crash. Evaluation of road safety using surrogate measures should be based on non-crash events that can be observed from a crash event in a predictable and reliable manner, and there is an accurate way for converting non-crash events into the crash frequency or severity. As a result of a scoping analysis of past studies on surrogate safety assessment (SSM), various research gaps in earlier studies were identified. Hence the aim of this study addresses research gaps in the present literature review by carrying out a systematic literature review of existing studies on the surrogate safety assessment.

It is essential that a systematic approach need to be adapted to identify the contributing factors of road crashes based on selecting the most appropriate treatments and implementation on road sites. It is necessary to conduct an in- depth analysis of hazardous sites including a detailed analysis of traffic flow characteristics and driver behaviour, especially at an uncontrolled intersection, to identify the traffic conflict area.

The aim of this article is to conduct a comprehensive study of existing research study on surrogate safety assessment using a systematic literature review by the following research question:

1. What are the different categories of surrogate safety measures used in road safety?

2. How effective is the proactive method in assessing road safety?
3. How surrogate safety measures (SSMs) are used to measure traffic conflict?
4. How can SSMs be used to measure traffic conflict using a micro-simulation approach?

Our focus will be on articles on road safety using "surrogate safety measure" published in a scientific peer-reviewed journal until July 2021. As a result, several definitions of surrogate safety measures have been presented over time. Tarko et al. [9] discussed conflict, as well as other critical safety events. However, in the last decade number of studies were increased rapidly so need to conduct a more updated and complete analysis of previous studies. A secondary goal of this study was to identify research gaps in the current literature. The following is the study process for this paper structure: The first stage in identifying relevant studies is to have a discussion about the research aim questions, followed by a search technique, inclusion and exclusion criteria, and ultimately collecting relevant literature. Finally, compile a list of related literature. Further, the current literature was divided into areas and a detailed discussion was done to identify limitations and research gaps. Finally, the study wraps up with a review of the findings and recommendations for further research.

2 Methodology

A Systematic Literature Review (SLR) is often conducted to provide a comprehensive summary of present evidence related to research questions. It is a systematic, repeatable, and transparent method for synthesizing past research conducted by academics, researchers, and practitioners. The aim of conducting systematic literature reduces occurrence bias in conducting a comprehensive literature search over multiple databases [10] and answers to the pre-specified specific research question [11]. Mostly at the beginning, systematic reviews were used in existing synthesize studies and described decision making in health care systems [12, 13] further progressively used in different domains like business and management [14], tourism system [15] and road safety analysis [16]. The process of data gathering is described in depth in the following sections, as is the quality of study selection.

2.1 Data collection

Studies were included that identified relevant literature review by searching on the following database: Web Science, Scopus, Pub-Mate, and Google Scholar using the following keyword 'traffic conflict', 'conflict indicators', 'surrogate safety measure', 'severity', 'near-crash' or 'near-miss', with some literature paper search individual

Table 1 Database and search choices

Database	Search choices
Scopus,	Search: in title, keyword, abstract
Web of Science (WoS),	Limit: peer-reviewed academic publications
Google Scholar,	Source type: academic journal
Science Direct,	Data type range- all year up to July 2021
Research Gate	Language—English

from Google then the total number of paper from each journal reported with the description search options provided in Table 1.

2.2 Data Extraction

Relevant data for each study were extracted from the citations database by study titles, keywords, abstract, name of authors, name of Journal, and year of publication. Identified data records were exported in an MS Excel spreadsheet. Eligibility citations were addressed from search question(s) by two independent reviewers screening full-text identified data independently during differences between critics are disputed and resolved through mutual agreement. To minimize biases while adding literature from the database to our manuscript we followed existing studies [14, 15, 17].

2.3 Study selection

Here are the following different steps to select the relevant study. Duplicate kinds of literature were removed from the database in the first step. After that, we looked at the title and abstract of each article to determine which ones were applicable to the studies and which parts were not. In the process finally, potentially relevant 213 articles were included in the full-text search.

In which 130 articles were discarded from the study of the content was not relevant or full-text was not available, end of the procedure, 83 articles were included for the systematic literature review. For the selection of study procedure, different steps are reported in Fig. 1, where n is the number of articles. During the selection process, inclusion criteria were selected for the study as follows. Studies published in English language, articles published in conferences and peer-reviewed journals, and articles explaining key concepts of such as surrogate measure safety, traffic conflict, severity, near-miss with specifying the method of surrogate measurement. Although for knowing the practical application of surrogate safety measures (SSMs) a technical report, Dissertation was also included in the study. However, non-relevant studies

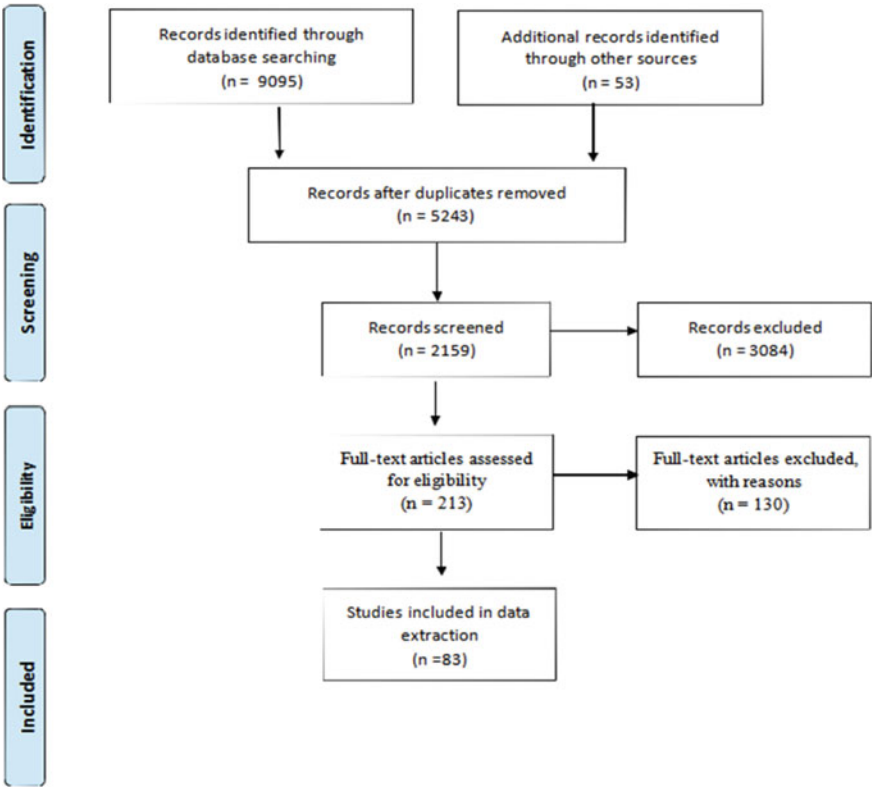

Fig. 1 Flow chart of the inclusion articles in the review (*Source* Liberati et al. [13])

identify as follows. First, all studies focused on surrogate measure safety in medical science dealing with patient safety were excluded. Also, papers focused on crash data identification on road safety were not included (Table 2).

3 Analysis of the Result

This study report is represented in Fig. 2 which depicts the name of the study as well as a list of the journal-reviewed articles that were published. In a systematic literature review, a large number of research studies were published in "Accident analysis and prevention" (Number of studies = 14) and "Technical Report" (Number of report = 9), followed by "conference proceedings" (Number of studies = 9) and "Transportation Research Board" (Number of studies = 8). Furthermore, 43 research studies have been published in 27 national and international journals. The systematic reviews of 83 studies were published in 31 journals and conference proceedings. Figure 3 is showing the evolution of studies over time. The earliest publication

Table 2 Selection of literature review using inclusion and exclusion criteria

Basic criteria	Final decision
Predetermined keyword exit as full or at the minimum in title/abstract part of an article	Inclusion
An article published in a scientific peer-reviewed journal/conference	Inclusion
An article should be written in the English language	Inclusion
Studies presented on traffic conflict technique/ micro-simulation using SSM	Inclusion
An accessible technical report, dissertation	Inclusion
An article is inaccessible, review papers	Exclusion
An article that is duplicated within the database search documents	Exclusion
Papers that are not primary/original research	Exclusion
Studies focus on crash data identification/ surrogate measure in medical science	Exclusion

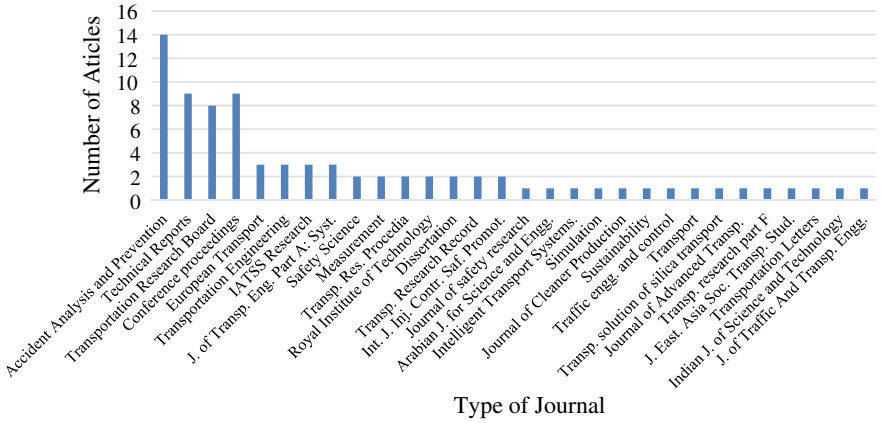

Fig. 2 Number of articles included in each journal's review

included in this study dates back to 1976 [18]. From 1976 to 2004, there was little research published, however, after 2004, the number of studies published increased rapidly, and in recent years published work was at its peak as shown in the graph. This pattern suggests there's a growing interest in the research for surrogate safety measure assessment in road safety.

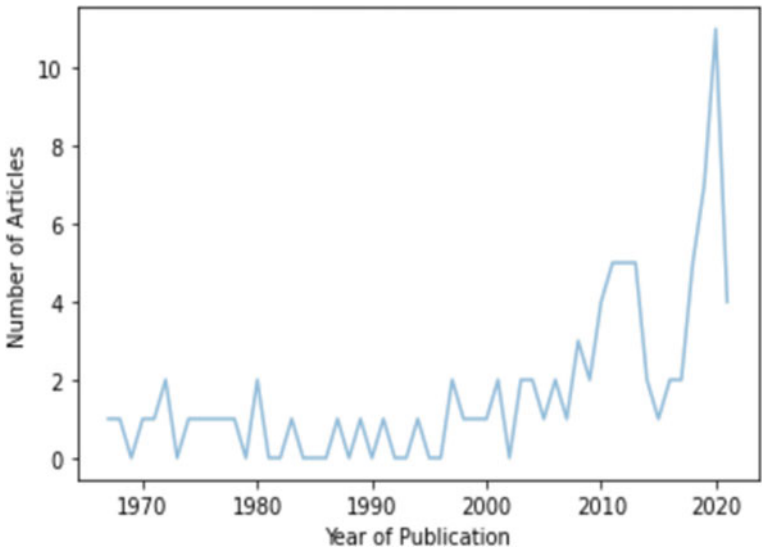

Fig. 3 Evolution of the number of articles over time

3.1 Safety Evaluation Using Surrogate Measures for Motorized and Non-Motorized Traffic

Several researchers applied surrogate measures of safety to alleviate frequent adequate crash data. Studies done by Allen et al. [19] and Cooper [20] used post-encroachment time (PET) as a surrogate measure to do road safety analysis. Also, previous researchers used traffic conflicts as a surrogate safety measure (SSM) for road safety evaluation [21–25] and Chin et al. (1992). Some studies were considered free speeding, aggressive lane merging and risk involving a crash [26, 27] for road safety evaluation. Hayward [28], Minder houd and Bovy [29] used time-integrated Time-to-Collision (TTC) as SSMs for Road safety assessment. Songchitruksa and Tarko [30] estimated the crash frequency based on measured crash proximity using the Extreme Value Method (EVM). The concept of this approach is explained in detail and preliminarily evaluated by Songchitruksa [31], Songchitruksa and Tarko [32], Harwood et al. [33] conducted a comprehensive review of a different intersection in their study, taking into account contributing factors such as vehicular volume, pedestrian volume, roadway crossing width, presence of raised pedestrian crosswalks, pedestrian-signing, median refuge islands, crosswalk markings, crosswalk illumination, raised intersections, and a pedestrified intersection. Preusser et al. [34] showed that allowing right turns on red (RTOR) had a minor influence on pedestrian-right turn vehicle crashes. However, some researchers studied the ability to measure conflict levels in traffic simulation mode [35, 36]. The first workshop conducted by ICTCT (International Co-operation in Traffic Conflict Techniques) was in Oslo city (Norway), the definition was suggested by Amundsen and Hyden [37] "A traffic

conflict is an observable situation in which two or more road users approach each other in space and time to such an extent that there is a risk of collision if their movements remain unchanged". Moreover, the study was done to describe the traffic conflict [38] potential to access near-miss events directly in real-time traffic conditions that provide an accurate way to predict the evaluated number of accidents and outcomes. Laureshyn et al. [39] describe the severity parameter as the closeness of an intersection to collision and various measure of traffic conflict adopted by Allen et al. [19], Gettman et al. [40], are for instance Post Encroachment Time (PET), Encroachment Time (ET), Proportion of Stopping Distance (PSD), Initially Attempted Post Encroachment Time (IAPE), Gap Time (GT) and Deceleration Rate (DR). Chin et al. [22] analyze traffic conflict data (TTC) to investigate the expressway on-ramp merging process. Gettman et al. [40] studied the conflict technique application along with the developed tool "Surrogate Safety Assessment Model" (SSAM) which identifies potential traffic conflicts. Lamm et al. [41] conducted a study, several safety criteria and an evolving composite method were used to assess the safety of two-lane rural roads. Ghanim and Shaaban [42] studied to investigate the feasibility of using SSAM to identify conflicts between pedestrians and vehicles by analyzing simulated trajectories. Kathuria and Vedagiri [43] evaluated the interaction of pedestrians and vehicles by using the pattern-based approach with surrogate measures TTC and PET. Moreover using Import Vector Machine, (IVM) evaluated the severity level at an uncontrolled intersection. Pedestrian safety is a major component of the design of a signalized intersection. Marisamynathan and Vedagiri [44] plotted cumulative frequency distributions to define severity levels, as well as crosswalk PET thresholds between pedestrians and vehicles. PET values of less than 2 s were found to be dangerous, while PET values of 5.5 s were found to be normal.

3.2 Safety Evaluation of Surrogate Safety Measure using Traffic Conflict Techniques

First-time traffic conflict technique (TCT) was conducted by the researcher of General Motors Corporation Laboratories [18] in road safety research. Traffic conflict is an operational tool based on evasive action by road users to avoid collisions on the site. Perkins and Harris [45] analyzed the behavior of road users in accident situations concerning safety. Baker [46], Malaterre and Muhlrad [47] estimated the significant relationship between conflict and crash databased field study, it provides countermeasure before and after the studies. Evasive action was identified by taking sudden action by Braking or lane change by one and more vehicles to avoid collision [19, 48–52].

The proximity between road users can be measured physically in spatial/temporary dimensions, and limits could be used to identify traffic conflicts. The most used surrogate measure indicator is the (TTC) [28], which was defined as "the time for two vehicles to collide if they continue at their present speed and

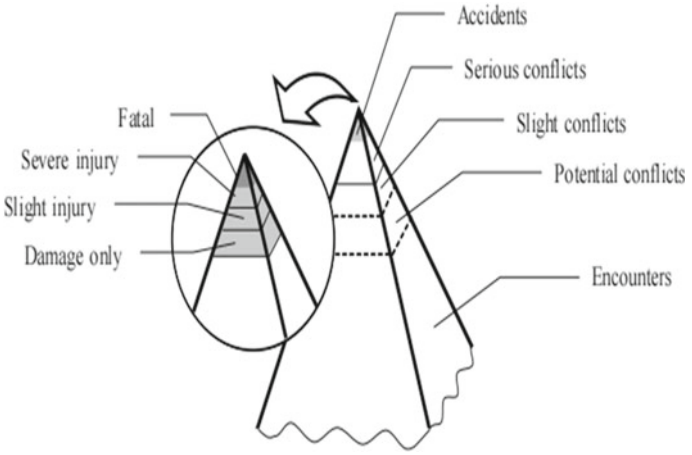

Fig. 4 The safety pyramid (S*ource* Hydén [54])

on the same path" with the proposed time remain potential collision between two vehicles found that if time remains below 1 s, a better criterion for near accidents. There Hydén [53, 54] developed a model to describe the risk of cyclists and pedestrians. Further Campbell and King [55] and Hydén [54] suggested that determines conflict severity from time to crash and time. The relationship between severity and frequency of interaction of road users is illustrated by a pyramid [54]. It describes relationships between traffic conflicts, events in traffic, and accidents, as depicted below in Fig. 4, top of the pyramid depicts the most severe events in traffic such accidents where an accident can divide into injury, fatal, vehicle damage in an accident, however, the decrease accident severity which is increase accident frequency [54, 56]. Sayed [57] observed that a decrease in PET and Delta t (Δt), would increase the conflict severity index (CSI) of critical crossing and rear-end crossing at multiple uncontrolled intersections. Jiang et al. [58] found that conflict consequence severity rates correlate superior with crash data than conventional conflict rates moreover TTC threshold influence correlation where low and high TTC threshold values have low correlation.

Basyouny and Sayed and Shelby [59], investigated the relation between predicted, conflict, and collisions with the proposed model for prediction conflict, Lognormal regression model, along with predict collision conflicts- based negative binomial (NB) regression model on a data set of the average hourly volume of 51 signalized intersection observed that conflict are more significant in the area, conflict is less significant in on minor approach where right turn lane is present. Tarko and Lizarazo [60] investigate crash probability from an observed data set of traffic conflict with Lomax-based method and observed that young male drivers or mature male drivers have involved in high crash probability compared to a mature female driver. Qi et al. [61] analyzed traffic characteristics of lane change merging vehicles using the modified post-encroachment time (PET) with the estimated value of PET < 0.7 s is a

serious conflict, value of PET between 0.7 and 2.25 s is a slight conflict and greater value of PET, 2.25 is a potential conflict. Shekhar Babu and Vedagiri [62] assess safety at an uncontrolled intersection using a risk threshold PET, the speed of the corresponding vehicle, and a proposed critical speed for analyzing critical conflict. It was observed that, aside from the right-turning of intersections, crossing maneuvers are heavily influenced by vehicular dynamic characteristics (TW).

Choudhary et al. [63], Goyani et. al. [64], Naidu and Chhabra [65] and Reddy et al. [66], observed traffic volume and operating vehicle speed have significant effects on crash probability at the uncontrolled intersection while an increase in vehicular speed would occur to lower PET threshold frequency for the reason that increases the spatial gap between moving vehicles. Kumar et al. [67] developed five temporal proximity indicators based on unsupervised K-means clustering to define crash severity levels. The authors found that pedestrian-vehicle conflict severity is influenced by pedestrian crossing behavior and demographic characteristics. Goyani et al. [68] observed proportion of two-wheeler has a significant influence on the percentage of critical conflict. Chaudhari A. [69] identified the risk threshold PET value as highly dependable on vehicular characteristics. It was found that the operating condition of small vehicles has a lower PET threshold in comparison to heavy vehicles because of vehicle maneuverability through the intersection. While adding one more lane or reducing the crossing speed of pedestrians would increase crash probability although the driving environment, as well as intersection geometry have a significant impact on the likelihood of a crash, Pawar et al. [70] found that the likelihood of a crash can be improved by improving the driving environment and road geometric condition, Pawar et al. [70], Shekhar Babu and Vedagiri [62, 71] and Vedagiri and Killi [72] examined vehicular safety on right turn movement at an uncontrolled junction. Paul and Ghosh [73]; Shekhar Babu and Vedagiri [62, 71] evaluated vehicular safety on right turn movement at an uncontrolled intersection. Studies revealed drivers take risks to accept the minimum gap in the conflict stream. Major critical conflicts were found between two-wheelers on through major roads and the right turn movement of heavy vehicles, Paul and Ghosh [73]. Mohanty et al. [74] used the PET threshold to assess severity collisions in the median opening portion of multi-lane divided urban roadways, as well as the critical safe ratio to assess traffic safety.

In mixed traffic, conflicting speeds of consecutively operating vehicles were analyzed, and it was discovered that the risk threshold time-to-collision (TTC) values for lateral headway is much lower than for longitudinal headway, and that maintaining a minimum lateral headway in mixed traffic generates negligible crash probability, according to Naidu and Chhabra [65]. Nadimi et al. [75] found that using a Mix Index (MI) combination of PET and TTC to identify rear-end collision likelihood on a motorway under mixed traffic conditions gives a more accurate result. Mahmud et al. [76] developed the model using the data count modeling process for detecting the likelihood of crashes on a two-lane rural highway. It was observed that the model can predict high-risk sections as well as prioritize road segments as reported by the probability of safety level. Predicting the likelihood of a crash using a model is a less expensive substitute to the collection of accident crash data in order to evaluate black spots on a rural highway.

3.3 Micro-Simulation Studies Based on Surrogate Safety Measures

Micro-simulation tools used in traffic safety widely in recent days is initially investigated by Cooper and Ferguson [77] simulated vehicles where number high traffic conflict. Darzentas et al. [78], Sayed et al. [57] investigated traffic collision risk between vehicles at different unsignalized intersections; Archer [38] develop a modeling of driver behaviors at an urban intersection to access road safety. Gettman and Head [23] investigated to obtain surrogate safety measures (SSMs) from previous simulation model studies along with each SSMs collected based on the occurrence of traffic conflict events, in their work surrogate safety measures are included as Post Encroachment Time (PET), Time-to-Collision (TTC), Deceleration Rate (DR), Speed Differential (Delta S), Maximum Speed (MaxS). where Post Encroachment Time (PET), Deceleration Rate (DR), and Speed Differential (Delta S) are used to measure conflict severity whereas Speed Differential (MaxS) and Maximum Speed (Delta S) are used in the severity of a collision. Furthermore [40] developed surrogate safety assessment software (SSAM) this can be used to analyze conflict and investigate the type of severity based on SSMs like TTC and PET obtained based on simulated vehicles trajectory.

Pirdavani et al. [79] evaluated the safety performance of different vehicle speed limits at an uncontrolled intersection using traffic proximity measure PET, and observed that speed limit and volume increase from both sides of the approach decrease PET value and arguably increase safety risk at the intersection. Ambros et al. [80], Caliendo and Guida [81] and Dijkstra [82] analyzed the relationship between observed crash data and simulated traffic conflict. Fan et al. [83] and Huang et al. [84] analyzed different traffic conflicts such as rear-end, crossing and lane changing by using simulation software VISSIM and SSAM. They found a significant relationship between observed and simulated traffic conflict. Cunto and Saccomanno [85], Ozbay et al. [86], Yang et al. [87] introduced a new surrogate safety indicator is Crash Potential Index (CPI), Modified Time-to-Collision (MTTC) to analyze rear-end traffic collisions and their severity furthermore argued that at the low traffic volume, were difficult to identify a potential conflict. Bachmann et al. [88] suggested a revised definition of TTC for traffic conflict simulation as "two vehicles interact in the same lane for a period of time" using their revised definition of TTC to observe the effect on traffic conflict along with founding that providing separate lane for trucks were reduce truck affiliated conflicts and increase car lane change conflict.

Astarita et al. [89] and Guido et al. [90] used TITRONE Software to estimate Deceleration Rate to Avoid a Crash (DRAC), TTC. Caliendo and Guida [81] investigated traffic conflict using SSAM software at the unsignalized intersection. However critical conflict was identified based on simulation traffic and compared with field data of the intersection. Sayed et al. [91] estimated traffic conflict at unsignalized intersection using proximity indicator TTC analyzes vehicle rear-end as well as merging

conflict. A study done by Giuffrè et al. [92] investigates roundabout safety performance using Software VISSIM and AIMSUN where traffic conflict was examined by SSAM. Astarita and Giofrè [93] was assessing traffic safety at an urban intersection using collision energy as new SSMs moreover examine the validity of new indicators based on a comparison between estimated SSMs from the micro-simulation trajectory and observed real crash data from a different intersection. Bulla Cruz et al. [94] verified event-based risk indicator in which their study evaluate traffic safety of roundabout by their independent techniques: using T-Analyst software Swedish Traffic Conflict Technique and conflict analyst using VISSIM, SSAM and further combination of three methods calibrated safety distance factor in VISSIM conflict area 0.5 along. Moreover, in their study that simulated traffic conflict, the severity value and compare with an observed value. The study was conducted by Alonso et al. [95] to evaluate traffic collisions in their case study based on real-time crash data and simulated data in SSAM in their study found a good correlation between simulated data and real data. Virdia et al. [96] investigated connected autonomous vehicles (CAVs) using micro-simulation techniques with surrogate indicators PET and TTC. In their study author observed that increasing CAV penetration decreases traffic conflict at the roundabout. Kili and Vedagiri [97] analyzed the level of safety at an uncontrolled intersection and found that the PET threshold is quite tiny, ranging from 25 to 40% negative, and the PET threshold 40–50% value is less than 5 s. It was established that the intersection was extremely dangerous and that it needed to be improved. The author also proposed that key preventative measures to be implemented to reduce heavy vehicles during peak hours. Furthermore, Vedagiri and Kili [72] analyzed management measure impact on uncontrolled intersection observed by applying a combination of raised table and rotary give the finest outcome in comparison to a single measure.

4 Conclusion

In recent years, traffic conflict techniques have been frequently employed to assess safety before and after studies, as well as to anticipate real-time safety. The use of multiple surrogate indicators in combination with semi-automated video analysis and traffic conflict methodologies to assess safety is faster, more reliable, and more successful than using past crash data.

There have also been different research discussed on dynamic traffic behavior for conflict, but it was found that most conflict analyzes were done utilizing PET and TTC to estimate conflict and severity, as well as studied the relationship between critical severity and recorded crash data. While some studies established a crash index to define severity level. Whereas existing studies mostly analyze rear-end traffic conflict, mid-block crossing conflict and right-turning conflict on motorized vehicles on urban roads/highways using driver behaviour like Gap acceptance, and lane change to analyze the compressive study. Studies explored the reliability of traffic

conflict techniques that could be improved by the application of micro-simulation techniques and long hour video sensor techniques.

The majority of research is conducted in developed countries with homogeneous traffic flow characteristics. However, in developing countries, driving behavior and traffic characteristics fluctuate due to driver performance and vehicle operating conditions. Apart from that, there is no clear guideline for using surrogate safety measures to assess road safety at the moment. The use of conflict strategies on a rural road with low traffic volume, single-car crashes such as overturns and tire bursts owing to road geometry or vehicle overloading, and a head-on collision appeared to be constrained.

To validate traffic conflict techniques few models were developed which correlate conflict to crashes are extreme value theory and the logarithm regression model although the application of these models in heterogeneous traffic conditions is limited, future work could be done using different surrogate indicators on urban or rural road traffic condition validate their result. Currently, risk-based indicators mostly focused on traffic operational attributes for safety analysis and further could be considered to other attributes of the vehicle and geometric condition of the road.

As previously stated, prior research has primarily focused on the conflict between two road users (motorized vehicle and pedestrian), however, there may be a research gap for a single vehicle and multi-vehicle conflict. Aside from that, the micro-simulation model's implications in a heterogeneous environment are limited due to a lack of experience in this field and a lack of funds. To increase the reliability of traffic conflict methodologies for evaluating road safety, more work on micro-simulation models on non-lane base heterogeneous environments is required. More study is needed on modeling of overtaking vehicle conflicts, single-car overturns, measuring and diverging of the vehicle in non-lane basis traffic conditions on urban and country roads, as well as calibration and validation of conflict approaches.

References

1. World Population Prospects: The 2019 revision. United Nations Department of Economic and social affairs (2019)
2. MoRTH (2019) Road accidents in India. Ministry of Road Transport & Highways, Transport Research Wing, New Delhi
3. World Road Association (2013) PIARC Annual Report–October 2013/ October 2014
4. Alsop J, Langley J (2001) Under-reporting of motor vehicle traffic crash victims in New Zealand. Accid Anal Prev 33:353–359
5. Archer J (2005) Indicators for traffic safety assessment and prediction and their application in micro-simulation modelling: a study of urban and suburban intersections. KTH Royal Institute of Technology
6. Salifu M, Ackaah W (2012) Under-reporting of road traffic crash data in Ghana. Int J Int Control Saf Promot 19:331–339
7. Watson A, Watson BC, Vallmuur K (2013) How accurate is the identification of serious traffic injuries by Police? In: The concordance between police and hospital reported traffic injuries, Proceedings of the 2013 Australasian road safety research, policing & education conference
8. Yang J (2012) Reactive silica transport in fractured porous media: analytical solution for a single fracture. Comput Geosci 38:80–86. https://doi.org/10.1016/j.cageo.2011.0

9. Tarko AP, Davis G, Saunier N, Sayed T, Washington S (2009) Surrogate measures of safety. In: White Paper ANB20 (3) Subcommittee on Surrogate Measures of Safety ANB20 Committee on Safety Data Evaluation and Analysis Contributors. Transportation Research Board
10. Bearman1 M, Dawson P (2013) Qualitative synthesis and systematic review in health professions education. Med Educ 47: 252–260. https://doi.org/10.1111/medu.12092
11. Moher D, Liberati A, Tetzlaff A, Altman D (2009) Preferred reporting items for systematic reviews and meta-analyses: the PRISMA statement. BMJ 339:b2535. https://doi.org/10.1136/bmj.b2535
12. Higgins J, Green S (2011) Cochrane handbook for systematic reviews of interventions Version 5.1.0
13. Liberati A, Altman DG, Tetzlaff J, Mulrow C, Gøtzsche PC, Ioannidis JPA, Clarke M, Devereaux PJ, Kleijnen J, Moher D (2009) The PRISMA statement for reporting systematic reviews and meta-analyses of studies that evaluate healthcare interventions: explanation and elaboration. BMJ 339:b2700
14. Dangelico, Vocalelli D (2017) Green marketing: an analysis of definitions, strategy steps, and tools through a systematic review of the literature. J Clean Prod 165:1263–1279
15. Pahlevan-Sharif S, Murab P, Wijesinghe NR (2019) J Hosp Tourism Manage 39:158–165
16. Arun A, Haque MM, Washington S, Sayed T, Mannering F (2021) A systematic review of traffic conflict-based safety measures with a focus on application context. Anal Methods Accid Res 32, 100185. https://doi.org/10.1016/j.amar.2021.100185
17. Almeida CP, Goular BN (2017) How to avoid bias in systematic reviews of observational studies. Rev CEFAC 19(4):551–555
18. Perkins SR, Harris JL (1967) Criteria for traffic conflict characteristics. Report GMR 632. General Motors Corporation, Warren Michigan
19. Allen B, Shin B, Cooper P (1978) Analysis of traffic conflict and collisions. Transportation research record no. 677, p 67–74
20. Cooper PJ (1983) Experience with traffic conflicts in Canada with emphasis on 'post-encroachment time' technique. In: Proceedings, international calibration study of traffic conflict techniques, Copenhagen, pp 75–96
21. Archer J (2004) Methods for the assessment and prediction of traffic safety at urban intersections and their application in micro-simulation modeling, Royal Institute of Technology
22. Chin H-C, Quek S-T (1997) Measurement of traffic conflicts. Saf Sci 26:169–185
23. Gettman D, Head L (2003) Surrogate safety measures from traffic simulation models: final report. Publication No. FHWA-RD-03–050. Federal Highway Administration, McLean. USA
24. Glauz WD, Migletz DJ (1980) Application of traffic conflict analysis at intersections. In: NCHRP Report 219, Transportation Research Board, National Research Council, Washington, DC
25. Parker MR, Zegeer CV (1989) Traffic conflict technique for safety and operation: engineers guide. Report FHWA-IP-88–026, FHWA, U.S. Department of Transportation
26. Porter BE, Berry TD, Harlow J (1999) A nationwide survey of red light running: measuring driver behaviors for the 'Stop Red Light Running' Program. Report, Daimler Chrysler Corporation
27. Kloeden CN, McLean AJ, Moore VM, Ponte G (1997) Traveling speed and the rate of crash involvement. Volume 1: findings. Report No. CR 172. Federal Office of Road Safety FORS, Canberra
28. Hayward JC (1972) Near-miss determination through use of a scale of danger. Highway Research Board. Report No. HRR 384:24–35
29. Minder houd MM, Bovy PHL (2001) Extended time-to-collision measures for road traffic safety assessment. Acc Anal Prevent 33(1):89–97
30. Songchitruksa P, Tarko A (2006) The extreme value theory approach to safety estimation. Accid Anal Prev 28:811–822
31. Songchitruksa P (2004) Innovative non-crash-based safety estimation: an extreme value theory approach. PhD dissertation, Purdue University, West Lafayette, Indiana

32. Songchitruksa P, Tarko AP (2004) Using imaging technology to evaluate highway safety. Report FHWA/IN/JTRP-2004, Grant No. SPR-2663, Purdue University
33. Harwood DW, Gilmore DK, Richard KR, Dunn JM, Sun C (2008) Passing sight distance criteria. NCHRP Report. Transp Res Board 605
34. Preusser DF, Leaf WA, DeBartolo KB, Blomberg RD (1981) The effects of right-turn-on-red on pedestrian and bicyclist accidents, Report No DOT HS 806:182 Dunlap & Associates Inc Darien Connecticut
35. Davis GA, Hourdos J, Xiong H, Chatterjee I (2011) Outline for a causal model of traffic conflicts and crashes. Accid Anal Prev 43:1907–1919
36. Mak KK, Sicking DL (2003) Roadside safety analysis program (RSAP)—engineering manual. In: National cooperative highway research program report 492. Transportation Research Board of the National Academies, Washington, USA
37. Amundsen F, Hydén C (1977) Proceedings of first workshop on traffic conflicts. Institute of Transport Economics, Oslo, Norway
38. Archer J (2000) Developing the potential of micro-simulation modeling for traffic safety assessment. ICTCT, Corfu, Greece
39. Laureshyn A, Svensson A, Hydén C (2010) Evaluation of traffic safety, based on micro-level behavioral data: theoretical framework and first implementation. Accid Anal Prev 42:1637–1646
40. Gettman D, Pu L, Sayed T, Shelby S (2008) Surrogate safety assessment model and validation: Final report. Report No. FHWA-HRT-08–051. Federal Highway Administration, McLean. USA
41. Lamm R, Psarianos B, Cafiso S (2002) Safety evaluation process for two-lane rural roads: a 10-Year Review, Transp Res Record 1796:51–59.https://doi.org/10.3141/1796-06
42. Ghanim MS, Shaaban K (2018) A case study for surrogate safety assessment model in predicting real-life conflicts. Arab J Sci Eng 44:4225–4231
43. Kathuria A, Vedagiri P (2020) Evaluating pedestrian-vehicle interaction dynamics at un-signalized intersections: a proactive approach for safety analysis. Accid Anal Prev 134:105316
44. Marisamynathan S, Vedagiri P (2020) Pedestrian safety evaluation of signalized intersections using surrogate safety measures. Transport 35(1):48–56
45. Perkins SR, Harris JI (1968) Traffic conflict characteristics: accident potential at intersections. Highway Research Record, vol 225. Highway Research Board, Washington DC, pp 45–143
46. Baker WT (1972) An evaluation of the traffic conflicts technique. In: 51st annual meeting of the Highway Research Board
47. Malaterre G, Muhlrad H (1977) A conflict technique. In Proceedings First Workshop on Trafic Conflicts. Oslo Norway pp 47–58
48. Dingus T, Neale V, Klauer S, Klauer A, Carroll R (2006) The development of a naturalistic data collection system to perform critical incident analysis: an investigation of safety and fatigue issues in long-haul trucking. Acc Anal Prevent 38:1127–1136
49. Phillips RO, Bjørnskau T, Hagman R, Sagberg F (2011) Reduction in car-bicycle conflict at a road- cycle path intersection: evidence of road user adaptation? Transp. Trans Res Part F Traffic Psychol Behav 14:87–95
50. Pugh DE, Halpin TJ (1974) Traffic conflicts in Washington State. Washington State Department of Highways
51. Spicer BR (1971) A pilot study of traffic conflicts at a rural dual carriageway intersection. RRL Report LR410. Road Research Laboratory, Crowthorne
52. Tarko AP. Estimating the expected number of crashes with traffic conflicts and the Lomax Distribution—a theoretical and numerical exploration. Acc Anal Prevent. https://doi.org/10.1016/j.aap.(2018).01.008
53. Hyden C (1975) Relations between conflicts and traffic accidents. Department of Traffic Planning and Engineering, Lund Institute of Technology Lund, Sweden
54. Hydén C (1987) The development of a method for traffic safety evaluation: the Swedish traffic conflicts technique. Bulletin 70, Dept. of Traffic Planning and Engineering, Lund University, Lund, Sweden

55. Campbell RE, King LE (1970) Rural intersection investigation for the purpose of evaluating the General Motors Traffic-Conflicts technique. HRB Spec Rep 107:60–69
56. Svensson Å (1998) A method for analyzing the traffic process in a safety perspective. Dissertation, Lund University
57. Sayed T, Brown G, Navin F (1994) Simulation of traffic conflicts at unsignalized intersections with TSC- Sim. Acc Anal Prev 5(26):593–607
58. Jiang R, Zhu S, Wang P, Chen Q, Zou H, Kuang S (2020) In search of the consequence severity of traffic conflict. J Adv Transp ID 9089817
59. Basyouny K, Sayed T (2012) Safety performance functions using traffic conflicts. Saf Sci 51(2013):160–164
60. Tarko P, Lizarazo CG (2021) Validity of failure-caused traffic conflicts as surrogates of rear-end collisions in naturalistic driving studies. Acc Anal Prevent 149:105863
61. Qi W, Wang W, Shen B, Wu J (2020) A modified post encroachment time model of urban road merging area based on lane change characteristic. IEEE Access
62. Shekhar Babu S, Vedagiri P (2016) Proactive safety evaluation of a multilane unsignalized intersection using surrogate measures. Transp Lett. https://doi.org/10.1080/19427867.2016.1230172
63. Coudhary A, Gore N, Arkatkar S, Joshi G, Pulugurtha S (2020) Exploring pedestrian surrogate safety measures by road geometry at midblock crosswalks: a perspective under mixed traffic conditions, IATSSR 248
64. Goyani J, Pawar N, Gore N, Jain M, Arkatkar S (2019) Investigation of traffic conflict at unsignalized intersection for reckoning crash probability under mix traffic condition. J Eastern Asia Soc Transp Stud 13
65. Naidu B, Chhabra RS. Safety indicators for heterogeneous non lane based traffic—a case study at outer ring road-Delhi 11(10). https://doi.org/10.17485/ijst/(2018)/v11i10/103552
66. Reddy S, Chepuri A, Arkatkar S, Joshi G (2019) Developing proximal safety indicators for assessment of un-signalized intersection—a case study in Surat city. Transp Lett
67. Kumar A, Paul M, Ghosh I (2019) Analysis of pedestrian conflict with right-turning vehicles at signalized Intersections in India. J Transp Eng Part A Syst 145(6):04019018
68. Goyani J, Paul AB, Gore N, Arkatkar S, Joshi, G (2021) Investigation of crossing conflicts by vehicle type at unsignalized t-intersections under varying roadway and traffic conditions in India. J Transp Eng Part A Syst 147(2):05020011
69. Chaudhari A, Gore N, Arkatkar S, Joshi G, Pulugurtha S (2021) Exploring pedestrian surrogate safety measures by road geometry at midblock crosswalks: a perspective under mixed traffic conditions. IATSS Res 45(1):87–101. https://doi.org/10.1016/j.iatssr.2020.06.00
70. Pawar N, Gore N, Arkatkar S (2019) Influence of driving environment on safety at un-signalized T-intersection under mixed traffic conditions. Innov Res Transp Infrastruct
71. Shekhar Babu S, Vedagiri P (2017) Traffic conflict analysis of unsignalized intersection under mix traffic condition. Eur Transp Transporti Europei 66(10)
72. Vedagiri P, Killi VD (2015) Traffic safety evaluation of uncontrolled intersections using surrogate safety measures under mixed traffic conditions. Transp Res Rec 2512(1):81–89
73. Paul M, Ghosh I (2018) Speed-based proximal indicator for right-turn crashes at unsignalized intersections in India. J Transp Eng Part A Syst 144(6):04018024
74. Mohanty M, Panda B, Dey PP (2020) Quantification of surrogate safety measure to predict severity of road crashes at median openings. IATSSR-00257, p 7
75. Nadimi N, Behbahani H, RezaShahbazi H (2016) Calibration and validation of a new time-based surrogate safety measure using fuzzy inference system. J Traffic Transp Eng (English Edition) 3(1):51–58
76. Mahmud SM, Ferreira L, Hoque Md, Tavassoli A (2019) Using a surrogate safety approach to prioritize hazardous segments in a rural highway in a developing country, R-00228, p 10
77. Cooper DF, Ferguson N (1976) Traffic studies at T-junctions: 2. a conflict simulation model. Traffic Eng Control 17(7):306–309
78. Darzentas J, Cooper DF, Storr PA, McDowell MRC (1980) Simulation of road traffic conflicts at T. junctions. Simulation 5(34):155–164

79. Pirdavani A, Brijs T, Bellemans T, Wets G (2010) Evaluation of traffic safety at un-signalized intersections using micro simulation: a utilization of proximal safety indicators. Adv Transp Stud Int J Sect A
80. Ambros J, Turek R, Paukrt J (2014) Road safety evaluation using traffic conflict: pilot comparison of micro-simulation and observation. In: International conference on traffic and transport engineering, Belgrade (2014)
81. Caliendo C, Guida M (2012) Micro simulation approach for predicting crashes at unsignalized intersections using traffic conflicts. J Transp Eng 138:1453–1467
82. Dijkstra A (2010) Do calculated conflicts relate to observed crashes? Retrieving conflicts from S-Paramics. In: The 10th Annual S-Paramics user group meeting & conference
83. Fan R et al (2013) Using VISSIM simulation model and surrogate safety assessment model for estimating field measured traffic conflicts at freeway merge areas. IET Intell Transp Syst 7(1):68–77
84. Huang F, Liu P, Yu H, Wang W (2013) Identifying if VISSIM simulation model and SSAM provide reasonable estimates for field measured traffic conflicts at signalized intersections. Accid Anal Prev 50:1014–1024
85. Cunto F, Saccomanno FF (2008) Calibration and validation of simulated vehicle safety performance at signalized intersections. Accid Anal Prev 3(40):1171–1179
86. Ozbay K, Yang H, Bartin B (20008) Derivation and validation of a new simulation-based surrogate safety measure. Transportation Research Board's 87th Annual Meeting, Washington, DC
87. Yang H, Ozbay K, Bartin B (2010) Application of simulation-based traffic conflict analysis for highway safety evaluation. Proc 1098 12th WCTR, July 11–15, Lisbon
88. Bachmann C, Roorda MJ, Abdulhai B (2011) Simulating traffic conflicts on truck-only infrastructure using an improved time-to-collision definition. In: 90th transportation research board annual meeting (CD-ROM), Transportation Research Board, Washington, DC
89. Astarita V et al (2012) A new microsimulation model for the evaluation of traffic safety performances. Eur Transp (51):1–16
90. Guido G, Saccomanno F, Vitale A, Astarita V, Festa D (2011) Comparing safety performance measures obtained from video capture data. J Transp Eng 137:481–491
91. Sayed T, Zaki MH, Autey J (2013) Automated safety diagnosis of vehicle–bicycle interactions using computer vision analysis. Saf Sci 59:163–172 https://doi.org/10.1016/j.ssci.2013.05.009
92. Giuffrè O, Granà A, Tumminello M, Giuffrè T, Trubia S, Sferlazza A, Rencelj M (2018) Evaluation of roundabout safety performance through surrogate safety measures from micro simulation. J Adv Transp 2018(4915970):14
93. Astarita V, Giofrè VP (2020) Trajectory perturbation in surrogate safety indicators. Transp Res Proc 8
94. Bulla-Cruz LA, Laureshyn A, Lyons L (2020) Event-based road safety assessment: a novel approach towards risk microsimulation in roundabouts. Measurement 165:108–192
95. Alonso B, Astarita V, DelÍOlio L, Giofré VP, Guido G, Marino M, Sommario W, Vitale A, (2020) Validation of simulated safety indicators with traffic crash data. Sustain 12:925. https://doi.org/10.3390/su12030925
96. Virdia N, Grzybowskaa H, Wallera S, Dixit V (2019) A safety assessment of mixed fleets with connected and autonomous vehicles using the surrogate safety assessment module. Acc Anal Prevent 131:95–111
97. Killi DV, Vedagiri P (2014) Proactive evaluation of traffic safety at an unsignalized intersection using micro simulation. J Traffic Logist Eng 2(2)
98. Paul M, Ghosh I (2021) Development of conflict severity index for safety evaluation serve crash type at unsignlized intersection under mix traffic condition. Saf Sci 144:105432

Effects of Bus Stops on Pedestrian Safety at Signalized Intersections

Srinivas Geedipally

Abstract Of all road users, pedestrians are considered the most vulnerable mainly due to the lack of body protection, mass, and speed. There are many factors that affect the occurrence of a pedestrian involved crash—exposure (e.g., pedestrian and traffic volume), injury severity (e.g., speed and vehicle type), roadway and environment (e.g., proximity to bus stops, presence/proximity of facilities (store, building, school)) and intersections. Among the factors, the presence and proximity of transit bus stops are the distinctive risk factors in the pedestrian involved crashes in urban areas. The objective of this study is to understand the influence of bus stop locations on pedestrian safety near signalized intersections. To accomplish the study objectives, pedestrian safety data collected at a sample of signalized intersections in Texas were used and a safety performance function was developed. It was found that bus stops within 300 ft from the center of the intersection increase pedestrian crashes by 48%. Other variables that also had an influence on pedestrian safety are entering vehicular volume, pedestrian crossing volume, the maximum number of lanes crossed by a pedestrian at an intersection, and left-turn signal phasing.

Keywords Pedestrian crashes · Safety performance functions · Crash modification factors · Bus stops · Signalized intersections · Negative binomial model

1 Introduction

Of all traffic fatalities worldwide, 22% of them are pedestrians [1]. This ratio is much higher in developing countries. In pedestrian crashes, millions of people are injured while walking, and a part of them become permanently disabled. In the United States, 6,283 people were killed in pedestrian/motor vehicle crashes in 2018, an increase of 3.4% from 2017 [2]. On average, a pedestrian was killed every 84 min, equivalent to around 120 people a week [2]. When compared to passenger vehicle occupants, on each trip, pedestrians are 1.5 times more likely to be killed in a car crash [3].

S. Geedipally (✉)
Texas A&M Transportation Institute, Arlington, USA
e-mail: srinivas-g@tti.tamu.edu

L. Devi et al. (eds.), *Proceedings of the Sixth International Conference of Transportation Research Group of India*, Lecture Notes in Civil Engineering 273,
https://doi.org/10.1007/978-981-19-4204-4_8

Importantly, more pedestrian fatalities occurred at non-intersections (74%) than at intersections (17%) in the country [2].

Of all road users, pedestrians are considered the most vulnerable mainly due to the lack of body protection, mass, and speed [4]. There are many factors that affect the occurrence of a pedestrian involved crash—exposure (e.g., pedestrian and traffic volume), injury severity (e.g., speed and vehicle type), roadway and environment (e.g., proximity to bus stops, presence/proximity of facilities (store, building, school)) and intersections [5–10]. Among the factors, the presence and proximity of transit bus stops are the distinctive risk factors in the pedestrian involved crashes in urban areas [6, 11]. The objective of this study is to understand the characteristics associated with the pedestrian crashes near signalized pedestrians. More specifically, this paper evaluates the role of bus stops within the vicinity of signalized intersections on pedestrian crashes.

2 Background

Having an understanding of roadway characteristics, exposure measures and traffic control devices that affect pedestrian crash frequency and severity are correlated with pedestrian crashes could assist in identifying locations with high potential for crashes.

Haleem et al. [7] used a mixed logit model and identified factors that affect pedestrian crash injury severity at signalized and unsignalized intersections using a mixed logit model. Their study used three years of pedestrian crash data from Florida (2008–2010) and included a total of 3038 pedestrian crashes. The study only included state roads and the authors recommended that additional research is needed for local roads. The following variables were associated with pedestrian severity risk for signalized intersections.

- Traffic volume,
- Speed limit,
- Trick percentage,
- Senior pedestrians,
- At-fault pedestrians,
- Rainy conditions. and
- Dark conditions.

Jermprapai and Srinivasan [12] reported on a planning-level model for assessing pedestrian safety. The study results were similar to other studies about the relationship between crashes and transportation, socioeconomic and land use characteristics. They found that a low-income location in a higher-income county is one of the riskiest factors. They also concluded that there is a high-risk at locations that have a larger volume of conflicting vehicular and pedestrian movements.

According to Haleem et al. [7], as annual average daily traffic (AADT) at signalized intersections increases, so does the probability of severe injuries, due to the

increased number of vehicle–pedestrian conflicts. Zahabi et al. [9] also found that pedestrian crashes at intersections have a lower probability of injury or fatality; intersection-related pedestrian crashes were 1.21 times less likely to result in a fatality than non-intersection-related pedestrian crashes. One possible explanation for this finding is that motorists operate at lower speeds near intersections. It could also be because both drivers and pedestrians are more likely to expect to interact at intersections, so they pay closer attention.

Passenger vehicles are more frequently involved in crashes with pedestrians, although other vehicles like trucks, buses, and emergency vehicles in pedestrian crashes cause more injuries that are severe or fatal. Trucks, vans and buses category are responsible for almost twice the percentage of crashes that resulted in a fatality, compared to passenger vehicles [5]. This finding is supported by Zahabi et al. [9] who found that trucks, vans, and buses involved in crashes resulted in more fatalities compared to passenger vehicles; the risk of pedestrian fatality is 1.2 higher with trucks and vans in a fatal crash. Hu and Cicchno [8] found that the increase in SUV-related fatal single-vehicle–pedestrian crashes was larger than the increases in the other vehicle types (such as cars, vans, pickups, or medium/heavy trucks). Zahabi et al. [9] also found that after controlling for other factors, a vehicle moving in a straight direction is significantly associated with 1.42 times higher risk of a fatality than a pedestrian crash involving a turning vehicle.

Crashes involving at-fault pedestrians were found to be associated with greater pedestrian injury severity than crashes where the driver was at-fault [7]. Alcohol and drug use by a pedestrian is also associated with higher pedestrian injury severity among pedestrian involved crashes [5]. According to Valaar et al. [13], 41% of pedestrians killed in crashes tested positive for alcohol in the U.S. The authors stated that though positive alcohol results among fatally-injured pedestrians have decreased, the numbers of total pedestrians with alcohol use remain as high as 40% based on 2012 Canada data, similar to that of the U.S. results. Additionally, 86.2% of the fatally-injured pedestrians who consumed alcohol had a blood alcohol content (BAC) of over 0.08 g/dL, which is the legal limit to operate a motor vehicle in Canada and the United States. Furthermore, 67.6% had registered BAC of over 0.16 g/dL, which is twice the legal limit, putting such pedestrians at a high level of risk in terms of crash involvement.

A study by Lindsay [14] analyzing fatal crashes in Australia from 2008 to 2010 found that out of 1,490 crash victims admitted to hospitals, alcohol tests were conducted for 1,204. Of that, a positive alcohol result was seen in 274 persons (18%). Additionally, among the people who has a positive result, alcohol impairment was particularly an issue with pedestrians (56%) compared to drivers (24%). When alcohol or drug use is present among pedestrians involved in crashes, a larger percentage of crashes result in injury or fatality. However, alcohol and drug use among pedestrians and other vulnerable road users has not been a much-studied issue when compared to drivers [5].

2.1 Roadway & Environment Characteristics

Zahabi et al. [9] found that the probability of a pedestrian fatality is affected by road type. Pedestrian crashes on arterial roads have a 1.12 times higher risk of fatality, compared to crashes on local roads. In 2002, McMahon et al. [15] analyzed pedestrian crashes that involved walking along the roadway. The researchers found that roadway characteristics such as higher traffic volume, higher speed limit, and lack of sidewalks/wide walkable areas all contributed to significantly higher crash risk for pedestrians.

Crash predictive models developed by Zeeger and Bushell [10] showed that multiple factors are associated with a greater probability of pedestrian crashes. The authors found that pedestrian crashes are more likely to occur:

- on higher traffic volume roads
- on roads with higher volumes of pedestrians
- at intersections where the ratio of minor road traffic and major road traffic is larger
- as the number of lanes to cross increases without the presence of a refuge island
- at intersections with a bus stop within 1000 feet
- within 1000 feet of a public or private school
- as the number of alcohol retail establishments within 1000 feet increases.

Pedestrian fatal crash risk also increased with exposure of pedestrians and increased traffic for signalized crossings. Other factors associated with increased pedestrian fatality risk included "a greater number of lanes, lack of a raised median or median island (for multi-lane roads), and for older pedestrians (65 years and older)" [10]. In multi-lane roads with higher volumes of traffic, there was a higher association between the presence of marked untreated (i.e., without any other traffic control devices) crosswalks and pedestrian crashes, in comparison to just the presence of unmarked crosswalks [10].

According to a study by Clifton et al. [5], over half of the pedestrians involved in crashes and two-thirds killed in crashes are not in crosswalks at the time of the crash. At unsignalized intersections, the presence of crosswalks and road surface conditions are significant predictors of pedestrian injury severity. When present, marked crosswalks are associated with a reduction in pedestrian injury severity, possibly by alerting drivers in advance.

Haleem et al. [7] in Florida identified environmental predictors of pedestrian injury severity using a mixed logit model. Significant environmental predictors identified in signalized intersections included weather and lighting conditions, and the hour of the crash. Significant environmental predictors related to pedestrian involved crashes identified at unsignalized intersections included dark lighting conditions and dry road surface conditions. The probability of severe injury is associated with night-time and dawn, both periods when there is poor visibility and high vehicle speeds [7]. This was true for both signalized and unsignalized intersections. However, pedestrian severity was found to be higher at unsignalized intersections. Also, rainy weather is associated with higher injury severity, possibly due to visibility restrictions and/or inability to

stop or slow before the collision [7]. Similarly, Zahabi et al. [9] found that pedestrian crashes occurring in the dark after sunset resulted in a higher probability of injury or fatality. The likelihood of fatality in pedestrian crashes after dark increased by 1.45 times according to their study.

Similar to the findings of Haleem et al. [7] and Zahabi et al. [9], Uttley and Foios [16] found that pedestrians faced increased risk in the roadway, especially in the dark. Interestingly, the researchers found that this risk increased when using a crosswalk in the dark compared to the crossing at non-crosswalk locations. The researchers attribute this to the confidence that pedestrians feel when using the crosswalks, where they are likely to overestimate their visibility to drivers on the road.

A noteworthy result found by Zahabi et al. [9] is that pedestrian crashes close to schools or parks had a significant association with crash severity. For example, pedestrian crashes around a school resulted in 1.13 times less likelihood of a severe injury or fatality, possibly due to the placement of calming traffic measures like lower speed limit around schools. However, if a pedestrian crash occurred around a park, the probability of fatality increased by 1.25 times, suggesting a need for calming traffic measures around parks just like in schools [9].

2.2 Transit/Bus Stop Characteristics

Among the factors affecting pedestrian involved crashes, the pedestrian crossing's proximity to transit bus stops is more likely to increase a pedestrian crash risk. Torbic et al. [17] developed the pedestrian safety prediction methodology of vehicle–pedestrian collisions at signalized intersections. The methodology includes crash modification factors associated with the number of bus stops, the presence and proximity of schools, the number of alcohol sales establishments, and neighborhood income level within 1000 ft. from the intersection. For the number of bus stops within 1000 ft. from the intersection, the pedestrian–vehicle collisions increased by up to 4 times at an intersection with one or more bus stops relative to an intersection without bus stops.

Specifically related to transit bus stops, the risk of pedestrian crashes increased with the number of bus stops around an intersection [18, 19]. A study by Walgren [19] presented that 89% of high crash locations were within 150 ft of a bus stop and 90% of these locations were within 70 ft of a crosswalk. The higher risk of pedestrian involved crashes near bus stops can be related to increased distraction and poor yielding behavior [6]. Craig et al. [6] analyzed whether the presence of a bus stop influences a driver yielding behavior to pedestrians at marked unsignalized crosswalks compared with other locations and whether a High-Visibility Enforcement (HVE) affects a driver yielding behavior. At the sixteen crosswalks in Saint Paul, MN, a driver yielding behavior to a pedestrian improved with HVE. In addition to HAV, Craig et al. [6] conducted public outreach and educational activities to increase awareness of pedestrian laws and safety tips for local residents and drivers,

and concluded that community outreach has been shown to measurably improve yielding behaviors to pedestrians at the studied crosswalks.

Although the proximity of transit bus stops leads to an increased risk of pedestrian involved crashes, the risk is not equal to all bus stops. Ulak et al. [11] developed a bus Stop Safety Index (SSI) to quantify and access pedestrian safety around bus stops for the purpose of screening the urban roadway network and identifying the high-risk bus stops similar with that of the Safety Performance Functions (SPFs) in the Highway Safety Manual. Ulak et al. [11] analyzed the pedestrian involved crashes in Palm Beach County, FL, and then each bus stop was assigned an SSI score based on injury severities and the spatial distance between the bus stop and the pedestrian involved crash. Then SSI scores are tabulated by using socio-demographic factors (i.e., median income, population), traffic indicators (i.e., traffic volume and speed), the proximity of facilities (i.e., supermarket, hospital, school), and bus stop metrics (i.e., daily boarding and frequency). Using the factors, the high-risk bus stops can be prioritized.

In addition to the location of bus stops, the design of bus stops can be influential on the risk of pedestrian involved crashes. Fitzpatrick and Nowlin [20] analyzed the effect of bus stop design (i.e., curbside versus bus bay/open bus bay, and queue jumper versus no queue jumper, as shown in Fig. 1) on travel time, speed and traffic volume. Results indicated that the bus bay and queue jumper design provided better benefits for traffic flow at the intersection.

Fitzpatrick and Nowlin [20] concluded that the collisions are more likely to occur when a transit stop is located immediately prior to an intersection (near-side transit stop) rather than immediately after passing through an intersection (far-side transit stop) as shown in Fig. 2. At intersections, near-side transit stops can increase the number of conflict points between the transit vehicles and right-turning vehicles. However, the far-side stop design may result in the intersections being blocked during peak hours by stopping buses or may obscure sight distance for crossing vehicles/pedestrians [21]. In addition, the presence of transit signal priority (TSP) technology at an intersection increased the probability of transit-involved collisions.

Miranda-Moreno et al. [22] investigated the relationship between pedestrian activity and the built environment and found that pedestrian activity is highly related to the number of bus stops and the presence of rail transit. In consequence, the frequency of pedestrian collision at signalized intersections significantly increased with the number of bus stops as well as traffic and pedestrian volume, intersection configuration (4-legged or 3-legged), and land use (commercial area).

Although previous research had studied the role of bus stops on the pedestrian crash risk, the effect on the number of crashes is not accurately quantified. In addition, not many previous studies included the signal characteristics in the regression models. This study tries to fill the knowledge gap by including the signal characteristics and bus stop presence among other variables in the model and presents the crash modification factor (CMF) for each variable.

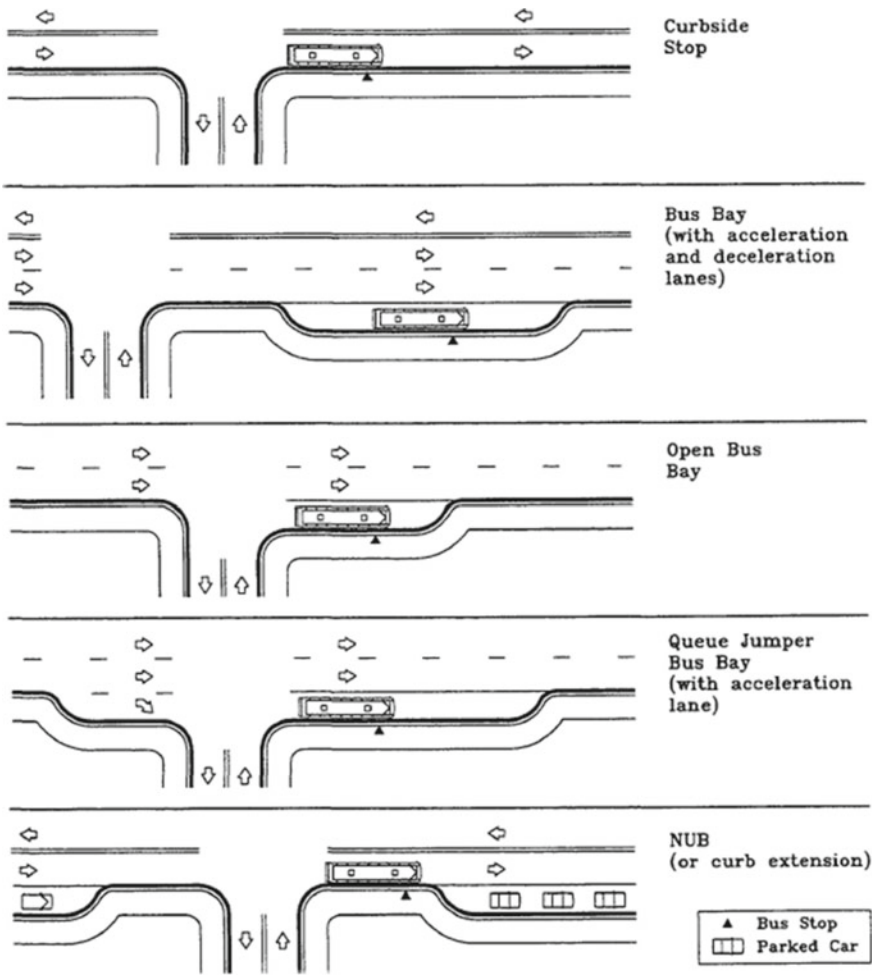

Fig. 1 Bus stop design [21]

3 Data Description

To provide a better understanding of the relationship between various intersection characteristics and pedestrian safety performance, it was first necessary to assemble a comprehensive database. As a part of this study, data were assembled for a sample of signalized intersections spanning over multiple years in Texas from multiple different sources. In total, 621 signalized intersections in four metropolitan cities (Houston, San Antonio, Austin and Dallas-Fort Worth) were randomly selected. Traffic volumes were obtained using the 2018 Texas Department of Transportation (TxDOT's) Road Inventory Network (i.e., RHINO) data.

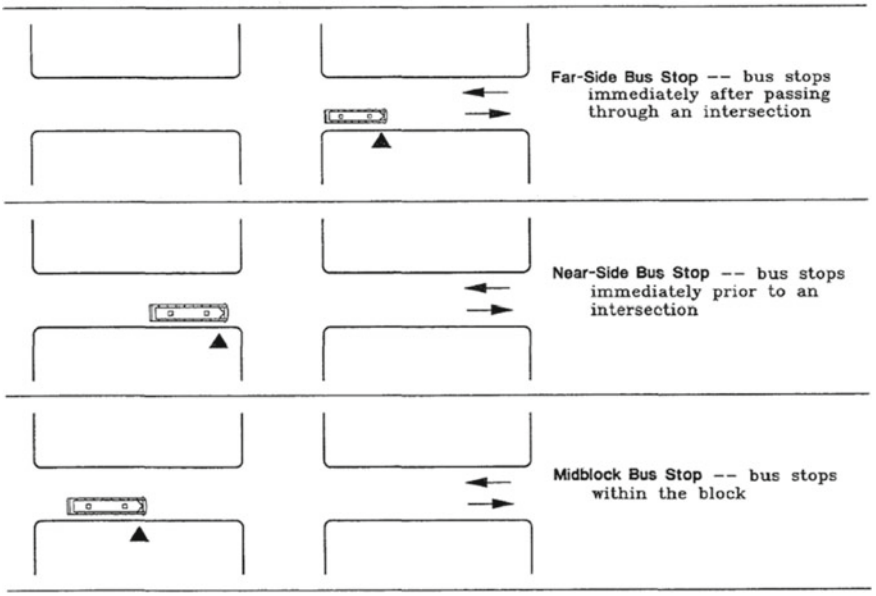

Fig. 2 Example of far-side, near-side, and midblock stops [21]

Intersection characteristics such as presence in the central business district (CBD), adjacent land uses (i.e., commercial, single and multifamily, industrial, and vacant), light rail stop presence, bus stop presence, sidewalks, and special generators within 300 ft of the intersection were extracted from aerial photography. Generally, the variables were quantified within the 300 ft buffer of the intersection. However, it was found that many of the school's coordinates did not locate them within the 300 ft buffer and given the number of potential pedestrians around schools, a variable that reflects the proximity of schools (K-12 and higher education) was created. The number of schools within ¼, ½, and 1 mile of each intersection, and along with the available street network, were counted. The number of lanes crossed by a pedestrian at an intersection is counted for all legs. The maximum number of lanes is then used in the model to quantify the distance a pedestrian needs to walk during a particular signal phase.

The most important variable that influences pedestrian safety is pedestrian volume. We conducted 2 h pedestrian counts at intersections in addition to the 24 h counts at two signalized intersections in each city. The 2 h counts were often started in the middle of a clock-hour (e.g., 1:30–3:30 pm), such that the expansion factors, time durations, and counts within each clock-hour needed to be considered separately. This approach was chosen based on a balancing of the competing objectives of (1) obtaining pedestrian volume estimates at a reasonable number of sites in each city and (2) obtaining estimates that are robust and defensible. The 24 h pedestrian count site was used to obtain a distribution of pedestrian volumes throughout the day, such

Table 1 Summary statistics for signalized intersections

Variable	Minimum	Maximum	Mean	Std. deviation
Major street AADT (vehicles per day)	460	72,868	23,336	14,269
Minor street AADT (vehicles per day)	70	67,599	7193	7615
Pedestrian crossing volume (pedestrian per day)	10	22,044	1169	2349
Maximum number of lanes crossed	2	10	4.67	1.32
Indicator for presence bus stops within 300 ft	0	1	0.88	0.33
Indicator for protected signal operation	0	1	0.59	0.49
Maximum posted speed limit (miles/h)	25	50	35.2	4.8
Pedestrian crashes	0	8	1.14	1.25
Number of intersections	621			

that expansion factors could be derived for each hour of the day. These adjustment factors are used to obtain daily volumes at every intersection.

All fatal to possible injury (KABC) pedestrian-related crashes were obtained for the years 2017–2019 from TxDOT's Crash Record Information System (CRIS). Only crashes that were identified as TxDOT reportable are included in the analysis. TxDOT reportable is defined as a crash occurring on a public roadway and resulting in death or injury or $1,000 in damage. About 3% of the crashes were missing location coordinates. Various techniques were used to geo-code them based on available information such as street name, intersecting street, block number, etc. so that the dataset was as complete as possible. Descriptive statistics for important variables are provided in Table 1.

4 Modeling Results

The proposed model coefficients were estimated using the NLMIXED procedure in the SAS software (SAS, 2015). The negative binomial (NB) distribution log-likelihood function was used to determine the model coefficients. Different variable combinations and various model forms were examined to identify the best possible relationship between crash frequency and independent variables. The model presented below was informed by findings from several preliminary regression analyzes. This model form includes variables that are intuitive, in-line with previous findings and best fit the data. The predicted average pedestrian crash frequency of a signalized intersection is calculated as shown below.

$$N_i = N_{base} \times CMF_{ltph} \times CMF_{lanesX} \times CMF_{bus}. \quad (1)$$

$$N_{base} = n \times e^{b_0 + b_1 \ln(TotEntVol) + b_2 \ln(PedVol)}. \quad (2)$$

with,

$$CMF_{ltph} = e^{b_{pt} \times I_{pt}}.$$

$$CMF_{lanesX} = e^{b_{lanesX}(n_{lanesX}-4)}.$$

$$CMF_{bus} = e^{b_{bus} \times I_{bus}}.$$

where,

N_i = predicted annual average crash frequency at intersection i,

I_{pt} = protected signal phasing indicator variable (=1.0 if protected, 0.0 otherwise),

$TotEntVol$ = Total entering vehicular volume from all approaches (=$AADT_{\text{Major}} + AADT_{\text{Minor}}$ if 4-leg; =$AADT_{\text{Major}} + AADT_{\text{Minor}}/2$ if 3-leg),

$PedVol$ = Total pedestrian crossing volume for all legs combined,

n_{lanesX} = Maximum number of traffic lanes crossed by a pedestrian (in any crossing maneuver) at the intersection,

I_{bus} = presence of bus stop within 300 ft of the intersection,

b_i = calibration coefficient for variable i.

The variable coefficients for signalized intersections are presented in Table 2. Some variables that are not statistically significant at the 5% level are included if they are intuitive and within logical boundaries. Although many other signal characteristics such as signal cycle length, pedestrian push button type, and walk length were considered, they were not statistically significant in the model.

Table 2 Calibrated coefficients for pedestrian crashes at signalized intersections

Coefficient	Variable	Int. type	Value	Std. Dev	t-statistic	p-value
b_0	Intercept	4-Leg	−4.8428	1.0113	−4.79	<0.0001
		3-Leg	−5.0672	1.0126	−5	<0.0001
b_1	Total entering vehicle vol.	All	0.2272	0.09336	2.43	0.0152
b_2	Pedestrian vol.	All	0.1955	0.03172	6.16	<0.0001
b_{pt}	Protected signal phasing	All	−0.1881	0.1016	−1.85	0.0646
b_{lanes}	Max. number of lanes crossed	All	0.06504	0.04067	1.6	0.1103
b_{bus}	Bus stop presence	All	0.3897	0.1598	2.44	0.015
k	Inverse dispersion parameter	All	0.4018	0.1063	3.78	0.0002
Number of intersections						621

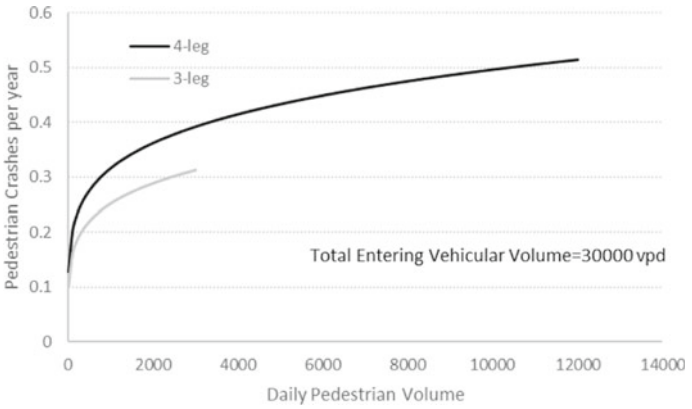

Fig. 3 Predicted crashes at different types of signalized intersections

The relationship between pedestrian crash frequency and pedestrian demand for base conditions, as obtained from the calibrated models, is illustrated in Fig. 3 for signalized intersections.

4.1 Crash Modification Factors

The following paragraphs present the CMFs for the variables significant in the model.

Intersection Left-Turn Signal Phasing. The base condition for this CMF is permissive or permissive/protected left-turn signal phasing. The CMF is determined as:

$$CMF_{ltph} = e^{-0.1881 \times I_{pt}}. \tag{3}$$

The CMF values are presented in Table 3. During the permissive phase, drivers mostly concentrate on the opposite direction vehicles to find a gap and often miss seeing the pedestrian crossing the street. This results in an increased chance for pedestrian crash occurrence. The results show that protected signal phasing reduces crashes by 17%.

Number of Lanes. This variable represents the maximum number of traffic lanes crossed by a pedestrian (in any crossing maneuver) at the intersection. The base

Table 3 CMF for left-turn signal phasing

Left-turn signal phasing	CMF
Permissive	1.00
Protected/Permissive	1.00
Protected	0.83

Table 4 CMF for number of lanes

Maximum number of lanes crossed	CMF
2	0.88
4	1.00
6	1.14
8	1.30
10	1.48

Table 5 CMF for bus stop presence

Bus stop present	CMF
No	1.00
Yes	1.48

condition for this CMF is four lanes. This CMF is applicable for all signalized intersections. Table 4 presents the relationship between the number of lanes and pedestrian crash frequency.

Bus Stop Presence. The base condition for this CMF is the absence of bus stops within 300 ft from the center of the intersection. This CMF is applicable for all signalized intersections. Table 5 presents the relationship between the presence of bus stops and pedestrian crash frequency.

5 Conclusions

Pedestrians are more likely than passenger vehicle occupants to sustain fatal or severe injuries in a vehicle–pedestrian collision. Identifying the high-risk locations (or hot-spots) is an important step to reduce the pedestrian crashes. In the traditional hot-spot identification process, crashes that occurred on a highway network or a geographical area are routinely considered. Since pedestrian crashes are rare and random, the traditional approaches could potentially identify very few to no sites where pedestrian crashes might occur. Crash prediction models (also called SPFs) play a critical role in predicting the number of pedestrian crashes that occur at a site. This study developed the SPFs for signalized using the Texas intersection data. The variables that are found to be significant in influencing the pedestrian crashes at intersections are the following.

- Sum of major and minor street AADT,
- Intersection left-turn signal phasing,
- Pedestrian crossing volume,
- Presence of a bus stop within 300 feet from the center of the intersection, and
- Maximum number of lanes crossed by the pedestrian.

The study results showed that the presence of a bus stop within the vicinity of an intersection increases pedestrian crashes by 48%. In addition, if the bus stop is present at an intersection with 10 lanes on a particular street, then the pedestrian crashes increase by 119% when compared to a four-lane street with no bus stops. Similarly, the results suggest that the agencies should try to avoid constructing bus stops if the signal left-turn operation is permissive. The results of this study will assist the planners in their safety activities and identifying hazardous signalized and stop-controlled intersections. It is recommended to conduct further research to explore the transferability of the SPFs in this study to other geographical and if an adjustment factor is needed.

Acknowledgements The author is grateful to TxDOT for sponsoring the data collection project and to the Center for Transportation Safety at Texas A&M Transportation Institute for sponsoring a project to conduct data analysis. The conclusions are those of the author only and may not necessarily reflect the views of the sponsors. Additionally, the author is grateful to Michael Pratt and Myunghoon Ko for their assistance in the data collection.

References

1. WHO (2013) Pedestrian safety: a road safety manual for decision-makers and practitioners. WHO, Geneva
2. NHSTA. Traffic safety facts-2018 fatal motor vehicle crashes: overview. U.S. Department of Transportation, National Highway Traffic Safety Administration. https://crashstats.nhtsa.dot.gov/Api/Public/ViewPublication/812826. Accessed 11 Nov 2020
3. Beck LF, Dellinger AM, O'Neil ME (2007) Motor vehicle crash injury rates by mode of travel, United States: using exposure-based methods to quantify differences. Am J Epidemiol 166:212–218
4. Li D, Ranjitkar P, Zhao Y, Yi H, Rashidi S (2017) Analyzing pedestrian crash injury severity under different weather conditions. Traffic Inj Prev 18(4):427–430
5. Clifton KJ, Burnier CV, Akar G (2009) Severity of injury resulting from pedestrian–vehicle crashes: what can we learn from examining the built environment? Transp Res Part D 14:425–436
6. Craig CM, Morris NL, Houten RV (2019) Pedestrian safety and driver yielding near public transit stops. Transp Res Rec: J Transp Res Board 2673(1):514–523
7. Haleem K, Alluri P, Gan A (2015) Analyzing pedestrian crash injury severity at signalized and non-signalized locations. Accid Anal Prev 81:14–23
8. Hu W, Cicchino JB (2018) An examination of the increases in pedestrian motor vehicle crash fatalities during 2009–16. Insurance Institute for Highway Safety, Arlington, VA
9. Zahabi SAH, Strauss J, Manaugh K, Miranda-Moreno LF (2011) Estimating potential effect of speed limits, built environment, and other factors on severity of pedestrian and cyclist injuries in crashes. Transp Res Rec: J Transp Res Board 2247:81–90
10. Zeeger CV, Bushell M (2012) Pedestrian crash trends and potential countermeasures from around the world. Accid Anal Prev 44(1):3–11
11. Ulak MB, Kocatepe A, Ozguven EE, Kumar A (2021) A stop safety index to address pedestrian safety around bus stops. Saf Sci 133
12. Jermprapai K, Srinivasan S (2014) Planning-level model for assessing pedestrian safety. Transportation Research Record No. 2464, pp 109–117

13. Valaar W, Hing MM, Brown S, McAteer H, Crain J, McFaull S (2016) Fatal and serious injuries related to vulnerable road users in Canada. J Saf Res 58:67–77
14. Lindsay VL (2012) Characteristics of alcohol impaired road users involved in casualty crashes. In: Australasian road safety research, policing and education conference 2012, 4–6 October 2012, Wellington, New Zealand
15. McMahon PJ, Zegeer CV, Duncan C, Knoblauch RL, Stewart JR, Khattak AJ (2002) An analysis of factors contributing to "Walking Along Roadway" crashes: research study and guidelines for sidewalks and walkways (FHWA-RD-01-101). Federal Highway Administration, McLean, VA
16. Uttley J, Fotios S (2017) The effect of ambient light condition on road traffic collisions involving pedestrians on pedestrian crossings. Accid Anal Prev 108:189–200
17. Torbic DJ, Harwood DW, Bokengroger GD, Srinivasan R, Carter D, Zegeer CV, Lyon C (2010) Pedestrian safety prediction methodology for urban signalized intersections. J Transp Res Board 2198:65–74
18. Harwood DW, Bauer KM, Richard KR, Gilmore DK, Graham JL, Potts IB, Torbic DJ, Hauer E (2008) Pedestrian safety prediction methodology. Publication NCHRP Project 17–26. Transportation Research Board, Washington DC
19. Walgren S (1998) Using geographic information system (GIS) to analyze pedestrian accidents. In: Paper presented at 68th annual meeting of the institute of transportation engineers, Toronto, ON, Canada
20. Fitzpatrick K, Nowlin RL (1997) Effects of bus stop design on suburban arterial operations. Transp Res Rec 1571:31–41
21. Transit Cooperative Research Program (TCRP) (1996) Report 16. Guidelines for the location and design of bus stops. Transportation Research Board, National Academy Press, Washington, DC
22. Miranda-Moreno LF, Morency P, El-Geneidy AM (2011) The link between build environment, pedestrian activity and pedestrian–vehicle collision occurrence at signalized intersections. Accid Anal Prev 43(2011):1642–1634

Identifying Habitual Driving Styles of Heavy Passenger Vehicle Drivers Using Driving Profile Data

Jahnavi Yarlagadda and Digvijay S. Pawar

Abstract This study aims to explore the range of driving patterns and the habitual driving styles exhibited by 33 professional HPV drivers. The driving data is collected using a high-frequency (10 Hz) GPS device for multiple trips in a naturalistic environment. The data is segmented as events of accelerations and decelerations and a similar pattern of events is identified using the K-means clustering technique. Further, the principal component analysis revealed that the identified five driving patterns are characterized by the level of acceleration/deceleration behavior, speed behavior and speed consistency during the maneuver. The results show that, each driving pattern represents a unique driving behavior and drivers are exhibiting a minimum of three patterns within the driving period. The proportion of patterns are changing within and among the individuals showing intra-driver and inter-driver behavioral variability. The study insights are useful in developing driver specific safety models accounting for the heterogeneity in driving patterns.

Keywords Acceleration profiles · Driving behavior · Exploratory analysis · K-means clustering

1 Introduction

Road traffic fatalities result in 1.35 million deaths every year in the world and India accounts for approximately 11% of the total accident related deaths [1]. The Indian ministry of road transport and highways reported a total of 449,002 road accidents killing almost 151,113 people in the year 2019 [2]. The statistics related to the causes of accidents show the fault of the driver as a major cause in 82% of accidents and over-speeding is the dominating traffic violation [2]. A study conducted on road

J. Yarlagadda · D. S. Pawar (✉)
Transportation Systems Engineering, Department of Civil Engineering, Indian Institute of Technology Hyderabad, Kandi, Medak 502285, India
e-mail: dspawar@ce.iith.ac.in

J. Yarlagadda
e-mail: ce17resch11013@iith.ac.in

L. Devi et al. (eds.), *Proceedings of the Sixth International Conference of Transportation Research Group of India*, Lecture Notes in Civil Engineering 273,
https://doi.org/10.1007/978-981-19-4204-4_9

traffic accidents in Bhutan [3] stated that human factors (87%) are the leading cause of accidents, in which careless driving and drunk driving are the significant causes. Similar studies across the world indicated that, approximately 90% of road crashes resulted due to the fault in driver behavior [4, 5]. Driving behavior indicates the manner of drivers' decisions in maneuvering the vehicle. The pattern of executing various maneuvers is termed as driving patterns or driving styles, and many studies aimed to classify the driving patterns/styles.

Surprisingly, most of the literature on driving style classification was dealt predominantly on passenger car drivers and no studies are found on the bus or heavy passenger vehicle drivers. As per the Ministry of Road Transport and Highways, buses (HPV) share about 6.6% of road accidents, which are resulting in 43,000 person injuries in India [6]. Across the world, non-collision injuries are significant in number and are as important as crash injuries [7, 8]. The non-collision injuries indicate the passengers falling or stumbling by standing in moving buses and result mainly from the forces exerted to the occupants by horizontal acceleration and deceleration maneuvers [7–9]. The sudden acceleration or deceleration may result in a risk of injury to the standing passengers, even when there is no traffic crash [10]. The driving style of bus drivers is a significant aspect which influences the risk of losing balance or injury for the standing passengers [11]. Thus, the present study aimed to explore the acceleration and deceleration behavior of bus (HPV) drivers. The data is collected using a high-frequency (10 Hz) GPS instrumentation in real-road driving conditions.

The next section of the paper details the literature review and the third section presents data collection and data extraction techniques. The fourth section presents the methodology and the fifth section details the results of clustering and principle component analysis. The sixth section details the visualization of driver behavioral heterogeneity. The conclusions and future scope of the work are discussed in the last section of the paper.

2 Literature Review

The definition of driving style or the driving pattern used across the studies is not uniform and is subjected to change concerning the objectives of the research (safety, comfort and economy) [12]. In this study, the literature on driving style classification from the perspective of road safety is detailed and the research gaps are highlighted.

The driving styles or the driving patterns were initially conceptualized using a set of questionnaires which captures the self-reported frequency of driving errors and violations [13–15]. The questionnaires were modified over years across the countries and widely used to differentiate driving styles [16, 17]. The questionnaire based assessment was subjective and found to be prone to reporting bias and also lacks the real-time driving performance data. Thus, the real-time driving data was collected by instrumenting the vehicle with multiple sensors. The 100-car naturalistic driving study (NDS) was the first large-scale study, which captured 43,000 h of driving data

corresponding to 241 drivers [18]. As part of the 100-car study, an event database was developed which details the critical incidents, near-crashes, and crashes observed over the study period. The frequency of crash and near-crash rate was considered as a means of assigning risk-level to individuals to classify drivers concerning driving safety [19, 20]. Similarly, some studies classified drivers based on the recorded crash and near-crash data and examined the correlation with the respective driving performance features such as maximum deceleration and jerk [21, 22]. The drivers associated with high crash or near-crash rates exhibited significant variation in driving performance data, which further guided the research to conceptualize the driving styles using driving performance features.

Constantinescu et al. [23] analyzed the abstract driving performance features related to speed and acceleration over the entire trip to classify the drivers. The abstract driving data of 23 drivers were compared against two additional test drivers and the drivers were classified into five groups indicating non-aggressive to aggressive driving styles. Similarly, Johnson and Trivedi [24] classified driving styles based on the pre-defined thresholds of critical driving events recorded using a smartphone-based application. Few studies constructed a g-g diagram and defined the safety domains for classifying the driver behavior [25, 26]. The frequency of data points exceeding the safety domain was considered as a means to assign safe or unsafe characterization to individuals. Murphey et al. [27] characterized the driving styles as calm, normal, and aggressive using the jerk feature on 11 standard drive cycles. The trial and error based reference thresholds were used for classification, which was related to fuel efficiency. In these studies, the driving style assessment was predominantly dependent on the pre-defined ground truth used to identify critical maneuvers. Moreover, the thresholds used across the studies were not consistent.

Given the lack of a uniform basis to define the thresholds, few studies used machine learning techniques to classify driving styles [28–30]. Kalsoom and Halim [28] clustered the driving simulator data using hierarchical and k-means techniques and grouped driving styles into slow, normal, and fast categories. The features like maximum and average speed, number of brakes, and number of horns were aggregated over the entire trip and used as clustering attributes. Similarly, Mantouka et al. [29] clustered the aggregated driving performance features and categorized the trips into six levels of safety. The percentage of mobile usage, speeding, number of harsh brakes and harsh accelerations were considered as the cluster attributes. The authors emphasized the need for a personalized feedback system, as the stability in driving behavior was observed to be low from one trip to another. Fugiglando et al. [30] introduced a new approach based on a set of CAN bus signals and their derived statistical features to cluster the individuals. The derived feature of each signal was clustered independently using k-means clustering. However, the complexity in driving behavior is not well indicated by the univariate approach. Few studies explored the driving patterns using multivariate techniques, representing the driver behavior by means of the combination of driving features [31, 32]. Higgs and Abbas [31] segmented the driving profiles into car-following periods and the corresponding state-action variables were clustered using k-means clustering. The authors used the driving profile data of 10-car and 10-truck drivers collected as part of the 100-car

naturalistic driving study. The authors reported a total of 30 clusters representing different driving patterns and the proportion of patterns was observed to be varied from one driver to another. Chen and Chen [32] analyzed the base-line event data recorded as a part of the SHRP-2 study and represented each event using a set of derived features of speed and acceleration. The authors classified the base-line events into three groups, representative of the habitual driving styles. However, these studies considered the driving style/driving pattern to be uniform for the entire trip and also the driving pattern variations in the individual are still not conclusive.

In most of the studies, the drivers were classified using the pre-defined thresholds of either subjective or objective performance measures and also, the driving style is assumed to be uniform throughout the driving period. Also, the drivers and driving styles were characterized by a single score or classification of safe or aggressive for the entire trip. Very limited research is available which speaks of individual's driving pattern variations within the trip. It is worth noting that, the nature of driving decisions depends not only on the external conditions but also on the driver specific factors like driving skills and personality traits. The variability in the driving environment and driver attributes manifests the existence of various driving patterns within the driving period [31, 33]. Therefore, the application of the same set of thresholds over the aggregated data for each driver neglects the diversity in driving patterns [34]. This motivates the present study to explore the variety of driving patterns exhibited by each driver without any pre-defined thresholds.

Considering the research gaps, the present study objectives are formulated as follows: (1) To identify the existence of various driving patterns exhibited by heavy passenger vehicle drivers (2) To explore the habitual driving styles of individuals and present the driver behavior variation at intra & inter-driver-level.

3 Data Collection and Data Extraction

3.1 Study Stretch and Instrumentation

Over years, various techniques and a variety of sensors are used to collect the driver behavior data under different driving states. However, capturing all the influencing factors with respect to driving states and human behavior is a challenging task [31]. So, this study considered the most fundamental motion attributes of driving i.e., speed and acceleration [26], which represent the kinematic behavior of the vehicle on road.

The study route chosen for this study is a 23 km stretch on a four-lane divided national highway (NH-65) near Hyderabad city (India). A high-frequency global positioning system (GPS) instrumentation (Video VBox—HD2) is used to capture the continuous driving profiles in the naturalistic driving environment over a defined road stretch. The instrumentation consists of a GPS data logger supported by two-video cameras (Fig. 1). The data logger provides the kinematic data, positional coordinates,

Fig. 1 The instrumentation and camera positions in the study vehicles

and synchronized video data at a frequency of 10 Hz. The data was collected for 33 different professional heavy passenger vehicle drivers. The selected HPV's had a seating capacity for 35–40 passengers, and the occupancy during data collection varied from 70 to 100%.

The selected drivers were middle-aged (25–40 years) having a driving experience of minimum five years. The drivers were not imposed of any speed restrictions, but rather instructed to drive as they would naturally do. Total of 33 drivers participated in the study, in which the multiple-trip data was collected for 5 drivers (20 trips each), and the single trip data was collected for 28 drivers. A total of 142 trip data was considered for analysis after eliminating GPS errors. More details regarding the data collection and data extraction can be found in [35].

3.2 Event Data Extraction

The methodology of the present study is designed to differentiate driving patterns based on the nature of longitudinal accelerations and decelerations performed during the trip. Thus, an algorithm is designed for segmenting the driving profiles into events of acceleration and deceleration maneuvers. The identified maneuvers are termed as events, which are characterized using a set of features shown in Table 1. The features are selected based on the existing literature to reflect the drivers' decisions [31, 32].

The process of segmentation is depicted in Fig. 2 [35]. In the first step of segmentation, the acceleration and deceleration maneuvers are identified by referencing the speed profile. The segments of the speed profile with a positive slope are considered

Table 1 Performance features of acceleration and deceleration events [35]

Feature description	Variable
Minimum speed (kmph)	V_{min}
Maximum speed (kmph)	V_{max}
Change in speed (kmph)	ΔV
Duration of event (sec)	ΔT
Mean speed (kmph)	V_{mean}
Standard deviation of speed	V_{sd}
Maximum longitudinal acceleration/deceleration (g)	LA_{max}/LA_{min}
Mean longitudinal acceleration/deceleration (g)	LA_{mean}
Standard deviation of longitudinal acceleration/deceleration	LA_{sd}
Maximum yaw rate (°/s)	Yr_{max}

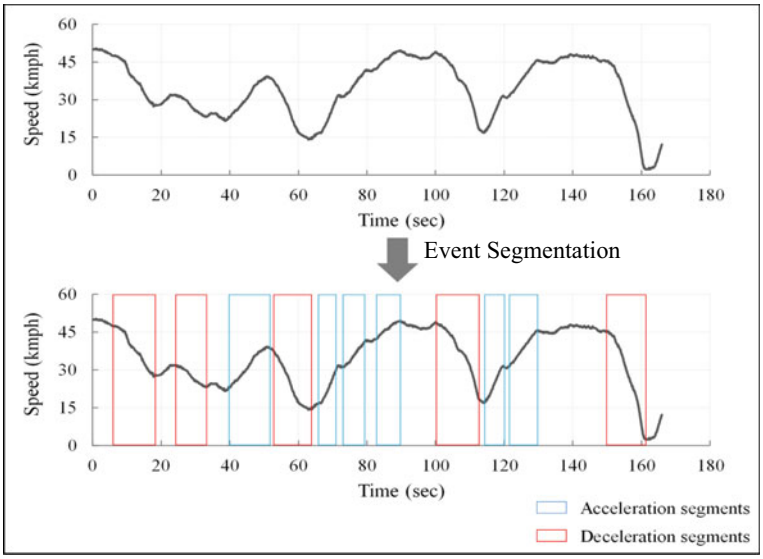

Fig. 2 Illustration of segmentation process [35]

under accelerations and the negative slope segments are categorized under decelerations. For all the segmented events, the corresponding characteristic features (see Table 1) are extracted from the respective profile data [35].

In the second step, the insignificant maneuvers corresponding to lower speed values (less than 15 kmph) and small speed fluctuations (less than 5 kmph) are eliminated. The limitations on the speed value and the change in speed are to eliminate the events corresponding to congested situations and to avoid the arbitrary fluctuations.

In the third step, the free decelerations resulting from the release of the acceleration pedal are separated from the braking events. In this condition, the segments with deceleration values less than 0.05 g are deducted. These thresholds are framed based on the manual video observation of 300 randomly chosen acceleration and deceleration events. The final dataset consists of 8295 acceleration events and 7151 deceleration events corresponding to 142 driving profiles. As each event is a multi-dimensional element, the data should be scaled prior to clustering. In this study, the Z-score standardization is used, which standardizes the data using the mean and standard deviation of the respective feature. The algorithm for event extraction and data preparation is coded in Python 3.7. The detailed process of event data segmentation can be found in [35].

4 Methodology

4.1 Overview of the Proposed Method

The methodology is developed to group similar patterns of accelerations and decelerations and interpret the attributes of different groups. The dataset contains a number of events characterized by the respective driving performance features. As there are no pre-defined-labels, the acceleration and deceleration events are analyzed using unsupervised machine learning techniques to cluster similar events. After the groups are identified, the principal component analysis is performed on the event dataset to reduce the dimensionality and identify the correlation between principal components and the features. Finally, the meaning of each cluster is interpreted using the attributes which speak of major variation between the groups. The R statistical software is used to perform clustering and principal component analysis. The methodology of the current study is shown in Fig. 3.

4.2 Multivariate K-means Clustering

Clustering is a machine learning technique which is used to group the unlabeled data based on the intrinsic similarity. As per the literature on driving style classification, the hierarchical, fuzzy k-means and K-means are the popular algorithms used for the classification of unlabeled performance data. Among these, k-means was observed to outperform the other clustering methods [28]. Thus, in this study, we used the multivariate K-means clustering technique, which groups “n” data points into “k” clusters based on the minimum Euclidean distance to the centroids. The optimal k value is decided based on indices such as WSS (within cluster sum of squares) and average silhouette value which measures the cluster compactness.

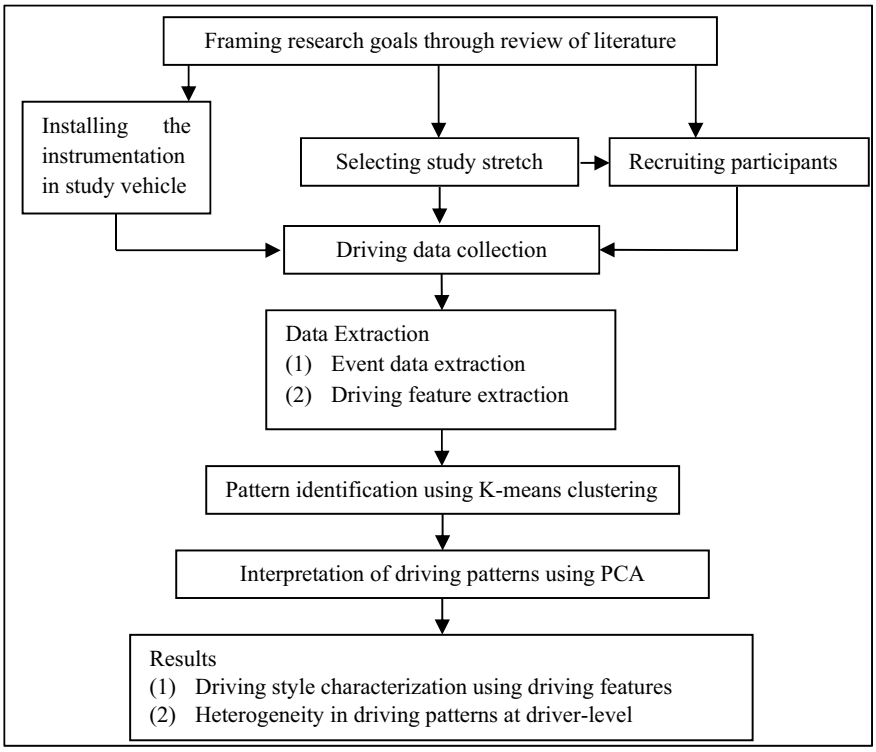

Fig. 3 Study methodology for identifying driving styles

4.3 Principal Component Analysis

The results of the clustering yield 'k' distinct groups and the respective centroids. In the current data set, the centroids are 10-dimensional in nature representing the centers of ten driving performance features. To facilitate the interpretation of this high-dimensional data, the principal component analysis (PCA) is performed after clustering. PCA is a dimensionality reduction method where the original features are transformed into a set of uncorrelated variables termed as principal components (PC). In order to understand the meaning of PCs, the loadings are computed which shows the correlation between the PCs and original features. Higher loadings represent stronger correlations between features and the respective PCs.

5 Results

5.1 Clustering Results

In this study, the acceleration and deceleration events are considered as independent datasets for clustering similar patterns. The driving performance data is scaled using the Z-standardization technique prior to performing cluster analysis. Given that the datasets are unlabeled, the optimal number of clusters should be determined in advance to group the data. The K-means algorithm is repeated multiple times for a different number of clusters ranging from 2 to 15, and the corresponding average total within cluster sum of squares (TWSS) and silhouette values are obtained. Thus, considering the results of both elbow curve and silhouette values, an optimal k value of 5 is chosen for both acceleration and deceleration datasets. The silhouette values are computed for individual clusters and shown in Fig. 4a, b.

In the case of both acceleration and deceleration datasets, there are a few negative silhouette points under different clusters. However, the positive average silhouette values of all the clusters indicate good separation from neighboring clusters. Thus, k-means clustering is performed with an optimum k value of 5 on both datasets. The clusters are formulated based on the intrinsic similarity of events in ten-dimensional space. The centroids of acceleration and deceleration clusters are shown in Table 2.

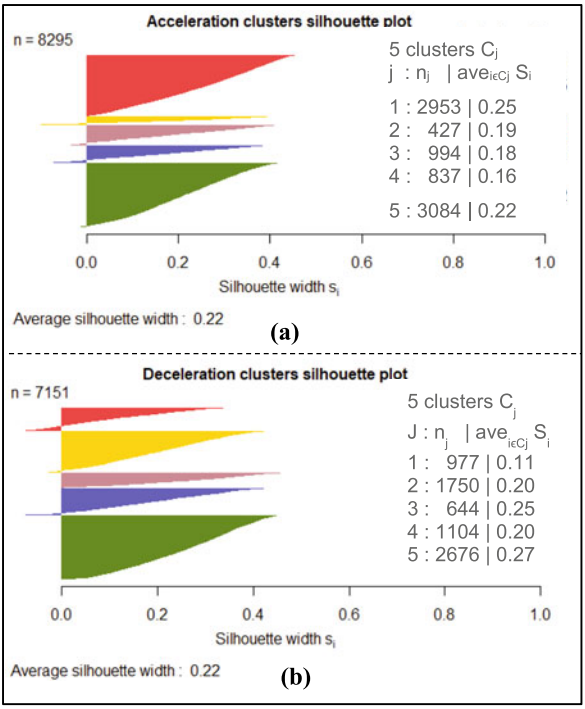

Fig. 4 Silhouette values of (**a**) acceleration clusters and (**b**) deceleration clusters

Table 2 Centroids of acceleration and deceleration clusters

Acceleration clusters	V_{min}	V_{max}	ΔV	ΔT	V_{mean}	V_{sd}	LA_{max}	LA_{mean}	LA_{sd}	Yr_{max}
AC1	44.73	53.19	8.45	7.70	38.81	13.36	0.16	0.06	0.04	7.63
AC2	24.03	41.74	17.71	3.58	34.78	12.94	0.48	0.19	0.13	20.63
AC3	22.66	45.73	23.07	16.46	34.22	13.20	0.22	0.07	0.05	14.54
AC4	6.38	23.30	16.92	7.41	29.81	12.85	0.29	0.10	0.07	36.61
AC5	21.42	30.79	9.37	5.44	31.77	12.90	0.21	0.08	0.05	12.70
Deceleration clusters	V_{min}	V_{max}	ΔV	ΔT	V_{mean}	V_{sd}	LA_{min}	LA_{mean}	LA_{sd}	Yr_{max}
DC1	19.60	35.88	16.28	4.74	34.28	13.79	0.39	0.14	0.10	19.24
DC2	10.59	22.00	11.40	5.38	29.26	13.81	0.24	0.09	0.06	22.25
DC3	46.03	56.35	10.32	7.29	51.73	7.02	0.21	0.08	0.05	7.89
DC4	12.20	45.63	33.43	13.70	33.87	14.32	0.31	0.11	0.07	21.07
DC5	38.74	48.74	10.01	7.02	35.34	14.87	0.19	0.07	0.05	8.49

The obtained clusters are a representation of driving performance indicated by ten driving features, whose values are varying across the clusters. Given the lack of standards against the levels of driving features, we need to know (a) the set of driving performance features that differentiates driving patterns and (b) the levels of features to characterize the driving performance. Thus, the clustering is followed by PCA for better interpretation of the clusters through dimensionality reduction.

5.2 PCA Results

The principal component analysis is performed on both acceleration and deceleration datasets. The original features are transformed to a set of principal components (PC), such that the variance explained by the successive PCs is maximized. A minimum of 80% variance in the data is considered as a limit to choose the PCs [23]. In the case of both acceleration and deceleration datasets, we have chosen four PCs, as these are explaining 84.3% and 85.6% of the variance respectively. For both the datasets, most of the features are cross-loaded on each PC, thus the Varimax rotation is used to aid the interpretation [36]. The "varimax" function in the R statistical software is used to rotate the loadings. The rotated component (RC) loadings of acceleration and deceleration datasets are shown in Table 3. The stronger correlations between original features and rotated components are represented by the higher absolute loading values, which are highlighted in bold in Table 3.

In the case of the acceleration dataset, RC1 is showing a high positive correlation with the acceleration related features (Table 3). The RC2 is positively correlated with the maximum and minimum speed over the event, and negatively correlated with the

Table 3 The rotated component loadings of acceleration and deceleration events

RC loadings of acceleration events					RC loadings of deceleration events				
Features	RC1	RC2	RC3	RC4	Features	RC1	RC2	RC3	RC4
V_{min}	−0.210	**0.926**	−0.181	−0.073	V_{max}	−0.088	**−0.898**	−0.307	−0.013
V_{max}	−0.080	**0.932**	0.235	−0.078	V_{min}	−0.304	**−0.871**	0.246	−0.042
ΔV	0.309	−0.206	**0.877**	0.007	ΔV	0.373	0.104	**−0.869**	0.049
ΔT	−0.308	0.094	**0.897**	−0.001	ΔT	−0.198	−0.036	**−0.929**	−0.006
V_{mean}	0.010	0.482	0.004	**−0.634**	V_{mean}	0.042	**−0.670**	−0.026	−0.120
V_{sd}	−0.039	−0.070	−0.006	**−0.912**	V_{sd}	0.009	0.098	−0.027	**0.989**
LA_{max}	**0.935**	−0.158	0.117	0.016	LA_{min}	**0.920**	0.126	−0.169	0.001
LA_{mean}	**0.913**	−0.195	−0.080	0.022	LA_{mean}	**0.917**	0.163	0.019	0.018
LA_{sd}	**0.957**	−0.129	−0.042	0.015	LA_{sd}	**0.947**	0.125	0.040	−0.005
Yr_{max}	0.360	**−0.675**	0.273	−0.008	Yr_{max}	0.306	**0.716**	−0.236	−0.048

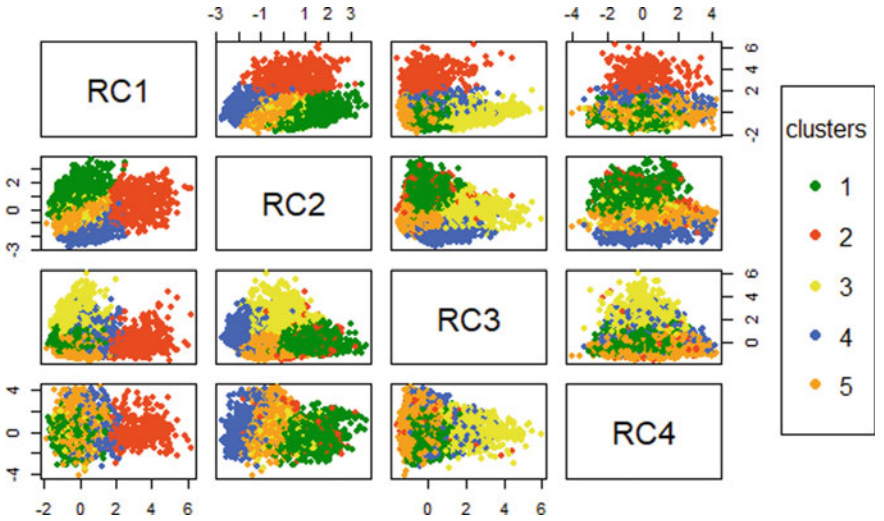

Fig. 5 The scatter plots of the clustered points after Varimax rotation for acceleration events

respective maximum yaw rate. The RC3 shows a significant positive correlation with the duration of the event and the change in speed, whereas RC4 is negatively correlated with the mean speed and the standard deviation of speed. To summarize, RC1 speaks of longitudinal acceleration behavior and RC2 explains the speed choices and steering action. RC3 indicates the speed surge exhibited over the full duration of the event and RC4 shows the variability in speed behavior or the consistency in driving speed over the acceleration event.

To understand the variation among the clusters and to interpret the underlying pattern of each cluster, the bi-plots of RCs are developed. Figure 5 shows the two-dimensional visualization of clustered data points (rotated component scores) scattered over pairs of rotated components. To interpret the variation among clusters, RCs are segmented based on the separation exhibited by clusters. The first row of the plot (Fig. 5) shows the variation of RC1 against RC2, RC3 and RC4. Similarly, the consequent rows show the variation of each RC against the others.

RC1 is taking values from −2 to 6, in which clusters 1, 3 and 5 have a lower limit of −2 and cluster 2 has an upper limit of 6. Cluster 4 is ranging from −0.5 to 2.5 and other clusters are showing separations at 1.5 and 2. By analyzing the separations and the values of RC1, three levels are assigned to RC1 representing three levels of longitudinal acceleration behavior which are: low (−2 to 1.5), moderate (1.5 to 4) and high (>4).

RC2 exhibits positive correlations with the speed related features and negative correlation with the yaw rate, thus the higher values of RC2 represents high speed and low lateral steering actions. RC2 is ranging from −3 to 3.5, in which cluster 4 has a lower limit of −3 and cluster 1 has an upper limit of 3.5. The other clusters are changing over −2 to 2.5 showing separations at −1.5, 0 and 1.5, thus with the similar segmentation approach, RC2 can be considered under four levels representing the speed behavior as: very low (−3 to −1.5), low (−1.5 to 0), moderate (0 to 1.5) and high speed (>1.5).

RC3 is varying over −2 to 6, representing the state of driving and the level of traffic interruption. Clusters 2 and 5 are observed to have a lower limit of −2, and cluster 3 shows an upper limit of 6. The other clusters are ranging from −1 to 4 parting at 0.5, 1 and 2. By observing the partitions and correlation with the features, three levels are suggested in the case of RC3 indicating, low (−2 to 1), medium (1 to 4) and high (>4) traffic interruption.

RC4 is varying from −4 to 4 and shows a negative correlation with speed variation exhibited over the event. The higher the RC4 value, the lower is the variation in speed and thus higher speed consistency. Cluster 1 and cluster 5 have a lower limit at −4 and upper limits at 2 and 4 respectively. Cluster 4 is ranging from −2 to 4, and other clusters change from −1.5 to 3 with the separation at 2. Thus, RC4 is divided into three levels representing the speed consistency such as: low (−4 to −2), moderate (−2 to 2) and high (>2). The details of segmented levels of rotated components and the respective share of clusters are summarized in Table 4.

Similarly, the deceleration clusters are interpreted with the help of rotated loadings and bi-plots of rotated components. The rotated loadings of the deceleration dataset (see Table 3) indicates that the deceleration features are highly correlated with RC1, the speed features and yaw rate are correlated with RC2, the duration of event and speed reduction are negatively correlated with RC3 and the speed variance is positively correlated to RC4. Further relation between clusters and rotated components can be interpreted from Fig. 6. The segmentation process for deceleration events is done in a similar manner as explained for acceleration events. The detailed segmentation of rotated components of the deceleration database is presented in Table 4.

Table 4 The segmentation of rotated components of acceleration and deceleration datasets

Acceleration RCs	Segmentation	Clusters
RC1	Low (−2 to 1.5) Moderate (1.5 to 4) High (>4)	1, 3, 4, 5 2, 4, 5 2
RC2	Very low (−3 to −1.5) Low (−1.5 to 0) Moderate (0 to 1.5) High speed (>1.5)	4, 5 2, 3, 4, 5 1, 2, 3, 5 1, 2
RC3	Low (−2 to 1) Moderate (1 to 4) High (>4)	1, 2, 4, 5 1, 2, 3, 4 3
RC4	Low (−4 to −2) Moderate (−2 to 2) High (>2)	1, 5 1, 2, 3, 4, 5 2, 4, 5
Deceleration RCs	Segmentation	Clusters
RC1	Low (−2 to 1) Moderate (1 to 3) High (>3)	2, 3, 4, 5 1, 3, 4 1
RC2	High (−3 to −1) Moderate (−1 to 2) Low (>2)	1, 3, 5 1, 2, 3, 4, 5 2
RC3	High (−5 to −2) Moderate (−2 to 1) Low (>1)	4 1, 2, 3, 4, 5 1
RC4	Low (−4 to −2) Moderate (−2 to 2) High (>2)	2, 3 1, 2, 3, 4, 5 5

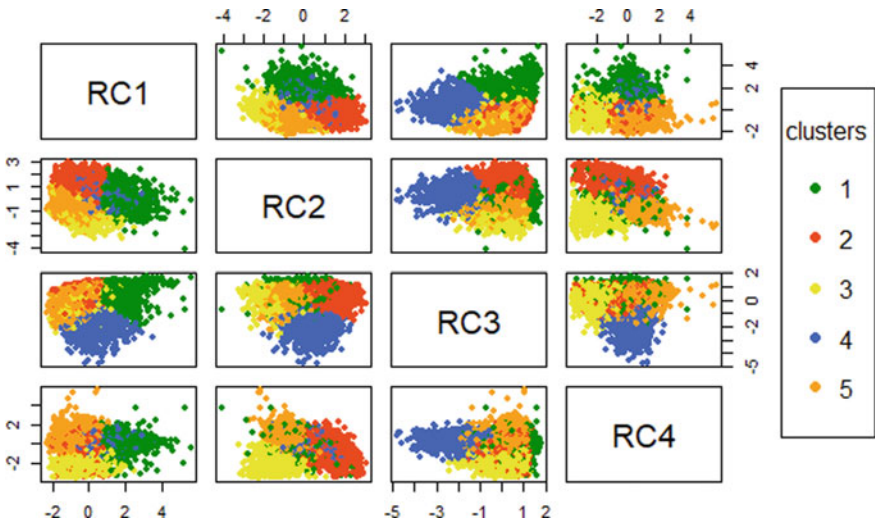

Fig. 6 The scatter plots of the clustered points after Varimax rotation for deceleration events

Making use of the segmentation and the levels of rotating components, the driving patterns associated with each cluster are interpreted. The driving patterns of clusters for acceleration and deceleration events are summarized in Table 5. The identified clusters represent the patterns of performing acceleration or deceleration maneuvers in terms of the acceleration/deceleration and speed behavior, lateral steering action, speed surge or reduction and the consistency in speed maintained over the duration of the respective maneuver.

The RC2 and RC3 represent the driver's speed choice whereas RC1 and RC4 show the nature of the driver's responses. The levels of behavioral features (RC1, RC2, RC3 and RC4) and their combination varies from one cluster to another, representing a unique driving pattern of each cluster. The acceleration clusters represent three levels of responses varying from smooth to sudden accelerations with low to high speed consistency at low to high speed choices. The cluster AC1 speaks of moderate acceleration maneuvers exhibited at high speeds with moderate speed surge and speed variability. The clusters AC2 and AC4 represent the moderate speed surge performed at low speeds with high consistency. However, cluster AC2 is observed to

Table 5 Interpretation of driving patterns of acceleration and deceleration clusters

Acceleration clusters	RC1 (acceleration)	RC2 (speed)	RC3 (speed surge and maneuver duration)	RC4 (speed consistency)
AC1	Smooth to moderate	Moderate to high	Low to moderate	Low to moderate
AC2	Moderate to sudden	Very low to low	Low to moderate	Moderate to high
AC3	Smooth	Low to moderate	Moderate to high	Moderate
AC4	Smooth to moderate	Very low to low	Low to moderate	Moderate to high
AC5	Smooth to moderate	Very low to moderate	Low	Low to high
Deceleration clusters	RC1 (deceleration)	RC2 (speed)	RC3 (speed reduction and maneuver duration)	RC4 (speed consistency)
DC1	Moderate to sudden	Moderate to high	Low to moderate	Moderate
DC2	Smooth	Low to moderate	Moderate	Low to moderate
DC3	Smooth to moderate	Moderate to high	Moderate	Low to moderate
DC4	Smooth to moderate	Moderate	Moderate to high	Moderate
DC5	Smooth	Moderate to high	Moderate	Moderate to high

present sudden acceleration behavior, and AC4 shows smooth to moderate acceleration behavior. The cluster AC3 indicates smooth acceleration maneuvers performed at low to moderate speeds associated with high speed surge and moderate speed consistency. The cluster AC5 represents low to moderate level of speed behavior and moderate acceleration behavior with the entire range of speed consistency.

Similarly, the behavioral features of deceleration clusters are observed to understand the nature of driving patterns concerning speed choices and driving responses. The clusters DC1, DC3 and DC5 present high speed behavior associated with harsh, moderate and smooth deceleration behavior respectively. The speed consistency is observed to be moderate for clusters DC1 and DC3, and high for cluster DC5. The cluster DC2 represents smooth deceleration maneuvers performed at low to moderate speeds associated with moderate speed reduction and speed consistency. The cluster DC4 indicates smooth to moderate decelerations of longer duration and high speed reduction performed at moderate speeds and speed consistency.

The aggregated proportions of each driving pattern observed for all the drivers are presented in Fig. 7. The acceleration clusters AC1 and AC5 are observed to be the dominating driving patterns sharing the major proportion (72.2%) of events followed by AC3 and AC4 sharing together about 22.1% of events. Both clusters AC1 and AC5 indicate smooth to moderate acceleration behavior. However, the respective speed choices are higher in AC1 and low to moderate in AC5. The cluster AC2, which represents the sudden acceleration behavior is observed to share about 5.1% of total events indicating the rare occurrences of aggressive accelerations. In the case of deceleration events, the clusters DC2 and DC5 are the dominating patterns observed in the entire dataset explaining 61.9% of total events, implying that the majority of the deceleration maneuvers are smooth in nature. However, the speed choices are observed to be higher under cluster DC5 compared with low to moderate speed behavior exhibited by cluster DC2. The clusters DC1, DC3 and DC4 together represent 38.1% of events, in which DC1 shares 13.7% of total events indicative of sudden decelerations performed at higher speeds.

The HPV professional drivers are predominantly exhibiting two driving patterns of acceleration and deceleration each. The dominating acceleration patterns indicate that 72.2% of accelerations are moderate in nature of which 35.6% are associated with high speed behavior. In the case of deceleration maneuvers, 61.9% are represented

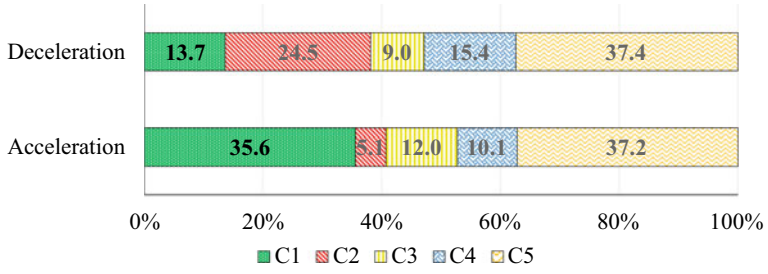

Fig. 7 Proportion of each driving pattern for acceleration and deceleration datasets

by two dominating patterns and indicate smooth deceleration behavior. However, 60.1% of decelerations are observed to happen at high speeds, in which 13.7% of events are associated with sudden deceleration behavior as well.

The identified acceleration patterns are taking the longitudinal acceleration values varying from 1.6 to 4.8 m/s^2, in which 27% and 9% of events exhibit accelerations greater than 2.5 m/s^2 and 3.5 m/s^2 respectively. Whereas, deceleration values were found to vary from 1.9 to 3.9 m/s^2, in which 47% events are higher than 2.5 m/s^2 and 14% are above 3.5 m/s^2. Thus, the observed longitudinal accelerations and decelerations are found to be beyond the acceptable limits (1.1–1.5 m/s^2) for passenger safety and comfort given by Hoberock [37]. Indicating in general aggressive acceleration and braking behavior of the HPV drivers. However, the correlation between the identified patterns and passenger safety and comfort is out of the scope of this study.

6 Intra-Driver & Inter-Driver Behavior

The proportions of identified acceleration and deceleration patterns in each trip are computed for individuals to understand the behavioral variations. The proportion of acceleration patterns and deceleration patterns for the first 28 drivers (D1 to D28, made one trip each) are shown in Figs. 8 and 9 respectively. The proportions are computed by standardizing the number of events in one cluster using the total number of events per trip.

Looking at the proportions of acceleration clusters (Fig. 8) for individual drivers, a total of 22 drivers are exhibiting dominance in cluster AC1, four drivers (D5, D7, D8 and D19) show a higher proportion of pattern AC5, driver D17 is observed to exhibit equal proportions of AC1 and AC5 and driver D21 shows AC2 as the dominating pattern. In the case of deceleration clusters (Fig. 9), a total of 21 drivers are showing dominance in cluster DC5, five drivers (D1, D13, D15, D18 and D27) in cluster DC3 and drivers D3 and D25 in DC1 and DC4 respectively. Each driver showcases

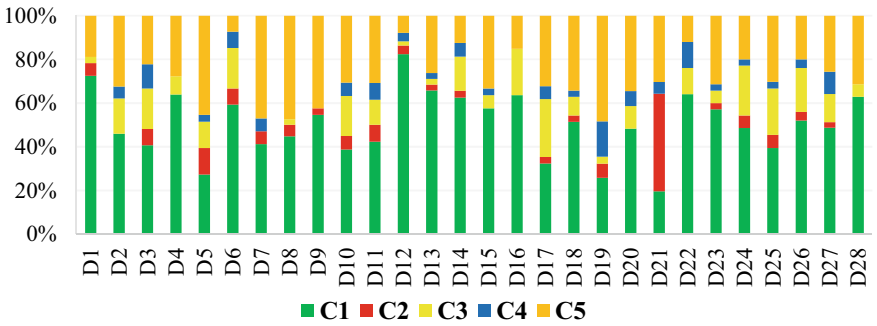

Fig. 8 Proportion of acceleration patterns in individual drivers

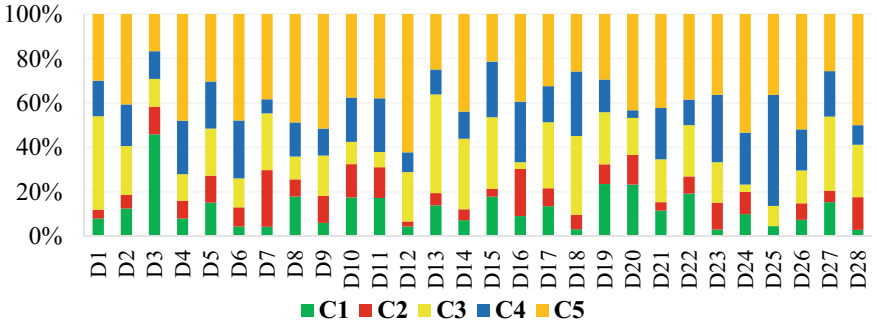

Fig. 9 Proportion of deceleration patterns in individual drivers

a minimum of three driving patterns with different proportions. The varying proportions of each pattern within the driver indicate the intra-driver behavioral variability. And each driver exhibits different proportions of driving patterns from one another suggesting the inter-driver variation (see Figs. 8 and 9). In the first group of drivers, AC1 and AC5 are found to be the dominating behaviors while accelerating and DC3 and DC5 are found to dominate while decelerating.

To explore the presence of habitual driving styles of individuals, the proportion of driving patterns over multiple trips is computed for the second group of drivers (D29 to D33). Figure 10 shows the driving pattern variations exhibited by individuals averaging over 20 trips. Observing the acceleration patterns (Fig. 10a), the drivers D29, D30 and D33 show major dominance in cluster AC1 and the next dominance in cluster AC5. Whereas drivers D31 and D32 show significant proportions in cluster AC5 and the following predominance in clusters AC1 and AC4. Both the clusters AC1 and AC5 represent moderate acceleration behavior. However, cluster AC1 indicates speedy behavior and volatility in speed consistency, and AC5 shows moderate speeds and a full range of speed variability. The clusters AC2 and AC4 indicate the low speed

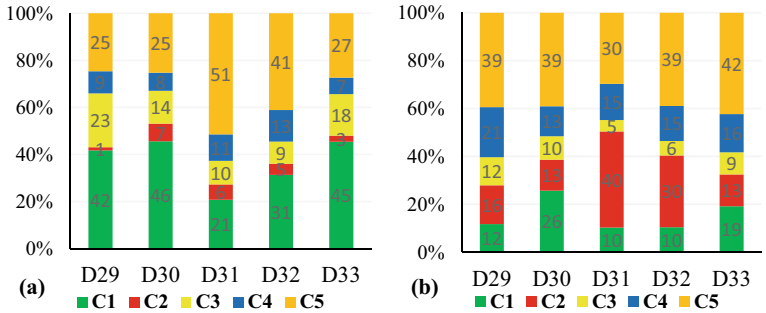

Fig. 10 Proportion of (**a**) acceleration patterns and (**b**) deceleration patterns for individuals over multiple trips

behavior with high consistency. However, the cluster AC2 represents the sudden acceleration behaviors and AC4 shows moderate acceleration behavior.

Similarly, the variation in deceleration patterns (Fig. 10b) indicates that the driver D31 shows a significant proportion in cluster DC2 followed by cluster DC5. Whereas, the drivers D29, D30, D32 and D33 display primary dominance in cluster DC5. However, the subsequent predominating clusters are different among the drivers. The clusters DC2 and DC5 exhibit smooth deceleration behavior at moderate speeds and high speeds respectively. The cluster DC5 shows high consistency in speed behavior and cluster DC2 shows moderate consistency. The cluster DC1 indicates sudden deceleration, speedy behavior and volatility in speed consistency. The cluster DC3 also indicates volatile speedy behavior except that, the respective decelerations are moderate in nature. The predominant driving patterns observed in the aggregated proportions of 20 trips are indicating the presence of the habitual driving style of the respective driver. However, from one trip to another trip, the proportions of the driving pattern may vary. The distribution of the proportions of each driving pattern observed for multiple trips is presented in Fig. 11.

The accelerations patterns AC1 and AC5 are showing higher means and deviations as well. Whereas the remaining acceleration patterns are consistently showing lower proportions. In the case of deceleration patterns, except DC4 the remaining patterns are showing varying means and deviations among individuals. It can be observed that the drivers are exhibiting each driving pattern with different proportions from one trip to another. The amount of deviation from the mean proportion is varying among the patterns and also among the drivers. Thus, the stability in driving behavior

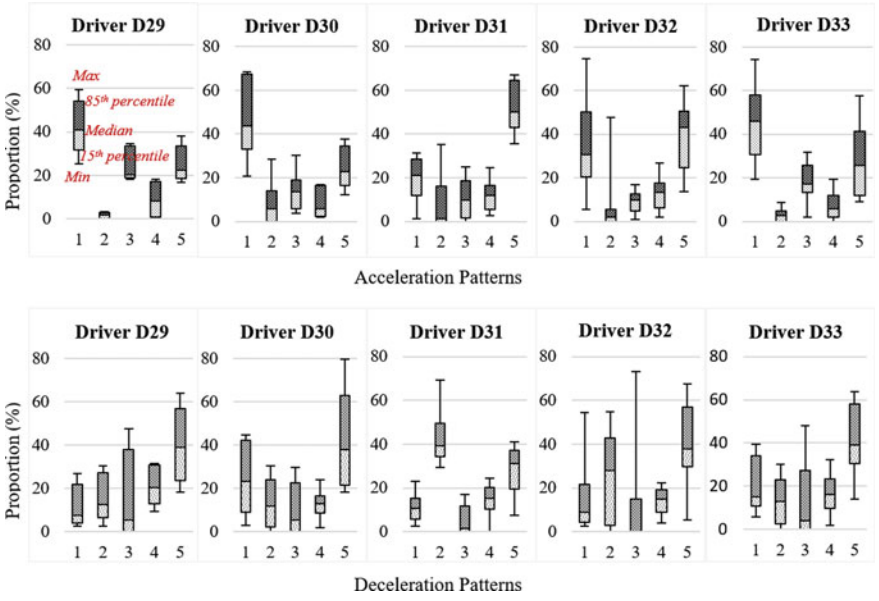

Fig. 11 Proportion of each driving pattern observed over multiple trips for individual drivers

is different from one driver to another and needs further analysis to identify the consistency in driving patterns. The observed behavioral heterogeneity is consistent with the findings of the previous studies on passenger car drivers. In the studies of Mantouka et al. [29], Higgs and Abbas [31], and Chen and Chen [32] each driver was exhibiting varying proportions of different patterns over the observed period. Also, Mantouka et al. [29] reported that the stability in driving behavior from one trip to another was low and emphasized the need for a personalized feedback system.

The present study provides a detailed investigation of individual's driving pattern variations in different driving regimes. Given the variability in driving patterns exhibited by individuals, the study emphasizes the need for continuous assessment, rather than assigning a single score to drivers. The identified patterns can be further studied to correlate with the different implications, such as driving safety, comfort and economy. Depending on the objective of the assessment, a set of thresholds can be derived from the observed clusters to identify the at-fault behaviors of individuals. The data-driven thresholds would be more indicative of diversity in driving behaviors which cannot be directly measured, such as the behavioral variations pertained to driving habits and driving skills.

7 Conclusions

This study explored the presence of different patterns in the longitudinal acceleration and deceleration maneuvers of professional drivers of heavy passenger vehicles. The continuous real-time driving data was collected for 33 drivers using a high-frequency GPS instrument. The driving performance features related to acceleration and deceleration events were considered to recognize the different driving patterns. A total of five patterns of accelerations and decelerations were identified using the multivariate k-means clustering technique. The principal component analysis after clustering revealed four behavioral features which distinguish the driving patterns from one another. The patterns were characterized by the nature of respective acceleration/deceleration, speed, lateral steering action, change in speed over the event and speed consistency. The observed driving patterns were found to vary over the levels of characterizing components, indicating that each driving pattern is representative of unique driving behavior. The exploratory analysis of individual driver's driving data shows the presence of a minimum of three driving patterns in each trip. The proportion of driving patterns is different among drivers and also varies among the trips of an individual driver. The study findings show that different patterns are exhibited by each driver within the driving period (or trip) indicating the intra & inter-driver behavioral variations. The study findings are implicating that driver behavioral heterogeneity should be considered to assess and characterize the individuals.

The aggregated data of multiple trips displayed the presence of two dominating driving patterns in both acceleration and deceleration maneuvers of professional HPV drivers. The major acceleration patterns constituted 72.2% of total events and indicated moderate accelerations at high speeds with variable speed consistency.

And the predominant deceleration patterns represented 61.9% of events and showed smooth decelerations at high speeds with low variability in speeds. The moderate, and sudden maneuvers are observed to be 88% in acceleration events and 36.1% in deceleration events. Moreover, the respective speed choices are higher in 35.6% of accelerations and 22.7% of decelerations.

To summarize the key aspects of this study,

1. The driving styles are conceptualized based on the longitudinal vehicle control exhibited by professional HPV drivers.
2. The similarities in the acceleration and deceleration behaviors are explored separately using unsupervised learning techniques without any pre-defined thresholds.
3. The behavior trends of each driver are presented in terms of the frequency of each driving pattern over the observed period (proving that, driving pattern is not constant and varies within the driving period).
4. Majority of the events are falling under two clusters, representing a relatively uniform behavior among the HPV drivers. However, the proportion of each driving pattern varied among individuals showing the inter-driver variability.
5. The explorative analysis shows that, different driving patterns exist within an individual and the frequency with which one performs a driving pattern is varying and might depend on several factors and represents their habitual way of driving.

The insights from the study aid in identifying the driving patterns and the habitual driving styles of individuals without pre-defined ground truth. In addition, the study aids in developing driver assistance programs for modifying driver behavior and to provide personalized feedback.

This study accounts few limitations with respect to the number of drivers studied and the unaccountability of the number of passengers in the vehicle. An additional number of drivers and the multiple trip data help in deeper insights about the habitual driving styles and influencing factors. The exact number of passengers travelling in HPV and their comfort thresholds were not considered in this study. The future scope of the study is extended to understand the correlations between different driving patterns and passenger safety and comfort for different vehicle types.

References

1. World Health Organization (2018) Global status report on road safety 2018: summary (No. WHO/NMH/NVI/18.20). World Health Organization
2. Ministry of Road Transport and Highways, Transport Research Wing (2019) Ministry of Road Transport and Highways, Transport Research Wing. Road accidents in India
3. Wangdi C, Gurung MS, Duba T, Wilkinson E, Tun ZM, Tripathy JP (2018) Burden, pattern and causes of road traffic accidents in Bhutan, 2013–2014: a police record review. Int J Inj Control Saf Promot 25(1):65–69

4. Treat JR, Tumbas NS, McDonald ST, Shinar D, Hume RD, Mayer RE, Castellan NJ (1979) Tri-level study of the causes of traffic accidents: final report. Exec Summ
5. Ansari S, Akhdar F, Mandoorah M, Moutaery K (2000) Causes and effects of road traffic accidents in Saudi Arabia. Public Health 114(1):37–39
6. Ministry of Road Transport and Highways, Transport Research Wing (2018) Ministry of Road Transport and Highways, Transport Research Wing. Road accidents in India
7. Bjoernstig ULF, Bylund PO, Albertsson P, Falkmer T, Björnstig J, Petzäll J (2005) Injury events among bus and coach occupants: non-crash injuries as important as crash injuries. IATSS Res 29(1):79–87
8. Albertsson P, Falkmer T (2005) Is there a pattern in European bus and coach incidents? A literature analysis with special focus on injury causation and injury mechanisms. Accid Anal Prev 37(2):225–233
9. Halpern P, Siebzehner MI, Aladgem D, Sorkine P, Bechar R (2005) Non-collision injuries in public buses: a national survey of a neglected problem. Emerg Med J 22(2):108–110
10. Elvik R (2019) Risk of non-collision injuries to public transport passengers: synthesis of evidence from eleven studies. J Transp Health 13:128–136
11. Silvano AP, Ohlin M (2019) Non-collision incidents on buses due to acceleration and braking manoeuvres leading to falling events among standing passengers. J Transp Health 14:100560
12. Sagberg F, Selpi, Bianchi Piccinini GF, Engström J (2015) A review of research on driving styles and road safety. Hum Factors 57(7):1248–1275
13. Reason J, Manstead A, Stradling S, Baxter J, Campbell K (1990) Errors and violations on the roads: a real distinction? Ergonomics 33(10–11):1315–1332
14. French DJ, West RJ, Elander J, Wilding JM (1993) Decision-making style, driving style, and self-reported involvement in road traffic accidents. Ergonomics 36(6):627–644
15. Taubman-Ben-Ari O, Mikulincer M, Gillath O (2004) The multidimensional driving style inventory-scale construct and validation. Accid Anal Prev 36(3):323–332
16. De Winter JCF, Dodou D (2010) The driver behaviour questionnaire as a predictor of accidents: a meta-analysis. J Saf Res 41(6):463–470
17. Wang X, Xu X (2019) Assessing the relationship between self-reported driving behaviors and driver risk using a naturalistic driving study. Accid Anal Prev 128:8–16
18. Neale VL, Dingus TA, Klauer SG, Sudweeks J, Goodman M (2005) An overview of the 100-car naturalistic study and findings. Natl Highw Traffic Saf Adm 5:0400
19. Guo F, Klauer SG, Hankey JM, Dingus TA (2010) Near crashes as crash surrogate for naturalistic driving studies. Transp Res Rec 2147(1):66–74
20. Guo F, Fang Y (2011) Individual driver risk analysis using naturalistic driving data. In: 3rd international conference on road safety and simulation
21. Zheng Y, Wang J, Li X, Yu C, Kodaka K, Li K (2014, October) Driving risk assessment using cluster analysis based on naturalistic driving data. In: 17th international IEEE conference on intelligent transportation systems (ITSC). IEEE, pp 2584–2589
22. Feng F, Bao S, Sayer JR, Flannagan C, Manser M, Wunderlich R (2017) Can vehicle longitudinal jerk be used to identify aggressive drivers? An examination using naturalistic driving data. Accid Anal Prev 104:125–136
23. Constantinescu Z, Marinoiu C, Vladoiu M (2010) Driving style analysis using data mining techniques. Int J Comput Commun Control 5(5):654–663
24. Johnson DA, Trivedi MM (2011, October) Driving style recognition using a smartphone as a sensor platform. In: 2011 14th international IEEE conference on intelligent transportation systems (ITSC). IEEE, pp 1609–1615
25. Vaiana R, Iuele T, Astarita V, Caruso MV, Tassitani A, Zaffino C, Giofrè VP (2014) Driving behavior and traffic safety: an acceleration-based safety evaluation procedure for smartphones. Mod Appl Sci 8(1):88
26. Eboli L, Mazzulla G, Pungillo G (2016) Combining speed and acceleration to define car users' safe or unsafe driving behaviour. Transp Res Part C: Emerg Technol 68:113–125
27. Murphey YL, Milton R, Kiliaris L (2009, March). Driver's style classification using jerk analysis. In: 2009 IEEE workshop on computational intelligence in vehicles and vehicular systems. IEEE, pp 23–28

28. Kalsoom R, Halim Z (2013, December) Clustering the driving features based on data streams. In: INMIC. IEEE, pp 89–94
29. Fugiglando U, Massaro E, Santi P, Milardo S, Abida K, Stahlmann R, Ratti C (2018) Driving behavior analysis through CAN bus data in an uncontrolled environment. IEEE Trans Intell Transp Syst 20(2):737–748
30. Mantouka EG, Barmpounakis EN, Vlahogianni EI (2019) Identifying driving safety profiles from smartphone data using unsupervised learning. Saf Sci 119:84–90
31. Higgs B, Abbas M (2014) Segmentation and clustering of car-following behavior: recognition of driving patterns. IEEE Trans Intell Transp Syst 16(1):81–90
32. Chen KT, Chen HYW (2019) Driving style clustering using naturalistic driving data. Transp Res Rec 2673(6):176–188
33. Higgs B, Abbas M (2013, October) A two-step segmentation algorithm for behavioral clustering of naturalistic driving styles. In: 16th international IEEE conference on intelligent transportation systems (ITSC 2013). IEEE, pp 857–862
34. Chen C, Zhao X, Zhang Y, Rong J, Liu X (2019) A graphical modeling method for individual driving behavior and its application in driving safety analysis using GPS data. Transport Res F: Traffic Psychol Behav 63:118–134
35. Yarlagadda J, Jain P, Pawar DS (2021) Assessing safety critical driving patterns of heavy passenger vehicle drivers using instrumented vehicle data—an unsupervised approach. Accid Anal Prev 163:106464
36. Kaiser HF (1958) The varimax criterion for analytic rotation in factor analysis. Psychometrika 23:187–200
37. Hoberock LL (1976) A survey of longitudinal acceleration comfort studies in ground transportation vehicles. Council for Advanced Transportation Studies

Age and Gender Differences in Motorized Two-Wheeler Safety Perceptions

Teena Roy, Darshana Othayoth, and B. K. Bhavathrathan

Abstract Motorized two-wheeler users are a rapidly increasing but vulnerable group of road users. A survey was conducted among different road users in Kerala to study the perceived safety about motorized two-wheeler users. The survey asked individuals to rate the level of risk associated with activities that can cause accidents and their agreement with increasing law enforcements. The survey responses were analysed using structural equation modelling to understand the relationship between risk perception, user's confidence and law enforcement. The study showed that risk perception and user's confidence are correlated (−0.51) but not user's confidence and law enforcement (−0.06). Risk perception positively influences user's agreement with stricter law enforcement (0.21). There is higher correlation between risk perception and user's confidence among males (−0.52) than females (−0.31). Both user's confidence and risk perception influence females' agreement with higher law enforcement. The study suggests improving risk perception for safer driving habits.

Keywords Motorized two-wheeler safety · User perception · Structural equation modelling

1 Introduction

Motorized two-wheelers are a primary mode of transportation in developing countries and their usage is increasing every year. In India, it has grown from 8.8% of the total vehicles in use in 1951 to 73.86% in the financial year 2017 [1]. Motorized two-wheeler riders and users are more vulnerable to road accidents and fatalities than other types of road users. In 2017, two-wheelers accounted for the majority of the accidents (33.9%) in India while cars, jeeps and taxis together contributed 24.5% [2].

T. Roy · B. K. Bhavathrathan (✉)
Indian Institute of Technology Palakkad, Kozhippara, India
e-mail: bhavathrathan@iitpkd.ac.in

D. Othayoth
National Institute of Technology Tiruchirappalli, Tiruchirappalli, India

L. Devi et al. (eds.), *Proceedings of the Sixth International Conference of Transportation Research Group of India*, Lecture Notes in Civil Engineering 273,
https://doi.org/10.1007/978-981-19-4204-4_10

Previous studies have shown that human behaviour plays a major role in traffic accidents [3]. It is seen that driver attitude and safety perception influence driver actions, which is a primary cause for traffic accidents [4]. The driver behaviour, attitude and perceptions vary across various age and gender groups. For example, studies have shown that the attitude of risk taking and sensation seeking is higher among males and among young people [5]. Young drivers are more likely to be involved in risky driving [6] as they underestimate the risk involved and overestimate their driving skills [7] more.

Thus, the attitude and risk perception of road users greatly affect their behaviour and actions. Hence, understanding this would help us develop better methods to reduce risky driving behaviour and accidents in turn. In this study, we consider the variables risk perception, user's confidence and law enforcement and the relationship between them. We also try to investigate how age and gender of the road user influence the motorized two-wheeler safety perceptions.

1.1 Variables Considered in the Study

Risk perception: Risk perception refers to the severity and extent of risk a user associates with an activity. It is a subjective judgement as it depends on the person's individual feelings, past experiences as well as the social constructs [8]. People adjust their actions based on the risk they perceive. The theory of risk compensation suggests that higher the risk perceived, more cautious or safer the action. Past studies show that risk perception and perception of driving tasks affect the safety attitude of drivers [9]. Higher the risk perceived, more is the safety attitude. Risk perception is seen to be higher across females than in males. Across various age groups, young drivers have a lower risk perception and hence lower safety attitude [7].

User's confidence: User's confidence refers to the level of surety and self-confidence the road user has. This is the self-rated confidence and driving ability of the user. User's confidence can affect the risk-taking level of the user and is seen to increase with experience. This perceived driving ability is seen to differ across ages, in men. The confidence level is higher in younger men than older men, and both groups view the driving ability of the other as lower than their own [10].

Law enforcement: Violating traffic laws, just like risky driving, goes against human nature to self-preserve [11]. Certain theories suggest that the motivation of rewards and punishments for obeying or disobeying laws is not as successful as one's attitude, values and personal beliefs as a motivation to follow the rules and regulations. Hence, it is important to form policies based on these factors. These motivation levels are seen to vary across the age and gender groups. The motivation of penalties against violation of laws seems to be higher across females [12].

It has been found that risk perception influences the risk-taking behaviour [13, 14]. For example, a study conducted among electric bike riders in China showed that riders with higher risk perception had more positive attitude towards traffic safety, which led to lesser aberrant driving behaviour [15]. Law enforcement is also seen

to improve the drivers following rules [16]. The relations between these factors are studied based on the differences in age, gender and whether the user has been involved in an accident. The present study focuses on arriving at a relationship between risk perception, user's confidence and law enforcement and the influence of age and gender on them. This paper is divided into the following sections: Sect. 2 contains the literature review, Sect. 3 describes the methodology and factors contributing to risk perception, user's confidence and legal affinity, Sect. 4 presents the results of the analysis and discusses the inferences and Sect. 5 is the conclusion.

2 Literature Review

From past studies, it was found that human actions are the primary cause for two-wheeler accidents [17] and that there are two types of aberrant driving behaviours that can lead to accidents, namely, errors and aggressive driving behaviours. Analysis using structural equation modelling shows that safety attitudes and risk perceptions affect these aberrant driving behaviours [15]. Risk perception level has been identified as a major factor in accidents between two-wheelers and cars [18] and has been found to have a negative effect on the attitude towards risky driving [19]. A past study conducted among young novice drivers showed a poorer perception of safety was associated with increased crash risk [20]. Studies have shown that the safety attitude towards the risk level perceived by drivers differs across genders in young people, with females having more positive attitudes [21]. The risk perception differs not just across age and gender, but across different types of road users too [22]. It is also seen from a past study that those involved with three or more accidents tend to have lesser risk perception and more unsafe behaviour [23].

Proper training, traffic knowledge and following the traffic laws are primary to reduce and prevent accidents. Particularly in countries with a huge number of motor vehicles, traffic law enforcement can bring down the frequentness of fatal motor vehicle accidents [24]. A recent study conducted in Delhi [25] showed that though the majority of the two-wheeler drivers wore helmets, many did not wear it properly, and many wore it only around traffic police to avoid fines. Though they have established five traffic training centres across the city, only 19.7% used it. Out of those used, 68.7% have no traffic offences till now. Almost half of the two-wheeler riders (45%) reported past traffic offences. This implies that a significant proportion of motorized two-wheeler drivers does not follow traffic laws. Thus, it is vital to ensure that drivers have sufficient traffic knowledge, training, and practice. Interventions by the traffic police and traffic tickets reduce traffic law violations to a good extent [26, 27]. From a previous study, it is seen that the perception of the possibility of arrest and the user's alignment with the laws to prevent drunk driving is much more effective in curbing drunk driving than the regulations itself [28].

While we know risk perception and user's confidence and self-rated driving ability are related, how they affect the level of law enforcement among road users is not much looked into. A past study in conducted between two counties in Norway showed

traffic safety campaigns brought about better risk perception, lesser risky behaviour and fewer crashes due to speeding [29]. Also, most of these studies take into account the perceptions of only the drivers, though they interact with all other road users. Hence, analysing the perceptions of other types of road users also would help us gain more insight into better implementation of traffic guidelines. Through this study, we try to understand how risk perception, user's confidence and law enforcement are related. We see this for two-wheelers specifically and taking into account the perceptions of various types of road users. We also try to investigate how age and gender of the road user influence the motorized two-wheeler safety perceptions. Since we know risk perception to be a main factor in driver behaviour, we look into how accident history affects the risk perception and confidence level.

3 Methodology

To obtain the user's perception, a questionnaire survey was conducted among different types of road users, like pedestrians, car users, two-wheeler users, etc. The survey collected the demographics of the user and the user's perceived risk level about various factors that can lead to accidents and traffic violations. The factors considered include driver behaviour, road condition, weather condition and the vehicle condition. Driver behaviour implies unsafe driving actions like over speeding, drunk driving, etc. Vehicle condition refers to the state of vehicle, like presence of front mirrors, rear view mirror, age of vehicle, etc. Road condition refers to the state of the road, like presence of potholes, geometric features like presence of curves, junctions, etc. Users were asked to rate the associated risk level in a 5-point scale. 1 being not risky at all to 5 being highly risky. The survey also gathered the user's agreement on a 1–5 scale about implementing stricter laws and penalties to curb traffic violations. The survey was distributed as online forms through the state of Kerala.

The methodology consists of two parts—(1) Preliminary analysis of the survey responses and (2) Path analysis. Path analysis was done using structural equation modelling. Structural Equation Modelling (SEM) is a statistical analysis tool that combines confirmatory factor analysis (CFA) and multiple regression analysis to study relations between latent and observed variables. Observed variables are those that can be directly measured while latent variables are measured using two or more observed variables. SEM consists of two parts—the measurement model, which relates and analyses the latent constructs to their observed variables, and the structural model, which checks the relations between the latent constructs. SEM provides the advantage of being able to look into both direct and indirect relationships between latent constructs and also to ensure satisfactory fit at both measurement and structural model stages separately or individually.

We formed the three study variables by taking various survey questions as the observed variables. Risk perception is evaluated by considering the risk perceived with drunk driving, driving without helmets and using mobile phones while driving. A higher number would imply higher risk perception. Law enforcement is measured

in the form of users' agreement with stricter laws to reduce crashes and increased penalties against the offences of drunk driving, over speeding, driving with no helmets and using mobiles while driving. The user's confidence is evaluated by considering the negative of the risk perceived by the user at curves and at junctions, points which should not be perceived as risky by a good driver. A higher value would imply a higher confidence level. We then develop the structural model and then a multigroup analysis and done based on age, gender and past involvement in accidents.

4 Results and Discussion

The survey was distributed online in the state of Kerala and a total of 980 responses were collected. After cleaning the data, the number of valid responses are 949, of which 237 (25%) were female. 376 (39.6%) of the respondents belong to the age group 18–25, 479 (50.4%) of 25–35 age, 71 (7.5%) of 35–45 and 23 (2.4%) of the age group 45 and above.

The Cronbach's alpha value obtained for the survey response is 0.9, which implies excellent reliability of the survey responses. From the survey responses, it is observed that driver actions are perceived as riskier than the vehicle, road or weather conditions. Drunk driving, unofficial races and over speeding (mean = 4.829, 4.683 and 4.673) are considered the riskiest. Risk perception is seen higher among females and among older people.

C.R (>0.70) and AVE (>0.50) values suggest consistent data, as seen in Table 1. Thus, the usage of SEM is justified. For the structural modelling, we used AMOS 26 for modelling and the method employed was maximum likelihood estimation. The measurement model gets an adequate fit, with a CFI of 0.951 and TLI of 0.932. The RMSEA value obtained was 0.083 and the ECVI is 0.324. The structural model had a CFI value of 0.958 and TLI of 0.936. RMSEA value is 0.08 and 0.298 is the ECVI value.

Table 1 explains the standardized regression weights or loading and the error obtained in the measurement model for each latent variable. Figure 1 explains the measurement model, which analyses the relationship of the latent variables, namely, user's confidence, risk perception, and law enforcement to their respective observed variables. All the observed variables have sufficiently good factor loadings and squared multiple correlations, as given in the figure. The correlations between the latent variables are also given in the figure. When we analyse the complete survey response as a single group (Fig. 2), user's confidence and risk perception are negatively correlated (−0.46). Risk perception (0.18) positively affects the law enforcement twice as much as user's confidence (−0.09). This implies that as the user's confidence level increases, the desire for more law enforcement reduces. As the perceived risk increases, people tend to agree more to enforce law. The risk level and confidence level complement each other moderately.

Figure 3 represents the variables in multigroup analysis. In multigroup analysis, the pathway is analysed by considering each age, gender, and involvement in accident

Table 1 Standardized factor loading, error, composite reliability and average variance extracted of the measurement model

Observed variable	Unobserved variable	Loading	Error	Composite reliability (C.R)	Average variance extracted (AVE)
Risk at curves (curves)	User confidence	0.91	0.206	0.884	0.791
Risk at junctions (junctions)	User confidence	0.904	0.228		
Risk in using mobile while driving (mobil_drv)	Risk perception	0.862	0.175	0.845	0.65
Risk in not wearing helmet (no_hlmt)	Risk perception	0.654	0.453		
Risk in drunk driving (drnk_drv)	Risk perception	0.627	0.216		
Increased penalty for over speeding (speed_penalty)	Law enforcement	0.728	0.378	0.896	0.634
Increased penalty for drunk driving (drnk_penalty)	Law enforcement	0.799	0.204		
Increased penalty for not wearing helmet while driving (helmet_penalty)	Law enforcement	0.715	0.437		
Increased penalty for using mobile while driving (mobile_penalty)	Law enforcement	0.84	0.231		
Stringent laws to reduce road crashes (law_crash)	Law enforcement	0.681	0.398		

as a separate group to see how the relationship varies across them. In the figure, b1 represents the factor loading for the effect of user's confidence on law enforcement. When we consider age, b1_1 represents the factor loading for the first group 18–25, b1_2 represents 25–35, etc. b2_1 represents the effect of risk perception on law enforcement for the age group 18–25, b2_2 for the group 25–35 and so on. A significant p value for the comparison between an unconstrained (all variables are free to vary) and a constrained model (here, we keep the structural weights constant across all age groups) implies that the pathway varies across the particular variable we have considered, like age and gender. Multigroup analysis of the model across age

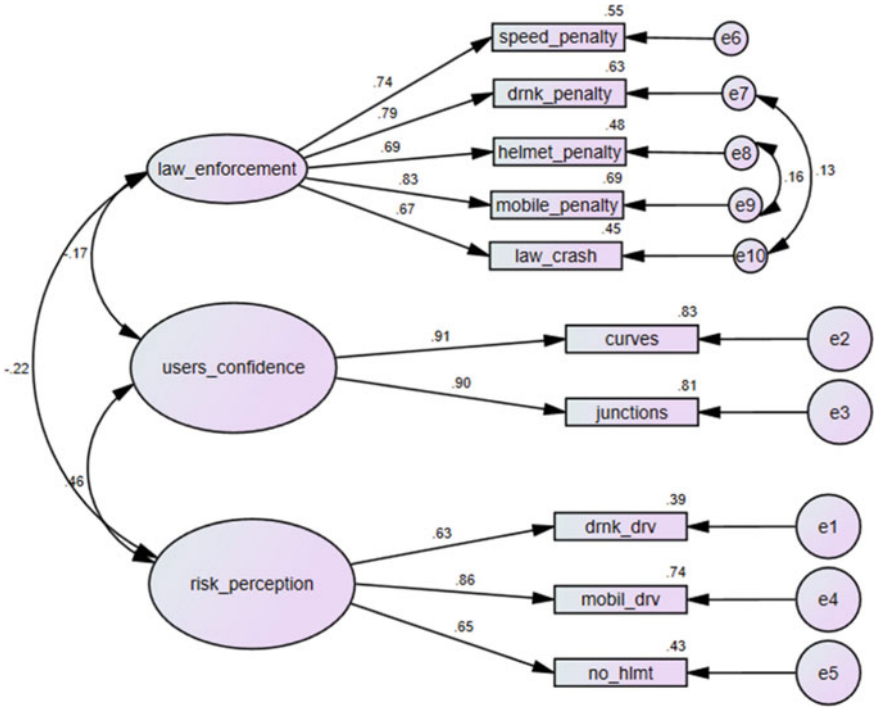

Fig. 1 Measurement model with factor loadings and squared multiple correlations for the observed variables

and gender shows a similar pattern. However, in gender, there is higher correlation between risk perception and user's confidence among males (−0.52) than females (−0.31) and both user's confidence and risk perception influence females' agreement with higher law enforcement. The coefficients do not vary significantly across various age groups. The effect of user's confidence and risk perception on law enforcement seems to be higher among the younger generation even though risk perception is higher among older generations. The effect of risk perception on law enforcement is higher among those who have been in an accident than those who have not. The factor loadings and significance are given in Table 2.

Though there is a good amount of correlation between risk perception and user's confidence, there seems to be very little effect of users' confidence level on law enforcement. Risk perception, on the other hand, exerts a moderate influence. Females are more open to law enforcement, which can be explained by the higher effect of risk perception in case of females. Higher the risk perception, more are they open to stronger enforcement of law. Though risk perception increases across age groups, the associated law enforcement seems to decrease. From the analysis, we see that while the pathway varies for different age and gender groups, involvement in an

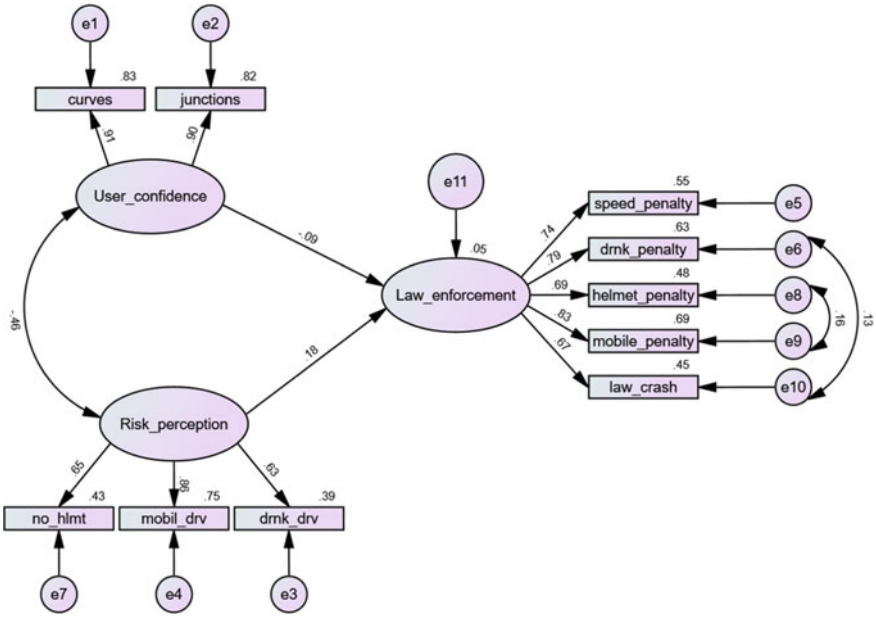

Fig. 2 Structural model of the complete sample

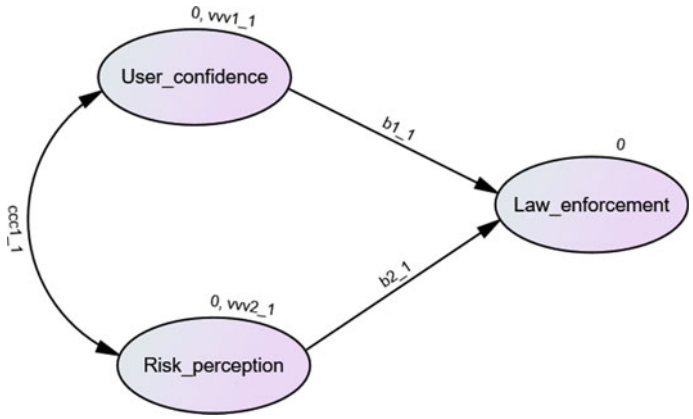

Fig. 3 Multigroup analysis factor loadings

accident does not affect the pathway as the p value obtained is 0.221 > 0.1. Thus, accidents do not affect the pathway.

Table 2 Multigroup analysis factor loadings and significance

Category	Structural weight between user confidence and law enforcement (b1_1)	Structural weight between risk perception and law enforcement (b2_1)	Covariance between user confidence and risk perception (ccc1_1)	P value of model comparison between constrained and unconstrained model
Gender				0.0
All	−0.06	0.21	−0.51	
Male	−0.06	0.20	−0.56	
Female	−0.07	0.24	−0.34	
Age				0.028
All	−0.07	0.21	−0.51	
18–25	−0.09	0.29	−0.52	
25–35	−0.06	0.20	−0.49	
35–45	−0.07	0.13	−0.54	
Accident history				0.221
All	−0.06	0.21	−0.51	
Involved in accident	−0.08	0.31	−0.46	
Not involved in accident	−0.06	0.19	−0.53	

5 Conclusions

Motorized two-wheeler riders and users are more vulnerable to road accidents and fatalities than other types of road users. The present study was conducted to develop the pathway between user's confidence, risk perception, and law enforcement. A survey was conducted online across the state of Kerala in which people rated the risk associated with various driver, environment and vehicle factors in a 1–5 scale. A total of 949 responses were obtained. From the survey responses, it is observed that driver actions are perceived as riskier than the vehicle, road or weather conditions, in agreement with past studies. Drunk driving, unofficial races and over speeding (mean = 4.829, 4.683 and 4.673) are considered the riskiest. Risk perception is seen higher among females and among older people. Using structural equation modelling, it was found that though user's confidence and risk perception are correlated, and risk perception affects law enforcement, there is no significant effect between user's confidence and law enforcement. Risk perception plays an important role as it primarily affects the young people and the males. Hence, if we can improve the risk perception of these groups, it can lead to safer driving habits and more users following traffic laws. These can be brought about by proper education and motor training. A past

study also suggests proper traffic education and training along with better enforcement to improve road safety [30]. Thus, we should focus more on ensuring motor drivers have good traffic knowledge and training.

Since the survey was conducted online using digital forms, the digital-divide in the population would reflect in the responses as well. Therefore, it is likely that the respondents do not cover the entire sociodemographic spectrum. Also, though we collected responses from over 55 years old, due to a lesser number of responses, we could not model for those age groups separately. In this study, we have not looked into any moderation effect between the three variables. These aspects present immediate future scope for this work.

References

1. Ministry of road transport and highways (India) (2019) Ministry of road transport and highways transport research wing (India): road transport year book 2016–17. Ministry of road transport and highways (India), New Delhi
2. Ministry of road transport and highways transport research wing (India) (2018) Ministry of road transport and highways transport research wing (India): road accidents in India-2017. Ministry of road transport and highways transport research wing (India), New Delhi
3. Evans L (1996) The dominant role of driver behaviour in traffic safety. Am J Public Health 86(6):784–785
4. Burgut HR, Bener A, Sidahmed H, Albuz R, Sanya R, Khan WA (2010) Risk factors contributing to road traffic accidents in rapidly developing countries: neglected health problems. Turk J Trauma Emerg Surg 16(6):497–502
5. Bachoo S, Bhagwanjee A, Govender K (2013) The influence of anger, impulsivity, sensation seeking and driver attitudes on risky driving behaviour among post-graduate university students in Durban, South Africa. Accid Anal Prev 55(7):67–76
6. Quimby AR (1988) In-car observation of unsafe driving actions. Australian Road Research Report ARR 153, Melbourne
7. Deery HA (1999) Hazard and risk perception among young novice drivers. J Saf Res 30(4):225–236
8. Slovic P (2016) Understanding perceived risk: 1978–2015. Environment 58(1):25–29
9. Ram T, Chand K (2016) Effect of drivers' risk perception and perception of driving tasks on road safety attitude. Transp Res Part F: Traffic Psychol Behav 42:162–176
10. Cohn LD, Macfarlane S, Yanez C, Imai WK (1995) Risk-perception: differences between adolescents and adults. Health Psychol 14(3):217–222
11. Yagil D (2005) Drivers and traffic laws: a review of psychological theories and empirical research. Traffic Transp Psychol 487–503
12. Matthews ML, Moran AR (1986) Age differences in male drivers' perception of accident risk: the role of perceived driving ability. Accid Anal Prev 18(4):299–313
13. Ma M, Yan X, Huang H, Abdel-Aty M (2010) Safety of public transportation occupational drivers: risk perception, attitudes, and driving behavior. Transp Res Rec 2145(1):72–79
14. Fishbein M (2018) The relation between perceived risk and preventive action. J Appl Soc Psychol 20(19):1541–1557
15. Yao L, Wu C (2012) Traffic safety for electric bike riders in China. Transp Res Rec 2314:49–56
16. Stanojević P, Jovanović D, Lajunen T (2013) Influence of traffic enforcement on the attitudes and behavior of drivers. Accid Anal Prev 52:29–38
17. Vlahogianni EI, Yannis G, Golias JC (2012) Overview of critical risk factors in power-two-wheeler safety. Accid Anal Prev 49:12–22

18. Penumaka AP, Savino G, Baldanzini N, Pierini M (2014) In-depth investigations of PTW-car accidents caused by human errors. Saf Sci 68:212–221
19. Teye-Kwadjo E (2019) Risky driving behaviour in urban Ghana: the contributions of fatalistic beliefs, risk perception, and risk-taking attitude. Int J Health Promot Educ 57(5):256–273
20. Ivers R, Senserrick T, Boufous S, Stevenson M, Chen HY, Woodward M, Norton R (2009) Novice drivers' risky driving behavior, risk perception, and crash risk: findings from the DRIVE study. Am J Public Health 99(9):1638–1644
21. Cordellieri P, Baralla F, Ferlazzo F, Sgalla R, Piccardi L, Giannini AM (2016) Gender effects in young road users on road safety attitudes, behaviors and risk perception. Front Psychol 7(September):1–11
22. Chaurand N, Delhomme P (2013) Cyclists and drivers in road interactions: a comparison of perceived crash risk. Accid Anal Prev 50:1176–1184
23. Ngueutsa R, Kouabenan DR (2017) Accident history, risk perception and traffic safe behaviour. Ergonomics 60(9):1273–1282
24. Redelmeier DA, Tibshirani RJ, Evans L (2003) Traffic-law enforcement and risk of death from motor-vehicle crashes: case-crossover study. Lancet 361(9376):2177–2182
25. Thombre A, Ghosh I, Agarwal A (2020) Examining road safety compliance among motorised two-wheelers in Delhi—a cross-sectional study. In: Second ASCE India conference on "Challenges of Resilient and Sustainable Infrastructure Development in Emerging Economies" (CRSIDE2020), pp 1–11
26. Luca DL (2014) Do traffic tickets reduce motor vehicle accidents? Evidence from a natural experiment. J Policy Anal Manag 34(1):85–106
27. Soori H, Royanian M, Zali AR, Movahedinejad A (2009) Road traffic injuries in Iran: the role of interventions implemented by traffic police. Traffic Inj Prev 10(4):375–378
28. Bertelli AM, Richardson LE Jr (2008) The behavioral impact of drinking and driving laws. Policy Stud J 36(4):545–569
29. Rundmo T, Iversen H (2004) Risk perception and driving behaviour among adolescents in two Norwegian counties before and after a traffic safety campaign. Saf Sci 42(1):1–21
30. Verma A, Velumurugan S, Chakrabarty N, Srinivas S (2011) Recommendations for driver licensing and traffic law enforcement in India aiming to improve road safety. Curr Sci 100(9):1373–1385

Safety Assessment of Urban Uncontrolled Intersections Using Surrogate Safety Measures

Tanvi Gupta, Siddhartha Rokade, and Pravesh Gautam

Abstract There are several proximal safety indicators that help determine the safety of uncontrolled intersections without using past accident data. This study is based on post encroachment time (PET) as safety indicator. This analysis aims to find out the percentage of critical conflicts by combining post encroachment time with the conflicting speed of vehicles. Research has been done firstly by considering all the right-turning vehicles together and then all classes of right-turning vehicles separately. Among multiple crossing scenarios, the maximum proportions of conflicts occur between right-turning two-wheeler (2w) and through moving 2w and right-turning 4w and through vehicle 2w, and found a relationship between traffic volume and PET, after seeing the correlation between them, which is found to be negatively correlated and there developed a model, and R square values are compared for the best fit model.

Keywords Proximal safety indicator · Critical conflicts · Post encroachment time (PET)

1 Introduction

Intersections present distinct safety concerns because of unsafe driver actions and maneuvers that outcome in traffic conflict with a potential for avoidable crashes. This includes car trajectory conflicts with multiple crossing approaches, pedestrian conflicts, sudden modifications in vehicle velocity, unintended lane changes, etc. These crossing points see more traffic clashes as traffic lights are absent, and drivers of self-sorting out traffic streams need to make proper choices for completing different moves. Curiously, for non-industrial nations, these crossing points carry on diversely

T. Gupta (✉) · S. Rokade
Maulana Azad National Institute of Technology, Bhopal, India
e-mail: tanvigupta2617@gmail.com

P. Gautam
Indian Institute of Technology Bombay, Mumbai, India

L. Devi et al. (eds.), *Proceedings of the Sixth International Conference of Transportation Research Group of India*, Lecture Notes in Civil Engineering 273,
https://doi.org/10.1007/978-981-19-4204-4_11

in contrast with their western counterparts [1]. The non-prioritized traffic, that is, minor street traffic, just as right-turning vehicles (for the left-hand drive) from the significant street, don't respect the option to proceed vehicles and embrace unsafe intersection or turning moves by accepting smaller gaps in the middle through rush hour gridlock along significant streets. Right-turning traffic has to wait to accept suitable gaps between through traffic along a major road to cross the road. Despite the fact that road accident count is altogether high, accident imprint frequencies isolated by areas, time, and type are, for the most part, low. It is hard to determine measurable surmises by only analyzing accident counts with this intense event pace. Additionally, these strategies require a longer time span to approve safety measures genuinely. Henceforth, there is a distinct requirement for a safety assessment strategy that is quicker, more asset viable, dependable, and doesn't need any accident information.

Evaluating safety by using surrogate measures to investigate conflicts is the best way to resolve the above problems. The focus of conflict research is to observe major conflicts or near-miss accidents. Traffic engineers use the idea of traffic conflict to identify dangerous locations on the country's highways. Conflicts are defined as the following events: The road conflict method can directly determine near-miss accidents in real time in the traffic flow. It provides a faster and more representative way of evaluating the expected frequency of accidents and accident results [2]. In addition, the conflicting data can be recorded with the camera in a short time. It takes less time to assess safety. In addition, these methods can also be used to evaluate the Safety of road structures that have not yet been built or traffic control strategies that have not been implemented through simulation. Because of this disruptive traffic environment, uncontrolled intersections where vehicles from all directions attempt crossing and turning simultaneously, thereby increasing the probability of crashes.

This study is more beneficial because it is not easy for us to have all the accident data and all the crash data of the intersection. Hence, it's essential to have surrogate safety measures that don't need any accident data for intersection safety. Therefore the objective of the study is to determine the critical conflicts for uncontrolled intersection and to develop a relation between PET and Traffic volume.

2 Literature Review

Past researchers had done traffic conflict studies to identify harmful traffic conditions by observing situations when the driver took ambiguous actions to avoid being involved in any accident due to sudden breaking, lane changing, etc. For conflict studies, we have to study surrogate safety measures and their quantitative measurements. PET is the time difference between two vehicles when a vehicle leaves the conflicting grid, and another vehicle just enters the conflicting grid [3]. When PET is small, there are chances of a major collision, ultimately resulting in a severe accident [4].

2.1 Former Studies on Surrogate Safety Measures

In this study, Babu and Vedagiri [5], an unsignalized intersection safety assessment will be undertaken using two substitute steps, PET and the corresponding speed of vehicle confrontation. To define critical contradictions, a vital speed concept is proposed. Using stop/braking distance definition, critical speed for a specific PET value is calculated. The findings suggest that a large percentage of disputes at the intersection are serious. This indicates that right-hand drivers are taking chances as they accept minor gaps in traffic at the crossing, which is risky. In recognizing the right-turning vehicle category, higher risk concerning heavy vehicles (HV) and TW is observed with right-turning light motor vehicles (LMV). Conflicting cars lower their speed when an HV turns; hence the low percentage of crucial conflicts for HV conflicts are registered. As TW turns, it clears the conflict area more rapidly than LMV, enabling high PET values to be recorded.

In [6], the efficiency is measured by microsimulation, creating models for the intersection. The average delay was regarded as the parameter for the study of the intersection accuracy calculation. For conflicting vehicles and vehicles entering the minor lane, negative binomial regression models are created. In this study, [7, 8], a comparative study mainly examining all classes of vehicles and then considering the individual share of the three classes of vehicles (2 W, LMV, and HV). Several CDFs (cumulative distribution functions) can be used between the overall number of PET threshold crossing conflicts and the cumulative number of right-hand turn and right-hand head-on crashes. In both cases, the CDF values for a single PET threshold of 3.5 s to below 0.5 s, with a decrease in the value of 0.5 s, are examined. Considering all vehicle types, for the threshold of PET at 1 s or below, the most significant association is found between crossings disputes and associated crash data. Given each vehicle class, a PET threshold of 1 s with an R2 value of 0.793 is found for 2 W, while a PET threshold of 1.5 s at the higher side than 2 W for LMV and HV is observed.

Paul and Ghosh [1], in this analysis, a new indicator by using conflicting vehicle speed with the traditional conflict-indicator time-proximity PET. Therefore, on certain PET values dependent on the principle of a braking distance and on critical crossing disputes, another speed metric known as critical speed is determined. Detailed research showed the highest proportion of critical conflicts between turning HVs and through moving PTWs accompanied by turning LMVs and through moving PTWs (Power two wheelers). In comparison, PTW is the smallest size vehicles, which may have encouraged larger size vehicle drivers to turn right in the failure of the rules of priority. A statistical research is carried out for validity of the proposed predictor, and there is a statistically important relationship between recorded right-turn accidents and vital crossing conflicts.

This study, Peesapati et al. [7], proposes a semi-automated data collection technique, which makes it possible for profile-based proxy measurements such as speed and DR (Deceleration rate) to be more easily carried out in the field. Video analysis software was developed for collecting valuable data from the video and can also be used to retrieve videos from small angles over a longer approach path. After video

processing and interpretation, the time and location of each vehicle are produced. From the built time and space profiles, speed and acceleration/deceleration profiles can be reliably measured. The study also demonstrates that, should the average speed of the vehicles be lower, the presented technique will generate less error and/or noise in data gathered (and the resulting acceleration deceleration profile). Therefore, for such arterial and other low-speed road trials, this approach produces more precise findings.

In [9], the simulation-based approach of evaluating traffic safety of unsignalized intersection under various traffic conditions was implemented in their analysis. The PET values for various traffic volumes and variable speed are observed by the micro simulator on both roads. The chance of finding large gaps in through traffic decreases as traffic becomes more at major roads and thus, smaller gaps are being taken over by crossing vehicles on minor roads, thus showing low PET values. Results indicate that PET expectations decline and exacerbate the protection of the intersection with increased traffic levels and posted speeds.

In [10], a crash vulnerability measured that takes into consideration both the likelihood and the predicted magnitude of the crash incident in his research. It proposes a term conflict index that derives from the difference in overall kinetic energy before and after the collision, angle of collision and PET. The conflict features estimated are likened to accounts of serious accidents. The safety measure proposed has been shown to be effective at the same level as the seriousness of the crashes that happened at each location. CI (Conflict Index) increases as the angle of conflict increases, showing harsher circumstances. This is presumably that, as the angle of the colliding cars changes, energy is released at the time of collide.

This paper, Archer and Young [11], focuses on the estimation and evaluation of road safety using proximal safety metrics and related calculation techniques. It reviews three separate proximal safety indicators, namely time-to-accident (TTA), TTC (Time to collision) and PET, in definition and system. It demonstrates how field data can be calculated. Simulation modeling may also have similar interventions. The paper indicates that proximal security interventions by observation or video analyses are helpful for assessing safety at individual locations in order to enforce adequate countermeasures. In addition, it was indicated that simulation models for intersection security measurement and prediction provide a fast, detailed and resource-efficient safety analysis procedure that yields accurate and safe steps. In fact, predictive modeling may be based on proximal measures.

In [12], the critical gap for 3-W (as for the subject vehicle) has been found to be smaller in contrast to vehicles, and the critical gap has been reduced as the leading vehicle speed rises and critical gaps have been increased as vehicles' lagger speed increases. The report also says that, as the waiting time of the subject vehicle increases, the driver continues to take short distances and converge with the mainstream. In the study, critical gap values increase and critical gaps increase with the lag vehicle in stagnant proportions, as the main road volume increases.

This study, Chandra and Mohan [13], shows that, if driver behavior is the primary cause of accidents at unsignalized intersections in India. An analysis of vital holes is made using data obtained at unsignalized intersections in India and the United States

of America. Critical gaps were estimated using the maximum probability process. The critical differences between cars at an intersection in India were compared to those at a comparable intersection in the United States of America and to the values specified in the Highway Capacity Manual (HCM). Additionally, critical gap estimates for motorized two-wheelers were produced. It was discovered that at intersections of identical geometry, the critical distance between cars for different motions was significantly smaller in India than in the United States, ranging between 20 and 31%. The critical gaps between cars performing various motions at Indian intersections were consistently smaller (by up to 57%) than the base values defined in HCM. Motorized two-wheelers, which were implicated in the bulk of intersection collisions, had much smaller vital differences than automobiles. Indian drivers' less important differences in contrast to their western parts represent their reckless and risk-taking nature, which often results in road accidents.

It can be concluded after these studies that majorly 2w are at higher risk and drivers of right-turning vehicles take evasive actions due to impatience when they have to wait for long a time and it occurs in accidents when they don't get required gap to cross the intersection.

3 Methodology

Three three-legged intersections, all of which are uncontrolled, have been finalized for the purpose of calculating critical conflicts. After a thorough field inventory of geometrical and traffic characteristics, intersections are finalized. Data are obtained at peak hours at all three intersections and over a period of 7–8 h using a high-definition camera. Morning and evening peak hours are known to ensure that high-quality data are extracted. The video graphic data were gathered over many days to ensure that we provide accurate peak hour data and that any conflicts can be found, resulting in an overall positive outcome. Grids are used to retrieve data using the software Kenovia (https://www.kinovea.org/setup/kinovea.0.8.27/Kinovea-0.8.27-x64.exe). Five vehicle classes were considered, i.e., the five vehicle classes are 2w, 3w, 4w, HCV, LCV. A large amount of data was extracted using the software Kenovia and then critical conflicts are found out by noting the time interval of vehicle leaving the conflicting grid and another vehicle entering the conflicting grid. In analysis, a number of critical are found by using breaking distance concept and relation is established for same. PET is related to traffic volume and model has been developed which will ultimately help in finding safety of that intersection and which class of vehicle is at more dangerous side. Nonlinear regression model has been developed.

4 Data Collection and Data Extraction

The intersection under investigation is a standard three-arm uncontrolled intersection in Bhopal and Indore. The intersection is divided into two arms that run parallel to the major path and a third arm that connects to a minor road. The main road is a separated two-lane carriageway, though the minor road is also a divided two-lane carriageway in Bhopal. Figure 1 illustrates three-legged intersection. At the intersection, light commercial vehicles (LCV), heavy commercial vehicles (HCV), two-wheelers (2 W), three-wheelers (3 W), and auto-rickshaws move.

The intersection has clear approaches and is free of bus stops, parking, and other obstructions. Left-turning cars from the major road usually take the left-most lane and diverge into the minor road at the intersection. Similarly, cars making a left turn from a minor road merge into the left-most lane of the main road. According to the left-hand rule in India, these maneuvers do not cause significant damage to protection, but right-turning traffic on a major road heading towards a minor road must pass through traffic on the major road. Similarly, traffic turning right from a minor road must pass across traffic on a main road. As a result, these actions do pose a danger to the intersection's safety. Additionally, right-turning traffic from the minor road would connect with the main roads through traffic. As a result, only crossing collisions caused by right-turning vehicles from minor roads and main roads with through traffic on the major road were analyzed.

The video-graphic technique is used to gather data at the chosen uncontrolled intersection destinations. A high-definition handy camera is mounted in suitable positions (on top of buildings and on top of shops located at the intersection's corner)

Fig. 1 Intersection of Bhopal on which study is done

to record the necessary information for calculation of necessary data. The video camera is mounted in the front building so that the whole confrontation region is available. By determining the PET and speeds of conflicting across cars, we were able to observe conflicts caused by crossing maneuvers. PET is described as the time difference between crossing vehicles exiting a conflict zone and through vehicles approaching the same conflict zone. The PET value of a conflict is dependent on many variables, including the direction, acceleration, and duration of the right-turning car, as well as the Speed of the conflicting through vehicle. As a result, the category of turning vehicle is often included in this analysis when deciding conflicts. Data has been collected at all the four intersections in peak hours morning (9:00 am to 11:00 am) and evening (5:00 pm to 6:00 pm). After considering the dimensions of intersections, grids were placed at the intersection using the software Kenovia, divided the conflict area into grids of 2.5 m $\times$ 2.5 m which I found more precise to be placed at the intersection. After that video was played at Kenovia itself and it is played at 25 frames per second, and the accuracy for the measurement of PET is 0.040 s. Frame by frame video is played, and after that situation of conflict was examined and PET is calculated as the time difference when right-turning vehicle just leaves the grid and through vehicle just enters the conflicting grid. This is the two-time events we have been calculating to collect all the data set for all the intersection. Speed is the parameter used for calculating the percentage of critical conflicts. So, it's important to know the speed of conflicting vehicle or through vehicle that is the vehicle coming from the major road. When vehicle enters the conflicting grid time is noted down as t1 and when vehicle the conflicting grid again time is noted down as t2. The difference between t1 and t2 is the time required by the conflicting vehicle to cross the grid and as we have discussed earlier, we know the size of grid, so, after calculation of time and distance traveled in one grid and time took to cross one grid. After considering the dimensions of intersections, grids were placed at the intersection using the software kenovia divided the conflict area into grids of 2.5 m $\times$ 2.5 m which I found more precise to be placed at the intersection. After that video was played at Kenovia itself and it is played at 25 frames per second, and the accuracy for the measurement of PET is 0.040 s. Frame by frame video is played. And after that situation of conflict was examined and PET is calculated as the time difference when right-turning vehicle just leaves the grid and through vehicle just enters the conflicting grid. This is the two-time events we have been calculating to collect all the data set for all the intersection. Speed is the parameter used for calculating the percentage of critical conflicts. So, it's important to know the speed of conflicting vehicle or through vehicle that is the vehicle coming from the major road. When vehicle enters the conflicting grid time is noted down as t_1 and when vehicle the conflicting grid again time is noted down as t_2. The difference between t_1 and t_2 is the time required by the conflicting vehicle to cross the grid and as we have discussed earlier, we know the size of grid. So, after calculation of time and distance traveled in one grid and time took to cross one time, we will get the speed of conflicting vehicle and this is what is done to calculate the speed of all classes of through vehicle.

5 Analysis and Results

All the conflicts are determined based on the PET and speed of conflicting vehicle and relation is developed based on pet and traffic volume.

5.1 Frequency Distribution of Observed PET

The frequency distribution and relative frequency distribution of PET values that are calculated for three-legged intersection are shown in Fig. 2 and Fig. 3, respectively. From Fig. 1, it can be observed that maximum number of PET values can be found between interval (0.5–0.6), (0.3–0.4), and (0.1–0.2), respectively, and after PET of 1 s, there is a sudden decrease in the frequency. From Fig. 2, it can be concluded that relative to all other PET value 0.3–0.4 is taken by a greater number of vehicles,

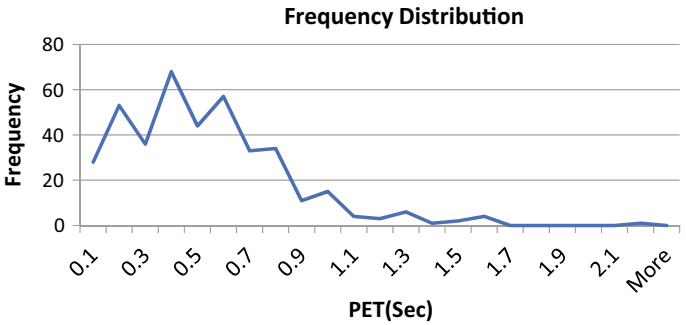

Fig. 2 Frequency distribution graph

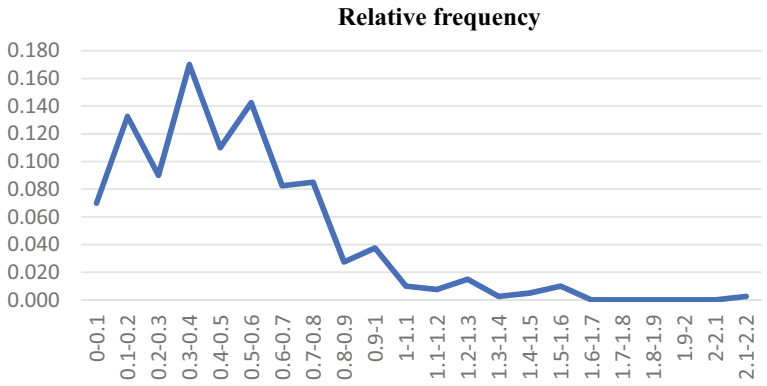

Fig. 3 Relative frequency distribution graph

which tends for the maximum number of conflicts because right-turning vehicles are accepting smaller gaps which will lead to a conflict.

5.2 Determination of Percentage of Conflicts Using Critical Speed

To find out the critical conflict, when right-turning vehicle exits the conflicting grid and the distance available through vehicle to enter the conflicting zone is speed of through vehicle/conflicting vehicle multiply by Post encroachment time (Speed of conflicting vehicle*PET). Whenever the calculated is more than the distance required to stop the conflicting vehicle, i.e., stopping distance, then this conflict is said to be non-critical and if calculated distance is less than the stopping distance it is said to be a critical one.

$$\text{Available distance} = \text{Stopping distance } v * \text{PET} = v^2 * 2gf$$

$$v = \text{PET}/2gf$$

where, v = Speed of conflicting through vehicle (m/s)

g = Gravitational acceleration (m/s^2) = 9.8

f = Coefficient of friction b/w road surface and tyre = 0.35

PET = post encroachment time [5].

In the present study, this concept has been used to find out the percentage of critical conflicts using critical Speed. In the present study, PET values are taken from 0 to 2.2 s. More than 2.5 s are common and no risky disputes because the driver is able to monitor the vehicle enough to avoid measures if necessary.

In this study, 400 conflicts whose pet is less than 2.5 s and conflicting or through vehicle speed are determined. All the conflicts are observed from the data and the disputes observed were divided by PET values in 11 groups as you can see in Table 1 from 0 to 2.5 s with a rise of 0.2 s. By taking the lower PET values for that category, the critical speeds for that particular class are calculated. Table 1 also shows critical speeds for each PET category. The conflicts found are further classified in five classes depending on the speeds of through vehicle, i.e., ≤ 4.9, $4.9 \leq 9.9$, $9.9 \leq 14.8$, $14.8 \leq 19.8$, $19.8 \leq 24.7$, $24.7 \leq 29.7$, $29.7 \leq 34.6$, $34.6 \leq 39.6$, $39.6 \leq 44.5$, $44.5 \leq 49.4$, these speed categories are classified based on critical speed.

All the through vehicle whose speed is greater than critical speed as are considered as critical conflicts and all the through vehicle whose speed is less than the critical speed for that particular is taken as non-critical ones. Since 5% vehicle speed is less than 4.9 km/h so they are non-critical conflicts. Now if we see the group (0–0.2) in Table 2 itself, we can see the critical speed for that particular group is 0 km/h. it means all the conflicting vehicle speed is more than the critical speed and hence

Table 1 Classification of all right-turning vehicles with through traffic

Conflict distribution of all right-turning vehicles with through vehicles														
			Percent conflicts											
			Conflicting vehicle speed in Km/h											
Class	Frequency	Critical speed (Km/h)	% Conflicts	≤4.9	4.9 ≤ 9.9	9.9 ≤ 14.8	14.8 ≤ 19.8	19.8 ≤ 24.7	24.7 ≤ 29.7	29.7 ≤ 34.6	34.6 ≤ 39.6	39.6 ≤ 44.5	44.5 ≤ 49.4	% Critical conflicts
0–0.2	81	–	20	1	4	3	5	–	3	2	2	1	–	20
0.2–0.4	104	5	26	5	3	3	3	3	3	2	2	1	2	21
0.4–0.6	101	10	25	4	5	4	3	2	2	1	2	2	1	16
0.6–0.8	67	15	17	2	3	–	4	3	3	1	1	–	–	8
0.8–1	26	20	7	1	1	–	2	2	–	1	1	–	–	4
1–1.2	7	25	2	–	0	0	1	–	–	–	0	0	–	1
1.2–1.4	7	30	2	–	–	–	0	1	0	1	0	–	–	1
1.4–1.6	6	35	2	–	–	–	–	0	–	0	1	–		1
1.6–1.8	–	40	–	–	–	–	–	–	–	–	–	–	–	–
1.8–2	–	44	–	–	–	–	–	–	–	–	–	–	–	–
2–2.2	1	49	0	–	–	–	–	–	–	0	–	–	–	–
	400		100	12	16	10	18	11	10	9	8	4	2	71

Table 2 Classification of all right-turning 2w vehicles with through traffic

Conflict distribution of all right-turning 2w with through vehicles														
				Percent conflicts										
				Conflicting vehicle speed in Km/h										
Class	Frequency	Critical speed (Km/h)	% Conflicts	≤4.9	4.9 ≤ 9.9	9.9 ≤ 14.8	14.8 ≤ 19.8	19.8 ≤ 24.7	24.7 ≤ 29.7	29.7 ≤ 34.6	34.6 ≤ 39.6	39.6 ≤ 44.5	44.5 ≤ 49.4	% Critical conflicts
0–0.2	42	18.83	–	–	–	2.69	1.79	4.48	3.14	3.59	1.79	1.35	–	18.83
0.2–0.4	58	26.01	4.94	–	1.35	1.79	2.69	3.59	5.38	4.04	2.24	2.69	2.69	26.46
0.4–0.6	66	29.60	9.89	0.9	1.79	2.69	3.14	4.48	4.93	2.69	3.59	3.14	2.24	26.91
0.6–0.8	40	17.94	14.83	–	–	4.04	3.59	2.69	–	2.24	2.69	2.69	–	13.90
0.8–1	9	4.04	19.78	–	–	–	0.45	–	0.90	1.35	–	1.35	–	3.59
1–1.2	3	1.35	24.72	–	–	–	–	–	0.45	–	0.45	0.45	–	1.35
1.2–1.4	2	0.90	29.67	–	–	–	–	–	–	0.45	–	–	0.45	0.90
1.4–1.6	2	0.90	34.61	–	–	–	–	0.45	–	–	–	0.45	–	0.45
1.6–1.8	–	–	39.55	–	–	–	–	–	–	–	–	–	–	–
1.8–2	–	–	44.50	–	–	–	–	–	–	–	–	–	–	–
2–2.2	1	0.45	49.44	–	–	–	–	–	–	–	–	–	0.45	–
	223	100		0.9	3.14	11.2	11.7	15.7	14.8	14.3	10.76	12.1	5.83	92.38

all the conflicts are considered as critical speed, i.e., 20.25% of conflicts are critical. Similarly for all the other groups critical conflicts are determined and based on critical speed and conflicting speed of through vehicle critical conflicts are shown. All the shaded cells that are shown in all the tables show that those percent of vehicles whose speed is more than critical speed for that particular pet class and addition of all the shaded cells of same row gives us the sum of percentage of critical conflicts. It is found that below pet 2.2 s 71% of conflicts are critical one hence the intersection is at higher risk. This is how we will calculate the percentage of critical conflicts for different classes of right-turning vehicles. From the above-shown table, it can be concluded that different vehicle drivers show different behavior, and due to its relevant, results can be seen and these results show that drivers of right-turning vehicle are accepting critical gaps and due to their acceptance of smaller gap we can see large number of critical conflicts, which is very risky for the safety of that intersection. It can also be concluded from the above scenario that all together 2w are at major risk it can be due to the driver behavior of 2w and its size also as we have discussed earlier, this tends to accept smaller gaps all together more than 90% of critical conflicts are found compared to 3w and 4w. This can be due to characteristics of right-turning vehicle [5]. From the above tables, it can also be seen that for all the speed significant count of conflicts can be found (Tables 3 and 4).

5.3 Development of Relation Between Traffic Volume and Post Encroachment Time

Model fitting is done to analyze the data and check the accuracy of data and develop a relationship. Curve fitting helps us in finding the relation between two dependent variables. It can be done by curve fitting tool (MATLAB). Model can be of various form means we can fit the equation using different forms of curve, for e.g., polynomial fit, exponential, logarithmic, linear fitting, power etc. and the best curve fit is chosen by its goodness of fit. Depending on its goodness of fit, different curves are plotted and best fit curve is shown in my study. Various models were tried and the best results were shown in 4-degree polynomial and have checked the goodness of fit for it. Plot for the polynomial of 4th degree is shown in Fig. 4 and residual plot for the same is shown in Fig. 5. This plot is also collectively for all types of vehicles. Results and outputs are shown in Table 5. From the table, it can be seen that R square value of it is 0.9623, which shows that 4-degree polynomial also best fits the model.

From the above graphs and its values, it can be seen that 4-degree polynomial best fits the model as its R square value is significantly high that is 0.9623, which means a best fit, and it shows that high traffic volume can call for lesser pet, which is very dangerous for the intersection.

Table 3 Classification of 3w right-turning vehicles with through traffic

Conflict distribution of all right-turning 3w with through vehicles														
				Percent Conflicts										
				Conflicting vehicle speed in Km/h										
Class	Frequency	Critical speed (Km/h)	% Conflicts	≤4.9	4.9 ≤ 9.9	9.9 ≤ 14.8	14.8 ≤ 19.8	19.8 ≤ 24.7	24.7 ≤ 29.7	29.7 ≤ 34.6	34.6 ≤ 39.6	39.6 ≤ 44.5	44.5 ≤ 49.4	% Critical conflicts
0–0.2	5	14.29	–	–	–	–	2.86	5.71	2.86	2.86	–	–	–	14.29
0.2–0.4	2	5.71	4.94	–	–	–	–	2.86	2.86	–	–	–	–	5.71
0.4–0.6	9	25.71	9.89	2.86	5.71	2.86	5.71	2.86	–	2.86	2.86	–	–	17.14
0.6–0.8	9	25.71	14.83	2.86	2.86	5.71	8.57	2.86	2.86	2.86	–	–	–	17.14
0.8–1	6	17.14	19.78	–	–	–	5.71	2.86	2.86	2.86	–	2.86	–	11.43
1–1.2	2	5.71	24.72	2.86	2.86	–	–	–	–	–	–	–	–	–
1.2–1.4	2	5.71	29.67	–	–	2.86	–	–	–	–	2.86	–	–	2.86
1.4–1.6	–	–	34.61	–	–	–	–	–	–	–	–	–	–	–
1.6–1.8	–	–	39.55	–	–	–	–	–	–	–	–	–	–	–
1.8–2	–	–	44.50	–	–	–	–	–	–	–	–	–	–	–
2–2.2	–	–	49.44	–	–	–	–	–	–	–	–	–	–	–
	35	100		8.57	11.43	11.43	22.86	17.14	11.43	11.43	5.71	2.86	–	68.57

Table 4 Classification of 4w right-turning vehicles with through traffic

Conflict distribution of all right-turning 4w with through vehicles														
				Percent conflicts										
				Conflicting vehicle speed in Km/h										
Class	Frequency	Critical speed (Km/h)	% Conflicts	≤ 4.9	4.9 ≤ 9.9	9.9 ≤ 14.8	14.8 ≤ 19.8	19.8 ≤ 24.7	24.7 ≤ 29.7	29.7 ≤ 34.6	34.6 ≤ 39.6	39.6 ≤ 44.5	44.5 ≤ 49.4	% Critical conflicts
0–0.2	26	22.2	–	0.0	0.0	1.7	5.1	6.0	2.6	4.3	2.6	0.0	0	22.2
0.2–0.4	35	29.9	4.94	3.4	0.0	3.4	4.3	6.0	4.3	0.0	3.4	2.6	2.6	26.5
0.4–0.6	19	16.2	9.89	2.6	1.7	3.4	0.0	3.4	2.6	0.9	0.0	0.9	0.0	11.1
0.6–0.8	18	15.4	14.83	1.7	2.6	3.4	0.0	2.6	3.4	0.9	0.0	0.9	0.0	7.7
0.8–1	10	8.5	19.78	0.9	1.7	0.0	0.0	0.0	2.6	0.9	1.7	0.0	0.9	6.0
1–1.2	2	1.7	24.72	0.0	0.0	0.0	0.9	0.9	0.0	0.0	0.0	0.0	0.0	0.0
1.2–1.4	3	2.6	29.67	0.0	0.0	0.9	0.9	0.0	0.0	0.0	0.0	0.9	0.0	0.9
1.4–1.6	4	3.4	34.61	0.9	0.0	0.0	0.0	0.9	0.9	0.0	0.9	0.0	0.0	0.9
1.6–1.8	0	0.0	39.55	0.0	0.0	0.0	0.0	0.0	0.0	0.0	0.0	0.0	0.0	0.0
1.8–2	0	0.0	44.50	0.0	0.0	0.0	0.0	0.0	0.0	0.0	0.0	0.0	0.0	0.0
2–2.2	0	0.0	49.44	0.0	0.0	0.0	0.0	0.0	0.0	0.0	0.0	0.0	0.0	0.0
	117.0	100.0		9.4	6.0	12.8	11.1	19.7	16.2	6.8	8.5	5.1	3.4	75.2

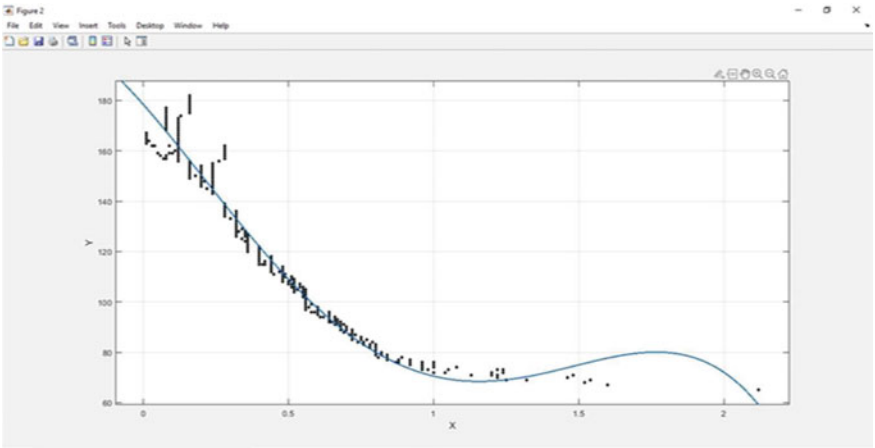

Fig. 4 Plot between PET and traffic volume

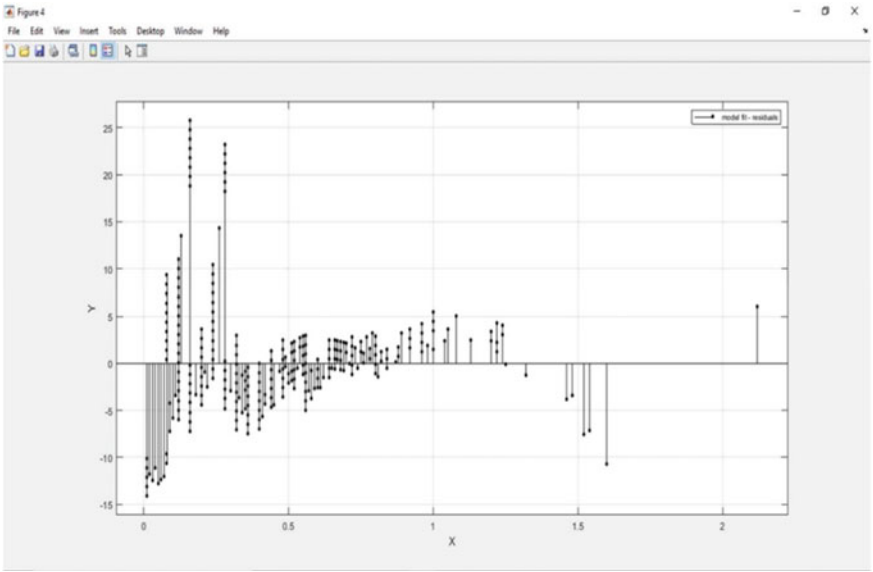

Fig. 5 Residual plot

6 Conclusion and Recommendations

Due to the high prevalence of disciplined traffic maneuverability in India, unsignalized intersections basically act as unregulated ones. By disobeying the preference laws, right-turning cars from major and minor roads make dangerous crossing movements in front of right-of-way vehicles. Non-prioritized vehicles obstruct the flow of

Table 5 Goodness of fit

Linear model polynomial with 4 degree	
$f(x) = p1 * x^4 + p2 * x^3 + p3 * x^2 + p4 * x + p5$	
Coefficients (with 95% confidence bounds)	
$\mathbf{P_1}$	−41.72 (−51.67, −31.77)
$\mathbf{P_2}$	141.4 (103.6, 179.2)
$\mathbf{P_3}$	−77.43 (−123.1, −31.76)
$\mathbf{P_4}$	−130.2 (−150.1, −110.2)
$\mathbf{P_5}$	178.5 (175.8, 181.1)
Goodness of fit	
SSE	1.43e+04
R-square	0.9623
Adjusted R-square	0.9619
RMSE	6.018

right-of-way vehicles in certain cases. As a result, using PET alone to assess dispute is insufficient for assessing the protection of intersections on highways where traffic travels at varying speeds. The aim of this analysis is to find out the percentage of critical conflicts by combining post encroachment time with the conflicting speed of vehicle. Analysis has been done firstly by considering all the right-turning vehicles together and then after that considering all classes of right-turning vehicle separately. Four uncontrolled intersections have been chosen. A speed parameter referred to as critical speed is measured and used to define critical disputes based on the definition of braking time. As a result, the present analysis evaluates the protection of an unsignalized intersection using two proxy measures PET and the pace of the conflicting through vehicle and after that a model is developed between traffic volume and pet showing how traffic volume variation can affect the post encroachment time. Now talking of percentage of critical conflicts when all right-turning vehicle are considered percentage of critical conflicts were found 71% similarly considering all different classes of right-turning vehicle different results were obtained, i.e., when RTV is 2w % is 92.38, when RTV is 3w % is 68.57 and when RTV is 4w % is 75.21. So, it can be said that percentage of critical conflicts are more when RTV is 2w.

The model developed between post encroachment time and traffic volume is best fitted using R square value. Different models were fitted and based on R square value best fit model is chosen because R square value for the model is quite high which is 4-degree polynomial whose R square value is 0.9623 which shows good fit for this model.

This study is mainly focused on four uncontrolled intersections, i.e., two in Bhopal and two in Indore. For further study, this can be done for different parts of the country and other type of intersections can also be considered, which may help us in predicting more better and accurate results. This study can be further extended to developing model based on traffic volume and PET considering all the vehicle classes separately, which will give more better and safer results. The intersections

in this study are having Speed of conflicting vehicle up to <50 km/h. so this can be further used for the intersections having higher Speed of conflicting vehicle and study of critical conflicts can be carried out. Based on one proximal indicator, we cannot purely define the safety level of intersection like I have considered Pet as surrogate measure and based on that all the results are concluded for further study various surrogate safety measures can be considered and concluding all the results a mixed index can be developed based on different parameters of safety.

References

1. Paul M, Ghosh I (2018) Speed-based proximal indicator for right-turn crashes at unsignalized intersections in India. J Transp Eng Part A: Syst 144(6):04018024
2. Archer J (2000). Developing the potential of micro-simulation modelling for traffic safety assessment. In: Proceedings of the 13th ICTCT workshop, vol. 44. Citeseer, October 2000
3. Cooper PJ (1984) Experience with traffic conflicts in Canada with emphasis on "post encroachment time" techniques. In: International calibration study of traffic conflict techniques. Springer, Berlin, Heidelberg, pp 75–96
4. Vogel K (2003) A comparison of headway and time to collision as safety indicators. Accid Anal & Prev 35(3):427–433
5. Shekhar Babu S, Vedagiri P (2018) Proactive safety evaluation of a multilane unsignalized intersection using surrogate measures. Transp Lett 10(2):104–112
6. Caliendo C (2014) Delay time model at unsignalized intersections. Transp Eng 140(9):04014042
7. Peesapati LN, Hunter M, Rodgers M, Guin A (2011) A profiling based approach to safety surrogate data collection. In: The 3rd international conference on road safety and simulation
8. Paul M, Ghosh I (2020) Post encroachment time threshold identification for right turn related crashes at unsignalized intersections on intercity highways under mixed traffic. Int J Inj Control Saf Promot 27(2)
9. "Pirdavani A, Brijs T, Bellemans T, Wets G (2010) Evaluation of traffic safety at un-signalized inter- sections using microsimulation: a utilization of proximal safety indicators. Adv Transp Stud 22:43–50
10. Alhajyaseen WK (2015) The integration of conflict probability and severity for the safety assessment of intersections. Arab J Sci Eng 40(2):421–430
11. Archer J, Young W (2010) The measurement and modelling of proximal safety measures. Proc Inst Civ Eng-Transp 163(4):191–201. Thomas Telford Ltd
12. Kanagaraj V, Srinivasan KK, Sivanandan R (2010) Modeling vehicular merging behavior under heterogeneous traffic conditions. Transp Res Rec 2188(1)
13. Chandra DS, Mohan DM (2018) Analysis of driver behaviour at unsignalized intersections. J Indian Roads Cong 5

Factors Affecting the Risk of Urban Road Traffic Crashes: A Case–Control Study Based on Wardha City Police Data

Sarfaraz Ahmed, Vikas Ravekar, Bandhan Bandhu Majumdar, and Siddardha Koramati

Abstract Road safety is a topic of concern for both health and development. Road traffic crashes are a disaster for humans. In terms of untimely deaths and injuries, it entails high human suffering and monetary costs. Road traffic crashes are controllable to corrective measures. It is, therefore, necessary to examine the causes of road traffic crashes and recommend corrective measures at a potential segment, particularly in developing countries such as India where road traffic crashes are prevalent and data on road crashes are scarce. The objective of this study is to identify risk factors related to the vehicle and the environment, that are associated with a road traffic crash on urban roads in India, based on police data records (FIR). Analyzing this basic but important data, when other geometric and land use information is missing, could help to determine the risk factors involved in road traffic crashes that are responsible for the fatal or non-fatal crash. For this study, crash data for the year 2014–2019 was collected from the Wardha City Police Department for seven road segments. A case–control study is conducted where the case is: a fatal road traffic crash; the control was a non-fatal crash. A case–control analysis is designed to assess whether exposure is related to an outcome. The risk analysis was calculated by the odds-ratio (OR) estimate, with a 95% confidence interval. Bicycles and pedestrians as victims, heavy motor vehicles as accused vehicle categories, and crossing types of vehicle maneuver were found to be major risk factors for fatal crashes, as were a few other statistically insignificant variables. Identifying factors related to the risk of being involved in a roadway traffic crash on a specific road segment aids us in recommending primary preventive measures and resolving this major threat to human health, particularly in the Indian context.

S. Ahmed (✉)
CSIR-Central Road Research Institute, New Delhi, India
e-mail: sarfaraz.crri@nic.in

V. Ravekar
Bajaj Institute of Technology Wardha, Wardha, India

B. B. Majumdar · S. Koramati
Birla Institute of Technology & Science, Pilani Hyderabad Campus, Hyderabad, India

L. Devi et al. (eds.), *Proceedings of the Sixth International Conference of Transportation Research Group of India*, Lecture Notes in Civil Engineering 273,
https://doi.org/10.1007/978-981-19-4204-4_12

Keywords Road traffic crash · Case–control study · Risk factors · Odds-ratio

1 Background

India has the highest number of traffic crashes among the 199 countries, followed by China and the United States [1]. According to the Ministry of Road Transport and Highways of the Government of India (GOI), there were 4,67,044 incidents and 1,51,417 deaths in 2018, averaging 1,280 accidents and 415 deaths per day and approximately 53 accidents and 17 deaths per hour. Road fatalities increased by 0.46% in 2018 relative to the previous year, 2017, and the number of people killed increased by 2.37% [2]. This data suggests that in India, fatal road traffic crashes are increasing significantly in comparison to non-fatal crashes, which must be addressed by developing preventive actions. To improve road safety, GOI introduced Motor Vehicle Amendment Bill 2019, amending the Motor Vehicle Act 1988. After its enactment, the Motor Vehicle Amendment Act 2019 has focused on road safety and included provisions such as penalties for traffic violations, improved coverage for hit-and-run cases, cashless care during the golden hour, vehicle health and driving checks, and more. Despite the passage of this law, India's unregulated vehicle growth and diverse traffic conditions may continue to be an issue [3]. Road traffic crashes are complicated incidents that are caused by a combination of human, mechanical, and environmental causes. The case–control analysis is the most common method of research design used in epidemiology to analyze factors and estimate injury risks [4]. Controls are a category of non-fatal crash-involved vehicles, while cases are a group of fatal crash-involved vehicles. We analyzed crash data obtained from Wardha police department FIR records for seven urban traffic corridors in Wardha city, India, for this study. Crash data was gathered over six years, from 2014 to 2019, during which 30 people were killed and 174 were injured. It is important to define risk factors that influence fatal crashes to administer effective steps to reduce the fatality rate. In India, where accident reports from city police stations are the only credible source of evidence, information about the road geometry and traffic characteristics for crash sites is usually not available. The crash reports include information such as the date of the crash, the time of the crash, the identification of the accused and victim vehicles, the number of injuries and deaths, the road type, type of road geometry, vehicle maneuver, the cause of the crash, and the type of accident. The study's key goal was to determine risk factors associated with fatal injuries caused by traffic crashes in the urban section that were linked to the driver, the vehicle, or the environment in the absence of other primary data.

2 Literature Review

Several previous studies examined the factors that influence traffic collisions. Using odds-ratio analysis, Híjar et al. [5] identified pedestrian, truck, and environmental risk factors associated with road accidents on the Mexico–Cuernavaca highways. They discovered that young drivers, regular driving, work trips, alcohol use, weekday trips, and inclement weather all play a role in fatal crashes on that route. Based on police reports, Valent et al. [6] used logistic regression to determine the main risk factors for fatal crashes in Udine, Northeast Italy. Male drivers, older drivers, cyclists, time of the incident (between 1:00 and 5:00 a.m.), lack of seat belt use, etc. were all linked to fatal crashes. In Yau [7] used stepwise logistic regression models to identify factors that influence traffic accidents by vehicle type. District board, gender, age of the vehicle, time of the accident, and street light conditions were found to be dominant attributes correlated with seriousness in private vehicles; seat-belt use and weekday incident were found to be dominant attributes in goods vehicles; and age of the vehicle, weekday, and time of the accident was found to be dominant attributes in motorcycles. Using odds-ratio analysis, Vorko-Jović et al. [8] established nighttime, junctions, and overspeeding as the key causative factors for fatal accidents in Zagreb, Croatia. To identify the key causative factors specific to serious traumatic brain injury caused by traffic accidents, Javouhey et al. [9] performed a population-based study based on five-year accident results (1996–2001) obtained from the Rhone region of France's road trauma registry. To measure their impact on crash propensity, odds-ratios were determined for all associated factors due to the accident. The most prevalent risk factors were found to be gender: man, elderly male (age more than 55 years), and un-helmeted motorcyclists, accompanied by an accused vehicle, location of the incident, time of the collision, and so on. A cross-sectional analysis was undertaken in Dubai by Al Marzooqi et al. [10] to recognize traffic accident risk factors such as high-speed limits and truck volume. Moskal et al. [4] investigated the impact of risk factors on injury injuries involving powered two-wheeler (PTW) riders in France. They performed a case–control analysis considering the odds-ratio using ten years of police data. Sex, helmet use, alcohol consumption, driving license, and transporting passengers in PTWs and leisure trips were found to be the most important risk factors for crashes.

3 Methodology

The research methodology includes selecting a study area, collecting crash data, extracting information, and analyzing it. Figure 1 depicts the overall research methodology.

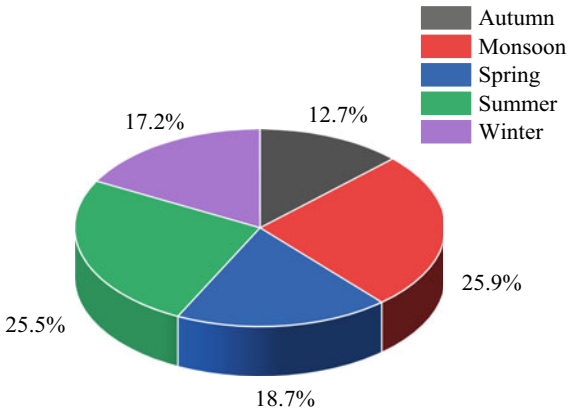

Fig. 1 The proportion of crashes that occurred during each season

3.1 Study Area Characteristics and Data Collection

Wardha city, the study area, is a municipal body in Maharashtra's Wardha district, India. Wardha is well-linked by road to the rest of Maharashtra's cities. The city is crossed by National Highway No.361 (Nagpur–Wardha–Yavatmal–Nanded–Latur–Tuljapur). It is also crossed by the Nagpur–Aurangabad–Mumbai Express Highway. As a result, heavy traffic is expected to flow through the area, and road traffic collisions seem to be on the rise. Hence, Wardha City was selected as the study area to determine risk factors specific to fatal crashes to help avoid potentially fatal crashes. Between 2014 and 2019, police records of 204 crashes on seven crash-prone road segments were used to create a road accident database [11]. The seven road segments are: Bajaj Chowk to Ambedkar Putla; Bajaj Chowk to Deoli Naka; Bajaj Chowk to Shivaji Chowk; Shivaji Chowk to Dhuniwale Math; Ambedkar Putla to Mahatma Gandhi Putla; Shivaji Chowk to Arvi Naka; and Dhuniwale Math to Nalwadi Road. After ensuring that no geometric changes (lane form, horizontal curvature, or vertical gradient) had occurred during the research period, these seven road segments were chosen for the study.

3.2 Data Description

There were two forms of crash severity included in the database: fatal and non-fatal. From 2015 to 2019, fatal and non-fatal crashes accounted for 14.7% and 85.83% of total crashes for seven segments, respectively. According to preliminary analysis, total, fatal, and non-fatal crashes were at their peak in 2016. From 2014 to 2016, the crash proportion rose, but decreased in 2018, before increasing again in 2019.

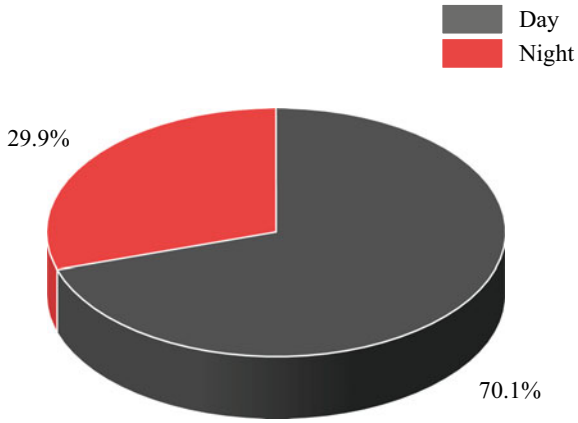

Fig. 2 Crash proportions as a function of time

Season of crash

Seasonal data could be extracted based on the date of a crash's occurrence. Summer, monsoon, autumn, winter, and spring are defined as the five seasons in this study. According to a descriptive investigation, the monsoon season (25.9%) is correlated with the highest number of fatal crashes, followed by summer (25.5%), spring (18.6%), winter (17.2%), and autumn (12.7%) as shown in Fig. 1.

Time of occurrence

The time of the crash event is determined by police reports. The 24-h day is split into two phases based on natural sunlight availability: daytime (6:00 AM–5:59 PM—when natural light is available) and nighttime (6:00 PM–5:59 AM—when artificial illumination is required for vehicular movement). Figure 2 shows that daytime crashes account for 70.1% of all crashes and nighttime crashes account for 29.9% of all crashes, respectively.

Accused vehicle details

There are many vehicle types in the database. Two-wheelers (bikes and scooters), three-wheelers, four-wheelers, heavy motor vehicles (buses, trucks, tankers, etc.), others (cyclists, pedestrians, hand carts), and unknown vehicles are the six types of vehicles. Two-wheelers, led by four-wheelers, and HMVs, were the most often involved vehicles in all crashes during the 6-year sample period (51.9%, 13.7%, and 12.3%, respectively) as shown in Fig. 3.

Victim vehicle details

Two-wheelers, led by others (pedestrians, bicycles, etc.) were the most common victim vehicles, accounting for 35.3% and 34.3% of all crashes, respectively, as shown in Fig. 4. Both of these classes of road users are considered Vulnerable Road Users (VRU), and they need special precautions to protect their lives.

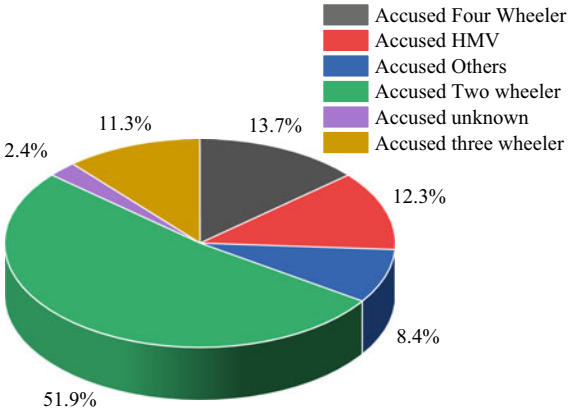

Fig. 3 The proportion of accused vehicles that were involved in a crash

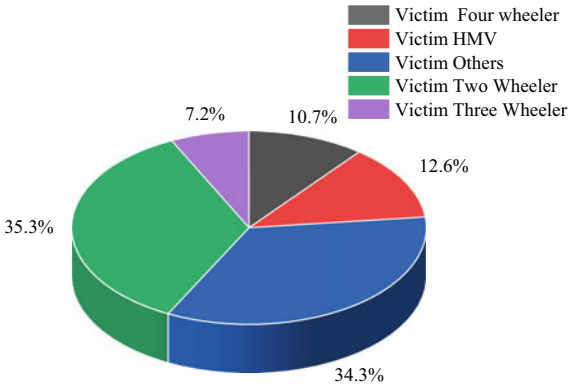

Fig. 4 The proportion of victim vehicles that were involved in a crash

Road Type

The three types of roads are arterial roads, state highways, and major district routes. Arterial roads accounted for 69.1% of all crashes, followed by state highways and major district roads, which accounted for 22.5% and 8.4% of all crashes, respectively, as shown in Fig. 5.

Road Geometry information

The four-arm lane, the curved road, and the straight road are the three forms of road geometry. More than half of the crashes, 54.9%, occurred on straight roads, 37.2% occurred on curved roads, and 7.9% occurred on four-arm roads as shown in Fig. 6.

Vehicle maneuver

Several vehicle maneuvers have been registered by the police to the database. Crossing, diverging, merging, heading straight, overtaking, U-Turn, weaving, and driving on the wrong side of the road was among the datasets. Crossing paths and

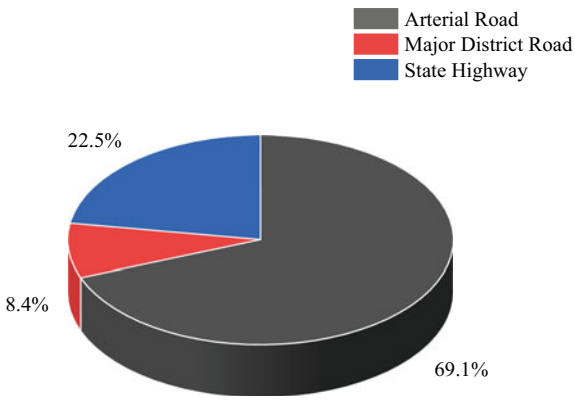

Fig. 5 The proportion of crashes on various types of roads

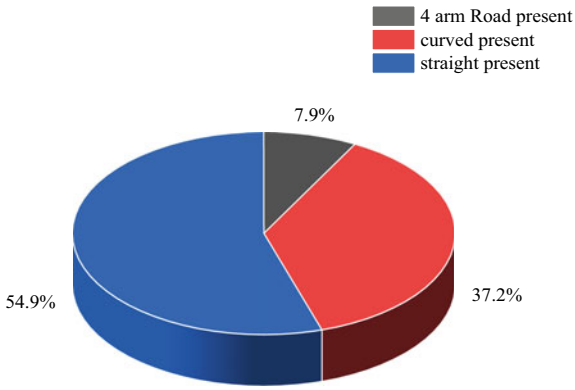

Fig. 6 The proportion of crashes that occurred on different road geometries

going straight are similarly responsible for collisions (26.4% and 26.4%, respectively) as shown in Fig. 7, which is surprising given that traveling straight is believed to be a lower risk factor than crossing, and was followed by wrong-side driving, which is also very common in Indian cities.

Cause of crash

The police report detailed the causes of the crash, which involved overspeeding, using a mobile phone while driving, vehicle skidding, and negligence, among other things. As a result, the variables were classified into four groups based on their characteristics. Negligence, overspeeding, mobile phone use, drunken driving, and signal jumping are all aspects of human causes. Similarly, vehicle defects and vehicle overturn are classified as vehicle faults, while road repairs, road distresses, road runoff, and skidding are classified as road conditions, and wrong-side driving/merging/crossing/U-turn is classified as directional related. As is widely believed, human error was a major factor in a large number of collisions, accounting for 67.1% of all crashes. Directional-related causes accounted for 24.1% of the

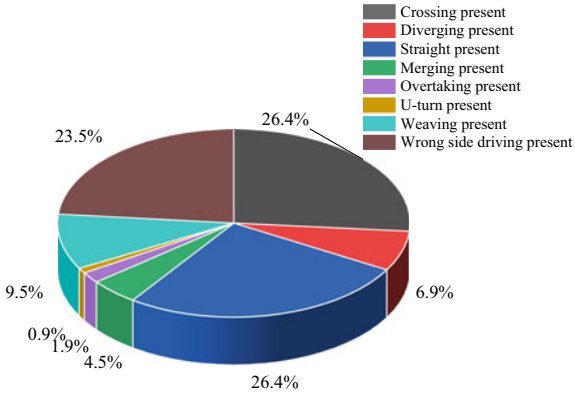

Fig. 7 The proportion of crashes for various vehicle maneuvers

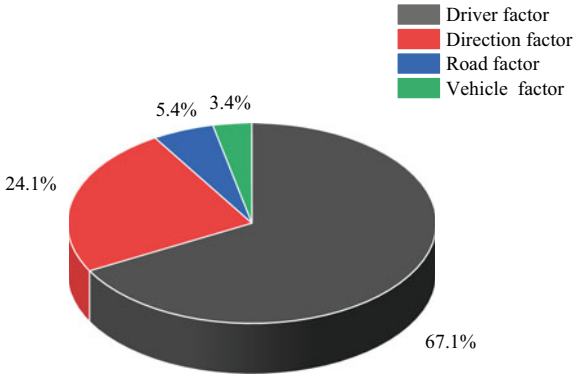

Fig. 8 The Proportion of crash causes

total, while road conditions and vehicle faults only accounted for 5.4% and 3.4%, respectively, as shown in Fig. 8.

Type of accident

Head-on collisions, rear-end collisions, hit-and-runs, side-impact collisions, and collisions with parked vehicles are all mentioned in the data. With 33.8%, the hit from the side had the biggest share, confirming prior findings on crossing route maneuver-related collisions. Other categories of crashes, such as head-on collisions, rear-end collisions, and hit-and-run, accounted for 27.9%, 18.2%, and 13.7 cents of all crashes, respectively, as shown in Fig. 9.

3.3 Case–control Study

The following vehicle, person, and environmental variables were investigated, according to traffic police reports: (a) season (summer, winter, monsoon, fall, spring);

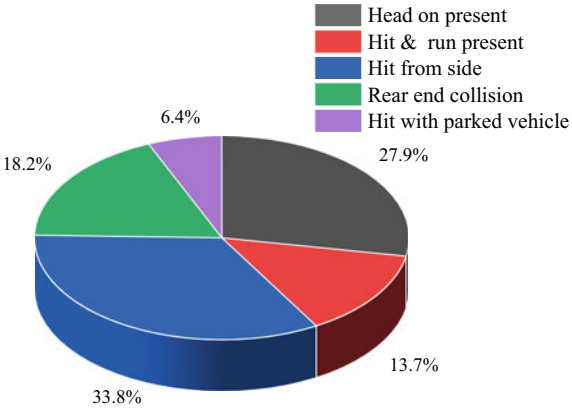

Fig. 9 Accident-type proportion

(b) the day of the accident (day or night); (c) type of accused vehicle; (d) type of victim vehicle; (e) road geometry (straight road, curved route, junction); (f) road type (arterial, state highway, Major District Road); (h) cause of the crash condition (driver, route, vehicle); (g) vehicle maneuver (crossing, merging, diverging, etc.); (i) Cause of the crash (Head-on, Rear-end collision, hit and run, Hit from the side, hit with parked vehicles). The two outcome groups have been compared:1. Fatal-persons who died 2. Non-Fatal- injured persons. Since the studied event is rare, the approximate odds-ratios for each variable provide a good prediction of the potential chances of being involved in a fatal accident. Case–control studies are used to determine whether a single exposure is linked to a specific outcome [12]. Case–control studies look at whether a single exposure is unequally spread in cases and controls, meaning that the exposure is a risk factor for the outcome under examination. Identifying case and control, or consequence and cause, is a crucial step in a case–control analysis. Following that, the proportions of cases and controls that show the exposure of concern must be identified. If the exposed cases and controls are a and b, and the unexposed cases and controls are c and d, then the exposure odds-ratio (OR) can be calculated using Eq. 1 [13].

$$OR = \frac{Odds\ of\ exposure\ among\ cases}{Odds\ of\ exposure\ among\ Controls} = \frac{a/c}{b/c} \tag{1}$$

The upper and lower confidence intervals can be calculated at 5% significance using Eqs. 2, 3 to approximate the significance of OR.

$$\text{Upper}\,95\%\,\text{CI} = e\text{^}(\ln(\text{OR}) + 1.96\sqrt{((1/\text{a} + 1/\text{b} + 1/\text{d}))} \tag{2}$$

$$\text{Lower}\,95\%\,\text{CI} = e\text{^}(\ln(OR) - 1.96\sqrt{((1/a + 1/b + 1/d))} \tag{3}$$

4 Results and Discussions

Based on the theoretical framework outlined in the methodology section, the case–control analysis is carried out. It compares how much each group is exposed to a risk factor to see whether there is an association between the risk factor and the fatal outcome. When each component is present and absent, the fatal and non-fatal crash frequency is compared, and a case–control analysis is conducted. Exposure is a risk factor if the OR value is greater than one, indicating that the existence of that variable may result in a high fatality rate. For example, when Accused HMVs are involved, the risk of being involved in fatal rather than non-fatal outcomes are higher (odds-ratio OR = 3.35 (>1); and associated CI being in the range of 1.29–8.69 (both upper and lower limit > 1) can be defined as a significant risk factor (Sig. RF).

When other victim category vehicles were involved in crashes (pedestrians, bicycles, and hand carts), the chance of death is higher (OR = 2.91; 95% CI, 1.32–6.42). The crossing maneuver can result in more deaths than injuries (OR = 3.46; 95% CI, 1.55–7.69). Monsoon has an OR of 1.26 (>1), but the related CI is in the range of 0.5399–2.9697 (lower limit < 1), indicating that it is a minor risk factor (Insig. RF). Spring has an OR of 0.85 [1] and a lower CI limit of less than 1 (0.3044–2.3991), rendering it a non-risk factor (NRF). All other factors are similarly defined and interpreted to classify risk factors associated with fatal crash outcomes. The case–control study's results are presented in Tables 1, 2,3, 4, 5 and 6.

Table 1 Fatal versus non-fatal environmental risks

Attributes	Risk variables	Outcomes	Total	OR	CI	Inference
Season	Spring	Fatal	5	0.8545	0.3044–2.3991	NRF
		Non-fatal	33			
	Summer	Fatal	8	**1.0744**	0.4463–2.5862	Insig. RF
		Non-fatal	44			
	Monsoon	Fatal	9	**1.2662**	0.5399–2.9697	Insig. RF
		Non-fatal	44			
	Autumn	Fatal	1	0.2055	0.0268–1.5774	NRF
		Non-fatal	25			
	Winter	Fatal	7	**1.587**	0.6213–4.0534	Insig. RF
		Non-fatal	28			
Time	Day	Fatal	17	0.4982	0.2250–1.1032	NRF
		Non-fatal	126			
	Night	Fatal	13	**2.0074**	0.9065–4.4451	Insig. RF
		Non-fatal	48			

Table 2 Fatal versus non-fatal type of vehicle risks

Attributes	Risk variables	Outcomes	Total	OR	CI	Inference
Accused Vehicle	2W	Fatal	11	0.4814	0.0913–1.8111	NRF
		Non-fatal	95			
	3W	Fatal	5	**1.3333**	0.2163–1.0718	Insig. RF
		Non-fatal	18			
	4W	Fatal	2	0.4379	0.0980–1.9573	NRF
		Non-fatal	28			
	HMV	Fatal	8	**3.3583**	**1.2969–8.6962**	Sig. RF
		Non-fatal	17			
	Others	Fatal	2	0.7571	0.1641–3.4936	NRF
		Non-fatal	15			
	Unknown	Fatal	2	**4.0714**	0.8311–45.4028	Insig. RF
		Non-fatal	3			
Victim Vehicle	2W	Fatal	7	0.498	0.2025–1.2247	NRF
		Non-fatal	66			
	3W	Fatal	1	0.3655	0.0465–2.8753	NRF
		Non-fatal	15			
	4W	Fatal	0	0.1111	0.0066–1.8816	NRF
		Non-fatal	22			
	HMV	Fatal	5	**1.4571**	0.5033–4.2186	Insig. RF
		Non-fatal	21			
	Others	Fatal	16	**2.9155**	**1.3236–6.4220**	Sig. RF
		Non-fatal	54			

Table 3 Fatal versus Non-Fatal Road-related risks

Attributes	Risk variables	Outcomes	Total	OR	CI	Inference
Road type	Arterial Road	Fatal	19	0.7362	0.3274–1.6556	NRF
		Non-fatal	122			
	MDR	Fatal	1	0.3405	0.0435–2.6684	NRF
		Non-fatal	16			
	SH	Fatal	10	**1.9167**	0.8249–4.4534	Insig. RF
		Non-fatal	36			
Road geometry	4 arm Road present	Fatal	2	0.8163	0.1759–3.7891	NRF
		Non-fatal	14			
	curved	Fatal	14	**1.5806**	0.7235–3.4534	Insig. RF
		Non-fatal	62			
	straight	Fatal	14	0.6786	0.3119–1.4763	NRF
		Non-fatal	98			

Table 4 Fatal versus non-fatal vehicle movement-related risks

Attributes	Risk variables	Outcomes	Total	OR	CI	Inference
Vehicle maneuver	Crossing	Fatal	15	**3.4615**	**1.5562–7.6998**	Sig. RF
		Non-fatal	39			
	Diverging	Fatal	0	0.1815	0.0105–3.1236	NRF
		Non-fatal	14			
	Merging	Fatal	1	0.7155	0.0862–5.9372	NRF
		Non-fatal	8			
	Straight	Fatal	6	0.6563	0.2527–1.7043	NRF
		Non-fatal	48			
	Overtaking	Fatal	0	0.6211	0.0862–5.9372	NRF
		Non-fatal	4			
	U turn	Fatal	0	**1.1311**	0.0530–24.142	Insig. RF
		Non-fatal	2			
	Weaving	Fatal	2	0.6597	0.1444–3.0142	NRF
		Non-fatal	17			
	Wrong side driving present	Fatal	6	0.7857	0.3010–2.0513	NRF
		Non-fatal	42			

Table 5 Fatal versus non-fatal cause-related risks

Attributes	Risk variables	Outcomes	Total	OR	CI	Inference
Cause of crash	Human factor	Fatal	23	**1.7293**	0.7017–4.2618	Insig. RF
		Non-fatal	114			
	Direction	Fatal	6	0.7616	0.2920–1.9864	NRF
		Non-fatal	43			
	Road condition	Fatal	0	0.2331	0.0134–4.0606	NRF
		Non-fatal	11			
	Vehicle fault	Fatal	1	0.9655	0.1121–8.3172	NRF
		Non-fatal	6			

4.1 Season

Based on the OR estimates, none of the seasons were statistically significant risk factors causing fatal crashes from 2015 to 2019. At a 95% confidence interval, summer, monsoon, and winter were found to be marginal risk factors. This demonstrates that severe weather has had an impact on the occurrence of road crashes. In general, Monsoon (OR = 1.26), Winter (OR = 1.58), and Summer (OR = 1.07) are linked to a higher risk of fatal crashes than other seasons as shown in Table 1,

Table 6 Fatal versus non-fatal accident type-related risks

Attributes	Risk variables	Outcomes	Total	OR	CI	Inference
Type of accident	Head on	Fatal	11	**1.611**	0.7128–3.6411	Insig. RF
		Non-fatal	46			
	Hit and run	Fatal	4	0.9615	0.3083–2.9989	NRF
		Non-fatal	24			
	Hit from side	Fatal	14	**1.8932**	0.8633–4.1517	Insig. RF
		Non-fatal	55			
	Rear-end collision	Fatal	1	0.0058	0.0008–0.0443	NRF
		Non-fatal	36			
	Hit with parked vehicle	Fatal	0	0.1961	0.0114–3.3874	NRF
		Non-fatal	13			

implying that they are important causes. In the winter, road accidents are more prevalent than in other months. This might be due to India's foggy weather in December and January, which causes poor road visibility [14]. People drive a little slower in foggy conditions, but they also retain a closer following distance to the vehicle in front of them. This, along with the narrower field of view, raises the danger of a collision [15]. The Indian monsoon season usually lasts from July to September. Rain can have a variety of effects on driving. Rain will decrease the output of headlamps, tail lights, brake lights, and other warning lights, as well as the driver's ability to see clearly [12]. Wet roads, from a technical standpoint, will reduce the traction of a vehicle's tires on the ground, making driving conditions riskier [16]. Summer in India lasts from April to June. Drivers are affected by high temperatures on both a psychological and physiological level. People get more irritated with others, they become fatigued, lose their focus, and their reaction time slows as the temperature rises [15]. This might explain why the odds of a traffic collision are higher in the summer. In India, the spring and autumn seasons are usually pleasant, which may explain why they were determined to be non-risk factors (OR 1).

4.2 Time

Time is split into two categories: Day (6 am–5:59 pm) and night (6 pm–5:59 am). As shown in Table 1, Nighttime is observed as an insignificant risk factor, with OR 2.07. This finding may be attributed to higher speed levels during night travel, which raises the risk of a crash. The main contributory risk factors associated with night travel are low night vision combined with poor visual direction on roads [17]. As a response, special attention must be paid to making nighttime driving safer. The daytime is determined to be non-risky (OR < 1). This might be because light and visual glare are not an issue for the driver's eyesight during daylight driving.

4.3 Type of Accused Vehicle

The distribution of incidents and OR Accused vehicles is seen in Table 2. The six types of accused vehicles include two-wheelers, three-wheelers, four-wheelers, HMV, others, and unknown. HMVs are found to be significant risk factors, with a greater risk of fatal crashes (OR = 3.35) than most of the accused vehicles. Because of their large size, mass, and greater momentum at a particular speed, fatal crashes are often more likely when smaller vehicles collide with heavy motorized vehicles (HMVs) such as buses and trucks [18, 19]. As a result, HMV movements must be given careful consideration. Three-wheelers and unknown accused vehicle categories were observed as insignificant risk factors associated with fatal crash outcomes. (OR = 1.33 for three wheelers, and OR = 4.07 for unknown, respectively). Despite their reputation for being extremely unstable, three-wheelers appear to have a negligible risk of causing a fatal collision. This is most likely since these vehicles are powered by scooter engines and so have modest average speeds, and because their floor levels are low, a fall from them does not typically result in fatal injuries [20]. In situations when the hitting vehicle is unknown, such as in hit-and-run accidents, the victim may not receive prompt medical attention. Due to their diminished physical power, as they age, older drivers are more likely to cause serious injuries [3]. As a result, three-wheeler movements and unknown vehicles must be closely monitored. Non-risk variables linked with fatal collision outcomes included two-wheelers, four-wheelers, and other vehicle types. (OR = 0.48 for two-wheelers, OR = 0.43 for four-wheelers, and OR = 0.75 for others.). Because two-wheelers and other vehicles (bicycles, for example) are so small, their impact on fatal collisions could be minimal. The severity of the offense increases as the accused vehicle goes from a two-wheeler to a truck [21]. Multi-vehicle two-wheeler collisions were caused by younger riders, improper vehicle speed, increased traffic congestion, and road design difficulties [22]. In the city, road designs should discourage excessive speeds. This might be accomplished by including safe and well-designed speed-limiting devices into the road design [20].

4.4 Type of Victim Vehicle

Other types of vehicles, such as cyclists, cyclists, and hand carts (slow-moving vehicles), were major risk factors (OR = 2.91) linked to a higher incidence of fatal collisions as shown in Table 2. Pedestrians and bicyclists are the most vulnerable road users, according to the findings, owing to their limited numbers and lack of security (Rifaat et al. 2011). Surprisingly, HMV was found to be a minor risk factor which might be due to an error while recording the data. From 2015 to 2019, Victim Two Wheelers, Three Wheelers, and Four Wheelers were shown to be non-risk factors based on OR estimations. When compared to other motorized vehicle users such as

two-, three-, and four-wheelers, bicycles and hand carts (slow-moving vehicles) are less protected during a crash, which might be resulting in more severity.

4.5 Road Type and Geometry

According to the findings, as shown in Table 3, state highway (SH) roads have a higher (OR = 1.961) but insignificant association with fatal crashes than major district roads (MDR) and arterial roads in Wardha city. Due to urban sprawl, state highways often become a part of the urban road network. They link the city with towns and districts, as well as national highways. Vehicles drive at high speeds as a result of the reduced traffic and increased number of lanes, making it more likely of a fatal crash. To avoid fatal crashes, highway segments that travel through concentrated land use must be prioritized [23]. As the number of intersections increases, the speed of traffic on arterial road segments decreases, resulting in fewer fatal collisions [24]. This might be one of the reasons why arterial roads are reported to have a lower risk of fatal crashes than non-fatal crashes. The low risk of fatal crashes on MDR can also be ascribed to the fact that they are the roads that connect production and market locations. As a consequence, the number of intersections may grow, while traffic speeds drop, resulting in fewer fatal incidents. As compared to straight and 4-arm junctions, curved roads (OR = 1.58) are found to be an insignificant risk factor. Drivers who are traveling at high speeds and are unaware of the magnitude of a turn can lose control of their vehicles, leave the lane, and slam into a barrier or tree, or another vehicle. Drivers will have a more dynamic driving situation on curves, requiring them to track more objects and spread their focus. In addition, constant curves on the roadway will inevitably trigger vehicle instability and safety concerns [25]. In general, roads in traffic networks are not always straight, and traffic phenomena on a curved road differ from traffic phenomena on a straight road because vehicles traveling on a curved road are impacted by centripetal force. This results in an erratic traffic flow that is more difficult than on straight roads [26].

4.6 Vehicle Maneuver

Concerning the factor of vehicle maneuver, crossing paths were observed to be associated with a 3.46 times higher probability of being involved in fatal crashes than other maneuvers as shown in Table 4. Crossing path collisions are a form of a traffic collision in which one moving vehicle cuts across the path of another as they were coming from either lateral or opposite directions, resulting in a collision at or near an intersection. Vehicle–vehicle crossing path collisions are common, but so are vehicle–pedestrian and vehicle–cyclist collisions. When there are no physical crossing facilities at intersections, drivers prefer to travel faster and pay less attention to crossing pedestrians [27]. This is can be attributed to unmarked roadways, where

people cross the road at different speeds and directions, resulting in a high risk of road injuries. U-turns were shown to be an insignificant risk factor for fatal collisions, with a 1.31 times higher chance of being involved. U-turns can be found at both junction and midblock (i.e., crossing U-turn intersections and median U-turns, respectively). The left turn (right turn in India), or angle, the crash is one of the most dangerous forms of junction collisions [28]. As a result, distinct phases for right-turn movements (i.e., protected right-turn phases) are given to reduce the likelihood of such crashes, particularly in heavy right-turn traffic. As a result, at junctions, higher cycle durations, and delays are recorded. As a response, optimal designs are necessary to improve traffic efficiency while also ensuring safety such as the prohibition of right-turn operations at the main junction in part or all. Diverging, merging, overtaking, weaving, and driving on the wrong side of the road were all found to have an OR less than one, indicating that they are not risk factors in study segments in Wardha city.

4.7 Cause of Crash

In general, the human factor is the most important factor that contributes to traffic collisions followed by road conditions and vehicle defects [29]. As shown in Table 5, human factors such as negligence, overspeeding, drunk driving, and so on were found to cause fatal crashes 1.72 times more often (OR = 1.72) than vehicle or road condition-related causes in this study. As a result, careful consideration must be paid to enforcement to ensure safe driving. With an OR of less than one, the direction, road condition, and vehicle fault were shown to be non-risk variables. It may seem paradoxical, but degraded pavements (one-way portions, four-legged/signalized junctions) may be beneficial to safety. Drivers may be more careful and drive at lower speeds on poorly maintained pavements, which might explain this [30]. Commercial vehicles, as opposed to non-commercial cars and motorbikes, were involved in more road crashes due to mechanical failure [31]. As a result, commercial vehicle maintenance should be given extra attention.

4.8 Accident Type

Type of accident is classified into four types as head-on, hit-and-run, hit from the side, rear-end collision. Head-on collisions (OR = 1.61) and side-impact collisions (OR = 1.89) were found to be risk factors for fatal crashes at greater chances than hit-and-run and rear-end collisions. Head-on crashes cause the most severe injury, while collisions with parked vehicles/objects have the least impact [32]. Side impact collisions are linked to both failures to yield and disobeying traffic signals [33]. Provisions can be made for opposing and side-by-side traffic streams to reduce head-on collisions and side-impact collisions. The variables including hit and run, rear-end

collision, and hit with the parked vehicle all had an OR less than one, indicating that they are minor risk factors. According to the Ministry of Road Transport and Highways (MoRTH), hit-and-run incidents accounted for over 14% of all accidents in India, up from 11.6% the year before (MoRTH, 2017) [34]. As a result, hit-and-run cases should be prioritized so that their number does not arise in the future, becoming a significant risk factor for fatal collisions. Researchers have long known that the danger of a fatal rear-end accident is more than twice as high in the dark as it is during the day. As a result, cars should be equipped with rear lights, rear marker plates, and retro-reflective tapes to make the vehicle's rear visible to oncoming traffic. To avoid being hit by a parked car, reflective warning signs must be used to make them visible [17].

As a result of the observations, each road section may be classified and prioritized as very high risk, high risk, and moderate risk by comparing the results of the case–control study variable and the frequency of a crash variable in each segment.

As indicated in table 7, segment 1 contains two major risk variables that might result in fatal collisions and is thus classified as a Very High-Risk Segment. Similarly, segments 2–4 have only one substantial risk factor that might result in a fatal collision and are thus classified as High-Risk Segments. Segments 5–7 have no significant risk concerns but do have minor risk variables that might result in a fatal crash, thus they are classified as Moderate-Risk Segments. As a result, the highest priority can be assigned to each section to prevent future fatal collisions as shown in Table 7.

Table 7 Risk factors across segments

Risk factor segment		Comparison with Case–control study output	
Segment name and no.	Description	significant risk factors	Insignificant risk factor
1. Bajaj Chowk to Ambedkar Putla	Very high-risk segment	Crossing, Accused -HMV	Hit from the side, human factor, monsoon
2. Dhuniwale Math to Nalwadi Road	High-risk segments	Crossing	Hit from the side, human factor
3. Bajaj Chowk to Deoli-Naka		Victim others	Human factor, hit from the side, monsoon, curved, SH
4. Ambedkar Putla to Mahatma Gandhi Putla		Crossing	Hit from side, monsoon, human factor
5. Shivaji Chowk to Dhuniwale Math	Moderate risk segment		Hit from the side, monsoon, summer, three-wheeler, human factor
6. Shivaji Chowk to Arvi- Naka			Head-on collision, monsoon, Human factor, nighttime
7. Bajaj Chowk to Shivaji Chowk			Head-on collision, summer,

4.9 Very-High-Risk Segments

The road connecting Bajaj Chowk and Ambedkar Putla is found to be a very high-risk region, with two major risk factors influencing crashes in this segment: crossing path maneuver and Accused HMV, as well as three other insignificant risk factors. As a consequence, this segment should be given the utmost priority to avoid any fatal collisions.

4.10 High-Risk Factors

The path that connects Dhuniwale Math to Nalwadi Road has been identified as a high-risk area, with one major risk factor affecting crashes in this segment: crossing path maneuver, as well as two minor risk factors such as hit from the side type of crash and human factor as a cause of the crash. The road from Bajaj Chowk to Deoli-Naka has been identified as a high-risk segment, with one major risk factor, other victim vehicles (pedestrians and bicycles), and six minor risk factors, including human factor as a cause of the crash, hit from the side type of crash, monsoon season, curved road geometry, crossing path maneuver, and state highway road impacting crashes in this segment. The Ambedkar Putla to Mahatma Gandhi Putla section is also found to be a high-risk segment, with one major risk factor: crossing path maneuver and three minor risk factors as causes of the crash: hit from the side, monsoon season, and human factor. As a result, these segments should be given the second-highest priority in order to avoid any fatal crashes.

4.11 Moderate Risk Factors

The road segments Shivaji Chowk to Dhuniwale Math, Shivaji Chowk to Arvi Naka, and Bajaj Chowk to Shivaji Chowk are affected by several minor risk factors such as head-on collisions, side-impact collisions, human factors, monsoon, and summer season. From Shivaji Chowk to Arvi Naka, three-wheelers were discovered to be a minor risk factor, so special attention should be paid to this segment to avoid three-wheeler-related crashes.

5 Conclusions

In urban India, road safety is a major concern, and this is especially true for both major and minor cities like Wardha. Although most road segment safety assessments are based on primary data and statistical analysis and modeling methods, only a

few studies have been conducted using secondary data, such as police data, which provides information on the different characteristics involved in an accident. In India, primary data such as traffic volume, speed, and other geometric measurements are seldom found in databases, making manual collection difficult in normal times and impossible during active pandemics. This study suggested a basic methodology for establishing a link between fatal crashes and driver, road, and environmental variables using the odds-ratio in the case–control study. The research based on seven road segments in Wardha, India, and identified several major and minor risk factors. It should be noted that since the data collection was small (204 cases), certain risk factors were discovered to be risk factors but were considered to be statistically insignificant. Larger datasets can yield better results. As a measure, risk factors that are insignificant but have a high likelihood of causing a fatal crash should be deemed risk factors so that they do not become major risk factors in the future.

Several studies have recommended some measures like HMV be prohibited from entering congested and high-crash-prone areas at peak hours in cities and conducting education and training campaigns primarily aimed at educating heavy-vehicle drivers about the safety of vulnerable road users may be a successful tactic [18]. Providing pedestrian travel infrastructures such as wide shoulders and footpaths with adequate lighting, especially in urban areas, and encouraging pedestrians to wear retroreflective clothing will help to alleviate this problem to some degree [34]. Kadali and Vedagiri [35] emphasized the significance of a street barrier or median to distinguish vehicular traffic and facilitate healthy pedestrian road crossing. To regulate human factors, such as driver behavior, efforts should be made to establish and enforce appropriate traffic laws and road safety regulations, as well as to raise public consciousness about traffic safety [29]. Adverse weather conditions during the monsoon and summer have been described as a risk factor that could result in a serious traffic accident injury. During inclement weather, drivers are urged to travel less and not exceed the posted speed limit. Additionally, drivers should inspect their tires daily to guarantee that they are in good condition [36]. Medians can be constructed to divide conflicting traffic to avoid head-on collisions and crashes caused by improper passing and lane changes. There have been suggestions for design features in braking that make halting or stopping for the striking vehicle smoother, in the struck vehicle's strength and energy-absorbing ability to shield the occupants from intrusion, in the design of interior surfaces of either vehicle and in the visibility of either vehicle to give drivers better notice to prevent a side impact collision [33]. In light of the findings of this study, Wardha city authorities should conduct a thorough safety audit of their roadways to recognize and implement countermeasures in crash-prone areas. Overall, it can be concluded that concentrating on the risk factors is beneficial. In urban Indian environments, appropriate strategies can be implemented to mitigate the severity of accident injuries and encourage a healthy road ecosystem.

Before concluding, the authors would like to point out that this report only included police-record-derived data with very small data and did not include geometric or traffic data, which are both important contributors to fatal crashes. As a result, defining risk factors, such as traffic and geometric variables, would be a potential focus of this research. Furthermore, the findings are city-specific for the case study.

However, the research method could be used as a preliminary step for cities with similar characteristics but it cannot be translated as it is.

References

1. India I (2021) Https://Irfnet.Ch/2020/12/04/Irf-India-Expresses-Concern-at-Increased-Number-of-Fatal-Road-Accidents-in-the-Country/. https://irfnet.ch/2020/12/04/irf-india-expresses-concern-at-increased-number-of-fatal-road-accidents-in-the-country/. Accessed 3 Feb 2021
2. MoRTH (2019) Road Accidents in India-2018. New Delhi
3. Panicker AK, Ramadurai G (2020) Injury severity prediction model for two-wheeler crashes at mid-block road sections. Taylor & Francis
4. Moskal A, Martin JL, Laumon B (2012) Risk Factors for injury accidents among moped and motorcycle riders. accid Anal Prev 49:5–11. https://doi.org/10.1016/j.aap.2010.08.021
5. Híjar M, Carrillo C, Flores M, Anaya R, Lopez V (2000) Risk factors in highway traffic accidents: a case control study. Accid Anal Prev 32(5):703–709. https://doi.org/10.1016/S0001-4575(99)00116-5
6. Valent F, Schiava F, Savonitto C, Gallo T, Brusaferro S, Barbone F (2002) Risk factors for fatal road traffic accidents in Udine Italy. Accid Anal Prev 34(1):71–84. https://doi.org/10.1016/S0001-4575(00)00104-4
7. Yau KKW (2004) Risk factors affecting the severity of single vehicle traffic accidents in Hong Kong. Accid Anal Prev 36(3):333–340. https://doi.org/10.1016/S0001-4575(03)00012-5
8. Vorko-Jović A, Kern J, Biloglav Z (2006) Risk factors in urban road traffic accidents. J Safety Res 37(1):93–98. https://doi.org/10.1016/j.jsr.2005.08.009
9. Javouhey E, Guérin AC, Chiron M (2006) Incidence and risk factors of severe traumatic brain injury resulting from road accidents: a population-based study. Accid Anal Prev 38(2):225–233. https://doi.org/10.1016/j.aap.2005.08.001
10. Al Marzooqi AH, Badi M, El Jack A (2010) Road traffic accidents in Dubai, 2002–2008. Asia-Pacific J Public Health 22(SUPPL 3):2002–2008. https://doi.org/10.1177/1010539510372834
11. Police W (2021) Wardha Police. http://wardhapolice.gov.in/
12. Sangkharat K, Thornes JE, Wachiradilok P, Pope FD (2021) Determination of the impact of rainfall on road accidents in Thailand. Heliyon 7(2):e06061. https://doi.org/10.1016/j.heliyon.2021.e06061
13. Alexander LK, Lopes B, Ricchetti-Masterson K, Yeatts KB (2015) Case-control studies. In: ERIC notebook. Epidemiologic Research and Information Center, Seattle
14. Singh SK (2017) Road traffic accidents in india: issues and challenges. Transp Res Procedia 25:4708–4719. https://doi.org/10.1016/j.trpro.2017.05.484
15. Bijleveld F, Churchill T (2009) The influence of weather on road safety. Swov 3(October):1–6
16. Bernardin F, Bremond R, Ledoux V, Pinto M, Lemonnier S, Cavallo V, Colomb M (2014) Measuring the Effect of the Rainfall on the Windshield in Terms of Visual Performance. Accid Anal Prev 63:83–88. https://doi.org/10.1016/j.aap.2013.10.008
17. Ackaah W, Apuseyine BA, Afukaar FK (2020) road traffic crashes at night-time: characteristics and risk factors. Int J Inj Contr Saf Promot 27(3):392–399. https://doi.org/10.1080/17457300.2020.1785508
18. Balakrishnan S, Moridpour S, Tay R (2019) Sociodemographic influences on injury severity in truck-vulnerable road user crashes. ASCE-ASME J Risk Uncertain Eng Syst Part A Civil Eng 5(4):04019015. https://doi.org/10.1061/ajrua6.0001023
19. Kim JK, Kim S, Ulfarsson GF, Porrello LA (2007) Bicyclist injury severities in bicycle-motor vehicle accidents

20. Mohan D, Bawa PS (1985) An analysis of road traffic in Delhi, India. Accid Anal Prev 17(1):33–45
21. Krishnan MJ, Anjana S, Anjaneyulu MVLR (2013) Development of hierarchical safety performance functions for urban mid-blocks. Procedia Soc Behav Sci 104:1078–1087. https://doi.org/10.1016/j.sbspro.2013.11.203
22. Allen T, Newstead S, Lenné MG, McClure R, Hillard P, Symmons M, Day L (2017) Contributing factors to motorcycle injury crashes in Victoria, Australia. Transport Res F Traffic Psychol Behav 45:157–168. https://doi.org/10.1016/j.trf.2016.11.003
23. Naqvi HM, Tiwari G (2020) Safety performance functions for fatal crashes on national highways in India. Transp Res Procedia 48(2019):1185–1189. https://doi.org/10.1016/j.trpro.2020.08.142
24. Prajapati P, Tiwari G (2013) Evaluating safety of urban arterial roads of medium sized Indian City. Proc Eastern Asia Soc Trans 9(December)
25. Kang X, Namgung M, Fujiwara A, Kim W, Wang W (2019) Analysis of vehicle maneuverability and driving characteristics on a curved road condition. KSCE J Civ Eng 23(1):420–432. https://doi.org/10.1007/s12205-018-1803-y
26. Kaur R, Sharma S (2017) Analysis of driver's characteristics on a curved road in a lattice model. Physica A 471:59–67. https://doi.org/10.1016/j.physa.2016.11.116
27. Wu P, Meng X, Song L, Zuo W (2019) Crash risk evaluation and crash severity pattern analysis for different types of urban junctions: fault tree analysis and association rules approaches
28. Al-Omari A, Shatnawi N, Khedaywi T, Miqdady T (2020) Prediction of traffic accidents hot spots using fuzzy logic and GIS. Appl Geomat 12(2):149–161. https://doi.org/10.1007/s12518-019-00290-7
29. Touahmia M (2018) Identification of risk factors influencing road traffic accidents. Eng Technol Appl Sci Res 8(1):2417–2421. https://doi.org/10.48084/etasr.1615
30. Intini P, Berloco N, Cavalluzzi G, Lord D, Ranieri V, Colonna P (2021) The variability of urban safety performance functions for different road elements: an Italian case study. Eur Trans Res Rev 13(1). https://doi.org/10.1186/s12544-021-00490-6
31. Hussain M, Shi J (2021) Modelling and examining the influence of predictor variables on the road crashes in functionally classified vehicles in Pakistan. Int J Crashworthiness. https://doi.org/10.1080/13588265.2021.1909839
32. Yannis G, Kondyli A, Mitzalis N (2013) Effect of lighting on frequency and severity of road accidents. Proc Inst Civ Eng Transp 166(5):271–281. https://doi.org/10.1680/tran.11.00047
33. Chipman ML (2004) Side impact crashes—factors affecting incidence and severity: review of the literature. Traffic Inj Prev 5(1):67–75. https://doi.org/10.1080/15389580490269218
34. Sivasankaran SK, Balasubramanian V (2020) Investigation of factors contributing to pedestrian hit-and-run crashes in India. Taylor & Francis
35. Kadali BR, Vedagiri P (2016) Proactive pedestrian safety evaluation at unprotected mid-block crosswalk locations under mixed traffic conditions. Saf Sci 89:94–105. https://doi.org/10.1016/j.ssci.2016.05.014
36. Mao X, Yuan C, Gan J, Zhang S (2019) Risk factors affecting traffic accidents at urban risk factors affecting traffic accidents at urban weaving sections: evidence from China. Int J Environ Res Public Health 16(9). https://doi.org/10.3390/ijerph16091542

Identification and Prioritization of Factors Responsible for Road Traffic Accidents in India

Nabanita Roy, Abhishek Chakraborty, Sudeshna Mitra, and Bhargab Maitra

Abstract Road Traffic Accident (RTA) is emerging as one of the predominant causes of death across the world. To address the road safety issues, the historical accident database might not be very helpful in developing countries such as India because of the unavailability of most of the data. In this regard, the present study focuses on the identification of the leading causes of RTAs in India, and the areas that need to be focused on priority-basis. Seven factors have been highlighted by the experts working in the field of road safety, as potential causes of the RTAs. Analytical Hierarchy Process (AHP) is applied to the data to prioritize the attributes through pair-wise comparison. Results revealed that 'over speeding' to be the most important factor; whereas 'unawareness of road rules' was observed to be the least prioritized. Necessary countermeasure strategies are discussed at the end, which would help to improve the road safety situation in India.

Keywords Road traffic accidents · Road traffic fatalities · Analytic hierarchy process

N. Roy · A. Chakraborty (✉)
Doctoral Research Scholar, Department of Civil Engineering, Indian Institute of Technology, Kharagpur 721302, India
e-mail: abhishekcivilchakraborty@gmail.com

N. Roy
e-mail: roynabanita91@gmail.com

S. Mitra
Transport Specialist, Global Road Safety Facility, The World Bank, Washington, D.C. 20433, USA
e-mail: smitra5@worldbank.org

B. Maitra
Department of Civil Engineering, Indian Institute of Technology, Kharagpur 721302, India
e-mail: bhargab@civil.iitkgp.ac.in

L. Devi et al. (eds.), *Proceedings of the Sixth International Conference of Transportation Research Group of India*, Lecture Notes in Civil Engineering 273,
https://doi.org/10.1007/978-981-19-4204-4_13

1 Introduction

Road Traffic Accident (RTA) is emerging as one of the predominant causes of death for people across the world [1]. At the same time, the share of road traffic deaths in low- and middle-income countries have been increased from 84 to 93% in the past three years [1, 2]. In India, which is one of the low- and middle-income countries, the motor vehicle population is growing at a faster rate than the economic and population growth. The surge in motorization coupled with the expansion of the road network has brought with it the challenge of addressing adverse factors such as the increase in road crashes.

In the year 2018, the number of RTAs and road fatalities have been increased in India, and in 2019, India experienced 449,002 RTAs involving 620,474 persons (151,113 fatalities) which is involving approximately 460 persons per million population [3]. In India, RTA is located in the 9th place in the table of causes of premature deaths and the proportion of such cases have been increased in the past 10 years [4]. This indicates the seriousness of the road safety scenario in the country, which needs to be addressed. To improve the road safety status, first, the causes or factors contributing to these RTAs are to be investigated, and then, the corresponding steps may be decided.

Similar to other low and middle-income countries, under-reporting of non-fatal crashes is observed in many cases in India [1, 2]. Even if the RTA cases are reported, many of the useful and relevant information regarding the crashes remain unreported, which creates difficulty to find out the actual reason for some crashes later. As per the reports published by the Ministry of Road Transport and Highways (MoRTH), 'over-speeding' causes most of the reported RTAs (70.4%), followed by 'driving on wrong side/ lane indiscipline' (6.3%). 'Drunken driving', 'use of mobile phones', and 'red light violation' are observed to be sharing 3%, 1.8, and 1.4% of RTAs respectively. However, in 17.1% of the cases, the reason for the crashes was either found to be 'in other categories' or unknown [3].

In such a situation, it is very difficult to assess the safety situation in India by solely depending on the historical crash data. Accumulation of all the relevant data such as road geometrics, traffic conditions, environmental conditions, road conditions, etc. would be quite difficult and in most of the situations, it would be impossible to gather all information. In line with that, it may not be appropriate to suggest countermeasures solely based on the historical crash data. Hence, instead of gathering information from police-reported crash records, it would be useful to involve various stakeholders such as police personnel, road safety experts, transport researchers, and academicians working in this field. In this regard, this present work focuses on exploring and prioritizing the leading causes or attributes of RTAs in India based on experts' suggestions. The subsequent section of the manuscript contains the summary of various causes of RTAs, followed by the methodology adopted, development of the questionnaire, data collection, and analysis of the data to prioritize the potential causes of RTAs. In the end, the conclusions are drawn and based on the results

obtained, and specific recommendations are suggested for the overall improvement of road safety.

2 Literature Review

A road traffic accident may cause due to human factors, external or environmental factors, and vehicular or mechanical factors acting individually or together in any combination. RTAs occurred due to the sole reason of vehicle malfunction or damage have been found to be very low with respect to the total number of RTAs across the world [5]. The environmental and human factors are, therefore, two main etiological factors of RTAs [6].

2.1 Environmental Factors

Weather Condition. Adverse weather may seriously influence RTAs. Chances of RTAs significantly increases with rainy or snowy weather condition as it increases the braking distance and reduces the visibility [7–9]. High cross-winds or gusts may overturn a vehicle [10]. However, dealing with such factors is difficult because they are nature-guided and cannot be prevented.

Road Infrastructure. Road environments such as infrastructures, road geometrics, and other roadside facilities can be the causes of RTAs. For example, the density of crossroad intersections and density of sharp bends have been found to be associated with the frequency of RTAs [11]. The presence of street lights increases the visibility at night and hence reduces the chances of crashes [12]. Deficiencies in the design of intersections also lead to chances of crashes and violations [13].

2.2 Human Factors

On the other hand, human factors are caused by the activities of the road users and researchers across the world have focused on attitudes, rule violation tendencies, and socioeconomic causes of the road users. Such individual-level attributes are described below:

Distraction. One of the common human factors identified by the researchers is the ‘distraction’. Distractions may cause ‘inside the vehicle’, such as due to ‘use of mobile phones’ [14], ‘talking to fellow co-passengers’, ‘eating/drinking’ as well as due to several reasons ‘outside the vehicle’. Distractions occurring outside the vehicle include crash scene, road construction, people, places, or things of interest alongside the road. Hands-free mobile phones are also found to be associated with

road crashes. A study by Stutts et al. (2001) revealed that close to 30% of the drivers were identified to be distracted by outside objects, persons, or events, and more than 11% of them were found to be distracted by adjusting radio or cassette or CDs [15]. In another study, based on an experiment conducted among drivers, Stutts et al. (2005) concluded that distractions negatively affect driving performance as drivers tend to remove their hands from the steering and their eyes focus on other things apart from the road in front [16]. Driving performance (in terms of both eye movements and vehicle movements) in work zones was found to be affected by the use of cell phones [17]. Due to performing secondary tasks, when young drivers are insisted to look away from the roadway in front, their driving performance decreased, and the chances of crash increases [18]. To reduce the distractions related to driving errors, Liang and Lee (2010) suggested minimizing the in-vehicle visual demands [19]. Distractions due to passengers and cell phones were found to be likely with angular crashes but on the other hand, chances of single-vehicle crashes were found to be associated with the distraction caused by electric devices [20].

Attitude. Another significant cause of RTAs are unruly road users. Drivers who have a positive attitude toward over speeding, were found to be associated with a greater number of self-reported accidents in the United Kingdom [21]. Drivers, who are highly biased toward the behaviors related to RTAs, were observed to have a negative attitude toward safety [22]. Among Norwegian people, it was observed that their safe attitude related to 'speeding' increases with increment in their traffic risk perception [23]. Another study reported that bigger vehicles sometimes show the attitudes of the 'right of the mighty' toward the smaller vehicles: which leads to road crashes. Unless road users realize their roles and responsibilities, other measures alone cannot change one's behavior [24].

Drinking and driving and rule violations. Many studies suggest that traffic law violations, whatever their origin, are contributing to an increased risk of crashes [25, 26]. All types of common law violations such as disregarding traffic laws, reckless driving, red-light violations, drinking and driving, driving without protective gear, etc. must be treated strictly without any compromises to control the safety situations on road [24]. Researchers have found out the consumptions of alcohol affect the reaction time, accelerating, and braking performances of drivers [12, 27]. The presence of alcohol in blood over a significant level increases the chances of an RTA [24, 28].

One of the common driving rule violations is found to be 'not wearing seatbelts' while driving [24, 29]. Not wearing seatbelts increases the chances of crash severities [30]. Helmets act as a protective device to reduce the crash severities [31]. Wearing helmets have been found to be effective in reducing the chances of head and neck injuries [32]. However, Kritsotakis et al. (2019) showed that young male drivers, who typically do not use seat belts or helmets, were found to be associated with risky driving behaviors [33]. This risk-taking attitude of young drivers might in turn increase the chances of crashes.

Most of the crashes at intersections caused by red-light running result in severe injuries and fatalities and vehicle behavior. That is why; traffic rule violations at intersections (such as stop sign violations or red light running) have evolved as a major safety concern [13, 34]. Researchers have observed that the number of traffic rule violations is correlated with intersection designs (geometrics, infrastructural deficiencies, traffic signal plans, etc.) [13, 35]. Drivers having a past record of violations or penalties are found to be more prone to be involved in consequent traffic accidents [26].

Reckless driving is a mental state in which the driver disregards the rules of the road. Hurry and error in judgment often lead to major crashes. Crash frequency has been reported to be increasing with increment in mean traffic speed [11]. Over speeding is the most common phenomenon, which leads to fatality. Authorities should take scientific and local condition-specific measures to control over speeding, which in term would reduce the number of RTAs [25, 36].

Age, Height, and Gender. Apart from distractions, several types of research have been conducted on drivers' age and gender in relation to RTAs. Women drivers generally drive slowly and cautiously [37]. Elderly drivers (over 50 years) were found to be associated with a lesser number of crashes in Jordan [38]. The same study also concluded that male drivers were associated with higher crash rates. In another study, it was reported that due to the average short height of female drivers, they sit closer to the steering wheel and so, in case of a crash, severity and fatality increase [39]. Automobile manufacturers should consider an average female's characteristics in vehicle designs and other contexts [40]. Both young and old drivers were found to be associated with stop sign violations [13].

Education or awareness. RTAs negatively affect the social and economic development of a country. Road safety education plays an important role in shaping the attitudes and behaviors of children and young people, ensuring they become responsible drivers, passengers, pedestrians, and cyclists [41]. Awareness of road RTAs and fatalities may increase the willingness of individuals toward road safety [42]. Both primary and secondary school students are required to be educated on road safety rigorously. Wherever possible, more focus is required on individual training as it has been found to be more effective [43]. Along with educational campaigning, stringent law enforcement is also required to influence human behavior [44].

The knowledge of these potential causes of crashes is utilized for preliminary shortlisting of the factors responsible for RTAs. The next steps involved in this present study are discussed in the subsequent sections.

3 Survey Designing

3.1 Copyright Forms

As the experts (road safety experts, police personnel, transport researchers, and academicians working in relevant fields) have the most professional experience of RTA related works, and they do visit various crash locations and black spots, they were asked to suggest the most important and leading causes of RTAs in India. Based on the evidence observed from the past literature and experts' advices, seven factors are shortlisted for this present study, which is most relevant in the Indian context. These factors are: 'poor infrastructure', 'over speeding', 'not using protective devices' such as seatbelts or helmets, 'drinking and driving', 'distractions', 'unskilled driving', and 'unawareness of rules of road'.

3.2 Selection of the Prioritizing Technique

For the present study, Analytical Hierarchy Process (AHP) has been chosen, which is extensively used by researchers for the prioritization of factors [45, 46]. Wong and Li, 2008). Cheng et al. (2002) quantitatively investigated construction partnering processes and several associated critical success factors based on expert perception and conducted an analytical hierarchy process [45]. Wong and Li (2008) also applied AHP in a multi-criteria analysis for the selection of intelligent building systems [46]. However, AHP is found particularly useful for analyzing expert perception, especially when the sample size is relatively smaller and the experiment is comparatively controlled. Cheng et al. (2002) have also suggested that the AHP method may be impractical for a survey with a large sample size as 'cold-called' respondents may have a greater tendency to provide arbitrary answers which are prone to high degrees of inconsistency [45].

3.3 Development of the Questionnaire

The responses given by experts are used in AHP for the evaluation of relative influences of the attributes [47]. This is because Saaty and Khouja (1976) showed that the general understanding of a person, who has a sound knowledge of a given problem, can be used to make fairly good estimates through paired comparisons [48]. In the present study, to compare the seven attributes among themselves, a pairwise comparison of attributes is required to be done. For this purpose, each of the experts is required to compare a total of ${}^{7}C_{2} = 21$ combinations of attributes. Based on these combinations, a questionnaire was prepared. The experts were supposed to compare

each of the 21 combinations between two factors on a nine-point scale (where 1 indicates 'equally important' and 9 indicates 'extremely important).

3.4 Data Collection

An online version of the questionnaire was sent electronically to fifteen different experts working in different locations in India. Thirteen experts out of them responded and the data was considered for further analysis. Since a large sample is not essential for using a subjective method such as AHP focusing on a specific issue [45, 47], the thirteen responses fit well to conduct the AHP analysis. The locations from where the experts responded to the questionnaire include Indian metropolitan cities such as Delhi, Kolkata, Hyderabad, and other large cities in the state of West Bengal, Kerala, Maharashtra, and Assam. Table 1 depicts the guideline conveyed to the experts for filling up the questionnaire. Each respondent is expected to fill up the questionnaire and mention how important they feel in between two given sets of factors. The data collection process was conducted in the year 2019. Most of the respondents sent back their responses within a day. Table 2 shows the sample questionnaire.

Table 1 Example showing filling up the questionnaire

How important is Factor A compared to Factor B?										
Score	9 - Extremely Important	7 - Strongly Important	5 - Moderately Important	3 – Somewhat Important	1 - Equally Important	3 - Somewhat Important	5 - Moderately Important	7 - Strongly Important	9 - Extremely Important	Score
If both FACTOR A and FACTOR B are EQUALLY IMPORTANT										
1	9	7	5	3	**1**	3	5	7	9	**1**
If FACTOR A is MODERATELY IMPORTANT than FACTOR B										
5	9	7	**5**	3	1	3	5	7	9	
If FACTOR B is EXTREMELY IMPORTANT than FACTOR A										
	9	7	5	3	1	3	5	7	**9**	**9**

Table 2 The AHP survey questionnaire

Fill up how important Factor A is compared to Factor B for all 21 combinations												
Factor A	Score										Score	Factor B
Poor infrastructure		9	7	5	3	1	3	5	7	9		Over speeding
Poor infrastructure		9	7	5	3	1	3	5	7	9		Not using protective devices
Poor infrastructure		9	7	5	3	1	3	5	7	9		Drinking and driving
Poor infrastructure		9	7	5	3	1	3	5	7	9		Distraction
Poor infrastructure		9	7	5	3	1	3	5	7	9		Unskilled driving
Poor infrastructure		9	7	5	3	1	3	5	7	9		Unawareness of the rules of the road
Over speeding		9	7	5	3	1	3	5	7	9		Not using protective devices
Over speeding		9	7	5	3	1	3	5	7	9		Drinking and driving
Over speeding		9	7	5	3	1	3	5	7	9		Distraction
Over speeding		9	7	5	3	1	3	5	7	9		Unskilled driving
Over speeding		9	7	5	3	1	3	5	7	9		Unawareness of the rules of the road
Not using protective devices		9	7	5	3	1	3	5	7	9		Drinking and driving
Not using protective devices		9	7	5	3	1	3	5	7	9		Distraction
Not using protective devices		9	7	5	3	1	3	5	7	9		Unskilled driving
Not using protective devices		9	7	5	3	1	3	5	7	9		Unawareness of the rules of the road
Drinking and driving		9	7	5	3	1	3	5	7	9		Distraction
Drinking and driving		9	7	5	3	1	3	5	7	9		Unskilled driving

(continued)

Table 2 (continued)

Fill up how important Factor A is compared to Factor B for all 21 combinations											
Drinking and driving		9	7	5	3	1	3	5	7	9		Unawareness of the rules of the road
Distraction		9	7	5	3	1	3	5	7	9		Unskilled driving
Distraction		9	7	5	3	1	3	5	7	9		Unawareness of the rules of the road
Unskilled driving		9	7	5	3	1	3	5	7	9		Unawareness of the rules of the road

4 Data Analysis and Results

Responses of thirteen experts have been analyzed using AHP to determine the rankings of the attributes. In this analysis section, the attributes have been represented by their attributes as: PI (poor infrastructure), OV (over speeding), PD (not using protective devices), DD (drinking and driving), DS (distraction), UD (unskilled driving), and UR (unawareness of rules of the road).

To determine the weights of the attributes, first, a standardized matrix is prepared based on the pair-wise comparison matrix for each of the respondents. Here in this case, for seven attributes (n = 7), a 7 × 7 matrix is developed for each respondent as they have filled the questionnaire. An example of the standardized matrix is shown in Table 3.

Here, the standardized matrix can be considered as an upper triangular or lower triangular in nature, because, if the relative importance of Factor A compared to Factor B is '5', the relative importance of Factor B w.r.t. Factor A must be 'one-fifth' (i.e., 0.2) and vice-versa. In this way, seven such standardized matrices (of dimension 7 × 7) have been developed.

Next, from the seven standardized matrices, normalized weight matrix is prepared by diving each cell of the standardized matrix with the sum of the columns containing that cell. Table 4 indicates an example of the normalized matrix which has been developed from the matrix mentioned in Table 3.

Average of the normalized weights is also calculated and shown in the last column. For each of the respondents, the normalized principal eigen vectors are calculated based on multiplying the average weights (as obtained from Table 4) by the corresponding sum from the standardized matrix. Seven such eigenvalues have been developed and the sum of them indicates the principle lambda value (λ_{max}) [49].

To check the consistency of the data, i.e., whether the responses provided by the experts are consistent or not, Consistency Index (CI) [50] is measured as mentioned in Eq. 1.

Table 3 Example: pair-wise (Standardized) matrix

	PI	OV	PD	DD	DS	UD	UR
PI	**1**	0.1429	0.2	0.2	0.3333	0.3333	1
OV	7	**1**	3	3	5	5	7
PD	5	0.3333	**1**	1	3	3	5
DD	5	0.3333	1	**1**	3	3	5
DS	3	0.2	0.3333	0.3333	**1**	1	3
UD	3	0.2	0.3333	0.3333	1	**1**	3
UR	1	0.1429	0.2	0.2	0.3333	0.3333	**1**
Sum	25	2.3524	6.0667	6.0667	13.667	13.6667	25

Table 4 Example: normalized weight matrix

	PI	**OV**	**PD**	**DD**	**DS**	**UD**	**UR**	**Average**
PI	0.04	0.0607	0.0330	0.0330	0.0244	0.0244	0.04	0.0365
OV	0.28	0.4251	0.4945	0.4945	0.3659	0.3659	0.28	0.3865
PD	0.2	0.1417	0.1648	0.1648	0.2195	0.2195	0.2	0.1872
DD	0.2	0.1417	0.1648	0.1648	0.2195	0.2195	0.2	0.1872
DS	0.12	0.0850	0.0549	0.0549	0.0732	0.0732	0.12	0.0830
UD	0.12	0.0850	0.0549	0.0549	0.0732	0.0732	0.12	0.0830
UR	0.04	0.0607	0.0330	0.0330	0.0244	0.0244	0.04	0.0365

$$CI = \frac{\lambda_{max} - n}{n - 1} \tag{1}$$

To compare the CIs, the parameter Consistency Ratio (CR) is calculated as mentioned in Eq. 2.

$$CR = \frac{CI}{RI} \tag{2}$$

where, RI is known as the random consistency index, here, for n = 7, the value of RI is considered to be 1.32 [50]. Based on these calculations, the CR values are calculated for each respondent and tabulated in Table 5. For consistent responses, the value of the CR must not exceed 0.1.

Inconsistent responses may occur due to several reasons. One of the reasons could be human errors while filling the survey sheet. The other probable cause could be a higher number of variables for pairwise comparisons. That is why, the number of variables is kept low in the present analysis. Inconsistencies may also arise from the comparison scale. Due to this, elements that are extremely different in priority, are avoided in the present study [51]. Eleven out of thirteen responses have been found to be significantly consistent (CR $\leq$ 0.1). Responses of the fourth and sixth experts are found to be associated with CR values of more than 0.1 (shown in italics in the table). These two sets of responses are omitted for further calculation.

Table 5 Consistency checks of the responses

Parameter	Respondent												
	1	2	3	4	5	6	7	8	9	10	11	12	13
Principle Lambda	7.32	7.29	7.38	8.68	7.60	8.23	7.22	7.84	7.68	7.66	7.70	7.80	7.80
CI	0.05	0.05	0.06	0.28	0.10	0.21	0.04	0.14	0.11	0.11	0.12	0.13	0.13
CR	0.04	0.04	0.05	*0.21*	0.07	*0.15*	0.03	0.10	0.08	0.08	0.09	0.10	0.10

Table 6 Ranking of factors based on AHP calculation

Factor	PI	OV	PD	DD	DS	UD	UR
Respondent 1	0.1126	0.4181	0.1126	0.2292	0.0256	0.0509	0.0509
Respondent 2	0.0578	0.2144	0.0578	0.4358	0.0578	0.1493	0.0271
Respondent 3	0.0317	0.2923	0.0776	0.2581	0.1438	0.1178	0.0786
Respondent 5	0.0488	0.2298	0.0727	0.1371	0.4498	0.0299	0.0320
Respondent 7	0.0365	0.3865	0.1872	0.1872	0.0830	0.0830	0.0365
Respondent 8	0.0347	0.4669	0.2103	0.1272	0.0591	0.0390	0.0627
Respondent 9	0.1065	0.3680	0.1531	0.2483	0.0488	0.0249	0.0504
Respondent 10	0.0618	0.3402	0.3172	0.1262	0.0657	0.0445	0.0445
Respondent 11	0.1691	0.3108	0.2888	0.1029	0.0472	0.0374	0.0438
Respondent 12	0.0732	0.3769	0.2067	0.1419	0.0651	0.0666	0.0695
Respondent 13	0.3748	0.2218	0.1370	0.0857	0.0502	0.0653	0.0653
Relative Priority Vector	0.1062	0.3259	0.1619	0.1916	0.0960	0.0624	0.0561
Ranking	4	1	3	2	5	6	7

The last column (average) of the normalized matrix has been utilized to prioritize the attributes. To do so, a new matrix has been prepared, where each row indicates the average weights of the normalized matrix corresponding to a particular respondent. The matrix is represented in Table 6. Finally, the relative priority vectors for the attributes are calculated. These values are obtained by averaging the weights of the respective attributes.

Based on this relative priority vector, the attributes are ranked. This analysis revealed that 'over speeding' is the most important attribute considered by the experts causing RTAs. Even if a crash initiates, if the impact speed can be brought down, it would drastically reduce the chances of fatalities. Hence, the issue of over speeding must be addressed properly. 'Drinking and driving' and 'not using protective devices' are observed to be positioned subsequently in the ranking table.

These findings support the fact that most of the reported crashes in India are found to be caused due to either over speeding or rule violations. In the same line, Nanda and Singh (2018) identified that the faults of drivers are the major cause of road traffic crashes in India [52]. The researchers stated that driving errors such as poor driving skills, drunken driving, and over speeding were found to be causes of 45% of overall road traffic crashes. In another study, a similar observation was drawn by Raja et al. (2021), where the researchers prioritized 28 different causal factors of road traffic crashes in India [53]. The researchers concluded 'drunken driving' to be the most influencing factor, followed by 'over speeding'.

'Poor infrastructure' and 'distraction' are observed to be moderately important in causing a crash. This might have been observed as the road users are accustomed to the road environment they are using. In the conditions of a developing country, road geometry and road environment are not well improved. In another study conducted in India, drunken driving and use of cell phones (i.e., distraction) were observed to be

the sixth and seventh most important attributes when ranked among twelve different attributes causing road traffic crashes [54].

'Unawareness of rules of road' and 'unskilled driving' are found to be the least important. The results are quite obvious as observed in the road conditions prevailed in a developing country, such as India. Drivers gain their knowledge of road rules and learn the skills of driving while getting their driving license, so it is unlikely that a driver will be unaware of the road rules and driving skills. Hence, they seem to be less likely to initiate a crash. Raja et al. (2021) also found unskilled driving to be the least influential in causing road crashes in India [53].

5 Conclusions

Based on the suggestions of the road safety experts in India, seven attributes were considered in the present study, potentially cause RTAs. A pair-wise comparison using the AHP technique revealed that 'over speeding' and 'drinking and driving' are predominant in causing RTAs. The results obtained from this study would help the engineers, administrators, policy-makers, and other stakeholders working in the field of road safety, to take necessary countermeasures. Stringent policy enforcement and traffic calming techniques may be adopted at the locations where vehicles generally ply at very high speed or drivers have the tendency to violate road rules. This will deter the drivers from practicing the most unsafe behaviors which were obtained from the present analysis; namely 'over speeding', 'drinking and driving', and 'not using protective devices'. Such countermeasure strategies do not involve huge investment and can be implemented on a short-term basis. At the same time, the driver-training and licensing procedures in India have evolved into a proper, stringent, and digital process that helps in proper drivers' education and also helps to track the records of a driver. In this way, the issues with 'unskilled driving' and 'unawareness of road rules' might be mitigated. On the other hand, improving the road infrastructure needs sufficient time and requires a substantiate amount of investment. Hence, improving the infrastructure to reduce the number of RTAs may be considered a secondary or long-term strategy.

As the experts involved in this study were approached from different corners of the country, the result of the present study may be considered general and the policymakers may consider the necessary strategies to implement in other parts of the country, as well as in places of other developing countries with similar road-traffic environment compared to India. In addition, further insights regarding the causal factors of RTAs would be obtained by considering different classes of vehicles, which might be interesting to look at. An econometric analysis considering the cost of implantation and cost saving in terms of saving the fatalities by implementing the strategies would be helpful in order to understand the effectiveness of such countermeasures for bringing down the overall RTA count.

References

1. World Health Organization (2018) Global status report on road safety. Geneva, 2018. Licence: CC BYNC-SA 3.0 IGO
2. World Health Organization (2015) Global status report on road safety. Geneva, 2015
3. Transport Research Wing, Ministry of Road Transport and Highways (2020) Road Accidents in India-2019
4. Institute for Health Metrics and Evaluation data. http://www.healthdata.org/india
5. Norman LG (1962) World Health Organization: road traffic accidents: epidemiology, control, and prevention
6. Agarwal PK, Kumar P, Singh H (2020) Causes and factors in road traffic accidents at a tertiary care center of Western Uttar Pradesh. Medico Legal Update 20(1):38–41
7. Satterthwaite SP (1976) An assessment of seasonal and weather effects on the frequency of road accidents in California. Accid Anal Prev 8(2):87–96
8. Chung E, Ohtani O, Warita H, Kuwahara M, Morita H (2005) Effect of rain on travel demand and traffic accidents. In: Proceedings. 2005 IEEE intelligent transportation systems, pp 1080–1083
9. Chen L, Wang P (2017) Risk factor analysis of traffic accident for different age group based on adaptive boosting. In: 2017 4th International Conference on Transportation Information and Safety (ICTIS), pp 812–817
10. Hermans E, Brijs T, Stiers T, Offermans C (2006) The impact of weather conditions on road safety investigated on an hourly basis. In: TRB annual meeting
11. Taylor, M. C., Baruya, A., Kennedy, J. V.: The relationship between speed and accidents on rural single-carriageway roads (Vol. 511). Crowthorne: TRL. (2002).
12. Keall MD, Frith WJ, Patterson TL (2005) The contribution of alcohol to night time crash risk and other risks of night driving. Accid Anal Prev 37(5):816–824
13. Retting RA, Weinstein HB, Solomon MG (2003) Analysis of motor-vehicle crashes at stop signs in four US cities. J Safety Res 34(5):485–489
14. Orlowske LL, Luyben PD (2009) Risky behavior: Cell phone use while driving. J Prev Interv Community 37(3):221–229
15. Stutts JC, Reinfurt DW, Staplin L, Rodgman E (2001) The role of driver distraction in traffic crashes
16. Stutts J, Feaganes J, Reinfurt D, Rodgman E, Hamlett C, Gish K, Staplin L (2005) Driver's exposure to distractions in their natural driving environment. Accid Anal Prev 37(6):1093–1101
17. Fisher DL, Knodler M, Muttart JW (2009) Driver-eye-movement-based investigation for improving work-zone safety. No NETCR71
18. Klauer SG, Ehsani JP, McGehee DV, Manser M (2015) The effect of secondary task engagement on adolescents' driving performance and crash risk. J Adolesc Health 57(1):S36–S43
19. Liang Y, Lee JD (2010) Combining cognitive and visual distraction: less than the sum of its parts. Accid Anal Prev 42(3):881–890
20. Ghazizadeh M, Boyle LN (2009) Influence of driver distractions on the likelihood of rear-end, angular, and single-vehicle crashes in Missouri. Transp Res Rec 2138(1):1–5
21. West R, Hall J (1997) The role of personality and attitudes in traffic accident risk. Appl Psychol 46(3):253–264
22. Nabi H, Salmi LR, Lafont S, Chiron M, Zins M, Lagarde E (2007) Attitudes associated with behavioral predictors of serious road traffic crashes: results from the GAZEL cohort. Inj Prev 13(1):26–31
23. Şimşekoğlu Ö, Nordfjærn T, Rundmo T (2012) Traffic risk perception, road safety attitudes, and behaviors among road users: a comparison of Turkey and Norway. J Risk Res 15(7):787–800
24. Gopalakrishnan S (2012) A public health perspective of road traffic accidents. J Famil Med Prim Care 1(2):144
25. Ayuso M, Guillén M, Alcañiz M (2010) The impact of traffic violations on the estimated cost of traffic accidents with victims. Accid Anal Prev 42(2):709–717
26. Factor R (2014) The effect of traffic tickets on road traffic crashes. Accid Anal Prev 64:86–91

27. Yadav AK, Velaga NR (2019) Modelling the relationship between different blood alcohol concentrations and reaction time of young and mature drivers. Transp Res F Traffic Psychol Behav 64:227–245
28. Pal R, Ghosh A, Kumar R, Galwankar S, Paul SK, Pal S, Sinha D, Jaiswal AK, Moscote-Salazar LR, Agrawal A (2019) Public health crisis of road traffic accidents in India: risk factor assessment and recommendations on prevention on the behalf of the Academy of Family Physicians of India. J Family Med Prim Care 8(3):775
29. Mohan D (2009) Seat belt law and road traffic injuries in Delhi, India. In: Proceedings of the Eastern Asia Society for transportation studies, vol 7 (The 8th international conference of Eastern Asia Society for Transportation Studies, 2009), pp 392–392
30. Febres JD, García-Herrero S, Herrera S, Gutiérrez JM, López-García JR, Mariscal MA (2020) Influence of seat-belt use on the severity of injury in traffic accidents. Eur Transp Res Rev 12(1):9
31. Sreedharan J, Muttappillymyalil J, Divakaran B, Haran JC (2010) Determinants of safety helmet use among motorcyclists in Kerala, India. J Injury Violence Res 2(1):49
32. Keng SH (2005) Helmet use and motorcycle fatalities in Taiwan. Accid Anal Prev 37(2):349–355
33. Kritsotakis G, Papadakaki M, Tumwesigye R (2019) Co-occurence of risky driving behaviours and associations with seatbelt and helmet use-a descriptive cross-sectional study among young adults. Epidemiol Biostat Public Health 16(2)
34. Lee Y, Li Z, Zhang S, Roshandeh AM, Patel H, Liu Y (2014) Safety impacts of red light running photo enforcement at urban signalized intersections. J Traffic Transp Eng (English edition) 1(5):309–324
35. Kulanthayan S, Phang WK, Hayati KS (2007) Traffic light violation among motorists in Malaysia. IATSS Res 31(2):67–73
36. Cheng W, Han C, Xi J (2010) Mechanism analysis of over-speeding impact on the road safety. In: 2010 international conference on intelligent computation technology and automation, IEEE, vol 2, pp 652–656
37. Polus A, Hocherman I, Efrat E (1988) Evaluation of the accident rates of male and female drivers. Transportation Research Board
38. Al-Balbissi AH (2003) Role of gender in road accidents. Traffic Inj Prev 4(1):64–73
39. McFadden J (1998) Development of design consistency evaluation models for two-lane rural highways. The Pennsylvania State University
40. Welsh R, Lenard J (2001) Male and female car drivers-difference in collision and injury risks. In: Proceedings of the 45th annual AAAM conference, Texas, pp 24–26
41. Hung KV, Huyen LT (2011) Education influence in traffic safety: a case study in Vietnam. IATSS Res 34(2):87–93
42. Wegrnan F (1992) Legislation, regulation and enforcement to improve road safety in developing countries
43. Dragutinovic N, Twisk D (2006) The effectiveness of road safety education: a literature review. SWOV Institute for Road Safety Research
44. Khorasani-Zavareh D, Mohammadi R, Khankeh HR, Laflamme L, Bikmoradi A, Haglund BJ (2009) The requirements and challenges in preventing of road traffic injury in Iran. A Qualitative study. BMC Public Health 9(1):1–9
45. Cheng EW, Li H, Ho DC (2002) Analytic hierarchy process (AHP): a defective tool when used improperly. Measuring Business Excellence
46. Wong JK, Li H (2008) Application of the analytic hierarchy process (AHP) in multi-criteria analysis of the selection of intelligent building systems. Build Environ 43(1):108–125
47. Majumdar BB, Mitra S (2015) Identification of factors influencing bicycling in small sized cities: a case study of Kharagpur India. Case Stud Transp Policy 3(3):331–346
48. Saaty T, Khouja M (1976) A measure of world influence. J Peace Sci Spring
49. Render B, Stair RM, Hanna ME, Hale TS (2018) Quantitative analysis for management, 13th edn. Pearson

50. Saaty RW (1987) The analytic hierarchy process—what it is and how it is used. Math Model 9(3–5):161–176
51. AHP Software (2021) Transparent Choice Ltd
52. Nanda S, Singh S (2018) Evaluation of factors responsible for road accidents in India by fuzzy AHP. In: Networking communication and data knowledge engineering. Springer, Singapore, pp 179–188
53. Raja KV, Ponnusamy M, Selvi GT, Saravanakumar R, Ashok M, Nagaraj V (2021) Assessment and prioritization of the critical factors triggering road accidents in India. Journal homepage: http://iieta.org/journals/ijsse 11(2):207–211
54. Gothane S, Sarode MV (2016) Analyzing factors, construction of dataset, estimating Importance of factor, and generation of association rules for Indian road accident. In: 2016 IEEE 6th International Conference on Advanced Computing (IACC). IEEE, pp 15–18

Investigating the Safety Scenario of a 4-Lane Divided National Highway in India: A Case Study on NH-2

Nabanita Roy, Abhishek Chakraborty, Sudeshna Mitra, and Bhargab Maitra

Abstract Road traffic accidents and fatalities have emerged as a serious problem over the world, as well as in India. Though National Highways (NHs) comprise less than 2% of the entire road network, they account for more than 35% of total traffic fatalities. In this regard, this study aims to identify and prioritize the hazardous locations on a 4-lane NH, find out the major risk factors, and recommend short-term and long-term countermeasures. Hazardous locations on a stretch on NH-2 were identified and prioritized through a comprehensive analysis of past accident data; based on total crash count (TCC), fatal crash count (FCC), and equivalent property damage only (EPDO) values. Probable risk factors such as illegal truck parking, insufficient storage lanes, improper pedestrian crossing facilities, design deficiencies at unsignalized minor junctions, etc. were identified from site visits. This study also recommends necessary crash mitigation and prevention strategies.

Keywords Road traffic accidents · Total crash count · Fatal crash count · Equivalent property damage only value

N. Roy · A. Chakraborty (✉) · B. Maitra
Department of Civil Engineering, Indian Institute of Technology, Kharagpur 721302, India
e-mail: abhishekcivilchakraborty@gmail.com

N. Roy
e-mail: roynabanita91@gmail.com

B. Maitra
e-mail: bhargab@civil.iitkgp.ac.in

S. Mitra
Global Road Safety Facility, The World Bank, Washington D.C. 20433, USA
e-mail: smitra5@worldbank.org

L. Devi et al. (eds.), *Proceedings of the Sixth International Conference of Transportation Research Group of India*, Lecture Notes in Civil Engineering 273,
https://doi.org/10.1007/978-981-19-4204-4_14

1 Introduction

1.1 Background

Fatalities and injuries due to road traffic accidents are a major and growing public health problem worldwide. As per the reports published by World Health Organization (WHO), more than 1.35 million people are killed and nearly 50 million people are injured globally each year due to road traffic accidents [1, 2]. WHO has also estimated that without increased efforts and new initiatives, the total number of road traffic fatalities and injuries would rise by 65% by 2020, while in low- and middle-income countries, fatalities are expected to increase by as much as 80% [3]. India, being one of such 'low- and middle-income' countries, has been going through a transitional state of economic growth and witnessed an unprecedented increase in the rate of motorization in recent years. India has faced serious challenges in the improvement of road safety as with the rapid expansion in the road network and urbanization, road traffic injuries (RTIs) and fatalities (RTFs) have gradually increased over the years. According to the reports published by the Ministry of Road Transport and Highways (MoRTH), it has been observed that the number of road traffic accidents (RTAs) or the corresponding injuries and fatalities are not gradually decreasing every year, rather in the past year (2018), the numbers have been increased. However, it can be assumed that the actual number of accidents is on the higher side because of underreporting of data in developing countries [4].

Out of the entire road network system in India, National Highways (NHs) comprise of only 2.03% of the total road network, but the percentage share of persons killed and persons injured are higher on NHs as compared to other roads [5]. Road accident has gone up on National Highways from 28.2% in 2014 to 30.55% in 2019. Moreover, RTFs on NHs has been increased from 34.1 to 35.7% during the same period [5]. The primary reason behind this may be the higher speed facilities on National Highways to provide high-speed mobility rather than accessibility.

However, high-speed facilities without proper access-control facilities increase the chances of RTAs [6]. It has been observed that 4-lane National Highways are, many times, not access controlled which leaves a number of major and minor at-grade intersections with cross-traffic. In addition, vulnerable road users (VRUs) such as pedestrians and bicyclists use the main carriageway of highways for commuting; all of which have contributed to the poor safety performance of National Highways in India. It is important to note that, such high-speed facilities are supposed to conform to high geometric design standards and operate as uninterrupted traffic flow facilities. These two important factors, i.e., higher geometric design standards and uninterrupted operations are among the important features in making these facilities safe and accident-free. However, this is clearly not the case in India and disproportionally high numbers of severe accidents are observed while comparing exposure in terms of road lengths and vehicle kilometers traveled.

In this regard, the objective of the present work is to investigate the safety scenario of a 4-lane national highway by identifying and prioritizing hazardous locations

based on accident data analysis; and to identify the major risk factors, followed by recommending necessary countermeasure strategies to mitigate the safety issues. The subsequent part of the manuscript summarizes traditional techniques for prioritizing hazardous locations, followed by the description of the project corridor and the accident data. Next, the analysis of the accident data along with the safety issues of the highway is highlighted. In the end, major conclusions are drawn for the overall improvement of the safety of the road users of the 4-lane highway.

1.2 Techniques for Identification of Hazardous Locations

Over the past few decades, road traffic safety has emerged as a major field of research with a goal of better understanding the scientific relationship between the crash frequency and severity with traffic volume and other variables such as geometric design and traffic operations and regulatory parameters of the road. Individual crashes are difficult to evaluate as they are random and unpredictable. However, over many years, safety analysts have developed different methods for selecting road segments, referred to as sites, for detailed analysis and improvements. The smallest length of a road segment with homogeneous characteristics which is associated with the maximum expected value of accident frequency may be considered a 'site'. Identification of such 'sites' in a scientific approach is necessary for the implementation of cost-effective countermeasures to site-specific safety issues. This is considered the first and most important step in the process of road safety improvement [7, 8]. This step must be done precisely, otherwise falsely identified high-priority locations might lead to lesser cost-effective solutions. Screening of the segments or sites highlights the locations where interventions are required to enhance safety. In addition, from the ranking of the locations, the areas can be identified where attention is required on a priority basis [7–10]. Such sites have generally been identified by various researchers as Blackspots or Hotspots [11], 'Hazardous Locations' [12], 'High Crash Locations' (HCLs) [13], 'Priority Investigation Locations' (PILs), 'Sites with Promise' (SWiP) [7], or 'Sites with high Potential for Safety Improvement' (PSI) [14]. A very early study by Deacon et al. (1975) suggested the use of total accident frequency or the total count of severe and non-severe accidents over a certain period as a metric for prioritizing accident-prone locations [15].

Hauer et al. (2002) suggested accident frequency as an important metric since the potential for site improvement is also proportional to the number of accidents experienced at the sites [8]. According to the authors, it is also more cost-effective to employ the 'crash count metric' for ranking hotspots. The metric 'crash count' or 'accident frequency' or 'crash frequency' (CF) is very popular among practitioners and road safety experts due to its simple approach. The Crash Frequency (CF) or Total Crash Count (TCC) method considers the frequency or number of crashes at a location and ranks the segments in descending order of their crash counts, i.e., the segment with a maximum frequency of crashes is placed in rank 1. The segments hence placed in the top ten positions are considered as blackspots. In this method, the

segments with high crash frequency can be identified easily, however, the severities of the crashes are not considered. Due to this, the locations with higher severity of crashes but with a lesser count of crashes remain undetected. That is why a modified version, namely Fatal Crash Count (FCC) or Fatal Crash Frequency (FCF) method has been introduced. The frequency of fatal crashes is only considered for ranking the segments in this method instead of the number of total crashes. However, a major drawback of this approach is that it does not consider the severity levels of the crashes and only considers the fatalities [9, 10].

Since, in conditions of low- and middle-income countries, underreporting of accidents is considered to be a major concern [2, 16–18], applying CF models may lead to erroneous results. Hence, for a comprehensive assessment of road safety, incorporation of accident severity with accident frequency would be appropriate [19, 20]. In this regard, the safety index called Equivalent Property Damage Only (EPDO) becomes a useful technique for prioritizing high accident locations. The EPDO method takes into account all levels of severity of crashes occurring at a particular location for deciding on a site as hazardous. For each of the segments, the total cost of the accident is estimated based on its cost of 'equivalent property damage'. The count of 'no-injury' or 'property damage only' crashes, the count of 'minor injuries', the count of 'grievous or major injuries', and the count of fatalities are multiplied by their corresponding 'equivalent property damage' weight factors and summed up to estimate the cost of EPDO corresponding to each of the segment [9, 20]. While this method considers different severity levels of the injuries that took place due to the crashes, this method also has a drawback. A site with a few numbers of fatalities gets highlighted easily and ranked higher in this method compared to a site associated with frequent severe injury crashes [9, 20]. This is because it assigns a very high weightage to the fatalities compared to other types of severities while calculating the EPDO value.

2 Data Collection and Database

2.1 Description of the Study Corridor and the Database

Three years past accident data is collected from a stretch of a 4-lane National Highways. The study corridor from Panagarh (Latitude: 23.434559, Longitude: 87.480875; Chainage: 520.103 km) to Dankuni (Latitude: 22.673621, Longitude: 88.300315; Chainage: 649.070 km) is a part of the National Highway 2 (NH-2) which connects Delhi to Kolkata. NH2 passes through different states namely, Delhi, Haryana, Uttar Pradesh, Bihar, Jharkhand, and West Bengal. The project corridor is 128.969 km long and lies completely in the state of West Bengal as shown in Fig. 1.

The project stretch passes through the district of Hooghly, East Bardhhaman, and West Bardhhaman and connects important cities (Asansol, Durgapur, Bardhhaman, Serampore, Howrah, and Kolkata) in the state of West Bengal. Land use in the project

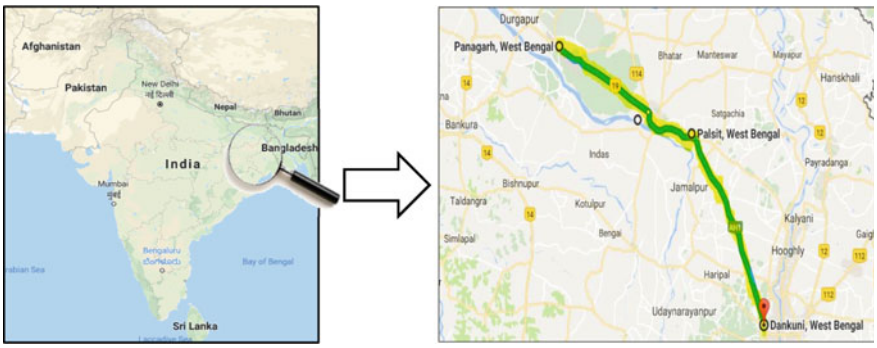

Fig. 1 Map of the project corridor

corridor is mainly industrial and agricultural. Additionally, a major military and air force base abuts the corridor. Four-laning of the stretch was completed during the early part of the decade and traffic operations started in June 2005. With the purpose of providing the necessary road safety consultancy services during the Operations and Maintenance of this section, it is important to perform, a thorough analysis of road accidents that have occurred on the study stretch, and identify the critical locations which need improvement. In order to identify the high crash locations, three years' crash data from January 2014 to December 2016 is used. This data has been obtained from the concessionaire who is legally required to keep a record of all accidents during operations and maintenance period. The accident database contains information classified into the following categories: Crash location, type of crash, causes of the crash/accident, type of maneuver, weather condition, time and day of the accidents, and the severity of the accident.

2.2 Description of the Study Corridor and the Database

For the purpose of accomplishment of the study objectives, three years' accident data is analyzed. The entire study section is divided considering a one kilometer chainage interval. However, it is important to note that the problem may be localized and the safety deficiency is over a smaller portion of the road than 1 km. To identify such local issues, 1 km segments with a high concentration of accidents were further investigated in detail and the critical locations were identified for a kilometer stretch. The nature of accidents has been classified into the following categories, namely overturning, head-on collision, rear-end collision, collision brush/side swipe, skidding, hit and run, run over, and others.

Figure 2a represents the distribution of accident severity over the three-year period on the entire project corridor. It can be observed that 5%, 30%, 20%, and 45% of the total crashes during 2014–2016 were fatal, grievous, minor, and non-injury type crashes respectively. Figure 2b represents the percentage share of fatal accidents

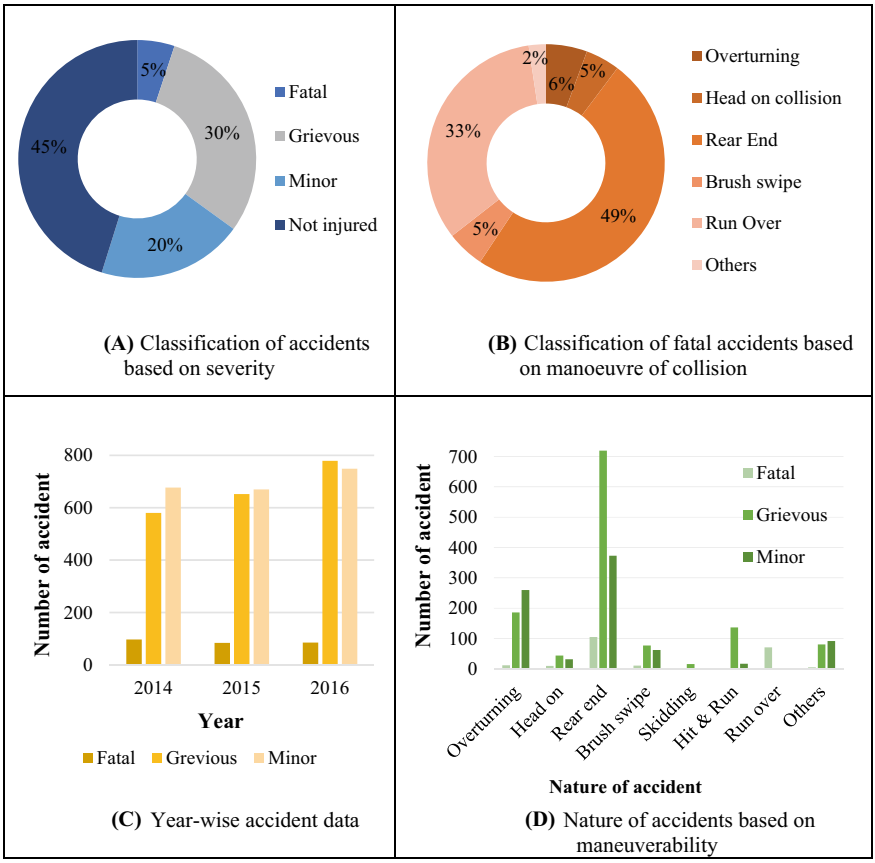

Fig. 2 **a–d** Descriptive statistics of the accident data of the project stretch

based on maneuver of collision. It is very evident that the rear-end-type collision is having the maximum share of accidents on this corridor, which is almost half of the total accidents. Further, it indicates a significant number of run-over-type accidents having a considerable share. In addition, 6%, 5%, and another 5% of fatal crashes are caused due to overturning, brush swipe, and head-on collision, respectively. After analyzing the year wise accident data, we can clearly depict that the number of accidents is continuously increasing every year (Fig. 2c)

Further, a preliminary analysis is conducted for the total crashes based on their respective crash maneuver. A detailed description of the distribution of accidents based on maneuver is given below with a graphical representation in Fig. 2d. From this figure, it can be observed that the majority of the accidents occurring in the corridor during the study period are because by rear-end collisions of vehicles that resulted in 105 fatal, 719 grievous, and 373 minor injuries, resulting in a total of 1197 rear-end collisions. The illegally parked trucks along the main carriageway

(MCW) are might be the major cause of rear-end collisions. The total number of accidents due to overturning is 458 of which 12 are fatal, 186 are grievous and 260 are minor injuries. The high number of accidents due to overturning could be due to the inability of heavy vehicles to safely maneuver while moving at high speed along horizontal curves. Apart from these two types of accidents, which are observed predominantly on the corridor, a comparatively lesser number of accidents are observed due to head-on collisions, brush swipe, skidding, hit-and-run, run-over, and other maneuver types. Head-on collision indicates contra flow of traffic which may be due to improper barricading at medians, lack of service lane, or improper median opening. Huge median opening, improper entry to MCW from a minor road, and inadequate width of storage lane may be the reasons of this type of collision. Sometimes skidding may occur due to over speeding or the driver losing control of the vehicle due to weather conditions. The presence of illegal median opening, where pedestrians generally cross in an unsafe manner, may be one of the reasons for run-over collisions. All types of accidents other than those mentioned above have been categorized as others. Such accidents account for 178 accidents of the total 2313 accidents, of which 5 are fatal, 81 are grievous, and 92 are minor injuries.

3 Results and Findings

3.1 Identification and Prioritization of the Hazardous Locations

In the following section, a detailed analysis is conducted to meet the above-mentioned objectives. For identification of the most critical locations, the Ministry of Road Transport & Highways (MoRTH) has given a definition of a black spot. As per a memorandum issued by MoRTH, Government of India, black spots on the NHs are the road segments of 500 m in length, where in the past three years at least 5 road crashes (involving major injuries or fatalities) took place. Alternatively, if 10 road accident fatalities took place in the past three years, the road segment can be called a black spot as per the MoRTH definition [21]. For site screening and identification of high crash locations, three different methods, namely total crash counts (TCC), fatal crash count (FCC), and equivalent property damage only (EPDO) have been used.

For this study, the costs of various types of accidents are considered to be: Rs. 16200 as the cost of property damage, Rs. 535489 as the cost of fatality, Rs. 242736 as the cost of major injury, and Rs. 18855 as the cost of minor injury; as proposed by several researchers [22, 23]. The weight factor for ‘equivalent property damage’ is considered 1 for ‘property damage only’ crashes and the equivalent property damage weight factors for other crash types are calculated as: 33 for each reported fatality, 15 for each reported grievous injury, and 1.16 for each reported minor injury. Multiplying a larger number with major injury crashes minimizes the error of underreporting minor and no-injury accidents [10, 19, 22, 23]. Mathematically, for a site location,

Table 1 Ranking of locations for NH-2 (520.103–649.07 km)

Location	TCC	Rank based on TCC	Location	FCC	Rank based on FCC	Location	EPDO	Rank based on EPDO
560–561	138	1	553–554	7	1	560–561	1011.6	1
640–641	75	2	560–561	7	1	640–641	500.2	2
582–583	68	3	568–569	6	3	569–570	467	3
568–569	62	4	569–570	6	3	591–592	452.6	4
625–626	62	4	627–628	6	3	627–628	438	5
627–628	61	6	557–558	5	6	558–559	433.2	6
565–566	57	7	591–592	5	6	565–566	425	7
586–587	56	8	631–632	5	6	582–583	424.6	8
558–559	55	9	534–535	4	9	568–569	411.2	9
591–592	53	10	552–553	4	9	557–558	409.8	10

$$EPDO = 33 \times F + 15 \times GI + 1.16 \times MI + PDC. \quad (1)$$

where

EPDO: equivalent property damage only,

F: number of fatal injuries,

GI: number of major injuries,

MI: number of minor injuries,

PDC: number of reported 'property damage only' or no-injury accidents.

The crash data was utilized for each of the crash-count-based methods. Finally, every single location is ranked based on TCC, FCC, and EPDO methods as shown in Table 1.

All locations on the project corridor are ranked based on total, fatal, and EPDO counts in Table 1. Based on the accident analysis, it can be observed that at least one fatal accident per year has taken place in thirty-three locations on the project stretch. A schematic representation of the positions of the black spots on the project corridor is provided in Fig. 3.

3.2 Identification of Major Risk Factors

With the aim of finding the risk factors and the major causes behind accidents detailed analysis is performed for all the locations considering the type of maneuverability. The proportions of accidents that took place at the top 16 hazardous locations based on maneuverability are represented in Fig. 4. It is observed from the detailed analysis

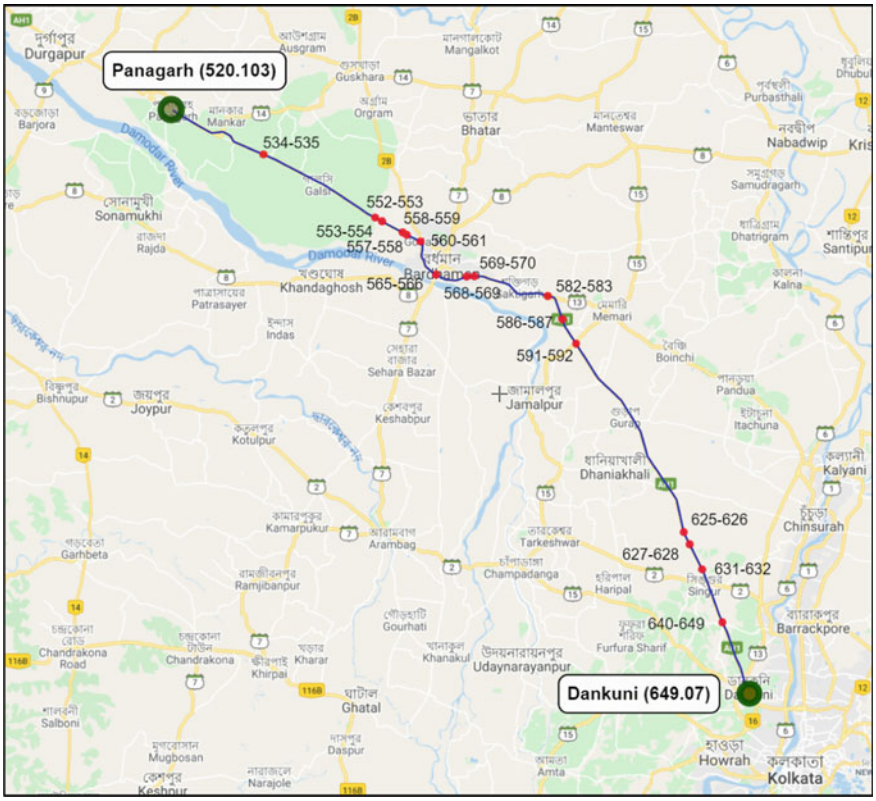

Fig. 3 Project stretch highlighting the black spots (with chainage)

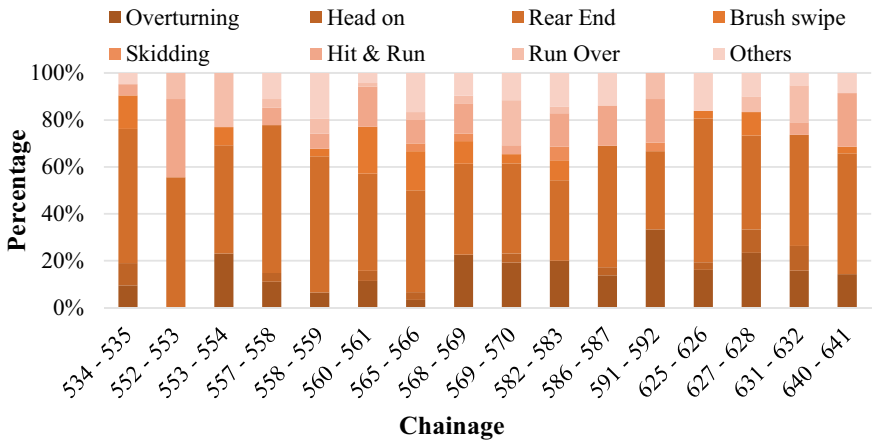

Fig. 4 Percentage of accidents based on maneuver type at top-ranked locations

that the 'rear end' type of collision is the most common type in terms of its frequency of occurrence. Frequent parking of trucks on the edge of the carriageway as well as the absence of overtaking zones throughout the highway stretch might be the major reasons behind such rear-end accidents.

3.3 Issues Identified at the Black Spots

The causes of such accidents remain unknown from the accident database due to the unavailability of all potential information related to the accidents. That is why, the historical crash data was utilized for the identification of the hazardous locations in a reactive manner. To identify and assess the safety issues in a proactive way, the authors conducted physical visits to the hazardous locations of the project site and searched for the potential causes of road accidents and their suitable countermeasures.

Based on the observation of the study sites, seven major risk factors were identified which were frequently observed, namely: illegal truck parking, insufficient storage lane, improper pedestrian crossing facility, contra-flow traffic, untreated intersections, frequent illegal access, and median openings and improper locations of bus stops. The 'risk-factor' specific issues and their corresponding countermeasures are also mentioned in the next section. The countermeasures mentioned in this present study are stated mostly based on the studies conducted by Mohan et al. (2009) and Chatterjee et al. (2020) in the Indian context [24, 25].

Illegal truck parking. The high percentage of rear-end collisions on the straight stretch might be due to the presence of trucks parked along the main carriageway (Fig. 5a). This might have been observed due to the truck entry restriction in Kolkata in the daytime. Parked trucks reduce the available width of the carriageway and block the sight distance as well as found to be damaging the shoulder.

To prevent illegal parking on the main carriageway, the provision of dedicated truck lay-byes needs to be evaluated. Police administration should be instructed to help remove illegal parking along the roadside and enforce the trucks to park at the designated truck lay-by. Facilities such as restrooms, dormitories, and eateries may be provided at such locations to attract truck drivers. Such locations clearly need additional parking space off the highway as well as adequate lighting so that if any vehicles are parked on the carriageway, are visible at night time. In the absence of street lights and proper separation between parked vehicles and traveled lanes, no parking on highways should be allowed.

Insufficient Storage Lane. On this corridor, at many intersections, untreated minor road approach and insufficient storage lane result in unsafe vehicular movement at several locations on the project stretch. As a result, the right-turning vehicles while waiting for a suitable gap to cross the highway partially blocks the fast lane, which poses a serious safety hazard to traveling vehicles. In addition to the lack of a storage lane, vehicles coming from the left, which generally takes a free left turn, do not have an adequate length of the acceleration lane. In such cases, proper treatment

Fig. 5 **a–f** Different issues identified at several locations on the project corridor

such as adequate delineations for median opening and storage lane must be provided for smooth maneuvering of traffic.

Absence of pedestrian crossing facility. Throughout the project stretch, the absence of a proper pedestrian crossing facility is a major safety concern (Fig. 5b). Although pedestrian crossing has been provided at a few locations, poor maintenance along with the absence of proper delineation with retro-reflective pavement markers (RRPM) causes the marking to become blurred. As a result, they are not visible to speeding vehicles, especially at night time. Moreover, at several locations due to the presence of educational institutions and commercial activities, pedestrians are observed to cross over a longer section of the highway in a haphazard manner.

This poses a high safety threat to these vulnerable road users as drivers don't expect pedestrians on an expressway.

Marked pedestrian crossing with advanced warning signs with the help of RRPM, raised pedestrian crossing facility is to be provided at locations of high pedestrian movement. Proper channelization and walking facility is to be provided for pedestrians with the help of PGR, sidewalk, and raised table crossing facility.

Contraflow of traffic. Contraflow is a form of reversible traffic operation in which vehicles move in the opposite direction as the nearest legal crossing is far away from the location and avoids the extra distance which is supposed to be covered (Fig. 5c). Contra-flow of traffic is a major cause of concern as it increases the chances of a head-on collision.

This problem must be resolved with changes in road design, which would be a long-term solution; however, with the help of speed calming measures, appropriate signage to pre-warn the MCW traffic about the possible contraflow movement, and police enforcement, the problem may be controlled until the design deficiencies persist.

Improper intersection design. At several unsignalized intersections, visibility remains a major issue for merging vehicles from minor/link roads. It has been observed during the site visits that vehicles from minor roads approach the highway at high speeds. This coupled with the absence of proper channelization and speed-calming measure poses a high risk of conflict and injury. The primary reason for such conflict is insufficient sight distance due to illegal encroachments near the intersection approach (Fig. 5d).

At unsignalized intersections, stop sign, intersection sign, and stop line along with a speed breaker should be provided such that the minor road traffic comes to a standstill before merging with the main stream traffic. At the same time, there should be proper signage showing the presence of a minor road on the MCW.

Illegal access and median openings. It was observed that there are very high number of illegal pedestrian and vehicular access along with unauthorized median openings at several places on the corridor. It was also observed that the illegal access is used to connect villages on either sides of the highway and is made by people from the nearby villages (Fig. 5e).

Locations with depressed median opening, where trucks are taking turns should be treated as illegal median openings and should be closed as soon as possible. Locations with unauthorized access should be closed as soon as possible. The broken fences and crash barriers should be fixed and reinstalled. If illegal access points cannot be closed, then the speed of the highway should be brought down by necessary speed-calming measures such as transverse rumble-strips, pre-warning signs, etc. It is impossible to operate this highway at an operating speed of 100 km/h when such frequent access points are present.

Improper boarding and alighting by buses. It has been observed that buses plying along this stretch do not stop at designated bus-stops. Bus-stops are absent at several locations, resulting in buses stopping at undesignated/undesired locations mainly near the intersections. Hence, designated bus-bays are to be planned and prevention of unsafe boarding alighting on the carriageway. Figure 5f shows how

illegally buses stop on roadside and creates congestion due to boarding and alighting of passengers.

Proper bus stops with bus bays are to be provided at locations where adequate space is available; preferably, at far-ends of an intersection to prevent unsafe boarding alighting on the carriageway. Where space is inadequate, the shoulder should be utilized as bus stop area to ensure safety. Police authorities should help in enforcing the stopping locations of buses.

4 Conclusions

The present study considers both reactive and proactive approaches of road safety. Prioritization the hazardous locations on the NH corridor based on different accident analysis techniques such as TCC, FCC, and EPDO methods highlights the areas of concern on the project highway. Through the site visit, some common safety deficiencies such as illegal median opening, untreated minor road approach, high volume of pedestrian crossing without grade separated facility, and illegal truck parking were observed on the hazardous locations and the necessary countermeasures are suggested on a proactive basis.

Although national highways are high-speed facilities meant to provide high-speed mobility rather than accessibility, it has been observed that the project corridor was not access controlled which increased the interaction of the main traffic with crossing pedestrians, and other cross traffic at various locations. Median openings, intended for left and U turning, encourage contraflow of traffic. In addition, vulnerable road users such as pedestrians and bicyclists use the main carriage way of highways for commuting; all of which have contributed toward the poor safety performance of the project corridor. Protection of critical structures is also another major issue in the project stretch. However, apart from the suggested low-cost short-term countermeasures, in order to achieve maximum long-term benefits, the safety concerns must be addressed considering the following:

- Geometric design of the road should be done in such a manner so that potential black spot locations may get eliminated as far as possible.
- Over-speeding tendencies of motorized vehicle may be deterred by designing suitable traffic calming measures and which in turn, would increase the safety of vulnerable road users.
- Periodic conduction of road safety audits, which would highlight the safety issues, if any. Crash barriers should be provided as necessary and especially where there are narrow bridges and culverts.

Suitable countermeasures need to be adopted by the stakeholders for safe vehicular movement to reduce the number of crashes as well as the severity on the 4-lane highways in similar road and traffic environment, where providing access-control facility is difficult. For safer vehicular mobility, such safety aspects must be addressed while upgradation of the highways. Further, considering the spot-speed data from

the hazardous locations as well as the drivers' behavior toward risky driving could lead to further interesting aspects while formulation of countermeasure strategies. This, in turn, would significantly contribute to the overall road safety improvements in India.

References

1. World Health Organization (2015) Global status report on road safety, Geneva
2. World Health Organization (2018) Global status report on road safety, Geneva. Licence: CC BYNC-SA 3.0 IGO
3. Hazen A, Ehiri JE (2006) Road traffic injuries: hidden epidemic in less developed countries. J Natl Med Assoc 98(1):73
4. Bener A, Abu-Zidan FM, Bensiali AK, Al-Mulla AA, Jadaan KS (2003) Strategy to improve road safety in developing countries. Saudi Med J 24(6):603–608
5. Transport Research Wing, Ministry of Road Transport and Highways (2020) Road accidents in India-2019
6. Brown HC, Tarko AP (1999) Effects of access control on safety on urban arterial streets. Transp Res Rec 1665(1):68–74
7. Hauer E, Allery BK, Kononov J, Griffith MS (2004) How best to rank sites with promise. Transp Res Rec: J Transp Res Board 2004:48–54
8. Hauer E, Kononov J, Allery BK, Griffith MS (2002) Screening the road network for sites with promise. Transp Res Rec: J Transp Res Board 1784:27–32
9. Bandyopadhyaya R, Mitra S (2015) Fuzzy cluster-based method of hotspot detection with limited information. J Transp Saf Secur 7(4):307–323
10. Bandyopadhyaya R, Mitra S (2011) Comparative analysis of hotspot identification methods in the presence of limited information. In: Paper presented at 3rd international conference on road safety and simulation, Indianapolis, Indiana
11. Mandloi D, Gupta R (2003) Evaluation of accident black spots on roads using geographical information systems (GIS). In: Map India conference
12. Kononov J, Bailey B, Allery B (2008) Exploratory examination of the functional form of the safety performance functions of urban freeways, Transport Research Board
13. Pulugurtha SS, Vanjeeswaran KKK, Uddaraju M (2004) Development of criteria to identify pedestrian high crash locations in Nevada (No. RDT 04-048). Nevada Department of Transportation
14. Tegge RA, Jo JH, Ouyang Y (2010) Development and application of safety performance functions for Illinois
15. Deacon JA, Zegeer CV, Deen RC (1975) Identification of hazardous rural highway locations. In: Transportation research record 543. TRB, National Research Council, Washington, DC
16. Kakkar R, Aggarwal P, Kakkar M, Deshpande K, Gupta D (2014) Road traffic accident: retrospective study. Indian J Sci Res 5(1):59–62
17. Mitra S, Mukherjee D, Subudhi T (2016) Development of a methodological framework of road safety management for Indian metro cities. In: Transportation planning and implementation methodologies for developing countries, p 19
18. Pareekh P, Mitra S, Mukherjee D, Wadhwaniya S, Gupta S, Hyder AA (2019) A study of road traffic injuries using data from trauma care facilities: additional perspectives from India. In: Paper presented at 98th annual meeting of Transportation Research Board, Washington DC
19. Washington S, Haque MM, Oh J, Lee D (2014) Applying quantile regression for modeling equivalent property damage only crashes to identify accident blackspots. Accid Anal Prev 66:136–146
20. Bandyopadhyaya R (2018) Systematic engineering approaches for ensuring safe roads. Integr Disaster Sci Manag 277–283

21. Ministry of Road Transport & Highways (MoRTH): Protocol for identification and rectification of road accident black spots on National Highways. Office Memorandum No. RW/NH/15017/109/2015/P&M (RSCE), issued on 28th October, 2015. https://morth.nic.in/sites/default/files/Protocol_for_identification_and_rectification_of_road_accident_black_spots_on_National_Highways_OM_dated_28_10_2015.pdf
22. Sen AK, Tiwari G, Upadhyay V (2010) Estimating marginal external costs of transport in Delhi. Transp Policy 17:27–37
23. Blincoe LJ, Seay AG, Zaloshnja E, Miller TR, Romano EO, Luchter S, Spicer RS (2002) The economic impact of motor vehicle crashes, 2000. National Highway Traffic Safety Administration, United States
24. Mohan D, Tsimhoni O, Sivak M, Flan-nagan MJ (2009) Road safety in India: challenges and opportunities. University of Michigan, Transportation Research Institute, Ann Arbor
25. Chatterjee S, Bandyopadhyaya PS, Mitra S (2020) Identifying critical safety issues on two-lane national highways in India—a case study from NH 117 and NH 60. Transp Res Procedia 48:3908–3923

Study of Techno-Legal Aspects of Accident Site Investigation—A Case Study from Bengaluru

Ashish Verma, P. Anbazhagan, and R. Babitha

Abstract After a major road crash, conducting crash investigation is generally the next step. But the road accident spot analysis is not carried out as per the procedure in most of the road crashes in India. Although crash spot studies are conducted by associated officers, the procedure, implementation, and post-investigation studies are charge framed, nontechnical, and not available in the public domain. The study aims to investigate the techno-legal aspect of the crash site investigation of a typical crash from Bengaluru which occurred between the motorbike and the car. Crash spot was studied, analysis of accident spot parameters, and vehicles inspection observations are correlated and used to infer the reason for the crash. This article aims to highlight the importance of scientific investigation of the road accident site and the sequence of activities happening after the occurrence of the road accident with a case study.

Keywords Urbanization · Motorization · Road accidents · Crash investigation · Legal aspects

1 Introduction

Crashes and fatalities on the road are the results of the interplay of several factors. Road users in India are heterogeneous with standard and nonstandard vehicles and drivers. Motor vehicle collisions cause more than 1.35 million deaths worldwide and an even greater number of non-fatal injuries each year [1]. As reported in [2], road traffic is a major issue and is a leading cause of death worldwide. The data released by the Ministry of Road Transport and Highways has highlighted road crashes to

A. Verma (✉) · P. Anbazhagan
Department of Civil Engineering, Indian Institute of Science Bangalore, Bangalore, India
e-mail: ashishv@iisc.ac.in

P. Anbazhagan
e-mail: anbazhagan@iisc.ac.in

R. Babitha
Department of Civil Engineering, MS Ramaiah University of Applied Sciences, Bangalore, India

L. Devi et al. (eds.), *Proceedings of the Sixth International Conference of Transportation Research Group of India*, Lecture Notes in Civil Engineering 273,
https://doi.org/10.1007/978-981-19-4204-4_15

be one of the biggest causes of unnatural deaths occurring in India. Developing countries account for 90% of these casualties. In India, the pace of development of the vehicle population is quicker than the economic and population growth. The surge in motorization coupled with an expansion of the road network has increased road crashes. Almost 1.5 lakh people in India lose their lives due to road crashes annually, and India accounts for nearly 11% of the road accident-related deaths in the world [3]. According to statistics released by the Karnataka state police, the number of persons who lost their lives due to road crashes in Bengaluru rose by 82 in 2019 with 768 deaths compared to 686 such deaths reported in 2018. The increasing number of road fatalities is a matter of concern, and it is essential to focus on road safety. At the same, most road crash cases are resolved by the case in-charge officer without highlighting the fundamental problem of road crashes, technical aspects and how to overcome the same. Most of the crash case reports is prepared by victimizing larger/insured vehicle than the real issue in the particular crash. Similarly, very limited technical studies of road crash spot analysis are reported in India finding out the real cause of the crash. Even though crash can be due to: (1) improper infrastructure (road surface, gradient and signs boards), (2) signaling, (3) faulty vehicles, and (4) driver behavior. All other aspects can be overridden if driver is intelligent and follows proper traffic rules. Most of the road crash reports only on vehicle or driver factors, which are investigated nontechnically and the driver behavior of the larger vehicle is quickly blamed as rash driving/negligence as it is difficult to prove both without any video records. So, in this study, we carried out a detailed analysis of road accident with technical aspects and explained how legal, technical aspects help determine the actual problem of crashes based on a typical road accident case in Bengaluru. This paper also aimed to understand the techno-legal aspects of road accident site investigation. It provided a detailed study with an example of how can an ordinary person collect data and effectively handle legal aspects to prove/disprove charges prepared nontechnically. Nontechnical reports are prepared in most of India's road accident cases by nonexperts and never reviewed or corrected by technical experts.

2 Literature Review

The detailed, objective investigation of the causes and mechanisms of injuries in traffic crashes originated in the United States. Mackay et al. [4] illustrated a fundamental problem of field accident investigation. The importance of the need of going to the accident scene within a few minutes of the occurrence of the accident and collecting every bit of information available and its analysis to provide a better insight into the causes of injury is discussed.

There is no theoretically underpinned framework for collecting and analyzing accident-related data in the road transport domain, which is universally accepted. The application of use systems theory-based human factors accident analysis methodologies is problematic for various reasons, including incompatible data collection procedures, a lack of detail in the following data collected, a lack of theoretically

underpinned analysis methods, and a lack of appropriately trained personnel. Paul and Michael [5] discussed the barriers preventing valid, reliable, and usable accident analysis within the road transport domain and, in closing, present a series of proposed solutions to the barriers discussed.

England [6] has described and evaluated Accident Investigation as a method of producing information to reduce the frequency of road accidents. Here the detailed investigation is done, looking both at the road user's interaction with the road environment and within the environment itself. The problem of a road accident and possible approaches to accident reduction is introduced, and the importance of the multidisciplinary approach to the second-level in-depth investigation of the accident to determine countermeasures is discussed. Hill et al. [7] considered detailed investigations focusing on all types of vehicles (including damage, failures, features fitted, and their contribution); the highway (including design, features, maintenance, and condition); the human factors (including drivers, riders, passengers, and pedestrians); and the injuries sustained for the study of new 'On-The-Spot' (OTS) accident research project which is now underway in the UK.

An in-depth database will permit analyses to better understand the causes of crashes and injuries and assist in the development of solutions, which is the main objective of this paper. Baldock et al. [8] focus on studying factors that contribute to road crashes, with an emphasis on the role of road infrastructure. The methodology of carrying out the detailed investigation of the crash scene is discussed in detail, and also the key road safety problems that need to be addressed are identified.

Mackay [9] has attempted to outline some of the benefits which might be obtained from a more thorough and comprehensive examination of transport, and particularly road traffic and accident. From the thorough investigation of the road accidents, detailed evidence which exactly explains the circumstances of a particular collision may be produced and also provides the car designer, traffic engineers and other concerned authorities with practical results to take up the right remedial measures.

Evans [10] raises ethical issues relating to drivers, industry, and government regarding the death in traffic accidents. Increased professional and public discussion of the ethical issues surrounding all causes of harm in traffic can make a major contribution to reducing this harm.

In short, very limited research papers are available on the crash investigation of the accident pinpointing the faulty driver/vehicle. The above papers describe the importance of carrying out the detailed investigation of the crash, and going to the crash spot within few hours of the occurrence of the crash which gives a better understanding of the crashes. It also states that there is no standard theoretical framework to carryout the crash investigation and this study comprises the framework of road crash investigation which can be used for understanding the techno legal aspects and issues involved in crashes.

3 Study Site and Information About Road Accident and Sequence of Events

In this study, a classical known crash case that occurred in Bengaluru has been taken for analysis. Even though crash is common to any two moving entities on the road, four- wheelers and two-wheelers are very common and frequent victim vehicles in developing countries like India. In this study, collision is between (four-wheelers) car and (two-wheelers) motorbike in the urban area. The crash spot with nearby location and origin spot of both vehicles before the crash is shown in Fig. 1. The motorbike coming from the Bio-Chemistry building collided with the car on its left side, which was going toward D-Gate of IISc Campus. Figure 2 shows the location of the accident spot with the direction of both the vehicles and the exact location of the collision. The car driver immediately applied the brake, and the car stopped. By the time bike went under the car (on the left side of the car), causing heavy damage to the car bumper, radiator, A/C components, oil pumps and associated spare parts in the left front of the car and also the bottom up to the left middle of the car. The driver of the two-wheeler was not wearing a helmet, and the bike indicator was off. The car had leakage of oil and water from the coolant and suffered damage due to the heavy impact of the bike. Bike was found below the car and had damages on the left side of the bike such as bumper and petrol tank, and headlight was intact. Further, both vehicles were moved away from the spot and the bike driver had injuries on the left hand, he walked to an ambulance and was sent to treatment at a nearby Health Center. Subsequently, the car was moved to the side of the road, and the car driver

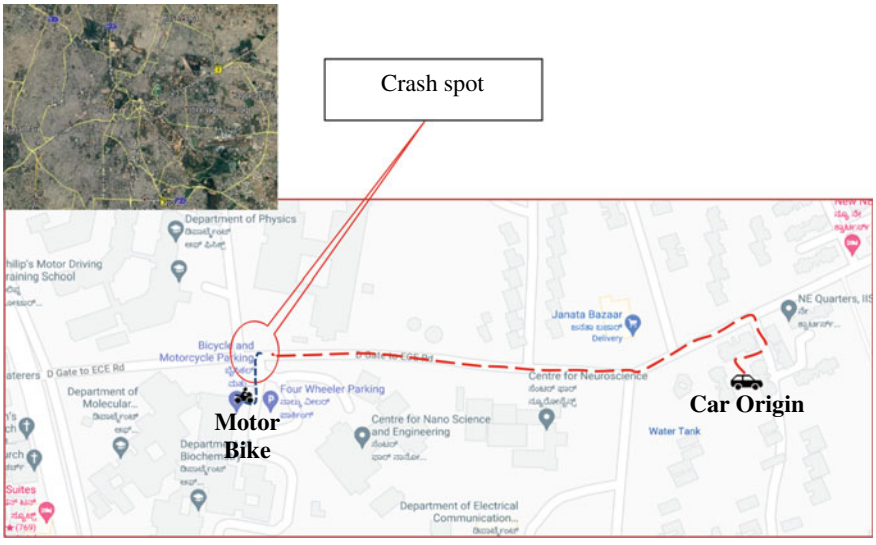

Fig. 1 IISc map showing the car moving path and the crash location (Figure prepared using Google Maps)

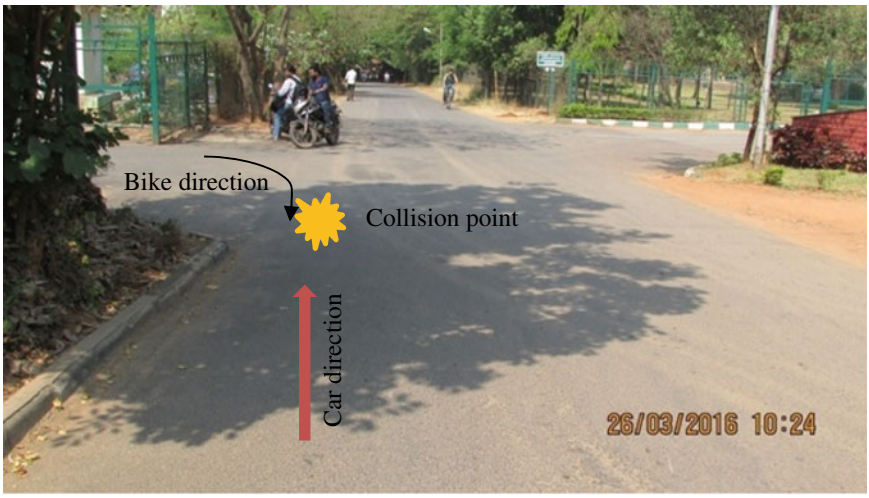

Fig. 2 Show view of the road from car direction (toward D-gate) with blind zone at the left of car due to fencing vegetation

left the crash spot. Later bike was moved to the parking area. Car was inspected by authorized service engineer and he suggested to move the car through tow vehicle and after few hours the car was towed to the nearest service station. Vehicle travel distance from origin spot is shown in Fig. 1, and it can be seen that car had crossed four junctions and about 270 m after the last junction point (Janatha Bazaar Circle). The bike just had one turn and approached, reaching gate and road junction after passing a steep-sloped ramp.

The marked portion of the road from Janatha Bazaar Circle to the entrance of the Centre for Nano Science and Engineering is having an upward grade. In this case, rising speed in a short duration (less than 300 m) is technically not feasible and reduces the possibility of rash driving. When a vehicle moves from Janatha Bazaar Circle toward D Gate, the left of the car is a blind zone due to dense vegetation and fencing. Figure 2 shows a photo of the blind zone close to the crash spot. As bike has to claim a steep slope (see Fig. 3a) before reaching gate and road, the bike might raise acceleration to claim the slope. The total incident was reported to the security office as the incident happened in the closed gate community. Since bike driver looks like a student and car driver being faculty, no police complaint was filed about the incident.

However, later it was found that the bike driver who does not belong to the campus had filed a case against the car driver at the police station in different sections. The car driver visited the station and explained the situation with evidence that he has not made any mistake and it was a mistake of the bike driver. However, the police did not register any complaint and asked the car driver to inform the court, but took few signatures in the document written in the local language, which was not known

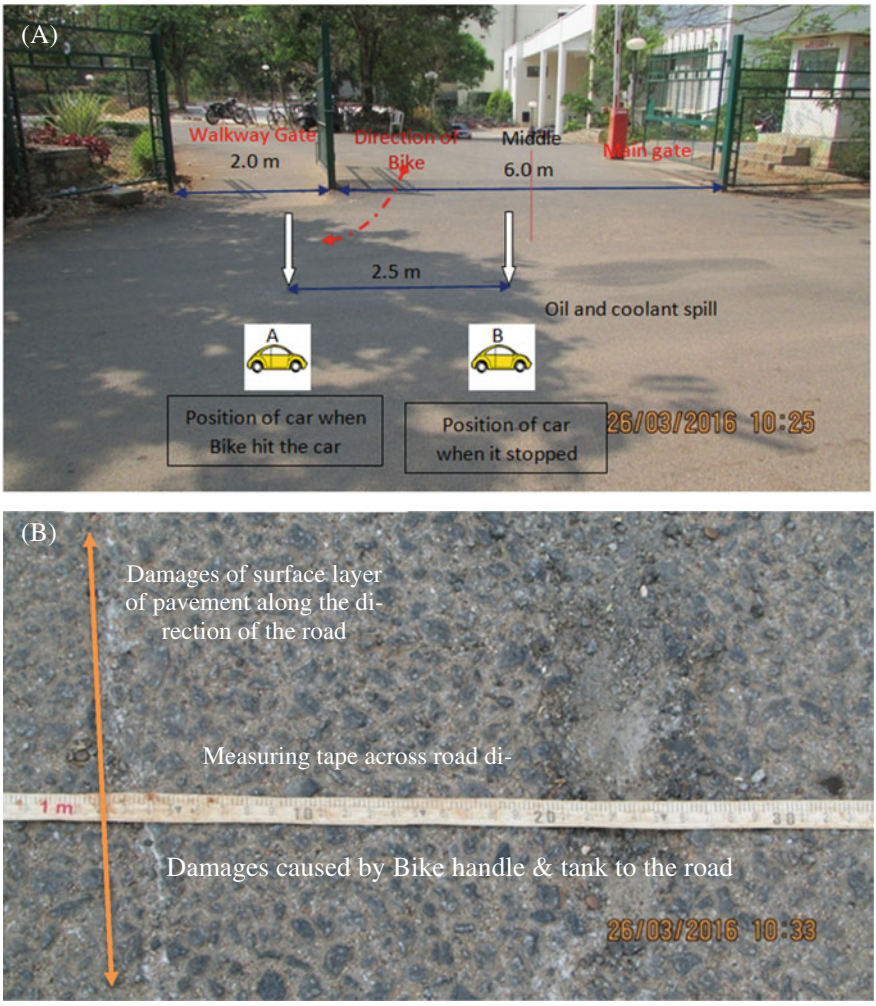

Fig. 3 **a** Crash spot with the marking of the initial position of the car at the time when the bike hit the car, final position where the car was stopped, gates and stopping distance marking and oil spill on the road. **b** Closer view of structural damage of road due to hitting bike handles and distance from the edge of the road (the left side toward D-Gate)

to the car driver. As car driver and owner were not happy with the police behavior, they asked the IISc team to study the accident and prepare a factual report.

4 Investigation of Road Accident Location

The authors personally visited the site and tried to understand the crash in technical detail before concluding the crash. The crash spot was studied, and data collected from the site are compiled to prepare the schematic location and vehicle position. Figure 3a shows the crash spot with information collected from the geometrical parameters. It was found that car was moving on the left side of the main road, and the bike was coming from the approach road to the main road. Crash spot was studied, and ground evidence was collected like soil, coolant spill location, and road damages caused by vehicles. The total width of the main road is 6.4 m, and damages on the road due to bike handle and tank hitting bitumen surface (Fig. 3b shows road damage with measurement) was noticed within 1.2 m from the left edge of the road. It indicates that during and after the crash, both vehicles are within the left lane of the main road. By tracing the beginning to end line of road damage along the left lane point of the road damage, we could arrive at the distance traveled by both vehicles after collision (initial damage location by bike handle) up to the halt position (final position where oil and coolant spill starting point and end of handle damage in the road). The bike left handle created an impression in the bituminous road surface up to 3.8 m followed by a patch mark on the road surface due to leakage of oil and coolant, which is the endpoint of the crash. Figure 3a shows the photos of road with bike handle impression, walkway gate, and main gate with oil and coolant spill on the road surface. Initial position at the time of the crash and the final position of the car after stopping are marked in Fig. 3a as A and B; we measured the distance between these two points as 3.8 m along the main road and 1.2 m from the left edge of the main road. Other geometric data are collected and marked in the crash spot photo in Fig. 3a. The position and direction of vehicles at the time of the crash and after both vehicles were halted were mapped. It can be clearly noted that there is a violation of traffic rules by bike driver, instead of exiting at the left lane of the approach road; bike exited at the right lane of the approach road, which is a violation of traffic as per Indian Traffic rules.

By carefully studying crash spot and road marks, the following conclusions can be drawn.

- The crash occurred about 1.2 m from the left edge of the main road in the left lane toward D Gate.
- Both car and bike were in motion at the time of the collision, which happened in front of the walkway in the left lane toward D gate fencing.
- After falling, the bike's left handle caused structural damage to a road opposite to walkway entry.
- No car wheel impression on the main road was observed, which mean that car has not applied sudden brake in high-speed.

Based on the above points, it is very clear that the two wheelers were in the right lane of the side road and turned right into the left lane, i.e., left side of the car rather than turning from the right side of the car.

The two-wheeler parking area entry and exit in approach road were also studied, and a Google Maps is shown in Fig. 4. Considering blind spot for a vehicle toward D Gate, the campus had separate parking and exit for two-wheelers as shown in Fig. 4.

Considering parking for two-wheelers and exit location, it is very clear that the bike should have come out on the main road from the dedicated exit gate for a two-wheeler to avoid blind spot and 90° turning at approach road in Fig. 3b.

As explained above and also as per the crash location marking, the bike was taking a right turn in the left lane towards the main road instead of taking a safe exit gate, which may be due to the bike driver is not familiar with campus and these traffic regulations, as he is not campus user or resident. Figure 5 presents the condition and

Fig. 4 Crash spot in Google Maps with entry and exit arrangement made as per traffic rules

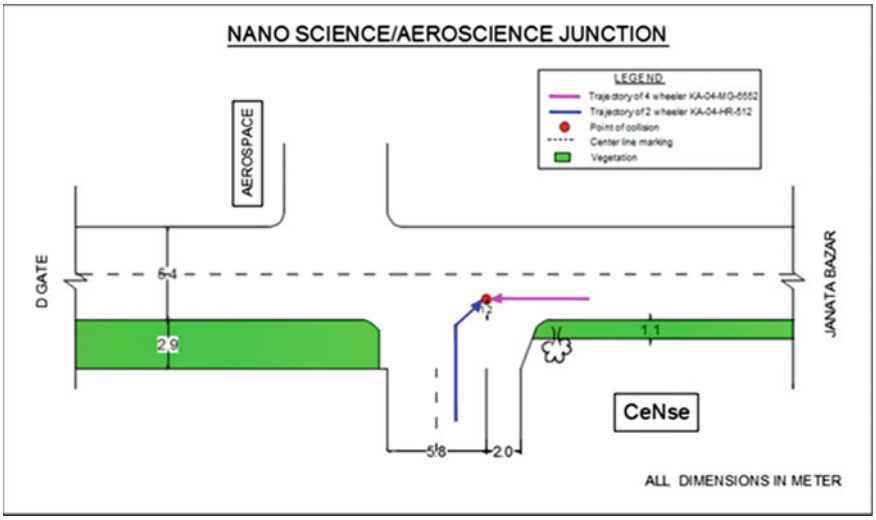

Fig. 5 Condition and collision diagram of the crash location

collision diagram of the crash prepared to explain the same after sufficient evidence and study discussed above.

Further, bike was entering the main road from the approach road and should ideally stop and watch on both sides of main road for a safe gap before proceeding further as per driving rules, the priority for movement goes to the vehicles on the main road, however, the bike was in motion at the time of the crash. As there was no car wheel impression on the road observed in photographs, it is plausible to assume that the car had stopped after normal breaking in the normal speed. Generally, the wheel impression of a vehicle is created on the road during accidents when applying sudden brake at high speed (for example, more than 60 km/h). Since the car stopped at 3.8 m from the initial point of the accident, it indicates that the car driver applied a brake on time, and car was stopped within the driver's reaction time, which is further explained later.

5 Investigation of Vehicles

As part of the crash investigation, vehicle damages should be studied apart from the geometric study of crash spots. Hence, the authors inspected both vehicles after the crash, took photos, and collected service reports of vehicles. Figure 6 shows typical photos of the bike taken during the inspection. The bike's right side, back, and front side are intact; no damages are noticed. The bike had damages in the left side, i.e., Bummer folded, headlight cover, and left-side handle damage and petrol tank left-side damage. No car paint or impression is noticed on any part of the bike, and no service report was available from the bike owner or in the case document.

Similarly, car was inspected at the service station as car was towed to the service station as per the service inspection report of the authorized car service station. We

Fig. 6 Typical photos of bike after the accident, parked within campus

have taken several photos and also collected on spot service report with recommendation and service station inspection and estimate. Figure 7 shows typical photos taken during the inspection. Quick visual observation of the car gives the impression that car was not damaged much, except for few scratches and dents (Fig. 7a) in the front between the number plate and left side of a car headlight. We also noticed the bike tyre impression next to the number plate. It indicates that bike hit a car in a straight and opposite direction of car driving direction. Further interaction with car driver and owner, service person and study of on-spot service report, we deepen our inspection. Figure 7b shows oil spill at a service station parked location similar to the oil spill marking in Fig. 3b. After seeing an oil spill, inspection shows the damage of car bumper, radiator, A/C components, oil pumps, and associated spare parts in the left front of the car and the bottom up to the left middle of the car. The photo was taken by placing a camera after lifting of damaged bumper and shown in Figs. 7c. Now, it is clear that damage of a major portion of radiator and front units results in car's non-operation driving status, which is why it was suggested to tow vehicle by inspection report. A study of the estimation of the service station revealed that replacement of most of the above spare parts of car was estimated to be Rs. 51,393.

By studying both vehicle photos, the following inferences were made.

- The bike's left handle bar damages were noticed due to the pavement surface, which is also confirmed as pavement damage reported in Sect. 4 of the accident location study.
- Other damages, scratches, and dent in the bike may be caused by bike interaction with the pavement surface. No evidence was found to say car hit the bike as the right side and front part of bike is intact.

- Bike wheel mark impression on car bumper and associated scratches, dent in Fig. 7a shows that bike hit the car. Further, car bumper was broken and damages in the major front assemblies of the car such as radiator, A/C components, and oil pumps (Fig. 7b) were observed. This clearly shows that the bike might have hit the car with higher acceleration than car i.e., speed of the bike might be more than the speed of the car.
- Bike damages on the left side indicate that after colliding with the car the bike fell on the left side, which caused damage to the left side of the bike and not on the right side, which is evident from structural damage to the main road.
- We can also infer that when a car hits a bike in a stopped position, the right side of the bike should be damaged, but in this case, the right side of the bike is intact and no damages are seen from Fig. 6. We can infer that the bike was also in motion at the time of the collision which hit the car, lost balance, turned left side, and moved under the car. So the left side of bike got damaged after hitting car on the main road and caused structural damages to the pavement surface.
- Figure 7 shows clearly that the number plate and left headlight of car (Fig. 7a) is intact after the collision. In general, when the car hits another vehicle like bike, the front portion of car such as the front number plate and head light will get damaged. In the present case, since the number plate of the car is intact and the

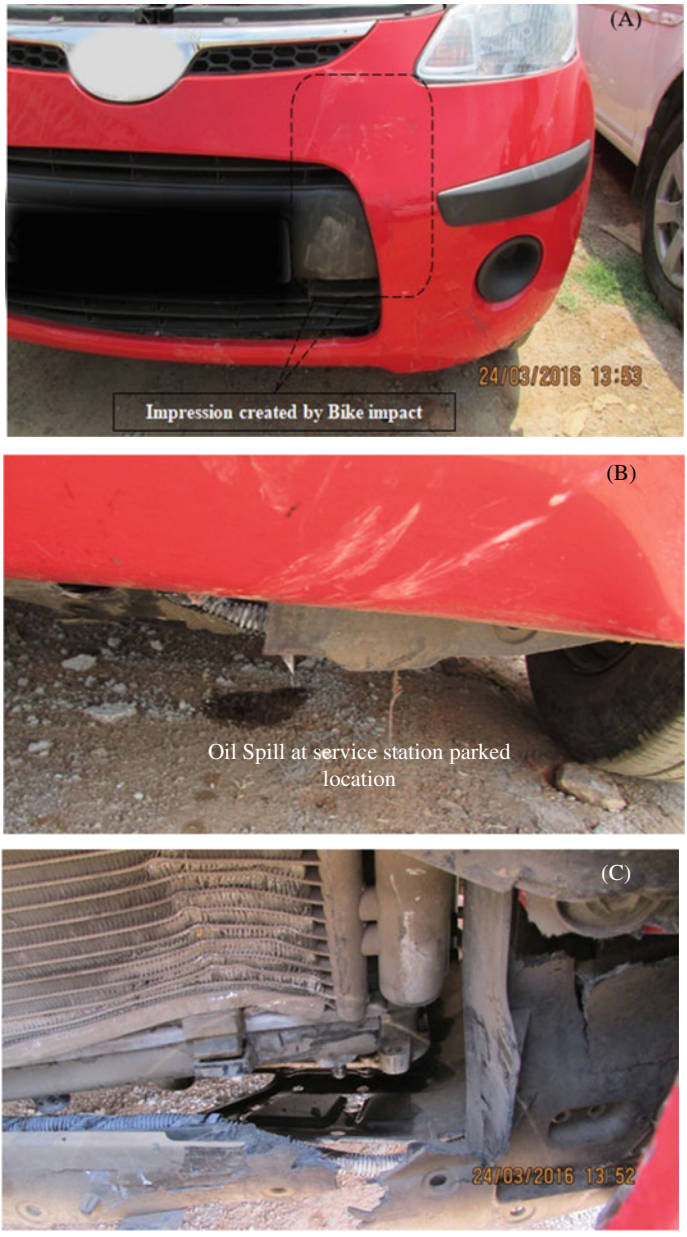

Fig. 7 Photos of car after the crash taken at the service station. **a** Car front with number plate, scratches and bike wheel impression created. **b** Oil and coolant leakage at the parked location and **c** damaged car radiator and A/C unit not visible outside

damages are on the left side of the bike, it suggests that the bike hit the car toward its left, i.e., between car number plate and headlight, which is possible only if bike hit the car and not when car hit the bike. Further, the bike was attempting to enter the main road toward the left of the car, which should ideally be from the right side. Bike should be damaged if car hit the bike, but it was not so.

- Figure 7c shows damages of radiator assembly and other parts of the car. Bigger damage impression on the radiator might be created by the impact of bike front wheel as the handle impression will be small. This suggests that the bike hit a car while in motion with a speed force that is above the design strength of the car radiator front panel.

6 Analysis of Geometric Data

After the study of crash spot and vehicles, we could come up with some inferences, but mostly qualitative and not quantitative parameters. Hence, available data collected are further studied and used to arrive at quantitative results helpful to support the qualitative hypothesis. The braking distance of the vehicle is the distance between the initial position of the car at the point where the impact happened and the final position of car after stopping by applying the brake.

In this study, structural damage to the road (impression and mark in Fig. 3a) caused by a bike can be taken as the initial point of crash, and the origin of oil and coolant leakage can be taken as the final vehicle position, i.e., halt of vehicles after the crash. Location of car after the crash, i.e., stopped position also confirmed with driver of car and eye witness on the spot, i.e., security person. There is no video recording in this location of the campus. Physical measurement in the accident spot of the initial and final position of the car was measured and found to be 3.8 m, as shown in Fig. 3a. The stopping distance or distance within a motor vehicle can be a function of (a) total reaction time of the driver, (b) speed of vehicle, (c) efficiency of brakes, (d) frictional resistance between the road, and (e) the tyres and gradient of the road. In this case, we have a stopping distance measurement of 3.8 m, which can be used to estimate the speed of the vehicle, and other parameters can be taken based on the accident spot. Indian Road Congress highlighted that the total reaction time of a good driver is 2.5 s. Based on this, the speed of car (km/h) can be calculated by the formula given below as per Khanna and Justo [11].

$$V = \sqrt{254 d \mu}$$

The speed of any vehicle (V in km/h) is a function of d = braking distance (m), which is 3.8 m in the present case, and μ = coefficient of friction (unitless). The friction of the accident road is assessed as per the Indian Road Congress Guidelines and varies from 0.4 to 0.35 depending on speed from 30 to 80 km/h. Variation of the possible speed of car based on 3.8 m stopping distance by variation of coefficient of friction is shown in Fig. 8. It can be noted from the analysis that car speed might be

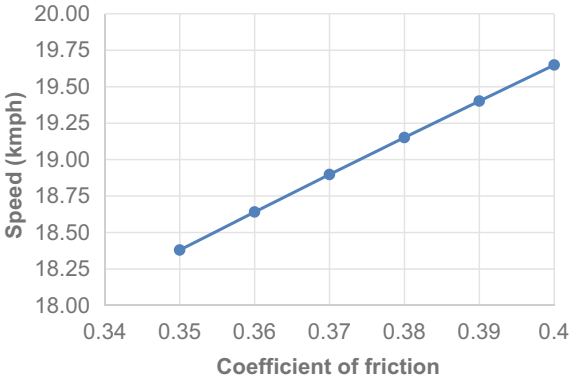

Fig. 8 Variation of car speed involved in the accident for the various coefficients of friction of the road

18 to 20 kmph. Even if maximum speed is taken, the estimated speed at the time of the accident is found to be 20 km/h, which is less than the speed limit of 30 km/h on the roads in campus and Bangalore city speed limit of 60 km/h. So, there is less chance that car might have caused accident.

7 Summary and Conclusion

Several accidents have occurred in different parts of India, but most accident are never technically studied and understood. In this study, for the first time, a detailed crash investigation was carried out for an accident between four-wheelers and two-wheelers. Analysis of accident spot parameters and vehicles inspection observations are correlated and used to infer the reason for the accident. Further, data collected from the accident spot was used to estimate the speed of one of the vehicles involved in the accident. Even though traffic rules violations and the speed of the bike caused the accident, but the cases of hit and run, over speed was booked against the car driver and owner despite sufficient evidence and data to the police. After about six months of the accident, the car owner and driver received court notice and then underwent court proceedings and procedures but did not accept police charges. After nearly two years, car driver and lawyer finally proved that all charges made by police, documents, and eyewitnesses were not correct by providing some evidence discussed in this paper without any eyewitness and cleared all charges. In summary, this paper highlights the importance and value of scientific accident site investigation and use it to conclude legal issues arising out of road accidents.

This study is based on one case study of the road crash. More case studies in different locations and different situations can be analyzed using a similar framework to understand the general applications of the proposed framework and also the framework can be modified to make it a more generalized framework in all the situations of road crashes.

References

1. World Health Organization (2018) World health statistics. https://www.who.int/docs/default-source/gho-documents/world-health-statistic-reports/6-june-18108-world-health-statistics-2018.pdf
2. World Health Organization (2018) Global status report on road safety. https://www.who.int/publications/i/item/9789241565684
3. Wing TR (2019) Road accidents in India. Ministry of Road Transport and Highways, MoRTH
4. Mackay GM, Ashton SJ, Galer MD, Thomas PD (1985) The methodology of in-depth studies of car crashes in Britain. Society of Automotive Engineers, Inc
5. Paul MS, Michael GL (2009) Systems-based human factors analysis of road traffic accidents: Barriers and solutions. In: Paul MS (eds) Australasian road safety research, policing and education conference. Sydney, New South Wales, pp 201–209
6. England L (1981) The role of accident investigation in road safety. In: Ergonomics. Taylor & Francis, England
7. Hill J, Thomas P, Smith M, Byard N, Rillie I (2019) The methodology of on the spot accident investigations in the UK. National Highway Traffic Safety Administration
8. Baldock, MRJ, Woolley JE, Ponte G, Wundersitz LN, Lindsay VL (2016) In-depth crash investigation at the centre for automotive safety research. Australasian road safety conference. Canberra, Australian Capital Territory, pp 15–23
9. Mackay GM (1970) The role of the accident investigator. Forensic Sci Soc
10. Evans L (2008) Death in traffic: why are the ethical issues ignored? Stud Ethics Law Technol 2
11. Khanna, Justo (1971) Text book – “highway engineering”

Analysis of Pavement and Geometric Factors of Selected Highways for Reduction in Road Accidents

Ankit Choudhary, Rahul Dev Garg, and Sukhvir Singh Jain

Abstract Road crashes are the major cause of unnatural deaths. Resultant, safety of road users has become one of the prime objectives of highway engineers apart from reliable and economic road network. This study is motivated to identify the safety requirements of different roads within the boundaries of Haridwar and Dehradun districts of Uttarakhand state, India. For analysis, six different roads were divided into 86 homogeneous segments of variable length. Essential traffic, geometric, and pavement surface variables, were selected and evaluated using Poisson regression (PR) and negative binomial regression (NB) model. Separate accident prediction models (APM's) were developed for total, rear-end and head-on crashes. The APMs delineated important risk factors in terms of positive and negative association. The probability of a crash was identified using risk ratios. Further, the models were compared in terms of goodness of fit. Akaike information criterion (AIC), Schwarz's Bayesian (SBC) value showed that the NB model performs better than the PR model as a former model allows additional over-dispersion parameters in the model.

Keywords Crash · Geometric design and pavement condition · PR and NB model

1 Introduction

In the past few years, India has witnessed a tremendous surge in road crashes. India ranks at the top with the highest number of RTAs deaths (1, 51,417) in the world, accounting for 11% of the total share [1]. However, most of these crashes occurred on rural highways (55% of RTAs and 63% of crash-related deaths), despite these rural highways constitute only 4.91% of the total road network (as shown in Fig. 1). Thus, the safety of highway users is a cause of concern for highway engineers and researchers. However, a couple of studies have been conducted in India to explore the risk variables associated with rural road safety for instance, [2–4]. These studies tried

A. Choudhary (✉) · R. D. Garg · S. S. Jain
Indian Institute of Technology-Roorkee, Roorkee, India
e-mail: achoudhary@ts.iitr.ac.in

L. Devi et al. (eds.), *Proceedings of the Sixth International Conference of Transportation Research Group of India*, Lecture Notes in Civil Engineering 273,
https://doi.org/10.1007/978-981-19-4204-4_16

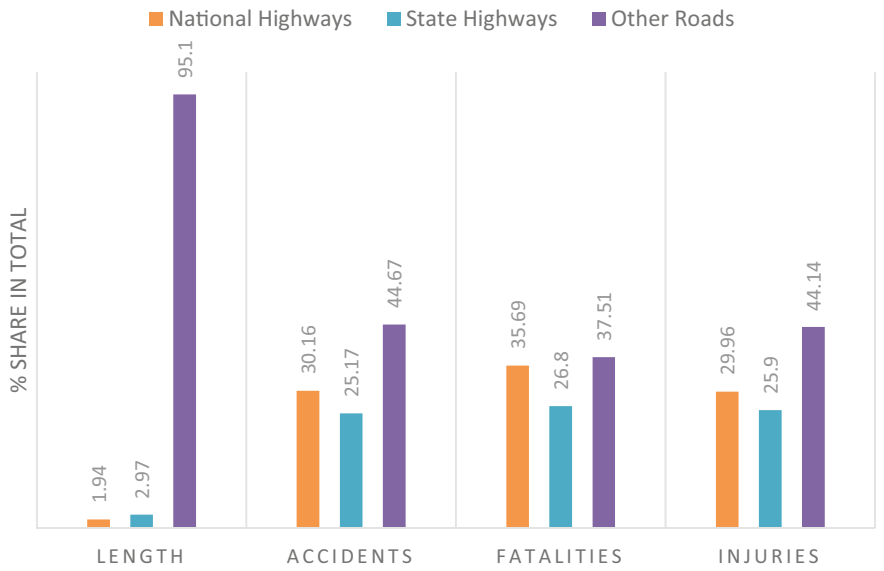

Fig. 1 Number of accidents, persons killed and injured as per the category of roads in 2018

to identify numerous variables that may impact crash frequency and their severity levels.

Accidents are random in nature and are influenced by a variety of risk factors. Generally, these risk factors are classified into, road infrastructure (for instance; pavement surface condition, roadside hazard, cross-sectional elements), occupancy characteristics (for instance, helmet use, driver distraction, sex), vehicle attributes (e.g., weight, vehicle height, and class of vehicle), crash attributes (for instance, collision type, instant speed), and environmental circumstances (for instance, weather condition, light condition, visibility). The objective of this paper is twofold. First, to develop safety performance function using Poisson regression (PR) and negative binomial (NB) model and, second, to compare the performance of developed models. The study was conducted in the Haridwar and Dehradun districts of Uttarakhand state, between January 2016 and December 2019.

In past, numerous researches have tried to enumerate the effect of infrastructure and traffic attributes on crash frequency. For instance, [5] had tried to develop a crash predication model for urban roads in Washington. The research concluded that steep curvature, increased vehicle volume wider lanes, and shoulder-width; increase the probability of crash. Similarly, [6] identified the association between the number of accidents and median width using the NB approach. The study concluded that increased median width (above 25ft) decreases the number of crashes. [7] used a hierarchical tree-based regression model and concluded that road geometrics and road surface condition significantly impact the safety of road users in terms of crash frequency. Similarly, [8] explored the efficiency of road design in terms of crash reduction for different categories of non-urban roads. The research concluded that

improved surface friction, wider lanes, and shoulder width improves the safety of road users in terms of crash reduction. In another study, [9] developed a generalized nonlinear model to analyze the efficacy of change in lane width on crash rates. The study predicted lower crash rates for segments having lane widths greater or less than 12-ft whereas, higher crash rates for 12-ft lane width. Similarly, [10] tried to identify the relationship between the number of crashes and shoulder width. The author developed two types of APMs, i.e., Negative-binomial and case–control models for different categories of collisions. The model suggested that up to 2.2 m shoulder width, crash risk increases; whereas, an increment above 2.2 m decreases the risk of a crash by 1–4% for each 0.1 m increase in shoulder width, for all types of crashes.

2 Modeling Approach

This study is an effort to quantify the effect of infrastructural variables on crash frequencies by developing different crash prediction models for divided/undivided roads and highways under mixed traffic conditions. The statistical analysis was conducted using the PR and NB regression modeling technique. In this study, six different roads were selected and were divided into homogeneous segments of variable length. It is suitable to use the NB/PR modeling technique to identify the co-relation among the number of accidents as conditional variable and infrastructural variables as un-conditional, because of the positive nature of crash events. These models represent an exceptional distribution of count data by preserving the legitimacy of statistical analysis [11]. To evaluate the fitness of the developed model, Akaike's Information Criteria (AIC) and likelihood ratio are utilized and the model which has the least AIC value is assumed to be the best fitted [12].

2.1 Poisson Distribution

The Poisson distribution is a discrete probability distribution function that applies to the occurrence of an event over a specified interval. The random variable Y is the frequency of events that occurred in an interval. The interval can be time, distance, area, volume, or some other similar units. Poisson regression is a novel approach that has a positive integer value and can be applied extensively to rare event count data [13]. The generalized form of the PR model is shown in Eq. (1).

$$\log(Y) = \text{Intercept} + \beta_1 x_1 + \beta_2 x_2 + \beta_3 x_3 \tag{1}$$

Explanatory variables $X = (X_1, X_2 \ldots\ldots X_k)$, can be continuous or a combination of continuous and categorical variables. The convention is to call such a model "Poisson Regression". The distribution of Poisson regression is shown in Eq. (2).

$$P(y_i) = \exp(-\lambda_i)\lambda_i y_i / y_i! \tag{2}$$

where λ_i is the PR parameter for crash frequency, which is equivalent to $E(y_i)$. The Poisson regression models are assessed by specifying λ_i as a function of explanatory factors. The relation between the Poisson parameter (λ_i) and explanatory factors is explained by a log-linear model as shown in Eq. (3).

$$\lambda_i = E(y_i) = \exp(\beta X_i) \tag{3}$$

where X_i is a vector of explanatory variables and β is a vector of estimated parameters. Similarly, the log-likelihood function LL(β) that is used to estimate the model is represented by Eq. (4).

$$LL(\beta) = \sum_{i=1}^{n} \left[-\exp(\beta X_i) + y_1 \beta X_i - L_n(y_i!) \right] \tag{4}$$

2.2 NB Distribution

Negative binomial or Poisson–gamma distribution is a generalized form of Poisson distribution, suitable for over-dispersed count data. The formulation is the same as that of the PR model, supplemented with an additional parameter α that adjusts the variance independently from the mean. The NB model rejects the assumption of equal mean and variance and is thus suitable for data having variance greater than the mean [11]. In general, the PR model is assumed to be a limiting model of NB because the value of α approaches 0 [13]. The choice of selection between these two models depends on the value of the additional parameter α. The probability function $L(\lambda_i)$ is given by Eq. (5).

$$L(\lambda_i) = \prod_i \frac{\Gamma\left[(1/\alpha) + y_i\right]}{\Gamma(1/\alpha) y_i!} \left[\frac{1/\alpha}{(1/\alpha) + \lambda_i} \right]^{1/\alpha} \left[\frac{\lambda_i}{(1/\alpha) + \lambda_i} \right]^{y_i} \tag{5}$$

2.3 Goodness of Fit

The term "goodness of fit" describes how well the model is fitted to the set of observed data. In general, the likelihood ratio, Akaike information criterion (AIC), Bayesian information criterion (BIC), and so on are commonly used to summarize the inconsistency between the performance of developed models.

Likelihood-ratio or sometimes known as Likelihood-ratio chi^2 is defined as a chi^2 distribution in which degrees of freedom are equivalent to the variance in the frequency of parameters in the controlled β_R and un-controlled β_u model. Similarly, the Akaike information criterion (AIC) value helps in the identification of the best fitted model and is given by Eq. (6). The model which has the least AIC value is assumed to be the best one among all the developed models [12].

$$\text{AIC} = [-2L_n(\beta_u+) + 2b]/N \tag{6}$$

where Ln (β_U) = log-likelihood value of the model, b = Number of factors, N = Number of observations.

3 Data Collection and Description

Accurate and precise data are base of traffic safety analysis. The effective use of this accident data depends on three factors, i.e., accuracy of time, date of occurrence, and accident location. The statistics used in this study was collected for 6 different rural roads and highways passing through the plain and hilly terrain of Uttarakhand state, India. These roads include:

a. Muzaffarnagar-Haridwar (NH-334),
b. Haridwar-Dehradun (NH-7),
c. Dehradun-Bhagwanpur (NH-72 A),
d. Roorkee-Laksar (SH-26),
e. Puhana-Jhabrera (SH-28),
f. Manglaur-Deoband (MDR-2 W).

These roads are 2/4-lane divided and undivided highways and accommodate mixed traffic conditions. The posted speed limit along these highways ranges from 50 km/h to 80 km/h for different locations. These roads are economic corridors of Uttarakhand state as connect important religious and tourist destinations which attract the travelers consistently. The maximum portion of these road segments (approximately 75%) passes through non-urban areas.

Crash history of four years (2017–2020) was collected for selected roads (as shown in Fig. 2) from concerned police stations. In India, accident data is collected by traffic police in transcribed format and was extracted as per IRC-53, 2015. This format comprises crash location, time, injures/fatalities, type of crashes, vehicle involved, and possible reason for crashes. After collecting crash data, it was compiled using Microsoft Excel and outliers. The outliers include crashes on intersections, urban areas, pedestrian crashes, or crashes for which required information is missing such as location or type of crash, etc. The total length of the study stretch was about 104 km, which were further divided into 86 homogeneous segments of variable length based on geometric and operational attributes of the road network.

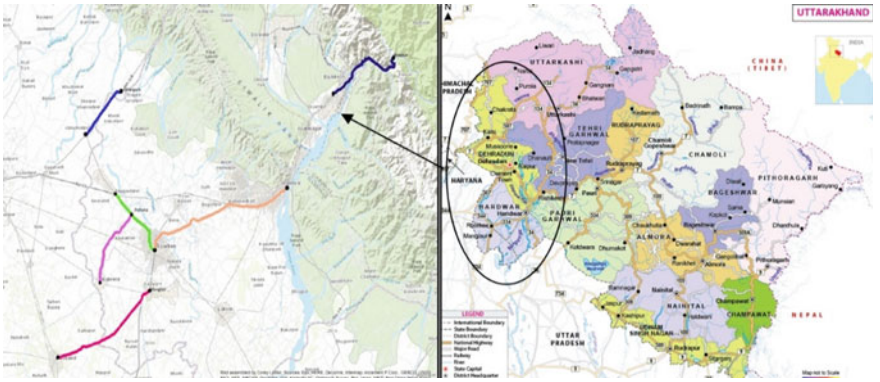

Fig. 2 Study area

In span of four years, total of 1130 crashes occurred on these highways. Crashes that occurred at intersections (within a buffer zone of 100 m) were not considered in the analysis. Resultant, 668 crashes were considered for analysis, out of which 247 were rear-end crashes and 271 were head-on crashes. The most difficult assignment for conducting systematic research in the framework of developing nations is the accessibility of reliable data. For this study, other than police stations data was collected through field surveys and from the database of different government and non-government agencies such as public work departments and toll tax booths respectively. The risk variables were broadly classified into three categories, i.e., traffic attributes, cross-sectional and spatial attributes, and roadway surface attributes. Table 1 represents the descriptive data of identified risk factors included in this research.

4 Results and Discussion

4.1 Pattern of Crashes

Crashes are random in nature; resultant, these does not show any fixed pattern or trend. However, some patterns/slight variations were observed on selected road segments. For instance, maximum accidents occurred in the month of July followed by august. It may be due to a sudden increase in traffic and pedestrian movement. This increase in movement is due to various yatras to holy shrines, Kawd yatra in Haridwar, Lord Badrinath, Kedarnath, and Hemkundsahib. Due to competition, drivers tend to make more possible trips, which increases rough and speedy driving. Investigating time variation, it was observed that maximum no. of accidents takes place in late evening hours i.e., between 18.00 h and 21.00 h. The possible reason is that in the evening, the driver tends to be in hurry to reach the destination before the sun sets, resultant motivates them to increase their speed. However, there may be other possible

Table 1 Descriptive data of identified risk factors

Factor name	Factor explanation	Min	Max	Mean	Std.dev
T_Crash	Total crashes	0.00	12.00	6.506	2.468
R_Crash	Total Rear-end crashes	0.00	7.00	2.948	1.746
H_Crash	Total Head-on crashes	0.00	6.00	2.194	1.701
S_length	Segment length (in kms)	0.30	1.80	1.115	0.494
AADT	Annual Average Daily Traffic/ 10,000	1.85	5.47	3.388	0.897
L_Width	Lane width (in meters)	2.75	3.75	3.311	0.295
S_Width	Shoulder width (in meters)	0.50	4.00	2.636	1.179
Acc_Density	No of access points per segment	0.00	7.00	2.545	2.036
Gradient	Average gradient	−5.4	7.15	1.972	2.270
S_Speed	Spot speed	41.0	80.0	59.06	10.546
Rutting	Rutting (in mm)	0.00	0.78	0.167	0.152
Potholes	Volume of potholes/segment	0.00	9.00	2.053	2.174
P_Distress	Pavement distress (in %)	0.00	1.56	0.207	0.402
Categorical variables				Count	%
S_Type	Type of segment				
	Straight	–	–	43	55.8%
	Curve	–	–	34	44.2%
Terrain	Type of terrain				
	Plain	–	–	64	83.1%
	Hilly	–	–	13	16.9%
Median	Presence of median				
	Yes	–	–	59	76.6%
	No	–	–	18	23.4%
Marking	Presence of road marking				
	Yes	–	–	47	61.0%
	No	–	–	30	39.0%
Sign_board	Presence of sign boards				
	Yes	–	–	59	76.6%
	No	–	–	18	23.4%
Built_area	Type of built-up area				
	Open area	–	–	52	67.5%
	Built up/business area	–	–	25	32.5%

reasons which may affect early or late evening hours crashes, for instance, roadside development, accessibility, lighting condition, etc.

From FIR reports, it was also analyzed that cars and bikes (48.84%) are more involved in the accident as compared to other vehicles. The reason found behind the involvement of cars and bikes in the accident is due to high operating speed, and drunk and drive cases. The report suggests that bikes that were involved in accidents were ridden by the age group of 26–40 years. After those trucks are the major defaulters. The main reasons found behind them were rash driving, not following traffic rules, overloading of vehicles and not proper maintenance of vehicles, etc. It has also been analyzed that unknown vehicles are also involved in accidents,, which are the results of hit and run cases. These hits and run cases mostly occurred in late night or early morning.

4.2 Discussion

As previously discussed, NB is superior to the PR model as it has an extra parameter α to model the over-dispersed data. However, in this analysis, NB and PR models exhibited comparable parameter approximations despite the fact that the NB model is more advance and provides a better understanding of individual impact than that of PR model. On the other side, the NB model is easy to interpret and more convenient for predication of road safety. Since there is a minimal marginal effect between the two models, therefore the results will be discussed on the basis of the NB model. Using PR and NB regression three different models were developed for separate types of collisions, i.e., for total crashes, rear-end crashes, and head-on crashes. The motivation behind developing separate models for head-on and rear-end crashes was to identify whether the impact of risk variables significantly varies with the type of crash or not. Risk variables were divided into traffic variables, road design, and pavement surface conditions for discussion. The safety performance functions were developed using 90% of crash statistics whereas 10% of the dataset was used for validation. Similarly, for interpretation of the result, risk ratios were calculated and inference of crash is determined on the basis of exp(β) values. Tables 2, 3, and 4 show changes in estimated constants, standard error, and exp(β) for total, rear-end, and head-on crashes (from significant to insignificant and vice-versa) under the PR and NB regression model framework, respectively.

The result indicates that the impact of risk variables changes as the type of crash changes. However, the sign of estimated coefficients remained almost constant for different types of crashes. Concerning the explanation of the model's outcomes, the estimated constant shows how independent factors are associated with the occurrence of total, head-on, and rear-end collisions. The estimated parameter indicates a co-relation between dependent and independent variables. For instance, the estimated coefficient of speed is 0.024, which shows a positive co-relation with the total number of accidents at 95% of the confidence interval.

Table 2 Parameter estimation for total crashes

Parameters		Poisson model			NB model		
		Est	Error[#]	Exp(β)	Est	Error[#]	Exp(β)
Traffic parameters	AADT	−0.18**	0.075	0.833	−0.12**	0.055	0.886
	S_Speed	0.039	0.010	1.039	0.024*	0.008	1.024
Pavement parameters	Rutting	−0.770**	0.365	0.463	0.804**	0.284	0.448
	Potholes	0.052	0.038	1.053	0.006	0.0300	1.006
	P_Distress	−0.633*	0.149	0.531	−0.424*	0.119	0.655
	Marking = 1	−0.302	0.190	0.740	0.276***	0.144	1.318
	Marking = 0	Ref	–	–	Ref	–	–
Geometric design parameters	S_length	−0.396**	0.147	0.673	−0.24**	0.107	0.787
	L_Width	−0.927*	0.238	0.396	−0.741*	0.172	0.477
	S_Width	0.271*	0.059	1.310	0.193*	0.047	1.213
	Acc_Density	−0.156*	0.041	0.856	−0.123*	0.033	0.884
	Gradient	0.113*	0.027	1.119	0.081*	0.023	1.085
	Median = 1	−0.587*	0.177	0.556	−0.25***	0.145	0.776
	Median = 0	Ref	–	–	Ref	–	–
	S_Type = 1	0.453**	0.221	1.573	−0.062	0.188	0.94
	S_Type = 0	Ref	–	–	Ref	–	–
	Terrain = 1	−0.269	0.259	0.765	−0.469*	0.137	0.625
	Terrain = 0	Ref	–	–	Ref	–	–
Road side attributes	Built_area = 1	−1.088*	0.175	0.337	0.322***	0.166	1.379
	Built_area = 0	–	–	–	Ref	–	–
	Sign_board = 1	0.540**	0.187	1.714	−0.775*	0.132	0.461
	Sign_board = 0	Ref	–	–	Ref	–	–
	Intercept	3.607	0.894	36.843	3.646	0.714	38.334

[#] Standard error

*, **, *** mean significant at 1%, 5%, and 10%, respectively

4.2.1 Traffic Conditions

Road crashes mainly occur due to the movement of traffic; resultant, it is natural to examine and understand the impact of traffic parameters on accidents. Traffic volume or flow can be defined as the frequency of vehicles crossing through a point location in unit time, whereas density is defined as the frequency of vehicles available per unit length of the road at an instant. These traffic parameters have adverse effects when they combine with engineering and behavioral characteristics. As anticipated, AADT were found significant at the 95% confidence interval and was negatively co-related with accident frequency. From statistical results, it can conclude that probability of total, head-on, and rear-end collision decreases with an increase in AADT. For instance, the number of total crashes increases by 0.886 times with a unit increase in

Table 3 Parameter estimation for Rear-End crashes

Parameters		Poisson model			NB model		
		Est	Error[#]	Exp(β)	Est	Error[#]	Exp(β)
Traffic parameters	AADT	−0.20**	0.087	0.816	−0.103	0.076	0.902
	S_Speed	0.041*	0.012	1.041	0.029**	0.01	1.03
Pavement parameters	Rutting	0.93 **	0.436	2.535	0.521	0.372	1.684
	Potholes	0.106**	0.043	1.111	0.062	0.04	1.064
	P_Distress	−0.902*	0.187	0.406	−0.599*	0.161	0.549
	Marking = 1	−0.066	0.225	0.936	0.775*	0.198	2.17
	Marking = 0	–	–	–	–	–	–
Geometric design parameters	S_length	−1.029*	0.164	0.357	−0.868*	0.13	0.42
	L_Width	0.316	0.281	1.372	0.567**	0.254	1.763
	S_Width	0.234*	0.067	1.264	0.153**	0.064	1.165
	Acc_Density	−0.175*	0.049	0.839	−0.166*	0.046	0.847
	Gradient	0.072**	0.032	1.074	0.079**	0.028	1.082
	Median = 1	0.253	0.199	1.287	−0.35***	0.202	0.704
	Median = 0	–	–	–	–	–	–
	S_Type = 1	0.125	0.261	1.133	−0.37	0.233	0.691
	S_Type = 0	–	–	–	–	–	–
	Terrain = 1	−0.69**	0.302	0.498	0.316***	0.19	1.371
	Terrain = 0	–	–	–	–	–	–
Road side attributes	Built_area = 1	−1.137*	0.197	0.321	−0.171	0.226	0.843
	Built_area = 0	–	–	–	–	–	–
	Sign_board = 1	1.039*	0.22	2.827	−1.025*	0.18	0.359
	Sign_board = 0	–	–	–	–	–	–
	Intercept	−1.038	1.101	0.354	−1.247	1.019	0.287

[#] Standard error

*, **, *** mean significant at 1%, 5%, and 10%, respectively

AADT. However, [14] concluded that with an increase in density and flow, accident frequency remains constant up to a threshold value. If this value increases above the critical value, then the accident frequency increases rapidly.

Similarly, the impact of speed on crashes had gained significant attention in previous research, and considerable investigation has been done so far. Speed is one of the critical components which directly impacts a crash in terms of crash occurrence and its severity level. Factors such as average speed and speed variance have been investigated in order to develop a relationship, which is to be considered one of the most influential and crucial factors. The present study identified a positive co-relation between the number of total and rear-end crashes. The statistics state that a unit increase in spot speed surges the frequency of crashes by 1.024 and 1.03 times. However, [15] concluded that speed and crash frequency are non-linearly. related,

Table 4 Parameter estimation for Head-On crashes

Parameters		Poisson model			NB model		
		Est	Error[#]	Exp(β)	Est	Error[#]	Exp(β)
Traffic parameters	AADT	−0.428*	0.188	0.652	−0.294**	0.146	0.745
	S_Speed	0.006	0.022	1.006	0.001	0.018	1.001
Pavement parameters	Rutting	−1.866*	0.828	0.155	1.861**	0.742	0.155
	Potholes	0.013	0.091	1.013	0	0.066	1
	P_Distress	0.149	0.328	1.161	− 0.017	0.289	0.983
	Marking = 1	−0.985*	0.454	0.373	−0.206	0.349	0.814
	Marking = 0	–	–	–	–	–	–
Geometric design parameters	S_length	0.548	0.36	1.729	0.483***	0.271	1.622
	L_Width	−1.183*	0.5	0.306	−1.412*	0.381	0.244
	S_Width	0.162	0.143	1.175	0.187	0.117	1.205
	Acc_Density	−0.17***	0.096	0.84	−0.117	0.081	0.89
	Gradient	0.138*	0.061	1.148	0.104***	0.058	1.109
	Median = 1	−0.623	0.394	0.536	−0.519	0.342	0.595
	Median = 0	–	–	–	–	–	–
	S_Type = 1	0.465	0.503	1.593	0.568	0.456	1.764
	S_Type = 0	–	–	–	–	–	–
	Terrain = 1	0.535	0.599	1.708	−0.671**	0.317	0.511
	Terrain = 0	–	–	–	–	–	–
Road side attributes	Built_area = 1	−0.905*	0.419	0.405	0.553	0.38	1.738
	Built_area = 0	–	–	–	–	–	–
	Sign_board = 1	−0.056	0.447	0.945	−0.55***	0.318	0.573
	Sign_board = 0	–	–	–	–	–	–
	Intercept	5.575	1.921	263.696	5.889	1.748	360.883

[#] Standard error

*, **, *** mean significant at 1%, 5%, and 10%, respectively

due to the presence of other parameters that impacts speed distribution factors and crashes. Contrary to this, [16] opined that accident rate and speed are positively related to a power function.

4.2.2 Geometric Conditions

Consistency in geometric design plays an important role in highway design. Therefore, treatment of any inconsistency in road design surely improves road safety. Past crash theories also conclude that improved road geometrics enhance transportation safety. Indeed, user safety is an essential objective of road design [17] such as designing an anticipated operative speed as per the developmental perspective of a

road. The outcomes of this research indicate that a section passing through an open area tends to be more hazardous than that of a section passing through hilly terrain or a built-up area. The study indicates that built-up/ business areas are negatively co-related with all types of crashes. Thus, from the results, it may be concluded that the presence of a built area decreases the probability of a vehicle to get involved in any type of crash. Similarly, the presence of hilly terrain can reduce the probability of rear-end crash by 1.37 times. However, it is quite understandable why these sections are more hazardous than those other sections. Driving in hilly or built area necessitates amplified attention and driving skills. Additionally, terrain highways are attributed with limited accessibility, controlled speed, manoeuvring, etc., which in turn motivates drivers for cautious driving. In contrast, plain terrain or segments passing through the open area are characterized by service lanes, diverging/merging ramps, wider lane, and shoulder widths. Thus, psychologically inspire drivers for weaving manoeuvre, speeding which in turn becomes an additional challenging safety condition and reduction.

Road accidents are the outcomes of inappropriate interface among motor vehicles, road attributes, and its users. For instance, lane and shoulder width are important cross-sectional parameters of roadway attributes, which significantly impact the safety of road users.

The analysis concluded that lane width is positively co-related with rear-end crashes. Thus, it can be concluded that the number of rear-end crashes will be 1.76 times greater for each unit increase in cross-sectional lane width. Consistent with the past result, [18] concluded that fatalities increase with the increment in the number of lanes and their width, because of increased possibilities of changing the lanes. The same study also suggests that on rural highways, increased shoulder width decreases the probability of crash occurrence. However, contradictory results were proposed by [5] and suggested that lane width less than 3.5 m tends to minimize crash rate. However, this study concluded that shoulder width is positively linked with all types of collisions. This shows that the number of total number of crashes will increase 1.213 times more for each unit increase in shoulder width. In other words, it can be stated that there will be a 21.3% increase in the number of crashes for each meter increase in shoulder width. Similarly, the frequency of head-on and rear-end collisions will increase 1.16 times, and 1.20 times for each unit increase in shoulder width respectively. The result seems to be plausible as the shoulder provides extra width, thus motivating drivers for overtaking and manoeuvring vehicles [2].

Considering the curve sections, [19] suggested that curve sections decrease the number of fatal crashes. This study also shows a negative co-relation between curve segments and total crashes. Hence, it can be concluded that the presence of curve segment decreases the probability of rear-end crash by 0.691 times, as the curve section increases the alertness and vigilance of the driver. However, it was observed that other types of crashes are positively associated with curve segments. Access density can be characterized as the summation of access weights of various access points on one road portion divided by the length of the road fragment. The

study concluded that with an increase in access points per kilometer, decreases the probability of total and rear-end crashes, whereas a per unit increase in gradient increases the probability of all types of crashes. Similarly, the presence of pavement marking decreases the probability of rear-end crashes as better longitudinal roadway marking retro-reflectivity levels increase drivers' visibility and detection distance [20]. Comparing the results of present and past research, it can be concluded that geometric parameters possess a mixed effect on road safety and hence needs further attempts of investigation.

4.2.3 Pavement Surface Condition

Tables 1 and 2 show that the distress ratio is negatively co-related with total and rear crashes. This indicates that a higher distress ratio is linked with a smaller number of crashes. The result suggested that with each 1 unit increase in distress ratio, the probability of total and rear-end crash decreases by 34.5 and 45.1%. This decrease may be because of an increase in alertness and vigilance in sections with the deprived surface condition [21]. This clarification seems to be reasonable because in this research maximum distress ratio was 1.56%, which is adequately large to increase rider's attentiveness yet at the same time far from making drivers fail to keep a grip on their vehicles.

Similarly, as anticipated rut depth (which can be defined as longitudinal depression in the pavement surface caused by regular wheel pressure, evaluated in mm) was found to be positively associated with the total and head-on collisions. Consistent with past studies [22] the result suggested that each 1 unit increase in rut depth, increases the probability of total and head-on crashes by 43.8% and 14.6% times, respectively. The result seems to be plausible as it is difficult to handle a vehicle on a road having extreme deep ruts. For instance, maneuvering of two-wheeler in adverse weather conditions or during changing lanes. However, the PR model shows a positive co-relation between rutting and the number of rear-end crashes. Thus, in results similar to [23] there is no distinctive connection between rut depth and accidents (Table 4).

4.3 Evaluation of Safety Performance Function (SPF)

Safety performance function (SPF) is basic criteria to statistically investigate the factors affecting the safety of rural roads. However, before the development of the safety performance function, a primary investigation was conducted to identify the association between crash frequency, gradient, and shoulder width. The results showed a significant dependency, thus motivating for further investigation to identify possible risk variables. To quantify the impact of identified risk variables, accident statistics for 4 years was used to develop different SPFs using SPSS software. The

final models were developed by regressing only significant variables as depicted in Table 5.

Using the PR and NB regression model, separate SPF was developed for each type of crash, i.e., for head-on, rear-end, and total crashes. Total crashes include all types (for instance., PDO, runoff, overturn, etc.) of crashes that occurred within the study segment including rear-end and head-on collisions. The recitals of Poisson regression as well as negative binomial regression models are shown in Table 5. The AIC and SBC (also called as Bayesian information criterion) test value indicate that NB models provide better goodness of fit than that of the PR model. However, aside from the AIC and SBC statistics, the number of distinguished significant variables are counted in each examined model. However, the results indicate that the PR model identified more significant factors than that of NB model.

Using the PR and NB regression model, separate SPF was developed for each type of crash, i.e., for head-on, rear-end, and total crashes. Total crashes include all types (for instance., PDO, runoff, overturn, etc.) of crashes that occurred within the study segment including rear-end and head-on collisions. The recitals of Poisson regression, as well as negative binomial regression models, are shown in Table 5. The AIC and SBC (also called as Bayesian information criterion) test value indicate that NB models provide better goodness of fit than that of the PR model. However, aside from the AIC and SBC statistics, the number of distinguished significant variables are counted in each examined model. However, the results indicate that the PR model identified more significant factors than that of the NB model.

To further assess the performances of the developed models, forecasts from the examined models are analyzed for the distinctive crash groups ordered by the kind of crash. Graphs 1 and 2 shows the performance of the developed model. As discussed, the safety performance function was developed using 90% of the data, whereas 10% of the data was used for validation. These graphs indicated the relation between observed and predicted values. The data set contains 77 samples of roadway segment, and the analysis period of analysis was for four years (2016–2019). From study segments, 8 (9.30%) segments have no crash at all, 13 (15.12%) had no rear-end crash at all, 11 (12.79%) had no head-on crashes. Results show that none of our models identified crash-free segment. A very crucial drawback of the Poisson model is that it cannot give a decent assessment of the probability that the fragment is in a specific zero group. However, in our analysis, it was observed that forecast biases are larger for the NB model.

Table 5 SPFs for different types of collisions

Model	Equation	Goodness of fit			Factors predicated significant
		AIC	SBC	LLV*	
NB (Head-on)	Exp (1.896 − 0.338* (AADT))	309.36	314.27	−152.6	1
NB (Rear-end)	Exp (0.652 + 0.524* (Sign_board) − 0.883* (Built_area) − 0.607* (S_length) + 0.176* (S_Width) − 0.125* (Ac_Density) + 0.049* (Gradient) + 0.018* (S_Speed) − 0.747* (P_Distress))	284.83	306.92	−133.4	8
NB (Total)	Exp (2.660 − 0.320* (Median) − 0.579* (Built_area) − 0.453*(L_Width) + 0.153* (S_Width) − 0.045* (Ac_Density) + 0.088* (Gradient) + 0.012* (S_Speed) + 0.714* (Rutting) − 0.419* (P_Distress))	380.35	404.89	−180.1	9
PR (Head-on)	Exp (1.743 − 0.291* (AADT))	340.68	345.59	−168.3	1
PR (Rear-end)	Exp (0.407 + 0.533* (Sign_board) − 1.037* (Built_area) − 0.619* (S_length) + 0.250* (S_Width) − 0.134* (Ac_Density) + 0.020* (S_Speed) − 0.928* (P_Distress) + 0.064* (Gradient))	377.06	399.14	−179.5	8
PR (Total)	Exp (3.946 + 0.403* (S_Type) − 0.644* (Median) + 0.284* (Sign_board) − 0.859* (Built_area) − 0.150* (AADT) − 0.955* (L_Width) + 0.233* (S_Width) − 0.069* (Ac_Density) + 0.103* (Gradient) + 0.023* (S_Speed) − 0.853* (Rutting) − 0.671* (P_Distress)	521.71	553.62	−247.8	12

* Log-Likelihood Values

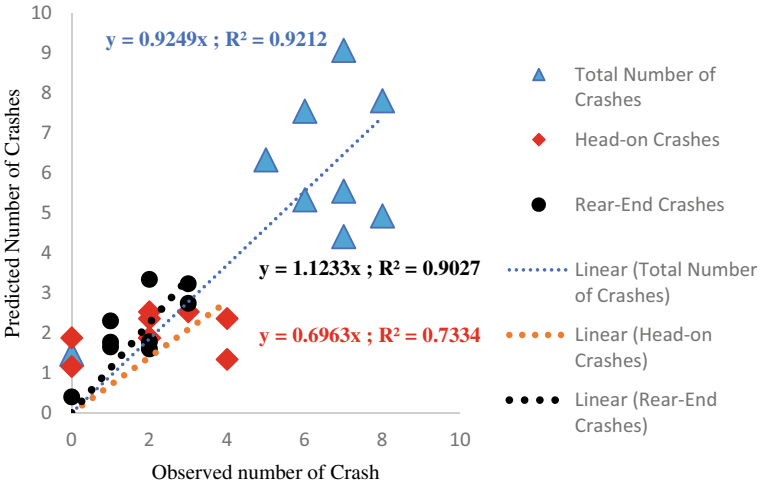

Fig. 3 Observed versus predicated (Poisson regression model)

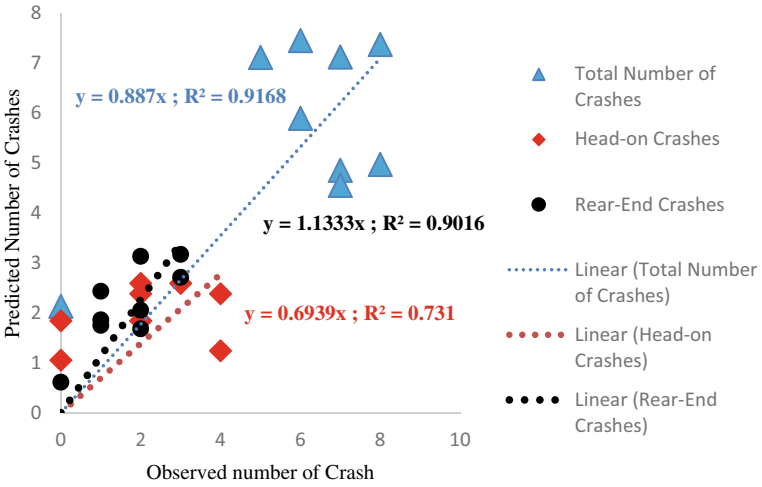

Fig. 4 Observed versus predicated (Negative binomial regression model)

5 Conclusions

This research applied the PR and NB regression model to examine the impact of geometric, traffic, and roadside attributes on rear-end, head-on, and total crashes along rural highways. The verdicts of this study shed substantial light on the factors affecting total, rear-end, and head-on crashes. These discoveries would be useful for professionals, road engineers, and appropriate authorities to configure the suitable

countermeasures as examined in the last section. The created safety execution function will likewise assist with distinguishing blackspots or high-risk destinations in rural areas. After cautious application and appraisal of the statistical model, joined by a definite assessment of the road crash model, the accompanying conclusions can be drawn,

- Impact of risk variables changes as the type of crash changes. For example, the statistics showed a significant relationship between potholes and rear-end crashes, but couldn't identify any relationship between potholes and other types of crashes (total and head-on). However, the sign of estimated coefficients remained almost constant for different types of crashes.
- Spot speed and AADT possess a significant impact on all types of crashes. However, these are positively and negatively associated with the total number of crashes, respectively.
- Increase in lane width decreases the frequency of head-on and the total number of the accidents, whereas shoulder width shows a positive significant co-relation for all types of crashes.
- Segments passing through hilly terrain or built-up area are less prone to accidents. Similarly, for all types of crashes, an increase in access points per segment length decreases the frequency of crashes.
- Pavement surface condition significantly impacts the safety of road users. Distress ratio and rutting were found positively and negatively associated with the number of crashes, respectively.
- Both models identified almost similar significant risk variables, but in terms of goodness of fit, NB regression model performed better than the PR regression model.

The study has tried to provide an improved understanding of the risk variables affecting the safety of roads under heterogeneous traffic conditions. Despite these significant efforts, the study is associated with some limitations. The major limitation is the availability of reliable and accurate crash data. Most of the crash data were collected manually, resultant manual data may be subject to error and is time-consuming.

Additionally, this study was limited to rural areas considering some specific risk variables despite the fact that accidents are associated with the number of risk variables and their interaction. For example, road surface conditions combined with weather conditions may significantly affect road safety. However, this study does not include variables associated with weather conditions (for instance, rainfall, visibility, etc.). For further research, pavement surface condition, surface run-off after precipitation, and visibility can be three crucial factors for analyzing road safety along rural highways in general, and for single-vehicle crashes specifically. Therefore, future research must focus on these factors as far as crash risk variables.

Acknowledgements The authors might want to express gratitude toward the Ministry of Education, Government of India, for financial help during the research as well as the concerned police

station of Uttarakhand, for their contribution in collecting the data and cooperation. The author also acknowledges Sanjay Kumar, Anjesh Saini, and Sudhir Kumar for help in field data collection.

References

1. Road safety Report, Ministry of Road Transport and Highways, India (2018)
2. Abdel-Aty MA, Radwan AE (2000) Modelling traffic accident occurrence and involvement. Accid Anal Prev 32(5):633–642
3. Dinu RR, Veeraragavan A (2011) Random parameter models for accident prediction on two-lane undivided highways in India. J Safety Res 42(1):39–42
4. Kaur Dhanoa K, Tiwari G, Manoj M (2019) Modelling fatal traffic accident occurrences in small Indian cities, Patiala, and Rajpura. Int J Injury Control Safety Promotion 26(3):225–232
5. Milton JC, Mannering FL (1996) The relationship between highway geometrics, traffic related elements, and motor vehicle accidents
6. Knuiman MW, Council FM, Reinfurt DW (1993) Association of median width and highway accident rates (with discussion and closure). Transp Res Rec 1401:70–82
7. Karlaftis MG, Golias I (2002) Effects of road geometry and traffic volumes on rural roadway accident rates. Accid Anal Prev 34(3):357–365
8. Labi S (2011) Efficacies of roadway safety improvements across functional subclasses of rural two-lane highways. J Safety Res 42(4):231–239
9. Lee J, Abdel-Aty M, Jiang X (2015) Multivariate crash modelling for motor vehicle and non-motorized modes at the macroscopic level. Accid Anal Prev 78:146–154
10. Gitelman V, Doveh E, Carmel R, Hakkert S (2019) The influence of shoulder characteristics on the safety level of two-lane roads: a case-study. Accid Anal Prev 122:108–118
11. Miller I, Freund JE (1977) Probability and statistics for engineers, 2nd edn. Prentice-Hall, Englewood Cliffs, NJ
12. Naderan A, Babaei M (2011) Assessment of statistical models for aggregate crash prediction. In: The 90th Transportation research board annual meeting, Washington DC
13. Vayalamkuzhi P, Amirthalingam V (2016) Influence of geometric design characteristics on safety under heterogeneous traffic flow. J Traffic Transp Eng (English edition) 3(6):559–570
14. Kononov J, Durso C, Reeves D, Allery BK (2012) Relationship between traffic density, speed, and safety and its implications for setting variable speed limits on freeways. Transp Res Rec 2280(1):1–9
15. Baruya A (1998) MASTER: Speed-accident relationship on European roads. In: Working Paper R 1.1. 3, Deliverable D7. Technical Research Centre of Finland VTT Espoo
16. Aarts L, van Schagen I (2006) Driving speed and the risk of road crashes: a review. Accid Anal Prev 38(2):215–224
17. Lamm R, Psarianos B, Mailaender T (1999) Highway design and traffic safety engineering handbook. McGraw-Hill Columbus, Ohio
18. Haynes R, Jones A, Kennedy V, Harvey I, Jewell T (2007) District variations in road curvature in England and Wales and their association with road-traffic crashes. Environ Plan A 39(5):1222–1237
19. Haynes R, Lake IR, Kingham S, Sabel CE, Pearce J, Barnett R (2008) The influence of road curvature on fatal crashes in New Zealand. Accid Anal Prev 40(3):843–850
20. Smadi O, Souleyrette RR, Ormand DJ, Hawkins N (2008) Pavement marking retro reflectivity: analysis of safety effectiveness. Transp Res Record 2056:17–24. https://doi.org/10.3141/2056-03
21. Buddhavarapu P, Banerjee A, Prozzi JA (2013) Influence of pavement condition on horizontal curve safety. Accid Anal Prev 52:9–18

22. Anastasopoulos PC, Mannering FL, Shankar VN, Haddock JE (2012) A study of factors affecting highway accident rates using the random-parameters tobit model. Accid Anal Prev 45:628–633
23. Hussein N, Hassan R, Fahey MT (2021) Effect of pavement condition and geometrics at signalized intersections on casualty crashes. J Safety Res 76:276–288

Investigating Surrogate Safety Measures Under Varying Roadway and Traffic Conditions Using Vehicular Trajectory Data

Omkar Bidkar, Shriniwas Arkatkar, and Gaurang Joshi

Abstract The present study investigates the effects of traffic volume on various surrogate safety measures (SSM) under varying roadway and traffic conditions both under work zone and without work-zone areas. The traffic data extractor is used to extract the collected traffic data. MATLAB coding tool was used to identify leader–follower pairs considering different vehicular movements. The potential SSM, such as post encroachment time (PET), time to collision (TTC), and de-acceleration rate to avoid collision (DRAC), are considered for the present study. Further, the Pearson correlation coefficient is computed to test the possible variations and dependence among SSMs. The analysis revealed a substantial variation between parameters for the selected pairs, PET and TTC, TTC, and DRAC, and PET and DRAC. Moreover, it is also inferred that the Pearson correlation coefficient result varies for different traffic volumes and roadway sections (work zone and without work zone) of roads.

Keywords Surrogate Safety Measures (SSMs) · Work-Zone (WZ) · Without Work-Zone (WWZ)

1 Introduction

Road transportation is the key element for every human being in most countries. Every person is well connected to road transportation directly or indirectly. According to the Ministry of Road Transport Highways (MoRTH), there is a total of 4,67,044 crashes in India, out of which 1,51,417 people are killed, and 4,69,418 caused injury to persons [1]. There is an increment of 0.46% road crashes and 2.37% of persons killed in 2018 for 2017. Therefore, it may be well realized that it is imperative to examine road safety-related issues for varying roadway and traffic conditions for work-zone (WZ) and without work-zone (WWZ) areas. Highway work zones are set up according to the type of road and the work to be done on the given road. Traffic

O. Bidkar · S. Arkatkar (✉) · G. Joshi
Department of Civil Engineering, Sardar Vallabhbhai National Institute of Technology (SVNIT), Ichchhanath, Surat 395007, India
e-mail: sarkatkar@gmail.com

L. Devi et al. (eds.), *Proceedings of the Sixth International Conference of Transportation Research Group of India*, Lecture Notes in Civil Engineering 273,
https://doi.org/10.1007/978-981-19-4204-4_17

safety issues will vary with normal roadway conditions and in the work-zone area. This motivation present study investigates the effects of traffic volume on various surrogate safety measures (SSM) under varying roadway and traffic conditions taking two roadway sections as WZ and WWZ.

Work-zone may be defined as an area where roadwork occurs and may involve lane closures, detours, and moving equipment [2]. Highway work zones are set up according to the type of road and the work to be done on the road. When there is new road construction, normal operating traffic will not be the case, but special care must be taken to avoid conflicts between workers and construction machinery. There are several kinds of literature available on work-zone capacity. The South Carolina Department of Transportation (DOT) carried out a research study to develop a methodology for deciding on a lane closure policy for highway work zones. They have developed a model that considers base capacity, PCEs for various speed groups, adjustment factors for specific work zone characteristics, and several open lanes [3]. Heaslip et al. developed an analytical model for computing the capacity of a freeway work zone by considering different geometric, traffic, and work-zone-related parameters [4]. Khattak et al. observed the correlation of safety parameters with various components of the work zone, and different crash frequency models were developed [5]. Raju et al. found the effect of construction WZ on macroscopic as well as microscopic traffic flow parameters. Further, they also plotted the hysteresis plots using identified vehicle trajectories of the vehicle pairs, which are slender in the WZ section compared to the WWZ section. This provides a very proactive approach to studying the driver's behavior [6]. Pawar et al. investigated the effect of the geometry of roads on traffic safety; the study is carried out using a surrogate safety measure, namely PET, especially at the un-signalized intersection [7]. Goyani et al. concluded that traffic safety at un-signalized varies for vehicle type, leader–follower pairs, and traffic composition**.** They also found that a motorized two-wheeler is a critical vehicle category among all the present vehicle categories, and they also inferred that the probability of crash would increase with the increase in its traffic composition [8]. Tarko et al. proved that crossing conflicts, head-on-collision, and rear-end conflicts are calculated easily using reliable surrogate safety measures, namely post encroachment time (PET) [9]. Guo et al. found a good correlation between conflicts calculated from the field and conflicts obtained from the simulation at the left-handed intersection. Results revealed that conflicts are transferrable to another intersection [10]. Caliendo et al. found that the micro-simulation approach is the best approach for assessing safety at a given intersection using critical conflicts. The authors developed the model helpful in calculating crashes in the field using critical conflicts established using simulation [11]. Rao et al. developed the model used for the direct estimation of critical conflicts at an uncontrolled intersection. They also observed that the number of conflicts increases with an increase in the flow rate for any percentage of turning flow [12]. Nayeem et al. revealed a significant relationship between hourly simulated conflicts and the number of crashes that occurred actually. Further, they also found that the number of crashes is reducing with the addition of non-motorized vehicles. This study can be particularly much helpful to the non-lane-based traffic streams rather than urban intersections [13]. John Older et al. revealed that automated traffic

conflicts are the best method than manual field observed methods; this could be a more pragmatic and efficient approach for solving critical conflicts [14]. The review of past studies mainly reflects that good numbers of studies are available in developing and developed nations involving SSM to reveal safety levels and suggest preventive measures proactively. However, very few studies involve computing different SSMs considering the comparison of roadway conditions of with-and-without work zones.

2 Motivation of the Study

Road transportation is an essential aspect of the Indian economy. Road crashes and conflicts are prevalent in India due to the involvement of vulnerable road users such as motorized two-wheelers. Hence, road safety is a critical issue on most Indian roads. There is a great demand for road transportation in India, so road construction and maintenance activities are very common in various countries. Work-zone may be defined as an area where roadwork occurs and may involve lane closures, detours, and moving equipment. WZ is very common on roads, where road construction and maintenance activities occur as a maintenance activity or new construction such as Metro construction. Traffic safety on roads varies concerning the type of road section, namely normal roads, and work-zone. Further, due to the mixed traffic condition and the presence of various static and dynamic vehicle types, variables such as traffic composition and traffic volume are significant both for the WZ and WWZ areas. Therefore, it is imperative to analyze traffic safety and vehicle operation in WZ and WWZ areas. With this motivation, the study attempts to examine the traffic conflicts using various SSM under mixed traffic conditions, taking both the cases as WZ and WWZ areas.

3 Research Methodology

The research methodology adopted for the present study is divided into various sections, as shown in Fig. 1. The Western Expressway of India is selected as a study region. Data collection was carried out in May 2017 from 8:00 AM to 6:00 PM on five-lane uninterrupted roads of the western expressway having a main carriageway width of 17.5 m in one direction of traffic flow. A year after metro construction was started on the same roads, road width is reduced from the road space of five lanes to three lanes. Therefore, with the intent of studying the impact of a work zone, the traffic flow data was collected in May 2018 once again on the same road with two-lane closures. Data is collected using a videographic survey for ten hours on both sections under normal and ideal weather conditions. Data is collected for three levels of volumes, namely high (V/C > 0.9), medium (0.5 < V/C < 0.9), and low (V/C < 0.3). After the data collection, traffic data extraction is carried out using traffic data extractor software with an accuracy of 0.01 s and a frame rate of 0.4 frames/sec.

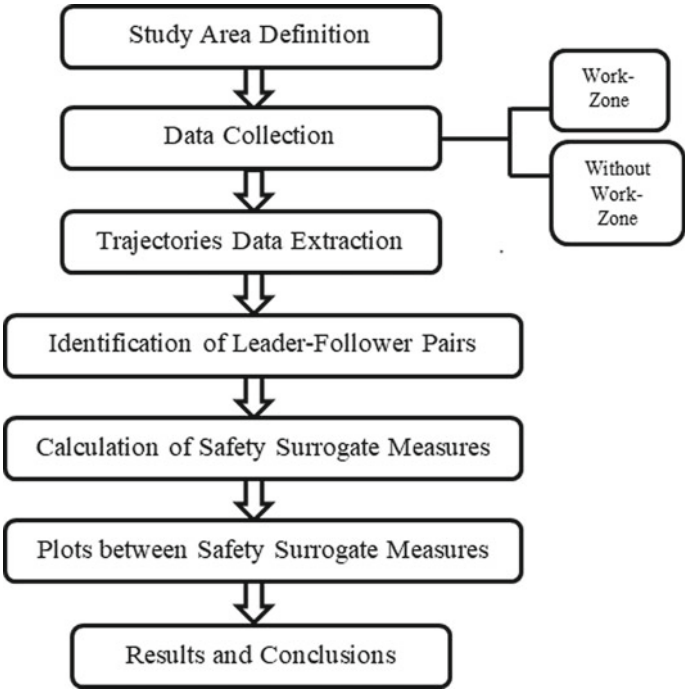

Fig. 1 Detailed step-wise research methodology

Input to the trajectories data extraction is the video of traffic data collected. The output of the data extraction process is the type of vehicle, the number of vehicles tracked, time, and positions of vehicles forming high-quality trajectory data under varying roadway and traffic conditions. Trajectories are developed for all volumes by using the time and space of the tracked vehicles. After trajectories data extraction and processing, various leader–follower pairs are identified for all possible combinations of vehicles tracked by the traffic data extractor. Leader–follower pairs are the main inputs for the computation of the different SSMs. Vehicles moving closer to each other both longitudinally and laterally are considered for analyzing potential conflicts. The non-lane-based movements, both with possible lateral and longitudinal combinations of traffic, were considered to analyze leader–follower vehicle pairs. Figure 2 depicts the heterogeneous nature of traffic, including non-lane-based positions with typical lateral as well as longitudinal combinations under a given traffic condition. To calculate leader–follower pairs, first define the potential leading vehicle (L_V) and following vehicle (F_V). Three important conditions are required to be considered for the calculation of leader–follower pairs: (1) Lv > Fv, (2) lateral clearance < lateral threshold, and (3) distance gap between Lv and Fv is minimum [15]. Lateral clearance is the sidewise minimum safety spacing maintained by a vehicle and a neighboring vehicle when it travels through a traffic stream [16]. It is assumed that a vehicle shall not move into the desired position if the lateral spacing

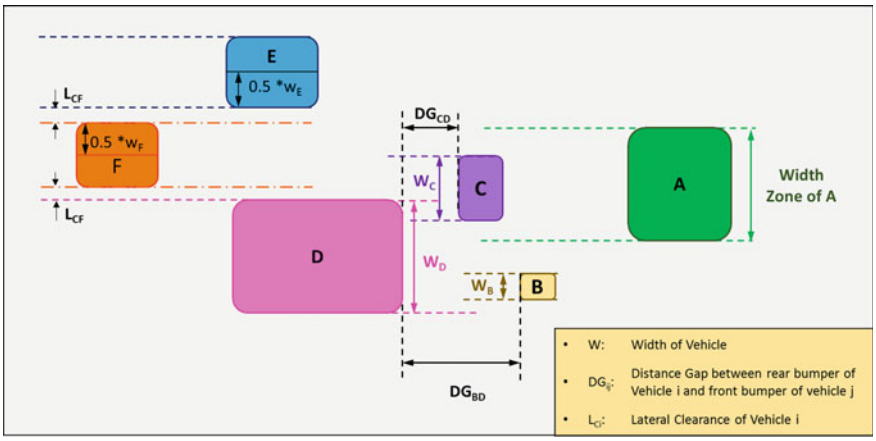

Fig. 2 Simultaneous interaction of different vehicles

available is less than the minimum required lateral clearance and shall aim to maintain its trajectory until the desired conditions are met ahead of moving in the traffic.

The first two conditions shown above are used to calculate the leader–follower vehicle pairs. It helps to find out leading and following vehicles with potential rear-end collisions due to fluctuations in the spacing between the vehicles over space and time. Interestingly, due to more dominant lateral movements, the third condition allows the condition of multiple leading vehicles present in the traffic streams with a lateral threshold zone. Once leader–follower pairs are calculated, various SSMs, namely post encroachment time (PET), time-to-collision (TTC), and de-acceleration rate to avoid collision (DRAC) as potential rear-end collisions are computed. After calculating SSMs, the relationships depicting the spread of PET and TTC, PET and DRAC, and TTC and DRAC are plotted. This is explained in the next section and some good insights about explaining the driver's behavior in the selected roadway sections of WZ and WWZ.

4 Calculation of Surrogate Safety Measures

Trajectory data and leader–follower vehicle pairs are the main input to the calculation of SSM. Surrogate Safety Measures namely PET, TTC, and DRAC are used because they are capable of simulating the field conditions. The mathematical formulation of TTC, PET, and DRAC are given below as Eqs. (1) through (3) [17].

$$TTC = \frac{X_L - X_F - l_L}{V_F - V_L} \tag{1}$$

$$PET = T2 - T1 \tag{2}$$

$$DRAC_t = \frac{(V_{F,t} - V_{L,t})^2}{2(X_{L,t} - X_{F,t} - l_L)} \tag{3}$$

where X_L, X_F represents the position of leader and follower, l_L is the length of the vehicle and, T1 represents the time required for the offending vehicle to leave the conflict area, T2 time required for the conflicting vehicle to enter the conflict area, V_F, V_L represent the speed of followers and leaders.

5 Relationship Between Various Surrogate Safety Measures

The relationship between PET and TTC, PET and DRAC, and TTC and DRAC are explained in detail in the subsequent sections. Two types of functional forms are tried for fitting plots between SSMs. The linear regression equation is framed to capture the relationship between PET and TTC which is shown in Eq. 4.

$$[\text{PET } = a0 + a1 * (\text{TTC})] \tag{4}$$

The exponential regression equation is also framed to capture the relationship between PET and DRAC, TTC and DRAC which are shown in equation no 5.

$$\left[\text{PET} = a1 * e^{a2*\text{DRAC}} \text{TTC} = \text{a1} * e^{a2*\text{DRAC}}\right] \tag{5}$$

5.1 Relationship Between PET and TTC for WWZ and WZ

Figure 3 shows the relationship between selected SSMs, PET, and TTC corresponding to the traffic volumes observed in the WWZ section. Table 1 shows the calibrated parameters of different plots for the WWZ section. Figure 3 depicts that PET is linearly co-related with TTC, and there is a positive correlation observed between them. It is found in Table 1 that the Pearson correlation coefficient varies as a function of traffic volume. It is also found that there is a wide variation in the coefficient of correlation among different volumes of the WWZ section than the WZ section. This may be attributed to the larger variations observed in the microscopic parameters such as relative velocity and spacing, particularly in the WWZ section due to better freedom and maneuverability of the vehicles on multiple lanes with higher lateral clearance shares and gaps.

Figure 4 shows the relationship between selected SSMs, PET, and TTC corresponding to the traffic volumes observed in the WZ section. Table 1 shows the calibrated parameters of different plots for the WZ section. Figure 4 depicts that PET is linearly co-related with TTC, and there is a positive correlation observed

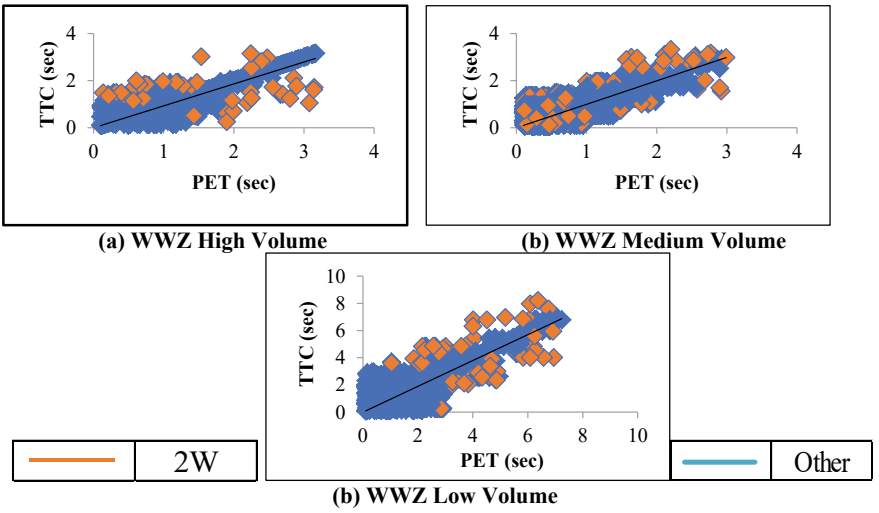

Fig. 3 Traffic volume-wise plots between PET and TTC for the WWZ section

Table 1 Traffic volume-wise calibration of plots between PET and TTC for WWZ and WZ

Parameters	Without Work-Zone			Work-Zone		
	High	Medium	Low	High	Medium	Low
A0	0.798	0.719	0.777	0.825	0.911	1.004
A1 (TTC)	0.211	0.322	0.519	0.514	0.233	0.0216
R^2	0.53	0.601	0.698	0.847	0.873	0.895

between them. It is found in Table 1 that the Pearson correlation coefficient varies as a function of traffic volume. However, it is also found that the variation in the coefficient of correlation for different volumes of the WZ section is substantially lesser. This may be attributed to the marginal variations in the microscopic parameters such as relative velocity and spacing, particularly in the WZ section, due to constrained freedom and maneuverability of the vehicles on the reduced lanes with relatively lower lateral clearance shares and gaps. The motorized 2 W drivers are observed to be generally aggressive by their smaller size and better maneuverability. Due to this ease, these smaller vehicles are highly vulnerable to conflicts, and hence should be evaluated with more detail. Accordingly, the data points about the 2 W are shown using red color, compared to the blue points depicting the rest of the vehicles in Figs. 3 and 4. From the figures, it may be noted that motorized 2 W tends to show more variation in PET and TTC than other vehicle categories, as the red color points are found to be placed away from the line established using the least-square method. The points in the WZ are placed closer in comparison to WWZ, a roadway section, which reveals the constrained behavior of motorized 2 W because of reduced road space due to metro construction.

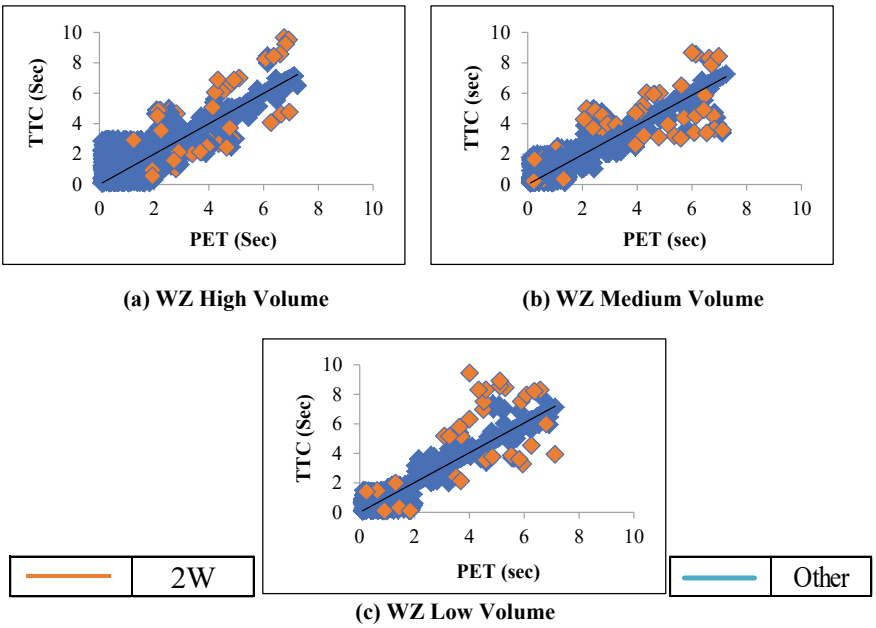

Fig. 4 Traffic volume-wise plots between PET and TTC for the WZ section

5.2 Relationship Between PET and DRAC for WWZ and WZ

Figure 5 shows the relationship between selected SSMs, PET, and DRAC corresponding to the traffic volumes observed in the WWZ section. Table 2 shows the calibrated parameters of different plots for the WWZ section. Figure 5 depicts that PET is exponentially co-related with DRAC, and there is a negative correlation observed between them. It is found in Table 2 that the Pearson correlation coefficient varies as a function of traffic volume. It is also found that there is a wide variation in the coefficient of correlation among different volumes of the WWZ section than the WZ section. This may be attributed to the larger variations observed in the microscopic parameters such as relative velocity and spacing, particularly in the WWZ section, due to better freedom and maneuverability of the vehicles on multiple lanes with higher lateral clearance shares and gaps.

Figure 6 shows the relationship between selected SSMs, PET, and DRAC corresponding to the traffic volumes observed in the WZ section. Table 2 shows the calibrated parameters of different plots for the WZ section. Figure 6 depicts that PET is exponentially co-related with DRAC, and a negative correlation is observed between them. It is found in Table 2 that the Pearson correlation coefficient varies as a function of traffic volume. However, it is also found that the variation in the coefficient of correlation for different volumes of the WZ section is substantially lesser. This may be attributed to the marginal variations in the microscopic parameters such

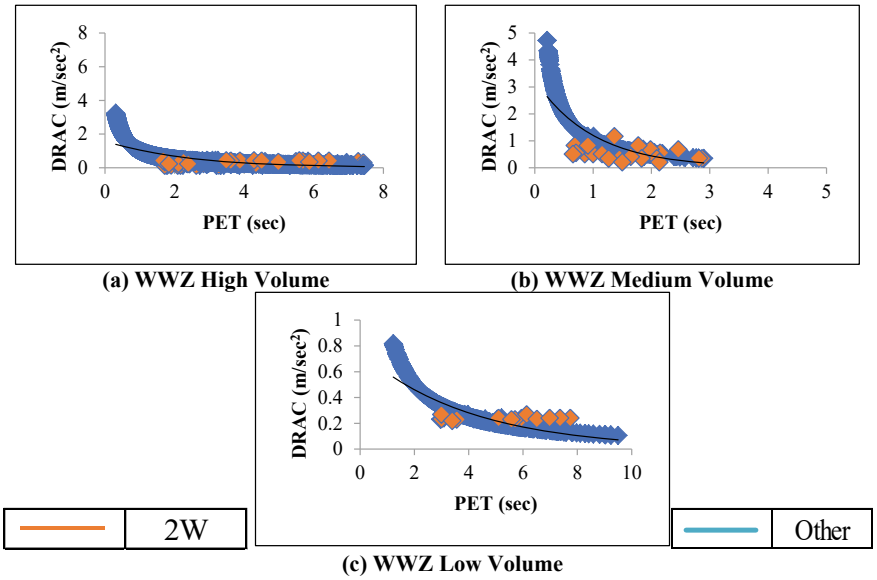

Fig. 5 Traffic volume-wise plots between PET and DRAC for the WWZ section

Table 2 Traffic volume-wise calibration of plots between PET and DRAC

Parameters	Without Work-Zone			Work-Zone		
	High	Medium	Low	High	Medium	Low
A1	1.51	3.27	0.754	1.94	1.74	1.7
A2 (DRAC)	-0.413	-1.003	-0.247	-0.512	-0.445	-0.414
R^2	0.573	0.638	0.705	0.801	0.817	0.848

as relative velocity and spacing, particularly in the WZ section, due to constrained freedom and maneuverability of the vehicles on the reduced lanes with relatively lower lateral clearance shares and gaps. The motorized 2 W drivers are observed to be generally aggressive by their smaller size and better maneuverability. Due to this ease, these smaller vehicles are highly vulnerable to conflicts, and hence should be evaluated in more detail. Accordingly, the data points about the 2 W are shown using red color compared to the blue points depicting the rest of the vehicles in Figs. 5 and 6. From the figures, it may be noted that motorized 2 W tends to show more variation in PET and DRAC as compared to other vehicle categories, as the red color points are found to be placed away from the line established using the least-square method. The points in the WZ are placed closer in comparison to WWZ, a roadway section, which reveals the constrained behavior of motorized 2 W because of reduced road space due to metro construction.

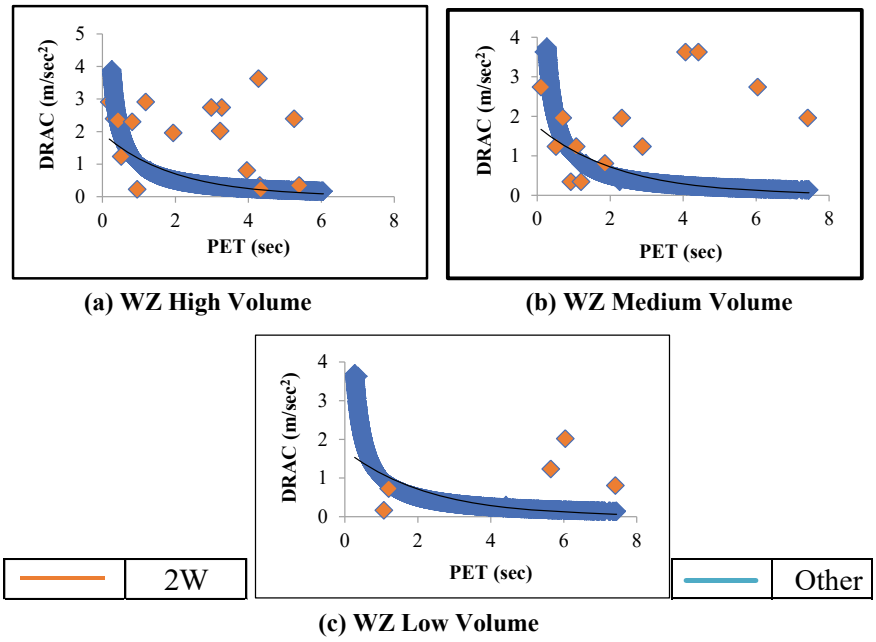

Fig. 6 Traffic volume-wise plots between PET and DRAC for the WZ section

5.3 Relationship Between TTC Versus DRAC for WWZ and WZ

Figure 7 shows the relationship between selected SSMs, TTC, and DRAC corresponding to the traffic volumes observed in the WWZ section. Table 3 shows the calibrated parameters of different plots for the WWZ section. Figure 7 depicts that TTC is exponentially co-related with DRAC, and there is a negative correlation observed between them. It is found in Table 3 that the Pearson correlation coefficient varies as a function of traffic volume. It is also found that there is a wide variation in the coefficient of correlation among different volumes of the WWZ section than the WZ section. This may be attributed to the larger variations observed in the microscopic parameters such as relative velocity and spacing, particularly in the WWZ section, due to better freedom and maneuverability of the vehicles on multiple lanes with higher lateral clearance shares and gaps.

Figure 8 shows the relationship between selected SSMs, TTC, and DRAC corresponding to the traffic volumes observed in the WZ section. Table 3 shows the calibrated parameters of different plots for the WZ section. Figure 8 depicts that TTC is exponentially co-related with DRAC, and there is a negative correlation observed between them. It is found in Table 3 that the Pearson correlation coefficient varies as a function of traffic volume. However, it is also found that the variation in the coefficient of correlation for different volumes of the WZ section is substantially

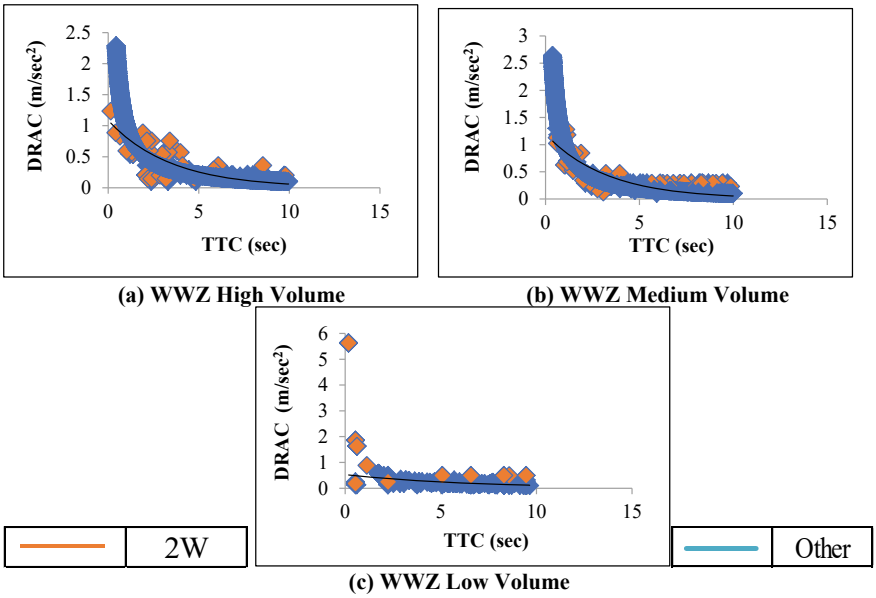

Fig. 7 Traffic volume-wise plots between TTC and DRAC for the WWZ section

Table 3 Traffic volume-wise calibration of plots between TTC and DRAC

Parameters	Without Work-Zone			Work-Zone		
	High	Medium	Low	High	Medium	Low
A1	1.086	1.19	0.53	1.1	1.13	1.11
A2 (DRAC)	-0.291	-0.309	-0.156	-0.294	-0.297	-0.294
R^2	0.647	0.73	0.851	0.811	0.872	0.903

lesser. This may be attributed to the marginal variations in the microscopic parameters such as relative velocity and spacing, particularly in the WZ section, due to constrained freedom and maneuverability of the vehicles on the reduced lanes with relatively lower lateral clearance shares and gaps. The motorized 2 W drivers are observed to be generally aggressive by their smaller size and better maneuverability. Due to this ease, these smaller vehicles are highly vulnerable to conflicts, and hence should be evaluated in more detail. Accordingly, the data points about the 2 W are shown using red color, compared to the blue points depicting the rest of the vehicles in Figs. 7 and 8. From the figures, it may be noted that motorized 2 W tends to show more variation in TTC and DRAC as compared to other vehicle categories, as the red color points are found to be placed away from the line established using the least-square method. The points in the WZ are placed closer in comparison to WWZ, a roadway section, which reveals the constrained behavior of motorized 2 W because of reduced road space due to metro construction.

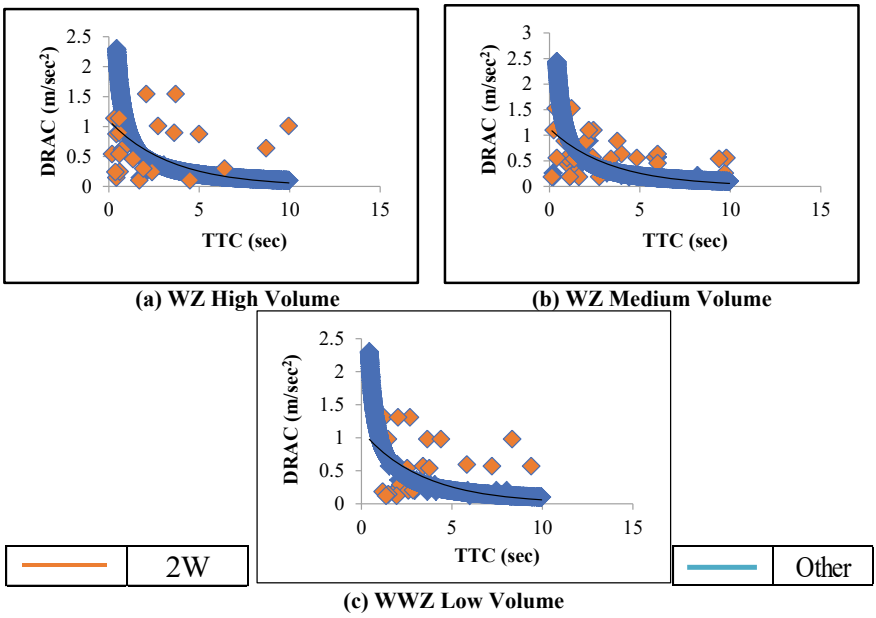

Fig. 8 Traffic volume-wise plots between TTC and DRAC for the WZ section

6 Results and Discussion

The investigation related to the variation in the SSMs was carried out based on vehicle type and traffic volume. For this purpose, it was decided to check the possible variation in relative spacing and acceleration rates by vehicle types while moving in different combinations. To examine the results of the sections, WWZ and WZ, volume levels by vehicle type, and the interquartile ranges of the variables such as relative spacing and acceleration rates are plotted as shown in Fig. 9. Figure 9a and b depict the box-whisker plots of the variation in relative spacing as a function of traffic volume considering WWZ and WZ sections, respectively. It is found that there is substantially less variation in the relative spacing (0.2–1.2 m.) in the case of the WZ section at different volumes in comparison to a large variation in relative spacing (5–25 m.) for the WWZ section at different volume levels. Hence, it is inferred that SSMs, namely PET, TTC, and DRAC, are better correlated in the WZ section than in the WWZ section.

Additionally, Fig. 10 depicts the variation of acceleration rates by different vehicle categories. From Fig. 10, it may be noted that the variation of acceleration rates including the range of values by motorized 2 W (2–6 m/s^2) is found substantially higher than other vehicle categories (0.4–4.5 m/s^2). Moreover, other smaller vehicles such as motorized 3 W and cars are also found to opt for higher acceleration rates in comparison to heavy vehicles such as heavy commercial vehicles (HCV), buses, and light commercial vehicles (LCV). These results further collaborate the finding

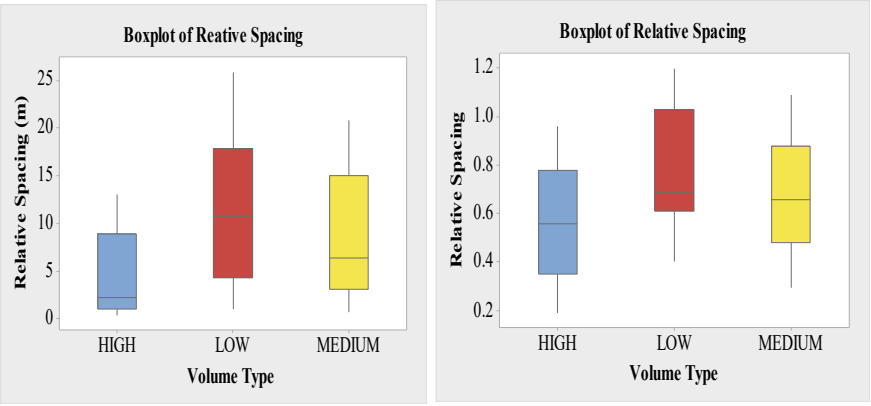

(a) Without Work-Zone (WWZ) Section **(b) Work-Zone (WZ) Section**

Fig. 9 Traffic volume-wise investigation for WZ and WWZ

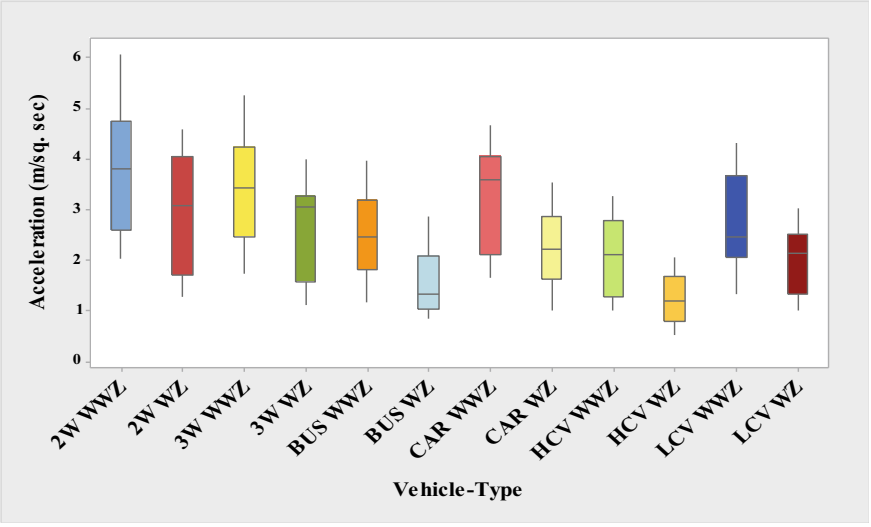

Fig. 10 Box–Whisker plots of observed acceleration rates by vehicle type on selected WZ and WWZ roadway sections

of aggressive behavior by motorized 2 W, particularly in comparison to other vehicle categories, resulting in a substantial variation as depicted by the plotted relationships among different SSMs. Hence, there is a need to perform more empirical observations on motorized 2 W behavior taking more work zones on different classes of roads and variations in its traffic composition.

7 Conclusions

The present study used vehicular trajectories data to identify the variation in the traffic conflicts, and hence the prevailing level of safety using different surrogate safety measures for varying roadway sections as work zone and without-work zone under non-lane-based heterogeneous traffic conditions. The important outcomes of the study are listed as follows:

1. Safety surrogate measures (SSM) such as post encroachment time (PET), time to collision (TTC), and de-acceleration rate to avoid collision (DRAC) are better correlated with each other for the work-zone section than without the work-zone roadway section. This may be attributed to a constrained performance of vehicles and hence lesser variation due to the operating characteristics of the vehicles on the work-zone sections. However, the impact of traffic volume and composition is quite evident.
2. PET is found to have negatively correlated with DRAC, while positively correlated with TTC for high, medium, and low traffic volume levels both for work-zone and without work-zone roadway sections.
3. TTC is found to have negatively correlated with DRAC for high, medium, and low traffic volume levels for the selected work-zone and without work-zone roadway sections.
4. There is a better correlation observed between SSMs, TTC, and DRAC, PET, and DRAC as compared to the correlation between SSMs PET and TTC for high, medium, and low traffic volumes for both the variants of roadway conditions as work-zone and without work-zone sections.
5. There is a wide variation in the computed correlation coefficients for the without work-zone section at different traffic volume levels; it infers that variation in driving behavior and diverse vehicular static and dynamic characteristics under different traffic volumes are the prime factors. To this end, motorized 2 W may be considered the most aggressive and vulnerable category by virtue of its smaller size and better maneuverability.
6. There is less variation in the computed correlation coefficients for the work-zone section at different traffic volume levels; this may be attributed to constrained movements and marginal variation in the driving behavior due to reduced roadway space.
7. The developed exponential relationships such as TTC and DRAC, PET and DRAC under non-lane-based heterogeneous traffic conditions in work zones could be much useful to derive the critical values of SSMs. This may be further useful in deciding the severity of the conflicts and the risk involved.

References

1. MoRTH (2018) Road accidents in India 2018. Ministry of Road Transport & Highways, Government of India
2. IRC SP 055: Guidelines on Traffic Management in Work Zones
3. Sarasua WA, Davis WJ, Chowdhury MA, Ogle JH (2006) Estimating interstate highway capacity for short-term work zone lane closures: development of methodology. Transp Res Record 1948(1):45–57
4. Heaslip K, Kondyli A, Arguea D, Elefteriadou L, Sullivan F (2009) Estimation of freeway work zone capacity through simulation and field data. Transp Res Record 2130(1):16–24
5. Khattak AJ, Khattak AJ, Council FM (2002) Effects of work zone presence on injury and non-injury crashes. Accident Anal Prevent 34(1):19–29
6. Raju N, Arkatkar S, Joshi G (2020) Effect of construction work zone on traffic stream parameters using vehicular trajectory data under mixed traffic conditions. J Transp Eng Part A Syst 146(6):05020002
7. Pawar N, Gore N, Arkatkar S (2019) Influence of driving environment on safety at un-signalized T-intersection under mixed traffic conditions. In: Innovative research in transportation infrastructure. Springer, Singapore, pp 23–31
8. Goyani J, Pawar N, Gore N, Jain M, Arkatkar S (2019) Investigation of traffic conflicts at unsignalized intersection for reckoning crash probability under mixed traffic conditions. J Eastern Asia Soc Transp Stud 13:2091–2110
9. Tarko AP (2018) Surrogate measures of safety. In: Safe mobility: challenges, methodology and solutions. Emerald Publishing Limited.
10. Guo Y, Li Z, Liu P, Wu Y (2019) Modeling correlation and heterogeneity in crash rates by collision types using full Bayesian random parameters multivariate Tobit model. Accident Anal Prevent 128:164–174
11. Caliendo C, Guida M (2012) Microsimulation approach for predicting crashes at unsignalized intersections using traffic conflicts. J Transp Eng 138(12):1453–1467
12. Rao VT, Rengaraju VR (1997) Probabilistic model for conflicts at urban uncontrolled intersection. J Transp Eng 123(1):81–84
13. Islam N, Faruk MO, Shimu TH, Hadiuzzaman M, Musabbir SR, Rahman F (2019) Safety assessment of heterogeneous traffic at urban intersections using simulated conflicts
14. Older SJ, Spicer BR (1976) Traffic conflicts—a development in accident research. Hum Factors 18(4):335–350
15. Mahapatra G, Maurya AK (2015) Study on lateral placement and speed of vehicles under mixed traffic condition. In Eastern Asia Society for transportation studies conference, Cebu City, Philippines
16. Budhkar AK, Maurya AK (2017) Characteristics of lateral vehicular interactions in heterogeneous traffic with weak lane discipline. J Modern Transp 25(2):74–89
17. Mahmud SS, Ferreira L, Hoque MS, Tavassoli A (2017) Application of proximal surrogate indicators for safety evaluation: a review of recent developments and research needs. IATSS Res 41(4):153–163

Emerging Travel Technologies

Automated Crowd Parameter Estimation and Crowd Movement Analysis in Kumbh Mela

Nipun Choubey, Ashish Verma, and Anirban Chakraborty

Abstract Understanding crowd behavior is essential in mass religious gatherings for crowd managers. Surveillance devices such as CCTV provide data in real time in the form of raw video, while the crowd manager estimates the crowd state from video based on their experience. In this study, we propose a methodology to automate the crowd parameter estimation process using an object detection model and tracking algorithm, which will assist crowd managers in estimating the state of the crowd. There are two key contributions to this study. First, the study proposes a methodology to automate crowd parameter estimation from video in a mass religious gathering. Second, the existing state-of-the-art object detection model has been improved to adapt to the challenging situation of mass religious gatherings with high density, high diversity crowd videos. CCTV videos from Kumbh Mela 2016 are used for this study.

Keywords Mass religious gatherings · Kumbh Mela · Neural networks · Computer vision · Pedestrian detection · Pedestrian count · Convolutional neural networks

1 Introduction

Mass gatherings is a planned or spontaneous event where people attending the event could strain the planning and response resources of the host community/region/country [1]. In the past, mass gatherings have experienced crowd disasters. For instance, during the Allahabad Kumbh Mela, a stampede in a railway station led to the loss of 36 lives, and 39 were injured [2]. In Maligawatta, Srilanka, stampede

A. Chakraborty
Department of Computational and Data Sciences, Indian Institute of Science, Bangalore, India

N. Choubey
Robert Bosch Center for Cyber-Physical Systems, Indian Institute of Science, Bangalore, India

A. Verma (✉)
Department of Civil Engineering, Indian Institute of Science, Bangalore, India
e-mail: ashishv@iisc.ac.in

L. Devi et al. (eds.), *Proceedings of the Sixth International Conference of Transportation Research Group of India*, Lecture Notes in Civil Engineering 273,
https://doi.org/10.1007/978-981-19-4204-4_18

occurred in a charity program that resulted in 3 deaths and 9 injuries [3]. Recently, 45 people died and 150 were injured in a crowd crush during the Lag Ba'omer celebration at Mount Meron, Israel [4]. To avoid crowd disaster in mass gatherings, crowd managers need to monitor the crowd movement continuously, and need to anticipate risky situations, and take necessary steps to avoid such fatalities and injuries.

Crowd parameters like density and flow can provide a quantitative measure of the state of the crowd. For example, increasing crowd density can indicate an accumulation of crowds at a location indicating the situation is more prone to crowd disaster. This could help crowd managers to anticipate and help in responding according to reduce the risk involved. Similarly, crowd flow can help in finding the direction of a major movement of the crowd and early warning can be sent to officials handling the important locations in that direction which can help the officials to take necessary actions to control the influx of pedestrians. Thus, the real-time crowd density of a location is more useful information than the CCTV video alone. However, estimating the crowd parameters from CCTV videos in mass gatherings is a challenging task. One of the critical reasons is raw data, i.e., though we are getting the data in real-time, this data is raw and needs to be processed to make video data more useful.

The motive of the study is to develop an autonomous model to extract crowd density and crowd flow from video data having a dense and heterogenous crowd. For this, Kumbh Mela 2016, which was held in Ujjain, is taken as the case study for estimating the crowd parameters from videos of a mass religious gathering. Kumbh Mela is the largest mass religious gathering in the world, which occurs in 4 cities every 12 years in India where pilgrims reach in millions. Kumbh Mela is attended by saints, monks, pilgrims, and tourists. There is a huge diversity of people attending the Kumbh Mela which spans over a month. The Kumbh Mela has witnessed many crowd disasters in the past. The study also tries to find the impact of demographic factors like gender and luggage on the parameters in mass religious gatherings like Kumbh Mela.

A brief review of related studies in the literature is presented in the following section. The methodology adopted is presented in Sect. 3. Section 4 describes the case study. While Sects. 5 and 6 mention the results and summary, respectively.

2 Related Works

For estimating the crowd parameter from video data, the autonomous model has three sub-modules, namely pedestrian detection, pedestrian tracking, and parameter estimation. Various researchers in the past have worked on these three aspects. Some of the significant achievements are mentioned in the respective subsections.

2.1 Pedestrian Detection

In the past decade, researchers have widely used image processing techniques to detect pedestrians. Hariyano and Jo [5] has applied the KLT tracker to find corresponding corner features of overlapping boxes in consecutive frames and used the Histogram of Oriented Gradients (HOG) [6] to recognize candidate box has pedestrians in the ETH and Caltech dataset. Peng et al. [7] has applied the Gaussian mixture model (GMM) for background subtraction and detected small objects, while using YOLO (You Only Look Once) [8] for detecting pedestrians covering a larger area in the frame. The authors claim the combined accuracy to be 20% higher than the individual model. To improve accuracy for pedestrians farther from a camera, Zhang et al. [9] used a region proposal network (RPN) [10] to extract probable regions and clustered them using K-Means clustering. Yin [11] has used a multi-resolution Generative Adversarial Network to detect pedestrians. Lan et al. [12] has taken the model and combined lower level features with the higher level to detect far-away pedestrians. A similar approach is applied by Liu et al. [13] on SSD (Single Shot multi-box Detector) [14] model. Du et al. [15] has improved the YOLOv2 model to detect pedestrians in infrared images accurately. The researchers have used pedestrian detection datasets such as PASCAL, VOC, INRIA, KITTI, CityScapes, and Caltech. These datasets have images/videos mostly from a car view angle with the autonomous driving primary application. While the Caltech dataset has a surveillance view, crowd density is lesser than what we observe in the Kumbh Mela case.

2.2 Pedestrian Tracking

Both image processing techniques and CNN techniques have been widely used for tracking pedestrians in the video. Boltes et al. [16] has applied the pyramidal Lucas–Kanade method for tracking. In his experiment, an overhead marker was installed on each pedestrian. Researchers have used the Kalman filter [17] and its variants to track pedestrians [18–20]. Bewley et al. [21] presented the detection-based tracking framework which focuses on frame-to-frame prediction and association. The framework performs better both in terms of accuracy and speed. Wojke et al. [22] presented a deepSORT approach for tracking pedestrians. The authors used a pretrained association metric to improve SORT. Yoon et al. [23] has used the Siamese network model and applied historical appearance matching for pedestrian tracking. Bergmann et al. [24] combined the regression technique with Faster R-CNN to track pedestrians. While Zhang et al. [25] has combined detection and re-identification tasks for pedestrian tracking.

2.3 Parameter Estimation

Gomes et al. [26] used optimization and Bayesian approaches to identify two parameters, maximum pedestrian density, and maximum speed, that appear in the fundamental diagram from individual trajectories. Hoogendoorn and Daamen [27] established a generic methodology using trajectory data for estimating pedestrian-specific parameters of different walker models that cannot be derived directly from the data. This elucidates the statistical features of the estimations as well as the performance of the models to which the calibration method is used. Walker models have been employed extensively in related research disciplines, such as the estimation of car-following models. Schultz and Rilett [28] suggested a method for generating input parameters for car-following sensitivity factors in microscopic traffic simulation models by using measurements of central tendency and dispersion (i.e., mean and variance). Hoogendoorn and Ossen [29] proposed both a static and dynamic technique (Kalman filter) for determining and tracking the (changing) parameters describing car-following behavior. Apart from this, image processing techniques have been employed for parameter estimation by various researchers. Yugendar and Ravishankar [30] has used background subtraction and ANOVA to track pedestrians. The authors found that gender, age, and luggage are significant factors in walking speed of individuals during sammakka-saralamma festival in Warangal.

3 Methodology

The entire crowd parameter estimation model is divided into three modules. The first module consists of a pedestrian detection/categorization model. The second module consists of a tracking model which uses the results of the detection model. The third module is estimation module, which takes the spatial information, and the pedestrian trajectories obtained from the tracking model to estimate the parameters. These modules are presented in the flowchart (Figs. 1, 2 and 3) and are discussed in brief in the following subsections.

3.1 Pedestrian Detection

For pedestrian detection, the state-of-the-art object detection model (Faster R-CNN) has been used. The model uses ResNet-50 as the backbone network. The model generates anchor boxes of different sizes and scales and learns if any object is present in the anchor boxes. The off-the-shelf model is trained on a publicly available dataset where the videos mostly have less density and larger objects and the pretrained weights do not capture the features available in Indian scenarios. For example, as shown in Fig. 4, pilgrims attending Kumbh Mela come with different attires than those available in

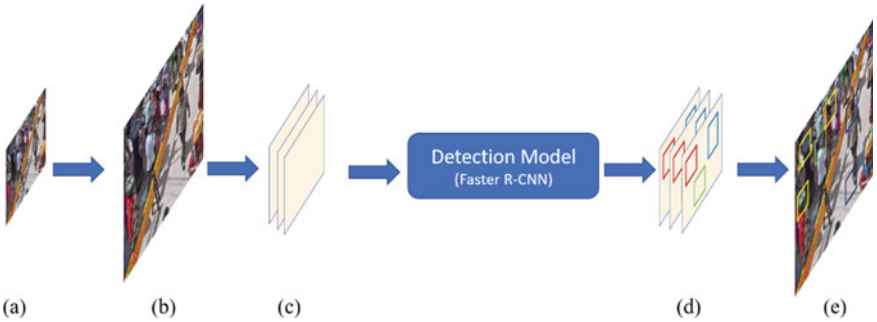

Fig. 1 Pedestrian detection module flowchart. **a** Original frame. **b** 2× upscaled frame. **c** Image split into tiles. **d** Predicted bounding boxes on tiles. **e** Combined tiles and corresponding bounding box to recover the upscaled frame

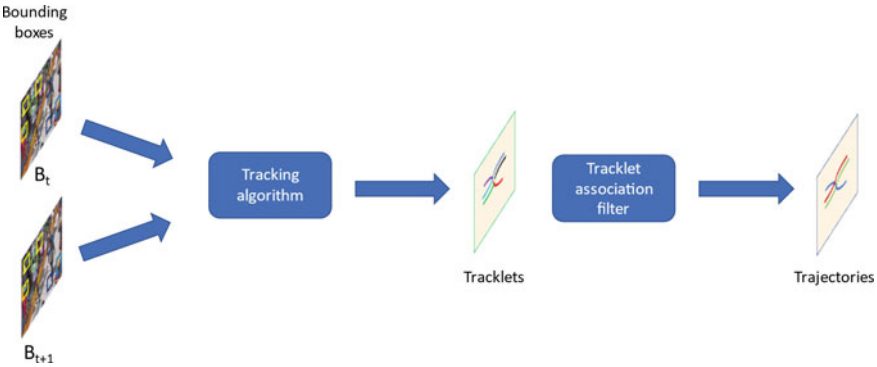

Fig. 2 Tracking module flowchart

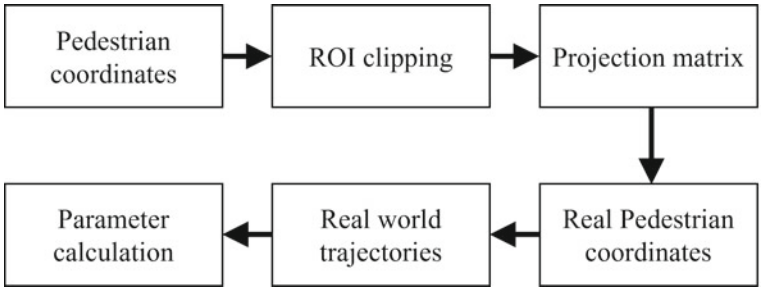

Fig. 3 Parameter estimation flowchart

Fig. 4 Snapshots of Nagchandreshwar mandir on 01st and 06th May 2016 during Kumbh Mela show the diversity, density, and complexity of the scenario

the publicly available dataset. Men are wearing turban, women are wearing veil, people are carrying head luggage and sometimes small child. The heterogeneity of the dataset is further discussed in detail. To incorporate the limitations of the model, we have applied a series of approaches. First, to increase the size of pedestrians in the image, the images were upscaled to twice their original dimensions, and tiles of the original image size were cropped from the upscaled image. Second, we reduced the anchor size to incorporate far-away pedestrians. Third, we applied data augmentation techniques to generate more data.

3.2 Tracking Model

The bounding box generated by the object detection model is fed into the tracking algorithm along with the corresponding video frame. These bounding boxes are considered as pedestrians detected and their centroids are used for tracking. These centroids will be referred as location of detected pedestrians. Short pedestrian tracklets were generated using tracking algorithm. These pedestrian tracklets are then fed to tracklet association filter for generating long trajectories (Fig. 2). Kalman filter and Optical flow methods are used as tracking algorithms for the study. Kalman filter uses the current state and new measurements to find the best estimate. For pedestrian tracking, the detected pedestrian centroids are considered the new measurement. While optical flow estimates the motion between frames and finds the probable location of pixels of the current frame in the next frame. The centroid of detected pedestrians in frame i is fed to the optical flow algorithm and probable locations of these detected pedestrians are estimated for frame $i+1$. These probable locations are then mapped with centroids of detected pedestrians in frame $i+1$ they are in spatial proximity. These pedestrians are named tracked pedestrians. In case no centroid is mapped in frame $i+1$, then the probable location is used for further tracking in subsequent frames. The pedestrian is marked as lost and removed from further tracking if

no centroid is mapped for the next n frames. For pedestrians detected in the frame and are not mapped with previously tracked pedestrians then these are considered new pedestrians. The pedestrian tracklets are mapped based on spatial and temporal proximity. Pedestrian tracklets which are not mapped and have detected pedestrian centroids less than a certain threshold are considered as noise and are removed. In this study, Lucas–Kanade optical flow method (LK) has been used. Trajectories obtained from both tracking algorithms are then fed to parameter estimation.

3.3 Parameter Estimation

The trajectories extracted in the previous step are composed of pixel coordinates. To estimate crowd parameters, the trajectories need to be projected to the real-world coordinate system. For this, a Region of Interest (ROI) is marked in the scene and its real-world dimensions were gathered. The camera intrinsic parameters were calculated based on the spatial dimension of the ROI and the trajectories are transformed into the real-world system. This is shown as a flowchart in Fig. 3. For each frame, the pedestrian location is calculated relative to ROI, i.e., whether a pedestrian is in the ROI or outside ROI. Crowd parameters are calculated as follows:

$$\text{Density} = \frac{N}{l \times w} \tag{1}$$

$$\text{Flow} = \frac{N}{(t_2 - t_1)} \tag{2}$$

where l, w are the length, width of ROI respectively. N is the number of pedestrians who crossed the ROI between the time steps t_1, t_2.

4 Case Study

For the study, the data collected in Kumbh Mela 2016 at Ujjain near Nagchandreshwar temple was used. Nagchandreshwar temple is a very crowded place. The arrival of pilgrims is higher on *snan* days (bathing days) than compared on regular days. Thus, data was collected on one of the regular days (01st May 2016) and one of the *snan* days (06th May 2016) [31]. Figure 4 demonstrates the high density, diversity of the crowd in one of the locations during the Kumbh Mela 2016 held at Ujjain. The video data was collected using a PTZ camera during the Kumbh Mela. The road was divided into two lanes using barricades. Pilgrims were carrying luggage on their heads, men wearing turbans, and women wearing veils with most of the bodies getting occluded due to the high-density crowd. The data collected possess unique features

and make the automation task more challenging. To train CNN models and validate the performance, the data is manually annotated.

4.1 Dataset Preparation

The video data was collected using a PTZ camera with 640 × 480 resolution at 25 fps during the Kumbh Mela. The road was divided into two lanes using barricades by the Mela authorities for better pedestrian flow. 250 sample frames were taken from the videos and were manually annotated. The dataset prepared has information about the bounding box (box marked on pedestrian), gender, and head luggage for every pedestrian in the frame. The bounding box is marked on each pedestrian's head if the pedestrian not carrying any head luggage, and the head luggage is marked in the case where the pedestrian's head is occluded. The gender information is marked only when the pedestrian head is not carrying head luggage. Thus, three classes, namely Male, Female, and head luggage are marked. Totally, 23,770 pedestrians among which 11,558 males, 6460 females, and 5752 pedestrians with head luggage were labeled. There was an average of 79 pedestriansper image with a minimum of 25 and a maximum of 138 pedestrians.

4.2 Model Training

The Nagchandreshwar scene has a dense crowd and high occlusion with only head/head-luggage visible for most of the pedestrians in the frame resulting in smaller bounding boxes. The object detection model was trained in two different ways. In the first approach, the model was trained with the images extracted from videos, and no alteration is made. The model trained is named model A further in this paper. While in the second, the following approaches were applied. The image was upscaled by a factor of 2 and 5 tiles of the size of the original image were extracted from the upscaled image. The bounding boxes were recalculated for these tiles. Then these 1250 tiles were used for training and evaluating the performance of the model. Out of 1250 tiles, 875 tiles were used for training, 125 for validation, and 250 for testing. Random data augmentation techniques such as horizontal vertical flips and rotation were used were applied for generalizing the training data. The model trained through this approach is named as model B further in this paper. Figure 5 shows the comparison of ground truth (a) with the model prediction (b).

Fig. 5 Bounding boxes (**a**) in the ground truth and (**b**) by model prediction. White, Red, and yellow boxes represent male, female, and head luggage class, respectively

5 Results

5.1 Pedestrian Detection

The object detection models predicted the bounding boxes in the test dataset. These bounding boxes were counted for each category (Table 1) and evaluation was done using Mean Absolute Error (MAE) (Table 2). From tables 1 and 2 it can be observed that model B performed much better than the model A and the effectiveness of approach can be clearly seen. Hence, all further calculations are done on model B. Precision and Recall of detections predicted by model B were calculated for the test dataset. For this, the extent of overlapping of bounding boxes predicted by the object detection model and ground truth were calculated. Then overlapping threshold of 0.5 is considered, i.e., if a predicted bounding box has overlapping higher than the overlapping threshold with the ground-truth bounding box, then it

Table 1 Comparison of ground truth and predicted pedestrian counts with different classes on train and test datasets. Here, pedestrian refers to all classes combined

Dataset	Class	Ground truth	Model A	Model B
Train (200 images)	Male	8600	1506	9683
	Female	3859	988	5090
	Head-luggage	5050	1006	2850
	Total	**17,509**	**3500**	**17,623**
Test (50 images)	Male	2109	128	2332
	Female	1387	65	1206
	Head-luggage	1028	182	713
	Total	**4524**	**375**	**4251**

Table 2 Mean absolute error of counts predicted by object detection models for different classes on train and test datasets

MAE	Model	Male	Female	Head-luggage	Pedestrian
Train (200 images)	Model A	35.47	15.075	21.08	70.05
	Model B	**9.335**	**11.375**	**13.89**	**13.93**
Test (50 images)	Model A	39.62	26.44	17.28	82.98
	Model B	**7.5**	**7.14**	**7.46**	**12.1**

is considered as True-positive. The precision of the object detection model on the test dataset was found to be 50.3% for head-luggage, 44.9% for male, and 28.6% for female; while the recall was found to be 40.2% for head-luggage, 54.7% for male and 29.8% for female on the same dataset. Though the training dataset has the least MAE value for the female class in the test dataset, the precision and recall are lower indicating lower performance for the female class. Though most of the images/frames have only head/head-luggage visible, the pedestrian hand predicted the hand as a pedestrian when the hand was visible. Also, it was found that objects on the street were considered head-luggage having a similar appearance to head-luggage.

5.2 Tracking Model

A video of 5 min has been taken for tracking and estimating the crowd parameters (separate from the dataset used for detection). The ROI (Region-Of-Interest) is marked as having dimensions 2 × 3.5 m (Fig. 6). The tracklets obtained from

Fig. 6 Region-of-interest (ROI) marked on the scene

Table 3 Density estimated by different models

Categories	Model B + Kalman (ped/m^2)	Model B + LK (ped/m^2)
Male	1.20	1.07
Female	1.22	0.58
Head-luggage	0.56	0.36
Total	2.98	2.02

the tracking algorithms were compared. It was found that the Kalman filter generated more tracklets than the LK method. Also, it was observed that the trajectories generated by Lucas–Kanade was better than those generated by the Kalman filter.

5.3 Parameter Estimation

The pedestrian density and flow parameters are estimated using the trajectories extracted from the tracking model. The results of the parameters are discussed in the following subsections.

Density. The density estimated using tracking algorithms is mentioned in Table 3. It can be observed that both the tracking algorithms have produced similar results of density for the male category. While for other categories the results differ significantly. One of the reasons is while trajectories were generated using two different algorithms smaller trajectories were considered as noise and were removed, which could have led to the difference in densities estimated. Figure 7 shows the temporal variation of density of pedestrians in the Nagchandreshwar scene for 5 min using the LK method. It can be observed from the figure that the overall density remained 1.5–3 ped/m^2 for the most amount of time and it can be considered a medium density situation.

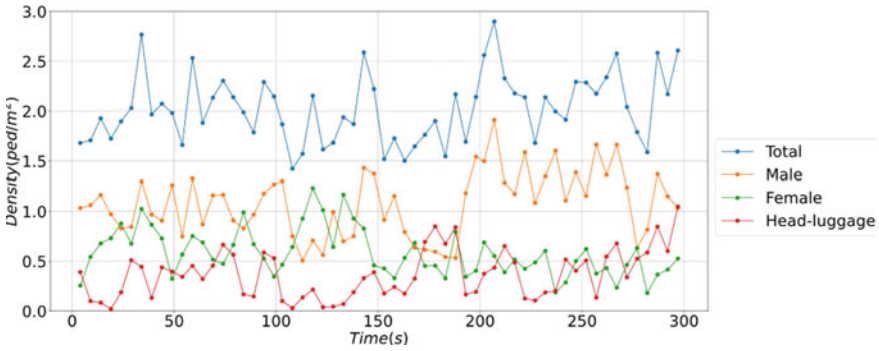

Fig. 7 Density versus time plot for Nagchandreshwar video

Flow. Flow parameters estimated using the trajectories generated by both the tracking algorithms. It was observed that the flow parameters estimated by using the trajectories generated by the Kalman filter were absurd and most of the flow was along line AD while the flow along line BC was negligible. It was observed the Kalman filter was not able to capture the pedestrian movement effectively. One of the possible reasons could be the pedestrian movement is more uncertain as compared to vehicular traffic. Thus, flow estimated using trajectories of LK method is reported here. The inflow is found to be 0.76 ped/s and 2.56 ped/s while the outflow is found to be 3.2 ped/s and 0.91 ped/s on AD and BC, respectively. Figure 8 shows the overall crowd inflow/outflow of pedestrians along sides AD and BC. It can be concluded that there are higher number pedestrians moving from BC to AD. The inflow and outflow of different categories of AD and BC are mentioned below in Table 4 and the same is plotted in Figs. 9 and 10.

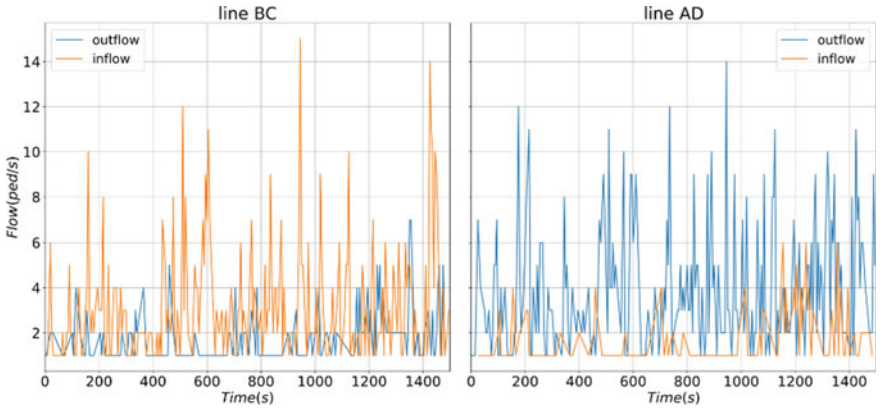

Fig. 8 Overall flow versus time plot for Nagchandreshwar video calculated on two lines

Table 4 Mean flow on two lines BC, AD of ROI ABCD

Side	Direction	Male (ped/s)	Female (ped/s)	Head-luggage (ped/s)	Total flow (ped/s)
BC	Inflow	0.77	1.36	0.43	2.56
	Outflow	0.27	0.11	0.53	0.91
AD	Inflow	0.25	0.10	0.39	0.76
	Outflow	1.25	1.32	0.63	3.2

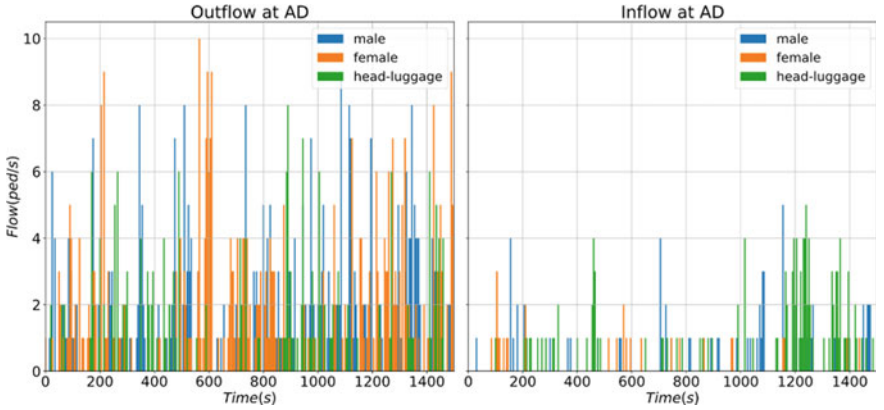

Fig. 9 Category-wise flow versus time plot for Nagchandreshwar video calculated on AD

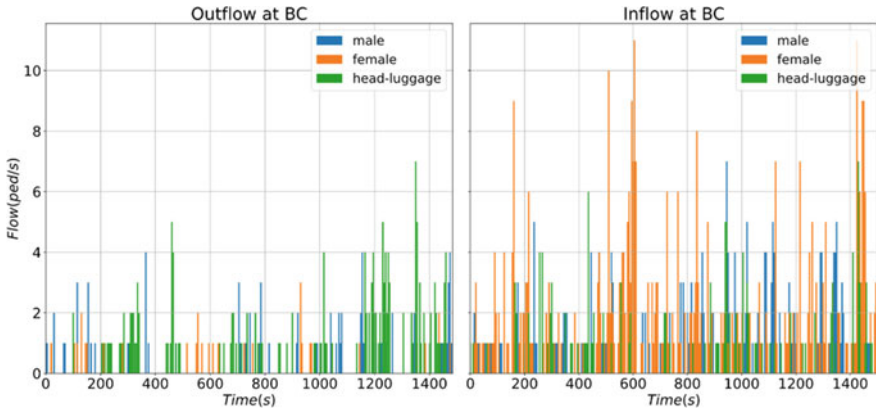

Fig. 10 Category-wise flow versus time plot for Nagchandreshwar video calculated on BC

6 Conclusion

Most of the crowd parameter estimation methods in the current literature have been done on low-density crowds, while there are few methods applied to Hajj which is also one of the largest mass religious gatherings, but there are very few in the Indian context. In the case of Kumbh Mela people from diverse backgrounds come to attend it. The visual appearances and attire of people are diverse, and the scenarios observed in Kumbh Mela are different from what has been studied. In this study, we proposed a methodology to automate crowd parameter estimation from video in mass religious gatherings and calibrated the existing Faster-RCNN model to adapt to the challenging situation of Kumbh Mela with videos consisting of a dense heterogenous crowd. Most of the existing literature focuses on estimating density, while very few have estimated

other crowd parameters such as crowd flow. The method is mostly automated and needs prior information about location such as the geometric dimension of ROI and hyper-parameter tuning such as bounding box confidence, overlapping threshold etc. The method can also adapt different scenarios and the accuracy heavily depends on the CNN model/weights used. The multi-pedestrian tracking did not perform well for long tracking in our case. The results were found to be inaccurate when we tried to associate short tracklets and create long trajectories. The multi-pedestrian tracking module needs to be improved for long tracking which is a challenging task in such a dense and highly occluded crowd. Long tracking would help in estimating the speeds of pedestrians, which could be another useful parameter for assessing crowd risk. One of the limitations of the proposed method is it works for static region-of-interest, which will not be the case if PTZ cameras' angle or zoom modified. Also, we would like to explore multi-scene crowd parameter estimation in the future.

Acknowledgements The work reported in this paper is part of the project titled "The Kumbh Mela Experiment: Measuring and Understanding the Dynamics of Mankind's largest crowd", funded by the Ministry of Electronics and IT, Government of India (MITO-0105), Netherlands Organization for Scientific Research, NWO (Project no. 629.002.202), and Robert Bosch Center for Cyber-Physical Systems, Indian Institute of Science, Bangalore (Grant No. RBCO001). The authors also express their gratitude toward the Kumbh Mela administration and Government of Madhya Pradesh, India, for providing constant support and official permissions to carry out research work and establish an Indo-Dutch collaborative research camp at Kumbh Mela 2016. We would like to thank Mr. Suman Michael for assisting in data annotation.

References

1. What is WHO's role in mass gatherings? https://www.who.int/news-room/q-a-detail/what-is-who-s-role-in-mass-gatherings. Accessed 10 Mar 2021
2. Kumbh Mela chief Azam Khan resigns over stampede (2013) https://www.bbc.co.uk/news/world-asia-india-21406879. Accessed 21 Aug 2021
3. Rizwie R (2020) 3 dead in a stampede in Maligawatta during aid distribution. http://www.dailynews.lk/2020/05/21/local/219065/3-dead-stampede-maligawatta-during-aid-distribution. Accessed 21 Aug 2021
4. Israel crush: dozens killed at Lag B'Omer religious festival (2021) https://www.bbc.com/news/world-middle-east-56938657. Accessed 21 Aug 2021
5. Hariyono J, Jo K (2015) Detection of pedestrian crossing road. In: IEEE international conference on image processing (ICIP), pp 4585–4588. https://doi.org/10.1109/ICIP.2015.7351675
6. Dalal N, Triggs B (2005) Histograms of oriented gradients for human detection. In: Proceedings of the 2005 IEEE computer society conference on computer vision and pattern recognition (CVPR'05)—volume 1, CVPR '05. IEEE Computer Society, San Diego, USA, pp 886–893. https://doi.org/10.1109/CVPR.2005.177
7. Peng Q, et al (2016) Pedestrian detection for transformer substation based on Gaussian mixture model and YOLO. In: 8th international conference on intelligent human-machine systems and cybernetics (IHMSC), pp 562–565. https://doi.org/10.1109/IHMSC.2016.130
8. Redmon J, Divvala S, Girshick R, Farhadi A (2016) You only look once: unified, real-time object detection. In: Proceedings: 2016 IEEE conference on computer vision and pattern recognition (CVPR). IEEE, pp 779–788. https://doi.org/10.1109/CVPR.2016.91

9. Zhang H, Du Y, Ning S, Zhang Y, Yang S, Du C (2017) Pedestrian detection method based on faster R-CNN. In: 13th international conference on computational intelligence and security (CIS), pp 427–430. https://doi.org/10.1109/CIS.2017.00099
10. Ren S, He K, Girshick R, Sun J (2016) Faster R-CNN: towards real-time object detection with region proposal networks. In: Proceedings: IEEE transactions on pattern analysis and machine intelligence, vol 39(6). IEEE, pp 1137–1149. https://doi.org/10.1109/TPAMI.2016.2577031
11. Yin R (2019) Multi-resolution generative adversarial networks for tiny-scale pedestrian detection. In: IEEE international conference on image processing (ICIP), pp 1665–1669. https://doi.org/10.1109/ICIP.2019.8803030
12. Lan W, Dang J, Wang Y, Wang S (2018) Pedestrian detection based on YOLO network model. In: IEEE international conference on mechatronics and automation (ICMA), pp 1547–1551. https://doi.org/10.1109/ICMA.2018.8484698
13. Liu S, Lv S, Zhang H, Gong J (2019) Pedestrian detection algorithm based on the improved SSD. In: 2019 Chinese control and decision conference (CCDC), pp 3559–3563. https://doi.org/10.1109/CCDC.2019.8832518
14. Liu W, Anguelov D, Erhan D, Szegedy C, Reed S, Fu C, Berg AC (2016) SSD: single shot MultiBox detector. In: Lecture notes in computer science, vol 9905. Springer, Berlin, pp 21–37. https://doi.org/10.1007/978-3-319-46448-0_2
15. Du C, Song P, Ma X (2020) Pedestrian detection in infrared images with improved YOLOv2 network. In: IEEE international conference on information technology, big data and artificial intelligence (ICIBA), pp 570–574. https://doi.org/10.1109/ICIBA50161.2020.9277234
16. Boltes M, Seyfried A, Steffen B, Schadschneider A (2010) Automatic extraction of pedestrian trajectories from video recordings. In: Klingsch WWF, Rogsch C, Schadschneider A, Schreckenberg M (eds) Pedestrian and evacuation dynamics 2008. Springer, Berlin, pp 43–54. https://doi.org/10.1007/978-3-642-04504-2_3
17. Kalman RE (1960) A new approach to linear filtering and prediction problems. J Basic Eng 82:35–45. https://doi.org/10.1115/1.3662552
18. Rosales R, Sclaroff S (1999) 3D trajectory recovery for tracking multiple objects and trajectory guided recognition of actions. In: IEEE computer society conference on computer vision and pattern recognition, vol 2, pp 123
19. Rodriguez M, Sivic J, Laptev I, Audibert J (2011) Data-driven crowd analysis in videos. In: Proceedings: 2011 international conference on computer vision. IEEE, pp 1235–1242. https://doi.org/10.1109/ICCV.2011.6126374
20. Bochinski E, Eiselein V, Sikora T (2017) High-speed tracking-by-detection without using image information. In: 2017 14th IEEE international conference on advanced video and signal based surveillance (AVSS), pp 1–6. https://doi.org/10.1109/AVSS.2017.8078516
21. Bewley A, Ge Z, Ott L, Ramos F, Upcroft B (2016) Simple online and realtime tracking. In: 2016 IEEE international conference on image processing (ICIP), pp 3464–3468. https://doi.org/10.1109/ICIP.2016.7533003
22. Wojke N, Bewley A, Paulus D (2017) Simple online and realtime tracking with a deep association metric. In: 2017 IEEE international conference on image processing (ICIP), pp 3645–3649. https://doi.org/10.1109/ICIP.2017.8296962
23. Yoon Y, Boragule A, Song Y, Yoon K, Jeon M (2018) Online multi-object tracking with historical appearance matching and scene adaptive detection filtering. In: 2018 15th IEEE international conference on advanced video and signal based surveillance (AVSS), pp 1–6. https://doi.org/10.1109/AVSS.2018.8639078
24. Bergmann P, Meinhardt T, Leal-Taixé L (2019) Tracking without bells and whistles. In: 2019 IEEE/CVF international conference on computer vision (ICCV), pp 941–951. https://doi.org/10.1109/ICCV.2019.00103
25. Zhang Y, Wang C, Wang X, Zeng W, Liu W (2020) FairMOT: on the fairness of detection and re-identification in multiple object tracking (submitted)
26. Gomes SN, Stuart AM, Wolfram MT (2019) Parameter estimation for macroscopic pedestrian dynamics models from microscopic data. SIAM J Appl Math 79(4):1475–1500

27. Hoogendoorn SP, Daamen W (2009) A Novel calibration approach of microscopic pedestrian models. In: Timmermans H (ed) Pedestrian behavior. Emerald Group Publishing Limited, Bingley, pp 195–214. https://doi.org/10.1108/9781848557512-009
28. Schultz G, Rilett L (2004) An analysis of the distribution and calibration of car-following sensitivity parameters in microscopic traffic simulation models. In: Transportation research board annual meeting, Transportation Research Board, Washington, DC
29. Hoogendoorn SP, Ossen S (2005) Parameter estimation and analysis of car-following models. In: Proceedings of the 16th international symposium on traffic and transportation theory, Maryland
30. Yugendar P, Ravishankar KR (2018) Crowd behavioural analysis at a mass gathering event. J KONBiN 46(1):5–20. https://doi.org/10.2478/jok-2018-0020
31. Kumbh Mela (2016) https://www.kumbhamela.net/kumbha-mela-ujjain.html. Accessed 30 Aug 2021

Application of On-Board Diagnostics (OBD) Data for Vehicle Trajectory Prediction

Nitin Navali, Lelitha Vanajakshi, and Darcy M. Bullock

Abstract This study explores the use of On-Board Diagnostics (OBD) data in the analysis and prediction of vehicle dynamics. Though various data sources are available for traffic data collection, these conventional approaches may not work for the complex traffic system in India, with its heterogeneity and lack of lane discipline. On-board units such as GPS and OBD are some devices, which perform independent of the traffic conditions. This study focuses on the use of OBD data along with GPS data for individual vehicle trajectory prediction. A machine learning tool, namely Long–Short-Term Memory (LSTM) model is employed and the prediction of speed and bearing for the next 1 s is done. Results obtained showed the OBD as a potential source of data that can be used for various real-time and offline applications.

Keywords On-Board Diagnostics (OBD) data · Vehicle Trajectory Prediction · Long–Short-Term Memory (LSTM) · Connected and Automated Vehicles (CAV)

1 Introduction

There has been extensive research in urban traffic management with the help of Intelligent Transportation Systems (ITS). However, it requires abundant data to understand the prevalent traffic condition. The application of a wide range of traffic sensors plays a vital role in getting such data. However, the majority of the commonly used sensors such as traditional loop detectors, do not work well under the heterogeneous and lane-less traffic conditions existing in many countries, including India.

To overcome this, alternative techniques and sensors for traffic data collection are being actively explored. One of the less explored data sources is the On-Board Diagnostics (OBD) sensors on vehicles. Vehicles these days have numerous sensors

N. Navali · L. Vanajakshi (✉)
Department of Civil Engineering, IIT Madras, Chennai, India
e-mail: lelitha@iitm.ac.in

D. M. Bullock
Department of Civil Engineering, Purdue University, West Lafayette, IN, USA
e-mail: darcy@purdue.edu

L. Devi et al. (eds.), *Proceedings of the Sixth International Conference of Transportation Research Group of India*, Lecture Notes in Civil Engineering 273,
https://doi.org/10.1007/978-981-19-4204-4_19

to measure wheel-based vehicle speed, accelerator pedal position, engine RPM, etc. With advancements in vehicle technology, many vehicles are having OBD, which makes it a cost-effective solution for such an application.

One of the earliest literature on OBD data for traffic applications was by [1], which proposed a method of collecting vehicle behaviour using OBD. The use of OBD data for accident analysis was reported in [2], and driving behaviour analysis using OBD data by [3] are some of the other reported studies. The use of OBD data for evaluating vehicular emissions [4], and to quantify the relationship between driving stress and traffic conditions [5], were some of the other reported studies.

This study explores the utilisation of OBD data for vehicle trajectory prediction. The methodology is to collect all the sensory data of a vehicle recorded through the OBD II port in real time to predict the vehicle trajectory using a deep learning based prediction technique and measure its performance.

Vehicle trajectory prediction is an essential aspect of vehicle interaction in autonomous vehicles, it helps in preventing collisions and assists in manoeuvring under different scenarios. Trajectory prediction and manoeuvre recognition were done by [6], and machine learning techniques were used by [7] for trajectory prediction. However, both of these were for lane disciplined traffic, where the uncertainties are minimal, and were not based on OBD data.

1.1 Experimental Setup and Data Collection

Present-day cars have multiple computers to control the engine, transmission, windows, locks, lights, etc. These computers are called Electronic Control Units (ECU) and they communicate with each other over a network, acting as the control center of all the sensors present in the vehicle. OBD II port acts as a gateway to receive the data from the ECU.

Most of the sensory data from the ECU is generally used for engine diagnostics while servicing the vehicle. A hardware setup is required to connect to the port and receive data. There are several devices that can scan the OBD port and list out various parameters such as speed, distance, fuel rate, throttle position, etc. Vehicle Spy Neo Fire IV [8] is one such device and is used in this study.

In this study, OBD data collection was done from two vehicle types—a truck and a passenger car. The study stretch consisted of major arterial roads in Chennai using a Swift Dzire 2012 model. This study stretch chosen is shown below (see Fig. 1).

The data received is in the form of packets that contain several rows with each row representing a Parameter ID (PID) containing data bytes of various lengths in the form of Bytes and Bits. Each of these PIDs represents some sensor data. There is no specific way of identifying them from the raw data. The process of sniffing the data for a required parameter is done as mentioned below.

PIDs have been identified by linking them to physical events. For example, if the PID for the brake pedal is to be found out, the brake pedal is repeatedly pressed and

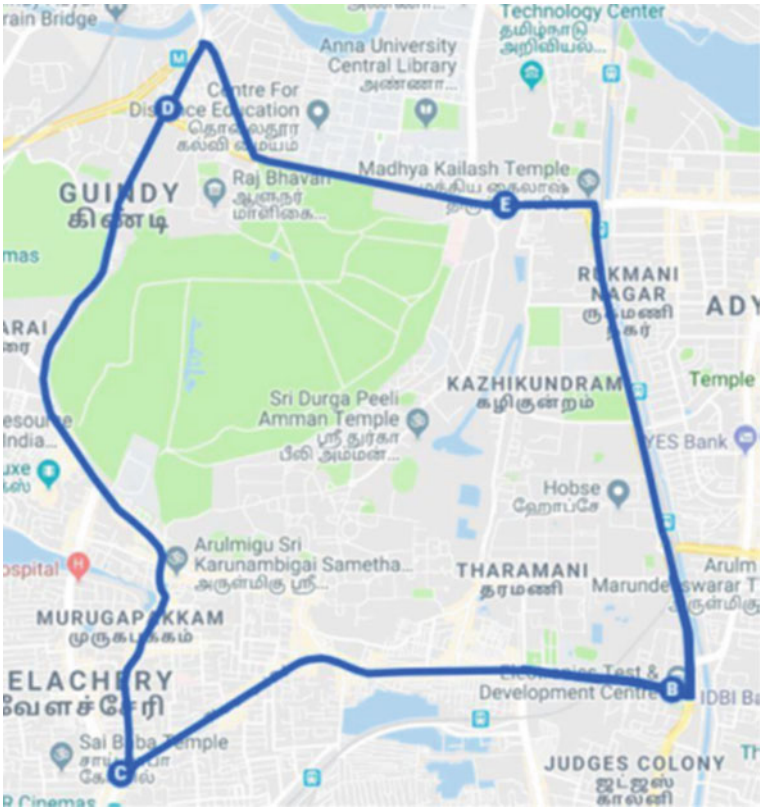

Fig. 1 Study stretch

released when the vehicle is at a standstill and a toggle in data is to be observed and matched. Similar controlled tests were performed to identify several PIDs.

After identifying a PID, scaling needs to be done with the help of external data sources. For example, in the case of speed data, the scale factor was found with the help of data from a hand-held GPS device, the speed values obtained from OBD were calibrated with speed from GPS and the scaling factor was found to be 0.0077. Table 1 shows the list of parameters that have been identified in this study and corresponding PIDs.

Similarly, several other parameters can be reverse engineered, but the availability of the parameters depends on the vehicle chosen. Luxurious cars have extra sensors than the regular ones, but some basic parameters are available in all the vehicles.

Table 1 Parameters and their corresponding IDs

‘	Wheel based vehicle speed (kmph)	Trip distance (m)	Accelerator pedal position	Brake pedal	Left/Right indicator
PID	314	314	120	318	3D0
Bytes	1–2	3–4	1–2	0	4
Bits	0–15	0–15	2–15	2	Left—6 Right—7
Factor for scaling	0.00766	0.0632	Min/Max scaling	Boolean	Boolean

2 Trajectory Prediction Methodology

2.1 Literature Review

Reported studies in the area of vehicle trajectory prediction include the use of Support Vector Machines (SVM) and Neural Networks (NN) to predict the lane change manoeuvre based on vehicle kinematics [9]. Prediction of vehicle's velocity time series using neural networks was reported in [10]. Mozaffari et al. [11] proposed an intelligent tool called evolutionary least learning machine (E-LLM) to predict upcoming power demands and employ the vehicle powertrain control systems to significantly improve the fuel economy and emission performance. Rezaei and Burl [12] discussed the benefit of using statistical methods with GPS/GIS information for predicting Driver Desired Velocity (DDV) and a time series method with prior knowledge of deterministic environmental factors. Recently, the use of deep learning techniques, such as the Long–Short-Term Memory (LSTM) for trajectory prediction is being widely explored. This study focuses on leveraging OBD data for trajectory prediction with the use of the Long– Short-Term Memory (LSTM) algorithm for trajectory prediction in lane-less traffic conditions.

LSTM is an upgraded version of Artificial Neural Networks (ANN). ANNs consist of a simple computational unit called node or neuron, which are connected with connections carrying some weights. Inputs are provided to a neuron through the incoming connections. These inputs are then multiplied by their corresponding connection weights. The weighted sum of the inputs is then applied with a non-linear function called activation function as an output [13]. In order to find the weights of each connection, ANN undergoes a training process. During training, the network is presented with input data along with their corresponding outputs. The training is done in such a way that a model is built, which gives the output as close to the known output corresponding to the input data. This is quantified by a loss function. Back-Propagation, which works on the principle of gradient descent proposed by [14] helps to optimise the training.

A Recurrent Neural Network (RNN) is a type of NN where the neurons in the hidden layer store all the previous elements of the sequence. This is done by a state

vector, which stores and acts as a memory of the previous elements of the sequence [15]. This means that the output from a neuron in an RNN is based on both inputs received in the current instance and also the memory of previous instances. RNNs are used for sequential data wherein information about the past is essential for the processing and making predictions.

Like ANN, RNN also requires training to implement the model, which is achieved by interpreting it as ANN. By unfolding RNN into several time steps, where each time step is a NN, can be trained in a similar way the NN are trained. This methodology of training RNN is called Back-Propagation Thought Time (BPTT) [16]. However, in practice, standard RNNs perform poorly when the outputs and relevant inputs are separated by a large number of time steps, which restricts them to be trained to learn dependencies across long intervals [17]. This can be explained as, at the training of an RNN with BPTT, the error gradient is calculated across several time steps. The recurrent connection has the same weight for each time step. Thus back-propagating the error involves multiplying the error gradient with the same value over and over again. This causes the gradients to either become too large or decay to zero. These problems are referred to as exploding gradients and vanishing gradients respectively [18]. In such situations, the model learning does not converge at all or may take an inordinate amount of time. To address this, LSTM was introduced. LSTM networks have proven to be very useful in learning long-term dependencies as compared to standard RNNs. LSTM overcomes the vanishing gradients problem by replacing an ordinary neuron with a complex architecture called the LSTM unit or block. The key feature of LSTM is the presence of input, forget and output gates [19, 20]. This helps in letting go of some dependency on earlier data, which are no longer important. This is very important in cases where values are changing randomly such that the data used for training might be a different scenario from what the model is being tested and utilised for.

LSTM is used for a wide range of applications such as text classification [21], speech recognition [22], handwriting recognition/generation [23], anomaly detection [24], time-series prediction [25], etc. Zahangir Alom Md et al. [26] has done a comprehensive survey on recent development advanced deep learning techniques in various fields.

Recently, the use of LSTM has been explored to predict the trajectory. In [27], the LSTM is used to analyse the temporal behaviour and predict the future coordinate of the surrounding vehicles. Kim B et al. [28] Predicted the location of the vehicle from the past trajectory data using LSTM. Future trajectories of different traffic agents were predicted from camera-based images in heterogeneous and lane-less traffic conditions using LSTM in [29].

2.2 Methodology

In this study, the high-frequency data from OBD is used as an input for the time-series prediction. The process of prediction using LSTM involves three steps which

are feature selection, parameter tuning, and validation of the model as discussed below.

Feature selection. In order to predict the trajectory, two features must be looked into; one is the bearing of the path and another is the length of the path the vehicle would traverse with that bearing. The speed data obtained from OBD has an interval of 0.1 s and since it is based on axle rotation, it can be assumed that there is very little error in speed measurement. The bearing was found using the hand-held GPS device.

It was observed that bearing after 360 degrees goes back to 0, which can be wrongly recognised by the model. In order to tackle this boundary condition, a change in bearing at a location was used in this study i.e. delta bearing (Δb).

Thus, the bearing of the next trajectory would be given by Eq. 1. The length of the next trajectory was calculated using Eq. 2. Once the bearing and the length are known, the location of the next point can be found with respect to the present point. The information of bearing and length is enough to give the location of the vehicle in the next instant.

$$\text{bearing}_{i+1} = \text{bearing}_i + \Delta b_{i+1} \tag{1}$$

$$\text{length}_{i+1} = \text{speed}_{i+1} * \text{time} \tag{2}$$

Tuning parameters. The data was scaled using min–max scaling to standardise the range of independent variables or features of data between 0 and 1. Later the predicted values are transformed back to get the values in the actual range.

Model validation. Training of the model was done using the training data, keeping 20:80 for testing and training. Table 2 shows the architecture of the LSTM model used in this study.

Once the bearing and the length are known, the location of the next point can be found with respect to the present point as shown in Fig. 2.

Table 2 Architecture of the LSTM model

Features	Speed	Delta bearing
Layers	3	3
Activation function	tanh	tanh
Dropout	0.2	0.2
Epochs	25	50
Batch size	512	256
Optimizer	Adam	Adam
Loss function	Mean squared error	Mean squared error

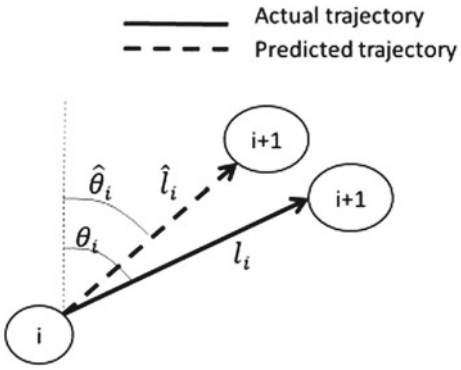

Fig. 2 Schematic of predicted trajectory, where, $\hat{\theta}_i$ and $\hat{l}_i$ are predicted values when the vehicle is at i. θ_i and l_i are the actual bearing and length of the path from i to $i + 1$

3 Results

To quantify the performance of the prediction model, Root Mean Squared Error (RMSE) was used, which is calculated as below.

$$\text{RMSE} = \sqrt{\frac{1}{n}\sum_{i}(y_i - \hat{y}_i)^2}, \tag{3}$$

RMSE for speed predictions for 1 s ahead came to be around 1.45 kmph. This value for bearing was found to be 0.54 deg. The model was also trained for multi-step predictions, and it can be seen that the RMSE increases with a multi-step prediction (see Fig. 3).

Figure 4 shows the actual and predicted path from a sample of test data and it can

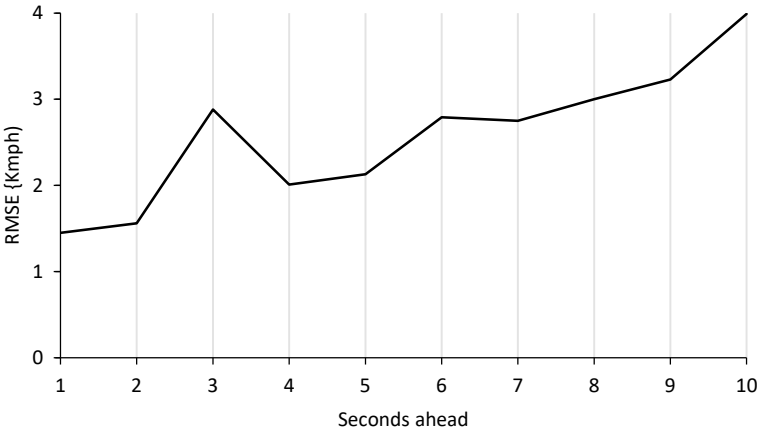

Fig. 3 RMSE for multi-step predictions of speed

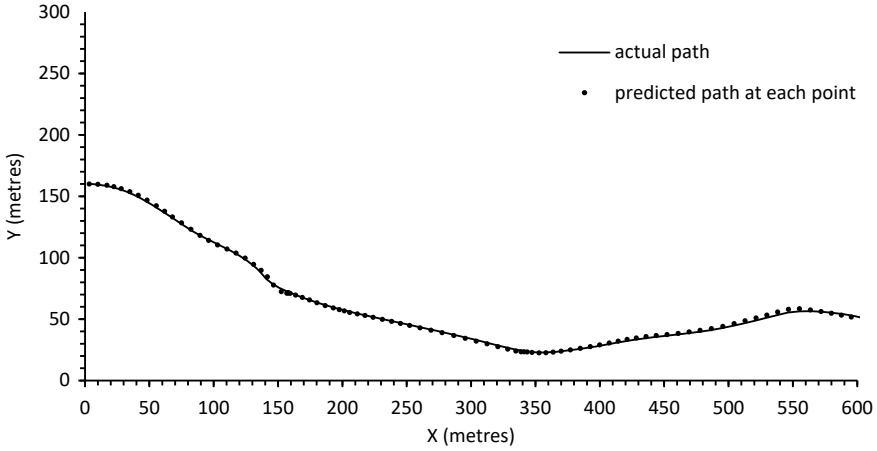

Fig. 4 Actual and Predicted path at each point in test data

be seen that the actual and predicted paths are in close agreement. It can be observed that the model performance is slightly reduced in curved sections.

4 Conclusion

The use of OBD data in traffic engineering is an emerging topic. With the introduction of V2V technologies, the OBD data becomes more relevant for better traffic management. As the data is obtained from the sensors in the vehicle, it is very rare to get imprecise data and the use of this data improves the performance of any traffic application. Under complex traffic conditions such as the one in India, where a majority of the traditional traffic sensors fail to perform, OBD data becomes more relevant.

Though the original purpose of OBD was for monitoring engine performance in a vehicle, the data from the in-vehicle sensors can provide a better understanding of the traffic behaviour, especially at the microscopic level. However, due to the unwillingness of the vehicle manufacturers to share the codes for these sensor data, there is a need to reverse engineer through controlled tests in order to get the required information. However, once they are identified, the data can be used for several applications without any external resources. In the current study, OBD data was used as an input to a deep learning technique namely, LSTM. The performance of the model was promising indicating the OBD data as a very good source of information in the domain of connected vehicles and automated vehicles.

There is scope to develop numerous other applications leveraging OBD such as pollution mapping, which will help in identifying areas of high pollution. Another example is the use of fuel consumption data as a function of speed and accelerations

for implementing an eco-friendly drive mode, where the ride is done with minimal fuel consumption.

Acknowledgements The authors acknowledge K Jijo and Howell Li from Purdue University for their assistance in the Hardware setup. The authors also acknowledge the support for this study as a part of the SPARC project funded by the Ministry of Human Resource Development, Government of India, through Project Number CIE1819289SPARLELI.

References

1. Alessandrini A, Filippi F, Orecchini F, Ortenzi F (2006) A new method for collecting vehicle behaviour in daily use for energy and environmental analysis. Proc Inst Mech Eng Part D. J Automob Eng 220(11):1527–1537
2. Zaldivar J, Calafate C, Manzoni P (2011) Providing accident detection in vehicular networks through OBD-II devices and android-based smartphones. In: IEEE 36th conference on local computer networks
3. Chen SH, Pan JS, Lu K (2015) Driving behavior analysis based on vehicle OBD information and AdaBoost algorithms. In: International multiconference of engineers and computer scientists, vol I
4. Ortenzi F, Costagliola M (2010) A new method to calculate instantaneous vehicle emissions using OBD data. SAE technical paper 2010-01-1289
5. Bitkina O, Kim J, Park J, Park J, Kim HK (2019) Identifying traffic context using driving stress: a longitudinal preliminary case study. Sensors 19:2152. https://doi.org/10.3390/s19092152
6. Houenou A, Bonnifait P, Cherfaoui V, Yao W (2013) Vehicle trajectory prediction based on motion model and maneuver recognition. In: 2013 IEEE/RSJ international conference on intelligent robots and systems, Tokyo, pp 4363–4369. https://doi.org/10.1109/IROS.2013.6696982
7. Jiang H, Chang L, Li Q, Chen D (2019) Trajectory prediction of vehicles based on deep learning. In: 2019 4th international conference on intelligent transportation engineering (ICITE), Singapore, pp 190–195. https://doi.org/10.1109/ICITE.2019.8880168
8. Intrepid control systems, vehicle spy enterprise. https://www.intrepidcs.com/products/software/vehicle-spy/. Accessed 12 May 2021
9. Izquierdo R et al (2017) Vehicle trajectory and lane change prediction using ANN and SVM classifiers. In: IEEE 20th international conference on intelligent transportation systems (ITSC), pp 1–6
10. Fotouhi A, Montazeri-Gh M, Jannatipour M (2011) Vehicle's velocity time series prediction using neural network. Int J Automot Eng 1:21–28
11. Mozaffari L, Mozaffari A, Azad NL (2015) Vehicle speed prediction via a sliding-window time series analysis and an evolutionary least learning machine: a case study on San Francisco urban roads. Eng Sci Technol Int J 18(2)
12. Rezaei A, Burl JB (2015) Prediction of vehicle velocity for model predictive control. IFAC-PapersOnLine 48(15)
13. Maind SB, Wankar P (2014) Research paper on basic of artificial neural network. Int J Recent Innov Trends Comput Commun 2(1):96–100
14. Williams D, Hinton G (1986) Learning representations by back-propagating errors. Nature 323(6088):533–538
15. Lipton ZC, Berkowitz J, Elkan C (2015) A critical review of recurrent neural networks for sequence learning. arXiv:1506.00019
16. Werbos PJ (1990) Backpropagation through time: what it does and how to do it. Proc IEEE 78(10):1550–1560

17. Hochreiter S et al (2001) Gradient flow in recurrent nets: the difficulty of learning long-term dependencies
18. Pascanu R et al (2013) On the difficulty of training recurrent neural networks. ICML 3(28):1310–1318
19. Greff K et al (2017) LSTM: a search space odyssey. IEEE Trans Neural Netw Learn Syst PP(99):1–11
20. Gers F, Schmidhuber J, Cummins F (2000) Learning to forget: continual prediction with LSTM. Neural Comput 12:2451–2471. https://doi.org/10.1162/089976600300015015
21. Zhou P, Qi Z, Zheng S, Xu J, Bao H, Xu B (2016) Text classification improved by integrating bidirectional LSTM with two-dimensional max pooling. arXiv:1611.06639
22. Graves A, Mohamed A-R, Hinton G (2013) Speech recognition with deep recurrent neural networks. In: ICASSP, IEEE international conference on acoustics, speech and signal processing – proceedings, vol 38. https://doi.org/10.1109/ICASSP.2013.6638947
23. Surya K (2013) Recognition of handwritten text using long short term memory (LSTM) recurrent neural network (RNN). AIP Conf Proc 2095:030011
24. Chauhan S, Vig L (2015) Anomaly detection in ECG time signals via deep long short-term memory networks. In: 2015 IEEE international conference on data science and advanced analytics (DSAA), Paris, pp 1–7
25. Duan Y, Lv Y, Wang F-Y (2016) Travel time prediction with LSTM neural network. In: 2016 IEEE 19th international conference on intelligent transportation systems (ITSC), Rio de Janeiro, pp 1053–1058
26. Zahangir Alom Md et al (2018) The history began from AlexNet: a comprehensive survey on deep learning approaches. arXiv:1803.01164
27. Park SH, Kim B, Kang CM, Chung CC, Choi JW (2018) Sequence-to-Sequence prediction of vehicle trajectory via LSTM encoder-decoder architecture. In: 2018 IEEE intelligent vehicles symposium (IV), pp 1672–1678
28. Kim B et al (2017) Probabilistic vehicle trajectory prediction over occupancy grid map via recurrent neural network. arXiv:1704.07049
29. Ma Y, Zhu X, Zhang S, Yang R, Wang W, Manocha D (2019) TrafficPredict: trajectory prediction for heterogeneous traffic-agents. AAAI 33(01):6120–6127

Platoon and Red Light Violation Detection Using Image Processing

Bharathiraja Muthurajan, Sidharth Sudheer, Bhargav Ram, and Lelitha Vanajakshi

Abstract Intersections account for most road accidents and delay in a road network. The intersection's efficiency and safety concerns can be addressed by collecting vehicle platoon size, queue length, and delay data and implementing a red light violation detection technique (RLVDS) to reduce accidents. It is challenging to collect this traffic information in heterogeneous and less lane disciplined traffic, a scenario often observed in developing countries such as India. Traditional sensors such as inductive loop, infrared, radar, or magnetic sensors and image processing solutions do not work well under these conditions. Hence the current work presents a set of robust techniques developed for heterogeneous traffic. First, the platoons were detected using foreground extraction, connected component analysis, and a density-based clustering algorithm. Then, the queue length was extracted using a progressive block processing technique. Separately the RLVD was performed using corner point tracking and user-defined detection zones.

Keywords Platoon detection · Red light violation detection · Image processing

1 Introduction

Road safety is one of the major concerns for transportation engineers and intersections account for half of road accident fatalities [1]. A report in 2003 by the National Cooperative Highway Research Program (NCHRP) examined studies from the previous 30 years in Australia, the UK, Singapore, and the USA, and concluded that red light cameras improve the overall safety of intersections [2]. An automated

B. Muthurajan · S. Sudheer · B. Ram · L. Vanajakshi (✉)
Transoportation Division, Department of Civil Engineering, Indian Institute of Technology Madras, Chennai, India
e-mail: lelitha@civil.iitm.ac.in

L. Vanajakshi
Transportation Engineering Division, Department of Civil Engineering, Indian Institute of Technology Madras, Chennai, India

L. Devi et al. (eds.), *Proceedings of the Sixth International Conference of Transportation Research Group of India*, Lecture Notes in Civil Engineering 273,
https://doi.org/10.1007/978-981-19-4204-4_20

Red Light Violation Detection System (RLVDS) detects violations based on pre-specified conditions and triggers response action. Most of these RLVD systems have been built as a response to western traffic condition, which does not handle the complexity specific to heterogeneous traffic conditions.

A traffic signal manages conflicts in opposing movements by separating them over time. It gathers vehicles arriving at the red time and discharges them as dense packets during the green time. Thus, a traffic signal forces the movement of vehicles as groups during the green light. Such a group is called a vehicle platoon. The present study concentrates on these two aspects of a signalized intersection, namely safety and efficiency.

Some of the indicators that are in general used to quantify the performance of a signal are queue length, delays, and platoon size. However, extracting this information is challenging due to their spatial characteristic and is extremely difficult when the traffic is heterogeneous and do not follow lane discipline, as is the case in countries like India. Extreme occlusion that happens due to different sized vehicles is another associated problem. Automated collection of traffic variables under such a situation is difficult using any of the traditional sensors such as inductive loop, infrared, radar, or magnetic sensors as well as using traditional image processing solutions. The present study concentrates on this problem using image processing based traffic data extraction at signalized intersections under Indian traffic conditions for estimating queue length, delay, platoon detection, and red light violation.

2 Literature Review

There are several reported studies on vehicle identification using image processing for the purpose of extracting traffic information such as vehicle count and classification at midblocks [3]. However, reported studies on counting the vehicles near the intersection are limited. A method to obtain turning counts using an optical flow algorithm in a complex crossroad was developed in [4]. A framework to track vehicles to estimate turning movement counts obtained by placing virtual loops or zones was presented in [5]. A detection signal is generated each time a vehicle crosses the zone.

Queue length detection using image processing was reported in the following studies. Agarwal and Hickman [6] developed a method to estimate queue lengths using queue polygons created using airborne images. The polygon was developed by identifying all the static vehicles near an intersection. The vehicles were identified from the binary mask and a boundary polygon was created around the mask. Siyal and Fathy [7] used a motion detection algorithm and a presence detection algorithm for queue detection. Similar studies were reported by Zanin and Messelodi [8] and Yao, Wang and Xiong [9] but with different thresholding techniques. The former used a “severity index” whereas the latter used the popular Otsu’s method [10] for thresholding. Cheek [11] developed a method to estimate queue lengths from video data using a linear regression model and applied a Kalman filter to reduce the errors.

Z. Li, N. Li, and Liu [12] conducted a study to estimate queue length and delay at a signalized intersection by placing two virtual detection zones, one upstream of the road, farther from the last vehicle in the queue, and one near the stop line. The vehicles were tracked and the crossing times were extracted to estimate queue length and delay. Another interesting and novel study by Shirazi and Morris [13] used a tracking algorithm based on the optical flow method [14] to identify stopped vehicles at intersections.

Reported studies on platoon detection using image processing are limited. Thomas [15] suggested a cluster-based platoon detection approach, a modified approach for Indian traffic conditions. A study conducted by Kogut and Trivedi [16] discussed platoon detection using image processing. However, this was tested only in homogeneous traffic conditions and traffic with lane discipline, this may not work in Indian conditions.

The methods adopted for Red Light Violation Detection Systems (RLVDS) using image processing can be broadly classified into two categories: the stop line method and the region-based method. The stop line method detects violators by identifying occlusion over the stop line or trip line. Tarko and Naredla [17] investigated the feasibility of using an Autoscope-based vision system to monitor red light running. Saha et al. [18] presented similar work by using a stop line as a tripwire for the detection of violators. However, these methods have several drawbacks. The stop line at the site should be clearly visible for the system to use it as a virtual tripwire. Moreover, since the area of processing is very small, the system is more susceptible to noise. These algorithms usually involve background subtraction, which also makes them susceptible to illumination changes.

The region-based violation detection approach analyses vehicular movement in the region close to the intersection. These methods are more robust and accurate than trip line methods since they utilise additional information to detect violators. Lim, Choi and Jun [19] proposed a method of RLVDS using multiple features like travelling trajectory, approach lane, and speed. Klubsuwan, Koodtalang, and Mungsing [20] investigated the use of mean square displacement (MSD) for the evaluation of vehicular trajectories to detect red light violations. Complications in this method arise from the need for vehicle detection and lack of lane discipline.

From the literature review, it was observed that not many studies have been reported for traffic data extraction and the development of applications using image processing for signalized intersections under Indian traffic conditions. This study aims to develop one such image processing solution based on a spatial data clustering technique to detect platoons. In the case of queue length measurement, the majority of the studies that used image processing based approaches were tested for homogeneous and lane-based traffic conditions. However, the queue length estimation under heterogeneous and lane-less traffic conditions is much more complex, and the reported approaches may not be able to perform well under such conditions. The current study develops a vehicle tracking based technique to estimate average speeds and maximum queue lengths under heterogeneous and lane-less traffic conditions. Finally, an RLVD application was also developed based on image processing.

3 Study Site and Data Collection

The study site selected for the platoon estimation was a stretch of road along Rajiv Gandhi Salai in Chennai, India, starting from Madhya Kailash (MK) intersection. Figure 1 shows a schematic sketch of the study site used. Permanently fixed video cameras at selected locations along the road to record traffic flow. Videos collected from two cameras, one at First Foot Over Bridge (FFOB) and the second at the Second Foot Over Bridge (SFOB) were used. The south bound traffic was recorded by both these cameras. The length of the section MK-FFOB section was 200 m and FFOB-SFOB was 1000 m. Video data for these sections were collected for two days, (referred to as Day 1 and Day 2 hereon) during the morning period, 06:30 AM – 08:00 AM.

The study site used for the evaluation of queue length and red light violation detection was the Tidel park intersection, which is the intersection that comes after SFOB. A camera fixed at a pole at the intersection captured the video of the complete intersection. However, the region of interest for the present study was the road stretch very close to the intersection starting from the stop line, upstream for a length of around 20 m. Videos were collected on two days (Day 1 and Day 2) from 6:30 AM to 8:00 AM for computing queue lengths. Figure 2a and b show sample images from this study site. The delay estimation was carried out on videos recorded on three different days from the Tidel park intersection. The actual delay was obtained using Bluetooth sensors.

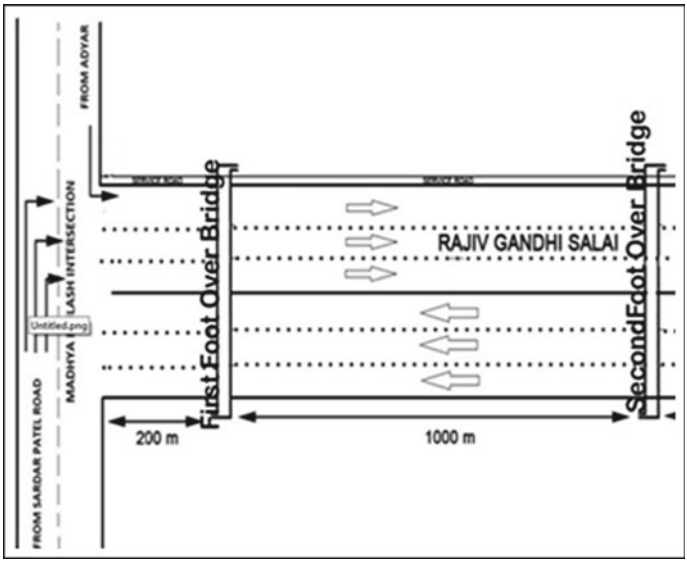

Fig. 1 An Layout of the Study site

Fig. 2 **a** Traffic approaching the Tidel Park intersection **b** Tidel Park intersection

4 Detection—Individual Vehicle and Platoon

Platoon detection was carried out based on basic object detection algorithms in image processing as discussed below.

4.1 Individual Vehicle Detection

The platoon identification and any other image processing solution for vehicle traffic analysis start with detecting individual vehicles. Vehicle detection has the following steps: foreground extraction, connected component analysis, and blob detection. Any object that is not a fixed scene attribute is considered the foreground. Several techniques are available for background extraction [21], among which GMMs are most common [22, 23]. In the GMM model, the pixel of the background of a scene is considered a mixture of Gaussian models. Pixels are evaluated against each one of the 3–5 different distributions. If the pixel is not associated with a distribution, it is identified as a foreground. Research has shown that this technique, particularly used with the Kalman filtering technique, shows high accuracy in vehicle detection and tracking [24]. To remove noise in the image for obtaining an accurate foreground, morphological operations such as median filter opening and closing are applied [25]. Figure 3a shows a sample image after applying these steps. In the next step, connected

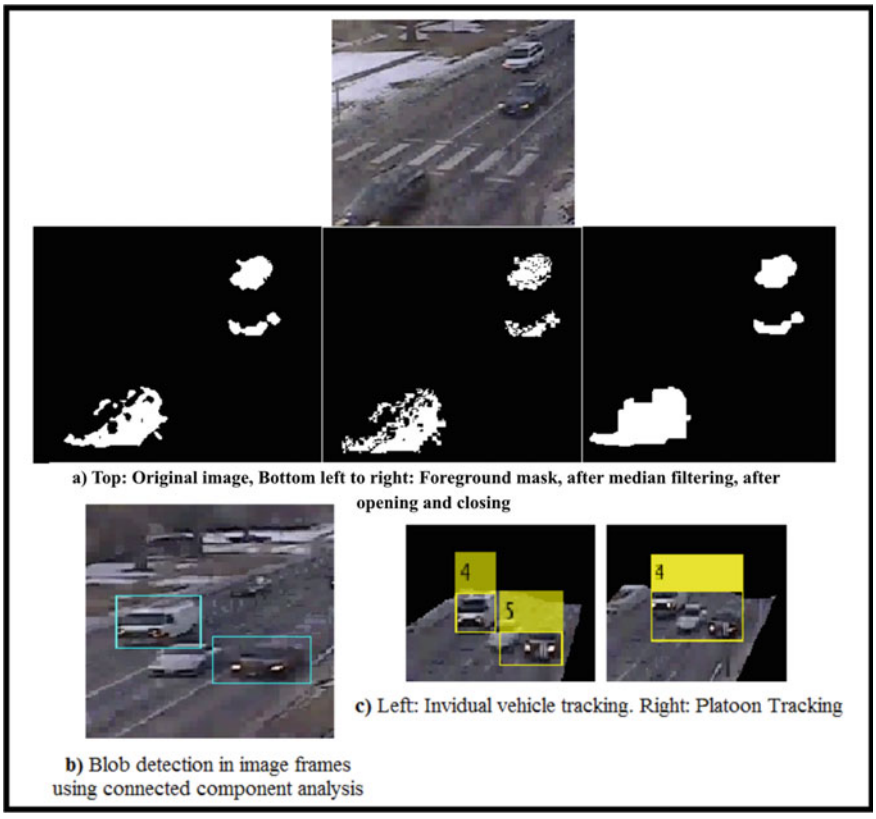

Fig. 3 Images after the application of various steps of image processing

component analysis [26] was applied to the obtained foreground. The connected component analysis technique searches for connected white pixels indicating the foreground and identifies it with a rectangular marker implying the location of a moving object, in our case a vehicle. The identified blob has centroid coordinates, and dimension information of which can be extracted. The centroids are tracked and this information is used in vehicle tracking, speed estimation, and platoon detection. Some blobs are removed based on the blob area threshold. The result of this step is shown in Fig. 3b.

4.2 Platoon Detection

Platoons are a group of vehicles that move as a single unit on a roadway. The current study detected platoons by clustering the vehicle centroids located in the previous step. Each cluster is identified as a platoon. Density-based spatial clustering of applications with noise (DBSCAN) [27], a density-based clustering technique, was used to identify platoons from the centroid information. This algorithm groups the centroids by using thresholds for a number of centroids and distance between centroids of platoon and non-platoon centroids. The thresholds were set at 7 and 50, based on Thomas [15] and Aziza et al. [28] observations. The algorithm aggregates multiple centroids and we can mark the cluster as a platoon using bounding boxes. The centroid of the bounding box will serve as the base for the rest of the application in this work. Figure 3c shows vehicle and platoon tracking results.

5 Tracking—Speed, Queue Length, and Delay

Queue length can be defined as the number/ length of vehicles that are waiting to be serviced at a signalized intersection. This study estimated the maximum queue length at an intersection during every cycle using image processing techniques. The process of estimating maximum queue length at signalized intersections can be subdivided into three major phases. The first phase is individual vehicle detection, which has already been discussed in the previous section. The other two phases are discussed below.

5.1 Speed Measurement

Speed measurement involves extracting the trajectories of individual vehicles/ vehicle centroids, based on feature-based tracking. Chan et al. [29] adopted the particle filter technique to detect and track the moving vehicles based on cues such as vertical edge, underneath shadow, symmetry, and taillights. The “feature” used in this study is the

vehicle centroids obtained during individual vehicle detection and the "tracking" procedure used in the study is based on a Kalman filtering technique [30, 31]. The core purpose of the filter is to predict the location of the centroid of the object (the bounding box) in the current frame based on its location in the previous frames. This involved predicting the new locations of the tracks—the new centroid coordinates of the vehicle—and defining the bounding box for the predicted centroid. This was done by allocating detections in the current frame to the tracks using a cost optimisation problem based on a Hungarian Algorithm [32]. Cost in this study is defined as the negative log-likelihood of detection to a track based on the Euclidean distance between the predicted centroid (by the Kalman filter) and the actual detections in the frame. The output of the allocation for a particular frame would be a 2-dimensional matrix with sizes such as the number of detections and the number of tracks. This matrix is optimised to minimise the total cost using Munkre's version [33] of a Hungarian algorithm. It is not mandatory that all the detections in the frames need to be allocated to different existing tracks in the frame. It may happen that the detections are far enough from all tracks and the cost function may be high as a result. In such a situation, the unassigned detection becomes a new track. Hence, a minimum cost for allocation is predefined based on the study by Trinayani and Sirisha [34] such that any cost function exceeding this minimum cost is said to be associated with a new track.

Once the allocations have been done, it is important to update these tracks, both assigned and unassigned with the new bounding box and its centroid. It is also important that the tracks, like how they get created by unassigned detections, also need to be deleted. This could result in a discrepancy between the number of frames in which the tracks were observed and the number of frames in which tracks were not observed, i.e., when the former is too small compared to the latter. This issue is captured by defining a variable called "visibility index". This index is the ratio of the total number of consecutive frames where the track was observed, and the number of frames covered since the track was first detected. A threshold index value of 0.6 was used in this study [33].

Once these trajectories were developed, the dataset was analysed to obtain the average speed in each video frame. It is important to note that the trajectories are merely an array of centroid locations of a vehicle in the image frame. However, these coordinate points are on the image plane; they are not actual coordinates. As a result, these coordinates have to be converted. For this, distances in the orthogonal directions were scaled and converted to actual distances. The scaling was carried out using known dimensions and their corresponding image distances like the width of the road, length of road markings, length of car, etc. After scaling these distances, the actual distance moved by the centroid of vehicles was calculated, taking into account the frame rate. The following equation was used in speed computation:

$$S = \sqrt{(F_x(x, y)D_x)^2 + \left(F_y(x, y)D_y\right)^2}\frac{FR}{FL} \tag{1}$$

where

S is the speed of an individual vehicle in m/s,

Fx and Fy are the scaling factors in the x- and y-direction,

Dx and Dy are the distance moved by the centroid of the vehicle in the x- and y-direction in the image plane from the initial frame to the final frame in which the vehicle was detected.

FL is the frame length or the total number of frames in which the vehicle was detected.

FR is the frame rate or the conversion ratio which converts the speed from m/frame to m/s. This value is the inverse of the rate at which MATLAB runs the video file.

5.2 Queue Length Measurement

Maximum queue length is computed by identifying the static vehicle, which lies at a maximum distance from the signal intersection. The main idea behind computing the average speed was to identify the static vehicles in each time interval. The method adopted to estimate maximum queue length in this study is a progressive block processing technique [35]. The progressive block processing technique is based on dividing the road stretch into blocks and then processing them in a progressive manner beginning from the stop line of the intersection. When a camera is mounted at a traffic junction, the position of the camera with respect to the road remains fixed. Once this is done, regions of interests (ROI) were defined which are limited to the road surface, devoid of features like buildings, trees, etc. This helps to reduce the sample space of the image for processing. Now, each ROI is further divided into small ROIs or blocks which are non-overlapping. Care has to be taken to ensure that each block is of uniform length and width in the real-world coordinate system. This is ensured by the scaling distances from image to real-world coordinate systems. In the present study, 5-m blocks were considered. Traffic queues at signalized intersections exhibit a unique behaviour of developing systematically starting from the stop line. This behaviour of traffic is what helps in exercising this technique of progressive block processing. To begin with, the average speed of the nearest block from the stop line is computed and if it is found to be below 5 km/h, the processing progresses to the next block and proceeds to the block where the average speed threshold is exceeded. The maximum queue length is defined as the distance of the vehicle in this block from the stop line. The main advantage of using this method is that it reduces computational time. Instead of analysing the entire road stretch, only sections of road (blocks) are analysed.

5.3 Delay Estimation

Delay estimation is started by defining an entry and exit zone manually. The entry zone is defined upstream to the maximum queue length. The exit zone will be downstream of the stop line, where a vehicle reaches its desired speed after it crosses an intersection being the ideal point. The algorithm starts by detecting corner points in the entry zone for each frame. The location of its first detection is stored along with the time stamp. This point gets tracked through the approach until it enters the exit zone. The last detected location of the tracked corner point is also saved along with the timestamp. The distance between the first and last detected point in world coordinates is calculated using the camera calibration matrix beforehand. So, the travel time for that distance is obtained by observing the difference between the stored values. Assuming the free-flow speed for a vehicle, the delay can be calculated as the difference between the actual time taken for the vehicle to cross the intersection and the travel time corresponding to the free-flow speed. Figure 4 shows the test video and the delay estimates in seconds. These results were validated using data obtained from Bluetooth sensors.

6 Application Development—Red Light Violation Detection

The present study also developed a field implementable solution using the detection and tracking described in the earlier sections for RLVDS. The violation detection is performed using corner point tracking. To implement this, user input was obtained to manually demarcate the intersection approaches into different zones. Each zone is numbered and also assigned the direction of flow, stop line, and violation line as arguments. The direction of flow is required to differentiate potential violators. The stop line is the location on the road near intersections to inform drivers of the point,

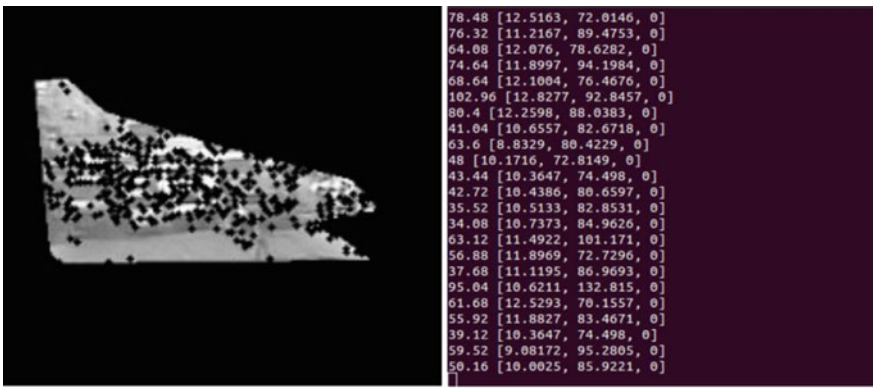

Fig. 4 Non-zero speed corner points and delay estimates

where they are required to stop. However, this condition is not strictly followed in India. Also, these lines are not properly maintained on roads. Hence, a surrogate for the stop line was introduced in the video, far into the intersection area, beyond which vehicles cannot go during red. This can be called the violation line, which is a virtual line drawn downstream of the actual stop line to identify vehicles that have jumped the red signal. The zone defined within the stop line and violation line is termed a critical zone. After defining these site-specific parameters, the red light violation detection system can be run on a video sequence.

Points that enter the critical zone are added to a set of potential violators and tracked in successive frames. When these potential violators exit the critical zone violating the signal, all the trajectory points are updated onto a cluster. Once the vehicle crosses the violation line, the entire cluster of points is added to a set called probable violators. These are filtered based on the cluster threshold and a picture of the violator is stored as an output.

The RLVD analysis was carried out using red starting times. Figure 5 shows red light violations detected by the program. Figure 5a captured a two-wheeler running a red light and Fig. 5b shows the corresponding output image saved with the violating two-wheeler. Figure 5c shows a false detection of a pedestrian as a violator, which happens as the pedestrian is moving in the direction of vehicle flow defined for that zone. This false detection can be handled by addressing vehicle and pedestrian classification in the future. Figure 5d shows the output obtained with the pedestrian. Figure 5e shows a false positive that was detected because the detected points had crossed the violation line although it later stopped. This can be avoided by moving the violation line or by analysing the complete movement of the vehicle through the intersection. Figure 6 presents the algorithm utilised to detect violations.

7 Implementation and Results

7.1 Platoon Identification

To apply the algorithm, the image coordinates were first converted to ground coordinates through a simple linear scaling technique. The linear scaling technique was implemented because the DBSCAN algorithm uses the distance between vehicle centroids as inputs. A linear scaling factor for orthogonal directions was built, after which the actual distances were computed and platoon detection was carried out. Figure 7 shows a representative plot for platoons identified by the image processing technique compared with the ground truth values for the section MK-FFOB for Day 1.

Performance of the algorithm was quantified using Root Mean Square Errors (RMSE) and three other measures, namely:

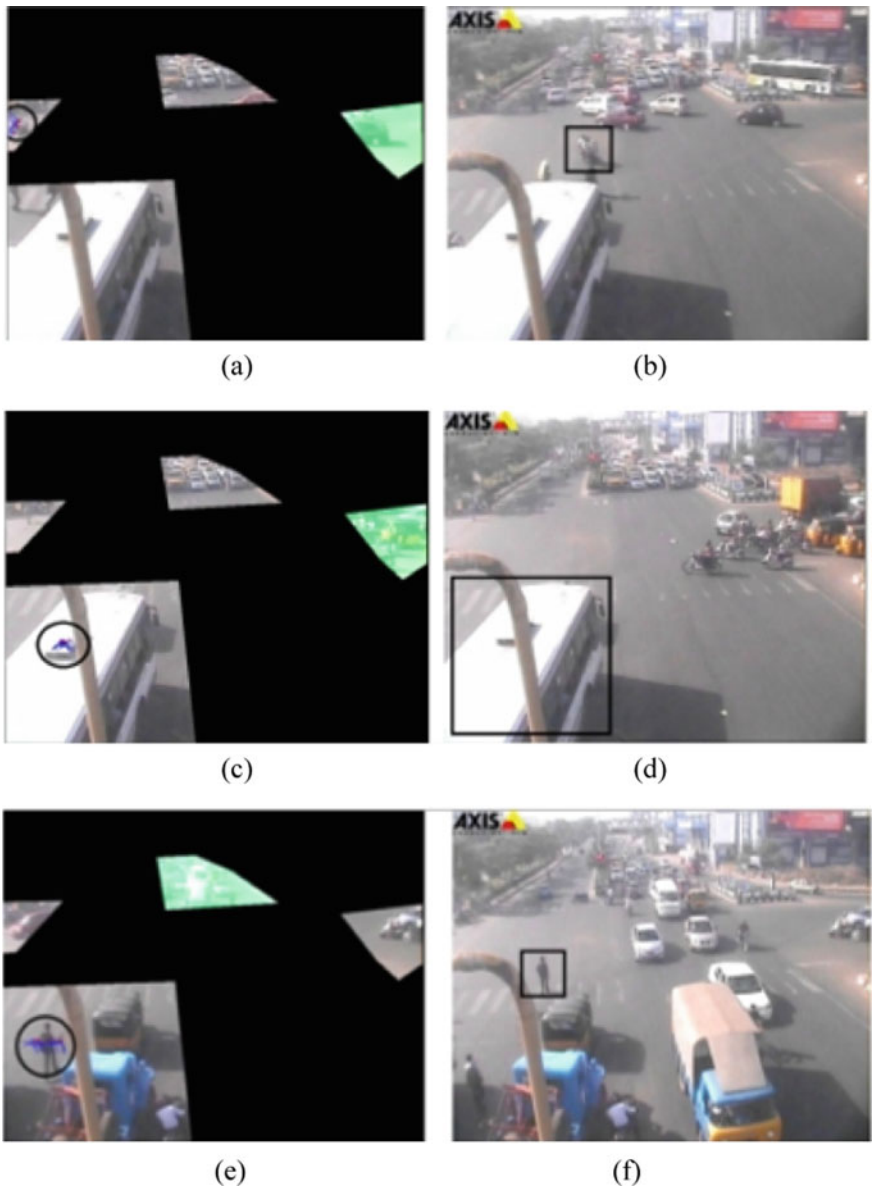

Fig. 5 Violators detected by RLVDS algorithm **a**, **b** RLV detected and resulting output, **c**, **d** Pedestrian detected as RLV and resulting output, **e**, **f** Bus detected as RLV and the resulting output

```
PROGRAM RedLightViolationDetectionSystem:
Initiate site specific parameters;
Read Video;
WHILE (Video did not end)
        Extract a frame;
        Detect interest points in approach zones;
        FOR (Each interest point)
                IF (Point has non-zero motion vector)
                        THEN Add to M (set of moving points) and track;
                        ELSE Discard point;
                ENDIF;
        ENDFOR;
        FOR (Each point in M)
                Find zone j, in which the point is located;
                IF (Point enters critical zone)
                        THEN Add point to PVj, potential violator in zone j and remove from
M;
                        ELSE Continue tracking;
                ENDIF;
        ENDFOR;
        FOR (Each zone j)
                IF (zone j is in red signal)
                        FOR (Each point p in PVj)
                                IF (p Exists the critical zone) THEN
                                        SET violatedj_true;
                                        Add point to cluster Cj_;
                                        Remove p from PVj;
                                ENDIF;
                        ENDFOR;
                ENDIF;
        ENDFOR;
        IF (violatedj_EQUAL true in previous step AND violatedj_EQUAL false in current
step)
                Add cluster Cj_to set V (Probable Violators);
                SET cluster Cj_zero;
        ENDIF;
        FOR (Each cluster in V)
                IF (Cluster size is greater than th)
                        THEN Violation detected, save frame as output;
                        ELSE Discard cluster;
                ENDIF;
        ENDFOR;
ENDWHILE;
END.
```

Fig. 6 Red light violation detection system algorithm

1. Detection Rate (DR)—It is the ratio of the number of correct detections observed by the algorithm and the actual number of detections observed manually, expressed as a percentage.
2. False Detection (F)—This is the number of false detections by the algorithm.

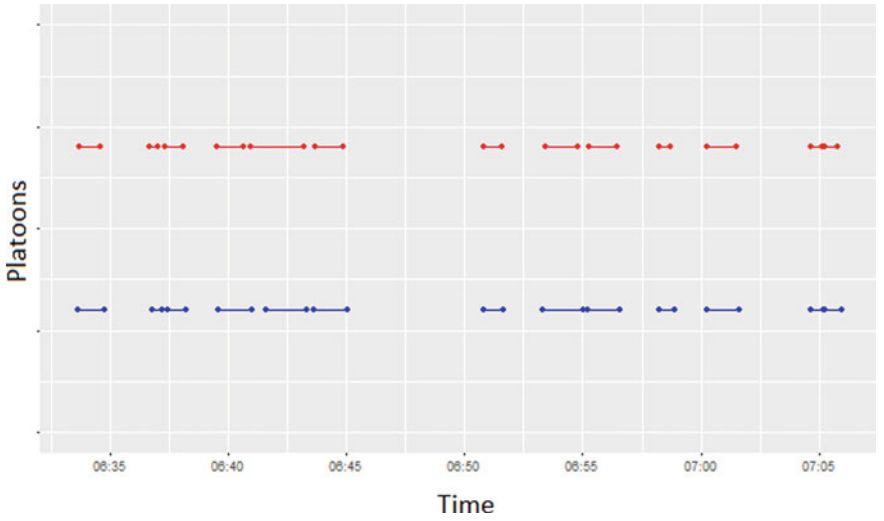

Fig. 7 Platoon identification result using cluster-based technique

3. Missed Calls (M)—It is the number of detection missed by the algorithm or the detections observed in the ground truth data but not by the proposed method.

The RMSE values for the algorithm for the Indian dataset are shown in Table 1.

RMSE values of the algorithm shows a fair performance of the algorithm. The results for the algorithm based on DR, M, and F for the Indian traffic condition are shown in Table 1. Here also, it can be seen that the results are promising for Indian traffic conditions.

7.2 Speed, Maximum Queue Length, and Delay

The developed algorithm was tested on the Indian data at the Tidel park intersection for two days. Both average speeds and queue lengths were computed and compared with the ground truth values.

Average Speed

Ground truth speed values were obtained by noting down the crossing times of vehicles across the region of interest. Average speed for 5-s intervals obtained from image processing and the actual ground truth values for the two days were compared. Figure 8 shows a sample comparison for Day 1 in the Indian dataset. Errors were quantified using Mean Absolute Error (MAE) and Mean Absolute Percentage Error (MAPE). MAE values of 2.9 km/h for Day 1 and 3.3 km/h for Day 2 were observed. Corresponding MAPE values were 7.91% for Day 1 and 5.78% for Day 2. The results are tabulated in Table 1.

Table 1 Platoon detection, average speeds, and maximum queue lengths for the Indian dataset

Section	RMSE(s) of platoon detection				Platoon detection performance					
	Day 1		Day 2		Day 1			Day 2		
	Start	End	Start	End	DR	M	F	DR	M	F
MK—FFOB	8.14	8.5	6.26	15.98	100%	0	2	100%	0	0
FFOB—SFOB	10.99	14.87	8.34	13.41	90.10%	1	2	81.80%	2	0
	Error analysis of average speed				Error analysis of average queue length					
	Day 1		Day 2		Day 1			Day 2		
	MAE(km/h)	MAPE	MAE(km/h)	MAPE	MAE(m)	MAPE		MAE(m)	MAPE	
	2.9	7.91%	3.3	5.78%	0.36	10.10%		2.81	2.52%	

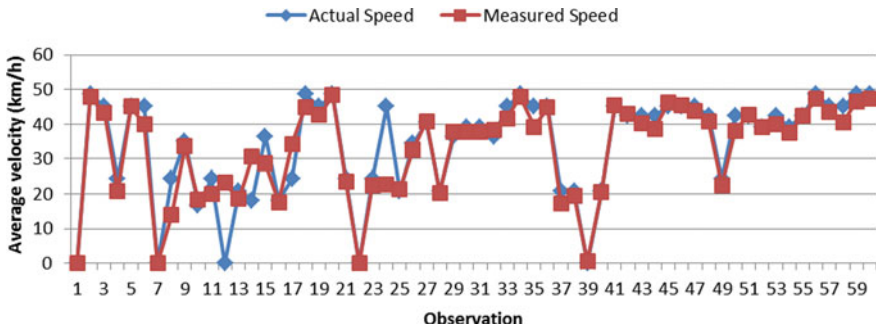

Fig. 8 Comparison of average speed on Day 1 for the Indian dataset

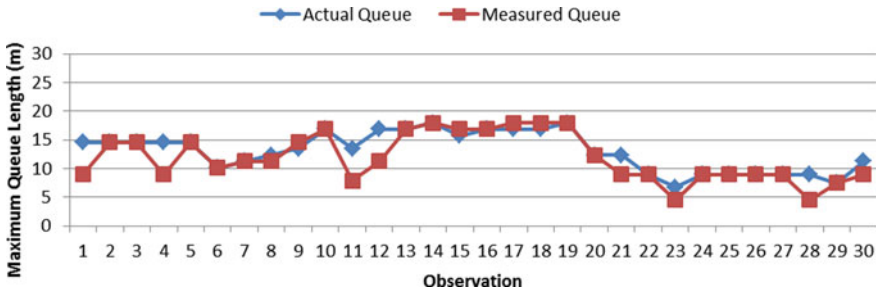

Fig. 9 Comparison of maximum queue length on Day 1 for Indian dataset

Maximum Queue Length

Similar to average speed, a time window of 5 s was used for maximum queue length. The obtained numbers were compared to the actual maximum queue length observed in the field. The algorithm was tested in the same dataset used for average speed. Figure 9 shows a comparison between the actual and measured values of maximum queue lengths for a sample scenario.

The MAE values obtained were 0.36 m and 2.81 m for Day 1 and Day 2, respectively, and MAPE values of 10.10% and 2.52% for Day 1 and Day 2, respectively, as shown in Table 1. The results from the algorithm clearly show that it is able to estimate the queue length accurately for Indian traffic conditions.

The results obtained from the proposed algorithm are compared with data from Bluetooth sensors installed at the site. Table 2 presents an overview of the data. A consistent similarity in the trend can be observed in all three datasets obtained from Bluetooth sensors and the image processing method. Though the descriptive statistics obtained from both Bluetooth data and image processing are comparable, the values from the Bluetooth data are slightly lower. The median value of the Bluetooth data is low indicating that the majority of data points obtained from these sensors have lower travel time values. This skew may have resulted due to the sampling effect. It

Table 2 Summary statistics for delay estimates

	Type of sensor	Average travel time (s)	Mean absolute percentage error (%)
Peak period—April 30th 9:09 AM to 11:28 AM	Image processing	296.3	19.23
	Bluetooth sensor	248.5	
Off-Peak period—May 1st 1:38 PM to 6:20 PM	Image processing	98.9	13.28
	Bluetooth sensor	87.3	
Transition period—May 2nd 8:40 AM to 9:50 AM	Image processing	187.3	17.06
	Bluetooth sensor	160	

can be seen that the sample size of Bluetooth data is around 7% of the size of the data obtained from image processing.

8 Summary and Conclusion

The aim of the study was to use image processing to extract required data for the performance evaluation of signalized intersections and to develop a novel red light runner detection algorithm that can perform well in Indian conditions in real time. The study focuses on extracting traffic parameters namely, platoons, speed, and maximum queue lengths and analysing the movement of corner points from vehicles detected in pre-specified detection zones to identify red light violations.

The platoon detection algorithm had a vehicle detection module and a data clustering module. The algorithm was tested on Indian traffic conditions and delivered promising results. The queue length estimation part of the study consisted of two main tasks, one for computing average speed, and the other for estimating maximum queue lengths. Average speeds were calculated by generating trajectories of vehicles by tracking them using a Kalman filter. The speed profiles for each vehicle were generated and the average speed for predefined time intervals was computed. The second part of the study evaluated queues. The queue length algorithm was implemented using a progressive block processing technique, an efficient method to compute queue lengths. The evaluation of average speed and queue lengths was carried out on the dataset. The results for both average speed and queue lengths have shown the proposed algorithms working well in Indian traffic conditions.

Algorithms for estimating the delay values and queue length (in terms of distance) values at an intersection were developed. The estimated delay was the time spent by the vehicle at the intersection in a queue. Subtracting the ideal time taken to pass through the section gives the delay experienced by users. The queue length estimation is done in terms of the distance at which the farthest stationary vehicle is standing from the stop line. Hence, it gives the length of the queue in terms of distance units. The travel time values obtained from the delay estimation algorithm were compared against the values obtained from Bluetooth sensors. A consistent similarity in the

trends is seen in the plots of the values from both sensors. The data obtained from the Bluetooth sensors are found to be lower than that obtained from the image processing technique by 10–15%.

In the final part, a Red-Light Violation Detection application was developed based on corner point tracking. The algorithm is designed to handle the complex conditions in Indian traffic such as heterogeneity and lack of lane discipline. The use of corner points for the analysis resulted in fast implementation of the algorithm by eliminating computationally intensive steps like background subtraction, etc. An image of the detected red light runner is saved as the output from the program. The information collected by the system can then be used for the effective penalisation of red light violators.

Acknowledgements The authors acknowledge the support for this study as a part of the SPARC project funded by the Ministry of Human Resource Development, Government of India, through Project Number CIE1819289SPARLELI.

References

1. Times of India indiatimes (2014) Traffic junctions account for half of road deaths in India. Accessed 20 February 2021
2. NCHRP (National Cooperative Highway Research Program) (2003) Impact of red light camera enforcement on crash experience. Synthesis 310. Washington D.C.: Transportation Research Board
3. Kamkar Shiva, Safabakhsh Reza (2016) Vehicle detection, counting and classification in various conditions. IET Intell Transp Syst 10(6):406–413. https://doi.org/10.1049/iet-its.2015.0157
4. Abdagic A, Tanovic O, Aksamovic A, Huseinbegovic S (2010) Counting traffic using optical flow algorithm on video footage of a complex crossroad. In: ELMAR. IEEE, pp 41–45
5. Tarko AP, Lyles RS (2002)Development of a portable video detection system for counting turning vehicles at intersections. https://doi.org/10.5703/1288284313185
6. Agarwal A, Hickman M (2004) Automated extraction of queue lengths from airborne imagery. In: 7th International IEEE Conference on Intelligent Transportation Systems, pp 297–302. Washington D.C. https://doi.org/10.1109/ITSC.2004.1398914
7. Siyal, M, and M Fathy.(1995). "Real-Time Measurement of Traffic Queue Parametres By Using Image Processing Techniques". In 5Th International Conference on Image Processing and Its Applications, 450–454. Edinburgh. https://doi.org/10.1049/cp:19950699
8. Zanin M, Messelodi S (2003) An efficient vehicle queue detection system based on image processing. In: 12th IEEE International conference on image analysis and processing, pp 232–237. https://doi.org/10.1109/ICIAP.2003.1234055
9. Yao Y, Wang K, Xiong G (2013) Embedded technology and algorithm for video-based vehicle queue length detection. In: IEEE international conference on service operations and logistics and information, pp 45–50. https://doi.org/10.1109/SOLI.2013.6611379
10. Kumar S, Pant M, Ray A (2011) Differential evolution embedded Otsu's method for optimized image thresholding. In: World congress on information and communications technologies (WICT), pp 325–329. Mumbai. https://doi.org/10.1109/WICT.2011.6141266
11. Cheek Marshall T (2006) Improvements to a queue and delay estimation algorithm utilized in video imaging vehicle detection systems. Texas A&M University, M.S.
12. Li Z, Li N, Liu F (2009) An effective calculating method of signalized intersection delay. In: International conference on digital image processing, pp 211–215. Bangkok. https://doi.org/10.1109/ICDIP.2009.41

13. Shirazi M, Morris B (2014) Vision-based turning movement counting at intersections by cooperating zone and trajectory comparison modules. In: 17th International IEEE conference on intelligent transportation systems, pp 8–13. Qingdao. https://doi.org/10.1109/ITSC.2014.6958188
14. Zhang QN, Sun YD, Yang J, Liu HB (2016)Real-time multi-class moving target tracking and recognition. IET Intell Transp Syst 10(5):308–317. https://doi.org/10.1049/iet-its.2014.0226.
15. Thomas H (2013)Real time identification of platoons under indian traffic conditions. M. Tech, Indian Institute of Technology Madras
16. Kogut G, Trivedi M (2002) A wide area tracking system for vision sensor networks. In: 9th World congress on intelligent transport systems. Chicago
17. Tarko A, Naredla L (2002) Monitoring red light running using tripwire video detection systems. In: 81st Annual meeting. Transportation Research Board
18. Saha S, Basu S, Nasipuri M, Basu D (2009) Development of an automated red light violation detection system (RLVDS) For Indian vehicle. In: IEEE National conference on computing and communication systems (COCOSYS-09), Burdwan, pp 59–64
19. Lim D, Choi S, Jun J (2002) Automated detection of all kinds of violations at a street intersection using real time individual vehicle tracking. In: IEEE southwest symposium on image analysis and interpretation. https://doi.org/10.1109/IAI.2002.999903
20. Klubsuwan K, Koodtalang W, Mungsing S (2013) Traffic violation detection using multiple trajectories evaluation of vehicles. In: 4th International conference on intelligent systems modelling & simulation (ISMS), pp 220–224. https://doi.org/10.1109/ISMS.2013.143
21. Talab AM, Huang ZC, Jiang X (2014) Video background extraction using improved mean algorithm and frame difference method. Research J Appl Sci Eng Technol 7(22):4795–4800. https://doi.org/10.19026/rjaset.7.866
22. Zivkovic Z (2004) Improved adaptive Gaussian mixture model for background subtraction. In: 17th International conference on pattern recognition. Cambridge, pp 28–31. https://doi.org/10.1109/ICPR.2004.1333992
23. Zhang Y, Zhao C, He J, Chen A (2016) Vehicles detection in complex urban traffic scenes using Gaussian mixture model with confidence measurement. IET Intell Transp Syst 10(6):445–452. https://doi.org/10.1049/iet-its.2015.0141
24. Srilekha S, Swamy G, Krishna A (2015) A novel approach for detection and tracking of vehicles using Kalman Filter. In: Proceeding of the international conference on computational intelligence and communication networks. Kolkata, pp 234–236. https://doi.org/10.1109/CICN.2015.53
25. Kaehler A, Bradski GR (2008) Learning Opencv, 1st edn. O'Reilly, Sebastopol
26. Shapiro, Linda G, Stockman GC (2001) Computer vision. 1st ed. Pearson
27. Ester M, Kriegel HP, Sander J, Xu X (1996) A density-based algorithms for discovering clusters in large spatial databases with noise. In: 2nd International conference on knowledge discovery and data mining. Oregon, pp 226–231
28. Aziza RS, Karim MR, Saifizul A, Yamanaka H (2014) The effect of gross vehicle weight on platoon speed and size characteristics on two-lane road. In: 2nd International conference on Innovative Trends in Multidisciplinary Academic Research (ITMAR). Istanbul, pp 708–724
29. Chan YM, Huang SS, Fu LC, Hsiao PY, Lo MF (2012) Vehicle detection and tracking under various lighting conditions using a particle filter. https://doi.org/10.1049/iet-its.2011.0019
30. Coifman B, Beymer D, McLauchlan P, Malik J (1998) A real-time computer vision system for vehicle tracking and traffic surveillance. https://doi.org/10.1016/s0968-090x(98)00019-9
31. Lu G, Kong L, Wang Y, Tian D (2014) Vehicle trajectory extraction by simple two-dimensional model matching at low camera angles in intersection. https://doi.org/10.1049/iet-its.2013.0151
32. Korsah G, Stentz A, Dias MB (2007) The dynamic Hungarian algorithm for the assignment problem with changing costs. Robotics Institute, Pittsburgh, PA, Technical Report

33. Munkres J (1957) Algorithms for the assignment and transportation problems. J Soc Indus Appl Math 5(1):32–38. https://doi.org/10.1137/0105003
34. Trinayani K, Sirisha B (2015) Moving vehicle detection and tracking using GMM And Kalman filter on highway traffic. Int J Eng Technol Manage Appl Sci 3(5):309–315
35. Satzoda R, Suchitra S, Chia J (2012) Vision-based vehicle queue detection at traffic junctions. In: 7th IEEE conference on industrial electronics and applications (ICIEA). Singapore

Comparison of Delay Estimation Techniques for Advanced Traffic Management

P. B. Renju, Nitin Navali, and Lelitha Vanajakshi

Abstract Estimating delays at different road segments and intersections is a primary step in any traffic management system. Delay along a path can be estimated using sensors such as Global Positioning System (GPS) sensors, Camera sensors, Wi-Fi sensors and On-Board Diagnostics (OBD) data of the vehicle. The former three techniques have been used for some time now, but the latter one has not been explored much, especially for estimating delay. The accuracy of methodologies using OBD, Wi-Fi and Camera was calculated using data from GPS as ground truth. Results obtained showed the performance of all these methods to be comparable. Choice of the right sensor may depend on various other factors such as cost, weather factors, accuracy, range, etc. Sometimes more than one sensor needs to be used for the desired results. This paper explores three techniques in more detail and summarizes the advantages and disadvantages of each one of them in various scenarios.

Keywords Delay estimation · Image processing · On-Board Diagnostics (OBD) data · Wi-Fi sensors · Global Positioning System (GPS)

1 Introduction

Traffic congestion is one of the most concerning issues in almost every city in the world. In addition to the wastage of productive time, congestion also contributes to air and noise pollution and wastage of fuel. Thus, there is an increasing demand for transport management systems for reducing delays, accidents and environmental problems. A major part of urban congestion can be attributed to the presence of intersections. Currently, major intersections in India are operated by traffic police

P. B. Renju · N. Navali
Department of Civil Engineering, Indian Institute of Technology Madras, Chennai, India

L. Vanajakshi (✉)
Department of Civil Engineering, and Faculty, Robert Bosch Centre for Data Science and Artificial Intelligence, IIT Madras, Chennai, India
e-mail: lelitha@civil.iitm.ac.in

L. Devi et al. (eds.), *Proceedings of the Sixth International Conference of Transportation Research Group of India*, Lecture Notes in Civil Engineering 273,
https://doi.org/10.1007/978-981-19-4204-4_21

personnel based on their perception of the prevalent traffic condition. This might be reasonably effective at the local level but renders ineffective at a network level. There has been extensive research on mitigating this issue with the help of Intelligent Transportation Systems (ITS). However, it requires abundant data to understand the prevalent traffic conditions. Application of a wide range of traffic sensors plays a vital role in getting such data. However, majority of the commonly used sensors, such as traditional loop detectors, do not work well under the heterogeneous and laneless traffic conditions existing in many countries, including India [1].

Alternative solutions include the use of GPS sensors, Wi-Fi sensors and Camera sensors. With industry 4.0 and the Internet of Things, vehicles on the road are expected to be connected and share data with each other. Vehicles these days have numerous sensors to measure speed, accelerator pedal position, engine rpm, etc. Such sensor data can be obtained from OBD II port. These sensor values can be used to estimate the approach delays at intersections, which then can be communicated to the vehicles around. This study explores the utilization of OBD data for the estimation of intersection delay.

One of the earliest literatures on OBD data for traffic applications was [2], which proposed a method of collecting vehicle behaviour using OBD. The use of OBD data for accident analysis was reported in [3], where they developed an android-based application to detect accidents using G force and airbag trigger data from OBD II. Driving behaviour analysis using OBD data, which included vehicle speed, engine RPM and throttle position, was reported in [4]. Use of OBD data for evaluating vehicular emissions [5], and quantifying the relationship between driving stress and traffic conditions [6], were some of the other reported studies.

Since the original use of OBD was to monitor vehicle status, research using OBD data was mainly at microscopic levels. In addition, all the reported studies on the use of OBD data for traffic analysis were from homogeneous and lane-disciplined traffic. No studies were reported on the use of OBD data under heterogeneous and laneless traffic. Leveraging additional information about the traffic conditions from OBD will be useful in analysing complex traffic conditions, such as heterogeneous and non-lane-based traffic conditions.

Researchers have been analysing traffic behaviour using conventional techniques such as ground-based time-lapse photography [7], moving car observer method [8], etc. However, these required specific infrastructures, which may not be very cost-effective. There has been a shift in measurement techniques towards advanced sensors [9], such as GPS, Wi-Fi and Bluetooth sensors, which are relatively inexpensive and provide extensive coverage. Several researchers have used GPS sensors to estimate intersection delay. For example, the speed profile from GPS trajectory data to identify stopped time delay were used in [10, 11]. Acceleration profiles were used in [12] to identify the points at which deceleration begins while approaching an intersection and acceleration ends after crossing the intersection, to obtain the intersection control delay. However, all these studies were done for lane-based traffic.

Similar studies under heterogeneous and laneless traffic conditions are limited. Khadhir et al. [13] had estimated delay from Wi-Fi sensors and camera data, and gave a comparative analysis. Anusha et al. [14] reported a model-based estimation

scheme to estimate queue and, in turn, delay using traditional detector data. Accurate estimation of delay under heterogeneous and non-lane-based traffic using emerging sensors which are less infrastructure intensive is not reported and is the objective of this study. In this study, high-fidelity GPS is used as ground truth in order to assess the performance of other emerging techniques such as OBD, Wi-Fi and Camera sensor.

2 Estimating Delay Using On-Board Diagnostics Sensors

Present-day cars have multiple computers to control the engine, transmission, windows, locks, lights, etc. These computers are called Electronic Control Units (ECU) and they communicate with each other over a network, acting as the control centre of all the sensors present in the vehicle. The OBD II port acts as a gateway to receive the data from the ECU. There are several devices which scan the OBD port and list out various parameters such as speed, distance, fuel rate, throttle position, etc. Vehicle Spy Neo Fire IV [15] is one such device and is used in this study. A hardware set-up is required to connect to the port and collect data. This is discussed in the next section.

2.1 Experimental Set-up and Data Collection

In this study, two vehicles were tested—a truck and a passenger car. The study stretch chosen is shown in Fig. 1. The data from truck was decrypted using a standard set-up file available as J1939 recordings. However, the car manufacturers are reluctant to share these codes and hence there was a need to reverse engineer the data from car OBD, which is obtained in the form of data packets. Data collection was done in two stages. First, a test ride was done using a Swift Dzire 2012 model.

The data received is in the form of packets as shown in Fig. 2, which contains several rows with each row representing a Parameter ID (PID) containing data bytes of various lengths. Each of these PIDs represents a particular sensor data in the car. However, there is no specific way of identifying them from the raw data. The process of sniffing the data for a required parameter is done by linking them to physical events. For example, if the PID for brake pedal is to be found out, press and release the brake pedal when the vehicle is at a standstill and identify the PID that shows variation corresponding to braking. Once the PID is identified, it can be mapped with the brake pedal sensor. Similarly, for many other parameters also, controlled tests were performed to identify their corresponding PIDs.

Each PID is a bunch of bytes and each byte consists of 8 bits that take the value of 0 or 1. Once a PID is identified and associated with a physical activity, particular bits for the event need to be filtered out. This is done by testing manually. For example, applying the brake pedal will toggle some bits to vary between 0 and 1. Some sensory data is stored in one bit, which is either 0 or 1. A sequence of bits corresponds to a parameter. The length of sequence is the number of consecutive bytes being triggered

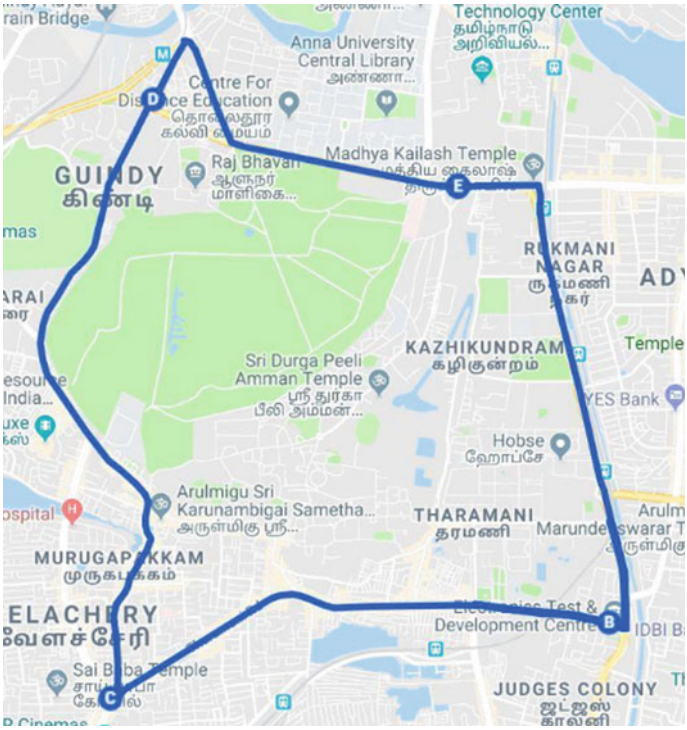

Fig. 1 Test ride route

Time (abs/rel)	Tx	Er	Description	Arbld/Header	Len	DataBytes	Network	Node	ChangeCnt	Timestamp
			Ethernet Status	162	3	00 00 00	neoVI		0	2019/03/27 08:17:56:072148
10.028 ms			HS CAN $120	120	6	00 03 1C 03 1C 03	HS CAN		808	2019/03/27 08:21:18:516686
10.028 ms			HS CAN $122	122	8	00 0F 0F 03 00 00 00 00	HS CAN		808	2019/03/27 08:21:18:516936
10.024 ms			HS CAN $124	124	8	00 1D 14 00 00 00 27 00	HS CAN		808	2019/03/27 08:21:18:517177
10.024 ms			HS CAN $136	136	4	00 00 40 78	HS CAN		92	2019/03/27 08:21:18:517347
20.046 ms			HS CAN $13F	13F	4	00 1D 20 00	HS CAN		155	2019/03/27 08:21:18:517515
12.009 ms			HS CAN $1AD	1AD	8	10 00 70 00 A4 44 02 00	HS CAN		673	2019/03/27 08:21:18:523565

Fig. 2 Snap from software displaying raw data

by a particular event. For example, vehicle speed was identified as 314 as its PID. It was seen that bits 0–15 changed, with changing speed. As speed increases, the bits from the right, i.e. from bit 0, change their value to 1. Visualizing this sequential bunch of 0s and 1s from the respective bits as a binary number and converting it to decimal gives an unscaled value of speed.

After identifying the bit position and length of the signal and converting the binary message to decimals, scaling needs to be done with the help of external data sources. If the required data is just a Boolean such as ON/OFF of the Left/Right indicator, there is no need of scaling. However, in cases such as speed, acceleration, RPM, fuel rates, etc., controlled tests with a recognized instrument for measuring the variable of

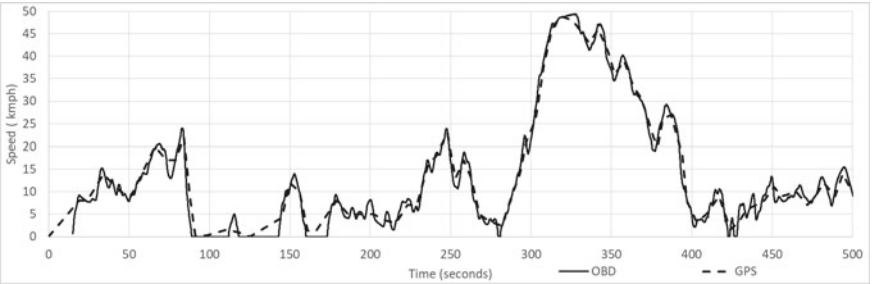

Fig. 3 Speed comparison of scaled OBD with GPS

Table 1 List of parameters and their corresponding IDs

	Wheel-based vehicle speed (kmph)	Trip distance (m)	Accelerator pedal position	Brake Pedal	Left/Right indicator
PID	314	314	120	318	3D0
Bytes	1,2	3,4	1,2	0	4
Bits	0,15	0,15	2,15	2	Left-6 Right-7
Factor for scaling	0.00766	0.0632	Min/Max scaling	Boolean	Boolean

interest has to be done to calibrate the sensor data obtained from OBD. For example, in the case of speed data, the scale factor was found with the help of a high-fidelity GPS unit. Figure 3 shows the plot of speed values obtained from OBD, after applying the scale factor along with speeds from GPS. A scaling factor of 0.0077 was found to give the closest speeds to the GPS.

Table 1 shows the list of parameters which have been identified in this study and corresponding PIDs and Bits. The factor for scaling is also given. Note that this is specifically for the probe vehicle under consideration and may vary with vehicle model. Hence, for every new vehicle model, this calibration may have to be done.

For the other PIDs, min–max scaling was used. For example, accelerator pedal position, where 0 represents the fully released pedal and 100 represents the pedal when it was pressed maximum, was converted using this method. Similarly, for brake pedal, 0 indicates released and 1 indicates brake applied. The same holds for left and right indicators where 0 indicates OFF and 1 indicates ON.

Similarly, several other parameters can be reverse-engineered, but the availability of the parameters depends on the vehicle chosen. Luxurious cars have extra sensors than the regular ones, but some basic parameters are available in all the vehicles. From the vehicle chosen in this study, speed, trip distance, accelerator pedal position, brake pedal and left/right indicators were identified.

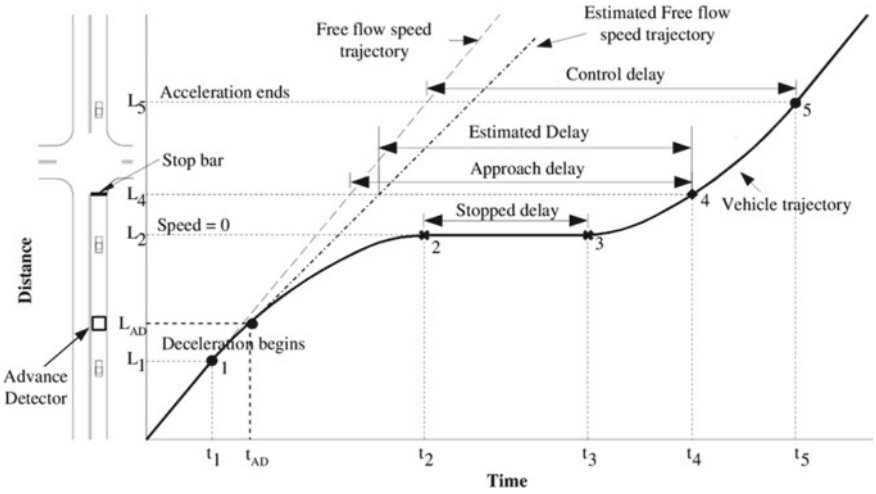

Fig. 4 Schematic distance–time diagram depicting all delay terms at a signalized intersection

2.2 Delay Estimation Using OBD Data

In this section, delay is computed using wheel-based vehicle speed and accelerator pedal position obtained from OBD unit. The delay calculated is compared with delay obtained using data from high-fidelity handheld GPS.

In order to calculate delay at an intersection using data at the microscopic level, such as the one obtained from OBD, the method suggested by [16] was used. Critical points as shown in Fig. 4 are identified first. The approach delay is then calculated by finding the timestamps of critical points as per Eq. 1.

$$Approach\ Delay = (t_4 - t_1) - \frac{L_4 - L_1}{s_f} \tag{1}$$

where,
t_1 = timestamp of start of deceleration on viewing the queue at the intersection
t_4 = timestamp of crossing the intersection stop line
L_1 = trip distance at start of deceleration
L_4 = trip distance at the intersection stop line
s_f = free-flow speed, taken as 40 kmph (11.11 ms^{-1}).

To identify the point of start of deceleration (t_1), it is evident that the accelerator pedal is released when the driver begins to decelerate on the approaching congestion at the intersection. Time corresponding to the pedal position (in percentage) being zero, as shown in Fig. 5, indicating fully released, is used for identifying this. From Fig. 5, t_1 is found to be 1986 s seconds. Speed plot can be used to find the point at which vehicle stops (the time at which the plot reduces to 0) and t_3, is the time when

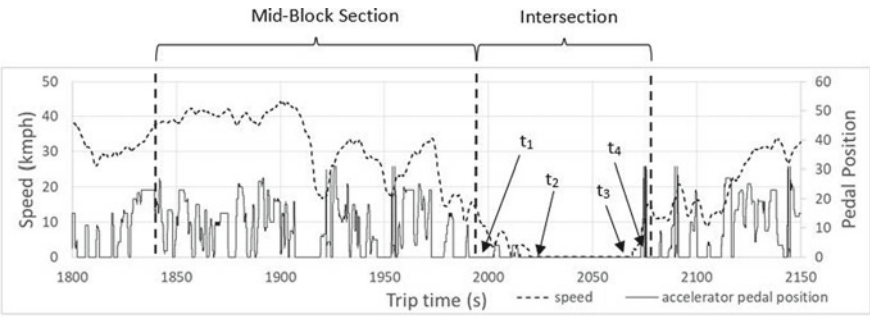

Fig. 5 Speed and acceleration pedal position plot from OBD unit

Table 2 Delay in the test route calculated through OBD and GPS

OBD (s)	GPS (s)	Absolute error (s)
132.7	130.8	1.9
40.0	33.1	6.9
87.4	79.5	7.9
154.7	153.0	1.7
183.5	192.4	8.9
89.9	90.6	0.7
22.5	20.6	1.9
156.3	152.9	3.4

speed becomes non-zero. The time point of crossing the intersection (t_4) is calculated with the help of trip distance data from OBD.

In order to evaluate the performance of the delay estimation from OBD, high-fidelity handheld GPS device was used in the test rides. GPS coordinates and timestamp data from the handheld GPS device were used to calculate delay. Table 2 shows the comparison of delays from OBD and GPS. It can be seen that the delay calculated through OBD is comparable to GPS. Mean absolute percentage error (MAPE) for this data set came out to be 5.63%, which shows that OBD is a very good source for delay estimation.

3 Estimating Delay Using Camera Sensors

Single pole-mounted camera was used for tracking individual vehicles over a 100m stretch of the road. Delay estimations were based on how much time individual vehicles took to enter the frame and leave the frame.

Figure 6a shows the location of the camera that was used for the experiment. It was placed on a foot over bridge near Indiranagar station in Chennai so that top-down

Fig. 6 **a** Location of the camera used for experiment. **b** Actual image captured by the camera

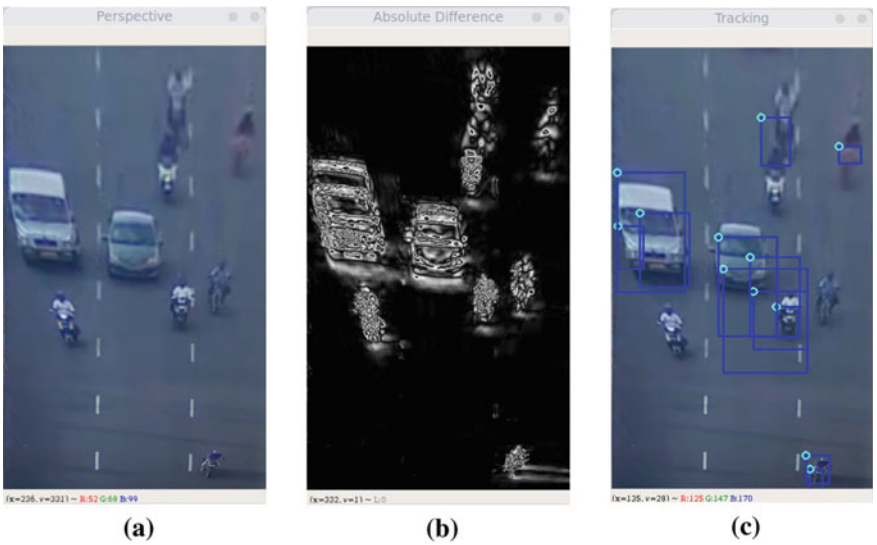

Fig. 7 **a** Cropped frame. **b** Grayscale frame after detecting moving vehicles. **c** Tracking of vehicles in progress

view along the length of the road could be captured. A 90m stretch of the road was captured as shown in Fig. 6b.

Figure 6b shows a sample frame captured by the camera for the experiment. Camera has a high field of view as seen from the image, but only a small portion of the scene covering road is required for further processing. This region of interest is manually marked, which is of trapezoidal shape due to the perspective view of the camera. Perspective transform is then performed on this region of interest to get

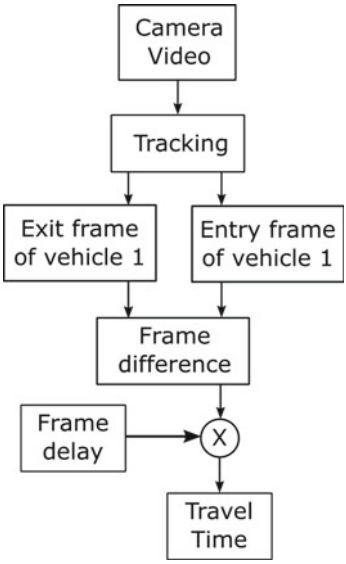

Fig. 8 Block diagram for the tracking mechanism

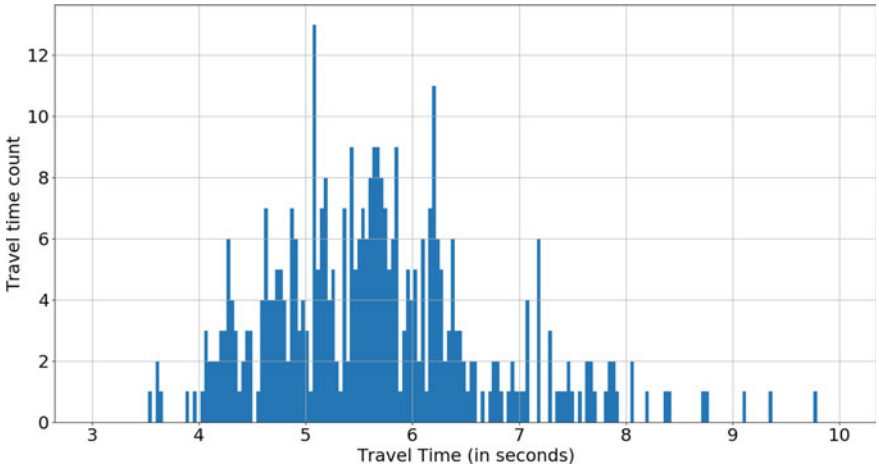

Fig. 9 Histogram of travel times of the vehicles

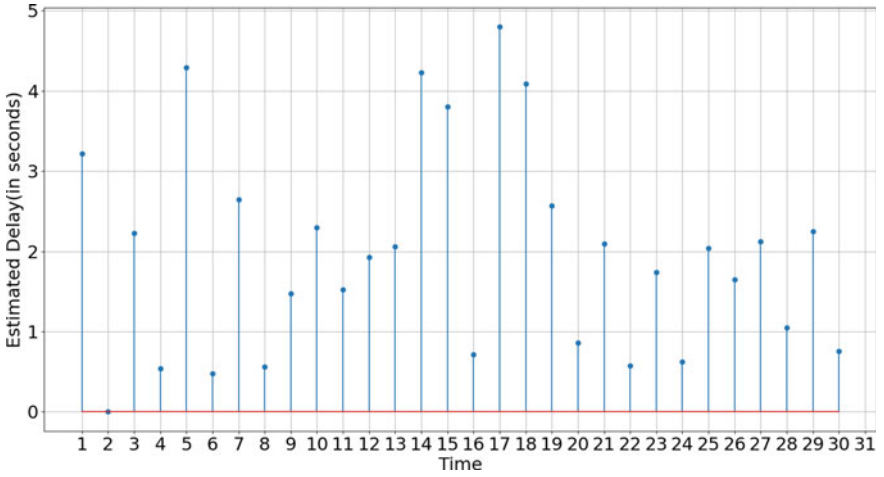

Fig. 10 Delays estimated using camera sensor

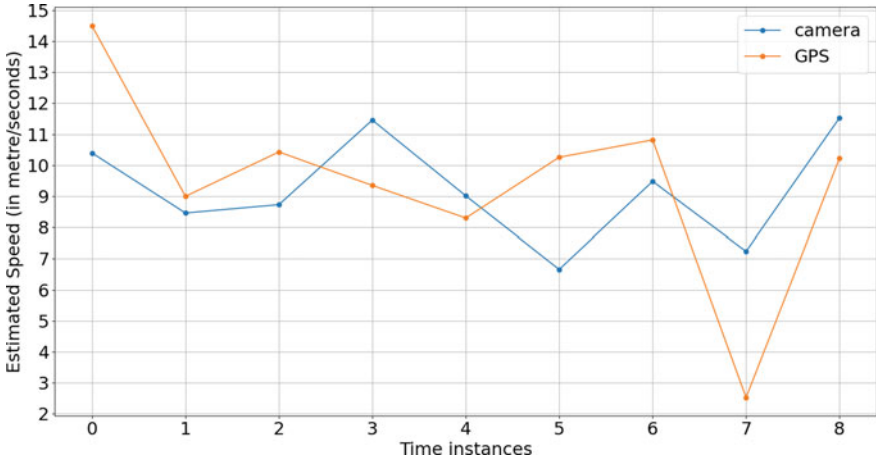

Fig. 11 Speed estimated using camera sensor and GPS

Fig. 7a. Since a video is nothing but a sequence of frames, it is possible to detect moving vehicles by subtracting adjacent frames along with some normalization and threshold operations. In this way, vehicles in motion will appear as shown in Fig. 7b. TrackCSRT module of OpenCV is used for tracking the vehicles. Tracking module is based on a discriminative correlation filter tracker with channel and spatial reliability [17]. It is then possible to obtain the exact frame at which vehicle entered the region of interest and the exact frame at which vehicle left the region of interest.

Figure 8 illustrates the block diagram of travel time estimation of individual vehicles. Initially, vehicles moving in the region of interest need to be detected. Once the

entry frame and exit frame of a particular vehicle have been found out, the difference in frames multiplied by frame delay, i.e. 40 ms (1/25th of a second, which is the property of the camera), will result in travel time within the region of interest, which is approximately 75 m long in our case.

For calculating delay within the region of interest, free-flow speed has to be estimated first. Travel times of vehicles were obtained within a span of 24 h in the region of interest. From this data, a histogram of travel time was plotted as shown in Fig. 9. The least time taken by the vehicle to cross the region was found to be 3.6 s and was taken as free-flow travel time. Free-flow speed is calculated using this number and the corresponding delay is then calculated as the difference between the actual travel time obtained and the free-flow travel time. Figure 10 shows the corresponding delay values for various time instances.

These estimated delays were validated with speeds obtained using GPS sensors. Travel speeds using GPS data were estimated through the haversine formula [18]. A sample plot is shown in Fig. 11. Root Mean Square Error (RMSE) obtained in this case was 2.65 m/s.

4 Estimating Delay Using Wi-Fi Sensors

Wi-Fi access points have the capability to detect Wi-Fi MAC (Media Access Control) addresses of mobile phones, laptops and other gadgets equipped with Wi-Fi hardware. If two Wi-Fi access points are kept at two locations on the same roadway, it is possible to detect the MAC ids at both locations. By taking the time stamp difference, the travel time between those two locations can be obtained. This idea has been used to estimate the travel times of vehicles in previous works of Khadhir et al. [13].

The data from Wi-Fi sensors consist of MAC IDs and respective timestamps. However, the vehicle might be travelling either upstream or downstream. Thus, a filtering mechanism is needed to filter out travel times in one direction. The mean travel time of all the vehicles crossing both Wi-Fi access points can be obtained for every minute. If the free-flow speed along this route is known, then the delay in the section of the road can be estimated.

For the purpose of this experiment, two Wi-Fi access points were fixed at two locations separated by a distance of 900 m as shown in Fig. 12. Devices under consideration were placed at Tidel Park Junction and PTK Nagar. As and when a device with Wi-Fi signal passes this route, the unique MAC address of the device and the time stamps get registered at both access points. Using the unique MAC ids and timestamps, the travel time and speed were calculated. To identify the free-flow speed in the selected study stretch, travel times were plotted as shown in Fig. 13.

From Fig. 13, it can be seen that the travel time values range from 61 to 164 s. Taking 61 s as the minimum travel time, the free-flow speed was found to be 53.11 km/h. Then,

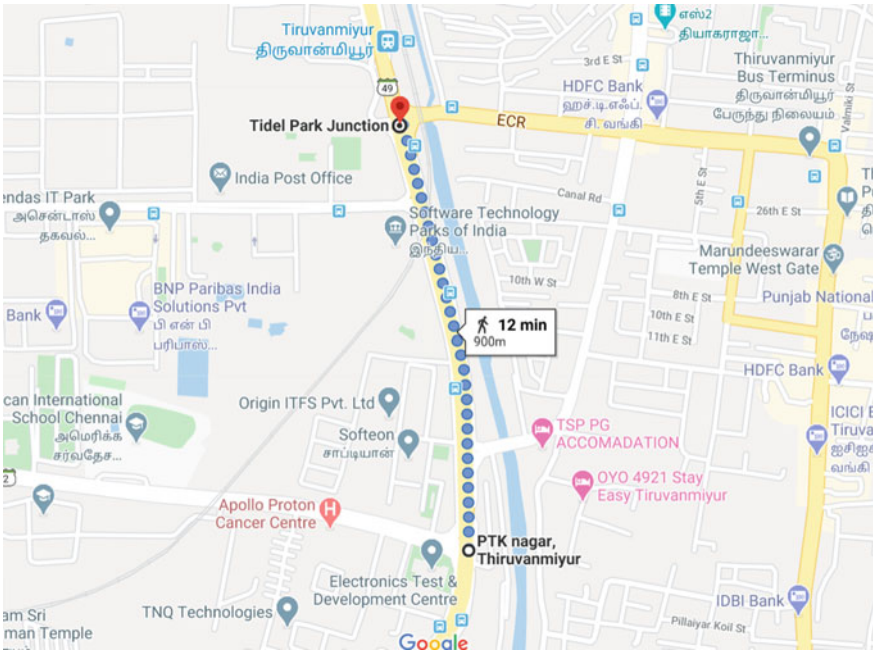

Fig. 12 Locations of the Wi-Fi access points

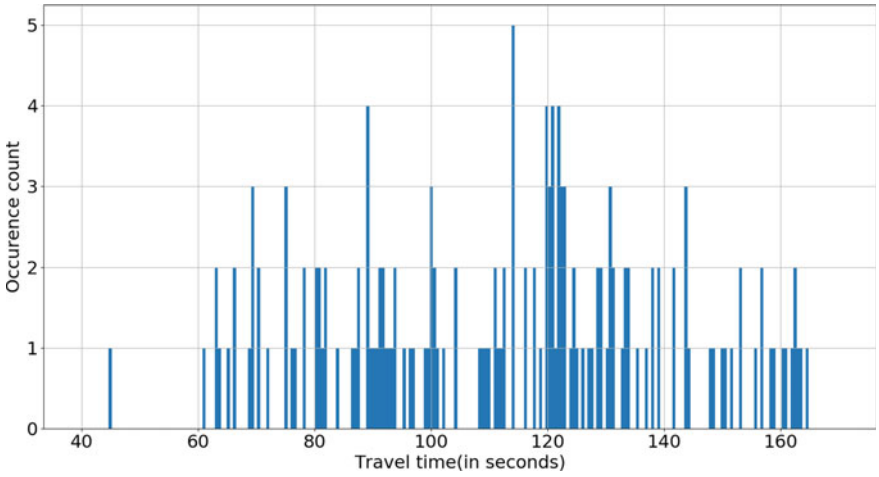

Fig. 13 Histogram of travel times between Wi-Fi access points

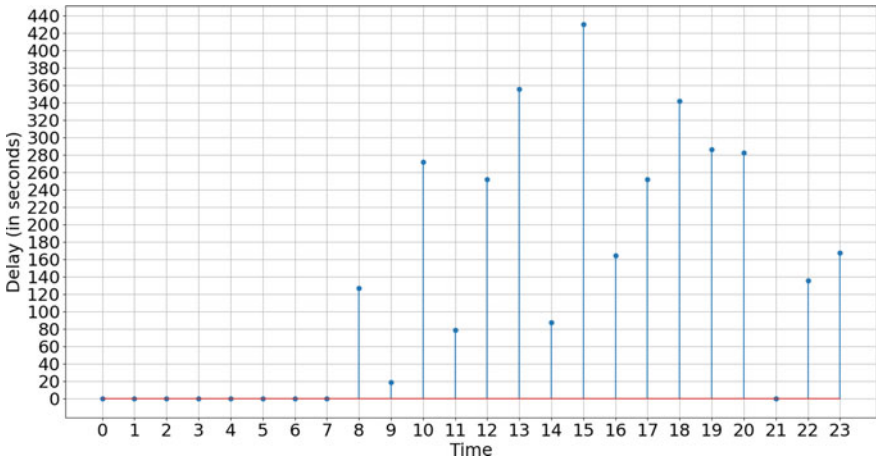

Fig. 14 Delay calculated using Wi-Fi sensors

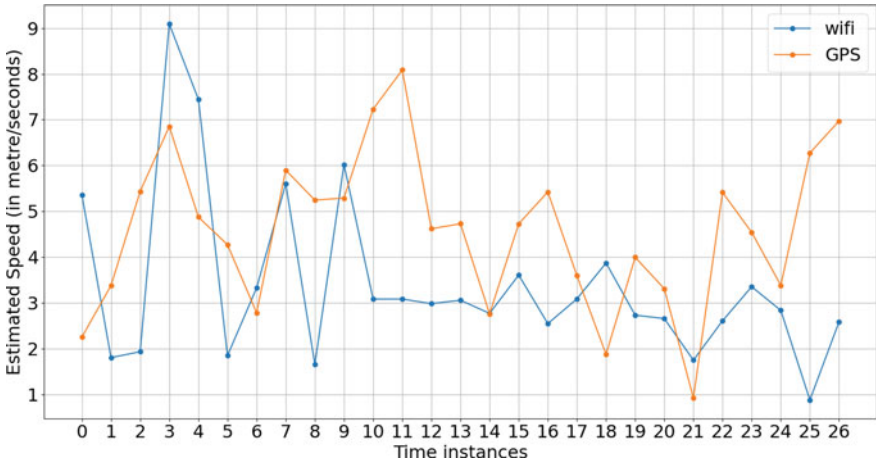

Fig. 15 Speed estimated using Wi-Fi sensor and gps sensor

$$Delay\ (s) = Mean\ travel\ time(s) - \frac{Distance\ (m)}{free\ flow\ speed\ (m/s)}. \tag{2}$$

As per the above equation, delay has been estimated from 5AM to 7AM, for every 5 min. Figure 14 shows a plot of the obtained delays. For validation purposes, speeds obtained using GPS were used again [18]. Figure 15 shows the comparison and the corresponding RMSE was found to be 2.56 m/s indicating a very high accuracy in delay estimates.

5 Comparison of Methodologies

All the above techniques for estimating delay are compared qualitatively on the basis of Accuracy, Sampling Rate, Cost of Installation, Weather and Time dependency, Operation Range and Bandwidth requirements in this section.

5.1 Sensing Accuracy

On-Board Diagnostic data have the highest accuracy among the four techniques, but such technology is not available in market now. The second best technique is using camera sensors accompanied by a good image processing algorithm. Of course, GPS with high sampling rate 1 Hz or more is always a direct way to obtain delays. However, GPS units of such fidelity are not commonly used for data collection. The use of Wi-Fi sensors showed the lowest accuracy, as expected. However, it is a cost-effective solution for large-range network-level data collection without user participation and hence can still be considered for field implementations.

5.2 Sampling Rate

Depending on the frame delay, camera sensor tends to have the highest sampling frequency 24 Hz. This is followed by OBD sensor which comes 10 Hz. This is followed by the high-fidelity GPS sensor 1 Hz and the Wi-Fi sensor, which captures data as and when a vehicle with an active Wi-Fi device crosses the sensor. Single Wi-Fi access point has a sampling rate of a few milliseconds, but since the same vehicle needs to register at both access points, the effective sampling rate will be lower.

5.3 Weather and Time Dependency

OBD sensors, GPS sensors and Wi-Fi sensors work irrespective of the time of the day and the weather conditions. However, camera sensing algorithm needs lighting for it to work. From experience, it has been shown that the detection accuracy of camera sensors reduces with climate change also.

5.4 Installation Cost

With the introduction of the Internet of Things, every car will be connected to the internet in future. With that, OBD data will be easily accessible for delay calculation with literally no installation cost. GPS sensors due to their easy accessibility are affordable solutions. This is followed by Wi-Fi sensors. Camera sensors have the highest installation cost of all the techniques.

5.5 Operation Range

Single-camera sensor has the least range of operation with only 90m. Wi-Fi sensors can be used in the range of 100–1000 m. GPS sensors and OBD sensors being tracking devices, do not have such constraints.

5.6 Bandwidth Requirement

Wi-Fi and GPS sensors have low bandwidth requirements for communicating to the server. OBD sensor has higher bandwidth requirement in comparison. Camera sensor has the highest bandwidth requirement as it is communicating close to 25 frames every second.

Table 3 summarizes the above comparisons.

Table 3 Summary of advantages and disadvantages

	OBD sensors	GPS sensor	Wi-Fi sensor	Camera sensor
Accuracy	High	Medium	Low	High
Sampling rate	High	Low	Low	Very High
Weather dependency	No	No	No	Yes
Installation cost	Lowest	Low	Medium	High
Operation range	NA	NA	1 km	90 m
Bandwidth	High	Low	Low	Highest

6 Conclusion

This paper explored different methods of estimating delay of vehicles at an intersection. Estimating delay with OBD data has been done, which is relatively a new approach and has great advantages over other techniques if put into use. Advantages and disadvantages of all the techniques have been discussed. This work should serve as a basis for engineers to plan the right technique to adopt for better traffic management.

Acknowledgements Authors acknowledge the 'Connected Intelligent Urban Transportation Lab', funded by the Ministry of Human Resource Development, Government of India, through project number CEMHRD008432.

References

1. Srivastava B (2011) A new look at the traffic management problem and where to start
2. Alessandrini A, Filippi F, Orecchini F, Ortenzi F (2006) A new method for collecting vehicle behaviour in daily use for energy and environmental analysis. Proc Inst Mech Eng Part D-J Automob Eng - PROC INST MECH ENG D-J AUTO 220:1527–1537
3. Zaldivar J, Calafate C, Cano J-C, Manzoni P (2011) Providing accident detection in vehicular networks through OBD-II devices and android-based smartphones, pp 813–819
4. Chen S-H, Pan J-S, Lu K (2015) Driving behavior analysis based on vehicle OBD information and AdaBoost algorithms. Lect Notes Eng Comput Sci 1:102–106
5. Ortenzi F, Costagliola M (2010) A new method to calculate instantaneous vehicle emissions using OBD data. SAE technical papers
6. Bitkina OV, Kim J, Park J, Park J, Kim HK (2019) Identifying traffic context using driving stress: a longitudinal preliminary case study. Sensors 19(9)
7. Buehler M, Hicks T, Berry DS (1976) Measuring delay by sampling queue backup. Transp Res Rec
8. Wardrop JG, Charlesworth G (1954) A method of estimating speed and flow of traffic from a moving vehicle. Proc Inst Civ Eng 3(1):158–171
9. Leduc G (2008) Road traffic data: collection methods and applications
10. Jiang Y, Li S, Zhu KQ (2005) Traffic delay studies at signalized intersections with global positioning system devices. ITE J (Inst Transp Eng) 75:30–39
11. Macababbad RJR, Regidor J (2011) A study on travel time and delay survey and traffic data analysis and visualization methodology
12. Ko J, Hunter M, Guensler R (2008) Measuring control delay components using second-by-second GPS speed data. J Transp Eng 134(8):338–346
13. Khadhir A, Himabindu M, Sreedhar S, Chilukuri BR, Vanajakshi L (2018) Comparative study of delay estimation methods at signalized intersections. In: Third national conference on recent advances in traffic engineering (RATE), SVNIT, Surat, India, pp 1–16
14. Anusha SP, Sharma A, Vanajakshi L, Subramanian SC, Rilett LR (2016) Model-based approach for queue and delay estimation at signalized intersections with erroneous automated data. J Transp Eng 142(5):04016013
15. Intrepid control systems, vehicle spy enterprise (2021). https://intrepidcs.com/products/software/vehicle-spy/. Accessed 12 May 2021
16. Quiroga CA, Bullock D (1999) Measuring control delay at signalized intersections. J Transp Eng 125(4):271–280

17. Lukežič A, Vojir T, Zajc LČ, Matas J, Kristan M (2017) Discriminative correlation filter with channel and spatial reliability. In: Proceedings of the IEEE conference on computer vision and pattern recognition, pp 6309–6318
18. Singla L, Bhatia P (2015) Gps based bus tracking system. In: 2015 international conference on computer, communication and control (IC4). IEEE, pp 1–6

Traffic Congestion Prediction Using Categorized Vehicular Speed Data

Manoj Kumar and Kranti Kumar

Abstract Traffic congestion has become a problem which is associated with our day-to-day life. Industrialization, urbanization, and the increasing population of cities have the main role in this problem. Transportation agencies in almost all the countries are trying their best to alleviate the traffic congestion problem. This study develops a traffic congestion evaluation method, which is categorized into four states named low, medium, congestion, and serious congestion. Convolutional long short-term memory (Conv-LSTM) neural network (NN) was trained to learn multivariate features as the inputs like categorized vehicular speed, time, and day of the week with respect to the traffic speed as an output of the whole stream. Trained model was used for short-term traffic speed prediction. Also, the prediction accuracy and stability of the Conv-LSTM NN has been compared with other neural network models, e.g., multi-layer perceptron (MLP), cascade forward back-propagation (CFBP), recurrent neural network (RNN), long short-term memory (LSTM) NN, and convolutional neural network(CNN). Results confirm that the Conv-LSTM NN achieves higher prediction performance than the compared models. Python 3.8.3 was used for programming purpose. Model code automatically selects 80% and 20% time intervals of the datasets in a random way for training and testing, respectively, from the traffic data. Furthermore, Conv-LSTM NN was combined with the developed congestion evaluation method and then the traffic congestion state was predicted. Study results confirm that the Conv-LSTM NN can be successfully applied for the prediction of traffic speed and traffic congestion status with non-homogeneous traffic in the Indian context.

Keywords Traffic congestion · Congestion index · Conv-LSTM neural network · Speed prediction

M. Kumar (✉) · K. Kumar
School of Liberal Studies, Dr. B. R. Ambedkar University Delhi, Delhi, India
e-mail: manojk.18@stu.aud.ac.in

K. Kumar
e-mail: kranti@aud.ac.in

L. Devi et al. (eds.), *Proceedings of the Sixth International Conference of Transportation Research Group of India*, Lecture Notes in Civil Engineering 273,
https://doi.org/10.1007/978-981-19-4204-4_22

1 Introduction

Traffic congestion affects the economy of a city and its environment as a direct and indirect effect [20]. A study conducted by the Council of Scientific and Industrial Research-Central Road Research Institute (CSIR-CRRI), Delhi, clearly suggests that commuters have to pay more for extra fuel consumption while driving on congested roads in Delhi. CSIR-CRRI preliminary estimate puts the wastage on fuel expenses at Rs 960 crore a day across India [7]. In another study done by CSIR-CRRI, it was found that poor upkeep encroachments cause traffic jams on internal roads in Delhi [6].

Traffic congestion directly affects an individual in the form of time loss, mental stress, increased travel cost, etc., whereas it affects the global level in the form of added pollution which leads to global warming. Traffic congestion prediction in advance provides the traffic management agencies, with the required time to divert the traffic on less congested routes or to take other suitable steps to make a smooth journey for travelers. Initial traffic forecasting models mainly focused on traffic parameter prediction such as flow, speed, and density under homogeneous traffic conditions. Most of the developed countries have homogeneous traffic and lots of research is available for homogeneous traffic prediction to mitigate traffic congestion [1, 21]. However, developing countries like India follow non-homogeneous (mixed) traffic. Research findings from homogeneous traffic can not be applied for mixed traffic scenarios, because vehicles do not follow proper lane discipline in a heterogeneous traffic stream. Traffic data collection is an important part to check the accuracy and reliability of developed models. Developed countries use modern equipment like road sensors, inductive loops, and installed video cameras to collect the real-world traffic data. However, these data collection equipment and techniques are costly [12].

Through the study of several models/algorithms on traffic prediction, it was noticed that most existing deep learning models [16, 25, 28] ignore the internal relationship between spatial and temporal information. Thus, the existing research seems insufficient for the prediction of traffic information in terms of traffic flow, speed, and congestion under mixed traffic conditions. This study presents a methodology to predict traffic congestion using the time series data of multi-locations. It predicts traffic congestion in four states namely low, medium, congestion, and serious congestion. Proposed traffic congestion states evaluation method is inspired by the method of Kong et al. [11]. In this paper, we applied the Conv-LSTM NN for traffic congestion prediction. The vehicular categorized data was employed to learn mixed traffic features and traffic speed was used as the target parameter. After training the model, target parameter from selected time steps was predicted. Then the congestion evaluation method was applied with the target parameter for the traffic congestion states forecast.

2 Literature Review

In this section, a brief overview is presented associated with ideas in the prediction of traffic flow, speed, and congestion. With the availability of big data, the development of artificial intelligence has led researchers to apply various models in this research area.

The autoregressive integrated moving average (ARIMA) model was applied to motorway data from France to predict traffic flow using previous traffic data [27]. Su et al. [24] proposed an incremental support vector regression (SVR) method for traffic flow prediction. A traffic flow prediction model named the Kalman filtering technique (KFT) was presented[13] and evaluated which can be applied to small input datasets. Hidden Markov model has been applied [30] for traffic congestion prediction during peak hours and its accuracy was checked with a neuro-fuzzy approach. MLP neural network was applied [14] for traffic flow prediction using past data collected from mixed vehicular traffic. Ma et al. [19] tested the effectiveness of LSTM NN with several traditional networks for speed prediction using the same real-time speed data collected from microwave sensors in Beijing. Bhatia et al. [3] implemented an LSTM architecture for real-time traffic flow prediction with an accuracy of 97% on the overall dataset. Gated recurrent units (GRU) NN and LSTM NN were used for traffic flow prediction and the experimental results demonstrate their better performance than ARIMA model [8]. Liu et al. [17] developed a deep learning model formed by combining CNN and LSTM NN, called Conv-LSTM for traffic flow prediction. A deep learning model was presented [9] to predict the traffic speed using RTMS sensors in Beijing. Boukerche and Wang [4] developed a deep learning model by combining the CNN and GRU models for traffic flow prediction. Mixed deep learning (MDL) model was introduced [18] for forecasting lane-level short-term traffic speed. MDL was constructed by using the Conv-LSTM layers. In the study of Inner Ring Road, Delhi, Rao and Rao [23] established the congestion thresholds on urban arterials to identify the traffic congestion in terms of speed using floating car data. Kong et al. [11] proposed a fuzzy evaluation method for traffic congestion estimation using trajectory data. Chakraborty et al. [5] used CNN, to detect traffic congestion from image-based data. Ranjan et al. [22] constructed a hybrid neural network by adding CNN, LSTM, and transpose CNN to predict the city-wide traffic congestion. A model named SG-CNN was proposed by Tu et al. [26] for traffic congestion prediction, which is inspired by the road segment grouping algorithm to optimize the training process. The aforementioned mentioned statistical methods like ARIMA models, nonparametric regression models, KFTs, and traffic flow theory-based models are primary models [1] which were used for traffic prediction problems. The statistical methods consider only time-series information of parameters, therefore these methods become inadequate to capture the changes in traffic parameters. To mitigate the drawbacks of statistical methods, various machine learning-based methods including SVR, k-nearest neighbor, locally weighted learning, and traditional neural networks (like MLP and CFBP, etc.) were applied. These models also appear weak to solve time-series problems having large data with variations. RNN was able

to learn the time-series information with the input of the previous time intervals from time-series data. However, RNN has failed to deal with gradient vanishing problems like remembering long-term historical information [2]. LSTM NN is known to deal with temporal problems over long sequence data. But, LSTM NN has some disadvantages: (1) it is challenging to use and (2) it is slow in processing when input and output sequences have a number of features. Similarly, CNN is known to deal with image processing problems by extracting the effective pixels from the image and it has been successful in object detection, segmentation, and image understanding. Unlike LSTM NN, CNN is capable of processing high-resolution multi-feature data because it has three abilities like local connectivity, weight sharing, and pooling. Thus, a combined network of LSTM and CNN i.e. Conv-LSTM can be successful to learn long-term time series data with a number of input features.

Till date, limited research exists associated with the deep learning approach to deal with traffic congestion prediction. The aim of this study is the accurate prediction of traffic congestion for short-term duration. In this article, Conv-LSTM neural network has been applied for traffic speed prediction. The network uses time-series data, which was collected at two different locations in Delhi city using video cameras. Then, the developed congestion evaluation method was applied to the predicted speed for the prediction of traffic congestion class.

3 Methodology

3.1 Study Data

Traffic data were collected from Majnu ka Tila, Delhi. Figure 1a shows the identified location. Selected location was having straight roads, clear site distance, and no traffic restrictions like intersections and mid-blocks. Outer Ring Road is one of the most important highways in Delhi. Its length is 47 km with a three-lane road. It connects Delhi areas as encircles like ISBT Kashmere Gate, Majnu ka Tila, Azadpur, Rohini, Vikash Puri, IIT Delhi Gate, Kalkaji, Okhla, and ISBT Kashmere Gate (Azadpur $\rightleftharpoons$ ISBT Kashmere Gate). Traffic data were collected from the foot over bridge at Majnu ka Tila using Sony Handycam 16.6 megapixels video cameras as shown in Fig. 1b. These cameras were fixed at a suitable height using camera stands. Data collection was done without disturbing the moving vehicles in the full traffic stream from 16 to 22 November 2020 (during 8:00 am–11:00 am in the morning peak and 4:00 pm-7:00 pm in the evening peak). Vehicles were classified into seven categories like Car/Van/Jeep, Motorcycle/Scooty, three-wheeler, Bus, Light Commercial Vehicle/Minibus/ambulance, Truck, and Cycle/Rickshaw. Data extraction was done using Kinovea window software from the recorded video film. Categorized vehicular travel time was calculated from a marked 30m road trap length and its corresponding speed was obtained by using speed, time, and distance relationship. For further analysis,

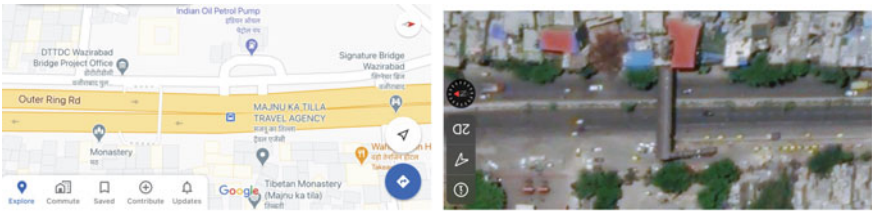

Fig. 1 Data collection locations with direction at the foot over bridge, Majnu Ka Tila, Delhi

Table 1 Summary of observed speed (in km/h) for different vehicle categories

	Intervals of 5 min				Intervals of 10 min			
Vehicle category	Min.	Max.	Mean	SD	Min.	Max.	Mean	SD
C/J/V	2.13	83.08	30.76	11.05	5.89	81.82	30.76	10.12
S/M	3.56	81.82	32.67	12.06	10.06	70.26	32.68	11.10
3W	3.08	69.23	28.07	10.38	4.79	51.92	28.08	9.33
Bus	3.77	63.16	22.23	8.16	4.89	56.25	22.24	7.37
LCV	2.35	67.50	25.38	10.03	4.07	70.34	25.61	9.66
Truck	1.66	61.02	22.13	7.59	4.52	71.76	22.29	7.72
Cycle	0.18	14.03	13.09	4.76	3.68	16.42	13.09	4.30
Average speed	4.46	49.56	24.96	7.24	7.97	43.46	24.97	6.91

[a] C/J/V—Car/Jeep/Van, S/M—Scooty/Motorcycle, 3W—Three-wheeler, LCV—Light commercial vehicle, Min—Minimum, Max—Maximum, SD—Standard deviation

extracted data in the intervals of 5 and 10 min were entered in an excel sheet for both directions.

As per location information, two datasets named input dataset and target dataset were prepared. Input datasets have 1008-time intervals and 504-time intervals (as rows) for time intervals of 5 min and 10 min, respectively, and 9 features (as columns) including time of day, day of the week, and categorized vehicular speed. Target dataset has 1008-time intervals and 504-time intervals (as rows) of 5 min and 10 min, respectively, and one features the average speed of categories vehicular speed. Variation of categorized vehicular speed is represented in Table 1. For all the models, previous data was used for predicting traffic speed in the upcoming 5 and 10 min of interval.

3.2 Conv-LSTM Neural Network

In this section, first, we give a brief introduction to LSTM NN and CNN. Then, we describe the structure of the Conv-LSTM model. To deal with the research gaps

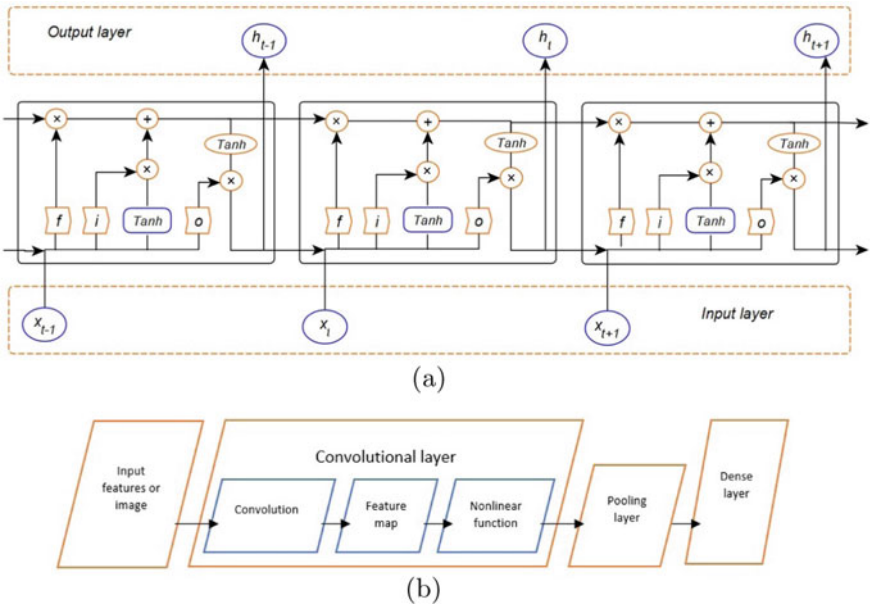

Fig. 2 Representation of structures **a** LSTM **b** CNN

described in the Sect. 2, LSTM neural network was originally proposed by Hochreiter and Schmidhuber [10]. LSTM neural network was proved more efficient than traditional RNN [19]. The hidden layer of the LSTM neural network is a memory block (LSTM block), which consists of the cell state c_t. The memory block also has three special gates, which are known as the input gate i_t, forget gate f_t, and output gate o_t. Due to the presence of gates and cell state, the output of LSTM NN gets influenced at every moment. These gates are activated using the Sigmoid activation function which produces the information in terms of a value lying in the interval of [0, 1], which can be understood from Fig. 2a. The network processes input sequence $x = (x_1, x_2, \ldots, x_N)$ by iterations from $n = 1$ to N in following equations (1)–(4):

$$i_t = \sigma(U_i x_t + V_i h_{t-1} + W_i C_{t-1} + b_i) \tag{1}$$

$$f_t = \sigma(U_f x_t + V_f h_{t-1} + W_f C_{t-1} + b_f) \tag{2}$$

$$g_t = \tanh(U_g x_t + V_g h_{t-1} + b_g) \tag{3}$$

$$o_t = \sigma(U_o x_t + V_o h_{t-1} + W_o C_t + b_o) \tag{4}$$

where Us, Vs, and Ws respectively are the weight matrices of input, recurring connections, and cell state, bs are the bias vectors. σ and $tanh$ are the Logistic (Sigmoid) and Hyperbolic tangent activation functions, which have been used for gates activation and cell activation, respectively. Along with these gates, the current internal cell state C_t and current hidden state (or output) h_t is defined as in the Eqs. (5) and (6).

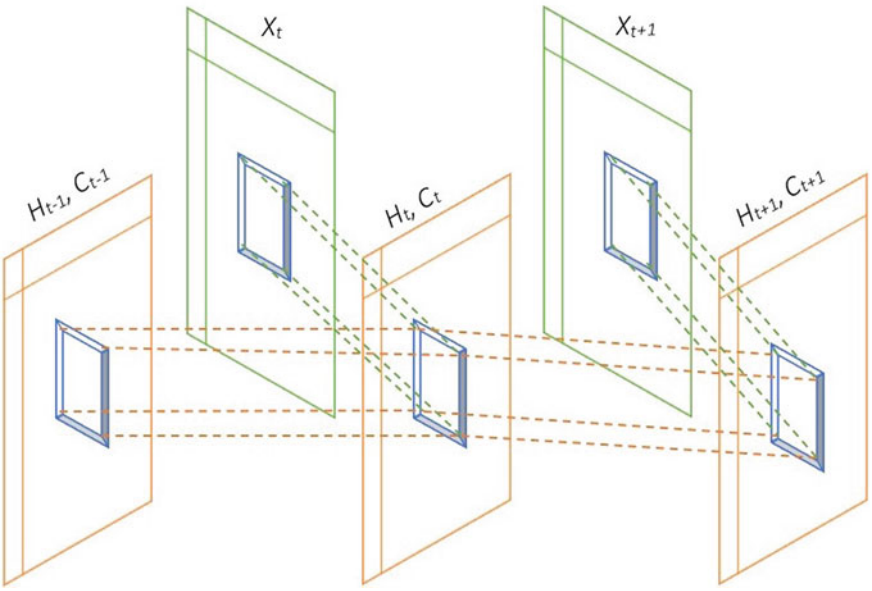

Fig. 3 Representation of Conv-LSTM NN

$$C_t = f_t \odot C_{t-1} + i_t \odot g_t \tag{5}$$

$$h_t = o_t \odot tanh(C_t) \tag{6}$$

During the training process, the weights and biases were initialized first. Afterward, the parameters were trained using back-propagation and gradient boost method was used to optimize the loss that occurred during this process. More description about the LSTM neural network can be found in [19].

The Conv-LSTM NN has the advantage of both CNN and LSTM. It also captures the spatial and temporal information of the traffic simultaneously. CNN is a type of deep learning network, which is specialized for feature extraction (or processing data). Detailed description about CNN can be found in [15]. The structure of CNN is shown in Fig. 2b. Conv-LSTM has similar processing equations to LSTM processing equations (1)–(6), but the variable dimension is different from the LSTM. $\mathcal{X}_1, \mathcal{X}_2, \ldots, \mathcal{X}_t$ are the input tensors, and their corresponding $\mathcal{C}_1, \mathcal{C}_2, \ldots, \mathcal{C}_t$ are cell states, and $\mathcal{H}_1, \mathcal{H}_2, \ldots, \mathcal{H}_t$ are hidden states. Note that $\mathcal{I}_t, \mathcal{F}_t$, and $\mathcal{O}_t$ are respectively three gates named input, forget, and output while all lie in $R^{P \times Q \times R}$ where P and Q respectively are the total rows and the total columns in the dataset; R is the length of each feature vector. The methodology of Conv-LSTM NN is expressed by Eqs. (7)–(11)

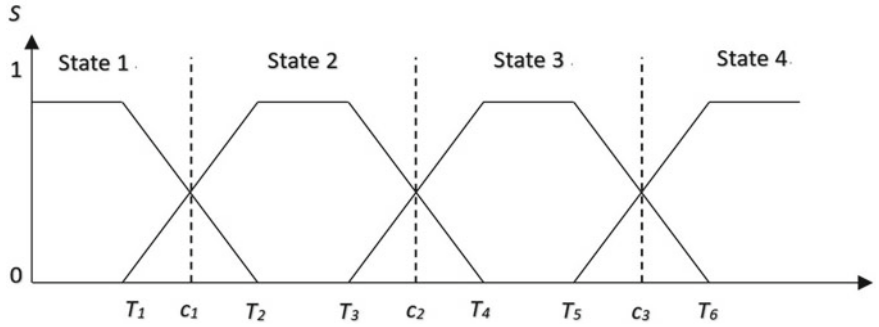

Fig. 4 Representation of membership function with congestion states

$$\mathcal{I}_t = \sigma_a(U_i \oplus \mathcal{X}_t + V_i \oplus \mathcal{H}_{t-1} + W_i \odot \mathcal{C}_{t-1} + b_i) \tag{7}$$

$$\mathcal{F}_t = \sigma_a(U_f \oplus \mathcal{X}_t + V_f \oplus \mathcal{H}_{t-1} + W_f \odot \mathcal{C}_{t-1} + b_f) \tag{8}$$

$$\mathcal{C}_t = \mathcal{F}_t \odot \mathcal{C}_{t-1} + \mathcal{I}_t \odot tanh(U_c \oplus \mathcal{X}_t + V_c \oplus \mathcal{H}_{t-1} + b_c) \tag{9}$$

$$\mathcal{O}_t = \sigma_a(U_o \oplus \mathcal{X}_t + V_o \oplus \mathcal{H}_{t-1} + W_o \odot \mathcal{C}_t + b_o) \tag{10}$$

$$\mathcal{H}_t = \mathcal{O}_t \odot tanh(\mathcal{C}_t) \tag{11}$$

where $\oplus$ represents the convolutional operator, $\odot$ represents the matrix multiplication; Us, Vs, and Ws are the weight tensors; bs are the bias tensors. Structure of Conv-LSTM is represented in Fig. 3 and more details about the network can be found in [18].

3.3 Traffic Congestion Measure

In this section, we derive a traffic congestion evaluation method, which is inspired by the fuzzy method. Developed congestion evaluation method was applied to generate evaluation sets in the form (low, medium, congestion, and serious congestion). In this method, first, membership function is determined along with the weight coefficients of the evaluation factor. Congestion evaluation method considers one or more traffic parameters as the evaluation factor. For simplicity and due to the availability of data, only one traffic parameter was considered, i.e., traffic speed. It is believed that the selected traffic speed parameter can characterize the traffic state accurately. Traffic congestion state was measured by exploring the traffic speed parameter. Identified traffic states play an effective role in the trips and traffic management system. Low, medium, congestion, and serious congestion categories were considered as the evaluation set.

To achieve this objective, the trapezoidal membership function was selected. It is a combination of piecewise linear and trapezoidal [29] as shown in Fig. 4, which can express knowledge of ambiguity caused by linguistic assessments by objectively

converting them into numerical variables. It determines the relationship between the evaluation factor (traffic speed) and the evaluation set for traffic congestion. Graph of membership function along with congestion states is shown in Fig. 4. In Fig. 4, $T_1, T_2, \ldots T_6$ are the linear ending values of the four clusters and are obtained by the K-means clustering technique and c_1, c_1, c_3 are thresholds for four congestion states corresponding to $T_1, T_2, \ldots T_6$. The expression of the proposed functional is represented as

$$S_1(v) = \begin{cases} 1, & v \le T_1 \\ \frac{T_2 - v}{T_2 - T_1}, & T_1 \le v \le T_2 \\ 0, & v \ge T_2 \end{cases} \quad S_2(v) = \begin{cases} \frac{v - T_1}{T_2 - T_1}, & T_1 \le v \le T_2 \\ 1, & T_2 \le v \le T_3 \\ \frac{T_4 - v}{T_4 - T_3}, & T_3 \le v \le T_4 \\ 0, & v \ge T_4 \end{cases}$$

$$S_3(v) = \begin{cases} \frac{v - T_3}{T_4 - T_3}, & T_3 \le v \le T_4 \\ 1, & T_4 \le v \le T_5 \\ \frac{T_6 - v}{T_6 - T_5}, & T_5 \le v \le T_6 \\ 0, & v \ge T_6 \end{cases} \quad S_4(v) = \begin{cases} \frac{v - T_5}{T_6 - T_5}, & T_5 \le v \le T_6 \\ 1, & v \ge T_6 \end{cases}$$

where $S_1(v)$, $S_2(v)$, $S_3(v)$, and $S_4(v)$, respectively, with the range of [0,1] are equivalant to traffic congestion states like serious congestion, congestion, medium, and low. Here, v_1 is the value of traffic speed, and its corresponding set $S = \{s_1, s_2, s_3, s_4\}$ correspond to serious congestion, congestion, medium, and low (called evaluation set). The value of proposed membership function r_{1j}, $j = 1, 2, \ldots, 4$ is determined for jth element of S with respect to traffic speed. Fuzzy evaluation set for a single parameter is expressed as in Eq. (12).

$$R = \begin{pmatrix} r_{11} & r_{12} & r_{13} & r_{14} \end{pmatrix} \tag{12}$$

After determining the fuzzy evaluation matrix, we can obtain the fuzzy comprehensive evaluation matrix B, which is represented in Eq. (13).

$$B = W \circ R = \begin{pmatrix} r_{11} & r_{12} & r_{13} & r_{14} \end{pmatrix} = (b_1, b_2, b_3, b_4) \tag{13}$$

where $\circ$ denote the fuzzy compositional operation and b_j denote the jth element of B. Applying max-membership principle, the biggest element $b = b_j$ of B represent traffic congestion state, as follow in Eq. (14)

$$b = b_j = \max(b_1, b_2, b_3, b_4). \tag{14}$$

4 Experiments

4.1 Performance Evaluation Metrics

This section describes the evaluation metrics, which have been utilized to determine the prediction performance and stability of applied models. During the experiments, metrics values were calculated from the predicted and the actual traffic speed. Equation (15)–(18) define the following metrics:

$$Mean\ squared\ error\ (MSE) = \frac{1}{n}\sum_{i=1}^{n}(\widehat{y}_i - y_i)^2 \quad (15)$$

$$Mean\ absolute\ error\ (MAE) = \frac{1}{n}\sum_{i=1}^{n}|\widehat{y}_i - y_i| \quad (16)$$

$$Mean\ absolute\ percentage\ error\ (MAPE) = \frac{1}{n}\sum_{i=1}^{n}\left|\frac{\widehat{y}_i - y_i}{y_i}\right| 100\% \quad (17)$$

$$Coefficient\ of\ correlation\ (CC) = \frac{\sum_{i=1}^{n}(\widehat{y}_i - \bar{\widehat{y}})(y_i - \bar{y})}{\sqrt{\sum_{i=1}^{n}(\widehat{y}_i - \bar{\widehat{y}})^2 \sum_{i=1}^{n}(y_i - \bar{y})^2}} \quad (18)$$

where y_i and $\widehat{y}_i$, respectively, are the actual and predicted speed during the ith time step from the test dataset; $\bar{y}$ is the mean of values of the y-variable and $\bar{\widehat{y}}$ is the mean of values of the $\widehat{y}$-variable; n is the total munber of predicted samples. Python 3.8.3 with the Keras 2.3.1, Tensorflow 2.0 was used for programming purpose.

4.2 Results and Discussion

To examine the prediction performance of applied NN models, each network was trained on 80% time intervals of datasets and tested (validated) on randomly selected 20% time intervals from the same datasets. All models were generated having similar architectures like input layers, output layers, and the number of the epoch which is shown in Table 2.

In a model, input layer receives the 9 features information (inputs) which includes time of the day, day of the week, and categorized vehicular speed and the output layer has one output i.e. traffic speed. In the process of information from inputs of the input layer into the output of the output layer, we need the activation function. The activation function produces a computer-understandable value. ReLU is a non-linear function and its range is between 0 and infinity.

Five different configurations of each network were designed for the prediction of traffic speed. Each configuration was having a single hidden layer and 150 epochs, while the number of hidden nodes were different. Each network performance was

Table 2 Structures of neural networks

Neural networks	Input feature	Output feature	Hidden layer	Epoch number	Activation function
MLP	Vehicular speed	Speed	1	150	Tansig
CFBP	Vehicular speed	Speed	1	150	Tansig
RNN	Vehicular speed	Speed	1	150	Tansig
LSTM	Vehicular speed	Speed	1	150	ReLU
CNN	Vehicular speed	Speed	1	150	ReLU
Conv-LSTM	Vehicular speed	Speed	1	150	ReLU

[b] Tansig—Hyperbolic tangent sigmoid, ReLU—Rectified linear unit

analyzed using metrics like MAE, MSE, MAPE, and CC. These models were trained by using the same training data of 5 min and 10 min intervals. Training and testing progress of Conv-LSTM model is shown in Fig. 5.

Prediction accuracy in 5 min and 10 min of interval for Conv-LSTM NN with other five neural network models MLP, CFBP, RNN, LSTM, and CNN is shown in the Tables 3 and 4. Best train of each model is highlighted in terms of hidden unit number, MAE, MSE, MAPE, and CC. Difference in the values of MAE, MSE, and MAPE between the best-performing model (LSTM) and Conv-LSTM are 0.2851, 0.2668, and 0.0124.

Table 3 shows that models MLP, CFBP, RNN, LSTM, CNN, and Conv-LSTM have highest coefficient of correlation values 97.47% (Train 4), 97.45% (Train 3), 96.46% (Train 1), 99.76% (Train 3), 99.49% (Train 2) and 99.98 % (Train 1) respectively for speed prediction in 5 min of interval. Table 4 shows that models MLP, CFBP, RNN, LSTM, CNN, and Conv-LSTM have highest coefficient of correlation values 97.12% (Train 1), 97.70% (Train 5), 97.59% (Train 1), 99.79% (Train 4), 99.88% (Train 4) and 99.93 % (Train 1), respectively, for speed prediction in 10 min of interval. Experimental results clearly show that the Conv-LSTM can capture both weekday and weekend time-series patterns. Furthermore, Conv-LSTM NN outperforms the other applied models in terms of accuracy and stability.

To analyze the congestion pattern for time intervals of testing dataset, developed congestion evaluation method was used. Congestion evaluation method has been described in Sect. 3.3. K-means clustering technique was used to determine the variables of congestion evaluation method which are shown in Table 5. In the values of the cluster, the first and second entries are the minimum and maximum values of the clusters, respectively.

Proposed congestion evaluation method classifies the traffic state (i.e., level of congestion) into four different categories namely low, medium, congestion, and serious congestion based upon traffic stream speed. Figure 6 represents a framework to

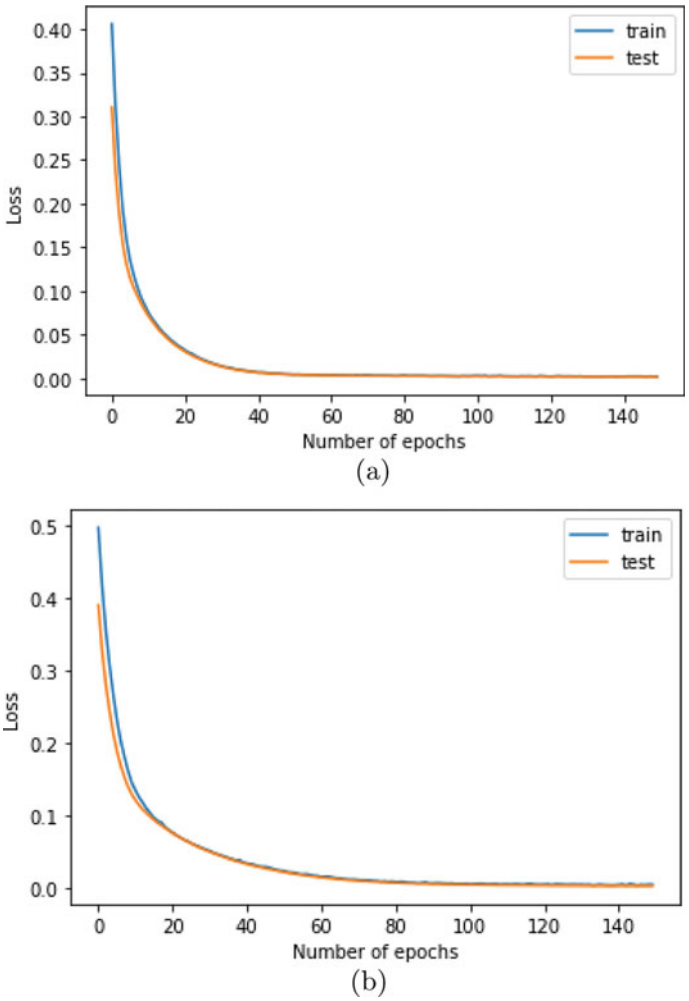

Fig. 5 Training progress and validation of Conv-LSTM model **a** for 5 min of intervals (Train 1) **b** for 10 min of intervals (Train 1)

predict the congestion state, in which the Conv-LSTM NN predicts traffic speed, and then developed evaluation method analyzes the type of traffic congestion state on the basis of the predicted speed. Table 6 shows some congested and non-congested time intervals using the developed congestion evaluation method. As per the time intervals, observed speed (average speed of categorized vehicular speeds) is taken from testing data, and predicted speed is the forecast speed corresponding to categorized vehicular speed (excluding average speed) from Conv-LSTM neural network. After that developed congestion evaluation method determines the congestion state according to traffic speed in terms of s_1, s_2, s_3, and s_4; where s_1, s_2, s_3, and s_4 represent serious

Table 3 Speed prediction for 5 min of intervals

	MLP					CFBP				
Model	Train 1	Train 2	Train 3	**Train 4**	Train 5	Train 1	Train 2	**Train 3**	Train 4	Train 5
HUN	10	25	40	**65**	80	10	25	**40**	65	80
MAE	1.1631	1.2130	1.1751	**1.1427**	1.2136	1.1300	1.2470	**1.1212**	1.2080	1.1781
MSE	4.7519	5.2385	4.8316	**4.7216**	5.0793	5.6828	5.9179	**5.5840**	5.6148	5.6079
MAPE	0.0649	0.0628	0.0637	**0.0623**	0.0755	0.0293	0.07668	**0.02346**	0.1319	0.0867
CC	0.9743	0.9675	0.9733	**0.9747**	0.9690	0.9744	0.9655	**0.9745**	0.9725	0.9736
	RNN					LSTM				
Model	**Train 1**	Train 2	Train 3	Train 4	Train 5	Train 1	Train 2	**Train 3**	Train 4	Train 5
HUN	**10**	25	40	65	80	10	25	**40**	65	80
MAE	**1.5213**	1.5607	1.5795	1.5926	1.5703	0.5507	0.5217	**0.3684**	0.4043	0.4447
MSE	**5.3077**	5.3228	5.3325	5.3380	5.3257	0.5429	2.0247	**0.2946**	0.7866	1.9515
MAPE	**0.0978**	0.1750	0.1391	0.1269	0.1179	0.0250	0.02221	**0.0165**	0.0181	0.0199
CC	**0.9646**	0.9634	0.9630	0.9624	0.9633	0.9958	0.9841	**0.9976**	0.9939	0.9852
	CNN					Conv-LSTM				
Model	Train 1	**Train 2**	Train 3	Train 4	Train 5	**Train 1**	Train 2	Train 3	Train 4	Train 5
HUN	10	**25**	40	65	80	**10**	25	40	65	80
MAE	0.9609	**0.5041**	0.6867	0.5051	0.9023	**0.0833**	0.2865	0.4987	0.0921	0.7470
MSE	1.7442	**0.6429**	2.5866	0.9664	1.7014	**0.0278**	0.1371	0.3616	0.0271	0.7685
MAPE	0.0439	**0.0223**	0.0309	0.0227	0.0557	**0.0041**	0.0136	0.0272	0.0054	0.0409
CC	0.9861	**0.9949**	0.9814	0.9934	0.9927	**0.9998**	0.9998	0.9998	0.9998	0.9997

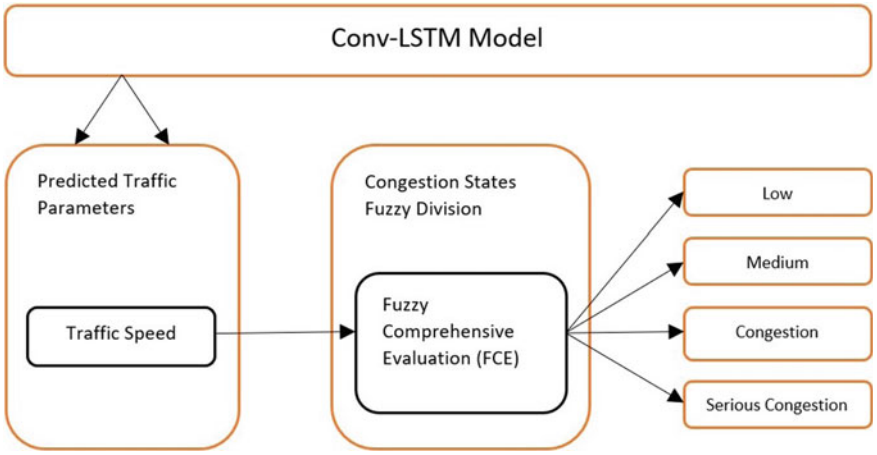

Fig. 6 Flow chart of traffic congestion state prediction with Conv-LSTM

Table 4 Speed prediction for 10 min of intervals

	MLP					CFBP				
Model	**Train 1**	Train 2	Train 3	Train 4	Train 5	Train 1	Train 2	Train 3	Train 4	**Train 5**
HUN	**10**	25	40	65	80	10	25	40	65	**80**
MAE	**1.0239**	1.0438	1.0430	1.0675	1.0535	0.9908	1.0345	1.0551	1.0256	**0.9708**
MSE	**3.8924**	4.1762	4.1719	4.1937	4.1788	4.2053	4.2750	4.0466	3.9742	**3.8195**
MAPE	**0.0718**	0.0762	0.1073	0.1266	0.0812	0.1217	0.0869	0.0621	0.04963	**0.02848**
CC	**0.9712**	0.9661	0.9663	0.9659	0.9662	0.9767	0.9720	0.9658	0.9711	**0.9770**
	RNN					LSTM				
Model	**Train 1**	Train 2	Train 3	Train 4	Train 5	Train 1	Train 2	Train 3	**Train 4**	Train 5
HUN	**10**	25	40	65	80	10	25	40	**65**	80
MAE	**1.0525**	1.1281	1.2525	1.3118	1.3263	0.9589	0.4232	0.3988	**0.3373**	0.3612
MSE	**3.6755**	3.7780	3.9629	4.0637	4.1008	1.7984	0.4566	0.5137	**0.2785**	0.2642
MAPE	**0.0994**	0.1027	0.0996	0.1185	1.1441	0.0478	0.0196	0.0179	**0.0159**	0.0187
CC	**0.9759**	0.9742	0.9710	0.9690	0.9687	0.9836	0.9958	0.9954	**0.9979**	0.9978
	CNN					Conv-LSTM				
Model	Train 1	Train 1	Train 3	**Train 4**	Train 5	**Train 1**	Train 2	Train 3	Train 4	Train 5
HUN	10	25	40	**65**	80	**10**	25	40	65	80
MAE	0.6871	0.3371	0.3468	**0.3013**	0.3261	**0.1167**	0.2827	0.2941	0.3428	0.1525
MSE	0.8405	0.2885	0.2465	**0.2210**	0.2382	**0.1002**	0.1945	0.1946	0.1956	0.1005
MAPE	0.0379	0.0151	0.0153	**0.0144**	0.0186	**0.0069**	0.0162	0.015	0.0205	0.0074
CC	0.9924	0.9982	0.9985	**0.9988**	0.9988	**0.9993**	0.9992	0.9992	0.9992	0.9993

[c] HUN—Hidden unit number, MAE—Mean absolute error, MSE—mean square error, MAPE—Mean absolute percentage error, and CC—Coefficient of correlation

Table 5 Linear values of four clusters

No of cluster	Values of cluster	Variable
1	07.97, 15.41	T_0, T_1
2	15.45, 20.88	T_2, T_3
3	20.98, 28.21	T_4, T_5
4	28.39, 43.46	T_6, T_7

congestion (SC), congestion (C), medium (M), and low (L), respectively. Testing datasets of 5 min intervals and 10 min intervals were used to generate Fig. 7 and it shows the comparison between predicted congestion state by predicted speed and estimated congestion state by observed speed. Figure 7 confirms that the predicted congestion state and observed congested state is almost the same. It affirms that the proposed method can be applied successfully to the prediction of traffic congestion state in non-homogeneous traffic.

Table 6 Congestion class prediction

Time intervals	Datetime	Obs. speed	*b* value	Obs. state	Pred. speed	*b* value	Pred. state
1	16-02-2021 10:25	13.92	1	s_1	14.12	1	s_1
2	16-02-2021 10:55	27.05	1	s_3	26.96	1	s_3
3	16-02-2021 16:25	23.92	1	s_3	23.90	1	s_3
4	16-02-2021 16:55	22.31	1	s_3	22.30	1	s_3
5	16-02-2021 17:25	30.29	1	s_4	29.92	1	s_4

[d] Obs.—Observed, Pred.—Predicted, s_1—Serious congestion, s_2—Congestion, s_3—Medium, s_4—Low

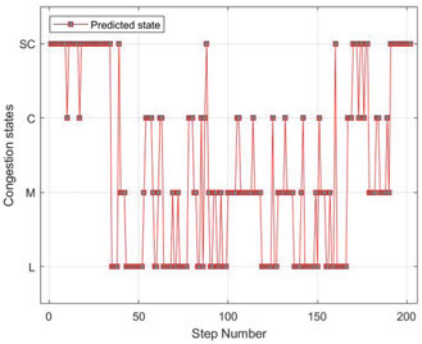

(a) Prediction with test data for 5 minutes

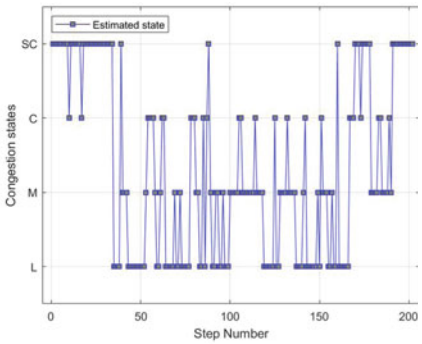

(b) Estimation with test data for 5 minutes

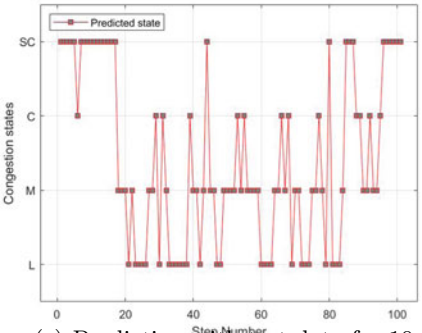

(c) Prediction with test data for 10 minutes

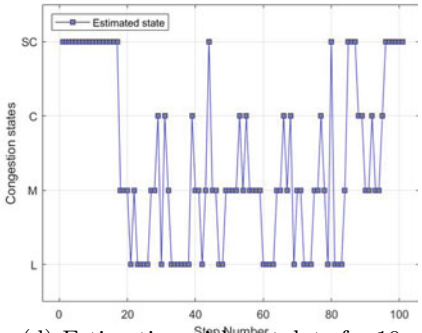

(d) Estimation with test data for 10 minutes

Fig. 7 Comparision between predicted and estimated congestion states

5 Conclusion

In this study, six neural network architectures were constructed with required properties having the same training and testing datasets. Each lag of datasets contains nine input features (e.g., Time of the day, day of the week, categorized vehicular average speed) and one output (e.g., average stream speed or traffic speed). For short-term traffic speed prediction, the performance of the networks was evaluated. The prediction accuracy of these networks was measured by metrics such as MSE, MAE, and MAPE, and stability by the coefficient of correlation (CC). Study results suggest that the Conv-LSTM neural network can be successfully applied for short-term prediction of traffic speed. In this article, our second aim was traffic congestion state prediction. For this purpose, we developed a congestion evaluation method based on the traffic speed using fuzzy comprehensive evaluation scheme. Finally, the developed congestion evaluation method was combined with the Conv-LSTM neural network which then predicted the traffic congestion state using categorized vehicular speed data. Study results clearly demonstrate that the Conv-LSTM neural network and congestion evaluation method can be successfully applied for traffic congestion prediction.

More datasets are required to test the efficiency and robustness of the proposed traffic congestion prediction method under diverse traffic conditions. Due to COVID-19-induced conditions, it was difficult for us to collect more amount of data. Future studies will focus on the collection of more data so that the proposed traffic congestion prediction method can be tested under different types of traffic conditions.

Acknowledgements This study was supported by the University Grants Commission (UGC), New Delhi, India, through the start-up grant research project "Modelling and simulation of vehicular traffic flow problems" through grant No. F.30-403/2017 (BSR), which is thankfully acknowledged. Financial support to the first author from UGC in the form of a Junior Research Fellowship (JRF) is also thankfully acknowledged.

Conflict of Interest Authors declare that they have no conflict of interest.

References

1. Bai M, Lin Y, Ma M, Wang P, Duan L (2021) Prepct: traffic congestion prediction in smart cities with relative position congestion tensor. Neurocomputing 444:147–157
2. Bengio Y, Simard P, Frasconi P (1994) Learning long-term dependencies with gradient descent is difficult. IEEE Trans Neural Netw 5:157–166
3. Bhatia J, Dave R, Bhayani H, Tanwar S, Nayyar A (2020) SDN-based real-time urban traffic analysis in vanet environment. Comput Commun 149:162–175
4. Boukerche A, Wang J (2020) A performance modeling and analysis of a novel vehicular traffic flow prediction system using a hybrid machine learning-based model. Ad Hoc Netw 106:102224
5. Chakraborty P, Adu-Gyamfi YO, Poddar S, Ahsani V, Sharma A, Sarkar S (2018) Traffic congestion detection from camera images using deep convolution neural networks. Transp Res Rec 2672:222–231

6. CSIR-CRRI: the council of scientific and industrial research-central road research institute conducted the study (2016). http://www.hindustantimes.com/delhi/poor-upkeep-encroachment-cause-jams-on-internal-delhi-roads-says-study/story-UlwR5FYUrmW2EUjtqJQtcK.html
7. CSIR-CRRI: the council of scientific and industrial research-central road research institute conducted the study (2017). http://www.hindustantimes.com/delhi-news/people-pay-more-for-extra-fuel-consumption-while-driving-on-delhi-s-roads/story-68rK37RfWJHX30UpFBFqWM.html
8. Fu R, Zhang Z, Li L (2016) Using LSTM and GRU neural network methods for traffic flow prediction. In: 2016 31st youth academic annual conference of chinese association of automation (YAC). IEEE, pp 324–328
9. Gu Y, Lu W, Qin L, Li M, Shao Z (2019) Short-term prediction of lane-level traffic speeds: a fusion deep learning model. Transp Res Part C: Emerg Technol 106:1–16
10. Hochreiter S, Schmidhuber J (1997) Long short-term memory. Neural Comput 9:1735–1780
11. Kong X, Xu Z, Shen G, Wang J, Yang Q, Zhang B (2016) Urban traffic congestion estimation and prediction based on floating car trajectory data. Future Gener Comput Syst 61:97–107
12. Kumar M, Kumar K, Das P (2021) Study on road traffic congestion: a review. In: Recent Trends in Communication and Electronics, pp 230–240
13. Kumar SV (2017) Traffic flow prediction using Kalman filtering technique. Procedia Eng 187:582–587
14. Kumar SV, Vanajakshi L (2015) Short-term traffic flow prediction using seasonal ARIMA model with limited input data. Eur Transp Res Rev 7:1–9
15. LeCun Y, Boser B, Denker JS, Henderson D, Howard RE, Hubbard W, Jackel LD (1989) Backpropagation applied to handwritten zip code recognition. Neural Comput 1:541–551
16. Li L, Qin L, Qu X, Zhang J, Wang Y, Ran B (2019) Day-ahead traffic flow forecasting based on a deep belief network optimized by the multi-objective particle swarm algorithm. Knowl-Based Syst 172:1–14
17. Liu Y, Zheng H, Feng X, Chen Z (2017) Short-term traffic flow prediction with conv-lstm. In: 2017 9th international conference on wireless communications and signal processing (WCSP). IEEE, pp. 1–6. https://doi.org/10.1109/WCSP.2017.8171119
18. Lu W, Rui Y, Ran B (2020) Lane-level traffic speed forecasting: a novel mixed deep learning model. IEEE Trans Intell Transp Syst 1–12. https://doi.org/10.1109/TITS.2020.3038457
19. Ma X, Tao Z, Wang Y, Yu H, Wang Y (2015) Long short-term memory neural network for traffic speed prediction using remote microwave sensor data. Transp Res Part C: Emerg Technol 54:187–197
20. Mahmuda Akhtar SM (2021) A review of traffic congestion prediction using artificial intelligence. J Adv Transp 2021. https://doi.org/10.1155/2021/8878011
21. Mohanty S, Pozdnukhov A, Cassidy M (2020) Region-wide congestion prediction and control using deep learning. Transp Res Part C: Emerg Technol 116:102624
22. Ranjan N, Bhandari S, Zhao HP, Kim H, Khan P (2020) City-wide traffic congestion prediction based on CNN, LSTM and transpose CNN. IEEE Access 8:81606–81620
23. Rao M, Rao KR (2016) Identification of traffic congestion on urban arterials for heterogeneous traffic. Transp Probl 11. https://doi.org/10.20858/tp.2016.11.3.13
24. Su H, Zhang L, Yu S (2007) Short-term traffic flow prediction based on incremental support vector regression. In: Third international conference on natural computation (ICNC 2007), vol 1. IEEE, pp 640–645
25. Tian Y, Zhang K, Li J, Lin X, Yang B (2018) LSTM-based traffic flow prediction with missing data. Neurocomputing 318:297–305
26. Tu Y, Lin S, Qiao J, Liu B (2021) Deep traffic congestion prediction model based on road segment grouping. Appl Intell 1–23
27. Williams BM (2001) Multivariate vehicular traffic flow prediction: evaluation of ARIMAX modeling. Transp Res Rec 1776:194–200
28. Wu Y, Tan H, Qin L, Ran B, Jiang Z (2018) A hybrid deep learning based traffic flow prediction method and its understanding. Transp Res Part C: Emerg Technol 90:166–180

29. Xiao Z, Xia S, Gong K, Li D (2012) The trapezoidal fuzzy soft set and its application in MCDM. Appl Math Model 36(12):5844–5855
30. Zaki JF, Ali-Eldin A, Hussein SE, Saraya SF, Areed FF (2020) Traffic congestion prediction based on hidden Markov models and contrast measure. Ain Shams Eng J 11:535–551

Data Imputation for Traffic State Estimation and Pre-diction Using Wi-Fi Sensors

Sarthak Chaturvedi, S. Deepak, Dhivya Bharathi, and Bhargava Rama Chilukuri

Abstract Real-time monitoring of traffic conditions is essential to support control strategies and provide useful information to travelers. With the accelerated development in transportation management systems (TMSs), traffic data collection methods have progressed rapidly. Despite the development in the data collection systems, there is missing data due to occasional sensor damage, trans-mission error, or a low penetration rate of the probe vehicle, thereby affecting the reliability and effectiveness of the Intelligent Transportation Systems (ITS). There is a need for effective data imputation methods to ensure the integrity and quality of traffic data. Two clustering-based methods for such traffic imputations are proposed in this paper—one using *k*-means clustering and the other using speed bins. Mean Absolute Percentage Error (MAPE) is used as a performance efficiency index for both methods. The Speed bin method was found to be more effective with a maximum MAPE of 13.8%. The maximum MAPE observed for the *k*-means clustering method is 22.6%.

Keywords Traffic data · Imputation · Clustering

1 Introduction

Traffic state monitoring is gaining potential interest from traffic management authorities. Travel time and the average speed of vehicles along a corridor are significant in understanding the traffic state of the corridor at any time of the day. Transportation managers and engineers use it for analyzing the performance of the corridors while travelers use it to decide their routes and mode of transport. Missing traffic data has been a cause of great concern and challenge for transportation professionals. Traffic state prediction could be extremely limited and wrong in the presence of missing traffic data. Hence, there is an urgency to find efficient traffic data imputation method to fill the missing data.

S. Chaturvedi (✉) · S. Deepak · D. Bharathi · B. R. Chilukuri
Indian Institute of Technology Madras, Chennai, India
e-mail: sarthakc97@gmail.com

L. Devi et al. (eds.), *Proceedings of the Sixth International Conference of Transportation Research Group of India*, Lecture Notes in Civil Engineering 273,
https://doi.org/10.1007/978-981-19-4204-4_23

It has been observed that transportation institutes in different countries have suffered different degrees of information deficit on traffic data starting from 15% in the US to 10% in China [1, 2]. Such missing values hamper the task of traffic forecasting. A random estimation or discarding of the cells with such missing values will affect the subsequent results. However, there are numerous other fields, such as statistics, medicine, hydro climatology, etc., which face similar problems. In recent years, many ITS engineers and researchers have found out that most of the imputation methods used in other domains are suitable for traffic imputation [3, 4] however, it lacks the theoretical reasoning/background. Imputation ideologies should be dealt with more than just replacing a number and they should reflect the prevailing traffic conditions in specific.

In this study, static Wi-Fi sensors capable of observing surrounding vehicles by the Media Access Control (MAC) identifier are used for data collection. These sensors can communicate traffic data to the server for real-time analysis. However, such systems are highly prone to missing and erroneous data, resulting in diminished datasets for analysis and real-time operation. Imputation is a technique to fill such missing data points with suitable estimated/predicted values. In this study, the feasibility and applicability of imputing missing data from static sensors along the corridor are studied. Further, imputation techniques used for homogeneous traffic conditions are straightforward and commonly based on the average speed of all vehicles across a period, as the speed variations are minimal. Heterogeneous traffic condition is a challenging case wherein the speed ranges are different for different classes of vehicles. This raises the need for analyzing the data for separate vehicle classes followed by imputation. The present study hypothesizes speed-based clustering to represent vehicle classes that reflect similar dynamic characteristics. In this study, a traffic flow theory-based background is framed to understand the prevailing traffic condition and imputation is carried out for individual vehicle classes. Overall, this study proposed an imputation methodology based on heuristics based on the traffic flow theory concept and clustering-based on speeds to represent vehicle classes.

The paper is organized as follows. The paper is organized as follows. Section 2 discusses the reported studies on imputation methodologies, Sect. 3 describes the data collection, description, and methodology while Sect. 4 discusses the results and inferences.

2 Literature Review

The imputation methods are commonly classified into four categories: prediction-based, interpolation-based, statistical learning-based method, machine learning-based and tensor-based methods. Prediction methods use the historical database to build models to predict the missing values in the database. A few studies [5–7] carried out prediction-based imputations for traffic data. ARIMA models are the most commonly used methods under prediction-based imputation. However, such models are site-specific and require training at different locations [8]. The interpolation-based

method uses the weighted average value of neighboring or historical data points to handle a missing value. Averaging can be based on temporal neighboring, which uses data from the same location, neighboring periods, or pattern neighboring, which uses data from locations/times having similar patterns. In this, K-NN is a commonly used method to identify suitable neighbors using appropriate distance metrics [9, 10]. A few studies [11, 12] have explored the feasibility and applicability of imputing missing traffic data using heuristic and statistical imputation techniques.

Statistical learning-based methods use the observed data to identify statistical properties like distributions and then inference the corrupted or missing value in an iterated fashion. A classical method used for the imputation is the Markov chain Monte Carlo (MCMC) method which generates a series of values to impute corrupted data points [13, 14]. Machine learning-based methods estimate the value by learning some complex relations between data points in history [15]. However, many of these methods fail to account for the spatial and temporal nature of the traffic data. They either consider just the temporal or just the spatial relation in the traffic data. Tensors-based methods have become increasingly popular in complex transportation datasets as they can develop multi-dimensional tensors that can explore a cross-functional relationship in spatiotemporal data [16]. However, such methods are highly data-intensive to learn the multi-dimensional relationships and may not be suitable for real-time implementations. Also, all of the above-said methods are based on data and have not considered the traffic flow theory concepts to understand the nature of prevailing traffic conditions. In addition, all of the above studies are carried out under homogenous traffic conditions. Heterogeneous traffic conditions like the one in India, are characterized by different vehicle classes traveling at different speeds. However, traditional methods impute a single value for a period, but there are no methods to address a range of values observed under heterogeneous traffic. Therefore, there is a need to develop a method for imputing missing values under heterogeneous conditions. In this regard, the present study attempts to develop an imputation methodology based on basic shock wave theory which infers the traffic condition. In the light of the shortcomings in various methods discussed above and traffic segments with a greater percentage of missing values for this end, we have proposed two clustering-based methods that can explore the scheme of travel time relation for various classes of vehicle in the traffic stream as a means to impute individual class speed and provide traffic planners with more comprehensive information on the traffic speed of the entire stream of vehicle.

3 Methodology

3.1 Data Attributes

Data from three consecutive sections of the road installed with static Wi-Fi sensors at each end of the sections are considered for this study. The data were obtained from the

road sections Madhya Kailash to FOB1, FOB1 to Tidel Park, and Tidel Park to SRP Tools which lay along the Old Mahabalipuram Road in Chennai, India, and is taken from January and February of 2020. The lengths of the sections are 0.7 km, 1.9 km, and 0.9 km respectively, and are three laned and contain three signals between them. The data used for imputation is the speed of the vehicles corresponding to the travel times as the three sections are of unequal length.

A network of static Wi-Fi sensors capable of sensing vehicles by their Media Access Control (MAC) address is installed at signalized intersections approximately 1 km apart [17]. MAC Ids recorded at sensor 1 are re-identified at sensor 2 to calculate the travel time of the vehicle in the section between these two sensors. The data obtained from these sensors is then used to prepare a comprehensive travel time database with missing and corrupted data in between which needs to be imputed.

The MAC address captured at location A at time $T1$ and location B at time $T2$ would have T2–T1 as the travel time in the section between A and B. The number of hits of a particular device's MAC address at the Wi-Fi sensor are generally high and spread across a few seconds. To pinpoint the timestamps $T1$ and $T2$, recording corresponding to maximum signal strength is used. The recording which has the maximum signal strength is assumed as the one closest to the sensor. This recording at the largest signal strength is then taken into consideration for further calculation. A minimum speed threshold of 5 km/h is kept during peak hours and 15 km/h during off-peak hours to neglect the travel time of pedestrians. A maximum speed threshold of 90 km/h (95th percentile value) is maintained in both cases to ignore errors. The above thresholds remove the errors from vehicles that have detoured from the route and have arrived at a later time, hence contributing to a slower speed. The thresholds thus ensure that we filter the data of vehicles that pass through the sensors at location A and location B without any stoppage or detour. The travel times are segregated into five-minute time bins, thus contributing to 288 bins over 24 h. Figure 1 shows the scatterplots of sample five-minute bin data at different periods. It can be seen the travel time ranges from the 90s to the 1200s reflecting the nature of heterogeneity in the samples observed.

The present study considered three consecutive sections of the road at three consecutive five-minute bins to experiment with the proposed imputation methodology. Table 1 shows the complete data setup required for a single imputation. The cells a11 to a33 comprise all the travel time data corresponding to that particular section at that particular period. The value to be imputed is a22 and will be done with the help of up-stream traffic (a11, a21, a12) and downstream traffic (a32, a13, a23). Cells a11, a21, a12 contribute to the traffic properties from the upstream side. Cells a32, a13 and a23 contribute to the traffic properties from the downstream side in a congested scenario.

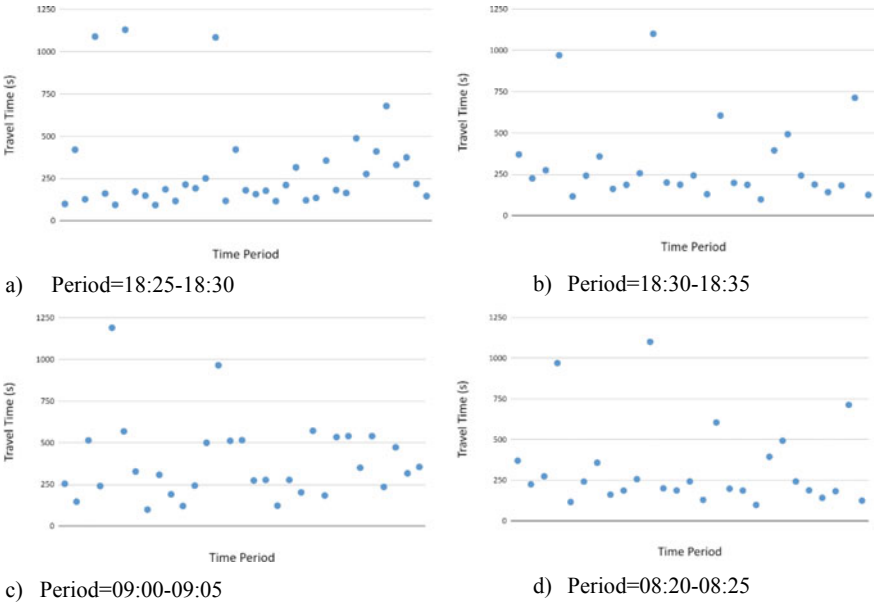

Fig. 1 Scatterplot of samples in different periods

Table 1 Sample imputation data representation

Interval	Section 1	Section 2	Section 3
T1–T2	a11	a12	a13
T2–T3	a21	a22	a23
T3–T4	*a31*	a32	a33

3.2 K-Means Clustering Method

The cell to be imputed is bordered by three cells from the upstream traffic and three cells from the downstream traffic. Each cell represents a five-minute bin for that particular section of the road. Each of these six cells is clustered by the speed of all the vehicles contributing to them to separate them into vehicle classes using the *k*-means algorithm. Brief pseudocode is shown in Algorithm 1. The optimal k used in the algorithm is obtained by finding the silhouette score [18] for different values of k. The value of k for which the silhouette score is maximum is considered the optimal k for the given data set. The silhouette score s(i) for point i is defined in Eq. 1.

$$s(i) = (b - a)/\max(a, b), \tag{1}$$

where a = Mean intra-cluster distance, b = Mean nearest-cluster distance.

Algorithm: 1 Pseudocode of k means clustering

Let v_i be the speed of the vehicle *i* observed during a five-minute interval.
Input: Speed of all the vehicles (v_1, v_2, …., v_n) in an interval,
the initial number of clusters *k* obtained using Silhouette score
(*k*<=5).
Output: Final number of clusters *k* and cluster centroids (c_1, c_2, …, c_k)

1. Place the centroids c_1, c_2, …, c_k randomly within the data points (vehicle speeds)
2. for each vehicle speed v_i:
   - find the nearest centroid (c_1, c_2, …, c_k)
   - assign the point to that cluster
3. for each cluster *j* = 1, ..., *k*
   - new centroid = mean of all points assigned to that cluster.
4. Repeat steps 3 and 4 until convergence or until the end of a fixed number of iterations
5. End

The present study assumed the maximum *k*-value as five, limiting to five vehicle classes on the section of the road considered. Table 2 shows a sample speed dataset from a five-minute bin segregated into two clusters based on the *k*-means algorithm. The silhouette scores obtained for this case are shown in Table 3.

As clustering of speed data does not directly take the vehicle class-specific features and interactions, the clusters are combined in case the mean cluster values are similar. The clusters of the three cells upstream are combined to match clusters based on similar properties. The heuristics comprise of the following set of rules:

Table 2 Sample clustered data

Speed data	Clustered data	Cluster number	Cluster centroids
8.99	23.90	–	–
23.90	32.70	–	–
32.70	19.24	–	–
19.24	23.31	–	–
5.82	22.04	1	22.65
14.47	27.07	–	–
23.31	17.57	–	–
22.04	20.05	–	–
27.07	17.94	–	–
17.57	8.99	–	–
20.05	5.82	2	9.76
17.94	14.47	–	–

Table 3 Sample silhouette score

k-value	Silhouette score
2	0.531
3	0.491
4	0.505
5	0.434

(1) Combine nearby clusters of the same cell if their difference is less than 3 km/h for speeds less than 25 km/h, less than 5 km/h for speeds less than 50 km/h, and less than 10 km/h for speeds greater than 50 km/h.
(2) Minimum cumulative difference of cluster centroids when combining different clusters across cells
(3) Combining should not happen if the difference between cluster centroids is greater than 5 km/h for speeds less than 30 km/h and greater than 10 km/h for speeds greater than 30 km/h, however, it should be treated as a separate cluster.

The reason for this heuristic is that different traffic regimes exist in different cells, but they may not be captured by the detector. Therefore, combining clusters with similar characteristics are done to determine the clusters for imputation. The speed of all the vehicles contributing to the matched clusters is combined to calculate an overall centroid. Similarly, the three cells contributing to the downstream traffic are clustered and combined to produce the output cluster centroids and are shown in Table 4.

The above heuristics are explained below using Table 4.

Class1: D1
Class 2: A1 + B1 + D2
Class 3: B2 + B3
Class 4: A2

Table 5 shows the sample of imputed data from upstream and downstream and the actual data. Vehicle classes 3 and 5 were not observed in the imputed data from downstream traffic. The aforementioned heuristics were implemented for ten

Table 4 Sample of upstream clusters

Cluster names	Cluster centroids
A1	22.65
A2	9.76
B1	21.21
B2	15.32
B3	14.02
D1	67.35
D2	21.70

Table 5 Comparison of upstream and downstream classes with the observed classes

Vehicle class	Speed (km/h)		
	Measured	Upstream	Downstream
Class 1	61.34	59.99	57.14
Class 2	38.80	39.54	32.24
Class 3	20.11	20.59	–
Class 4	12.05	14.85	10.76
Class 5	6.21	6.60	–

different periods, and the MAPE of the upstream and the downstream imputations were calculated.

3.3 Speed Bin Method

Another method explored for imputation is to classify the vehicles with a predefined number of clusters with predefined properties. To define the number of clusters, the upper and lower bound of the vehicle's speed captured by this network of static Wi-Fi sensors were analyzed. The maximum speed limit was found to be as high as 75 km/h, and the minimum speed was found to be 5–6 km/h. Considering the maximum speed that could be captured as 75 km/h, we equally divided the speed limits into five clusters, each representing a consecutive 15 km/h interval. To impute the missing cell, the vehicles from the upstream cells (explained before) are pooled together and classified based on their speeds into these five aforementioned clusters. This pooling was done as these vehicles were found to affect the traffic properties of the empty cell (a22) the most. Further, the mean of the speeds of each cluster is taken as the imputed speed value specific to that cluster for cell a22. Similarly, pooling was carried out in the downstream location, and clustering was performed on pooled data to get the imputed values. The following figure (Fig. 2) shows the upstream and downstream locations for the cell a22 (i.e., the red shaded cells are the upstream locations and the green shaded cells are the downstream locations).

Fig. 2 Data imputation based on speed bin method

3.4 Performance Efficiency (PE)

The accuracy of imputed data to the actual observed data is evaluated using the Mean Absolute Percentage Error (MAPE) method. To evaluate the performance efficiency of both the methods, some cells were randomly removed with known properties from the database and the results obtained from the *k*-mean clustering and the speed bin method were evaluated. The PE was obtained by comparing the values obtained in each cluster in both the methods with the respective values obtained in the original data. For this purpose, mean absolute percentage error (MAPE) was used as the performance index. Equation 2 defines the MAPE.

$$\text{MAPE} = \frac{1}{n}\sum_{t=1}^{n}\frac{|A_t - F_t|}{A_t} \tag{2}$$

where, At—Actual value, Ft—Forecast value, N—number of fitted points.

4 Results and Discussions

The scope of the present study is to impute the missing values in the real-time traffic speed/travel time database using static sensors. The data attributed using both the speed bin method and the *k*-means clustering method were statistically analyzed for fit by the Mean Average Percentage Error method. The results for the same are shown in Table 6.

Table 6 Comparison of speed bin and *k*-means clustering method

S. No	Time	MAPE			
		k-means clustering method		Speed bin method	
		Up-stream	Downstream	Up-stream	Downstream
1	18:05–18:20	0.87	13.37	7.65	4.8
2	18:10–18:25	15.6	18.5	4.93	10.85
3	18:15–18:30	10.46	4.93	8.38	4.43
4	18:20–18:35	7.2	11.47	2.6	7.44
5	18:25–18:40	11.34	6.95	4.38	2.77
6	18:30–18:45	12.04	15.82	7.54	8.57
7	18:35–18:50	16.04	7.22	3.13	3.97
8	18:40–18:55	10.62	22.66	7.24	6.61
9	08:20–08:35	14.45	13.73	10.37	13.82
10	10:20–10:45	9.36	10.3	7.92	6.68

The results suggest that the speed bin method performed significantly better than the *k*-means clustering method. The MAPE for the speed bin method was obtained in the range of 2–14%. For the same data, the *k*-means clustering showed a higher degree of variation from the original data, with MAPE ranging in the range of 0.8–23%. One reason for *k*-means clustering having lower imputation efficiency was that the properties and number of optimum clusters created in each surrounding cell differed from the other cells because of a different class of vehicles observed in the segments during the stipulated time interval. This problem is non-existent in the speed bin method as the number of clusters, and their properties are the same across all cells. One key observation made during this study suggests that the *k*-means clustering could be more efficiently used to represent greater vehicle classes as it can classify vehicles more efficiently in a closely spaced speed dataset. The predefined speed bin method fails when the speed difference in the observed dataset is less than the predefined limits. In such cases, *k*-means could make more and optimum number of clusters in such data.

It was observed in half of the instances that the downstream location performed better, whereas in another half upstream value was closer to the observed data on the ground. Such observation was because of congestion arising in either upstream or downstream locations, which doesn't let the traffic fleet reflect its similar behavior in the subsequent segment.

The results suggest that the speed bin method performed significantly better than the *k*-means clustering method. The MAPE for the speed bin method was obtained in the range of 2–14%. For the same data, the *k*-means clustering showed a higher degree of variation from the original data, with MAPE ranging in the range of 0.8–23%. One reason for *k*-means clustering having lower imputation efficiency was that the properties and number of optimum clusters created in each surrounding cell differed from the other cells because of a different class of vehicles observed in the segments during the stipulated time interval. This problem is non-existent in the speed-bin method as the number of clusters, and their properties are the same across all cells. One key observation made during this study suggests that the *k*-means clustering could be more efficiently used to represent greater vehicle classes as it can classify vehicles more efficiently in a closely spaced speed dataset. The predefined speed bin method fails when the speed difference in the observed dataset is less than the predefined limits. In such cases, *k*-means could make more and optimum number of clusters in such data.

It was observed in half of the instances that the downstream location performed better, whereas in another half upstream value was closer to the observed data on the ground. Such observation was because of congestion arising in either upstream or downstream locations, which doesn't let the traffic fleet reflect its similar behavior in the subsequent segment.

Acknowledgements The author acknowledges the Robert Bosch Centre for Data Science and Artificial Intelligence at the Indian Institute of Technology (IIT) Madras for their continuous

research support. We also thank The Ministry of Electronics and Information Technology (MeitY) for supporting this work through the project—Departure Time Planner using V2V and V2I communication.

References

1. Al-Deek HM, Venkata C, Chandra SR (2004) New algorithms for filtering and imputation of real-time and archived dual-loop detector data in I-4 data warehouse. Transportation research record 1867.1:116–126
2. Qu L, Li L, Zhang Y, Hu J (2009) PPCA-based missing data imputation for traffic flow volume: a systematical approach. IEEE Trans Intell Transp Syst 10(3):512–522
3. Van Buuren S (2018) Flexible imputation of missing data. CRC Press
4. Li Y, Li Z, Li L (2014) Missing traffic data: comparison of imputation methods. IET Intell Transp Syst 8.1:51–57
5. Zhong M, Sharma S (2006) Matching hourly, daily, and monthly traffic patterns to estimate missing volume data. Transp Res Rec 1957(1):32–42
6. Li L, Su X, Zhang Y, Lin Y, Li Z (2015) Trend modeling for traffic time series analysis: an integrated study. IEEE Trans Intell Transp Syst 16(6):3430–3439
7. Nihan NL (1997) Aid to determining freeway metering rates and detecting loop errors. J Transp Eng 123(6):454–458
8. Allison PD (2001) Missing data, vol 13. Sage Publications
9. Chen C, Kwon J, Rice J, Skabardonis A, Varaiya P (2003) Detecting errors and imputing missing data for single-loop surveillance systems. Transp Res Rec 1855(1):160–167
10. Liu Z, Sharma S, Datla S (2008) Imputation of missing traffic data during holiday periods. Transp Plan Technol 31(5):525–544
11. Smith BL, Scherer WT, Conklin JH (2003) Exploring imputation techniques for missing data in transportation management systems. Transp Res Rec 1836(1):132–142
12. Wang J, Zou N, Chang GL (2008) Travel time prediction: Empirical analysis of missing data issues for advanced traveler information system applications. Transp Res Rec 2049(1):81–91
13. Ni D, Leonard JD (2005) Markov chain monte carlo multiple imputation using bayesian networks for incomplete intelligent transportation systems data. Transp Res Rec 1935(1):57–67
14. Ni D, Leonard JD, Guin A, Feng C (2005) Multiple imputation scheme for over-coming the missing values and variability issues in ITS data. J Transp Eng 131(12):931–938
15. Duan Y, Lv Y, Kang W, Zhao Y (2014) A deep learning-based approach for traffic data imputation. In: 17th International IEEE conference on intelligent transportation systems (ITSC). IEEE, China, 2016, pp 912–917
16. Chen X, He Z, Sun L (2019) A Bayesian tensor decomposition approach for spatio-temporal traffic data imputation. Transp Res Part C: Emerg Technol 98:73–84
17. Patra SS, Muthurajan B, Chilukuri BR, Devi L (2019) Development and evaluation of a low-cost Wi-Fi media access control scanner as traffic sensor. In: 11th international conference on communication systems and networks (COMSNETS). IEEE, pp 777–782
18. Kaufman L, Rousseeuw P (1990) Finding groups in data: an introduction to cluster analysis. Wiley, Hoboken

Vehicle Actuated Signal Control System for Mixed Traffic Conditions

Chithra A. Saikrishna and S. P. Anusha

Abstract Actuated signal control (ASC) works based on vehicle actuations that utilize vehicle headway or count for signal control. However, under mixed traffic conditions, it is nearly impossible to obtain such data from all the vehicles in the traffic stream. Under such scenarios, the average delay of vehicles obtained from a representative sample of vehicles can be used as an input for signal control. This study evaluated the effectiveness of RFID sensors for real-time delay estimation where the average approach delay obtained from RFID sensors was used as the control variable for the working of an actuated signal control system at an isolated intersection. Based on the simulation results, it was observed that a penetration rate of 80% of total car volume in the traffic stream would effectively represent a vehicle actuated system that works based on delay from all vehicles in the traffic stream along with better performance in terms of percentage reduction in overall intersection delay.

Keywords Vehicle actuated signal control · Delay · Mixed traffic · RFID sensors

1 Introduction

Increasing vehicle congestion in urban cities has demanded smart and real-time traffic management strategies that would reduce the delay at an intersection thereby maximizing the efficiency of traffic network systems. For countries like India, where highly heterogeneous non-lane based traffic system prevails, implementation of traffic management measures is even more challenging. The inability of fixed signal control strategies in handling the rising traffic demand and urban infra-structure development paved the way for alternative, more responsive signal control systems. Integration of advanced vehicle detection techniques in signal control has also leveraged the research in dynamic signal control systems. Vehicle actuated signal control is one among the dynamic control strategy recommended for an isolated intersection with fluctuating demands. The applicability of Radio-Frequency Identification

C. A. Saikrishna (✉) · S. P. Anusha
College of Engineering Trivandrum, Thiruvananthapuram, India
e-mail: chithrasaikrishna@gmail.com

L. Devi et al. (eds.), *Proceedings of the Sixth International Conference of Transportation Research Group of India*, Lecture Notes in Civil Engineering 273,
https://doi.org/10.1007/978-981-19-4204-4_24

(RFID) technology in the estimation of traffic stream parameters also contributes to the better management of traffic congestion. In this paper, the suitability of delay obtained from RFID sensors for operating actuated signal control systems is evaluated through simulation studies.

2 Literature Review

Existing real-time traffic control strategies such as actuated or adaptive require information of the entire traffic. This necessitates an automated data collection process that can collect data from the entire traffic. For example, actuated signals need headway between vehicles and adaptive solutions need flow data. However, traditional location based sensors such as inductive loops or video image processing fail to produce accurate data under mixed traffic conditions. This is because the sensors fail to capture parallel vehicular movements passing through them and for the various vehicle classes involved. Few research had been carried out in the past to explore the feasibility of different sensors such as Radio-Frequency Identification (RFID) system in Jayan and Anusha [1] and Wu and Yang [2], Bluetooth sensors in Abbas et al. [3] and Mathew et al. [4] and Wi-Fi sensors in [5], for data collection under mixed traffic conditions. Jayan and Anusha [1] conducted a study on the suitability of using Bluetooth and RFID detectors in travel time prediction for mixed traffic conditions which possessed several ITS applications. Reliability analysis of the sensor data in travel time estimation along with determining the penetration rate and match rate was conducted to analyze the performance of RFID sensors under mixed traffic conditions. Based on the results of the study it was concluded that RFID sensors can be used for real-time data collection for travel time studies under heterogeneous, non-lane based traffic scenarios.

Several studies have explored the possibility of vehicle actuated (VA) signal control for efficient traffic signal management at intersections due to their adaptability to varying traffic demands. Wang et al. [6] developed an improved VA system that used critical gaps for green extension after the queue clearance. The signal performance using critical gap as the single control variable was analytically modelled and evaluated at an isolated intersection. Moghimi et al. [7] predicted the varying signal cycle length for an actuated signal control based on gap using time series models with changing traffic demand levels. VISSIM traffic simulation software was used to develop the different simulation scenarios where cycle length prediction was carried out using the proposed model. Though implementation of VA traffic signal controllers for homogeneous traffic conditions are relatively easier the case is different for heterogeneous, non-lane based traffic prevailing in countries like India. Few researches were conducted to adapt the VA control logic to heterogeneous vehicle mix so as to develop an efficient traffic signal system. Ravikumar and Mathew [8] developed a vehicle actuated signal control strategy based on headways for heterogeneous traffic having limited lane discipline. Their study demonstrated algorithms for signal control including changing the detector configuration and the loop size, logical grouping of

signal phases, and the use of dummy phases. Oertel and Wagner [9] developed an actuated signal control plan based on delay times obtained from vehicles entering an isolated intersection. From the experimental studies conducted using the Simulation of Urban MObility (SUMO) software, they demonstrated that for the efficient working of delay based vehicle actuated signal control, the penetration rate of detectors or the number of equipped vehicles in the traffic stream were not necessarily a significant parameter. If the position of at least one vehicle on the approach was determined, green times for the following phase can be estimated during the red phase.

Simulation studies are necessary to evaluate various traffic management strategies to improve the road transport network efficiency. Traffic simulators offer the possibility to experiment with an existing or non-existing traffic system in a safe and non-disturbing way [10]. Various traffic simulation softwares are available with microscopic, mesoscopic and macroscopic modelling approaches such as CORSIM, Paramics, AIMSUN, MATSim, SimTraffic, VISSIM, SUMO etc. Compared to other traffic simulation softwares which provides a licensed version, SUMO is an open source software, which is easy to understand and implement. The software provides several tools for generating multi-modal traffic networks including foreign network import, demand modelling and route generation from different sources, command line application as well as a graphical user interface application for simulation visualization. In order to model highly heterogeneous road traffic conditions prevailing in India, SUMO offers a variety of vehicle types in addition to the sublanes feature that renders traffic flows more realistic in the Indian scenario.

Lopez et al. [11] presented a methodology to prepare a simulation scenario in SUMO based on real-time traffic data. The different concepts, models, tools and applications available in SUMO to support the researchers to enhance the developed simulation model were explained. Limited literature discussed about the calibration of SUMO for heterogeneous traffic flow. In order to validate the output of the simulation with real data, it is necessary to calibrate the various parameters of SUMO. Sashank et al. [12] presented a methodology for calibration of SUMO for heterogeneous traffic by identifying the parameters that affect the model behavior using sensitivity analysis and one-way ANOVA test and an optimal combination of parameters using Genetic Algorithm (GA).

Based on the literature review, it is observed that there are limited studies that evaluated the performance of an actuated signal control using delay data obtained from sensors as an input. The present study focus on developing an actuated signal control that utilizes delay from RFID sensors for heterogeneous traffic condition.

3 Objective

The objective of the study is to evaluate the reliability of RFID sensors for estimation of delay at an isolated intersection and to analyze the performance of a vehicle actuated signal control system operated by the delay obtained from RFID sensors. The

challenges faced in the study are the poor lane discipline of the highly heterogeneous Indian traffic condition in addition to the relatively lower proportion of RFID tagged vehicles in Indian roads. The performance evaluation of a signalized intersection operated using actuated signal control was carried out under varying sensor penetration rates through traffic simulation carried out using an open source microscopic simulation software Simulation of Urban MObility (SUMO).

4 Methodology

The work methodology comprises of four parts: the first section discuss the techniques used for data collection and the data extraction process. The second section is devoted to the development of a simulation network in SUMO and calibration for field conditions. The third section involves the comparison of performance of Fixed Signal Control (FSC) with the in-built Actuated Signal Control (ASC) in SUMO. The last section illustrates the performance evaluation of ASC implemented via TraCI in SUMO using delay obtained from RFID tagged cars at different penetration rates.

4.1 Data Collection and Extraction

A four-legged signalized intersection at Pattom in Trivandrum city of Kerala, India was selected for the study. The approaches namely Kesavadasapuram, Marappalam, Plamoodu and Medical College are four lane roads with median and operate under pre-timed signal control. The traffic characteristics of the selected intersection are shown in Table 1. The saturation flow for each approach was estimated as per Indo-HCM 2017. The cycle wise variation of traffic parameters at the intersection is shown in Figs. 1 and 2. The proportion of RFID tagged vehicles in the traffic stream was found to be 11.9% of the total vehicles and 40% of the total cars respectively.

Data collection was done using two RFID detector units placed on the Plamoodu approach from 2:50 PM to 4:10 PM on a typical weekday. Each unit, comprising a RFID reader, Raspberry Pi and GPRS was positioned at the stop line and at 70 m upstream from the stop line. The time stamps of RFID tagged vehicles passing the

Table 1 Traffic characteristics for different approaches of the signalized intersection

Approach	Saturation flow (PCU/hr)	Turning Counts (PCU/hr)		
		Left	Through	Right
Kesavadasapuram	3155	387	1043	206
Marappalam	2678	59	290	255
Plamoodu	3919	640	1061	0
Medical college	3475	436	353	465

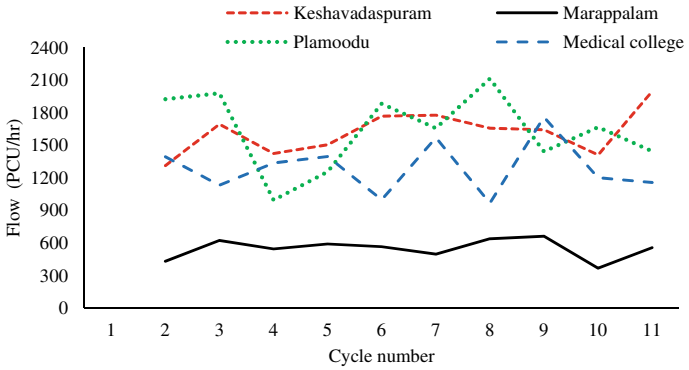

Fig. 1 Cycle wise variation of vehicle arrival flow

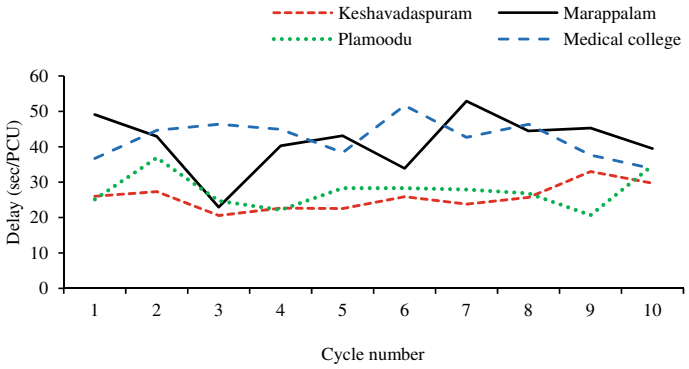

Fig. 2 Cycle wise variation of vehicle delay

two points were recorded and the travel time was determined from matching the unique ID of each vehicle obtained from the two detectors. The free flow travel times of vehicles were subtracted from the travel time obtained by RFID sensors to compute the delay experienced by the detected vehicles. The estimated vehicle delay in seconds averaged over each cycle was validated by comparing it with field delay obtained from video graphic techniques.

Traffic flow was recorded for the same duration as that of RFID detections on all four approaches. The vehicle entering a virtual trap of 70 m length extending upstream from the stop line at the intersection was counted manually for every 5 s interval to obtain the arrival count. Similarly, a vehicle leaving the stop line completely was considered as its exit from the virtual trap. The number of vehicles in the queue in Passenger Car Units (PCU) was determined from the arrival and departure counts using the Input–Output method [13] and were plotted against cycle time to construct a queue accumulation curve. Using Simpson's one-third rule, the area under the curve

was calculated and the average delay for each cycle was determined in seconds per vehicle. The data analysis and results are discussed in Sect. 5.1.

4.2 Simulation Network

The microscopic simulation tool Simulation of Urban MObility (SUMO) developed by the DLR institute in Germany was used to generate the road traffic network.

The signalized intersection under study namely, the Pattom intersection was imported using Open Street Map and modified in NETEDIT. The traffic scenario was built by adding the additional network elements including demand data, traffic lights and detector files (Fig. 3).

The classified vehicle counts obtained from the video graphic data for an hour constituted the input demand file. The traffic signal timings as observed in the field were given as input with a cycle time of 120 s as indicated in Table 2. Detectors were placed at the stop line and at a location of 70 m upstream from the stop bar for retrieving simulation output.

Calibration. Calibration is the process of refining the input parameters of the model to accurately replicate the observed traffic conditions [12]. The simulation software SUMO by default works for homogeneous, lane based traffic networks. In order to simulate the heterogeneous lane-less traffic condition that prevails in the field, the network has to be calibrated by changing the default network parameters of the software. The values were varied by trial and error method until the output results of

Fig. 3 Study site generated in SUMO

Table 2 Signal timing for different approaches of the signalized intersection

Name of approach	Red phase	Green phase	Amber phase
Kesavadasapuram (Right-turn)	**96**	**22**	**2**
Kesavadasapuram (Through)	**54**	**64**	**2**
Marappalam	**95**	**23**	**2**
Plamoodu	**78**	**40**	**2**
Medical college	**91**	**27**	**2**

the simulation matched with the field data. In order to represent the field condition, network parameters of the model including desired speed of vehicles, acceleration rate, deceleration rate, lateral resolution, minimum gap at jam conditions and driver imperfection value were adjusted. The simulation was run multiple times and for each simulation run the vehicle delay from the detector output was compared with the field delay value determined from the video graphic survey. The errors between the simulated values and the observed field data were quantified using Mean Absolute Percentage Error (MAPE). The calibration process was carried out until the MAPE values were within 20%. The results are shown in Sect. 5.2.

4.3 Delay Based Actuated Signal Control in SUMO

The calibrated network was used for the performance evaluation of vehicle actuated signal control. SUMO has an in-built actuated signal control plan based on time loss. The control system works based on the logic that a running green phase is terminated as soon as the first vehicle with a delay, d, smaller than a critical delay time, d_{min} (about zero), passes the stop line, bounded by a minimum and maximum green time (g_{min}, g_{max}). Based on this approach, the delay time of vehicles running on each approach were constantly measured at an interval of 1 s and if the time loss of a vehicle in an approach exceeds the threshold value of minimum time loss (by default 1 s) a phase prolongation is requested for the current active phase. The control switches to the next phase if the delay has dropped to zero [9].

The simulation run was performed for a duration of 90 min and output results of 60 min duration were obtained after eliminating the first and last 15 min time interval. The delay values obtained from the detectors for the four approaches were then used to calculate the total intersection delay. This was then compared with the intersection delay estimated from the calibrated network under fixed time signal control for performance evaluation. The results are discussed in Sect. 5.3.

4.4 Actuated Signal Control in SUMO Using TraCI

The in-built actuated signal control plan in SUMO utilizes the delay from all the vehicles. Since the objective of the study is to analyze the performance of a vehicle actuated signal control system operated by the delay obtained from RFID sensors, TraCI (Traffic Control Interface) was used to access the running simulation in SUMO. The interface provides a communication between the simulator and an external script (controller). It allows retrieval of traffic states along with the detector data to the controller where it is used to compute the signal timings. The adjusted signal timings are then sent back to the simulator thus providing the possibility of controlling running simulation online. In this study, a python script was developed to implement the vehicle actuated signal control in the SUMO network using TraCI.

The algorithm used in the python script for implementing actuated traffic signal based on delay from RFID sensors was developed based on the queue clearing policy. The flow chart for the signal control plan is illustrated in Fig. 4. The algorithm utilizes

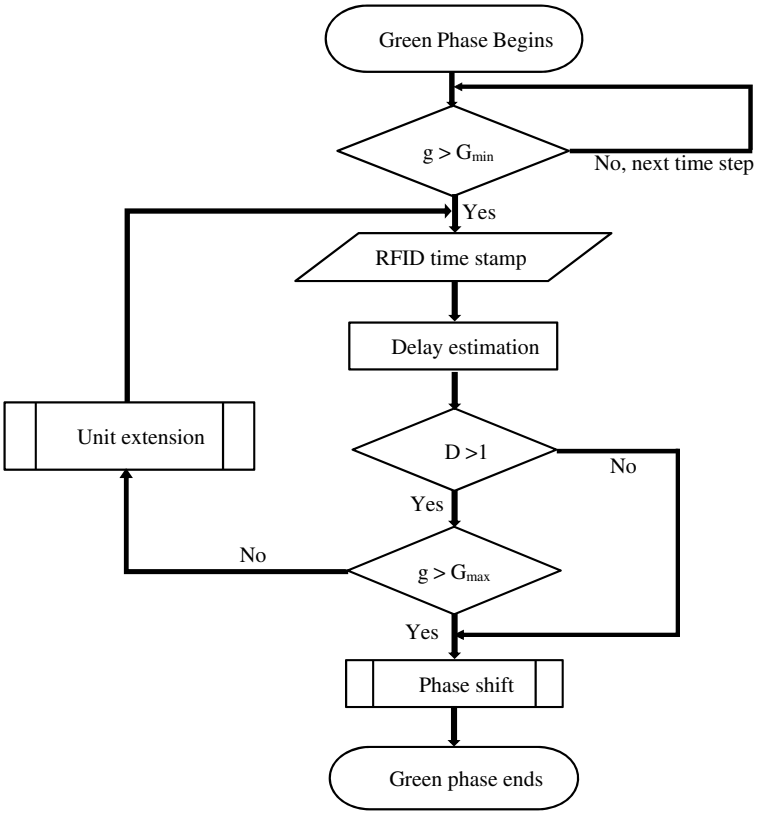

Fig. 4 Flow chart for actuated signal control based on delay from RFID sensors

the data obtained from two detectors, one unit placed at the stop line and the other 70 m upstream of the intersection on all the four approaches. Once the minimum green time in a running green phase is reached, the time stamps of the first vehicle approaching the stop line at the end of the minimum green time, obtained from RFID detectors, is sent to the controller for delay estimation. The travel time of that vehicle was calculated by finding the difference between the time stamps of stop line detection and upstream detection. The free flow travel time of vehicles was then subtracted from the actual travel time to determine the delay experienced by that vehicle. If there exists a delay i.e., the delay value is greater than zero (threshold delay value is set to 1 s), then the green phase is given a unit extension. If the delay value is equal to zero which implies that the queue has cleared, then the green phase is terminated and the right of way is shifted to the next phase. The signal controller thus checks the delay of each consecutive vehicle approaching the intersection. The green phase of an approach is terminated at the instant the first vehicle with a delay close to zero approaches the stop bar detector or the maximum green duration is reached.

The actuated signal control system implemented via TraCI, based on the above logic employed delay from RFID sensors as the control variable to operate phase shifts. Based on this, the overall intersection delay from actuated signal control was evaluated and compared with the delay from pre-timed signal control. The percentage reduction in overall intersection delay was also estimated. The results are shown in Sect. 5.4.

Actuated Signal Control at Different Penetration Rates. A sensitivity analysis was carried out to evaluate the optimum penetration rate of RFID cars that would replicate the ASC based on the delay of all the vehicles in the traffic stream and to identify their performance in terms of percentage reduction in overall intersection delay compared to fixed signal control. The performance of actuated signal control with different penetration rates of RFID cars with respect to the total cars in the traffic stream was evaluated. The overall intersection delay for each penetration rate was compared with that for an actuated signal control that used delay from all vehicles and the MAPE values were determined. The percentage reduction in intersection delay using actuated signal control for different penetration rates in comparison with fixed signal control was also estimated. The results are discussed in Sect. 5.4.

5 Results and Discussions

5.1 Comparison of RFID Delay with Field Delay

The delay obtained from RFID sensors were compared with the actual delay to estimate the effectiveness of RFID sensors for delay estimation under mixed traffic condition (Fig. 5). The Mean Absolute Percentage Error (MAPE) was found to be 10.4%. According to Lewis' scale of judgment of forecasting accuracy, any forecast

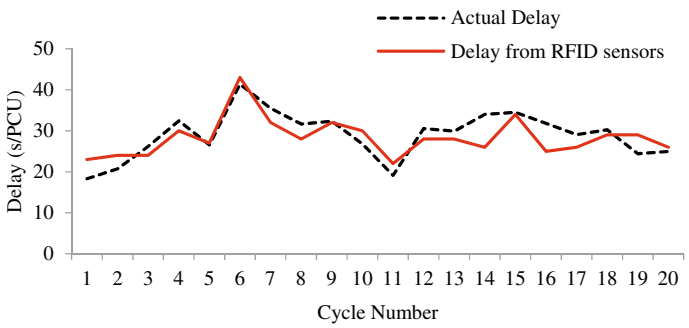

Fig. 5 Comparison of actual field delay with RFID delay

with a MAPE value of less than 10% can be considered highly accurate, 11–20% is good, and 21–50% is reasonable and 51% or more is inaccurate [14]. Thus it can be concluded that the delay data obtained from RFID tagged cars can be used to replicate the field delay.

5.2 Calibration Results of SUMO

The intersection was operated through fixed signal control by using the traffic signal timings observed in the field. The simulation model was run for 90 min with the calibrated parameters as input and the model was validated with field data. The approach delay of vehicles averaged over the signal cycle from the simulation output was validated by comparing it with the field delay extracted from the video graphic data (Fig. 6). The MAPE and MAE for the delay were obtained as 16% and 6.7% respectively indicating a good match between the simulated and field data. Thus, it can be concluded that the simulation model is calibrated and can be used for the evaluation of different traffic control strategies.

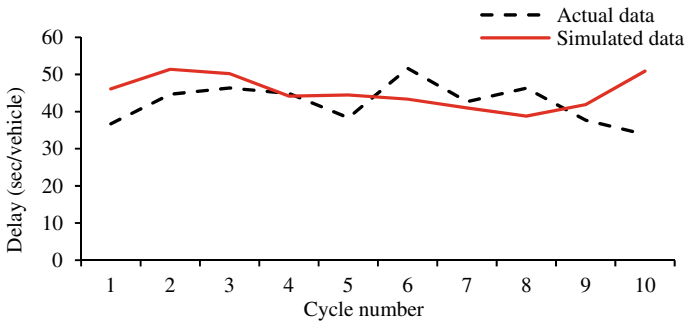

Fig. 6 Comparison of simulated delay with field delay

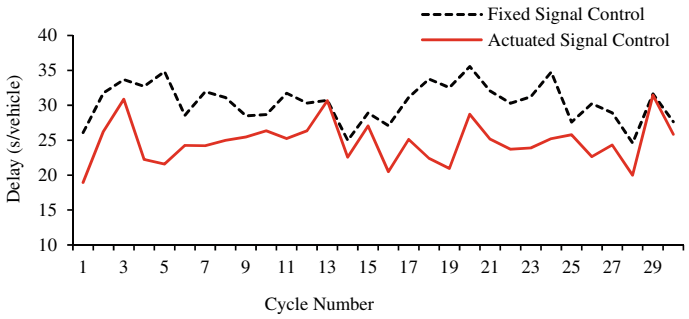

Fig. 7 Comparison of delay for actuated signal control with fixed signal control (Plamoodu approach)

5.3 Performance Evaluation of Actuated Signal Control in SUMO

Simulation was performed with the actuated signal control system available as in-built in SUMO which used delay from all vehicles in the traffic stream. The delay obtained from the simulation was compared with the delay obtained from the calibrated SUMO network operated using fixed signal control. The overall intersection delay was compared with the fixed signal control and it was found that there is a reduction in overall intersection delay of 12% while implementing the actuated signal plan at the intersection. For one of the study approach namely the Plamoodu approach the average reduction in delay for actuated signal control was 19% compared to fixed signal control (Fig. 7). Thus it can be concluded that for an isolated intersection actuated signal is performing well with a reduced delay compared to fixed signal control.

5.4 Performance Evaluation of Actuated Signal Control Using TraCI

The objective of the study was to utilize the delay obtained from RFID tagged cars as an input for actuated signal control. Since the signal control as illustrated in Sect. 5.3 utilized the delay from all the vehicles in the traffic stream, it was necessary to execute the simulation using delay from a sample of RFID cars in the traffic stream. For this purpose, the operation of actuated signal control was accessed using TraCI in SUMO as explained in Sect. 4.4. The performance of the actuated signal system implemented via TraCI was first evaluated by employing the proportion of RFID cars as 40% which corresponds to the proportion of RFID cars in the field and the results were compared with the delay obtained from fixed signal control delay from SUMO. The percentage reduction in overall intersection delay was estimated as 20%. For

one of the study approach namely Medical College approach the average reduction in delay for actuated signal control using TraCI was found to be 41% compared to fixed signal control (Fig. 8). This shows that in a heterogeneous traffic, ASC based on RFID car detection from a representative vehicle sample renders better performance compared to ASC utilizing delay from all vehicles in the traffic stream that resulted in a reduction in overall intersection delay of only 12%.

The above analysis used the proportion of RFID cars as 40% of the total cars (which corresponds to 11.9% of all vehicles in the traffic stream), based on the observations from the field. Further, in order to investigate the optimum proportion of RFID cars that would replicate the actuated signal control utilizing delay from all vehicles in the traffic stream, the actuated signal system was operated under varying penetration rates and the simulation was run via TraCI. The performance of the actuated signal control was evaluated for different penetration rates of RFID cars varying from 10 to 100% of total car volume in the traffic stream.

Table 3 shows the Mean Absolute Percentage Error (MAPE) of the delay values for different penetration rates for the four study approaches of the intersection. It can be observed that the MAPE value is lowest for the RFID penetration rate of 80% of total cars (which corresponds to 23.8% of all vehicles in the traffic stream). Hence actuated signal control based on RFID delay can be implemented in a heterogeneous traffic where it would fairly represent an ASC system that works utilizing delay from all vehicles in the traffic stream.

A performance analysis was also carried out to evaluate the percentage reduction in overall intersection delay for ASC at different penetration rates of RFID cars by comparing it with fixed signal control. Table 4 shows the reduction in overall intersection delay for actuated signal control under different penetration rates.

Based on the results obtained from Table 4, it can be observed that for 80% RFID car detection, the reduction in overall intersection delay was 22% which was superior to that obtained while implementing actuated signal control that utilized delay from all vehicles. Thus it can be concluded that delay based actuated signal control with 80% penetration rate among total car volume (23.8% of total vehicles) would represent an actuated signal control based on delay data from all vehicles in

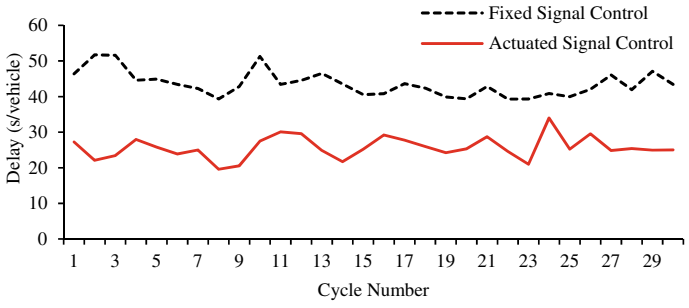

Fig. 8 Comparison of delay from fixed signal control with actuated signal control (Medical college approach)

Table 3 Variation in MAPE for delay for varying penetration rate of RFID cars

RFID car proportion (of total cars %)	MAPE (%)				
	Keshavadaspuram	Marappalam	Plamoodu	Medical college	Average MAPE
100	30	22	23	22	25
90	28	23	18	17	22
80	25	24	20	15	21
70	23	24	20	24	23
60	21	25	25	19	23
50	28	25	20	22	24
40	23	26	22	15	22
30	28	26	23	19	24
20	30	28	22	26	26
10	24	30	25	22	25

Table 4 Reduction in intersection delay for varying penetration rate of RFID cars

RFID car proportion (of total cars %)	Reduction in overall intersection delay
100	25
90	20
80	22
70	24
60	21
50	25
40	20
30	18
20	17
10	16

the traffic stream and also render higher performance on the basis of reduction in total intersection delay.

6 Conclusions

Traffic signal control plays an important role in managing the queue and delays at intersections. The actuated signal control system works based on vehicle actuations that utilize different parameters such as vehicle headway or count for signal control. However, such signal control is ineffective under mixed traffic conditions as prevailing in India where different vehicle classes move without lane discipline

thereby render the difficulty in obtaining real-time vehicle data. Under mixed traffic conditions, delays obtained from RFID sensors can be utilized for signal control.

This study evaluated the effectiveness of delay obtained from RFID sensors for actuated signal control system for an isolated intersection. A microsimulation software SUMO was used to replicate the signalized intersection under study. Delay obtained from RFID detectors placed at upstream and downstream locations of the intersection were compared with actual delay obtained and the MAPE value was observed to be 10.4% indicating that the delay obtained from RFID sensors are representative of the stream delay.

Based on this, evaluations were made to analyze the effectiveness of vehicle actuated signal control using delay obtained from RFID sensors at different penetration rates. The experiments were performed by controlling the simulation network under the in-built actuated signal plan in SUMO as well as actuated signal control based on delay for varying RFID car proportions operated via TraCI. The overall intersection delay evaluated using in-built vehicle actuated signal control in SUMO was compared with the fixed signal control and it was found that there is a reduction in overall intersection delay of 12% while implementing the actuated signal plan in the intersection. The performance of the actuated signal control employing delay from 11.9% RFID tagged vehicles as observed in the traffic stream in the field, implemented in SUMO via TraCI, was evaluated by comparing the average approach delay experienced by vehicles with the corresponding delay obtained for fixed signal control at the intersection. The percentage reduction in overall intersection delay was estimated as 20% while implementing vehicle actuated signal control based on RFID delay. Further, the performance of vehicle actuated signal control system utilizing delay from RFID sensors at different penetration rates of RFID cars was evaluated in SUMO via TraCI.

The results showed that even at penetration rates as low as 10%, actuated signal control resulted in a 16% reduction in total intersection delay when compared with the fixed signal control. From the simulation results, it was concluded that a penetration rate of 80% of RFID cars (which corresponds to a penetration rate of 23.8% with respect to total vehicles) would be effective in developing a delay based actuated signal control for a heterogeneous and non-lane based traffic condition at an isolated intersection.

The overall contributions of the study are as follows:

1. The study explored the applicability of delay from RFID sensors as input for vehicle actuated signal control for an isolated intersection.
2. Based on the results of the study, it was observed that even with a lower penetration rate, the delay based actuated signal control staged a better performance in terms of reduction in overall intersection delay compared to the fixed signal control.
3. Actuated signal control based on delay from a sample of RFID cars in the traffic stream can replicate the delay based actuated signal control system that utilizes delay from all vehicles in the traffic stream in addition to enhanced signal performance based on reduction in overall intersection delay.

Thus it can be concluded that vehicle actuated signal control system operated using delay from RFID detectors can be used as an application in Intelligent Transportation System (ITS) under mixed traffic conditions.

Acknowledgements The authors acknowledge the support for this study by Transportation Research Centre (TRC) set up at the College of Engineering, Trivandrum, Kerala through State Budget allotment 2016–2017 by the Kerala Government vide letter no. L4/30202/16/DTE dated 23/09/2016. The authors also acknowledge ITS Planners and Engineers for their technical support.

References

1. Jayan A, Anusha SP (2019) Evaluation of effectiveness of RFID and bluetooth sensors for travel time studies under mixed traffic conditions. Period Polytech Transp Eng 48(3)
2. Wu A, Yang X (2013) Real-time queue length estimation of signalized intersections based on RFID data. Procedia Soc Behav Sci 96:1477–1484
3. Abbas M, Rajasekhar L, Gharat A, Dunning JP (2013) Microscopic modeling of control delay at signalized intersections based on Bluetooth data. J Intell Transp Syst 17(2):110–122
4. Mathew JK, Devi VL, Bullock DM, Sharma A (2016) Investigation of the use of bluetooth sensors for travel time studies under Indian conditions. Transp Res Procedia 17:213–222
5. Gore N, Arkatkar S, Joshi G, Bhaskar A (2019) Exploring credentials of Wi-Fi sensors as a complementary transport data: an Indian experience. IET Intel Transport Syst 13(12):1860–1869
6. Wang XB, Yin K, Liu H Vehicle (2018) Actuated signal performance under general traffic at an isolated intersection. Transp Res Part C
7. Moghimi B, Safikhani A, Kamga C, Hao W (2018) Cycle-length prediction in actuated traffic signal control using ARIMA model. J Comput Civ Eng 32(2):04017083
8. Ravikumar P, Mathew TV (2011) Vehicle-actuated signal controller for heterogeneous traffic having limited lane discipline. ITE Journal 81(5):44–53
9. Oertel R, Wagner P (2010) Delay-time actuated traffic signal control for an isolated intersection. In: 90th annual meeting transportation research board, Washington, D.C
10. Bajpai A, Mathew TV (2011) Development of an interface between signal controller and traffic simulator. CTRG
11. Lopez PA, Behrisch M, Bieker-Walz L, Erdmann J, Flotterod YP, Hilbrich R, Lucken L, Rummel J, Wagner P, Wießner E (2018) Microscopic traffic simulation using SUMO. In: 21st international conference on intelligent transportation systems (ITSC), Maui, Hawaii, USA
12. Sashank Y, Navali NA, Bhanuprakash A, Kumar BA, Vanajakshi L (2020) Calibration of SUMO for Indian heterogeneous traffic conditions. In: Arkatkar SS et al. (eds.) recent advances in traffic engineering, lecture notes in civil engineering 69. Springer Nature Singapore Pte Ltd
13. May AD (1990) Traffic flow fundamentals prentice hall. Inc. Ebglewood Clieffs, NJ, USA
14. Klimberg RK, Sillup GP, Boyle KJ, Tavva V(2010) Advances in business and management forecasting. Emerald books, U.K

Design and Development of Bluetooth Based Vehicle Scanner for Real Time Traffic Control

Ashish R. Kulkarni, Narendra Kumar, and K. Ramachandra Rao

Abstract Measurement of traffic volume and control of traffic signal timing using various technologies like inductive loops, pressure plates or tubes and vision-based systems are common. Many of these sensing technologies are non-intrusive. In this paper, the Author's present an exploration of the Bluetooth devices and scanners and attempt to fabricate one such unit and the results of the deployment of the prototype in the field. The prototype Bluetooth vehicle scanner is based on an Arduino Mega microcontroller. It consists of a Bluetooth module and a Wi-Fi module interfaced with a microcontroller. Based on re-identification, filter rules and distance between the scanners, the average speed is calculated and conveyed to the traffic signal controller. The traffic signal controller determines the green time offset required for the main corridor under consideration within the set cycle time. The prototype system has shown promising results and can be used effectively in the existing traffic signal control system.

Keywords Bluetooth · BTS · MAC id · Hardware

1 Introduction

Urban traffic control is a challenge which mankind has tried to control using various methods or techniques in various eras. The mode of transport has changed or evolved, and so has the traffic control measures and devices. Still, the emphasis is on safety and smooth travel with minimum delay. The first traffic light dates back to the year

K. R. Rao (✉)
Department of Civil Engineering and Transportation Research and Injury Prevention Centre (TRIPC), IIT Delhi, New Delhi, India
e-mail: rrkalaga@civil.iitd.ac.in

A. R. Kulkarni · N. Kumar
Department of Electrical Engineering, Delhi Technological University, Delhi, India
e-mail: ashishkulkarni@dtu.ac.in

N. Kumar
e-mail: narendrakumar@dtu.ac.in

L. Devi et al. (eds.), *Proceedings of the Sixth International Conference of Transportation Research Group of India*, Lecture Notes in Civil Engineering 273,
https://doi.org/10.1007/978-981-19-4204-4_25

1868 [1]. Electric traffic lights started in 1914 and since then urban traffic control is seen as a challenge. Only mechanisms have changed, the problem still remains. It was a concern then and is still a concern till date. History also tells us that people at that time also thought about how to make road travel smooth and ensure that stoppage at intersections is a minimum. Vehicle actuated traffic lights became a reality in the year. Measurement of volume of traffic and control of traffic light timing accordingly using various methods like inductive loops, pressure plates or tubes, vision, Bluetooth etc., at an isolated intersection or group of intersections or an area or an arterial or a city wide network is still a work under progress. Problem is that no one method of traffic detection is seemingly complete in itself and secondly the nature of traffic is ever evolving. Today's developed methods may be inadequate or obsolete tomorrow.

If we review the literature, only the scale i.e., magnitude of the problem has changed. That the nature of traffic changes during the day, the week, period of the month, season or year on year, is a fact known to early researchers in the area. A series of articles have appeared in transactions of AIEE in the year 1932. It discusses the flexible progressive traffic signal systems and new developments in the area during that period [2]. For the record, the first progressive traffic light system was in place in 1918 in Salt Lake City, Utah. It was felt then also that the average traffic speed should be known for the satisfactory performance of the progressive traffic light system. This was essential to achieve maximum bandwidth in one particular direction based on the time of the day. Same is true today also. With the increase in population, both of people and automobiles, the fight for road space has become very difficult. Average speed has changed, traffic infrastructure and technology have changed from manual, synchronous motor based to fully electronic and computer based one. What remains constant is the quest for the best way to get a feedback about traffic conditions in real time.

Recent advances speak about camera vision, inductive loops, etc., eventually camera vision will prevail. Other sources of data are GSM based location services, GPS, Wi-Fi in smartphones and Bluetooth. This is all apart from the traditional road surveys. Camera vision suffers from the problem of processing time to be effective in real time. At the network level, the delay is only bound to increase. Also, the solution is costly as it includes costly night vision cameras, communication links, the cost of which will increase with video transmission and other components. The search for a cheap, easy to deploy and useful real time, traffic monitoring system is still on.

Bluetooth based vehicle scanners offer such features. The solution can be cheap, quickly deployable and really useful in real time. This paper discusses the design and development of a low cost Bluetooth based vehicle scanner for measuring average traffic speed and its use for controlling the green time of traffic lights in real time. The work done is specific to India, but can be used anywhere in the world. The main attraction is the low cost compared to the available professional systems.

2 Literature Survey

As mentioned in the above section electric traffic lights came into practice in 1914. The progressive traffic light system was operational in 1918. Vehicle actuated and pedestrian signals were also a reality by the 1930s.

A 1932 paper in Transactions of AIEE by Vickery and Leonard mentions that "sufficient flexibility should be built into traffic signal timing apparatus to insure that such apparatus shall not shortly become obsolete".

A very true statement. Despite all advances in various traffic light system schemes to make them adaptive and responsive in real time, the majority of the signals worldwide are fixed time signals. To make them traffic responsive in real terms is a mammoth task. The main element is the sensor which measures the traffic in real time and secondly the software-hardware to make it real time responsive. It's a huge investment.

A solution which is cheap and quickly deployable is the need of the hour. Albeit there are so many developed solutions worldwide. The main question is how to augment the infrastructure that is already in place. In the case of Delhi, there are more than 400 traffic light controlled intersections. Complete overhaul is a huge financial task, augmenting the capabilities of the existing infrastructure seems a good alternative.

Three colour four way traffic light, in operation officially since 1920, in itself hasn't changed much. Earlier lamps are now replaced with Led's to reduce power consumption and enhance visibility in all conditions, day or night. These changes are already accommodated in various places.

Feedback regarding traffic conditions is essential to make a traffic control system a responsive one. Various methods listed in the literature are:

i. Pressure plates
ii. Inductive loops
iii. Ultrasonic sensors
iv. Lasers
v. Camera vision
vi. ANPR
vii. GSM based
viii. GPS based
ix. Bluetooth
x. Wi-Fi based

Pressure plates were the first to be used. Inductive loops of single loop type are the most prevalent ones. Ultrasonic sensors are also used. Currently, more focus is on camera vision and ANPR. The problem with camera vision for intersection control is the file size for transmission, its processing and feature extraction and then the post processing to be implemented in real time. It's quite a challenging and costly affair. It's good for offline processing and issue of challans for traffic light violations.

With the advent of smartphones and the development of communication technologies, especially mobile communication, the use of wireless techniques for travel time detection, surveillance etc., is in demand. A recent paper discusses the use of crowd sourcing techniques using smartphones for generating data related to travel time and traffic conditions.

Of all the wireless techniques, Bluetooth based vehicle reidentification seems to be an attractive proposition.

Bluetooth, a short range communication protocol was under development since 1989 in Ericson and launched formally in 1994. It works in the unlicensed ISM band at 2.4 GHz with FHSS technology.

Out of all the communication modes supported by Bluetooth, Inquiry Scan is of particular interest and to be of use for ITS technology. Under Inquiry scan, a Bluetooth device set as a Master keeps on enquiring the devices in its vicinity. All devices which are discoverable are noted with their MAC (Media Access Control) ID which is unique to each Bluetooth device. A time-stamp needs to be put-up with each discovery, so that the data can be further used meaningfully. No formal communication or pairing is required as no data is to be transferred. Only the presence of a device is to be recorded with the time-stamp. Since no further enquiry or communication takes place, issues of privacy violations do not hold. This is similar to a person's presence being recorded in the crowd by the CCTV cameras placed at various locations. It doesn't amount to a privacy violation.

This simple approach has interested researchers and government agencies to use Bluetooth for various applications/uses in the field of ITS.

The use of Bluetooth in ITS has gathered interest since the year 2002. In a research paper published in 2002 [3], the utility of BT devices for RVC (road side to vehicle communication) has been discussed. It has discussed about three major characteristics of BT devices:

i. estimation of maximum range,
ii. effects of vehicle speed and multipath fading, and
iii. estimation of connection set up delays.

They have concluded that vehicle speed may not affect the detection, but SNR, the power dissipated and connection delay of the order of seconds may degrade the performance.

A research paper by Sawant et al. in the year 2004 has studied the use of Bluetooth for intra-vehicle communication, forming an ad-hoc sensor network for data exchange and enhancing road safety in view of increasing car crashes in the USA [4]. Since then, many applications of Bluetooth have been studied, early focus was on intra-vehicular communication, then trip generation, O–D formulation, travel time estimation, data fusion for instant traffic information, electronic toll system etc.

Extensive work on the use of Bluetooth, analysis of data generated, removal of duplicate data, methodology to be used for using collected data, filtering techniques etc., appear in the literature post the year 2012. Most of the work focuses on how to use Bluetooth as a complimentary source of data and how that data can be made reliable

[5]. How to increase the probability of capturing data correctly, the development of a simulation framework and microscopic modelling of control delay were the topics delved on by the researchers. Many papers and reports have discussed the deployment of BTS on arterials or urban intersections. Improvements in prototypes and the problems solutions encountered, development of software for collecting the field data and filtering the data for presentation are discussed in the 2011 report by Oregon DOT [6]. A 2019 paper discusses setting up a simulation framework considering multiple inquiry scans and distance from the detector [7].

In this proposed work we've developed an integrated end-to-end development of low cost BTS, online collection of data, filtering of data and working out green time offset of traffic signal for a particular approach and implementing the same on an intersection within 2–3 cycle times in real time. Details are presented in the next section. In order to support our view that Bluetooth devices can act as a good source of traffic data and to validate our findings presented in the following sections, we have done a traffic survey using a commercial grade Bluetooth/Wi-Fi/Xbee scanner and correlated it with the traffic videos recorded during the same time. The findings are presented in Table 1 below. The unique MAC ids are around 10–15% of the vehicle count recorded in the video and the same can be extrapolated to figure out the traffic volume on the road.

Table 1 Summary of comparison of video analysis and field data collection using commercial scanner

Date and day	Location	Start time	End time	Total no. of vehicles	Total mac ID scanned	Unique mac ID
02–03-2021 Tuesday	K.N. Katju Marg PS	9:30 AM	9:40 AM	1010	359	151
	GNDIT Gate-2	10:07 AM	10:08 AM	75	46	14
06–03-2021 Saturday	K.N. Katju Marg PS	9:15 AM	9:23 AM	714	207	46
	GNDIT Gate-2	10:10 AM	10:22 AM	988	489	145
07–03-2021 Sunday	K.N. Katju Marg PS	9:59 AM	10:09 AM	785	256	112
	GNDIT Gate-2	9:35 AM	9:40 AM	567	178	98
08–03-2021 Monday	K.N. Katju Marg PS	9:48 AM	9:58 AM	940	349	120
	GNDIT Gate-2	10:22 AM	10:30 AM	689	263	113
	GNDIT Gate-2	10:39 AM	10:49 AM	851	401	146
09–03-2021 Tuesday	K.N. Katju Marg PS	10:55 AM	11:02 AM	655	232	58

This development becomes all the more important and interesting in view of the data released in March 2020 by Bluetooth.com [8]. Their report projects that by the year 2024 2/3rd of the automobiles will have on-board Bluetooth modules. With the new automotive standards and solutions, each vehicle will have 3–4 Bluetooth devices. As such a huge data set will be readily available which can be leveraged to the fullest with minimum investment.

Considering that the driver has a smartphone, a wearable device (like fitness band), on-board hands-free Bluetooth connection, a tire pressure monitor and an internal sensor network of the car i.e., sensor mesh on Bluetooth; future vehicles can have more than 4 Bluetooth modules. There will be a problem of plenty. As such Bluetooth Traffic Scanners will be very useful in the near future.

3 System Description and Working

The prototype Bluetooth vehicle scanner is based on an Arduino Mega microcontroller. The prototype consists of the microcontroller, HC-05 Bluetooth module, EPS8266 Wi-Fi module and power supply board. The block diagram representation is shown in Fig. 1, whereas the actual hardware assembly is shown in Fig. 2. The HC-05 is set in Master configuration and continuous enquiry scan mode. No handshaking is done. It scans its vicinity for Bluetooth devices. The scanning is done every 5 s and MAC ids of all identified devices is communicated to the Arduino. Arduino then sends all the MAC ids with a time-stamp to the Server. The screenshot of the serial monitor response and the web page used to display the MAC id, Time-Stamp, Scanner id and time of first and last detection is shown in Fig. 3. The server screenshot displaying the Bluetooth addresses captured is shown in Fig. 4 separately. The server after collecting the data runs a filter algorithm and retains the last entry of a MAC id received from a particular scanner id. Further, it runs the reidentification algorithm to separate the MAC ids which are detected by multiple scanners in a time window of max of 30 min. Based on the physical distance between the scanner's deployment, the speed and direction of travel for a particular MAC id is calculated

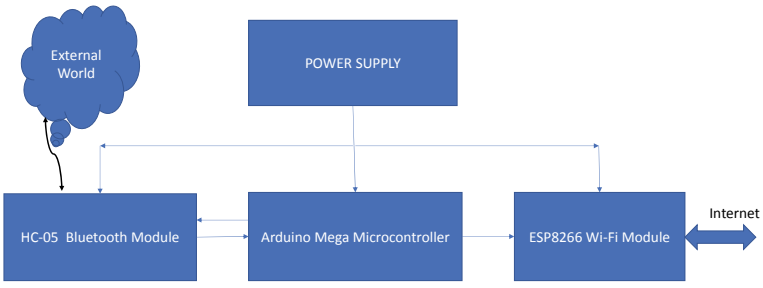

Fig. 1 Block diagram representation of the prototype Bluetooth scanner module

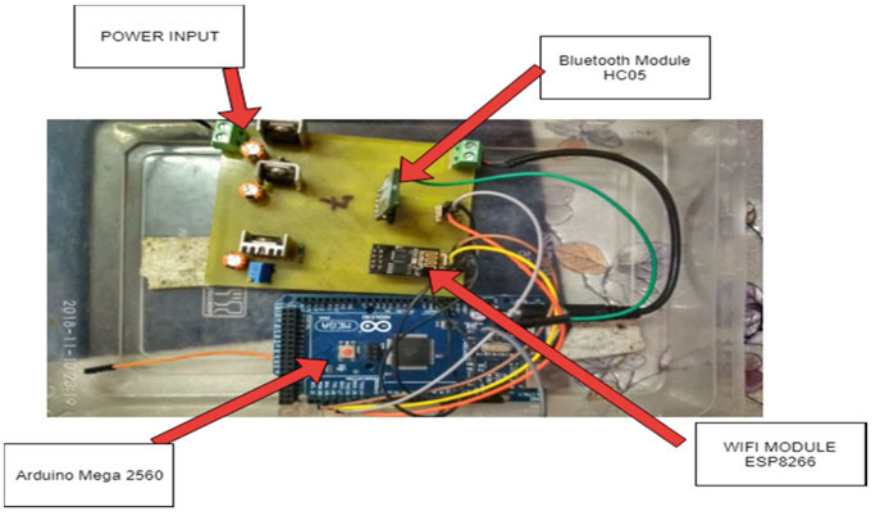

Fig. 2 Actual Hardware implementation of Bluetooth vehicle scanner

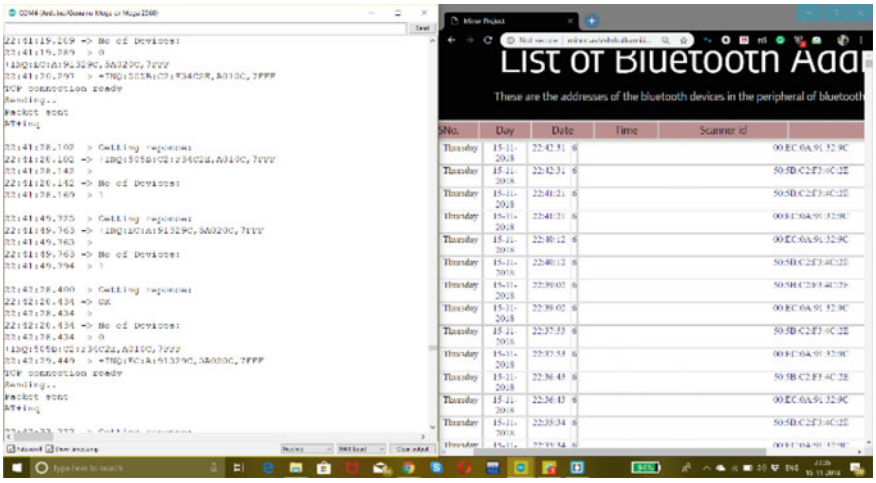

Fig. 3 Screenshot depicting the serial monitor response on left and web page displaying the Bluetooth addresses on right

and displayed on another web page of the same server. Screenshot of the web page is shown in Fig. 5. The process of finding the average travel speed is shown in Fig. 6 and the steps of the algorithm are as follows:

i. Sensors placed on the roadside scan the surroundings and collect the MAC ids of discoverable Bluetooth devices every 5 s.

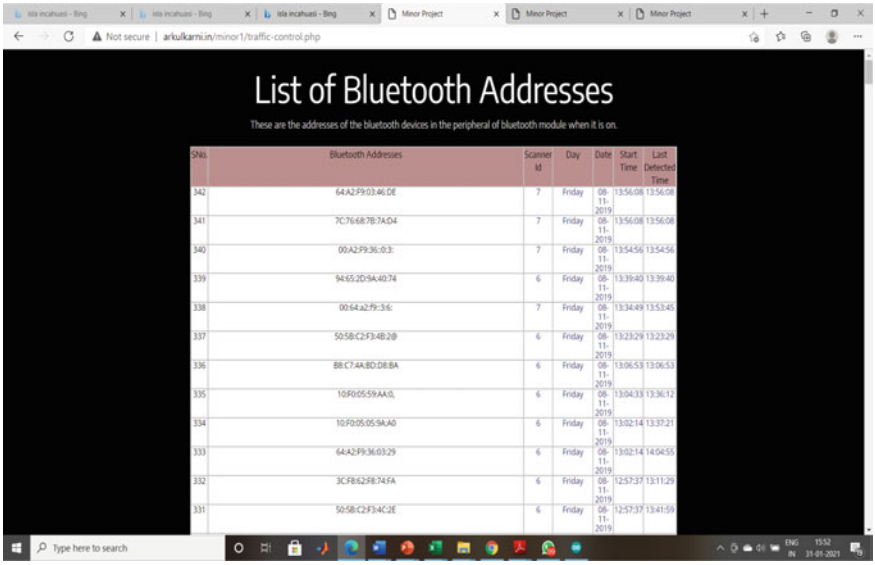

Fig. 4 Screenshot of webpage displaying the captured MAC addresses by the Bluetooth Scanner [10]

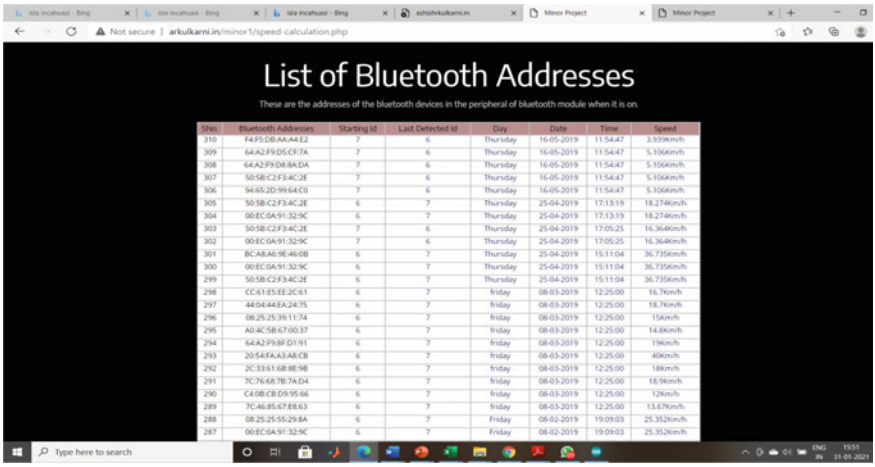

Fig. 5 Screenshot of web page displaying the direction and speed of travel for reidentified Bluetooth MAC addresses [11]

ii. Collected MAC ids are sent to the Arduino microcontroller over the serial port. The microcontroller sends the MAC ids along with the scanner id and time-stamp to the server using the Wi-Fi module EPS 8266.

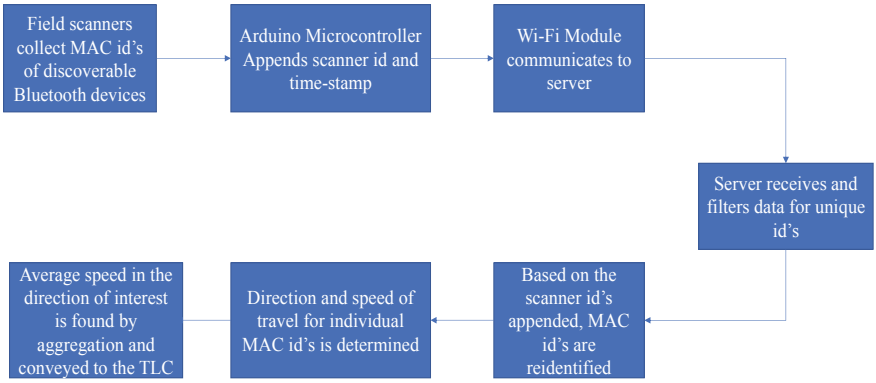

Fig. 6 Process flow for finding the average traffic speed on the server

iii. Time-stamp can also be appended at the server end. It can cause a delay of 2–3 s for every device.
iv. Server filters the received data for unique ids. Multiple detections of same MAC ids are quite possible within a scan cycle or in multiple scan cycles. The last entry for a given scanner id is retained and other instances are deleted.
v. Next, the server processes the filtered data for reidentification of devices across the two scanners ids in the vicinity. Based on the time difference, the direction of travel can be determined and speed can be calculated if the distance between the two scanners is known. The direction of travel can be determined based on which scanner out of the two (say, scanner A and B) identifies the device first: the direction can be from A to B or B to A.
vi. Average travel speed can be found out in a given time interval by aggregation. Before aggregation, the speeds are filtered and outliers like excessive high and low speeds are filtered out.
vii. Average speed thus calculated is sent to the traffic light controller at an interval of 5 min over SMS.

The workflow is depicted through the block diagram as shown in Fig. 7 Actual hardware implementation done in the controller cabinet is shown in Fig. 8 and the corresponding change in real time on a working traffic light is shown in Fig. 9.

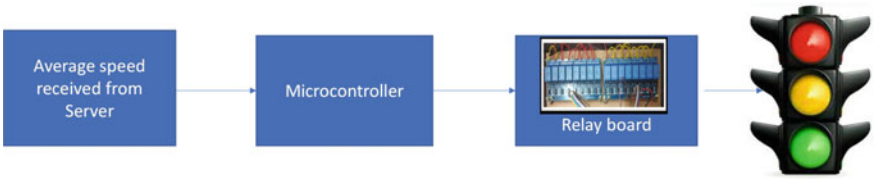

Fig. 7 Block diagram representation depicting the work flow for real time implementation of adaptive traffic lights

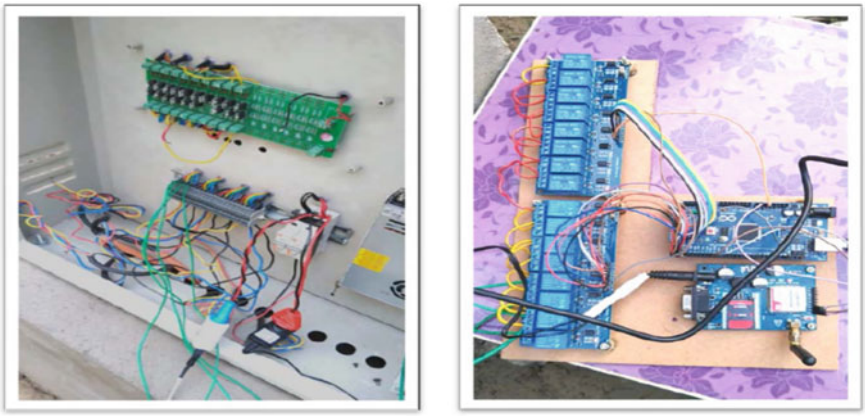

Fig. 8 External hardware connected to the Traffic Signal Controller to make it adaptive: **a** Components placed in controller cabinet **b** Relay board connections

Fig. 9 Real time control of existing Traffic Lights with modified hardware

The calculation for the green time offset for a particular approach based on the time of the day can be calculated as follows:

Average speed received from the server is 25 km/h.

Distance from the stop line to be cleared in the green time = 300 m.

Therefore green time offset is = dist/time = (0.3 km/25 km/h) * 3600 = 43.2 = 43 s.

Similarly, a speed of 30 km/h yields a green time offset of 36 s, whereas a speed of 20 km/h yields a green time offset of 54 s. The program will check for the solution to be within the minimum and maximum green time constraints. Limits need to be imposed so as to make the calculations realistic. The minimum green time is set to 15 s [9] and the maximum green time is 50 s. Traffic flow rate, saturation flow rate etc., are not considered here while deciding the minimum green time. They will be considered when we fine tune our algorithm and give weightage to the historical data as well. The purpose here is just to check if the limits are imposed properly or not. The calculated green time will change again after 5 min on receiving the new average speed from the server. So, the implementation algorithm will change accordingly. In this particular, the geometry and other details of the intersection under consideration are shown in Fig. 10.

In this particular project, there is one difference with respect to the normal progression algorithm. Normal progression assumes a definite speed of travel along the corridor and calculates the offset for subsequent signals based on the distance between the consecutive intersections. Here we calculate the upstream speed and then determine the green time. Based on this speed, the other offsets can be calculated, or each intersection can calculate its green time based on the upstream average speed. There are many variations to it, which can make the program more adaptive in real time. Authors are yet to apply the corridor level control and only single intersection control is considered.

Fig. 10 Three-way traffic signal at Sachdeva Public School

4 Conclusion

Bluetooth scanners deployed in the field are able to capture the MAC ids satisfactorily and send the same to the central server using the connected wi-fi module effectively.

The proposed hypothesis that a Bluetooth vehicle scanner can be used effectively, has been validated by correlating a vehicle survey done by deploying a state-of-the-art commercial Scanner capable of Bluetooth, Wi-Fi and XBee Scanning with video recordings of traffic at the same time and place. The findings are tabulated in Table 1. The penetration of Bluetooth devices without asking the commuters to turn-on their Bluetooth devices is between 10 and 15%. This can be further extrapolated to determine the traffic volume and used to determine the cycle time.

As such, Bluetooth vehicle scanners can prove to be a low cost and good source of traffic data and the same can be used to realize a low cost adaptive traffic light. This device acts as an input sensor to the existing traffic control system. The existing traffic light controller can be replaced by the modified controller proposed in this work enhancing the performance of the traffic light control system. Moreover, modification of existing traffic signal controllers without affecting the existing traffic light signal infrastructure is also possible.

References

1. Clark L Traffic signals: a brief history. Washington State Magazine. Washington State https://magazine.wsu.edu/web-extra/traffic-signals-a-brief-history/. Accessed 28 Aug 2021
2. Vickery HW, Leonard VW (1932) A recent development in traffic control. Trans Am Inst Electr Eng 51(3):796–800
3. Pasolini G, Verdone R (2002) Bluetooth for ITS? In: The 5th international symposium on wireless personal multimedia communications, vol.1. Honolulu, pp 315–319
4. Sawant H, Jindong T, Qingyan Y, Qizhi W (2004)Using Bluetooth and sensor networks for intelligent transportation systems. In: Proceedings of the 7th international IEEE conference on intelligent transportation systems (IEEE Cat. No.04TH8749). Washington, pp 767–772
5. Ashish B, Edward C (2013) Fundamental understanding on the use of Bluetooth scanner as a complementary transport data. Transp Res Part C: Emerg Technol 37:42–72
6. Porter JD, Kim DS, Magana ME Wireless data collection system for real-time arterial travel time estimates. OTREC 10–16. https://www.oregon.gov/ODOT/Programs/ResearchDocuments/WirelessData.pdf. Accessed 28 Aug 2021
7. Zarinbal Masouleh A, Hellinga BR (2019)Simulation of the bluetooth inquiry process for application in transportation engineering. IEEE Trans Intell Transp Syst 20(3):1020–1030
8. Bluetooth Market Update. https://www.bluetooth.com/bluetooth-resources/2020-bmu/. Accessed 28 Aug 2021
9. https://delhitrafficpolice.nic.in/sites/default/files/uploads/2014/04/B-46.pdf. Accessed 30 Aug 2021
10. https://arkulkarni.in/minor1/traffic-control.php. Accessed 28 Aug 2021 https://arkulkarni.in/minor1/speed-calculation.php
11. https://arkulkarni.in/minor1/speed-calculation.php. last accessed 2021/08/28

Characterisation and Prediction of Motorised Three Wheelers Travel Time in Urban Roadways

Durba Kundu, Hemant Mahour, Dhivya Bharathi, and Lelitha Vanajakshi

Abstract Motorised three wheeler is one of the most popular paratransit vehicles in India, due to its small size, cost-effectiveness, manoeuvrability, and availability. It provides the most flexible, rider-friendly, quick travel even in traffic-choked streets and narrow roads, exhibiting entirely different characteristics in terms of travel speed, and trip lengths compared to other paratransit modes like taxicabs. Reported studies on the behaviour of paratransit mainly concentrated on taxicabs and hence there is a need to analyse the travel behaviours of motorised three wheelers. In this regard, the present study aims to understand and characterise the travel patterns of motorised three wheelers. In addition, travel time prediction is an inevitable aspect for demand-responsive paratransit services like motorised three wheelers, taxicabs etc. It helps both the drivers and passengers to make smart choices about the routes by avoiding congested streets and to have information about the pickup and arrival time. The present study proposes a methodology using Support Vector Regression (SVR) to predict the travel time of motorised three wheelers by incorporating the trip characteristics under heterogenous lane less traffic conditions. The performance of the proposed method showed a clear improvement when compared with a Median based prediction methodology that was reported to be working well for travel time prediction problems.

Keywords Travel time prediction · Paratransit · Machine learning · Travel pattern

D. Kundu · H. Mahour · D. Bharathi · L. Vanajakshi (✉)
Indian Institute of Technology Madras, Chennai, India
e-mail: lelitha@iitm.ac.in

L. Devi et al. (eds.), *Proceedings of the Sixth International Conference of Transportation Research Group of India*, Lecture Notes in Civil Engineering 273,
https://doi.org/10.1007/978-981-19-4204-4_26

1 Introduction

Last-mile connectivity is an important factor that influences/encourages travellers to choose a particular mode of transport to reach their preferred destination. In this regard, paratransit is the most sought-after mode to travel to /from the mass transit services, due to its cost-effectiveness, last-mile connectivity, comfort, flexible routes, and timing. Though, taxi cabs are popular in western countries, motorised three wheelers (popularly known as Auto-rickshaws) are the most preferred paratransit in developing countries like India due to its lesser cost and flexibility. However, commuters prefer certain information like travel time, distance, fare, etc. to be known before the start of the trip to plan their activity. The availability of such information may help the commuters to make better trip-related decisions ahead of the journey. Also, the travel time predicted for the corridor/or the stream of vehicles may not match with the travel time experienced by the motorised three wheelers in real time, as they exhibit a completely different driving characteristic and travel behaviour. Hence, the travel time of motorised three wheeler needs to be analysed and predicted separately. The present study aims to analyse the travel time of motorised three wheelers to understand their trip characteristics and to develop a methodology to predict the same by incorporating the identified trip characteristics, under heterogeneous and lane less traffic conditions. The current study focused on route level travel time prediction for any given time and day, to enhance the mobility service and to reduce the travel time uncertainties of the motorised three wheelers on Indian roads.

Literature reported the use of various prediction methods such as historical methods, statistical methods like regression analysis and time series analysis, machine learning techniques like support vector machines and artificial neural networks, traffic flow theory-based methods etc. for the prediction of travel time in general. A few studies were reported on the prediction of travel times of paratransit vehicles like taxi cabs. However, there are no studies reported on the prediction of motorised three wheelers. In addition, almost all of them were tested on homogeneous and lane-based traffic conditions. The present study developed a methodology to predict the travel time of motorised three wheelers under heterogeneous lane less traffic conditions using support vector regression, a machine learning technique. The study analyses the travel time data of motorised three wheelers to understand the patterns that data exhibits and incorporated the same into the prediction methodology. Further, the proposed methodology is compared with a Median based prediction approach [1] to understand its efficiency. Results show the proposed methodology as a viable solution for the development of a route planner solution for paratransit service under Indian traffic conditions. The prediction methodology presented in this study can be readily implemented for real time implementations like the development of on-demand mobility applications.

The paper is organised as follows. Section 2 discusses the reported studies on travel time prediction, Sect. 3 describes the data collection and pre-processing carried out before the implementation, Sect. 4 details the methodology while Sect. 5 discusses

the results and comparison with the existing models. Finally, Sect. 6 concludes the paper by summarising the results and inferences.

2 Literature Review

Travel time prediction has been a major area of research for the past several years. Studies focusing on travel time prediction of public transport [2–10], car [11–13] and taxis [14–19] are reviewed here. Methodologies reported for travel time prediction can be broadly classified as parametric models (linear regression, time series models and Kalman filter) and non-parametric models (neural network, support vector regression, nearest neighbours and ensemble learning). Bai et al. [19] compared these methods in terms of data, prediction range and accuracy.

Several studies on predicting the travel time of buses were reported and some of the major ones are discussed here. Jeong and Rilett [2] introduced a historical average travel time model for predicting link travel time between two links of bus stops. Historical average models are mainly based on the historic travel time data and are useful where the traffic flow is relatively less. Patnaik et al. [3] developed a multivariate regression model to predict the bus arrival time, using the vehicle automatic passenger counting system combined with factors such as station distance, detention time, and station number. Bae and Kachroo [4] simulated the dynamic characteristics of a bus driver, based on passenger arrival rate and the passenger boarding rate. This study has used the least-squares estimation method to predict the boarding time and the parameter adaptation algorithm to predict the arrival time. Cathy and Dailiey [5] developed a prediction model based on the Kalman filter. Bie et al. [6] presented a forecast model based on the GPS data to predict the bus arrival time at a signalized intersection. Chen et al. [7] developed a neural network model considering the weather and time period to predict the bus arrival time. A few studies [8–10, 20] reported the SVR technique to be more accurate in predicting travel time than other machine learning algorithms. Yu et al. [8] proposed a SVM based prediction model to predict the travel times of buses. Yu et al. [9] compared four general models (SVM, ANN, *k*-nearest neighbours (*k*-NN) algorithm, and regression model). They reported that the SVM model outperformed the other models for the arrival time prediction of the bus. Thissen et al. [10] and Wu et al. [20] also used SVM as a prediction tool for bus arrival time. However, the above studies were on bus travel time. In the last decades, a few studies have been reported on the travel time prediction using data from floating cars and are discussed next.

Przemysław and Andrzej [11] have focused on the travel time prediction of personal car using online navigation system by creating a dynamic model. Mingjun and Shiru [12] used a non-parametric regression model for short-term travel time prediction of cars. Li et al. [13] used a gradient boosting model for travel time prediction of freight vehicles. A few studies on travel time prediction of taxi cab services in different regions were also reported [14–18]. Kankanamge et al. [14] and Gupta et al. [15] used an isolated XG Boost regression model for the travel time

prediction of a taxi. Dietmer and Mirsad [16] used the least square method for travel time prediction using floating car data. Jammula et al. [17] investigated travel time estimation under heterogeneous traffic conditions using a multi-linear regression. Gui and Yu [18] aimed to forecast the trip travel time of a certain origin and destination location at a future start time of a day based on the past trip travel time of that day using selective forgetting extreme machine learning techniques.

As discussed under the bus travel time prediction, several studies showed SVR as a good prediction model for travel time. Similar conclusions were made in the case of the prediction of taxi travel time in [21, 22]. Liu et al. [21] showed that the prediction method based on SVR has better tracking ability and dynamic behaviour compared to ANN models. Laha and Putatunda [22] suggested support vector regression as a good choice when the dataset is small to moderate. They have worked on NYC Yellow Taxi GPS Data, San Francisco black cars GPS traces and Porto GPS data. They compared different algorithms for travel time prediction in different situations and showed SVR working well with small size training dataset considering both prediction accuracy and total computation time. When continuous prediction of remaining travel time and continuous updating of total travel time along the trajectory of a trip was considered, the SVR method had the best predictive accuracy.

From the literature review, it was observed that for the travel time prediction of different vehicles (bus, taxi) support vector regression is a good prediction technique as it can handle high variability and can perform with sparse dataset [8–10, 20, 19, 21]. Support Vector Machines (SVM) is an advanced machine learning technique, introduced by Vapnik [23]. The key features of SVM include the capability of generalisation, efficiency in computation, and robust prediction with a smaller number of datasets. Bhaskar et al. [24] suggested that regression-based modelling is fast to compute and favourable for several transport applications. Vanajakshi and Rilett [25] and Wu et al. [26] used this technique for forecasting travel time for the limited dataset. The support vector regression technique was reported to have greater generalisation ability and guaranteed global minima for a given training data. Among various data-driven methods, support vector regression is shown to predict travel time with better accuracy [25–27]. SVR method is reported to be able to capture variations more efficiently than ANN and moving average method [27]. Vanajakshi and Rilett [25] reported that SVM is a viable alternative for short-term prediction problems when the amount of data is less or noisy in nature. Based on these, SVR is selected as the prediction tool in this study.

Thus, the objective of the current study is to predict segment wise travel times of paratransit vehicles. Based on the literature review, support vector regression is chosen, mainly because the data is sparse and dispersed, where SVR is recommended. Details of the data used are discussed next, followed by the analysis and results.

3 Data Description and Preliminary Analysis

The data used in this study is from a motorised three wheeler aggregator group from Chennai, India. GPS data from 10 motorised three wheelers collected for a period of three months (April, May and June) were used. The raw data consist of the month of the year, trip date, day of the week, trip number, start time of the trip, end time of the trip, latitude and longitude coordinates of the routes travelled for every time stamp and status of the trip (start, ready, end). The attributes of the raw data were 'IMEI_Number', 'curr_date', 'curr_time', 'msg_type', 'lat', 'long', 'trip_start_time'. A sample screenshot of the raw database is shown in Fig. 1.

Individual trips from each device were identified using the information from the "msg_type" column. If the "msg_type" is 'Ready', the trip has started whereas the "msg_type" = 'Place' denotes an ongoing trip, and the "msg_type" = 'End' implies the end of the trip. Similarly, the start time, end time, latitudes and longitudes of origin and destination are identified. The geographic distance between the origin and destination was obtained by calculating cumulative distances between the successive latitude and longitude coordinates using Haversine formula [28]. This distance is considered as trip length. Further, the data were processed to extract travel time and journey speeds for all the trips. Travel times of the trips were extracted by taking the difference between the starting and ending time stamps of the trip. The journey speeds are then calculated from the travel time and trip length. The raw data contained a total of 8,98,643 data points that resulted in 3208 trips among different origins and destinations. Out of the total trips, 2351 trips were made during weekdays and 857 trips were made on weekends. Out of all the data, 54% of the trips were in the month of May, 34% of the trips were in the month of April and 12% of the trips were in the month of June. Motorised three wheelers were marked as "Auto ID 1 to 10" based on the unique IMEI number and trips made by each "Auto ID" was separated for analysis. The number of trips made was found to vary from a minimum of 1 trip to a maximum of 28 trips in a day.

The present study conducted a preliminary data analysis to understand the characteristics and patterns in the data. The datasets were processed in three stages to remove the outliers. In stage one, IDs with very less data points are removed. In

imei_number	curr_date	curr_time	msg_type	lat	long	speed	heading	hicle_stat	vehicle_number	trip_number	p_start_dat	p_start_tir	signal_str	ttery_cha	version	month	week_day	curr_day	curr_hr	curr_min
861074025250245.00	16-05-2015	18:09:32	READY	13.0741	80.2693	0	13.54	0	TN 09 BT 6538	1	0015-05-16	18:09:32	0	0		May	Saturday	16	18	9
861074025250245.00	16-05-2015	18:09:36	PLACE	13.0741	80.2693	0	13.54	0	TN 09 BT 6538	1	0015-05-16	18:09:32	2	86	4	May	Saturday	16	18	9
861074025250245.00	16-05-2015	18:09:46	PLACE	13.0741	80.2693	0	13.54	0	TN 09 BT 6538	1	0015-05-16	18:09:32	2	86	4	May	Saturday	16	18	9
861074025250245.00	16-05-2015	18:09:56	PLACE	13.0741	80.2693	0	13.54	0	TN 09 BT 6538	1	0015-05-16	18:09:32	2	85	4	May	Saturday	16	18	9
861074025250245.00	16-05-2015	18:10:09	PLACE	13.0741	80.2693	0.35	13.54	0	TN 09 BT 6538	1	0015-05-16	18:09:32	2	86	4	May	Saturday	16	18	10
861074025250245.00	16-05-2015	18:10:20	PLACE	13.0741	80.2693	0.24	13.54	0	TN 09 BT 6538	1	0015-05-16	18:09:32	2	86	4	May	Saturday	16	18	10
861074025250245.00	16-05-2015	18:10:31	PLACE	13.0741	80.2693	0.38	13.54	0	TN 09 BT 6538	1	0015-05-16	18:09:32	2	86	4	May	Saturday	16	18	10
861074025250245.00	16-05-2015	18:10:41	PLACE	13.0741	80.2693	0.14	13.54	0	TN 09 BT 6538	1	0015-05-16	18:09:32	2	86	4	May	Saturday	16	18	10
861074025250245.00	16-05-2015	18:10:53	PLACE	13.0741	80.2693	0	13.54	0	TN 09 BT 6538	1	0015-05-16	18:09:32	2	86	4	May	Saturday	16	18	10
861074025250245.00	16-05-2015	18:11:03	PLACE	13.0741	80.2693	0	13.54	0	TN 09 BT 6538	1	0015-05-16	18:09:32	2	86	4	May	Saturday	16	18	11
861074025250245.00	16-05-2015	18:11:13	PLACE	13.0741	80.2693	0	13.54	0	TN 09 BT 6538	1	0015-05-16	18:09:32	2	86	4	May	Saturday	16	18	11
861074025250245.00	16-05-2015	18:11:24	PLACE	13.0741	80.2693	0	13.54	0	TN 09 BT 6538	1	0015-05-16	18:09:32	2	86	4	May	Saturday	16	18	11
861074025250245.00	16-05-2015	18:11:35	PLACE	13.0741	80.2693	0	13.54	0	TN 09 BT 6538	1	0015-05-16	18:09:32	2	86	4	May	Saturday	16	18	11
861074025250245.00	16-05-2015	18:11:46	PLACE	13.0741	80.2693	0	13.54	0	TN 09 BT 6538	1	0015-05-16	18:09:32	2	87	4	May	Saturday	16	18	11
861074025250245.00	16-05-2015	18:11:56	PLACE	13.0741	80.2693	0	13.54	0	TN 09 BT 6538	1	0015-05-16	18:09:32	2	86	4	May	Saturday	16	18	11
861074025250245.00	16-05-2015	18:12:08	PLACE	13.0741	80.2693	0	13.54	0	TN 09 BT 6538	1	0015-05-16	18:09:32	2	86	4	May	Saturday	16	18	12
861074025250245.00	16-05-2015	18:12:19	PLACE	13.0741	80.2693	0	13.54	0	TN 09 BT 6538	1	0015-05-16	18:09:32	2	87	4	May	Saturday	16	18	12
861074025250245.00	16-05-2015	18:12:30	PLACE	13.0741	80.2693	0	13.54	0	TN 09 BT 6538	1	0015-05-16	18:09:32	2	86	4	May	Saturday	16	18	12
861074025250245.00	16-05-2015	18:12:41	PLACE	13.0741	80.2693	0	13.54	0	TN 09 BT 6538	1	0015-05-16	18:09:32	2	87	4	May	Saturday	16	18	12

Fig. 1 Screenshot of raw database

this stage, Auto ID 2, 6 and 9 got removed from the database. In the second stage, trip lengths and journey speeds were analysed. Para transits are usually preferred for short distance commuting within the city and hence, longer trips are unusual. Hence, a threshold of 20 km was adopted and it was found that less than 1% of trips (11 trips) were beyond the threshold and were removed. Further, trips with trip lengths less than 0.5 km were also removed. A total of around 70 trips were removed based on longer and shorter trip length thresholds. In the next stage, trips with journey speed more than 60 km/hr (speed limit) and less than 0.5 km/hr were identified and removed. After this, outliers were detected using Median Absolute Deviation (MAD) method [29], which considers the distribution followed by the data. To identify the outliers in the data, standard z-score and modified Z-score are commonly used. In general, if the dataset follows a normal distribution, a standard z-score is used and if the dataset follows log-normal distribution modified z-score is used.

For this, distribution fitting was carried out using Easy-fit software [30] and the best fitting distribution was identified using Kolmogorov–Smirnov (K-S) test. Based on the K-S test statistic value, it was observed that the data follow a log-normal distribution. Figure 2 shows a sample distribution fitting for the considered data using normal and log-normal distribution and Table 1 shows the corresponding parameters of these distributions. From the values, it can be seen that the value of K-S Statistics for log-normal distribution (0.0745) is less than the value of K-S Statistics of Normal

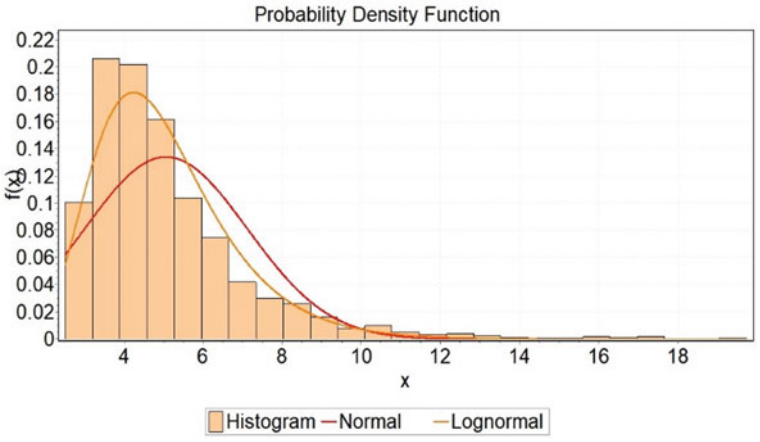

Fig. 2 PDF of the travel time distribution

Table 1 The parameters of the log-normal and normal distribution of the travel time data

Distribution	Number of samples	Parameters	K-S value	P-value
Log-normal	3021	$\sigma = 0.3175$, $\mu = 1.6234$	0.0745	0.000
Normal	3021	$\sigma = 2.3154$, $\mu = 5.6517$	0.1414	0.14

distribution (0.1414). It implies that Log-normal distribution better fits the travel time data than normal distribution.

As the data follow log-normal distribution, a modified z-score, which uses median as a measure instead of mean making it resistant to abnormally deviated values compared to the standard z-score, is used. The modified z-score was calculated for each day of the week separately and outliers were removed independently. Figure 3a and b show scatterplots of data with and without outliers for weekdays. Figure 4a and b show the scatterplot of data with and without outliers for weekends. It can be observed from the figures (after removing outliers) that weekdays data exhibit prominent morning and evening peak whereas weekend does not show any of such trends. Thus, it reveals weekdays and weekends may need separate models for prediction.

These cleaned data were analysed, and the descriptive statistics obtained for travel time, trip length, and journey speed are shown in Table 2. In the next stage, the number

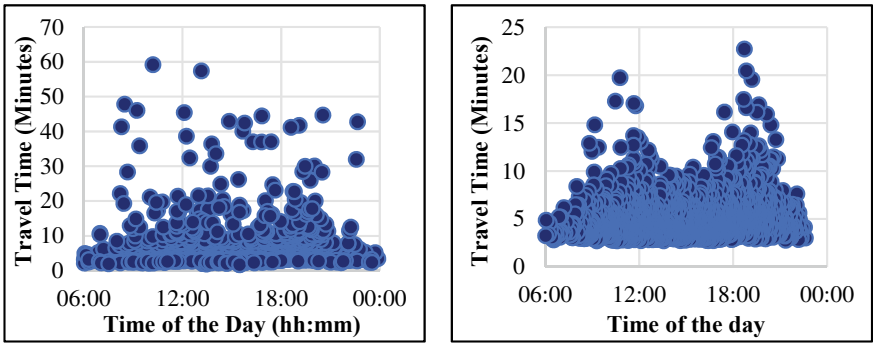

a) With outliers b) Without outliers

Fig. 3 Scatterplot of weekdays travel time data with and without outliers. **a** With outliers. **b** Without outliers

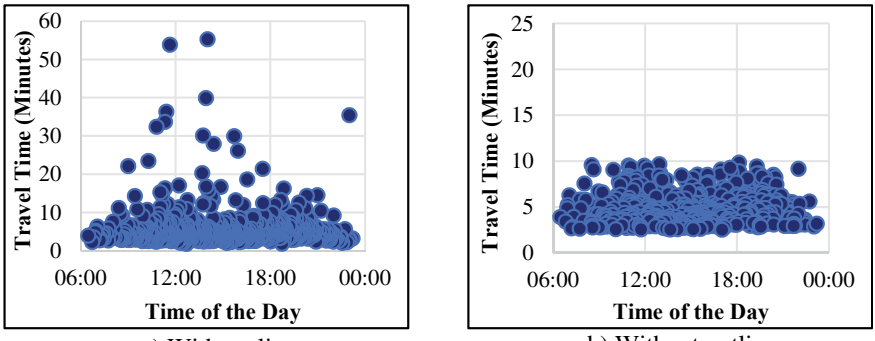

a) With outliers b) Without outliers

Fig. 4 Scatterplot of weekend travel time data with and without outliers. **a** With outliers. **b** Without outliers

Table 2 Descriptive statistics of the variables

Distribution	Variables		
	Travel time (minutes)	Speed (km/hr)	Trip length (km)
Mean	18.78	10.96	4.72
Median	13.27	16.16	3.66
Mode	10.36	11.4	3.23
Standard deviation	20.93	9.87	4.66
Minimum	5.07	4.51	2.231
Maximum	19.28	22.62	19.47
25th Percentile	7.4751	11.38	2.16
75th Percentile	23.3	21.53	4.98

of trips over different time periods of the day was analysed and it was observed that in the middle of the day (10 to 18 h), the number of trips was higher than the rest of the day. Also, it was found that the majority of trips (86.26%) were in the range of 0–30 min. 12.82% of trips were between 30–60 min. 93.89% of the trips were within 10 km. 32.23% of the trips had a speed within 10 km/hour. 59.10% of the trips had a speed range between 10–20 km/hour.

The data were further analysed to identify the peak and off-peak hours within a day. For this, the travel time data were grouped and averaged over an hour and analysed across different time periods of the day. Removing the late night and early morning hours in which trips were not there, there were 18-time bins from 6.00 AM to 11 PM. Figure 5 shows the variation in average journey time across different times of the day. From Fig. 6, it can be observed that the travel times from 9 AM to 1 PM and 4 PM to 9 PM are relatively high, indicating morning and evening peaks. Based on this, the travel times are grouped with respect to the starting time of the trip as:

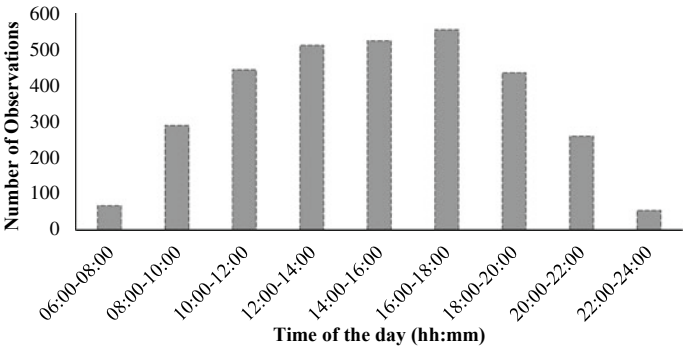

Fig. 5 Number of trips over time

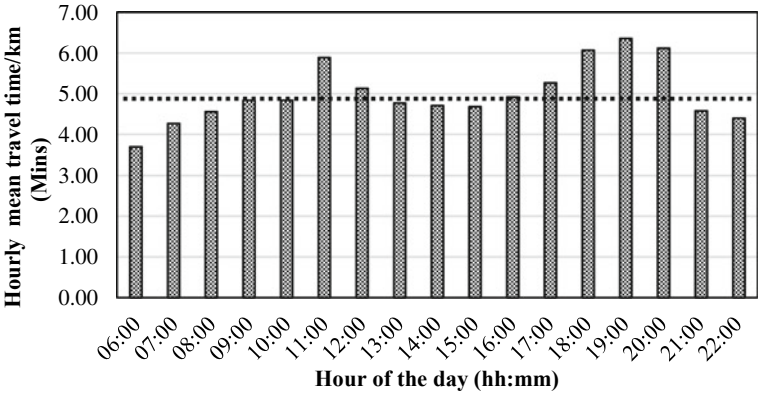

Fig. 6 Average hourly travel time over the time of the day for the weekdays trip

Morning off-peak (before 9 AM), morning peak (9 AM - 1 PM), afternoon off-peak (1 PM - 4 PM), evening peak (4 PM - 9 PM), and evening off-peak (after 9 PM).

Following this, the most travelled route was identified and selected from the list of origin–destination pairs for the implementation of the proposed prediction methodology. Maximum number of trips were observed from Besant Nagar, a recreational area, in the central part of the city, to Madipakkam, a residential area in the suburbs. Around 24 trips were found between this origin and destination during the study period of three months. Out of these 24 trips, 75% trips were kept for model building and the remaining for testing. To account for the travel time variations along the identified route, the selected route was disintegrated into 7 different segments of varied lengths using major landmarks. Figure 7 shows the map of the selected route with segments marked. Table 3 shows the list of segments with its details. The time taken by the motorised three wheelers to traverse each of these segments was calculated and used for modelling and prediction. To increase the data points for training, overlapping trips were also considered and segment travel times were extracted.

4 Prediction Methodology

The present study developed a support vector regression-based prediction methodology and compared the performance with the median based travel time prediction method.

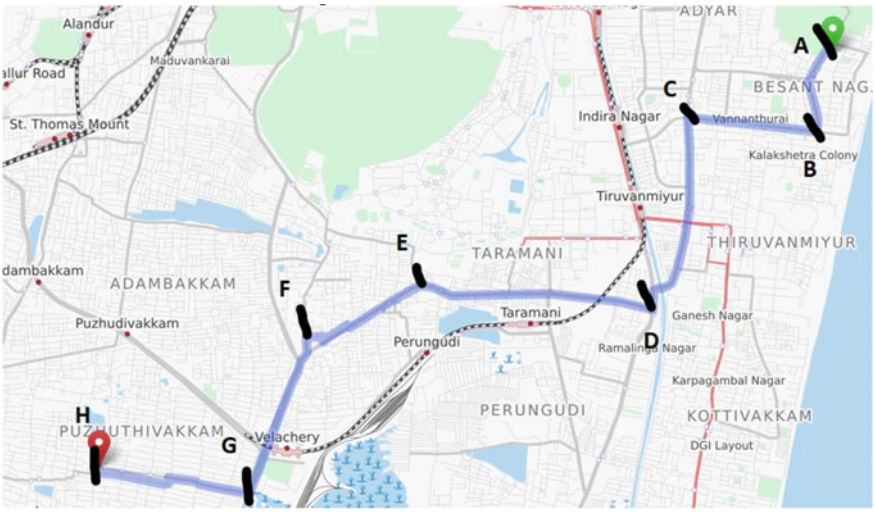

Fig. 7 Segmentation (A-B, B-C, C-D, D-E, E-F, F-G, G-H) of the most travelled Route. *Source* Open Street Maps

Table 3 Description of the segments

Description of the link	Number of trips	Number of overlapping trips	Length(km)
Link 1 (A-B)	24	38	1.08
Link 2 (B-C)	24	34	1.16
Link 3 (C-D)	24	24	1.12
Link 4 (D-E)	24	20	1.24
Link 5 (E–F)	24	28	1.91
Link 6 (F-G)	24	30	2.11
Link 7 (G-H)	24	24	2.78

4.1 Support Vector Regression

The baseline of a regression problem is to find a particular function that estimates mapping from the input features to real numbers on the basis of a training sample. The Support Vector Regression (SVR) uses the same principles as of the SVM for classification, with only a few minor differences. First of all, in SVR, the output is a real number. In the case of regression, a margin of tolerance (ε) is pre-defined. The main idea of SVR, as in SVM, is to minimise error, by individualising the hyper plane which maximises the margin. The performance of SVR depends on several hyperparameters such as penalty parameter, intensive loss function parameter and the parameter for kernel function. The cost function helps in controlling the trade-off

between the maximisation of the margins and the minimisation of error. The kernel function helps to map the non-linearity of the problem into feature space. In this study, radial-basis-kernel-function with a soft margin [22] was used to deal with the non-linearity of the dataset. The radial basis function uses a non-linear hyperplane for prediction.

In a linear SVM model, the general SVM equation is written as Eq. (1).

$$f(x) = w.x + b, \tag{1}$$

where 'w' is the weight vector and 'b' is the bias. f(x) is the function associated with the hyperplane. In this study, the training data, T has a set of n number of points Eq. (2), i.e.

$$T = \{(x_i, y_i)\} \mid x_i \in R^T, \tag{2}$$

where y_i belongs to -1 or 1, in which the point x_i belongs to a T-dimensional space R^t. A simple form of non-linear SVR model in higher dimensional space is given by Eq. (3)

$$y(x, w) = w\varnothing(x) + w_0, \tag{3}$$

where $\varnothing(x)$ represents the high dimensional feature spaces.

The travel time of a segment is predicted based on the input features, which include the historic travel time, real time data and the predicted value. The input features selected are travel time data of the previous trip of the same segment, average travel time of 30 min interval of that segment, travel time data of the same trip of the previous segment or Predicted travel time value of the previous segment, weekdays/weekend, and peak hour/off-peak hour. The performance of this model was compared with a median based model as discussed below.

4.2 Median Based Prediction Method

A median based model which uses particle filtering technique as a recursive estimation tool was developed for predicting travel time of auto-rickshaws. As stated already, the entire route was divided into smaller segments of different lengths and the time taken to travel each of these segments was considered for prediction. The model considers the predicted segment travel time as the sum of the median of historical travel times, and random variations in travel time over time, as shown in Eq. (4).

$$T^i_{t+1} = m^i_{t+1} + x^i_{t+1}, \tag{4}$$

where $T^{i}_{(t+1)}$ is the time taken to travel the section i in the next trip $(t + 1)$, m^{i} $(t + 1)$ is the median of the historical travel time of section i in the next trip $(t + 1)$, $x^{i}_{(t+1)}$ is the random variation of $(t + 1)^{\text{th}}$ trip travel time from the corresponding historical median travel time. The steps for obtaining the aforementioned variables are discussed next.

For any trip (t), the median was calculated using the one-hour of historical data considering $\pm$ 30 min around $(t - 30$ to $t + 30$ min). The one-hour time window changes with respect to the start time of the trip. The algorithm automatically detects the start time of the trip and calculates the median in real time. The model hypothesises that the median of historical travel times captures the primary traffic patterns specific to the time of the day and hence predicting the actual travel time will be equivalent to forecasting the variations in travel time according to the current conditions. The evolution of the random variation in travel time was modelled and represented in state space form as Eq. (5)

$$x^{i}_{(t+1)} = x^{i}_{(t)} + w^{i}_{(t+1)}, \tag{5}$$

where, $x_i{}^{(t+1)}$ is the variation of $(t + 1)^{\text{th}}$ trip travel time from the corresponding historical median travel time, $x_i{}^{(t)}$ is the variation of $(t)^{\text{th}}$ trip travel time from the corresponding historical median travel time, $w_i{}^{(t)}$ is the associated process disturbance with the $(t)^{\text{th}}$ trip travel time. The measurement process was assumed to be governed by Eq. (6)

$$z^{i}_{(t+1)} = x^{i}_{(t)} + v^{i}_{(t+1)}, \tag{6}$$

where $z^{i}{}_{(t)}$ is the measured variation of $(t)^{\text{th}}$ trip travel time from the corresponding historical median travel time for the section i, and $\mathrm{v}^{i}{}_{(t)}$ is the measurement noise associated with the $(t)^{\text{th}}$ trip travel time for the section i. As per the model, the previous trip connecting the same origin and destination would not have happened in the one-hour window of the same day. Hence, to identify significant inputs for the variation prediction, the current framework used the historical travel time of trips that happened in the one-hour window. The algorithm identifies the two closest trips based on the time of entry into the segment and assigns them as inputs to predict the variations in travel time over time. The prediction methodology was integrated with the particle filtering technique to recursively predict and update in real time. The above scheme was implemented in MATLAB and the results are discussed below.

5 Results

The performance of the proposed method was quantified using Mean Absolute Percentage Error (MAPE) and compared with the median based prediction methodology using the particle filtering technique. Figure 8 shows the comparison of the measured and predicted travel times using the SVR method and Median method for a sample trip. Figure 8 shows a very good matching of predicted travel time values with the measured travel time values by SVR based method compared to Median based method. It is very evident from the figure that SVR captures the variations in travel time better than the Median based method.

Further, the performance was evaluated for all the trips during the test period. Figure 9 shows the comparison of MAPE values of the SVR method and median method for all the considered test trips. From the figure, it can be seen that the trip

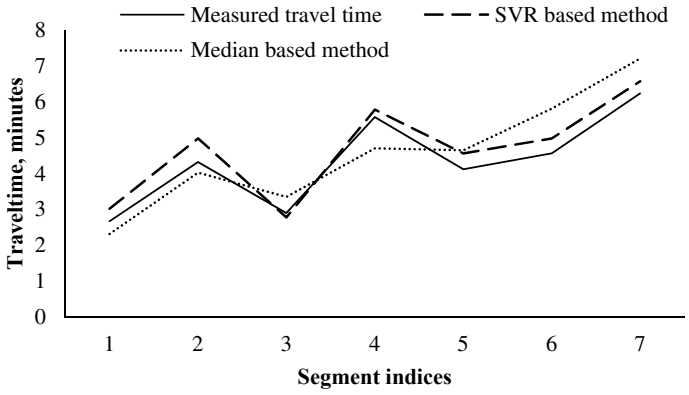

Fig. 8 Measured and predicted values of SVR method and Median method

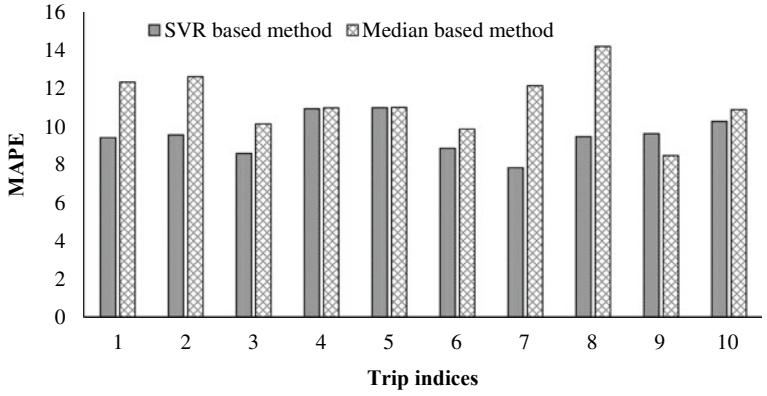

Fig. 9 MAPE values of SVR method and Median method across trip indices

wise performance of both the methods are comparable with slight superiority by SVR method with an error advantage up to 4% (Trip index no:8). Also, it can be seen that all the trip wise MAPE values are lesser than 12% for SVR method, which is considered to be good, as per Lewis's scale of prediction accuracy [31].

As the current methodology predicts the travel time of segments along the route, it is important to evaluate and compare the accuracy over segments. Hence, in the next stage, the performance of the individual segments was analysed for both the support vector regression-based method and median based method. Figure 10 shows the MAPE values of both the methods for all the trips that happened on each segment along the considered route. From the figures, it can be seen that SVR method outperforms the median method in majority of segments. In particular, MAPE values of SVR method are less than 15% on segment 6, which is one of the most congested corridors with an oversaturated signalized intersection. Next, the average MAPE values of each segment were analysed and shown in Fig. 11. A clear superiority by SVR method can be seen in most of the cases revealing the efficiency of the proposed method to predict the travel time of auto-rickshaws under heterogenous lane less traffic conditions.

6 Conclusion

The present study analyses the travel time data of motorised three wheelers collected from a heterogeneous lane less traffic condition to understand the patterns that data exhibits and incorporated the same into the prediction methodology. A machine learning based methodology was developed to predict the travel time of motorised three wheelers accurately in real time and compared the performance with an existing median based methodology. The raw data attributes were studied and analysed to understand the nature of the data and test bed. The pattern analysis of motorised three wheelers travel time revealed that the morning peak is around 09:00 AM to 01.00 PM and the evening peak is from 04.00 PM to 09.00 PM. These time periods showed higher travel times compared to the rest of the day. Further, different trip characteristics such as trip length, journey speed, and number of trips were analysed, and it was found that the majority of trip travel times (86.26%) were in the range of 0–30 min. 12.82% trips were between 30–60 min. 93.89% of the trips were within 10 km. 32.23% of the trips had a speed within 10 km/hour. 59.10% of the trips had a speed range between 10–20 km/hour. In the next stage, the study developed a SVR model for the real time prediction of the travel time of motorised three wheelers. The results derived from the study showed that the SVR model is able to predict the paratransit travel time with an accuracy of 15%. For comparison, an already existing median based model was used. Comparison results showed the SVR outperforming the median based modelling approach. The prediction methodology presented in this study can be readily implemented for real time implementations like the development of on-demand mobility applications. In the next stage, more data from multiple cities

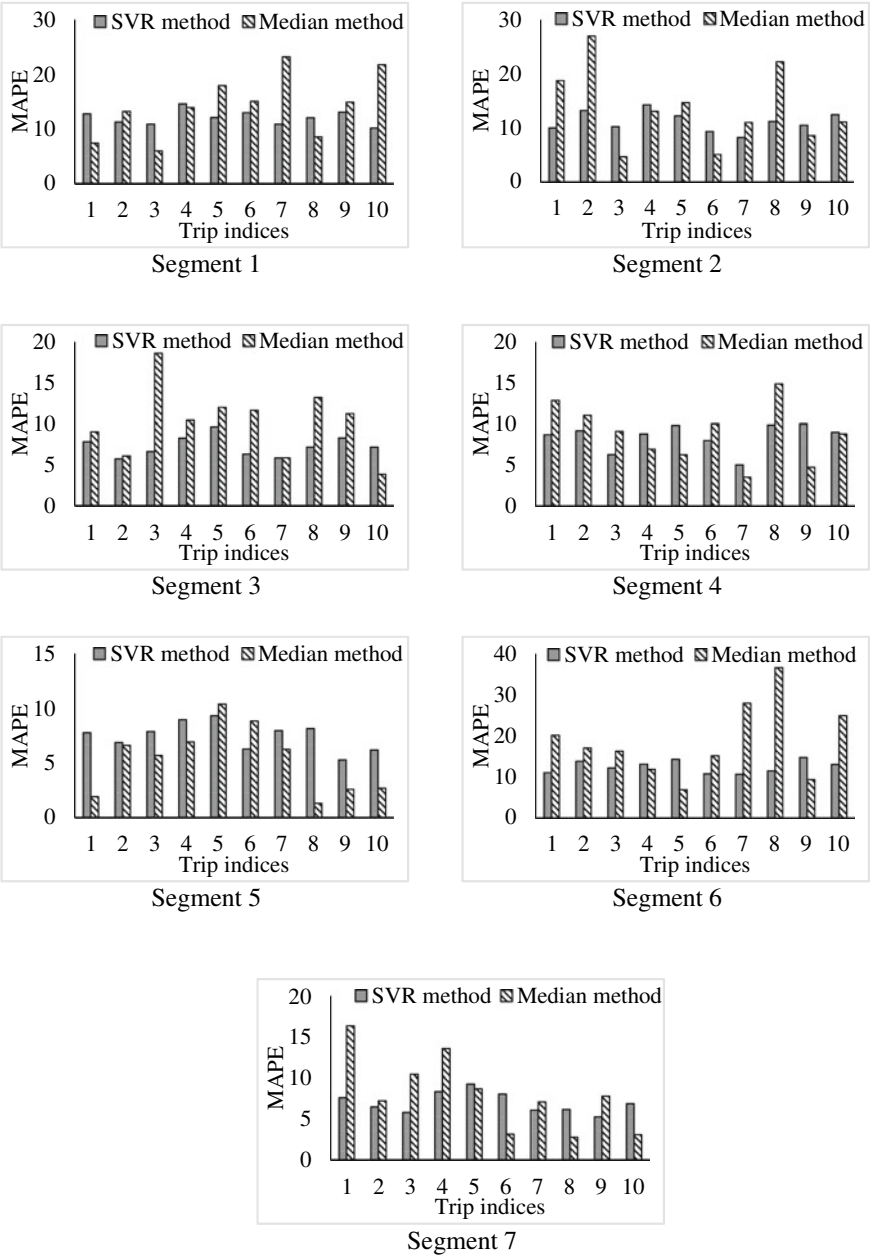

Fig. 10 MAPE values of SVR method and Median method over trips on individual segments

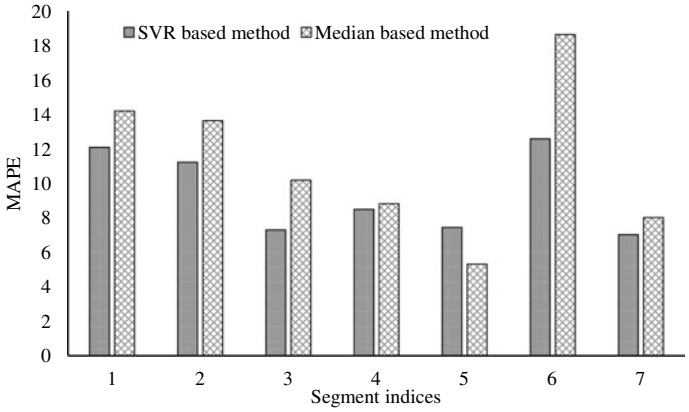

Fig. 11 MAPE values of SVR method and Median method for individual segments

can be used along with considering other influencing factors such as human and environmental characteristics.

Acknowledgements The authors acknowledge the support of for this study as a part of the IMPRINT project funded by SERB, Department of Science and Technology, Government of India, through sanction order number IMP/2018/001850.

References

1. Dhivyabharathi B, Kumar BA, Vanajakshi L (2016) Real time bus arrival time prediction system under Indian traffic condition, IEEE International Conference on Intelligent Transportation Engineering (ICITE), pp 18–22
2. Jeong R, Rilett L (2004) The prediction of bus arrival time using AVL data, in 83rd annual general meeting of transportation research board, national research council. Washington D.C, USA
3. Patnaik J, Chien S, Bladikas A (2004) Estimation of bus arrival times using APC data. J Public Transp 7(1):1–20
4. Bae S, Kachroo P (1995) Proactive travel time predictions under interrupted flow condition, vehicle navigation & information systems conference proceedings, 6th International VNIS. 'A Ride into the Future' 179–186. Institute of Electrical and Electronics Engineers
5. Cathey FW, Dailey DJ (2003) A prescription for transit arrival/departure prediction using automatic vehicle location data. Transp Res Part C Emerg Technol 11(3–4):241–264
6. Bie Y, Wang D, Qi H (2011) Prediction model of bus arrival time at signalized intersection using GPS data. J Transp Eng 138(1)
7. Chen M, Liu X, Xia J, Chien S (2004) A dynamic bus-arrival time prediction model based on APC data. Comp Aided Civil Infrast Eng 19(5):364–376
8. Yu B, Lam WHK, Tam ML (2011) Bus travel time prediction at bus stop with multiple routes. Transp Res Part C: Emerg Technol 19:1157–1170
9. Yu B, Yang ZZ, Chen K, Yu B (2010) Hybrid model for prediction of bus arrival time at next station. J Adv Transp 44:193–204

10. Thissen U, Brakel RV, Weijer APD, Melssen WJ, Buydens LMC (2003) Using support vector machines for time series prediction. Chemom Intell Lab Syst 69(1):35–49
11. Gaweł P, Jaszkiewicz A (2011) Improving short-term travel time prediction for on-line car navigation by linearly transforming historical traffic patterns to fit the current traffic conditions. Proc Soc Behav Sci 20:638–647
12. Deng M, Qu S (2016) Road short-term travel time prediction method based on flow spatial distribution and the relations. Mathem Probl Eng 2016(7626875):14
13. Li Q, Wen Z, He, B (2020) Practical federated gradient boosting decision trees. Proceedings of the AAAI Conference on Artificial Intelligence 34(04):4642–4649
14. Kankanamge KD, Witharanage YR, Withanage CS, Hansini N, Lakmal D, Thayasivam U (2019) Taxi trip travel time prediction with isolated XGBoost regression.: Moratuwa Engineering Research Conference (MERCon), pp. 54–59
15. Gupta, Bharat, Shivam Awasthi, Rudraksha Gupta, Likhama Ram, Pramod Kumar, Bakshi Rohit Prasad, Sonali Agarwal (2018) Taxi travel time prediction using ensemble-based random forest and gradient boosting model. In Advances in Big Data and Cloud Computing, pp 63–78. Springer, Singapore
16. Bauer D, Tulic M (2018) Travel time predictions: should one model speeds or travel times? European Transp Res Rev 10:46
17. Jammula JK, Bera R, Ravishankar KVR (2018) Travel time prediction modelling in mixed traffic conditions. Intern J Traffic Trans Eng 8(1):135–147
18. Yun MA, XIONG Gui-xi (2009) Analysis of travel time prediction based on BRT environment. Comput Modern 1(12)
19. Bai Mengting, Yangxin Lin, Meng Ma, Ping Wang (2018) Travel-time prediction methods: a review. In International Conference on Smart Computing and Communication, pp. 67–77. Springer, Cham
20. Wu T, Wang Y, Jiang R, Lu X, Tian J (2017) A pathways-based prediction model for classifying breast cancer subtypes. Oncotarget 8(35):58809–58822
21. Liu Yang, Yanjie Ji, Keyu Chen, Xinyi Qi (2019) Support vector regression for bus travel time prediction using wavelet transform. J Harbin Inst Technol (New Series) 3
22. Laha AK, Putatunda S (2017) Travel time prediction for GPS taxi data streams, thesis, W.P. No. 2017–03–03, March
23. Cortes C, Vapnik V (1995) Support-vector networks. Mach Learn 20:273–297
24. Bhaskar A (2009) A methodology (CUPRITE) for urban network travel time estimation by integrating multisource data. PhD, Ecole polytechnique fédérale de Lausanne EPFL. Retrieved from http://books.google.com.au/books?id=9FRHcgAACAAJ
25. Vanajakshi L, Rilett L (2004) A comparison of the performance of artificial neural networks and support vector machines for the prediction of traffic speed, IEEE Intelligent Vehicles Symposium, pp 194–199
26. Wu C, Ho J, Lee DT (2004) Travel-time prediction with support vector regression. In IEEE Transactions on Intelligent Transportation Systems, vol. 5, no. 4, pp. 276–281
27. Philip AM, Ramadurai G, Vanajakshi L (2018) Urban arterial travel time prediction using support vector regression. Trans Devel Econ 4(7)
28. Chamberlain RG (2013) Great circle distance between two points. http://www.movabletype.co.uk/scripts/gis-faq-5.1.html
29. Wu C, Zhao Y, Wang Z (2002) The median absolute deviations and their applications to Shewhart (X)over-bar control charts. Commun Statis Simul Comput 3131(3):425–442
30. Klaus S (2002) EASY-FIT: a software system for data fitting in dynamical systems. Struct Multidiscip Optim 23(2):153–169
31. Kenneth DL, Ronald KK (1982) Advances in business and management forecasting. Emerald books, U.K.